frontiers | Research Topics

The immunosuppressive tumor microenvironment and strategies to revert its immune regulatory milieu for cancer immunotherapy

Edited by
Mazdak Ganjalikhani Hakemi, Gulderen Yanikkaya Demirel, Yangqiu Li, Andrey Zamyatnin and Jayakumar Nair

Published in
Frontiers in Immunology

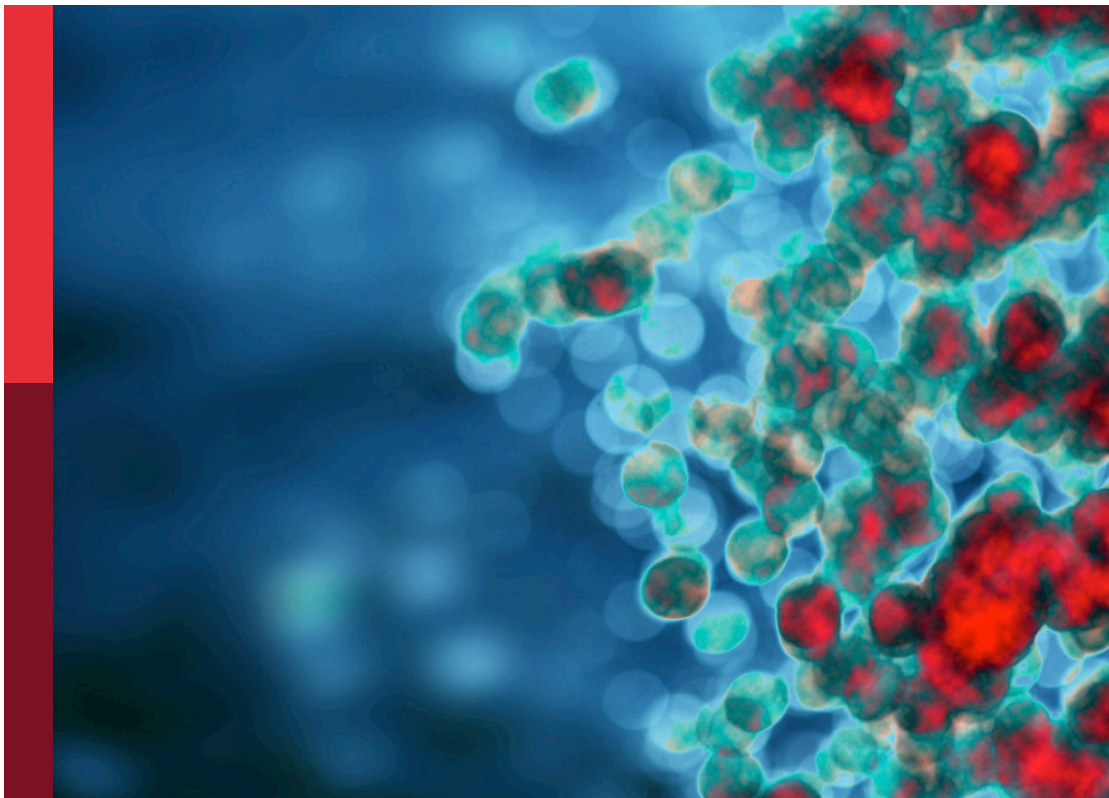

ISSN 1664-8714
ISBN 978-2-8325-2966-9
DOI 10.3389/978-2-8325-2966-9

About Frontiers

Frontiers is more than just an open access publisher of scholarly articles: it is a pioneering approach to the world of academia, radically improving the way scholarly research is managed. The grand vision of Frontiers is a world where all people have an equal opportunity to seek, share and generate knowledge. Frontiers provides immediate and permanent online open access to all its publications, but this alone is not enough to realize our grand goals.

Frontiers journal series

The Frontiers journal series is a multi-tier and interdisciplinary set of open-access, online journals, promising a paradigm shift from the current review, selection and dissemination processes in academic publishing. All Frontiers journals are driven by researchers for researchers; therefore, they constitute a service to the scholarly community. At the same time, the *Frontiers journal series* operates on a revolutionary invention, the tiered publishing system, initially addressing specific communities of scholars, and gradually climbing up to broader public understanding, thus serving the interests of the lay society, too.

Dedication to quality

Each Frontiers article is a landmark of the highest quality, thanks to genuinely collaborative interactions between authors and review editors, who include some of the world's best academicians. Research must be certified by peers before entering a stream of knowledge that may eventually reach the public - and shape society; therefore, Frontiers only applies the most rigorous and unbiased reviews. Frontiers revolutionizes research publishing by freely delivering the most outstanding research, evaluated with no bias from both the academic and social point of view. By applying the most advanced information technologies, Frontiers is catapulting scholarly publishing into a new generation.

What are Frontiers Research Topics?

Frontiers Research Topics are very popular trademarks of the *Frontiers journals series*: they are collections of at least ten articles, all centered on a particular subject. With their unique mix of varied contributions from Original Research to Review Articles, Frontiers Research Topics unify the most influential researchers, the latest key findings and historical advances in a hot research area.

Find out more on how to host your own Frontiers Research Topic or contribute to one as an author by contacting the Frontiers editorial office: frontiersin.org/about/contact

The immunosuppressive tumor microenvironment and strategies to revert its immune regulatory milieu for cancer immunotherapy

Topic editors

Mazdak Ganjalikhani Hakemi — Isfahan University of Medical Sciences, Iran
Gulderen Yanikkaya Demirel — Yeditepe University, Türkiye
Yangqiu Li — Jinan University, China
Andrey Zamyatnin — Lomonosov Moscow State University, Russia
Jayakumar Nair — National Institutes of Health (NIH), United States

Citation

Hakemi, M. G., Demirel, G. Y., Li, Y., Zamyatnin, A., Nair, J., eds. (2023). *The immunosuppressive tumor microenvironment and strategies to revert its immune regulatory milieu for cancer immunotherapy*. Lausanne: Frontiers Media SA.
doi: 10.3389/978-2-8325-2966-9

Table of contents

frontiers | Frontiers in Immunology

TYPE Editorial
PUBLISHED 26 June 2023
DOI 10.3389/fimmu.2023.1238698

OPEN ACCESS

EDITED AND REVIEWED BY
Ibrahim C. Haznedaroglu,
Hacettepe University Hospital, Türkiye

*CORRESPONDENCE
Mazdak Ganjalikhani Hakemi
mghakemi@med.mui.ac.ir
Gülderen Yanikkaya Demirel
gulderen.ydemirel@yeditepe.edu.tr
Yangqiu Li
yangqiuli@hotmail.com
Nair Jayakumar
jayakumar.nair@nih.gov

RECEIVED 12 June 2023
ACCEPTED 19 June 2023
PUBLISHED 26 June 2023

CITATION
Ganjalikhani Hakemi M, Yanikkaya Demirel G, Li Y and Jayakumar N (2023) Editorial: The immunosuppressive tumor microenvironment and strategies to revert its immune regulatory milieu for cancer immunotherapy.
Front. Immunol. 14:1238698.
doi: 10.3389/fimmu.2023.1238698

Editorial: The immunosuppressive tumor microenvironment and strategies to revert its immune regulatory milieu for cancer immunotherapy

Mazdak Ganjalikhani Hakemi[1]*, Gülderen Yanikkaya Demirel[2]*, Yangqiu Li[3]* and Nair Jayakumar[4]*

[1]Department of Immunology, Faculty of Medicine, Isfahan University of Medical Sciences, Isfahan, Iran, [2]Department of Immunology, Faculty of Medicine, Yeditepe University, Istanbul, Türkiye, [3]Institute of Hematology, School of Medicine, Jinan University, Guangzhou, China, [4]Women's Malignancies Branch, National Institutes of Health (NIH), Bethesda, MD, United States

KEYWORDS

cancer immunology, cancer immunotherapy, immunosuppression, immune regulation, tumor microenvironment

Editorial on the Research Topic

The immunosuppressive tumor microenvironment and strategies to revert its immune regulatory milieu for cancer immunotherapy

Despite advancements in tumor immunotherapy, inconsistent therapeutic effects and barriers impacting clinical outcomes highlight the need for a better understanding of the tumor microenvironment (TME) in cancer immunology (1). The TME plays a crucial role in anti-cancer immunity, influencing the effectiveness of immunotherapy and other treatments (2, 3). Interactions between cancer cells, the extracellular matrix, and stromal cells shape the TME, creating a heterogeneous environment that fosters chronic inflammation, immune suppression, and angiogenesis (4–6).

Limited understanding of immune suppression in cancer patients has hindered the success of immunotherapeutic strategies. Therefore, comprehending the TME, tumor immune evasion mechanisms, and the interplay between stromal and immune cells is vital for successful tumor immunotherapy (7, 8). Overcoming immune-suppressive networks and activation barriers within the TME is crucial for effective cancer cell eradication (9–11). Targeting key factors and reprogramming the TME to enhance T cell activity while reducing immune-suppressive cell accumulation are potential strategies.Further studies on TME composition and its impact on immune surveillance attenuation can guide the development of strategies to manipulate the TME and benefit cancer patients (12, 13).

Understanding the TME status, immune cell involvement, and key transcription factors is essential for developing therapies that target inefficient T-cells within the TME. In their study titled "*Regulatory effects of IRF4 on immune cells in the tumor microenvironment*,"

Lu et al. demonstrated the significant potential of targeting IRF4 and its interactions with BATF, TCF1, Roquin, or Regnase1 to regulate anti-tumor T-cell immunity and improve therapeutic efficacy. Polyamine metabolism is closely associated with tumor development and the TME. Wang et al. conducted a study on the "*development and validation of polyamine metabolism-associated gene signatures*" to predict prognosis and immunotherapy response in lung adenocarcinoma (LUAD) using machine learning. They identified specific genes related to polyamine metabolism that can predict patient survival and showed their association with immune cell infiltration and immunotherapy response in LUAD patients. Additionally, the role of adenosine triphosphate (ATP) in cellular energy metabolism and the contribution of CD39 and CD73 ectonucleotidases to inflammation, hypoxia, and cancer progression have been recognized as promising therapeutic targets (14, 15). Jiang et al. in a study entitled "*The ectonucleotidases CD39 and CD73 on T cells: The new pillar of hematological malignancy*" highlighted the potential of CD39 and CD73 as disease markers and prognostic indicators in hematological malignancies, contributing to the progression and expansion of leukemias.

Zhou et al. conducted a bibliometric and visual analysis on tumor-associated macrophage (TAM) research, evaluating its research status, focus areas, and development trends. The study covered 6,405 articles published between 2001 and 2021, primarily from the USA and China, providing valuable information for researchers in this promising field of cancer immunology. In their contribution, Zhu et al. explored the inhibition of immune response by stress hormones and its reversal through enhancing the anti-cancer functions of granulocytes using Ginsenoside Rg1, a traditional herbal medicine ingredient. They confirmed the immunoprotective effects of Ginsenoside Rg1 on granulocytes through cell culture and animal experiments. The study demonstrated the downregulation of ARG2, MMP1, S100A4, and RAPSN mRNA expression, as well as the upregulation of LAMC2, DSC2, KRT6A, and FOSB mRNA expression in noradrenaline-inhibited granulocytes. These findings suggest the potential use of Ginsenoside Rg1 as an adjuvant drug for cancer patients experiencing mental stress. Sarsembayeva et al. investigated the role of tumor microenvironment-derived Cannabinoid receptors (CB1 and CB2 receptors) in non-small cell lung cancer. They identified immune cells expressing cannabinoid receptors in the tumor microenvironment and observed that the absence of cannabinoid receptor 2 led to a favorable change in the composition of immune cell populations, favoring tumor-killing lymphocytes. The study indicated that the absence of this receptor significantly improved the response to immunotherapy, highlighting the relevance of microenvironment findings in immunotherapeutic approaches. In the context of immune suppression in solid tumors such as Glioblastoma (GBM), Ni et al. conducted a study titled "*Transcriptome and single-cell analysis reveal the contribution of immunosuppressive microenvironment for promoting glioblastoma progression*." This research identified immune suppressive subgroups, major cell types, signaling pathways, and molecules involved in the formation of the immune suppressive subgroup. The findings provide valuable insights for future personalized immunotherapy approaches targeting GBM.

In their review titled "*Targeting the Bone Marrow Microenvironment in Acute Myeloid Leukemia: Potential Use of Immune Checkpoint Inhibitors*," Aru et al. emphasized the impact of dual inhibition of the CXCL12-CXCR4 and PD-1-PD-L1 axes in alleviating the immunosuppressive tumor microenvironment of acute myeloid leukemia (AML). This highlights the potential of immune checkpoint blockade (ICB) as a therapeutic approach for modifying the bone marrow microenvironment (BMM) in AML. However, further research involving larger patient cohorts is needed to fully understand the integration of ICIs in hematological malignancy treatments. Yao et al. explored the immune characteristics of T-cell subsets in peripheral blood and bone marrow samples of chronic myeloid leukemia (CML) patients. They observed altered immune patterns, including increased levels of TIGIT and CD8+ tissue-residual T cells (TRM) in *de novo*-CML patients, while the level of CD8+TEMRA cells decreased in patients who did not achieve a molecular response. These findings suggest that tyrosine kinase inhibitor (TKI) therapy can reshape the T-cell repertoire when patients achieve a molecular response in CML. Lv et al. utilized single-cell RNA sequencing (scRNA-seq) to analyze immune cell dynamics and tumor cell infiltration in the bone marrow (BM) of multiple myeloma (MM) patients. They discovered aberrant metabolic processes associated with the immunosuppressive microenvironment in MM, particularly dysregulated amino acid metabolism that impaired the function of cytotoxic CD8 T cells. The authors propose that restoring metabolic balance should be a key focus for improving the efficacy of immune-based therapies in MM. In the context of B cell malignancies, including MM, B-cell lymphomas, and chronic lymphocytic leukemia, immunomodulatory drugs (IMiDs) such as thalidomide, lenalidomide, and pomalidomide have been employed. Guo et al. summarized the current advances in the use of IMiDs in regulating immune cell function and enhancing the efficacy of immunotherapies across different types of B-cell neoplasms. The authors highlight the importance of IMiDs-based tumor microenvironment re-education as a crucial mechanism for improving treatment outcomes. These studies collectively demonstrate the significance of understanding and targeting the immune disorder within the microenvironment of hematological malignancies, including AML, CML, MM, and B-cell neoplasms. By manipulating the tumor microenvironment, such as through immune checkpoint inhibitors or metabolic interventions, there is potential to enhance the effectiveness of immunotherapies in these diseases.

More recently, an old foe has come back to the forefront of the fight against cancer, namely oncolytic viruses and their more interesting cousins the arenaviruses. While oncolytic viruses have limited efficacy in tumors with intact IFN pathways, arenaviruses provide a promising alternative due to their ability to evade host immunity (16, 17). In their review titled "*Arenaviruses: Old viruses present new solutions for cancer therapy*," Stachura et al. discuss the resurgence of oncolytic viruses and the emerging use of arenaviruses in cancer treatment. The authors provide a comprehensive overview of arenaviruses, focusing on lymphocytic choriomeningitis virus (LCMV), a non-cytopathic virus with specific cancer tropism. They highlight the recent positive results from early clinical trials with arenavirus-based therapies, presented at the AACR and ASCO meetings in 2023. The review delves into

the biology of LCMV, its safety profile in patients, and various LCMV-based therapies and anti-cancer vaccines. The information presented in the review will be valuable for researchers in the field of cancer immunotherapy, providing insights into the potential of arenaviruses as a novel viral-based therapy.

At the whole, we received and enthusiastically reviewed several interesting reviews and research articles on this Research Topic, which shed light on new research directions related to one of the most important and multidisciplinary research subject: "*The Immunosuppressive Tumor Microenvironment and Strategies to Revert its Immune Regulatory Milieu for Cancer Immunotherapy*. "We hope that all the efforts of the editorial team and the articles presented in this Research Topic can be interesting, informative, and inspiring for all our readers, encouraging them to thoroughly explore the presented subject in this Research Topic.

Author contributions

All authors listed have made a substantial, direct, and intellectual contribution to the work and approved it for publication.

Acknowledgments

We extend our heartfelt gratitude to all the authors who contributed their studies to the current Research Topic, as well as to the reviewers who diligently assessed the manuscripts. Their dedicated efforts have greatly aided us in disseminating the latest knowledge on this subject to a global audience.

Conflict of interest

The authors declare that the research was conducted in the absence of any commercial or financial relationships that could be construed as a potential conflict of interest.

Publisher's note

References

1. Elmore LW, Greer SF, Daniels EC, Saxe CC, Melner MH, Krawiec GM, et al. Blueprint for cancer research: critical gaps and opportunities. *CA: A Cancer J Clin* (2021) 71:107–39. doi: 10.3322/caac.21652

2. Lee WS, Yang H, Chon HJ, Kim C. Combination of anti-angiogenic therapy and immune checkpoint blockade normalizes vascular-immune crosstalk to potentiate cancer immunity. *Exp Mol Med* (2020) 52:1475–85. doi: 10.1038/s12276-020-00500-y

3. Tang T, Huang X, Zhang G, Hong Z, Bai X, Liang T. Advantages of targeting the tumor immune microenvironment over blocking immune checkpoint in cancer immunotherapy. *Signal Transduction Targeted Ther* (2021) 6:72. doi: 10.1038/s41392-020-00449-4

4. Alsibai KD, Meseure D. Significance of tumor microenvironment scoring and immune biomarkers in patient stratification and cancer outcomes. *Histopathol Update* (2018), 11–31. doi: 10.5772/intechopen.72648

5. Oshimori N, Guo Y, Taniguchi S. An emerging role for cellular crosstalk in the cancer stem cell niche. *J Pathol* (2021) 254:384–94. doi: 10.1002/path.5655

6. Binnewies M, Roberts EW, Kersten K, Chan V, Fearon DF, Merad M, et al. Understanding the tumor immune microenvironment (TIME) for effective therapy. *Nat Med* (2018) 24:541–50. doi: 10.1038/s41591-018-0014-x

7. Farkona S, Diamandis EP, Blasutig IM. Cancer immunotherapy: the beginning of the end of cancer? *BMC Med* (2016) 14:1–18. doi: 10.1186/s12916-016-0623-5

8. Li X, Shao C, Shi Y, Han W. Lessons learned from the blockade of immune checkpoints in cancer immunotherapy. *J Hematol Oncol* (2018) 11:1–26. doi: 10.1186/s13045-018-0578-4

9. Marzagalli M, Ebelt ND, Manuel ER. Unraveling the crosstalk between melanoma and immune cells in the tumor microenvironment. *Semin Cancer Biology Elsevier* (2019) pp:236–50. doi: 10.1016/j.semcancer.2019.08.002

10. Wei F, Wang D, Wei J, Tang N, Tang L, Xiong F, et al. Metabolic crosstalk in the tumor microenvironment regulates antitumor immunosuppression and immunotherapy resisitance. *Cell Mol Life Sci* (2021) 78:173–93. doi: 10.1007/s00018-020-03581-0

11. Hanahan D, Coussens LM. Accessories to the crime: functions of cells recruited to the tumor microenvironment. *Cancer Cell* (2012) 21:309–22. doi: 10.1016/j.ccr.2012.02.022

12. Nakamura K, Smyth MJ. Myeloid immunosuppression and immune checkpoints in the tumor microenvironment. *Cell Mol Immunol* (2020) 17:1–12. doi: 10.1038/s41423-019-0306-1

13. Li K, Shi H, Zhang B, Ou X, Ma Q, Chen Y, et al. Myeloid-derived suppressor cells as immunosuppressive regulators and therapeutic targets in cancer. *Signal Transduction Targeted Ther* (2021) 6:362. doi: 10.1038/s41392-021-00670-9

14. Kepp O, Loos F, Liu P, Kroemer G. Extracellular nucleosides and nucleotides as immunomodulators. *Immunol Rev* (2017) 280:83–92. doi: 10.1111/imr.12571

15. Longhi MS, Robson SC, Bernstein SH, Serra S, Deaglio S. Biological functions of ecto-enzymes in regulating extracellular adenosine levels in neoplastic and inflammatory disease states. *J Mol Med* (2013) 91:165–72. doi: 10.1007/s00109-012-0991-z

16. Kaufman HL, Kohlhapp FJ, Zloza A. Oncolytic viruses: a new class of immunotherapy drugs. *Nat Rev Drug Discovery* (2015) 14:642–62. doi: 10.1038/nrd4663

17. de Vries CR, Kaufman HL, Lattime EC. Oncolytic viruses: focusing on the tumor microenvironment. *Cancer Gene Ther* (2015) 22:169–71. doi: 10.1038/cgt.2015.11

frontiers | Frontiers in Immunology

TYPE Review
PUBLISHED 12 October 2022
DOI 10.3389/fimmu.2022.1017990

OPEN ACCESS

EDITED BY
Yangqiu Li,
Jinan University, China

REVIEWED BY
Xiaofang Wang,
Guangzhou Medical University, China
Liang Lin,
Cytovia Therapeutics, United States

*CORRESPONDENCE
Keshu Zhou
drzhouks77@163.com

SPECIALTY SECTION
This article was submitted to Cancer Immunity and Immunotherapy, a section of the journal Frontiers in Immunology

RECEIVED 12 August 2022
ACCEPTED 27 September 2022
PUBLISHED 12 October 2022

CITATION
Guo H, Yang J, Wang H, Liu X, Liu Y and Zhou K (2022) Reshaping the tumor microenvironment: The versatility of immunomodulatory drugs in B-cell neoplasms.
Front. Immunol. 13:1017990.
doi: 10.3389/fimmu.2022.1017990

Reshaping the tumor microenvironment: The versatility of immunomodulatory drugs in B-cell neoplasms

Hao Guo, Jingyi Yang, Haoran Wang, Xingchen Liu, Yanyan Liu and Keshu Zhou*

Department of Hematology, The Affiliated Cancer Hospital of Zhengzhou University & Henan Cancer Hospital, Zhengzhou, China

Immunomodulatory drugs (IMiDs) such as thalidomide, lenalidomide and pomalidomide are antitumor compounds that have direct tumoricidal activity and indirect effects mediated by multiple types of immune cells in the tumor microenvironment (TME). IMiDs have shown remarkable therapeutic efficacy in a set of B-cell neoplasms including multiple myeloma, B-cell lymphomas and chronic lymphocytic leukemia. More recently, the advent of immunotherapy has revolutionized the treatment of these B-cell neoplasms. However, the success of immunotherapy is restrained by immunosuppressive signals and dysfunctional immune cells in the TME. Due to the pleiotropic immunobiological properties, IMiDs have shown to generate synergetic effects in preclinical models when combined with monoclonal antibodies, immune checkpoint inhibitors or CAR-T cell therapy, some of which were successfully translated to the clinic and lead to improved responses for both first-line and relapsed/refractory settings. Mechanistically, despite cereblon (CRBN), an E3 ubiquitin ligase, is considered as considered as the major molecular target responsible for the antineoplastic activities of IMiDs, the exact mechanisms of action for IMiDs-based TME re-education remain largely unknown. This review presents an overview of IMiDs in regulation of immune cell function and their utilization in potentiating efficacy of immunotherapies across multiple types of B-cell neoplasms.

KEYWORDS

Immunomodulatory drug, B-cell lymphoma, Multiple myeloma, Tumor microenvironment, Immunotherapy, CRBN

1 Introduction

B-cell neoplasms, which stem from distinct stages of B-cell development, are a heterogeneous set of cancers including B-cell lymphomas (BCLs), chronic lymphocytic leukemia (CLL), and plasma cell dyscrasias such as multiple myeloma (MM) (1). Despite great advances have been achieved in diagnosis and treatment, these hematologic disorders still cause significant global morbidity and mortality. The introduction of a safe and more effective new class of drugs, especially the monoclonal antibodies (mAbs) (e.g. anti-CD20 rituximab and anti-CD38 daratumumab), has made remarkable therapeutic progress in the past twenty years. Yet a large number of patients still fail to have response or relapse eventually. More recently, novel immunotherapies including immune checkpoint inhibitors (ICIs) and chimeric antigen receptor (CAR) T-cell therapy have made breakthroughs in treatment of refractory disease (2, 3). However, the success of immunotherapy is impeded by inhibitory signals which reside in cancer cells or that are generated from the tumor microenvironment (TME), which restricts the tumor-suppressive capacity of the immune system (4–6).

TME is a complex network consisting of both cellular and non-cellular compositions, which forms a physical barrier around malignant cells. Increasing evidence has established that components of TME play vital roles in a series of processes of tumor development, including carcinogenesis, progression, metastasis and treatment resistance (6–8). Recognition of the TME has paved the way for exploring novel strategies targeting the microenvironment as well as its interplays with tumor cells (9). Immunomodulatory drugs (IMiDs) are a group of anticancer agents including thalidomide and its analogs lenalidomide and pomalidomide. These compounds show pleiotropic effects in hematologic malignancies including anti-angiogenic, anti-proliferative and immunobiologic properties by direct cytotoxicity towards tumor cells and indirectly interfering with cellular components of the TME (10–12). Herein, we provide a comprehensive review of the immunomodulatory activities of thalidomide analogues towards T cells, tumor-associated macrophages (TAMs), natural killer (NK) cells, dendritic cells (DCs) and stromal cells. In addition, we also discuss the clinical efficacy of IMiDs in combination with the state-of-the-art immunotherapies to shed light on optimal TME–targeted treatment strategy.

Abbreviations: AML, Acute myeloid leukemia; ADCC, Antibody-dependent cell-mediated cytotoxicity; ADCP, Antibody-dependent cellular phagocytosis; APC, Antigen presenting cell; ASCT, Autologous stem cell transplantation; BCL, B-cell lymphoma; BsAb, Bispecific antibody; BiTE, Bi-specific T-cell engager; BMSC, Bone marrow-derived mesenchymal stromal cell; CK1α, Casein kinase 1 alpha; CRBN, Cereblon; CAR, Chimeric antigen receptor; CLL, Chronic lymphocytic leukemia; CR, Complete response; DC, Dendritic cell; DLBCL, Diffuse large B-cell lymphoma; FDC, Follicular dendritic cell; FL, Follicular lymphoma; FDA, Food and Drug Administration; ICI, Immune checkpoint inhibitor; IS, Immune synapse; IMiD, Immunomodulatory drug; IRF4, Interferon regulatory factor 4; MCL, Mantle cell lymphoma; MOA, Mechanism of action; mAb, Monoclonal antibody; MM, Multiple myeloma; MDS, Myelodysplastic syndrome; NK, Natural killer; ND, Newly diagnosed; NHL, Non-Hodgkin lymphoma; ORR, Overall response rate; PDX, Patient-derived xenograft; PCNSL, Primary central nervous system lymphoma; PEL, Primary effusion lymphoma; PFS, Progression-free survival; Treg, Regulatory T cell; R/R, Relapsed/refractory; SLE, Systemic lupus erythematosus; TME, Tumor microenvironment; TAA, Tumor-associated antigen; TAM, Tumor-associated macrophage; VEGF, Vascular endothelial growth factor.

2 Development of IMiDs

2.1 Drug repurposing and regeneration

Thalidomide (α-N-phthalimido-glutarimide) (Figure 1A), a synthetic glutamic acid derivative, was once infamous for its potent teratogen causing dysmelia when used for alleviating nausea during pregnancy in the late 1950s and early 1960s. Despite withdrawal from markets that time, thalidomide regained its new life four decades later when immunomodulatory and anti-tumor effects were discovered (10, 13, 14). The first evidence for the immunomodulatory functions of thalidomide was demonstrated that it was effective in the treatment of erythema nodosum leprosum due to its ability to inhibit TNFα secreted by activated monocytes (15, 16). Except for this anti-inflammatory property, thalidomide was subsequently shown to exert other immunomodulatory properties such as co-stimulation of T cells and activation of NK cells (17). Along with these findings, the recognition of thalidomide as an inhibitor of angiogenesis further fueled a surge of interest in repurposing thalidomide as a promising anti-neoplastic therapy (18). As such, a set of formal medicinal chemistry programs were then initiated to discover novel derivatives with enhanced efficacy while less toxicity compared with thalidomide (19). Lenalidomide and pomalidomide (Figure 1A), the two first-in-class IMiDs, are derived by adding an amino group to the fourth carbon of the phthaloyl ring of thalidomide (13).

Lenalidomide was the first thalidomide analogue developed, consequently dominating the clinical development in hematologic malignancies (14). Lenalidomide was also the first agent of this group of immunomodulatory drugs approved by US Food and Drug Administration (FDA) for the treatment of MM, relapsed/refractory (R/R) mantle cell lymphoma (MCL), and myelodysplastic syndrome (MDS) with deletion 5q (20–24). Recently, it has been approved for previously treated follicular lymphoma (FL) and marginal zone lymphoma (MZL) in combination with rituximab (25–27). Notably, in 2020, lenalidomide combined with tafasitamab (a CD19 targeting mAb) received accelerated approval for patients with R/R diffuse large B-cell lymphoma (DLBCL) (28).

10.3389/fimmu.2022.1017990

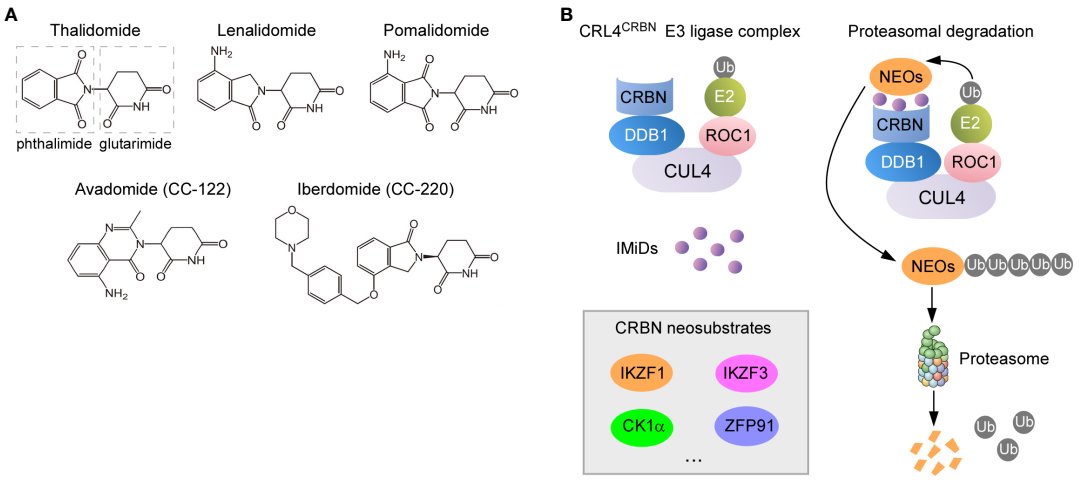

FIGURE 1
Molecular mechanisms of action for IMiDs. **(A)** Structure of thalidomide and its analogues. They all share a glutarimide ring that binds to CRBN while vary in the neosubstrate-binding moiety (phthaloyl ring). **(B)** Proteasomal degradation of CRBN neosubstrates redirected by IMiDs. IMiDs act as the molecular glue to recruit neosubstrate proteins to CRBN receptor component of the $CRL4^{CRBN}$ E3 ligase complex (left), which leads to the sequential ubiquitylation and degradation of neosubstrates (NEOs) (right).

As the third-generation thalidomide analogue, pomalidomide contains both the phthalimide and the glutarimide moieties like thalidomide but differs in an amino substituent at the four position of the phthalimide ring (Figure 1A) (29). Pomalidomide has been approved for the treatment of MM, which is more powerful than lenalidomide and shows efficacy in cases that are resistant to lenalidomide (30, 31). Furthermore, it is now under extensive exploration in preclinical or clinical studies on aggressive BCLs including DLBCL, primary effusion lymphoma (PEL) and primary central nervous system lymphoma (PCNSL) (32–37). Avadomide (also called CC-122) (Figure 1A), a novel modulator of cereblon E3 ubiquitin ligase (CELMoD) exhibiting potent anti-lymphoma and immunomodulatory activities, is currently in phase I trials (38, 39). Other new CELMoDs such as CC-220 (iberdomide) and CC-885 (Figure 1A) have shown efficacy in the treatment of systemic lupus erythematosus (SLE) and acute myeloid leukemia (AML) (40–42). The established applications and most common side effects of three approved IMiDs (thalidomide, lenalidomide and pomalidomide) are summarized in Table 1.

2.2 Mechanism of action

IMiDs exert their anti-tumor effects by a unique mechanism of action (MOA), not only killing the malignant cells directly, but also modulating nonmalignant immune cells (T cells, NK cells, TAMs, DCs etc.) within the TME, which are believed to contribute to lymphoma progression and survival (10, 11, 13). Due to the pleiotropic effects of IMiDs, their molecular targets were believed to be various. The direct target of IMiDs was unknown until Ito et al. identified cereblon (CRBN) as the sole molecular target underlying thalidomide teratogenicity (173). Thereafter, various studies have focused on elucidating the role of CRBN in the effects of thalidomide analogues, especially for lenalidomide (56, 80, 174–176). As a result, CRBN is currently regarded as a primary direct target for therapeutic activities of all IMiDs (13).

CRBN forms a cullin-4 RING E3 ubiquitin ligase complex ($CRL4^{CRBN}$) with DNA damage-binding protein 1 (DDB1), cullin 4 (CUL4), and regulator of cullins-1 (ROC1) (Figure 1B) (173, 177, 178). When bound by thalidomide derivatives, CRBN triggers protein ubiquitination and degradation of drug-specific neosubstrates. Substrate selectivity rests with the structure of IMiDs bond to CRBN (13, 179). IMiDs have a conserved glutarimide moiety that directly docks into a tri-tryptophan pocket on the surface of CRBN, which in turn activates its E3 ligase activity, modulates specificity of protein substrate and avoids autoubiquitylation (180, 181). In malignant B cells, IMiDs retarget CRBN-dependent ligase activity to Ikaros (IKZF1) and Aiolos (IKZF3), both of which are zinc finger–containing transcription factors in lymphoid development, resulting in their proteasomal degradation (14, 56, 88, 182, 183) (Figure 1B). The reduced abundance of Ikaros and Aiolos elicits direct anti-proliferative and anti-neoplastic effects against tumor cells. More importantly, a constellation of immunomodulatory effects arising from Ikaros and Aiolos degradation have been proposed to contribute to activities of IMiDs (14, 19), which include improved formation of immune synapse (IS) (184),

10.3389/fimmu.2022.1017990

TABLE 1 Applications of thalidomide analogues in hematologic malignancies and reported toxicities.

	Thalidomide	Lenalidomide	Pomalidomide
Preclinical activities	MM (43–45) NHL (46) CLL (47, 48) AML (49–53) ALL (54, 55)	MM (56–61) NHL (11, 61–71) CLL (72–77) AML (78, 79) MDS (78, 80–83)	MM (61, 84–87) NHL (34, 35, 37, 61, 88) AML (40, 89)
Clinical applications	MM* (90–95) FL (96, 97) MCL (98–100) HL (101, 102) TCL (103, 104) CLL (105–108) DLBCL (109) MALT lymphoma (110) AML (111–113) MDS (111, 114–117) CMML (118) CML (119)	MM* (120–125) MDS* (126, 127) MCL* (128–132) FL* (25–27, 128, 133–135) MZL* (26, 27, 128, 135) SLL (26, 27, 128, 135) CLL (136–141) DLBCL (128, 142, 143) MALT lymphoma (110, 144) PCNSL (145, 146) TCL (147–150) AML (127, 151–155) CMML (156–159)	MM* (160–163) CLL (164) DLBCL (32, 164) PCNSL (33) MPN (165, 166) MDS (167) AML (40, 167, 168)
Toxicities	Teratogenicity (169) Constipation (169) Hypothyroidism (169) ACTH stimulation (169) Hypoglycemia (169) Xerostomia (169) Fever (169) Mood changes (169) Headache (169) Peripheral neuropathy (169) Somnolence (169) Sedation (169) Rash (169) VTE (169)	Neutropenia (121) Anemia (121) Thrombocytopenia (121) Diarrhea (121) Fatigue (121) Muscle cramps (121) Rash (121) Infections (121) VTE (121) Myelosuppressive effects (170) Secondary MDS/AML (171) Secondary ALL (172)	Neutropenia (170) Anemia (170) Thrombocytopenia (170) Fatigue (170) VTE (170) Neuropathy (170) Infections (170)

MM, Mutiple myeloma; NHL, Non-Hodgkin lymphoma; CLL, Chronic lymphocytic leukemia; AML, Acute myeloid leukemia; ALL, Acute lymphoblastic leukemia; MDS, Myelodysplastic syndrome; FL, Follicular lymphoma; MCL, Mantle cell lymphoma; HL, Hodgkin lymphoma; TCL, T-cell lymphoma; DLBCL, Diffuse large B-cell lymphoma: MALT lymphoma, Mucosa-associated lymphoid tissue lymphoma; MZL, Marginal zone lymphoma; SLL, Small lymphocytic lymphoma; PCNSL, Primary central nervous system lymphoma; CMML, Chronic myelomonocytic leukemia; MPN, Myeloproliferative neoplasm; ACTH, Adrenocorticotropic hormone; VTE, Venous thromboembolism. *, FDA-approved applications.

potentiated co-stimulation of T cells (57), and enhanced release and function of anti-tumor cytokines (185).

It should be noted that different neosubstrate spectrum that are targeted for proteasomal degradation may account for the distinct activity of each thalidomide derivative (14). For instance, lenalidomide degrades casein kinase 1 alpha (CK1α, encoded by *CSNK1A1* gene) more efficiently than thalidomide and pomalidomide in myeloid neoplasms, thus providing a therapeutic window for lenalidomide in del (5q) MDS, where *CSNK1A1* haploinsufficiency due to genetic deletion sensitizes tumor cells to lenalidomide (80, 186, 187). A recent study showed that treatment with lenalidomide but not pomalidomide leads to expansion of pre-leukemic *Trp53*-mutant hematopoietic stem and progenitor cells (HSPCs) due to selective degradation of Ck1α, which offers a potential alternative strategy to mitigate the risk of therapy-related myeloid neoplasms (t-MNs) development (171). Accordingly, the efficacy and toxicity profiles of each IMiD and the precise use of these agents need to be thoroughly investigated.

3 The anti-tumor activities of IMiDs

3.1 Direct effects on malignant B cells

Direct anti-neoplastic activity of IMiDs against malignant B cells has been demonstrated in MM, CLL and aggressive non-Hodgkin lymphoma (NHLs) (12, 188). Degradation of Ikaros and Aiolos by lenalidomide and pomalidomide leads to specific and sequential downregulation of c-Myc followed by interferon regulatory factor 4 (IRF4), which results in subsequent cell death of myeloma cells (189). In addition, lenalidomide can upregulate p21WAF/Cip1 expression and lead to cell cycle arrest in CLL cells (72). In Namalwa CSN.70, a Burkitt's lymphoma cell line with chromosome 5 deletion, lenalidomide was shown to induce cell cycle arrest and inhibit Akt and Gab1 phosphorylation (190). Moreover, lenalidomide kills activated B cell-like (ABC) DLBCL cells by inhibiting IRF4 and the Ets transcription factor Spi-B while stimulating IFNβ production in a CRBN-dependent manner (191).

3.2 Pleiotropic effects of IMiDs on TME

Beyond the direct cytotoxicity towards malignant B cells, recent studies have emphasized the therapeutic implications of IMiDs-remodeled interplay between malignant cells and non-malignant immune cells in the TME within the lymph nodes and bone marrow (11, 12, 192). Despite these nursing cells usually build a supportive network for tumor development and drug resistance, they also have potential to drive antitumor immune responses in specific cases (5, 6). Early studies based on gene expression signature of FL patients found that the length of survival was associated with the molecular features of tumor-infiltrating immune cells at diagnosis, which was independent of clinically prognostic variables (193). This evidence was supported by direct studies demonstrating that TME cells such as follicular dendritic cells (FDCs), $CD4^+$ T cells and bone marrow stromal cells promoted lymphoma cell survival and proliferation (194, 195). In addition, tumor-associated monocytes/macrophages can attract and work in concert with other immune cells (e.g. T cells) by secretion of chemokines CCL3 and CCL4 (196, 197). As a result, TME shields malignant B cells from the immune recognition and elimination. The underlying mechanisms include the dampened expression of molecules (e.g. MHC I and II) required for interactions with immune cells, defected T-cell IS formation, and the recruitment of immunosuppressive cells such as regulatory T cells (Tregs) and TAMs (198–200). The immunomodulatory effects of IMiDs on the TME, especially the immune cells, are summarized in Table 2 and illustrated in Figure 2.

3.2.1 Effects on T cells

Compelling evidence suggests that malignant B cells can induce an immune-suppressed, largely exhausted and senescent T-cell phenotype through numerous mechanisms, such as upregulation of inhibitory ligands, downregulation of co-stimulatory molecules and production of immunosuppressive cytokines, which ultimately results in suppression the T-cell surveillance and immune escape (199, 235–237).

Preclinical studies have shown that treatment with IMiDs enhances co-stimulation and proliferation of T cells by inducing pro-inflammatory cytokine (e.g. IFN-γ, TNF-α and IL-2), decreasing anti-inflammatory cytokines (e.g. IL-6 and IL-10) and potentiating DC-antigen presentation in MM and CLL (12, 192, 238, 239). The degradation of Ikaros and Aiolos by IMiDs relieves the transcriptional repression of *Il2* promoter, thus promoting IL-2 production (175). Moreover, IMiDs can reduce immune tolerance of myeloma cells by binding to B7 co-stimulation molecular and activating B7-CD28 pathway (240). IMiDs can also upregulate transcriptional activity of DNA-binding protein AP-1 to increase T-cell cytokine production (212, 240, 241). These mechanisms collectively contribute to a primed T-cell activation (212, 242).

Due to the influence of malignant B cells, tumor-infiltrating $CD4^+$ and $CD8^+$ T cells usually display decreased IS formation and effector function (11). Ex vivo lenalidomide treatment of T cells co-cultured with CLL or FL cells repairs IS formation defect by restoring T-cell actin cytoskeletal signaling and enhancing actin polymerization (184, 198, 202). In addition, lenalidomide was shown to induce actin reorganization and γδT-MCL IS formation, as well as expansion and cytotoxicity of γδT cells against MCL (11). Another study reported that lenalidomide can repair defected T-cell adhesion and migration in CLL by restoring normal levels of Rho-GTPase family (Rho, Rac1 and Cdc42) and rescuing LFA-1 function (243).

Clinical investigations also provided evidence for the positive regulation of IMiDs on T-cell functions. Lenalidomide

TABLE 2 Modulatory effects of IMiDs on immune cells and implications for improving immunotherapies.

Cell types	Effects of IMiDs	Rational combinations with immunotherapies
T cells	1. Promoting co-stimulation and proliferation (175, 201) 2. Enhancing T-cell effector functions (153, 202) 3. Increasing pro-inflammatory cytokine levels (192) 4. Improving IS formation between T cells and tumor cells (65) 5. Inhibiting T-cell exhaustion and senescence (192, 203) 6. Modulating Th1/Th2 subsets and Treg function (201, 204, 205)	1. Anti-PD-1/PD-L1 therapy (59, 206) 2. CAR-T cell therapies (73, 207, 208) 3. Bi-specific T-cell engager (209–211)
NK cells	1. Increasing NK-cell number (212) 2. Stimulating NK-cell activation (216–218) 3. Enhancing NK-cell cytotoxicity (217, 218, 221, 222) 4. Restoring IS formation (217) 5. Promoting ADCC (62)	1. Monoclonal antibodies (25, 26, 213–215) 2. Bispecific antibodies (219, 220)
TAMs	1. Switching M2 to M1 type (35, 223) 2. Enhancing phagocytosis (35) 3. Promoting ADCP (213, 225)	1. Monoclonal antibodies (25, 215, 224–227) 2. Bispecific antibodies (227, 228)
DCs	1. Promoting antigen uptake antigen and presentation (229) 2. Increasing expression of MHC class I and II molecules (229) 3. Enhancing T-cell priming by DCs (229) 4. Potentiating DC-mediated T-cell responses (229)	1. DC vaccination (230–233) 2. Anti-PD-1/PD-L1 therapy (234)

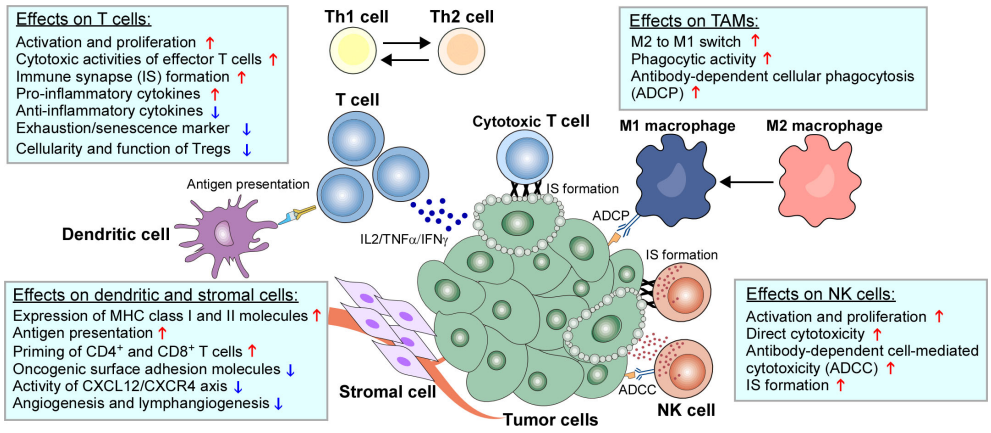

FIGURE 2
Immunomodulatory effects of IMiDs on the TME of B-cell neoplasms. The biological impacts of IMiDs on T cells, natural killer (NK) cells, tumor-associated macrophages (TAMs), dendritic cells and stromal cells are depicted.

maintenance therapy after autologous stem-cell transplantation (ASCT) increases $CD8^+$ T-cell numbers, upregulates co-stimulatory molecules and reduce inhibitory checkpoint molecules in MM patients (244). Similarly, Danhof et al. showed that lenalidomide maintenance post ASCT preserves $CD8^+$ T cells and reduces expression of PD-1, enabling synergetic efficacies with ICIs (203). These findings were further validated in patient-derived xenograft (PDX) models showing an enhanced anti-CLL activity by combining avadomide and anti-PD-1 or anti-PD-1 ligand (PD-L1) (245). Moreover, the tumor-promoting Th17/Th1 and Th22 cells and related cytokines (IL-17, IL-6, IL-1β etc.) were decreased in MM patients treated with IMiDs during induction chemotherapy compared to untreated patients, which was associated with a favorable clinical outcome (246). As a result, lenalidomide and obinutuzumab combination was shown to induce an activated T-cell phenotype and reshape gene signatures into effector memory T cell features in FL patients (202). While *in vitro* studies showed that lenalidomide and pomalidomide strongly inhibit generation, proliferation and function of Tregs possibly due to decreased FOXP3 expression, the impact of IMiDs on the cellularity of Tregs in patients with B-cell neoplasms remains controversial (11, 192). In a post-transplant MM setting, treatment with IMiDs during induction therapy pre-ASCT resulted in decreased Tregs while increased $CD8^+$ T cells in peripheral blood (247). In contrast, another study showed that lenalidomide maintenance after ASCT increased Treg numbers in relapsed MM patients (204). A similar pattern was observed in MCL patients treated with lenalidomide (248).

3.2.2 Effects on NK cells

NK cells are predominant innate lymphocytes that reject types of tumors and clear microbial infections (249), and more importantly, mediate antibody-dependent cell-mediated cytotoxicity (ADCC) against BCLs, which serves as the one of the major cytotoxic mechanisms for anti-CD20 mAb Rituximab (250). Numerous studies have demonstrated that the activity and function of NK cells can be potentiated by IMiDs in B-cell malignancies (212, 251). Lenalidomide treatment can increase NK-cell number, stimulate NK-cell activation, restore IS formation, and enhance direct NK-cell cytotoxicity as well as NK-dependent ADCC (212, 217, 221, 222, 234, 252). Mechanistically, the effect of lenalidomide on NK cells may be mediated indirectly *via* IL-2 produced by T cells. Either T-cell depletion or IL-2 blockade can completely abrogate NK-cell proliferation and cytotoxicity (212). The increased IL-2 and activation of NK cells correlate to increased IFN-γ synthesis and upregulation of CD69 (253). A recent study by Hideshima et al. demonstrated that pomalidomide directly binds to zeta-chain-associated protein kinase-70 (Zap-70) and triggers its phosphorylation to activate NK cells in a CRBN-independent manner. In addition, they also demonstrated a second mechanism whereby pomalidomide directly triggers granzyme-B and NK cytotoxicity which is mediated by CRBN-IKZF3 axis (218). Consistently, avadomide has shown to promote NK-cell proliferation and cytotoxicity by inducing IL-2 secretion and upregulating granzyme B and NKG2D receptor (254–256).

Lenalidomide was shown to enhance NK-dependent ADCC in BCL cell lines treated with rituximab (62). In this context, the increased expression of granzyme B and Fas ligand (FasL) may account for enhanced ADCC, which could be inhibited by a granzyme B inhibitor or FasL antibody (62). Moreover, lenalidomide lowers NK-cell activation thresholds by rituximab, thus augmenting NK-cell responses (217). On the other hand, lenalidomide synergistically enhances rituximab-induced phosphorylation of JNK and activates the

mitochondrial apoptotic pathway in MCL cells (63). *In vivo* studies using immunodeficient mice inoculated with MCL cells demonstrated that lenalidomide and rituximab combination decreased tumor burden and prolonged animal survival along with the increased number of splenic NK cells (63). These data provide compelling proof-of-concept for the clinical translation of lenalidomide combination with rituximab into B-cell lymphoma treatment.

3.2.3 Effects on TAMs

TAMs are the key cellular components of TME, which can produce chemokines, cytokines and growth factors to recruit immunosuppressive cells and support tumor progression (257–259). TAMs are typically classified into M1-like (anti-tumorigenesis) and M2-like (pro-tumorigenesis) types based on their different surface markers, gene expression signatures and metabolic traits. The conversion between M1 and M2 is a dynamic process named "macrophage polarization" which occurs in response to TME signals (257, 260). Repolarization of M2-like macrophages to M1 phenotype represents a novel promising therapeutic strategy (261).

A recent study showed that lenalidomide altered the M1/M2 polarization in myeloma-associated macrophages (MAMs) from MM patients. Mechanistically, lenalidomide interferes epigenetically with IRF4 and IRF5 *via* degradation of IKZF1 and shifts M2-like MAMs to a pro-inflammatory and tumoricidal phenotype that resemble M1 cells (223). Similarly, pomalidomide has shown to repolarize macrophages from M2 to M1 and increase their phagocytic activity in mouse models of PCNSL, which is probably mediated by the potentiated STAT1 signaling while inhibited STAT6 signaling (35).

Therapeutically, macrophages possess immense potential of eliciting antibody-dependent cellular phagocytosis (ADCP) to destroy tumor cells (224). Of note, ADCP was demonstrated as one of the driving cytotoxic mechanism for anti-CD20 and anti-CD38 therapeutic antibodies against B-cell neoplasms (224, 262, 263). Thus, harnessing and enhancing macrophage-mediated ADCP through repolarization of M1/M2 macrophages is poised to become a novel and effective strategy for immunotherapy. Lenalidomide was shown to improved MOR202 (an anti-CD38 mAb)-mediated tumoricidal activity of MAMs against primary MM cells by restoring the defective vitamin D pathway in these MAMs with reduced CYP27B1 level (225). In addition, lenalidomide and pomalidomide mediated a substantial CD38 upregulation on MM cell lines, which also contributes to a synergistic enhancement of cytotoxic activity by combining MOR202 with IMiDs (213). Despite the enhanced ADCP of anti-CD20 mAbs by IMiDs has not been fully studied, it deserves further investigation for clinical application especially considering that obinutuzumab, the third-generation type II humanized anti-CD20 mAb (264), has shown to induce stronger ADCP as compared to rituximab, which may be due to the increased activation of FcγRI (CD64) expressed on primary macrophages (226).

3.2.4 Effects on DCs

As the most powerful antigen presenting cells (APCs), DCs are key messengers and link between the innate and adaptive immune systems by capturing and presenting tumor antigens for T-cell recognition (265, 266). Evidence of immunomodulatory activity of IMiDs on DCs was first revealed in mouse, showing that lenalidomide and pomalidomide upregulated MHC class I molecules and CD86 on DCs derived from bone marrow, promoted antigen uptake antigen and presentation of DCs for naive $CD8^+$ T cells (229). Pomalidomide can also increase the expression of MHC class II molecules on DCs, resulting in increasing $CD4^+$ T cell priming (229). Recently, Phan et al. showed that IMiDs have the potential to shift the DC-mediated response from Th1 to Th2 humoral immunity in human. IMiDs potentially enhanced DC-mediated allergic Th2 responses (CCL17 secretion and memory Th2 response) through upregulated STAT6 and IRF4 (267). Interestingly, high CCL17 levels in serum at the onset of rash as a side effect correlate with clinical outcome of lenalidomide treatment, which suggests that DCs immunostimulation inextricably linked side effect and activity of IMiDs (267). These findings also provide evidence for the additional use of IMiDs in dendritic cell–based anti-tumor vaccines (230, 231).

3.2.5 Effects on stromal cells and angiogenesis

In pathological conditions, malignant B cells rely on interactions with nonmalignant stromal cells within bone marrow and secondary lymphoid organs for their survival and proliferation (237). In MM, cytokines derived from bone marrow-derived mesenchymal stromal cells (BMSCs), an integral part of the non-hematopoietic BM microenvironment, are considered important drivers of myeloma pathobiology (268). Treatment with IMiDs significantly abrogates the interaction between MM cells and BMSCs by decreasing the production of IL-6 by stromal cells and downregulating adhesion molecules including LFA-1/ICAM-1 and VLA-4/VCAM-1 (269). In addition, lenalidomide potentially inhibits the pro-survival activity of BMSCs in MCL by inhibiting IL-6-mediated STAT-3 signaling (270). Lenalidomide may also target CXCL12/CXCR4 axis by inhibiting production of CXCL12 by MSCs in NHL (271). To date, the exact impacts of IMiDs on other nonimmune components of TME in B-cell neoplasms such as cancer-associated fibroblasts (CAFs), extracellular matrix (ECM) and pericytes, are still unknown.

Angiogenesis is a constant hallmark from initiation to progression for both MM and BCLs (272, 273). The antiangiogenic activity of IMiDs have been well characterized in MM, which was initially thought as the major MOA of thalidomide analogs against myeloma progression (274).

Thalidomide impairs angiogenesis *via* suppression of vascular endothelial growth factor (VEGF) signaling (275). Similarly, lenalidomide exerts anti-angiogenic activity by downregulating basic fibroblast growth factor (bFGF) and VEGF due at least in part to inhibition of Akt phosphorylation (276). In CLL, lenalidomide was shown to inhibit CLL-mediated pro-angiogenic effect *in vitro* and modulates angiogenesis-related factors in patients with R/R CLL (277). Moreover, lenalidomide also exhibits inhibitory effects on VEGF-mediated angiogenesis and lymphangiogenesis in mouse models of B-cell lymphoma (64).

4 IMiDs in the era of immunotherapy

4.1 Antibody-based therapies

Due to extensive capacity of antibodies for targeting tumor-specific antigens, antibody-based therapies have become the most frequently used immunotherapeutic method for cancer treatment. The potent anti-tumor activity of rituximab in patients with various lymphoid malignancies has led to its widespread use in most indolent and aggressive $CD20^+$ BCLs (278). As shown in preclinical studies exhibiting synergistic anti-tumor activity, the chemotherapy-free combination of rituximab plus lenalidomide (R^2 regimen) proved to be effective in previously untreated indolent lymphoma (FL and MZL) and induced high molecular response (25, 279, 280). Similarly, obinutuzumab plus lenalidomide (GALEN regimen) has also been demonstrated as an active immunomodulatory combination with a manageable safety profile in both front-line and R/R FL (133, 281). Although the MOA of obinutuzumab favors it as a more effective anti-CD20 mAb (264), it remains uncertain whether rituximab or obinutuzumab is the better one when combined with lenalidomide in indolent lymphoma. In CLL, the combination of lenalidomide and ofatumumab was well-tolerated and induced durable responses in the majority of R/R patients with 71% ORR and a long progression-free survival (PFS) of 16 months (282). The ability to augment ADCC and ADCP suggests that lenalidomide should also cooperate with other therapeutic antibodies beyond anti-CD20 mAbs. Daratumumab (an anti-CD38 mAb) is approved as monotherapy or in combination with standard regimens for treatment of newly diagnosed (ND) or R/R MM (214). In RRMM, daratumumab in combination with dexamethasone and lenalidomide led to a significant PFS benefit over dexamethasone and lenalidomide alone (215, 283). The phase 3 MAIA study further demonstrated that daratumumab plus dexamethasone and lenalidomide increased OS and PFS of NDMM patients ineligible for transplantation (120). In addition, the anti-CD19 mAb MOR-28 (Tafasitamab) plus lenalidomide has shown outstanding clinical benefits with durable response rates in a phase 2 trial for R/R DLBCL (28).

Bi-specific T-cell engagers (BiTEs) are a new category of artificial bispecific antibodies (BsAbs) engineered to recognize specific tumor-associated antigen and CD3 at the same time (284, 285). Given the promising clinical efficacy of BiTEs in R/R BCLs (286), the combinations of lenalidomide with BsAbs such as Blinatumomab (a CD19/CD3 BiTE)and Mosunetuzumab (a CD20/CD3 BiTE) are currently being investigated in early-phase 1 clinical trials (209–211).

4.2 ICIs

The use of ICIs targeting PD-1 signaling pathway has ushered in a paradigm shift in cancer due to success in various high-risk solid tumors (287). However, the activity of ICIs in hematologic malignancies is currently restricted to certain subtypes of lymphoma, such as Hodgkin lymphoma (HL) and primary mediastinal B-cell lymphoma (PMBCL) (288). The severe T-cell tolerance and exhaustion within the TME is considered as the major contributor to disappointing clinical results for anti-PD-1 monotherapy in NHLs and CLL (289, 290). A recent study by Geng et al. showed that lenalidomide bypasses the requirement of CD28 for tumor-infiltrating $CD8^+$ T-cell activation and antitumor activity of PD-1 blockade, which suggests that lenalidomide combination is beneficial to overcome PD-1 resistant tumors infiltrated with $CD28^-$ exhausted T cells (206). In addition, another preclinical study demonstrated avadomide combination enhanced anti-CLL activity of anti-PD-1/PD-L1 therapy (245). Mechanistically, avadomide stimulated T-cell activation, motility, cytokine production, IS formation, and IFN-γ-inducible expression of PD-L1, thus reshaping a non-T cell-inflamed into a T cell-inflamed TME (245). Moreover, single blockade of PD-1 or dual blockade using anti-PD-1/PD-L1 antibodies plus lenalidomide blocked the cross-talk between myeloma cells and BMSC, thus inducing an anti-myeloma immune response to inhibit cell growth (291). Despite some early-phase 1/2 trials of pembrolizumab (an anti-PD-1 mAb) plus IMiDs and dexamethasone reported a ~50% ORR in patients with RRMM (292–294), however, phase 3 trials (KEYNOTE-183 and KEYNOTE-185) evaluating the combination of pembrolizumab with dexamethasone and an IMiD in RRMM (with pomalidomide) and NDMM (with lenalidomide) was eventually discontinued due to higher risk of death (295, 296). Further studies are needed to determine the mechanism underlying the unexpected toxicity, which will contribute to realize the therapeutic potential of ICIs and IMiDs combination in the clinic.

4.3 CAR-T cell therapy

CAR-T cell therapies have been approved for treatment of R/R B-ALL and aggressive B-NHLs. There are intensive bench-to-bedside studies underway to further improve the efficacy of CAR-T cells, focusing on recently described resistance mechanisms, such as T-cell exhaustion, immunosuppressive TME, defective IS, downregulation of target antigens, among others (297, 298). A strong rationale supports the combination of IMiDs and CAR-T therapy according to the enhanced activity of effector T cells and other cellular components in the TME re-educated by IMiDs. *In vivo* models have demonstrated that lenalidomide significantly enhances anti-lymphoma functions of CD19 and CD20 CAR-T cells, with decreased tumor burden and increased intratumoral $CD8^+$ T cells (207). Another study showed that lenalidomide improved the efficacy of CS1-directed CAR-T cells against MM by enhancing expansion, cytotoxicity, memory maintenance, Th1 cytokine production, and IS formation of CAR-T cells (208). In addition, lenalidomide has shown to maintain the *in vitro* activity of CD23 CAR-T cells, preserve functional CAR T-CLL cell immune synapses, and improve the therapeutic efficacy of CD23 CAR-T cells *in vivo* (73). Despite the evidence of synergistic efficacy, it should be noted that the specific toxicities associated with CAR-T cells plus IMiDs, such as severe cytopenias and cytokine release syndrome (299, 300), will need to be carefully examined. Current ongoing trials have included the combing IMiDs with CD19 or B cell maturation antigen (BCMA) CAR-T cell therapy in DLBCL and MM (301–304).

4.4 Conventional chemotherapy

Despite advances in treatment, conventional chemotherapy is still the mainstay to induce a fast clinical remission of most hematologic cancers in the age of targeted and immune therapies. The introduce of IMiDs to chemotherapy regimen for decades has dramatically increased CR ratio and improved prognosis of NDMM (121, 274). Currently, induction treatments for MM have traditionally relied on a backbone of a combinations of IMiDs (thalidomide, lenalidomide and pomalidomide), proteasome inhibitors, alkylators (or anthracyclines), and/or steroids (274). In this scenario, IMiDs are believed to improve the immune environment beyond direct anti-tumor activity, which ensures persistent minimal residual disease (MRD) negativity through enhanced immunological surveillance against myeloma cells (305). In addition, the recently approved anti-CD38 antibodies have also shown to reshape the MM immune environment *via* activation of T and NK cells and suppression of Tregs (305). These combined immunogenic chemotherapies are paving a promising way to "cure MM". Similarly, adding lenalidomide to R-CHOP (rituximab plus cyclophosphamide, doxorubicin, vincristine, and prednisone) (R^2-CHOP regimen) has recently shown improved outcomes in ABC-type DLBCL (306). As such, a deeper understating of immune dysfunction in B-cell malignancies has already led to the development of a more effective and less toxic immunotherapy-chemotherapy combinations to be given to cancer patients.

5 Conclusions and perspectives

Compelling evidence over last decades has shown the potent immunomodulatory effects of IMiDs on diverse cellular components (T cells, NK cells, TAMs, DCs, etc.) that reside within TMEs of B-cell neoplasms, which repurposes these agents to play a role in the era of immunotherapy (Table 2). The promising outcomes of chemotherapy-free regimen combining IMiDs with mAbs (e.g. rituximab or obinutuzumab) in treatment of both indolent and aggressive NHL types exemplify a shift of paradigm from the standard chemotherapy to a safer and more effective IMiD-intensified immunotherapy. Based on these findings in hematologic cancers, a number of studies have explored the potential applications of IMiDs in solid tumors. For instance, CC-885, a novel CRBN modulator, has shown to induce CRBN- and p97-dependent PLK1 degradation and synergizes with volasertib (PLK1 inhibitor) to suppress lung cancer (307). Moreover, pomalidomide can generate an immune-responsive and anti-tumorigenic environment and provide an ideal combination treatment with chemotherapeutic drugs or other immunotherapies in pancreatic cancer (308). Other studies also reported activities of lenalidomide in breast cancer (309), prostate cancer (310) and colon adenocarcinoma (206). Although IMiDs by themselves exhibit very limited anti-tumor activity against solid tumors in the clinic (311), their broad immunobiological properties revert the immune regulatory milieu of TME and create opportunities for other therapeutics to achieve better responses (206).

Of note, despite a series of preclinical studies have shed novel light on the synergistic effects and MOA, the clinical safety and efficacy of the combination of IMiDs with other novel immunotherapies such as BiTEs, ICIs and CAR-T cell therapy are not yet fully determined. In addition, since all MM patients inevitably develops resistance to IMiDs over time, it is a significant limitation and challenge for clinicians to make decisions about RRMM treatment. From a molecular point of view, IMiD resistance involves downregulation of CRBN expression, IKZF1/3 and CRBN mutations, deregulation of IRF4 expression, abnormal epigenetic mechanisms (CBP/EP300, BRD4 and HDAC) and aberrant signaling pathways (Wnt, STAT3 and MAPK/ERK) (312, 313). Fortunately, recent studies have discovered that some potential novel agents and PROTACs, which target the resistance mechanisms, can increase the sensitivity of MM cells to IMiDs or synergistically enhance the anti-myeloma activity of IMiDs (313). Further studies to verify the safety and efficacy of these strategies in clinic are urgently

needed to pave the way for the treatment of R/R settings. Moreover, although the E3 ubiquitin ligase CRBN is now considered as the major target that likely underlies the effects of IMiDs in tumor cells as well as immunomodulation, there are a range of key issues be addressed including: 1) the functions of CRBN in the absence of IMiDs and its physiological significance is still unknown; 2) the common and distinct neosubstrates of CRBN in tumor cells and immune cells are not fully identified; 3) the CRBN-independent mechanisms underlying the anti-tumor and immunomodulatory activities of IMiDs are reported and merit in-depth investigation. Further elucidation of these issues will contribute to optimize IMiDs-based immunotherapeutic combinations and overcome intractable drug resistance.

Author contributions

KZ conceived and designed the review. HG drafted and revised the manuscript. JY and HW helped with the literature collection. XL and YL proofread the manuscript and provided suggestions. All authors contributed to the article and approved the submitted version.

Funding

This study was supported by the National Natural Science Foundation of China (No. 81470336 to KZ).

Conflict of interest

The authors declare that the research was conducted in the absence of any commercial or financial relationships that could be construed as a potential conflict of interest.

Publisher's note

References

1. Cuenca M, Peperzak V. Advances and perspectives in the treatment of b-cell malignancies. *Cancers* (2021) 13(9):2266. doi: 10.3390/cancers13092266

2. Ayyappan S, Maddocks K. Novel and emerging therapies for b cell lymphoma. *J Hematol Oncol* (2019) 12(1):82. doi: 10.1186/s13045-019-0752-3

3. Wang L, Qin W, Huo Y-J, Li X, Shi Q, Rasko JEJ, et al. Advances in targeted therapy for malignant lymphoma. *Signal Transduct Target Ther* (2020) 5(1):15. doi: 10.1038/s41392-020-0113-2

4. Labani-Motlagh A, Ashja-Mahdavi M, Loskog A. The tumor microenvironment: A milieu hindering and obstructing antitumor immune responses. *Front Immunol* (2020) 11:940. doi: 10.3389/fimmu.2020.00940

5. Fowler NH, Cheah CY, Gascoyne RD, Gribben J, Neelapu SS, Ghia P, et al. Role of the tumor microenvironment in mature b-cell lymphoid malignancies. *Haematologica* (2016) 101(5):531–40. doi: 10.3324/haematol.2015.139493

6. Liu Y, Zhou X, Wang X. Targeting the tumor microenvironment in b-cell lymphoma: challenges and opportunities. *J Hematol Oncol* (2021) 14(1):1–17. doi: 10.1186/s13045-021-01134-x

7. Höpken UE, Rehm A. Targeting the tumor microenvironment of leukemia and lymphoma. *Trends Cancer* (2019) 5(6):351–64. doi: 10.1016/j.trecan.2019.05.001

8. Qu Y, Dou B, Tan H, Feng Y, Wang N, Wang D. Tumor microenvironment-driven non-cell-autonomous resistance to antineoplastic treatment. *Mol Cancer* (2019) 18(1):69. doi: 10.1186/s12943-019-0992-4

9. Jin M-Z, Jin W-L. The updated landscape of tumor microenvironment and drug repurposing. *Signal Transduct Target Ther* (2020) 5(1):1–16. doi: 10.1038/s41392-020-00280-x

10. Yamshon S, Ruan J. IMiDs new and old. *Curr Hematol Malignancy Rep* (2019) 14(5):414–25. doi: 10.1007/s11899-019-00536-6

11. Gribben JG, Fowler N, Morschhauser F. Mechanisms of action of lenalidomide in b-cell non-Hodgkin lymphoma. *J Clin Oncol* (2015) 33(25):2803. doi: 10.1200/JCO.2014.59.5363

12. Ioannou N, Jain K, Ramsay AG. Immunomodulatory drugs for the treatment of b cell malignancies. *Int J Mol Sci* (2021) 22(16):8572. doi: 10.3390/ijms22168572

13. Ito T, Handa H. Molecular mechanisms of thalidomide and its derivatives. *Proc Japan Academy Ser B* (2020) 96(6):189–203. doi: 10.2183/pjab.96.016

14. Jan M, Sperling AS, Ebert BL. Cancer therapies based on targeted protein degradation–lessons learned with lenalidomide. *Nat Rev Clin Oncol* (2021) 18 (7):401–17. doi: 10.1038/s41571-021-00479-z

15. Sampaio EP, Kaplan G, Miranda A, Nery JA, Miguel CP, Viana SM, et al. The influence of thalidomide on the clinical and immunologic manifestation of erythema nodosum leprosum. *J Infect Diseases* (1993) 168(2):408–14. doi: 10.1093/infdis/168.2.408

16. Sampaio E, Hernandez M, Carvalho D, Sarno E. Management of erythema nodosum leprosum by thalidomide: thalidomide analogues inhibit m. leprae-induced TNFα production *in vitro*. *Biomed Pharmacother* (2002) 56(1):13–9. doi: 10.1016/S0753-3322(01)00147-0

17. Haslett PA, Corral LG, Albert M, Kaplan G. Thalidomide costimulates primary human T lymphocytes, preferentially inducing proliferation, cytokine production, and cytotoxic responses in the CD8+ subset. *J Exp Med* (1998) 187 (11):1885–92. doi: 10.1084/jem.187.11.1885

18. D'Amato RJ, Loughnan MS, Flynn E, Folkman J. Thalidomide is an inhibitor of angiogenesis. *Proc Natl Acad Sci* (1994) 91(9):4082–5. doi: 10.1073/pnas.91.9.4082

19. Bartlett JB, Dredge K, Dalgleish AG. The evolution of thalidomide and its IMiD derivatives as anticancer agents. *Nat Rev Cancer* (2004) 4(4):314–22. doi: 10.1038/nrc1323

20. List A, Kurtin S, Roe DJ, Buresh A, Mahadevan D, Fuchs D, et al. Efficacy of lenalidomide in myelodysplastic syndromes. *New Engl J Med* (2005) 352(6):549–57. doi: 10.1056/NEJMoa041668

21. List A, Dewald G, Bennett J, Giagounidis A, Raza A, Feldman E, et al. Lenalidomide in the myelodysplastic syndrome with chromosome 5q deletion. *New Engl J Med* (2006) 355(14):1456–65. doi: 10.1056/NEJMoa061292

22. Dimopoulos M, Spencer A, Attal M, Prince HM, Harousseau J-L, Dmoszynska A, et al. Lenalidomide plus dexamethasone for relapsed or refractory multiple myeloma. *New Engl J Med* (2007) 357(21):2123–32. doi: 10.1056/NEJMoa070594

23. Habermann TM, Lossos IS, Justice G, Vose JM, Wiernik PH, McBride K, et al. Lenalidomide oral monotherapy produces a high response rate in patients with relapsed or refractory mantle cell lymphoma. *Br J Haematol* (2009) 145 (3):344–9. doi: 10.1111/j.1365-2141.2009.07626.x

24. Ruan J, Martin P, Shah B, Schuster SJ, Smith SM, Furman RR, et al. Lenalidomide plus rituximab as initial treatment for mantle-cell lymphoma. *New Engl J Med* (2015) 373(19):1835–44. doi: 10.1056/NEJMoa1505237

25. Morschhauser F, Fowler NH, Feugier P, Bouabdallah R, Tilly H, Palomba ML, et al. Rituximab plus lenalidomide in advanced untreated follicular lymphoma. *New Engl J Med* (2018) 379(10):934–47. doi: 10.1056/NEJMoa1805104

26. Leonard JP, Trneny M, Izutsu K, Fowler NH, Hong X, Zhu J, et al. AUGMENT: A phase III study of lenalidomide plus rituximab versus placebo plus rituximab in relapsed or refractory indolent lymphoma. *J Clin Oncol: Off J Am Soc Clin Oncol* (2019) 37(14):1188–99. doi: 10.1200/JCO.19.00010

27. Andorsky DJ, Coleman M, Yacoub A, Melear JM, Fanning SR, Kolibaba K, et al. MAGNIFY: Phase IIIb interim analysis of induction R2 followed by maintenance in relapsed/refractory indolent non-Hodgkin lymphoma. *Am Soc Clin Oncol* (2019) 37(15_suppl):7513. doi: 10.1016/j.htct.2020.10.372

28. Salles G, Duell J, Barca EG, Tournilhac O, Jurczak W, Liberati AM, et al. Tafasitamab plus lenalidomide in relapsed or refractory diffuse large b-cell lymphoma (L-MIND): a multicentre, prospective, single-arm, phase 2 study. *Lancet Oncol* (2020) 21(7):978–88. doi: 10.1016/S1470-2045(20)30225-4

29. Yeung AJ-T, Ling SC. "Pomalidomide". In: Ling SC, Trieu S. editors. *Resistance to Targeted Therapies in Multiple Myeloma. Resistance to Targeted Anti-Cancer Therapeutics*, Cham, Switzerland: Springer (2021) 22, 31–7. doi: 10.1007/978-3-030-73440-4_3

30. Richardson PG, Oriol A, Beksac M, Liberati AM, Galli M, Schjesvold F, et al. Pomalidomide, bortezomib, and dexamethasone for patients with relapsed or refractory multiple myeloma previously treated with lenalidomide (OPTIMISMM): a randomised, open-label, phase 3 trial. *Lancet Oncol* (2019) 20 (6):781–94. doi: 10.1016/S1470-2045(19)30152-4

31. Siegel DS, Schiller GJ, Song KW, Agajanian R, Stockerl-Goldstein K, Kaya H, et al. Pomalidomide plus low-dose dexamethasone in relapsed refractory multiple myeloma after lenalidomide treatment failure. *Br J Haematol* (2020) 188(4):501–10. doi: 10.1111/bjh.16213

32. Xu P, Wang L, Cheng S, Zhao WL. Trial in progress: Pomalidomide plus rituximab, ifosfamide, carboplatin, and etoposide for relapsed or refractory diffuse Large b-cell lymphoma (PRIDE). *Blood* (2021) 138:4562. doi: 10.1182/blood-2021-146851

33. Tun HW, Johnston PB, DeAngelis LM, Atherton PJ, Pederson LD, Koenig PA, et al. Phase 1 study of pomalidomide and dexamethasone for relapsed/refractory primary CNS or vitreoretinal lymphoma. *Blood J Am Soc Hematol* (2018) 132(21):2240–8. doi: 10.1182/blood-2018-02-835496

34. Park S, Jo S-H, Kim J-H, Kim S-Y, Ha JD, Hwang JY, et al. Combination treatment with GSK126 and pomalidomide induces b-cell differentiation in EZH2 gain-of-Function mutant diffuse Large b-cell lymphoma. *Cancers* (2020) 12 (9):2541. doi: 10.3390/cancers12092541

35. Li Z, Qiu Y, Personett D, Huang P, Edenfield B, Katz J, et al. Pomalidomide shows significant therapeutic activity against CNS lymphoma with a major impact on the tumor microenvironment in murine models. *PloS One* (2013) 8(8):e71754. doi: 10.1371/journal.pone.0071754

36. Tun HW, Johnston PB, Grommes C, Reeder CB, Omuro AMP, Menke DM, et al. Phase I clinical trial on pomalidomide and dexamethasone in treating patients with relapsed/refractory primary central nervous system lymphoma (PCNSL) or primary vitreoretinal lymphoma (PVRL). *Am Soc Clin Oncol* (2017) 35 (15_suppl):7516. doi: 10.1200/JCO.2017.35.15_suppl.7516

37. Shrestha P, Davis DA, Jaeger HK, Stream A, Aisabor AI, Yarchoan R. Pomalidomide restores immune recognition of primary effusion lymphoma through upregulation of ICAM-1 and B7-2. *PloS Pathogens* (2021) 17(1): e1009091. doi: 10.1371/journal.ppat.1009091

38. Hagner PR, Man H-W, Fontanillo C, Wang M, Couto S, Breider M, et al. CC-122, a pleiotropic pathway modifier, mimics an interferon response and has antitumor activity in DLBCL. *Blood J Am Soc Hematol* (2015) 126(6):779–89. doi: 10.1182/blood-2015-02-628669

39. Rasco DW, Papadopoulos KP, Pourdehnad M, Gandhi AK, Hagner PR, Li Y, et al. A first-in-human study of novel cereblon modulator avadomide (CC-122) in advanced malignancies. *Clin Cancer Res* (2019) 25(1):90–8. doi: 10.1158/1078-0432.CCR-18-1203

40. Piccolomo A, Schifone CP, Strafella V, Specchia G, Musto P, Albano F. Immunomodulatory drugs in acute myeloid leukemia treatment. *Cancers* (2020) 12 (9):2528. doi: 10.3390/cancers12092528

41. Merrill JT, Werth VP, Furie R, van Vollenhoven R, Dörner T, Petronijevic M, et al. Phase 2 trial of iberdomide in systemic lupus erythematosus. *New Engl J Med* (2022) 386(11):1034–45. doi: 10.1056/NEJMoa2106535

42. Schafer PH, Ye Y, Wu L, Kosek J, Ringheim G, Yang Z, et al. Cereblon modulator iberdomide induces degradation of the transcription factors ikaros and aiolos: immunomodulation in healthy volunteers and relevance to systemic lupus erythematosus. *Ann Rheum Diseases* (2018) 77(10):1516–23. doi: 10.1136/annrheumdis-2017-212916

43. Mitsiades N, Mitsiades CS, Poulaki V, Chauhan D, Richardson PG, Hideshima T, et al. Apoptotic signaling induced by immunomodulatory thalidomide analogs in human multiple myeloma cells: therapeutic implications. *Blood J Am Soc Hematol* (2002) 99(12):4525–30. doi: 10.1182/blood.V99.12.4525

44. Hideshima T, Chauhan D, Shima Y, Raje N, Davies FE, Tai Y-T, et al. Thalidomide and its analogs overcome drug resistance of human multiple myeloma cells to conventional therapy. *Blood J Am Soc Hematol* (2000) 96 (9):2943–50. doi: 10.1182/blood.V96.9.2943

45. Drucker L, Uziel O, Tohami T, Shapiro H, Radnay J, Yarkoni S, et al. Thalidomide down-regulates transcript levels of GC-rich promoter genes in multiple myeloma. *Mol Pharmacol* (2003) 64(2):415–20. doi: 10.1124/mol.64.2.415

46. Schlenzka J, Moehler TM, Kipriyanov SM, Kornacker M, Benner A, Bähre A, et al. Combined effect of recombinant CD19× CD16 diabody and thalidomide in a preclinical model of human b cell lymphoma. *Anti Cancer Drugs* (2004) 15 (9):915–9. doi: 10.1097/00001813-200410000-00013

47. Skórka K, Bhattacharya N, Własiuk P, Kowal M, Mertens D, Dmoszyńska A. Thalidomide regulation of NF-κB proteins limits tregs activity in chronic lymphocytic leukemia. *Adv Clin Exp Med* (2014) 23(1):25–32. doi: 10.17219/acem/37018

48. Pointon JC, Eagle G, Bailey J, Evans P, Allsup D, Greenman J. Thalidomide enhances cyclophosphamide and dexamethasone-mediated cytotoxicity towards cultured chronic lymphocytic leukaemia cells. *Oncol Rep* (2010) 24(5):1315–21. doi: 10.3892/or_00000988

49. Salemi M, Mohammadi S, Ghavamzadeh A, Nikbakht M. Anti-vascular endothelial growth factor targeting by curcumin and thalidomide in acute myeloid leukemia cells. *Asian Pacific J Cancer Prevention: APJCP* (2017) 18(11):3055. doi: 10.22034/APJCP.2017.18.11.3055

50. Kian MM, Salemi M, Bahadoran M, Haghi A, Dashti N, Mohammadi S, et al. Curcumin combined with thalidomide reduces expression of STAT3 and bcl-xL, leading to apoptosis in acute myeloid leukemia cell lines. *Drug Design Dev Ther* (2020) 14:185. doi: 10.2147/DDDT.S228610

51. Noman ASM, Koide N, Khuda II-E, Dagvadorj J, Tumurkhuu G, Naiki Y, et al. Thalidomide inhibits epidermal growth factor-induced cell growth in mouse and human monocytic leukemia cells *via* ras inactivation. *Biochem Biophys Res Commun* (2008) 374(4):683–7. doi: 10.1016/j.bbrc.2008.07.090

52. Girgis E, Mahoney J, Darling-Reed S, Soliman M. Arsenic trioxide enhances the cytotoxic effect of thalidomide in a KG-1a human acute myelogenous leukemia cell line. *Oncol Lett* (2010) 1(3):473–9. doi: 10.3892/ol_00000083

53. Liu P, Li J, Lu H, Xu B. Thalidomide inhibits leukemia cell invasion and migration by upregulation of early growth response gene 1. *Leukemia Lymphoma* (2009) 50(1):109–13. doi: 10.1080/10428190802588352

54. Czyżewski K, Zaborowska A, Styczyński J. Thalidomide increases *in vitro* sensitivity of childhood acute lymphoblastic leukemia cells to prednisolone and cytarabine. *Archivum Immunologiae Therapiae Experimentalis* (2006) 54(5):341–5. doi: 10.1007/s00005-006-0036-9

55. Styczynski J, Czyzewski K, Wysocki M. Ex vivo activity of thalidomide in childhood acute leukemia. *Leukemia Lymphoma* (2006) 47(6):1123–8. doi: 10.1080/10428190500467891

56. Krönke J, Udeshi ND, Narla A, Grauman P, Hurst SN, McConkey M, et al. Lenalidomide causes selective degradation of IKZF1 and IKZF3 in multiple myeloma cells. *Science* (2014) 343(6168):301–5. doi: 10.1126/science.1244851

57. Luptakova K, Rosenblatt J, Glotzbecker B, Mills H, Stroopinsky D, Kufe T, et al. Lenalidomide enhances anti-myeloma cellular immunity. *Cancer Immunol Immunother* (2013) 62(1):39–49. doi: 10.1007/s00262-012-1308-3

58. Breitkreutz I, Raab M, Vallet S, Hideshima T, Raje N, Mitsiades C, et al. Lenalidomide inhibits osteoclastogenesis, survival factors and bone-remodeling markers in multiple myeloma. *Leukemia* (2008) 22(10):1925–32. doi: 10.1038/leu.2008.174

59. Görgün G, Samur MK, Cowens KB, Paula S, Bianchi G, Anderson JE, et al. Lenalidomide enhances immune checkpoint blockade-induced immune response in multiple MyelomaLenalidomide in combination with checkpoint blockade in multiple myeloma. *Clin Cancer Res* (2015) 21(20):4607–18. doi: 10.1158/1078-0432.CCR-15-0200

60. Van Der Veer MS, de Weers M, van Kessel B, Bakker JM, Wittebol S, Parren PW, et al. Towards effective immunotherapy of myeloma: enhanced elimination of myeloma cells by combination of lenalidomide with the human CD38 monoclonal antibody daratumumab. *Haematologica* (2011) 96(2):284–90. doi: 10.3324/haematol.2010.030759

61. Escoubet-Lozach L, Lin I-L, Jensen-Pergakes K, Brady HA, Gandhi AK, Schafer PH, et al. Pomalidomide and lenalidomide induce p21WAF-1 expression in both lymphoma and multiple myeloma through a LSD1-mediated epigenetic mechanism. *Cancer Res* (2009) 69(18):7347–56. doi: 10.1158/0008-5472.CAN-08-4898

62. Wu L, Adams M, Carter T, Chen R, Muller G, Stirling D, et al. Lenalidomide enhances natural killer cell and monocyte-mediated antibody-dependent cellular cytotoxicity of rituximab-treated CD20+ tumor cells. *Clin Cancer Res* (2008) 14 (14):4650–7. doi: 10.1158/1078-0432.CCR-07-4405

63. Zhang L, Qian Z, Cai Z, Sun L, Wang H, Bartlett JB, et al. Synergistic antitumor effects of lenalidomide and rituximab on mantle cell lymphoma *in vitro* and *in vivo*. *Am J Hematol* (2009) 84(9):553–9. doi: 10.1002/ajh.21468

64. Song K, Herzog BH, Sheng M, Fu J, McDaniel JM, Ruan J, et al. Lenalidomide inhibits lymphangiogenesis in preclinical models of mantle cell LymphomaAnti-lymphangiogenesis by lenalidomide in MCL. *Cancer Res* (2013) 73(24):7254–64. doi: 10.1158/0008-5472.CAN-13-0750

65. Ramsay AG, Clear AJ, Kelly G, Fatah R, Matthews J, MacDougall F, et al. Follicular lymphoma cells induce T-cell immunologic synapse dysfunction that can be repaired with lenalidomide: implications for the tumor microenvironment and immunotherapy. *Blood J Am Soc Hematol* (2009) 114(21):4713–20. doi: 10.1182/blood-2009-04-217687

66. Qian Z, Zhang L, Cai Z, Sun L, Wang H, Yi Q, et al. Lenalidomide synergizes with dexamethasone to induce growth arrest and apoptosis of mantle cell lymphoma cells *in vitro* and *in vivo*. *Leukemia Res* (2011) 35(3):380–6. doi: 10.1016/j.leukres.2010.09.027

67. Verhelle D, Corral LG, Wong K, Mueller JH, Moutouh-de Parseval L, Jensen-Pergakes K, et al. Lenalidomide and CC-4047 inhibit the proliferation of malignant b cells while expanding normal CD34+ progenitor cells. *Cancer Res* (2007) 67(2):746–55. doi: 10.1158/0008-5472.CAN-06-2317

68. Sakamaki I, Kwak LW, Cha S, Yi Q, Lerman B, Chen J, et al. Lenalidomide enhances the protective effect of a therapeutic vaccine and reverses immune suppression in mice bearing established lymphomas. *Leukemia* (2014) 28 (2):329–37. doi: 10.1038/leu.2013.177

69. Zhang L-H, Schafer PH, Muller G, Stirling D, Bartlett B. Direct inhibitory effects of lenalidomide on the proliferation and VEGF production of non-Hodgkin lymphoma cells are associated with increased SPARC expression. *Am Soc Hematol* (2008) 112(11):2612. doi: 10.1182/blood.V112.11.2612.2612

70. Gunnellini M, Falchi L. Therapeutic activity of lenalidomide in mantle cell lymphoma and indolent non-hodgkin's lymphomas. *Adv Hematol* (2012) 2012:523842. doi: 10.1155/2012/523842.

71. Moros A, Bustany S, Cahu J, Saborit-Villarroya I, Martínez A, Colomer D, et al. Antitumoral activity of lenalidomide in *In vitro* and *In vivo* models of mantle cell lymphoma involves the destabilization of cyclin D1/p27KIP1 ComplexesLenalidomide targets cyclin D1/p27KIP1 in MCL. *Clin Cancer Res* (2014) 20(2):393–403. doi: 10.1158/1078-0432.CCR-13-1569

72. Fecteau J-F, Corral LG, Ghia EM, Gaidarova S, Futalan D, Bharati IS, et al. Lenalidomide inhibits the proliferation of CLL cells *via* a cereblon/p21WAF1/Cip1-dependent mechanism independent of functional p53. *Blood J Am Soc Hematol* (2014) 124(10):1637–44. doi: 10.1182/blood-2014-03-559591

73. Tettamanti S, Rotiroti MC, Giordano Attianese GMP, Arcangeli S, Zhang R, Banerjee P, et al. Lenalidomide enhances CD23.CAR T cell therapy in chronic lymphocytic leukemia. *Leukemia Lymphoma* (2022) 63(7):1566–79. doi: 10.1080/10428194.2022.2043299

74. Lapalombella R, Andritsos L, Liu Q, May SE, Browning R, Pham LV, et al. Lenalidomide treatment promotes CD154 expression on CLL cells and enhances production of antibodies by normal b cells through a PI3-kinase–dependent pathway. *Blood J Am Soc Hematol* (2010) 115(13):2619–29. doi: 10.1182/blood-2009-09-242438

75. Schulz A, Dürr C, Zenz T, Döhner H, Stilgenbauer S, Lichter P, et al. Lenalidomide reduces survival of chronic lymphocytic leukemia cells in primary cocultures by altering the myeloid microenvironment. *Blood J Am Soc Hematol* (2013) 121(13):2503–11. doi: 10.1182/blood-2012-08-447664

76. Fiorcari S, Martinelli S, Bulgarelli J, Audrito V, Zucchini P, Colaci E, et al. Lenalidomide interferes with tumor-promoting properties of nurse-like cells in chronic lymphocytic leukemia. *Haematologica* (2015) 100(2):253. doi: 10.3324/haematol.2014.113217

77. Lapalombella R, Yu B, Triantafillou G, Liu Q, Butchar JP, Lozanski G, et al. Lenalidomide down-regulates the CD20 antigen and antagonizes direct and antibody-dependent cellular cytotoxicity of rituximab on primary chronic lymphocytic leukemia cells. *Blood J Am Soc Hematol* (2008) 112(13):5180–9. doi: 10.1182/blood-2008-01-133108

78. He X, Dou A, Feng S, Roman-Rivera A, Hawkins C, Lawley L, et al. Cyclosporine enhances the sensitivity to lenalidomide in MDS/AML in vitro. *Exp Hematol* (2020) 86:21–7. e2. doi: 10.1016/j.exphem.2020.05.001

79. Hickey CJ, Schwind S, Radomska HS, Dorrance AM, Santhanam R, Mishra A, et al. Lenalidomide-mediated enhanced translation of C/EBPα-p30 protein up-regulates expression of the antileukemic microRNA-181a in acute myeloid leukemia. *Blood J Am Soc Hematol* (2013) 121(1):159–69. doi: 10.1182/blood-2012-05-428573

80. Krönke J, Fink EC, Hollenbach PW, MacBeth KJ, Hurst SN, Udeshi ND, et al. Lenalidomide induces ubiquitination and degradation of CK1α in del (5q) MDS. *Nature* (2015) 523(7559):183–8. doi: 10.1038/nature14610

81. Stahl M, Zeidan AM. Lenalidomide use in myelodysplastic syndromes: Insights into the biologic mechanisms and clinical applications. *Cancer* (2017) 123 (10):1703–13. doi: 10.1002/cncr.30585

82. Matsuoka A, Tochigi A, Kishimoto M, Nakahara T, Kondo T, Tsujioka T, et al. Lenalidomide induces cell death in an MDS-derived cell line with deletion of chromosome 5q by inhibition of cytokinesis. *Leukemia* (2010) 24(4):748–55. doi: 10.1038/leu.2009.296

83. Fink EC, Krönke J, Hurst SN, Udeshi ND, Svinkina T, Schneider RK, et al. Lenalidomide induces ubiquitination and degradation of CSNK1A1 in MDS with del (5q). *Blood* (2014) 124(21):4. doi: 10.1182/blood.V124.21.4.4

84. Yamamoto J, Suwa T, Murase Y, Tateno S, Mizutome H, Asatsuma-Okumura T, et al. ARID2 is a pomalidomide-dependent CRL4CRBN substrate in multiple myeloma cells. *Nat Chem Biol* (2020) 16(11):1208–17. doi: 10.1038/s41589-020-0645-3

85. Vo M-C, Yang S, Jung S-H, Chu T-H, Lee H-J, Lakshmi TJ, et al. Synergistic antimyeloma activity of dendritic cells and pomalidomide in a murine myeloma model. *Front Immunol* (2018) 9:1798. doi: 10.3389/fimmu.2018.01798

86. Rychak E, Mendy D, Shi T, Ning Y, Leisten J, Lu L, et al. Pomalidomide in combination with dexamethasone results in synergistic anti-tumour responses in pre-clinical models of lenalidomide-resistant multiple myeloma. *Br J Haematol* (2016) 172(6):889–901. doi: 10.1111/bjh.13905

87. Bolzoni M, Storti P, Bonomini S, Todoerti K, Guasco D, Toscani D, et al. Immunomodulatory drugs lenalidomide and pomalidomide inhibit multiple myeloma-induced osteoclast formation and the RANKL/OPG ratio in the myeloma microenvironment targeting the expression of adhesion molecules. *Exp Hematol* (2013) 41(4):387–97. e1. doi: 10.1016/j.exphem.2012.11.005

88. Gopalakrishnan R, Matta H, Tolani B, Triche T, Chaudhary PM. Immunomodulatory drugs target IKZF1-IRF4-MYC axis in primary effusion lymphoma in a cereblon-dependent manner and display synergistic cytotoxicity with BRD4 inhibitors. *Oncogene* (2016) 35(14):1797–810. doi: 10.1038/onc.2015.245

89. Le Roy A, Prebet T, Castellano R, Goubard A, Riccardi F, Fauriat C, et al. Immunomodulatory drugs exert anti-leukemia effects in acute myeloid leukemia by direct and immunostimulatory activities. *Front Immunol* (2018) 9:977. doi: 10.3389/fimmu.2018.00977

90. Singhal S, Mehta J, Desikan R, Ayers D, Roberson P, Eddlemon P, et al. Antitumor activity of thalidomide in refractory multiple myeloma. *New Engl J Med* (1999) 341(21):1565–71. doi: 10.1056/NEJM199911183412102

91. Richardson P, Anderson K. Thalidomide and dexamethasone: a new standard of care for initial therapy in multiple myeloma. *J Clin Oncol: Off J Am Soc Clin Oncol* (2005) 24(3):334–6. doi: 10.1200/jco.2005.03.8851

92. Barlogie B, Tricot G, Anaissie E, Shaughnessy J, Rasmussen E, Van Rhee F, et al. Thalidomide and hematopoietic-cell transplantation for multiple myeloma. *New Engl J Med* (2006) 354(10):1021–30. doi: 10.1056/NEJMoa053583

93. Rajkumar SV, Blood E, Vesole D, Fonseca R, Greipp PR. Phase III clinical trial of thalidomide plus dexamethasone compared with dexamethasone alone in newly diagnosed multiple myeloma: a clinical trial coordinated by the Eastern cooperative oncology group. *J Clin Oncol* (2006) 24(3):431–6. doi: 10.1200/JCO.2005.03.0221

94. Wijermans P, Schaafsma M, Termorshuizen F, Ammerlaan R, Wittebol S, Sinnige H, et al. Phase III study of the value of thalidomide added to melphalan plus prednisone in elderly patients with newly diagnosed multiple myeloma: the HOVON 49 study. *J Clin Oncol* (2010) 28(19):3160–6. doi: 10.1200/JCO.2009.26.1610

95. Rosiñol L, Oriol A, Teruel A, de la Guía A, Blanchard M, de la Rubia J, et al. Bortezomib and thalidomide maintenance after stem cell transplantation for multiple myeloma: a PETHEMA/GEM trial. *Leukemia* (2017) 31(9):1922–7. doi: 10.1038/leu.2017.35

96. Smith SM, Grinblatt D, Johnson JL, Niedzwiecki D, Rizzieri D, Bartlett NL, et al. Thalidomide has limited single-agent activity in relapsed or refractory indolent non-Hodgkin lymphomas: a phase II trial of the cancer and leukemia group b. *Br J Haematol* (2008) 140(3):313–9. doi: 10.1111/j.1365-2141.2007.06937.x

97. Grinblatt DL, Johnson J, Niedzwicki D, Rizzieri DA, Bartlett N, Cheson BD. Phase II study of thalidomide in escalating doses for follicular (F-NHL) and small lymphocytic lymphoma (Sll): CALGB study 50002. *Blood* (2004) 104(11):3284. doi: 10.1182/blood.V104.11.3284.3284

98. Damaj G, Lefrere F, Delarue R, Varet B, Furman R, Hermine O. Thalidomide therapy induces response in relapsed mantle cell lymphoma. *Leukemia* (2003) 17(9):1914–5. doi: 10.1038/sj.leu.2403058

99. Drach J, Kaufmann H, Woehrer S, Chott A, Zielinski C, Raderer M. Durable remissions after rituximab plus thalidomide for relapsed/refractory mantle cell lymphoma. *J Clin Oncol* (2004) 22(14_suppl):6583–. doi: 10.1200/jco.2004.22.90140.6583

100. Ruan J, Martin P, Coleman M, Furman RR, Cheung K, Faye A, et al. Durable responses with the metronomic rituximab and thalidomide plus prednisone, etoposide, procarbazine, and cyclophosphamide regimen in elderly patients with recurrent mantle cell lymphoma. *Cancer: Interdiscip Int J Am Cancer Society* (2010) 116(11):2655–64. doi: 10.1002/cncr.25055

101. Kuruvilla J, Song K, Mollee P, Panzarella T, McCrae J, Nagy T, et al. A phase II study of thalidomide and vinblastine for palliative patients with hodgkin's lymphoma. *Hematology* (2006) 11(1):25–9. doi: 10.1080/10245330500276592

102. García-Sanz R, González-López T, Vázquez L, Hermida G, Graciani I, San Miguel J. The combination of thalidomide, cyclophosphamide and dexamethasone is potentially useful in highly resistant hodgkin's lymphoma. *Eur J Haematol* (2010) 84(3):266–70. doi: 10.1111/j.1600-0609.2009.01375.x

103. Wu H, Zhao C, Gu K, Jiao Y, Hao J, Sun G. Thalidomide plus chemotherapy exhibit enhanced efficacy in the clinical treatment of T-cell non –Hodgkin's lymphoma: A prospective study of 46 cases. *Mol Clin Oncol* (2014) 2 (5):695–700. doi: 10.3892/mco.2014.307

104. Oxberry S, Johnson M. Response to thalidomide in chemotherapy-resistant cutaneous T-cell lymphoma. *Clin Oncol* (2006) 18(1):86–7. doi: 10.1016/j.clon.2005.08.006

105. Giannopoulos K, Dmoszynska A, Kowal M, Wąsik-Szczepanek E, Bojarska-Junak A, Rolinski J, et al. Thalidomide exerts distinct molecular antileukemic effects and combined thalidomide/fludarabine therapy is clinically effective in high-risk chronic lymphocytic leukemia. *Leukemia* (2009) 23(10):1771–8. doi: 10.1038/leu.2009.98

106. Chanan-Khan A, Miller KC, Takeshita K, Koryzna A, Donohue K, Bernstein ZP, et al. Results of a phase 1 clinical trial of thalidomide in combination with fludarabine as initial therapy for patients with treatment-requiring chronic lymphocytic leukemia (CLL). *Blood* (2005) 106(10):3348–52. doi: 10.1182/blood-2005-02-0669

107. Giannopoulos K, Mertens D, Stilgenbauer S. Treating chronic lymphocytic leukemia with thalidomide and lenalidomide. *Expert Opin Pharmacother* (2011) 12 (18):2857–64. doi: 10.1517/14656566.2011.635644

108. Furman R, Leonard J, Allen S, Coleman M, Rosenthal T, Gabrilove J. Thalidomide alone or in combination with fludarbabine are effective treatments for patients with fludarabine-relapsed and refractory CLL. *J Clin Oncol* (2005) 23 (16_suppl):6640–. doi: 10.1200/jco.2005.23.16_suppl.6640

109. Tueger S, Chen F, Ahsan G, McDonald V, Andrews V, Madrigal J, et al. Thalidomide induced remission of refractory diffuse large b-cell lymphoma post-allogeneic SCT. *Haematologica* (2006) 91(6_Suppl):ECR16–ECR. doi: 10.3324/%25x

110. Kiesewetter B, Raderer M. Immunomodulatory treatment for mucosa-associated lymphoid tissue lymphoma (MALT lymphoma). *Hematol Oncol* (2020) 38(4):417–24. doi: 10.1002/hon.2754

111. Raza A, Mehdi M, Mumtaz M, Ali F, Lascher S, Galili N. Combination of 5-azacytidine and thalidomide for the treatment of myelodysplastic syndromes and acute myeloid leukemia. *Cancer: Interdiscip Int J Am Cancer Society* (2008) 113 (7):1596–604. doi: 10.1002/cncr.23789

112. Steins MB, Padró T, Bieker R, Ruiz S, Kropff M, Kienast J, et al. Efficacy and safety of thalidomide in patients with acute myeloid leukemia. *Blood J Am Soc Hematol* (2002) 99(3):834–9. doi: 10.1182/blood.V99.3.834

113. Thomas DA, Estey E, Giles FJ, Faderl S, Cortes J, Keating M, et al. Single agent thalidomide in patients with relapsed or refractory acute myeloid leukaemia. *Br J Haematol* (2003) 123(3):436–41. doi: 10.1046/j.1365-2141.2003.04639.x

114. Strupp C, Germing U, Aivado M, Misgeld E, Haas R, Gattermann N. Thalidomide for the treatment of patients with myelodysplastic syndromes. *Leukemia* (2002) 16(1):1–6. doi: 10.1038/sj.leu.2402330

115. Raza A, Meyer P, Dutt D, Zorat F, Lisak L, Nascimben F, et al. Thalidomide produces transfusion independence in long-standing refractory anemias of patients with myelodysplastic syndromes. *Blood J Am Soc Hematol* (2001) 98(4):958–65. doi: 10.1182/blood.V98.4.958

116. Chung C-Y, Lin S-F, Chen P-M, Chang M-C, Kao W-Y, Chao T-Y, et al. Thalidomide for the treatment of myelodysplastic syndrome in Taiwan: results of a phase II trial. *Anticancer Res* (2012) 32(8):3415–9.

117. Leitch HA, Buckstein R, Shamy A, Storring JM. The immunomodulatory agents lenalidomide and thalidomide for treatment of the myelodysplastic syndromes: a clinical practice guideline. *Crit Rev Oncology/hematology*. (2013) 85 (2):162–92. doi: 10.1016/j.critrevonc.2012.07.003

118. Kenealy M, Patton N, Filshie R, Nicol A, Ho S-J, Hertzberg M, et al. Results of a phase II study of thalidomide and azacitidine in patients with clinically advanced myelodysplastic syndromes (MDS), chronic myelomonocytic leukemia (CMML) and low blast count acute myeloid leukemia (AML). *Leukemia Lymphoma* (2017) 58(2):298–307. doi: 10.1080/10428194.2016.1190971

119. Monroy RH, Vargas-Viveros P, Ceballos EC, Velazquez JC, Munos SC. Imatinib (IM) plus thalidomide (Thali), a effective combination for the treatment of chronic myeloid leukemia (CML) Philadelphia chromosomepositive (Ph+) in IM-resistant disease. Report of 14 new cases from a single center in Mexico. *Blood* (2013) 122(21):5172. doi: 10.1182/blood.V122.21.5172.5172

120. Facon T, Cook G, Usmani SZ, Hulin C, Kumar S, Plesner T, et al. Daratumumab plus lenalidomide and dexamethasone in transplant-ineligible newly diagnosed multiple myeloma: frailty subgroup analysis of MAIA. *Leukemia* (2022) 36(4):1066–77. doi: 10.1038/s41375-021-01488-8

121. Holstein SA, Suman VJ, McCarthy PL. Update on the role of lenalidomide in patients with multiple myeloma. *Ther Adv Hematol* (2018) 9(7):175–90. doi: 10.1177/2040620718775629

122. Attal M, Lauwers-Cances V, Marit G, Caillot D, Moreau P, Facon T, et al. Lenalidomide maintenance after stem-cell transplantation for multiple myeloma. *New Engl J Med* (2012) 366(19):1782–91. doi: 10.1056/NEJMoa1114138

123. Palumbo A, Hajek R, Delforge M, Kropff M, Petrucci MT, Catalano J, et al. Continuous lenalidomide treatment for newly diagnosed multiple myeloma. *New Engl J Med* (2012) 366(19):1759–69. doi: 10.1056/NEJMoa1112704

124. McCarthy PL, Owzar K, Hofmeister CC, Hurd DD, Hassoun H, Richardson PG, et al. Lenalidomide after stem-cell transplantation for multiple myeloma. *New Engl J Med* (2012) 366(19):1770–81. doi: 10.1056/NEJMoa1114083

125. Weber DM, Chen C, Niesvizky R, Wang M, Belch A, Stadtmauer EA, et al. Lenalidomide plus dexamethasone for relapsed multiple myeloma in north America. *New Engl J Med* (2007) 357(21):2133–42. doi: 10.1056/NEJMoa070596

126. List A, Bennett J, Sekeres M, Skikne B, Fu T, Shammo J, et al. Extended survival and reduced risk of AML progression in erythroid-responsive lenalidomide-treated patients with lower-risk del (5q) MDS. *Leukemia* (2014) 28 (5):1033–40. doi: 10.1038/leu.2013.305

127. Ossenkoppele G, Breems D, Stuessi G, van Norden Y, Bargetzi M, Biemond B, et al. Lenalidomide added to standard intensive treatment for older patients with AML and high-risk MDS. *Leukemia* (2020) 34(7):1751–9. doi: 10.1038/s41375-020-0725-0

128. Witzig TE, Nowakowski G, Habermann T, Goy A, Hernandez-Ilizaliturri F, Chiappella A, et al. A comprehensive review of lenalidomide therapy for b-cell non-Hodgkin lymphoma. *Ann Oncol* (2015) 26(8):1667–77. doi: 10.1093/annonc/mdv102

129. Ruan J, Martin P, Christos P, Cerchietti L, Tam W, Shah B, et al. Five-year follow-up of lenalidomide plus rituximab as initial treatment of mantle cell lymphoma. *Blood J Am Soc Hematol* (2018) 132(19):2016–25. doi: 10.1182/blood-2018-07-859769

130. Wang M, Fayad L, Wagner-Bartak N, Zhang L, Hagemeister F, Neelapu SS, et al. Lenalidomide in combination with rituximab for patients with relapsed or refractory mantle-cell lymphoma: a phase 1/2 clinical trial. *Lancet Oncol* (2012) 13 (7):716–23. doi: 10.1016/S1470-2045(12)70200-0

131. Goy A, Sinha R, Williams ME, Besisik SK, Drach J, Ramchandren R, et al. Single-agent lenalidomide in patients with mantle-cell lymphoma who relapsed or progressed after or were refractory to bortezomib: phase II MCL-001 (EMERGE) study. *J Clin Oncol* (2013) 31(29):3688. doi: 10.1200/JCO.2013.49.2835

132. Yamshon S, Martin P, Shah B, Schuster SJ, Christos PJ, Rodriguez A, et al. Initial treatment with lenalidomide plus rituximab for mantle cell lymphoma (MCL): 7-year analysis from a multi-center phase II study. *Blood* (2020) 136:45–6. doi: 10.1182/blood-2020-138731

133. Morschhauser F, Le Gouill S, Feugier P, Bailly S, Nicolas-Virelizier E, Bijou F, et al. Obinutuzumab combined with lenalidomide for relapsed or refractory follicular b-cell lymphoma (GALEN): a multicentre, single-arm, phase 2 study. *Lancet Haematol* (2019) 6(8):e429–e37. doi: 10.1016/S2352-3026(19)30089-4

134. Flowers CR, Leonard JP, Fowler NH. Lenalidomide in follicular lymphoma. *Blood* (2020) 135(24):2133–6. doi: 10.1182/blood.2019001751

135. Witzig TE, Wiernik PH, Moore T, Reeder C, Cole C, Justice G, et al. Lenalidomide oral monotherapy produces durable responses in relapsed or refractory indolent non-hodgkin's lymphoma. *J Clin Oncol* (2009) 27(32):5404–9. doi: 10.1200/JCO.2008.21.1169

136. Ferrajoli A, Lee B-N, Schlette EJ, O'Brien SM, Gao H, Wen S, et al. Lenalidomide induces complete and partial remissions in patients with relapsed and refractory chronic lymphocytic leukemia. *Blood J Am Soc Hematol* (2008) 111 (11):5291–7. doi: 10.1182/blood-2007-12-130120

137. Badoux XC, Keating MJ, Wen S, Lee B-N, Sivina M, Reuben J, et al. Lenalidomide as initial therapy of elderly patients with chronic lymphocytic leukemia. *Blood J Am Soc Hematol* (2011) 118(13):3489–98. doi: 10.1182/blood-2011-03-339077

138. Chen CI, Bergsagel PL, Paul H, Xu W, Lau A, Dave N, et al. Single-agent lenalidomide in the treatment of previously untreated chronic lymphocytic leukemia. *J Clin Oncol* (2011) 29(9):1175. doi: 10.1200/JCO.2010.29.8133

139. Shanafelt TD, Ramsay AG, Zent CS, Leis JF, Tun HW, Call TG, et al. Long-term repair of T-cell synapse activity in a phase II trial of chemoimmunotherapy followed by lenalidomide consolidation in previously untreated chronic lymphocytic leukemia (CLL). *Blood J Am Soc Hematol* (2013) 121(20):4137–41. doi: 10.1182/blood-2012-12-470005

140. Itchaki G, Brown JR. Lenalidomide in the treatment of chronic lymphocytic leukemia. *Expert Opin Investigational Drugs* (2017) 26(5):633–50. doi: 10.1080/13543784.2017.1313230

141. Strati P, Keating MJ, Wierda WG, Badoux XC, Calin S, Reuben JM, et al. Lenalidomide induces long-lasting responses in elderly patients with chronic lymphocytic leukemia. *Blood J Am Soc Hematol* (2013) 122(5):734–7. doi: 10.1182/blood-2013-04-495341

142. Zinzani PL, Rodgers T, Marino D, Frezzato M, Barbui AM, Castellino C, et al. RE-MIND: comparing tafasitamab+ lenalidomide (L-MIND) with a real-world lenalidomide

monotherapy cohort in relapsed or refractory diffuse large b-cell lymphoma. *Clin Cancer Res* (2021) 27(22):6124–34. doi: 10.1158/1078-0432.CCR-21-1471

143. Thieblemont C, Delfau-Larue M-H, Coiffier B. Lenalidomide in diffuse large b-cell lymphoma. *Adv Hematol* (2012) 2012:861060. doi: 10.1155/2012/861060

144. Kiesewetter B, Troch M, Dolak W, Müllauer L, Lukas J, Zielinski CC, et al. A phase II study of lenalidomide in patients with extranodal marginal zone b-cell lymphoma of the mucosa associated lymphoid tissue (MALT lymphoma). *Haematologica* (2013) 98(3):353. doi: 10.3324/haematol.2012.065995

145. Houillier C, Choquet S, Touitou V, Martin-Duverneuil N, Navarro S, Mokhtari K, et al. Lenalidomide monotherapy as salvage treatment for recurrent primary CNS lymphoma. *Neurology* (2015) 84(3):325–6. doi: 10.1212/WNL.0000000000001158

146. Ghesquieres H, Chevrier M, Laadhari M, Chinot O, Choquet S, Molucon-Chabrot C, et al. Lenalidomide in combination with intravenous rituximab (REVRI) in relapsed/refractory primary CNS lymphoma or primary intraocular lymphoma: a multicenter prospective 'proof of concept'phase II study of the French oculo-cerebral lymphoma (LOC) network and the lymphoma study association (LYSA). *Ann Oncol* (2019) 30(4):621–8. doi: 10.1093/annonc/mdz032

147. Hopfinger G, Nösslinger T, Lang A, Linkesch W, Melchardt T, Weiss L, et al. Lenalidomide in combination with vorinostat and dexamethasone for the treatment of relapsed/refractory peripheral T cell lymphoma (PTCL): report of a phase I/II trial. *Ann Hematol* (2014) 93(3):459–62. doi: 10.1007/s00277-014-2009-0

148. Dueck G, Chua N, Prasad A, Stewart D, White D, Vanderjagt R, et al. Activity of lenalidomide in a phase II trial for T-cell lymphoma: Report on the first 24 cases. *J Clin Oncol* (2009) 27(15_suppl):8524–. doi: 10.1200/jco.2009.27.15_suppl.8524

149. Sakamoto H, Itonaga H, Sawayama Y, Furumoto T, Fujioka M, Chiwata M, et al. Treatment with mogamulizumab or lenalidomide for relapsed adult T-cell leukemia/lymphoma after allogeneic hematopoietic stem cell transplantation: the Nagasaki transplant group experience. *Hematol Oncol* (2020) 38(2):162–70. doi: 10.1002/hon.2712

150. Ruan J, Zain JM, Palmer B, Jovanovic B, Mi X, Swaroop A, et al. Multicenter phase II study of romidepsin plus lenalidomide for patients with previously untreated peripheral T-cell lymphoma (PTCL). *Wolters Kluwer Health* (2021) 39(S2):98–9. doi: 10.1002/hon.55_2879

151. Fehniger TA, Byrd JC, Marcucci G, Abboud CN, Kefauver C, Payton JE, et al. Single-agent lenalidomide induces complete remission of acute myeloid leukemia in patients with isolated trisomy 13. *Blood J Am Soc Hematol* (2009) 113 (5):1002–5. doi: 10.1182/blood-2008-04-152678

152. Pollyea D, Kohrt H, Gallegos L, Figueroa M, Abdel-Wahab O, Zhang B, et al. Safety, efficacy and biological predictors of response to sequential azacitidine and lenalidomide for elderly patients with acute myeloid leukemia. *Leukemia* (2012) 26(5):893–901. doi: 10.1038/leu.2011.294

153. Govindaraj C, Madondo M, Kong YY, Tan P, Wei A, Plebanski M. Lenalidomide-based maintenance therapy reduces TNF receptor 2 on CD4 T cells and enhances immune effector function in acute myeloid leukemia patients. *Am J Hematol* (2014) 89(8):795–802. doi: 10.1002/ajh.23746

154. Pollyea DA, Zehnder J, Coutre S, Gotlib JR, Gallegos L, Abdel-Wahab O, et al. Sequential azacitidine plus lenalidomide combination for elderly patients with untreated acute myeloid leukemia. *Haematologica* (2013) 98(4):591. doi: 10.3324/haematol.2012.076414

155. Fehniger TA, Uy GL, Trinkaus K, Nelson AD, Demland J, Abboud CN, et al. A phase 2 study of high-dose lenalidomide as initial therapy for older patients with acute myeloid leukemia. *Blood J Am Soc Hematol* (2011) 117(6):1828–33. doi: 10.1182/blood-2010-07-297143

156. Buckstein R, Kerbel R, Cheung M, Shaked Y, Chodirker L, Lee CR, et al. Lenalidomide and metronomic melphalan for CMML and higher risk MDS: A phase 2 clinical study with biomarkers of angiogenesis. *Leukemia Res* (2014) 38 (7):756–63. doi: 10.1016/j.leukres.2014.03.022

157. Sekeres MA, Othus M, List AF, Odenike O, Stone RM, Gore SD, et al. Randomized phase II study of azacitidine alone or in combination with lenalidomide or with vorinostat in higher-risk myelodysplastic syndromes and chronic myelomonocytic leukemia: North American intergroup study SWOG S1117. *J Clin Oncol* (2017) 35(24):2745. doi: 10.1200/JCO.2015.66.2510

158. Kunacheewa C, Thongthang P, Ungprasert P, Utchariyaprasit E, Owattanapanich W. A systematic review and meta-analysis of the efficacy and adverse events of azacitidine-plus-lenalidomide treatment for patients with acute myeloid leukemia, myelodysplastic syndromes and chronic myelomonocytic leukemia. *Hematology* (2019) 24(1):498–506. doi: 10.1080/16078454.2019.1631425

159. Burgstaller S, Stauder R, Kuehr T, Lang A, Machherndl-Spandl S, Mayrbaeurl B, et al. A phase I study of lenalidomide in patients with chronic myelomonocytic leukemia (CMML)–AGMT_CMML-1. *Leukemia Lymphoma* (2018) 59(5):1121–6. doi: 10.1080/10428194.2017.1369070

160. Richardson PG, Siegel DS, Vij R, Hofmeister CC, Baz R, Jagannath S, et al. Pomalidomide alone or in combination with low-dose dexamethasone in relapsed and refractory multiple myeloma: a randomized phase 2 study. *Blood J Am Soc Hematol* (2014) 123(12):1826–32. doi: 10.1182/blood-2013-11-538835

161. San Miguel J, Weisel K, Moreau P, Lacy M, Song K, Delforge M, et al. Pomalidomide plus low-dose dexamethasone versus high-dose dexamethasone alone for patients with relapsed and refractory multiple myeloma (MM-003): a randomised, open-label, phase 3 trial. *Lancet Oncol* (2013) 14(11):1055–66. doi: 10.1016/S1470-2045(13)70380-2

162. Chanan-Khan A, Swaika A, Paulus A, Kumar S, Mikhael J, Rajkumar S, et al. Pomalidomide: the new immunomodulatory agent for the treatment of multiple myeloma. *Blood Cancer J* (2013) 3(9):e143–e. doi: 10.1038/bcj.2013.38

163. Offidani M, Corvatta L, Caraffa P, Leoni P, Pautasso C, Larocca A, et al. Pomalidomide for the treatment of relapsed–refractory multiple myeloma: a review of biological and clinical data. *Expert Rev Anticancer Ther* (2014) 14(5):499–510. doi: 10.1586/14737140.2014.906904

164. Mato AR, Schuster SJ, Foss FM, Isufi I, Ding W, Brander DM, et al. A phase Ia/Ib study exploring the synthetic lethality of the orally administered novel BTK inhibitor, dtrmwxhs-12 (DTRM-12), in combination with everolimus and pomalidomide in patients with relapsed/refractory CLL, DLBCL or other b-cell lymphomas. *Blood* (2019) 134:810. doi: 10.1182/blood-2019-126192

165. Begna K, Mesa R, Pardanani A, Hogan W, Litzow M, McClure R, et al. A phase-2 trial of low-dose pomalidomide in myelofibrosis. *Leukemia* (2011) 25 (2):301–4. doi: 10.1038/leu.2010.254

166. Gowin KL, Mesa RA. Profile of pomalidomide and its potential in the treatment of myelofibrosis. *Ther Clin Risk Management* (2015) 11:549. doi: 10.2147/TCRM.S69211

167. Zeidner JF, Knaus HA, Zeidan AM, Blackford AL, Montiel-Esparza R, Hackl H, et al. Immunomodulation with pomalidomide at early lymphocyte recovery after induction chemotherapy in newly diagnosed AML and high-risk MDS. *Leukemia* (2020) 34(6):1563–76. doi: 10.1038/s41375-019-0693-4

168. Montiel-Esparza R, Knaus HA, Zeidner JF, Vulic A, Prince GT, Smith BD, et al. Immune modulation with pomalidomide after induction chemotherapy in newly diagnosed acute myeloid leukemia (AML). *Blood* (2015) 126(23):1351. doi: 10.1182/blood.V126.23.1351.1351

169. Grogan DP, Winston NR. Thalidomide. In: *StatPearls*. StatPearls Publishing (2022). Treasure Island (FL)

170. Lacy MQ, McCurdy AR. Pomalidomide. *Blood* (2013) 122(14):2305–9. doi: 10.1182/blood-2013-05-484782

171. Sperling AS, Guerra VA, Kennedy JA, Yan Y, Hsu JI, Wang F, et al. Lenalidomide promotes the development of TP53-mutated therapy-related myeloid neoplasms. *Blood* (2022) blood.2021014956. Online ahead of print. doi: 10.1182/blood.2021014956

172. Khan SR, Tariq M, Fayyaz SM, Soomar SM, Moosajee M. Lenalidomide induced secondary acute lymphoblastic leukemia in a multiple myeloma patient: A case-report. *Leukemia Res Rep* (2022) 17:100315. doi: 10.1016/j.lrr.2022.100315

173. Ito T, Ando H, Suzuki T, Ogura T, Hotta K, Imamura Y, et al. Identification of a primary target of thalidomide teratogenicity. *science* (2010) 327(5971):1345–50. doi: 10.1126/science.1177319

174. Lopez-Girona A, Mendy D, Ito T, Miller K, Gandhi A, Kang J, et al. Cereblon is a direct protein target for immunomodulatory and antiproliferative activities of lenalidomide and pomalidomide. *Leukemia* (2012) 26(11):2326–35. doi: 10.1038/leu.2012.119

175. Gandhi AK, Kang J, Havens CG, Conklin T, Ning Y, Wu L, et al. Immunomodulatory agents lenalidomide and pomalidomide co-stimulate T cells by inducing degradation of T cell repressors I karos and a iolos *via* modulation of the e 3 ubiquitin ligase complex CRL 4 CRBN. *Br J Haematol* (2014) 164(6):811–21. doi: 10.1111/bjh.12708

176. Zhu YX, Braggio E, Shi C-X, Bruins LA, Schmidt JE, Van Wier S, et al. Cereblon expression is required for the antimyeloma activity of lenalidomide and pomalidomide. *Blood J Am Soc Hematol* (2011) 118(18):4771–9. doi: 10.1182/blood-2011-05-356063

177. Petroski MD, Deshaies RJ. Function and regulation of cullin–RING ubiquitin ligases. *Nat Rev Mol Cell Biol* (2005) 6(1):9–20. doi: 10.1038/nrm1547

178. Angers S, Li T, Yi X, MacCoss MJ, Moon RT, Zheng N. Molecular architecture and assembly of the DDB1–CUL4A ubiquitin ligase machinery. *Nature* (2006) 443(7111):590–3. doi: 10.1038/nature05175

179. Chamberlain PP, Cathers BE. Cereblon modulators: Low molecular weight inducers of protein degradation. *Drug Discovery Today: Technologies* (2019) 31:29–34. doi: 10.1016/j.ddtec.2019.02.004

180. Collins I, Wang H, Caldwell JJ, Chopra R. Chemical approaches to targeted protein degradation through modulation of the ubiquitin-proteasome pathway. *Biochem J* (2017) 474(7):1127–47. doi: 10.1042/BCJ20160762

181. Fischer ES, Böhm K, Lydeard JR, Yang H, Stadler MB, Cavadini S, et al. Structure of the DDB1-CRBN E3 ubiquitin ligase in complex with thalidomide. *Nature* (2014) 512(7512):49–53. doi: 10.1038/nature13527

182. Krönke J, Hurst SN, Ebert BL. Lenalidomide induces degradation of IKZF1 and IKZF3. *Oncoimmunology* (2014) 3(7):e941742. doi: 10.4161/21624011.2014.941742

183. Krönke J, Udeshi N, Narla A, Grauman P, Hurst S, McConkey M, et al. Lenalidomide promotes CRBN-mediated ubiquitination and degradation of IKZF1 and IKZF3. *Blood* (2013) 122(21):LBA–5. doi: 10.1182/blood.V122.21.LBA-5.LBA-5

184. Ramsay AG, Johnson AJ, Lee AM, Gorgün G, Le Dieu R, Blum W, et al. Chronic lymphocytic leukemia T cells show impaired immunological synapse formation that can be reversed with an immunomodulating drug. *J Clin Invest* (2008) 118(7):2427–37. doi: 10.1172/JCI35017

185. Muller GW, Corral LG, Shire MG, Wang H, Moreira A, Kaplan G, et al. Structural modifications of thalidomide produce analogs with enhanced tumor necrosis factor inhibitory activity. *J Medicinal Chem* (1996) 39(17):3238–40. doi: 10.1021/jm9603328

186. Petzold G, Fischer ES, Thomä NH. Structural basis of lenalidomide-induced CK1α degradation by the CRL4CRBN ubiquitin ligase. *Nature* (2016) 532(7597):127–30. doi: 10.1038/nature16979

187. Schneider RK, Ademà V, Heckl D, Järås M, Mallo M, Lord AM, et al. Role of casein kinase 1A1 in the biology and targeted therapy of del (5q) MDS. *Cancer Cell* (2014) 26(4):509–20. doi: 10.1016/j.ccr.2014.08.001

188. Fuchs O. Role of immunomodulatory drugs in the treatment of lymphoid and myeloid malignancies. *Front Clin Drug Res Hematol* (2018) 3:73. doi: 10.2174/9781681083674118030005

189. Bjorklund C, Lu L, Kang J, Hagner P, Havens C, Amatangelo M, et al. Rate of CRL4CRBN substrate ikaros and aiolos degradation underlies differential activity of lenalidomide and pomalidomide in multiple myeloma cells by regulation of c-myc and IRF4. *Blood Cancer J* (2015) 5(10):e354–e. doi: 10.1038/bcj.2015.66

190. Gandhi AK, Kang J, Naziruddin S, Parton A, Schafer PH, Stirling DI. Lenalidomide inhibits proliferation of namalwa CSN.70 cells and interferes with Gab1 phosphorylation and adaptor protein complex assembly. *Leukemia Res* (2006) 30(7):849–58. doi: 10.1016/j.leukres.2006.01.010

191. Zhang LH, Kosek J, Wang M, Heise C, Schafer PH, Chopra R. Lenalidomide efficacy in activated b-cell-like subtype diffuse large b-cell lymphoma is dependent upon IRF4 and cereblon expression. *Br J Haematol* (2013) 160(4):487–502. doi: 10.1111/bjh.12172

192. D'Souza C, Prince HM, Neeson PJ. Understanding the role of T-cells in the antimyeloma effect of immunomodulatory drugs. *Front Immunol* (2021) 12:632399. doi: 10.3389/fimmu.2021.632399

193. Dave SS, Wright G, Tan B, Rosenwald A, Gascoyne RD, Chan WC, et al. Prediction of survival in follicular lymphoma based on molecular features of tumor-infiltrating immune cells. *N Engl J Med* (2004) 351(21):2159–69. doi: 10.1056/NEJMoa041869

194. Küppers R. Mechanisms of b-cell lymphoma pathogenesis. *Nat Rev Cancer* (2005) 5(4):251–62. doi: 10.1038/nrc1589

195. Dogan A, Du M-Q, Aiello A, Diss TC, Ye H-T, Pan L-X, et al. Follicular lymphomas contain a clonally linked but phenotypically distinct neoplastic b-cell population in the interfollicular zone. *Blood J Am Soc Hematol* (1998) 91(12):4708–14. doi: 10.1182/blood.V91.12.4708

196. Zucchetto A, Tripodo C, Benedetti D, Deaglio S, Gaidano G, Del Poeta G, et al. Monocytes/macrophages but not T lymphocytes are the major targets of the CCL3/CCL4 chemokines produced by CD38(+)CD49d(+) chronic lymphocytic leukaemia cells. *Br J Haematol* (2010) 150(1):111–3. doi: 10.1111/j.1365-2141.2010.08152.x

197. Burger JA, Quiroga MP, Hartmann E, Bürkle A, Wierda WG, Keating MJ, et al. High-level expression of the T-cell chemokines CCL3 and CCL4 by chronic lymphocytic leukemia b cells in nurselike cell cocultures and after BCR stimulation. *Blood* (2009) 113(13):3050–8. doi: 10.1182/blood-2008-07-170415

198. Ramsay AG, Clear AJ, Fatah R, Gribben JG. Multiple inhibitory ligands induce impaired T-cell immunologic synapse function in chronic lymphocytic leukemia that can be blocked with lenalidomide: establishing a reversible immune evasion mechanism in human cancer. *Blood J Am Soc Hematol* (2012) 120(7):1412–21. doi: 10.1182/blood-2012-02-411678

199. Scott DW, Gascoyne RD. The tumour microenvironment in b cell lymphomas. *Nat Rev Cancer* (2014) 14(8):517–34. doi: 10.1038/nrc3774

200. Upadhyay R, Hammerich L, Peng P, Brown B, Merad M, Brody JD. Lymphoma: immune evasion strategies. *Cancers* (2015) 7(2):736–62. doi: 10.3390/cancers7020736

201. Aue G, Sun C, Liu D, Park J-H, Pittaluga S, Tian X, et al. Activation of Th1 immunity within the tumor microenvironment is associated with clinical response to lenalidomide in chronic lymphocytic leukemia. *J Immunol* (2018) 201(7):1967–74. doi: 10.4049/jimmunol.1800570

202. Ménard C, Rossille D, Dulong J, Nguyen T-T, Papa I, Latour M, et al. Lenalidomide triggers T-cell effector functions *in vivo* in patients with follicular lymphoma. *Blood Advances* (2021) 5(8):2063–74. doi: 10.1182/bloodadvances.2020003774

203. Danhof S, Schreder M, Knop S, Rasche L, Strifler S, Löffler C, et al. Expression of programmed death-1 on lymphocytes in myeloma patients is lowered during lenalidomide maintenance. *Haematologica* (2018) 103(3):e126. doi: 10.3324/haematol.2017.178947

204. Minnema M, van der Veer M, Aarts T, Emmelot M, Mutis T, Lokhorst H. Lenalidomide alone or in combination with dexamethasone is highly effective in patients with relapsed multiple myeloma following allogeneic stem cell transplantation and increases the frequency of CD4+ Foxp3+ T cells. *Leukemia* (2009) 23(3):605–7. doi: 10.1038/leu.2008.247

205. Nguyen-Pham T-N, Jung S-H, Vo M-C, Thanh-Tran H-T, Lee Y-K, Lee H-J, et al. Lenalidomide synergistically enhances the effect of dendritic cell vaccination in a model of murine multiple myeloma. *J Immunother* (2015) 38(8):330–9. doi: 10.1097/CJI.0000000000000097

206. Geng CL, Chen JY, Song TY, Jung JH, Long M, Song MF, et al. Lenalidomide bypasses CD28 co-stimulation to reinstate PD-1 immunotherapy by activating notch signaling. *Cell Chem Biol* (2022) 29(8):1260–1272.e8. doi: 10.1016/j.chembiol.2022.05.012

207. Otáhal P, Průková D, Král V, Fabry M, Vočková P, Latečková L, et al. Lenalidomide enhances antitumor functions of chimeric antigen receptor modified T cells. *Oncoimmunology* (2016) 5(4):e1115940. doi: 10.1080/2162402X.2015.1115940

208. Wang X, Walter M, Urak R, Weng L, Huynh C, Lim L, et al. Lenalidomide enhances the function of CS1 chimeric antigen receptor-redirected T cells against multiple myeloma. *Clin Cancer Research: an Off J Am Assoc Cancer Res* (2018) 24 (1):106–19. doi: 10.1158/1078-0432.CCR-17-0344

209. Poh C, Frankel P, Ruel C, Abedi M, Schwab E, Costello CL, et al. Blinatumomab/Lenalidomide in Relapsed/Refractory non-hodgkin's lymphoma: A phase I California cancer consortium study of safety, efficacy and immune correlative analysis. *Blood* (2019) 134(Supplement_1):760–. doi: 10.1182/blood-2019-124254

210. Robinson HR, Qi J, Cook EM, Nichols C, Dadashian EL, Underbayev C, et al. A CD19/CD3 bispecific antibody for effective immunotherapy of chronic lymphocytic leukemia in the ibrutinib era. *Blood* (2018) 132(5):521–32. doi: 10.1182/blood-2018-02-830992

211. Martens AWJ, Janssen SR, Derks IAM, Adams Iii HC, Izhak L, van Kampen R, et al. CD3xCD19 DART molecule treatment induces non-apoptotic killing and is efficient against high-risk chemotherapy and venetoclax-resistant chronic lymphocytic leukemia cells. *J Immunother Cancer* (2020) 8(1):e000218. doi: 10.1136/jitc-2019-000218

212. Hayashi T, Hideshima T, Akiyama M, Podar K, Yasui H, Raje N, et al. Molecular mechanisms whereby immunomodulatory drugs activate natural killer cells: clinical application. *Br J Haematol* (2005) 128(2):192–203. doi: 10.1111/j.1365-2141.2004.05286.x

213. Boxhammer R, Steidl S, Endell J. Effect of IMiD compounds on CD38 expression on multiple myeloma cells: MOR202, a human CD38 antibody in combination with pomalidomide. *Am Soc Clin Oncol* (2015) 33(15_suppl):8588. doi: 10.1200/jco.2015.33.15_suppl.8588

214. Offidani M, Corvatta L, Morè S, Nappi D, Martinelli G, Olivieri A, et al. Daratumumab for the management of newly diagnosed and relapsed/refractory multiple myeloma: current and emerging treatments. *Front Oncol* (2021) 10:624661. doi: 10.3389/fonc.2020.624661

215. Kaufman JL, Usmani SZ, San-Miguel J, Bahlis N, White DJ, Benboubker L, et al. Four-year follow-up of the phase 3 pollux study of daratumumab plus lenalidomide and dexamethasone (D-Rd) versus lenalidomide and dexamethasone (Rd) alone in relapsed or refractory multiple myeloma (RRMM). *Blood* (2019) 134:1866. doi: 10.1182/blood-2019-123483

216. Chang DH, Liu N, Klimek V, Hassoun H, Mazumder A, Nimer SD, et al. Enhancement of ligand-dependent activation of human natural killer T cells by lenalidomide: therapeutic implications. *Blood* (2006) 108(2):618–21. doi: 10.1182/blood-2005-10-4184

217. Lagrue K, Carisey A, Morgan DJ, Chopra R, Davis DM. Lenalidomide augments actin remodeling and lowers NK-cell activation thresholds. *Blood J Am Soc Hematol* (2015) 126(1):50–60. doi: 10.1182/blood-2015-01-625004

218. Hideshima T, Ogiya D, Liu J, Harada T, Kurata K, Bae J, et al. Immunomodulatory drugs activate NK cells *via* both zap-70 and cereblon-dependent pathways. *Leukemia* (2021) 35(1):177–88. doi: 10.1038/s41375-020-0809-x

219. Roider T, Brinkmann BJ, Kim V, Knoll M, Kolb C, Roessner PM, et al. An autologous culture model of nodal b-cell lymphoma identifies ex vivo determinants of response to bispecific antibodies. *Blood Advances* (2021) 5(23):5060–71. doi: 10.1182/bloodadvances.2021005400

220. Wang Z, Yin C, Lum LG, Simons A, Weiner GJ. Bispecific antibody-activated T cells enhance NK cell-mediated antibody-dependent cellular cytotoxicity. *J Hematol Oncol* (2021) 14(1):1–4. doi: 10.1186/s13045-021-01216-w

221. Acebes-Huerta A, Huergo-Zapico L, Gonzalez-Rodriguez AP, Fernandez-Guizan A, Payer AR, López-Soto A, et al. Lenalidomide induces immunomodulation in

chronic lymphocytic leukemia and enhances antitumor immune responses mediated by NK and CD4 T cells. *BioMed Res Int* (2014) 2014:265840. doi: 10.1155/2014/265840

222. Chiu H, Trisal P, Bjorklund C, Carrancio S, Toraño EG, Guarinos C, et al. Combination lenalidomide-rituximab immunotherapy activates anti-tumour immunity and induces tumour cell death by complementary mechanisms of action in follicular lymphoma. *Br J Haematol* (2019) 185(2):240–53. doi: 10.1111/bjh.15797

223. Mougiakakos D, Bach C, Böttcher M, Beier F, Röhner L, Stoll A, et al. The IKZF1-IRF4/IRF5 axis controls polarization of myeloma-associated macrophages. *Cancer Immunol Res* (2021) 9(3):265–78. doi: 10.1158/2326-6066.CIR-20-0555

224. Cao X, Chen J, Li B, Dang J, Zhang W, Zhong X, et al. Promoting antibody-dependent cellular phagocytosis for effective macrophage-based cancer immunotherapy. *Sci Adv* (2022) 8(11):eabl9171. doi: 10.1126/sciadv.abl9171

225. Busch L, Mougiakakos D, Büttner-Herold M, Müller MJ, Volmer DA, Bach C, et al. Lenalidomide enhances MOR202-dependent macrophage-mediated effector functions *via* the vitamin d pathway. *Leukemia* (2018) 32(11):2445–58. doi: 10.1038/s41375-018-0114-0

226. Elias S, Kahlon S, Kotzur R, Kaynan N, Mandelboim O. Obinutuzumab activates FcγRI more potently than other anti-CD20 antibodies in chronic lymphocytic leukemia (CLL). *Oncoimmunology* (2018) 7(6):e1428158. doi: 10.1080/2162402X.2018.1428158

227. Chen S, Lai SWT, Brown CE, Feng M. Harnessing and enhancing macrophage phagocytosis for cancer therapy. *Front Immunol* (2021) 12:635173. doi: 10.3389/fimmu.2021.635173

228. Weiskopf K, Weissman IL. *Macrophages are critical effectors of antibody therapies for cancer*. *MAbs* (2015) 7(2):303–10. doi: 10.1080/19420862.2015.1011450

229. Henry JY, Labarthe MC, Meyer B, Dasgupta P, Dalgleish AG, Galustian C. Enhanced cross-priming of naive CD8+ T cells by dendritic cells treated by the IMiDs® immunomodulatory compounds lenalidomide and pomalidomide. *Immunology* (2013) 139(3):377–85. doi: 10.1111/imm.12087

230. Palma M, Hansson L, Mulder TA, Adamson L, Näsman-Glaser B, Eriksson I, et al. Lenalidomide as immune adjuvant to a dendritic cell vaccine in chronic lymphocytic leukemia patients. *Eur J Haematol* (2018) 101(1):68–77. doi: 10.1111/ejh.13065

231. Lapenta C, Donati S, Spadaro F, Lattanzi L, Urbani F, Macchia I, et al. Lenalidomide improves the therapeutic effect of an interferon-α-dendritic cell-based lymphoma vaccine. *Cancer Immunol Immunother* (2019) 68(11):1791–804. doi: 10.1007/s00262-019-02411-y

232. Vo M-C, Jung S-H, Chu T-H, Lee H-J, Lakshmi TJ, Park H-S, et al. Lenalidomide and programmed death-1 blockade synergistically enhances the effects of dendritic cell vaccination in a model of murine myeloma. *Front Immunol* (2018) 9:1370. doi: 10.3389/fimmu.2018.01370

233. Luptakova K, Glotzbecker B, Mills H, Stroopinsky D, Vasir B, Rosenblatt J, et al. Lenalidomide decreases PD-1 expression, depletes regulatory T-cells and improves cellular response to a multiple myeloma/dendritic cell fusion vaccine in vitro. *Blood* (2010) 116(21):492. doi: 10.1182/blood.V116.21.492.492

234. Giuliani M, Janji B, Berchem G. Activation of NK cells and disruption of PD-L1/PD-1 axis: two different ways for lenalidomide to block myeloma progression. *Oncotarget* (2017) 8(14):24031–44. doi: 10.18632/oncotarget.15234

235. Crespo J, Sun H, Welling TH, Tian Z, Zou W. T Cell anergy, exhaustion, senescence, and stemness in the tumor microenvironment. *Curr Opin Immunol* (2013) 25(2):214–21. doi: 10.1016/j.coi.2012.12.003

236. Reiser J, Banerjee A. Effector, memory, and dysfunctional CD8+ T cell fates in the antitumor immune response. *J Immunol Res* (2016) 2016:8941260. doi: 10.1155/2016/8941260

237. Nicholas NS, Apollonio B, Ramsay AG. Tumor microenvironment (TME)-driven immune suppression in b cell malignancy. *Biochim Biophys Acta (BBA) - Mol Cell Res* (2016) 1863(3):471–82. doi: 10.1016/j.bbamcr.2015.11.003

238. Kater AP, Tonino SH, Egle A, Ramsay AG. How does lenalidomide target the chronic lymphocytic leukemia microenvironment? *Blood* (2014) 124(14):2184–9. doi: 10.1182/blood-2014-05-578286

239. Quach H, Ritchie D, Stewart AK, Neeson P, Harrison S, Smyth MJ, et al. Mechanism of action of immunomodulatory drugs (IMiDS) in multiple myeloma. *Leukemia* (2010) 24(1):22–32. doi: 10.1038/leu.2009.236

240. LeBlanc R, Hideshima T, Catley LP, Shringarpure R, Burger R, Mitsiades N, et al. Immunomodulatory drug costimulates T cells *via* the B7-CD28 pathway. *Blood* (2004) 103(5):1787–90. doi: 10.1182/blood-2003-02-0361

241. Schafer PH, Gandhi AK, Loveland MA, Chen RS, Man H-W, Schnetkamp PP, et al. Enhancement of cytokine production and AP-1 transcriptional activity in T cells by thalidomide-related immunomodulatory drugs. *J Pharmacol Exp Ther* (2003) 305(3):1222–32. doi: 10.1124/jpet.102.048496

242. McDaniel JM, Pinilla-Ibarz J, Epling-Burnette P. Molecular action of lenalidomide in lymphocytes and hematologic malignancies. *Adv Hematol* (2012) 2012:513702. doi: 10.1155/2012/513702

243. Ramsay AG, Evans R, Kiaii S, Svensson L, Hogg N, Gribben JG. Chronic lymphocytic leukemia cells induce defective LFA-1-directed T-cell motility by altering rho GTPase signaling that is reversible with lenalidomide. *Blood* (2013) 121(14):2704–14. doi: 10.1182/blood-2012-08-448332

244. Fostier K, Caers J, Meuleman N, Broos K, Corthals J, Thielemans K, et al. Impact of lenalidomide maintenance on the immune environment of multiple myeloma patients with low tumor burden after autologous stem cell transplantation. *Oncotarget* (2018) 9(29):20476. doi: 10.18632/oncotarget.24944

245. Ioannou N, Hagner PR, Stokes M, Gandhi AK, Apollonio B, Fanous M, et al. Triggering interferon signaling in T cells with avadomide sensitizes CLL to anti-PD-L1/PD-1 immunotherapy. *Blood* (2021) 137(2):216–31. doi: 10.1182/blood.2020006073

246. Di Lullo G, Marcatti M, Heltai S, Tresoldi C, Paganoni AM, Bordignon C, et al. Immunomodulatory drugs in the context of autologous hematopoietic stem cell transplantation associate with reduced pro-tumor T cell subsets in multiple myeloma. *Front Immunol* (2019) 9:3171. doi: 10.3389/fimmu.2018.03171

247. Chung DJ, Pronschinske KB, Shyer JA, Sharma S, Leung S, Curran SA, et al. T-Cell exhaustion in multiple myeloma relapse after autotransplant: optimal timing of immunotherapy. *Cancer Immunol Res* (2016) 4(1):61–71. doi: 10.1158/2326-6066.CIR-15-0055

248. Eve HE, Carey S, Richardson SJ, Heise CC, Mamidipudi V, Shi T, et al. Single-agent lenalidomide in relapsed/refractory mantle cell lymphoma: results from a UK phase II study suggest activity and possible gender differences. *Br J Haematol* (2012) 159(2):154–63. doi: 10.1111/bjh.12008

249. Vivier E, Tomasello E, Baratin M, Walzer T, Ugolini S. Functions of natural killer cells. *Nat Immunol* (2008) 9(5):503–10. doi: 10.1038/ni1582

250. Weiner GJ. Rituximab: mechanism of action. seminars in hematology. *Semin Hematol* (2010) 47(2):115–23. doi: 10.1053/j.seminhematol.2010.01.011.

251. Vogler M, Shanmugalingam S, Särchen V, Reindl LM, Grèze V, Buchinger L, et al. Unleashing the power of NK cells in anticancer immunotherapy. *J Mol Med* (2022) 100(3):337–49. doi: 10.1007/s00109-021-02120-z

252. Chanan-Khan A, Miller KC, Musial L, Lawrence D, Padmanabhan S, Takeshita K, et al. Clinical efficacy of lenalidomide in patients with relapsed or refractory chronic lymphocytic leukemia: Results of a phase II study. *J Clin Oncol* (2006) 24(34):5343–9. doi: 10.1200/JCO.2005.05.0401

253. Payvandi F, Wu L, Naziruddin SD, Haley M, Parton A, Schafer PH, et al. Immunomodulatory drugs (IMiDs) increase the production of IL-2 from stimulated T cells by increasing PKC-θ activation and enhancing the DNA-binding activity of AP-1 but not NF-κB, OCT-1, or NF-AT. *J Interferon Cytokine Res* (2005) 25(10):604–16. doi: 10.1089/jir.2005.25.604

254. Gandhi AK, Mendy D, Parton A, Wu L, Kosek J, Zhang L-H, et al. CC-122 is a novel pleiotropic pathway modifier with potent in vitro immunomodulatory and anti-angiogenic properties and *in vivo* anti-tumor activity in hematological cancers. *Blood* (2012) 120(21):2963–. doi: 10.1182/blood.V120.21.2963.2963

255. Carpio C, Bouabdallah R, Ysebaert L, Sancho J-M, Salles G, Cordoba R, et al. Avadomide monotherapy in relapsed/refractory DLBCL: safety, efficacy, and a predictive gene classifier. *Blood* (2020) 135(13):996–1007. doi: 10.1182/blood.2019002395

256. Cubillos-Zapata C, Cordoba R, Avendaño-Ortiz J, Arribas-Jiménez C, Hernández-Jiménez E, Toledano V, et al. CC-122 immunomodulatory effects in refractory patients with diffuse large b-cell lymphoma. *Oncoimmunology* (2016) 5(12):e1231290. doi: 10.1080/2162402X.2016.1231290

257. Pan Y, Yu Y, Wang X, Zhang T. Tumor-associated macrophages in tumor immunity. *Front Immunol* (2020) 11:583084. doi: 10.3389/fimmu.2020.583084

258. Lin Y, Xu J, Lan H. Tumor-associated macrophages in tumor metastasis: biological roles and clinical therapeutic applications. *J Hematol Oncol* (2019) 12(1):76. doi: 10.1186/s13045-019-0760-3

259. Zhu S, Yi M, Wu Y, Dong B, Wu K. Roles of tumor-associated macrophages in tumor progression: implications on therapeutic strategies. *Exp Hematol Oncol* (2021) 10(1):1–17. doi: 10.1186/s40164-021-00252-z

260. Boutilier AJ, Elsawa SF. Macrophage polarization states in the tumor microenvironment. *Int J Mol Sci* (2021) 22(13):6995. doi: 10.3390/ijms22136995

261. Li C, Xu X, Wei S, Jiang P, Xue L, Wang J. Tumor-associated macrophages: potential therapeutic strategies and future prospects in cancer. *J Immunother Cancer* (2021) 9(1):e001341. doi: 10.1136/jitc-2020-001341

262. van de Donk N, Usmani SZ. CD38 antibodies in multiple myeloma: Mechanisms of action and modes of resistance. *Front Immunol* (2018) 9:2134. doi: 10.3389/fimmu.2018.02134

263. VanDerMeid KR, Elliott MR, Baran AM, Barr PM, Chu CC, Zent CS. Cellular cytotoxicity of next-generation CD20 monoclonal AntibodiesCellular cytotoxicity of CD20 monoclonal antibodies. *Cancer Immunol Res* (2018) 6(10):1150–60. doi: 10.1158/2326-6066.CIR-18-0319

264. Tobinai K, Klein C, Oya N, Fingerle-Rowson G. A review of obinutuzumab (GA101), a novel type II anti-CD20 monoclonal antibody, for the treatment of

patients with b-cell malignancies. *Adv Ther* (2017) 34(2):324–56. doi: 10.1007/s12325-016-0451-1

265. Wang Y, Xiang Y, Xin VW, Wang X-W, Peng X-C, Liu X-Q, et al. Dendritic cell biology and its role in tumor immunotherapy. *J Hematol Oncol* (2020) 13(1):107. doi: 10.1186/s13045-020-00939-6

266. Patente TA, Pinho MP, Oliveira AA, Evangelista GC, Bergami-Santos PC, Barbuto JA. Human dendritic cells: their heterogeneity and clinical application potential in cancer immunotherapy. *Front Immunol* (2019) 9:3176. doi: 10.3389/fimmu.2018.03176

267. Phan V, Ito T, Inaba M, Azuma Y, Kibata K, Inagaki-Katashiba N, et al. Immunomodulatory drugs suppress Th1-inducing ability of dendritic cells but enhance Th2-mediated allergic responses. *Blood Adv* (2020) 4(15):3572–85. doi: 10.1182/bloodadvances.2019001410

268. Maiso P, Mogollón P, Ocio EM, Garayoa M. Bone marrow mesenchymal stromal cells in multiple myeloma: Their role as active contributors to myeloma progression. *Cancers* (2021) 13(11):2542. doi: 10.3390/cancers13112542

269. Chang X, Zhu Y, Shi C, Stewart AK. Mechanism of immunomodulatory drugs' action in the treatment of multiple myeloma. *Acta Biochim Biophys Sinica* (2014) 46(3):240–53. doi: 10.1093/abbs/gmt142

270. Zhang L, Yang J, Qian J, Li H, Romaguera JE, Kwak LW, et al. Role of the microenvironment in mantle cell lymphoma: IL-6 is an important survival factor for the tumor cells. *Blood* (2012) 120(18):3783–92. doi: 10.1182/blood-2012-04-424630

271. Wobus M, Benath G, Ferrer RA, Wehner R, Schmitz M, Hofbauer LC, et al. Impact of lenalidomide on the functional properties of human mesenchymal stromal cells. *Exp Hematol* (2012) 40(10):867–76. doi: 10.1016/j.exphem.2012.06.004

272. Ribatti D, Vacca A. New insights in anti-angiogenesis in multiple myeloma. *Int J Mol Sci* (2018) 19(7):2031. doi: 10.3390/ijms19072031

273. Menzel L, Höpken UE, Rehm A. Angiogenesis in lymph nodes is a critical regulator of immune response and lymphoma growth. *Front Immunol* (2020) 11:591741. doi: 10.3389/fimmu.2020.591741

274. Raza S, Safyan RA, Lentzsch S. Immunomodulatory drugs (IMiDs) in multiple myeloma. *Curr Cancer Drug Targets* (2017) 17(9):846–57. doi: 10.2174/1568009617666170214104426

275. Mercurio A, Adriani G, Catalano A, Carocci A, Rao L, Lentini G, et al. A mini-review on thalidomide: Chemistry, mechanisms of action, therapeutic potential and anti-angiogenic properties in multiple myeloma. *Curr Medicinal Chem* (2017) 24(25):2736–44. doi: 10.2174/0929867324666170601074646

276. Dredge K, Horsfall R, Robinson SP, Zhang L-H, Lu L, Tang Y, et al. Orally administered lenalidomide (CC-5013) is anti-angiogenic *in vivo* and inhibits endothelial cell migration and akt phosphorylation in vitro. *Microvasc Res* (2005) 69(1):56–63. doi: 10.1016/j.mvr.2005.01.002

277. Maffei R, Fiorcari S, Bulgarelli J, Rizzotto L, Martinelli S, Rigolin GM, et al. Endothelium-mediated survival of leukemic cells and angiogenesis-related factors are affected by lenalidomide treatment in chronic lymphocytic leukemia. *Exp Hematol* (2014) 42(2):126–36.e1. doi: 10.1016/j.exphem.2013.10.007

278. Pierpont TM, Limper CB, Richards KL. Past, present, and future of rituximab-the world's first oncology monoclonal antibody therapy. *Front Oncol* (2018) 8:163. doi: 10.3389/fonc.2018.00163

279. Delfau-Larue MH, Boulland ML, Beldi-Ferchiou A, Feugier P, Maisonneuve H, Casasnovas RO, et al. Lenalidomide/rituximab induces high molecular response in untreated follicular lymphoma: LYSA ancillary RELEVANCE study. *Blood Adv* (2020) 4(14):3217–23. doi: 10.1182/bloodadvances.2020001955

280. Becnel MR, Nastoupil LJ, Samaniego F, Davis RE, You MJ, Green M, et al. Lenalidomide plus rituximab (R(2)) in previously untreated marginal zone lymphoma: subgroup analysis and long-term follow-up of an open-label phase 2 trial. *Br J Haematol* (2019) 185(5):874–82. doi: 10.1111/bjh.15843

281. Bachy E, Houot R, Feugier P, Bouabdallah K, Bouabdallah R, Virelizier EN, et al. Obinutuzumab plus lenalidomide in advanced, previously untreated follicular lymphoma in need of systemic therapy: a LYSA study. *Blood* (2022) 139(15):2338–46. doi: 10.1182/blood.2021013526

282. Vitale C, Falchi L, Ten Hacken E, Gao H, Shaim H, Van Roosbroeck K, et al. Ofatumumab and lenalidomide for patients with relapsed or refractory chronic lymphocytic leukemia: Correlation between responses and immune characteristics. *Clin Cancer Research: an Off J Am Assoc Cancer Res* (2016) 22 (10):2359–67. doi: 10.1158/1078-0432.CCR-15-2476

283. Dimopoulos MA, San-Miguel J, Belch A, White D, Benboubker L, Cook G, et al. Daratumumab plus lenalidomide and dexamethasone versus lenalidomide and dexamethasone in relapsed or refractory multiple myeloma: updated analysis of POLLUX. *Haematologica* (2018) 103(12):2088–96. doi: 10.3324/haematol.2018.194282

284. Haas C, Krinner E, Brischwein K, Hoffmann P, Lutterbüse R, Schlereth B, et al. Mode of cytotoxic action of T cell-engaging BiTE antibody MT110. *Immunobiology* (2009) 214(6):441–53. doi: 10.1016/j.imbio.2008.11.014

285. Pishko A, Nasta SD. The role of novel immunotherapies in non-Hodgkin lymphoma. *Trans Cancer Res* (2017) 6(1):93–103. doi: 10.21037/tcr.2017.01.08

286. Goebeler M-E, Bargou RC. T Cell-engaging therapies — BiTEs and beyond. *Nat Rev Clin Oncol* (2020) 17(7):418–34. doi: 10.1038/s41571-020-0347-5

287. Hatic H, Sampat D, Goyal G. Immune checkpoint inhibitors in lymphoma: challenges and opportunities. *Ann Trans Med* (2021) 9(12):1037. doi: 10.21037/atm-20-6833

288. Salik B, Smyth MJ, Nakamura K. Targeting immune checkpoints in hematological malignancies. *J Hematol Oncol* (2020) 13(1):1–19. doi: 10.1186/s13045-020-00947-6

289. Nagasaki J, Togashi Y. A variety of 'exhausted' T cells in the tumor microenvironment. *Int Immunol* (2022) dxac013. Online ahead of print. doi: 10.1093/intimm/dxac013

290. Ansell SM, Lin Y. Immunotherapy of lymphomas. *J Clin Invest* (2020) 130 (4):1576–85. doi: 10.1172/JCI129206

291. Görgün G, Samur MK, Cowens KB, Paula S, Bianchi G, Anderson JE, et al. Lenalidomide enhances immune checkpoint blockade-induced immune response in multiple myeloma. *Clin Cancer Research: an Off J Am Assoc Cancer Res* (2015) 21 (20):4607–18. doi: 10.1158/1078-0432.CCR-15-0200

292. Badros AZ, Kocoglu MH, Ma N, Rapoport AP, Lederer E, Philip S, et al. A phase II study of anti PD-1 antibody pembrolizumab, pomalidomide and dexamethasone in patients with Relapsed/Refractory multiple myeloma (RRMM). *Blood* (2015) 126(23):506. doi: 10.1182/blood.V126.23.506.506

293. San Miguel J, Mateos M-V, Shah JJ, Ocio EM, Rodriguez-Otero P, Reece D, et al. Pembrolizumab in combination with lenalidomide and low-dose dexamethasone for Relapsed/Refractory multiple myeloma (RRMM): Keynote-023. *Blood* (2015) 126(23):505–. doi: 10.1182/blood.V126.23.505.505

294. Mateos MV, Orlowski RZ, Ocio EM, Rodríguez-Otero P, Reece D, Moreau P, et al. Pembrolizumab combined with lenalidomide and low-dose dexamethasone for relapsed or refractory multiple myeloma: phase I KEYNOTE-023 study. *Br J Haematol* (2019) 186(5):e117–e21. doi: 10.1111/bjh.15946

295. Mateos MV, Blacklock H, Schjesvold F, Oriol A, Simpson D, George A, et al. Pembrolizumab plus pomalidomide and dexamethasone for patients with relapsed or refractory multiple myeloma (KEYNOTE-183): a randomised, open-label, phase 3 trial. *Lancet Haematol* (2019) 6(9):e459–e69. doi: 10.1016/S2352-3026(19)30110-3

296. Usmani SZ, Schjesvold F, Oriol A, Karlin L, Cavo M, Rifkin RM, et al. Pembrolizumab plus lenalidomide and dexamethasone for patients with treatment-naive multiple myeloma (KEYNOTE-185): a randomised, open-label, phase 3 trial. *Lancet Haematol* (2019) 6(9):e448–e58. doi: 10.1016/S2352-3026(19)30109-7

297. Shah NN, Fry TJ. Mechanisms of resistance to CAR T cell therapy. *Nat Rev Clin Oncol* (2019) 16(6):372–85. doi: 10.1038/s41571-019-0184-6

298. Gumber D, Wang LD. Improving CAR-T immunotherapy: Overcoming the challenges of T cell exhaustion. *EBioMedicine* (2022) 77:103941. doi: 10.1016/j.ebiom.2022.103941

299. Neelapu SS. Managing the toxicities of car T-cell therapy. *Hematol Oncol* (2019) 37:48–52. doi: 10.1002/hon.2595

300. Pan B, Lentzsch S. The application and biology of immunomodulatory drugs (IMiDs) in cancer. *Pharmacol Ther* (2012) 136(1):56–68. doi: 10.1016/j.pharmthera.2012.07.004

301. Thieblemont C, Chevret S, Allain V, Di Blasi R, Morin F, Vercellino L, et al. Lenalidomide enhance CAR T-cells response in patients with Refractory/Relapsed Large b cell lymphoma experiencing progression after infusion. *Blood* (2020) 136:16–7. doi: 10.1182/blood-2020-136279

302. Neelapu SS, Kharfan-Dabaja MA, Oluwole OO, Krish P, Reshef R, Riedell PA, et al. A phase 2, open-label, multicenter study evaluating the safety and efficacy of axicabtagene ciloleucel in combination with either rituximab or lenalidomide in patients with refractory Large b-cell lymphoma (ZUMA-14). *Blood* (2019) 134:4093. doi: 10.1182/blood-2019-126369

303. Lemoine J, Morin F, Di Blasi R, Vercellino L, Cuffel A, Benlachgar N, et al. Lenalidomide exposure at time of CAR T-cells expansion enhances response of Refractory/Relapsed aggressive Large b-cell lymphomas. *Blood* (2021) 138:1433. doi: 10.1182/blood-2021-151109

304. Zhao G, Wei R, Feng L, Wu Y, He F, Xiao M, et al. Lenalidomide enhances the efficacy of anti-BCMA CAR-T treatment in relapsed/refractory multiple myeloma: A case report and revies of the literature. *Cancer Immunol Immunother* (2022) 71(1):39–44. doi: 10.1007/s00262-021-02959-8

305. Suzuki K, Nishiwaki K, Yano S. Treatment strategy for multiple myeloma to improve immunological environment and maintain MRD negativity. *Cancers* (2021) 13(19):4867. doi: 10.3390/cancers13194867

306. Nowakowski GS, Hong F, Scott DW, Macon WR, King RL, Habermann TM, et al. Addition of lenalidomide to r-CHOP improves outcomes in newly diagnosed diffuse Large b-cell lymphoma in a randomized phase II US intergroup

study ECOG-ACRIN E1412. *J Clin Oncol: Off J Am Soc Clin Oncol* (2021) 39 (12):1329–38. doi: 10.1200/JCO.20.01375

307. Li L, Xue W, Shen Z, Liu J, Hu M, Cheng Z, et al. A cereblon modulator CC-885 induces CRBN- and p97-dependent PLK1 degradation and synergizes with volasertib to suppress lung cancer. *Mol Ther - Oncolytics* (2020) 18:215–25. doi: 10.1016/j.omto.2020.06.013

308. Bastea LI, Liou GY, Pandey V, Fleming AK, von Roemeling CA, Doeppler H, et al. Pomalidomide alters pancreatic macrophage populations to generate an immune-responsive environment at precancerous and cancerous lesions. *Cancer Res* (2019) 79(7):1535–48. doi: 10.1158/0008-5472.CAN-18-1153

309. Brosseau C, Colston K, Dalgleish AG, Galustian C. The immunomodulatory drug lenalidomide restores a vitamin d sensitive phenotype to the vitamin d resistant breast cancer cell line MDA-MB-231 through inhibition of BCL-2: potential for breast cancer therapeutics. *Apoptosis* (2012) 17(2):164–73. doi: 10.1007/s10495-011-0670-5

310. Dahut WL, Aragon-Ching JB, Woo S, Tohnya TM, Gulley JL, Arlen PM, et al. Phase I study of oral lenalidomide in patients with refractory metastatic cancer. *J Clin Pharmacol* (2009) 49(6):650–60. doi: 10.1177/0091270009335001

311. Semeraro M, Vacchelli E, Eggermont A, Galon J, Zitvogel L, Kroemer G, et al. Trial watch: Lenalidomide-based immunochemotherapy. *Oncoimmunology* (2013) 2(11):e26494. doi: 10.4161/onci.26494

312. Barrio S, Munawar U, Zhu YX, Giesen N, Shi C-X, Da Viá M, et al. IKZF1/3 and CRL4CRBN E3 ubiquitin ligase mutations and resistance to immunomodulatory drugs in multiple myeloma. *Haematologica* (2020) 105(5): e237. doi: 10.3324/haematol.2019.217943

313. Zuo X, Liu D. Mechanism of immunomodulatory drug resistance and novel therapeutic strategies in multiple myeloma. *Hematology* (2022) 27(1):1110–21. doi: 10.1080/16078454.2022.2124694

frontiers | Frontiers in Immunology

TYPE Original Research
PUBLISHED 22 November 2022
DOI 10.3389/fimmu.2022.1046121

OPEN ACCESS

EDITED BY
Andrey Zamyatnin,
I.M. Sechenov First Moscow State Medical University, Russia

REVIEWED BY
Aimin Jiang,
The First Affiliated Hospital of Xi'an Jiaotong University, China
Ming Yi,
Zhejiang University, China

*CORRESPONDENCE
Li Zhang
343918320@qq.com
Zheng Gong
xblong2000@gmail.com

†These authors share first authorship

‡These authors have contributed equally to this work

SPECIALTY SECTION
This article was submitted to Cancer Immunity and Immunotherapy, a section of the journal Frontiers in Immunology

RECEIVED 16 September 2022
ACCEPTED 04 November 2022
PUBLISHED 22 November 2022

CITATION
Fan T, Lu J, Niu D, Zhang Y, Wang B, Zhang B, Zhang Z, He X, Peng N, Li B, Fang H, Gong Z and Zhang L (2022) Immune and non-immune cell subtypes identify novel targets for prognostic and therapeutic strategy: A study based on intratumoral heterogenicity analysis of multicenter scRNA-seq datasets in lung adenocarcinoma.
Front. Immunol. 13:1046121.
doi: 10.3389/fimmu.2022.1046121

Immune and non-immune cell subtypes identify novel targets for prognostic and therapeutic strategy: A study based on intratumoral heterogenicity analysis of multicenter scRNA-seq datasets in lung adenocarcinoma

Tianyu Fan[1†], Jian Lu[2†], Delei Niu[3], Yue Zhang[1], Bin Wang[3], Bei Zhang[1], Zugui Zhang[4], Xinjiai He[5], Nan Peng[6], Biao Li[6], Huilong Fang[6], Zheng Gong[7,8*‡] and Li Zhang[1*‡]

[1]The Department of Immunology, College of Basic Medicine, Qingdao University, Qingdao, Shandong, China, [2]Department of Orthopaedics, Suzhou Science and Technology Town Hospital, Suzhou, Jiangsu, China, [3]The Department of Pathogenic Biology, College of Basic Medicine, Qingdao University, Qingdao, Shandong, China, [4]Value Institute, Christiana Care Health System, Newark, DE, United States, [5]Department of Radiation Oncology, The Affiliated Hospital of Qingdao University, Qingdao, Shandong, China, [6]Department of Pathogenic Biology and Immunology, Xiangnan University, Chenzhou, Hunan, China, [7]Sino-Cell Biomed Institutes of Medical Cell and Pharmaceutical Proteins, Qingdao University, Qingdao, Shandong, China, [8]Department of Basic Medicine, Xiangnan University, Chenzhou, Hunan, China

Lung adenocarcinoma (LUAD) is the most common type of lung cancer and the leading cause of cancer incidence and mortality worldwide. Despite the improvement of traditional and immunological therapies, the clinical outcome of LUAD is still far from satisfactory. Patients given the same treatment regimen had different responses and clinical outcomes due to the heterogeneity of LUAD. How to identify the targets based on heterogeneity analysis is crucial for treatment strategies. Recently, the single-cell RNA-sequencing (scRNA-seq) technology has been used to investigate the tumor microenvironment (TME) based on cell-specific changes and shows prominently valuable for biomarker prediction. In this study, we systematically analyzed a meta-dataset from the multiple LUAD scRNA-seq datasets in LUAD, identified 15 main types of cells and 57 cell subgroups, and revealed a series of potential biomarkers in M2b, exhausted $CD8^+$T, endothelial cells, fibroblast, and metabolic patterns in TME, which further validated with immunofluorescence in clinical cohorts of LUAD. In the prognosis analysis, M0 macrophage and T cell activation were shown correlated to a better prognosis ($p<0.05$). Briefly, our study provided insights into the heterogeneity of LUAD and assisted in novel therapeutic strategies for clinical outcome improvement.

KEYWORDS

lung adenocarcinoma (LUAD), TCGA, scRNA-seq, immunotherapy, microenvironment

Introduction

Lung cancer is the leading cause of cancer death globally, and the most prevalent subtype of lung cancer is lung adenocarcinoma (LUAD) (1). Despite the great endeavors in traditional and complementary treatments, the clinical outcomes are still not satisfactory (2, 3). The process of oncogenesis and cancer development is influenced by the tumor microenvironment (TME) and the tumor cells through mutual and dynamic crosstalk. The TME is consisted of immune cells (like lymphocytes, macrophages, and microglia), tumor stromal cells (including stromal fibroblasts and endothelial cells), the non-cellular components of the extracellular matrix, and the tumor cells (4, 5). And a growing number of therapeutic strategies were focused on TME, such as cancer-associated fibroblasts (CAFs), tumor-associated macrophages (TAMs), and CTLA-4/PD-1/PD-L1 immune checkpoints (6–8). Due to the heterogeneity of LUAD, patients given the same treatment regimen had different responses and clinical outcomes. Therefore, the identification of targets based on intratumoral heterogenicity analysis is extremely crucial for novel and precise therapeutic strategies in LUAD.

The TME was so complex that essential to study further for clinical outcome improvement in LUAD (5, 9). RNA sequencing (RNA-seq) had already been independently made to predict the prognosis-related genes and assessment their correlation with clinical outcomes in TME. Reports showed immune subtypes in LUAD TME with prognostic and therapeutic implications (10). Currently, single-cell RNA sequencing (scRNA-seq) is widely used to identify biomarkers in diagnosing, treating patients, and studying the heterogeneity in TME. Intratumoral heterogeneity could be analyzed by scRNA-seq at the cell-type level; in contrast, the conventional bulk RNA-seq obtained the average expression of genes, and difficult to study the heterogeneity in TME. And due to the cancer heterogeneity, patients' response is different significantly to certain treatment. Recently the heterogeneity of stromal cells and tumor-infiltrating immune cells associated with immunotherapy responses had been widely reported (11). The knowledge about the mechanism responsible for the LUAD heterogeneity was still poor, even if many scientists were devoted to elucidating these issues. To date, although numerous scRNA-seq studies on LUAD had been reported, most of these studies were limited by small sample sizes and imperfect controls. In this study, we constructed a meta-dataset from multiple scRNA-seq datasets (GSE131907, GSE134355, and GSE148071) and analyzed the immune and non-immune diversity clusters in TME, dug out targets for treatment, and assessed their prognostic value in LUAD. Briefly, our study systemically provided insights into the heterogeneity of LUAD and assisted in precise and novel strategies for prognosis and target treatments.

Materials and methods

Acquisition of data

The expression matrix and patients' clinical information from three datasets (GSE134355, GSE131907, and GSE148071), which contained 19 normal and 53 LUAD samples, were downloaded from the GEO database (https://www.ncbi.nlm.nih.gov/geo/). The GSE134355 dataset was generated from Illumina HiSeq X Ten and GPL20795 platform. The GSE131907 dataset was generated from Illumina HiSeq 2500 and GPL16791 platform. The GSE148071 dataset was generated from Illumina HiSeq X Ten and GPL20795 platform.

QC and cell type recognition

Using Seurat (version 4.2.0) performed the QC process (12). We excluded cells with a mitochondrion-derived UMI count of more than 10% or less than 200 UMIs as low-quality cells. ScaleData was used to remove the influence of UMI counts and mitochondrion-derived UMI counts. The quality control (QC) process used the Seurat R package. The QC parameter setup and candidate cells filter by the following criteria: nFeatue_RNA>200 & <7000 percent.mt<25. We also used the VlnPlot function of the Seurat package to generate the QC figure (Figure S1A) and show the value (nFeaure_RNA, nCount_RNA, mito_RNA, and ribo_RNA) after QC. The Harmony R package was used to correct batch effects (Figure S1A down). The next step was using Seurat's FindClusters function (resolution = 1.1) to identify the main cell clusters and utilizing 2D tSNE or UMAP to visualize (13). Currently, for data dimension reduction, these algorithms were most commonly used. The downstream analysis did not perform on the primary cell cluster due to the difference in the cell cycle. Each cell cluster's markers were listed using the FindAllMarkers function. Based on the CellMarker database, the major cell types were identified and annotated (14).

Immune checkpoint gene analysis

To represent the gene expression levels in different cell clusters, we calculated the mean normalized immune checkpoint gene expression levels from cell clusters and then normalized them into row Z scores. The immune checkpoint gene heatmap analyses were performed using the ComplexHeatmap R package. We used the ComplexHeatmap:: pheatmap function and set-up parameters: scale = "row" to calculate the Z-score of genes mRNA expression level, then the heatmap was colored according to this Z-score.

Core transcription factors regulatory network analysis

The core regulatory transcription factors and their regulatory network were predicted using the R package SCENIC. The R software (version 4.0.2) was used to reconstruct the regulatory networks and display the transcriptional characterization (15). The value of the area under the curve (AUC) was estimated by SCENIC, then the Limma was used to identify differences in AUC among cell clusters or between normal and tumor-derived cells of each module. Regulators were investigated further through the adj. p val< 0.01.

Pseudotime trajectory analysis

We used Monocle 2 for single-cell trajectories analysis, an R package developed by Qiu et al. (16). We revealed the alteration of the $CD8^+$ T cell during tumor-educating. We optimized the input parameters as following: mean expression ≥ 0.125, num_cells_expressed ≥10, and in the differentialGeneTest function $q$val < 0.01 was considered as significant. 2D tSNE plots were used to visualize the trajectories and plot_pseudotime_heatmap was used for constructing the dynamic expression heatmaps.

InferCNV

The InferCNV R package was used for CNV analysis. Through InferCNV, you could visualize CNV in cells according to RNA-Seq expression data. Genes were analyzed, including their relative expression levels and chromosomal locations to estimate CNVs (17, 18). Cell types were initially classified by using the Seurat package. CNV was calculated for all euchromosome types using InferCNV. For 10× Genomics single-cell data, the cut-off value was 0.1.

Functional enrichment analysis

The FindMarkers function of Seurat was used to identify DEGs. The cut-off thresholds were adj. p value <0.01 and fold change (FC) >1.5. Then, GO enrichment analysis was carried out using clusterProfiler (19) on these DEGs. An enrichment adj. p val <0.05 was considered statistically significant.

Gene set was enrichment in each specific cell cluster and was performed by GSEA analysis. Only gene sets were significantly enriched with false discovery rate (FDR) p values <0.05 and nominal p values <0.05.

The GSVA package was adopted for performing gene set variation analysis (GSVA) and using default configuration parameters. The cytokine pathway gene sets or 50 hallmark gene sets were downloaded from the GSEA molecular signature database.

Cell-cell communication analysis

The CellChat R package provided a means for analyzing cell-to-cell communication at the molecular level through R software. First, 16 types were clustered from 24,550 single cells as described above. Analysis of 16 subclusters and major cell types was carried out using CellChat to examine molecular interaction networks. The CellChat estimated the ligand-receptor pairs. And the result with p values <0.05 would be retained for evaluating the cluster-by-cluster analysis.

Correlation to public datasets

The deconvolution analysis was performed on the integrated bulk RNA-seq data (TCGA-LUAD) against our scRNA-seq dataset, which was conducted using the BisqueRNA package with default settings (20). We labeled our cells into 15 categories, including macrophages, B cells, NK cells, DC cells, fibroblasts, $CD8^+$ T cells, $CD4^+$ T cells, epithelial cells, endothelial cells, Mast cells, smooth muscle cells, neutrophils, plasma cells, and myeloid. The group comparisons were then made using the composition of deconvolution cell types in each bulk sample. The Cox regression analysis to assess the prognostic value of different cell clusters. Visualization of Cox regression results was achieved using Z scores. To determine if the relative abundance of cell clusters' dynamical alteration was associated with the LUAD progression (WHO clinical stage).

Immunofluorescence assay on human LUAD tissue

Sections of tissue containing 25 pairs of para-tumors and tumors were obtained from the Affiliated Hospital of Qingdao University (NO: QDU-HEC-2022227). Patient information was listed in Figure S2. The immunofluorescence was performed on the same type of tissue sections for the analysis to be consistent.

The antibodies were applied to validate the specific markers were identified in this study as follows: anti-FGFBP2 (R&D system, catalog. AF9349-SP), anti-PRF1(abclone, catalog. A0093; RRID: AB-2749981), anti-CD163 (abclone, catalog. A8383; RRID: AB-10687227), anti-ATP5F1E (abclone, catalog. A7645; RRID: AB-2768505), RRID: AB-853002), anti-LAG3

(Abcam, catalog. 209236; RRID: AB-2162568), anti-CLDN4 (Abcam, catalog. ab53156), anti-CLDN1 (Abcam, catalog. ab211737), anti-ACTA2 (Abcam, catalog. ab264014), anti-RALA (Abcam, catalog. ab236314). Data analysis was performed with GraphPad Prism (version 9) software.

Flow cytometry

We mechanically separated and enzymatically digested the collected tumor tissue to prepare a single-cell suspension (collagenase (Solarbio), DNase I (Solarbio), and Dispase I (Solarbio); prepared in DMEM) at 37°C for 1 h. Filter with a 40 μm cell strainer. The lymphocytes are then isolated with a tumor-infiltrating lymphocyte isolation solution kit. The isolated cells are washed once with PBS at 4°C and stained with antibodies from 3 different channels for 1 h. The antibodies were applied as follows: anti-CD8 (Abcam, catalog. 233300; anti-TIM3(Abcam, catalog. ab28522), anti-PD 1 (Abcam, catalog. ab52587). Data analysis was performed with FlowJo (version 10) software.

Statistical analysis

Our analysis was conducted using the R software and package, Spearman correlation analysis was performed, and heatmaps and scatterplots were generated as a result. We also used the online tool GEPIA, which analyzes pan-cancer tissue-specific expression. The immunofluorescence results were statistically analyzed by ImageJ software and the flow cytometry results were statistically analyzed by CytExpert software. It was considered statistically significant if $p < 0.05$.

Results

The LUAD cell types and normal lung tissues

Three GEO datasets (GSE134355, GSE131907, GSE148071) were involved in this study. Of these, the dataset (GSE134355) originated from normal lung tissues, the dataset (GSE148071) was tumor-derived cells, and the dataset (GSE131907) originated from both normal and tumor-derived cells (Figure 1A). A total of 15 main cell types were identified in these cells (Figure 1B). Eleven major immune cell types ($CD45^+$) were identified, containing $CD4^+$ T cell, $CD8^+$ T cell, natural killer (NK) cell, B cell, regulatory T cell (Tregs), dendritic cell (DCs), plasma, myeloid, macrophages mast cell, and neutrophil, as well as the four non-immune cell types ($CD45^-$), including epithelial, smooth muscle cells, fibroblasts, and endothelial cells (Figures 1B, C). Furthermore, the known markers mentioned in the CellMarker database were also investigated (Figure S1B). The differences in the cell cycle stages at the level of the single cells were not analyzed in the downstream analysis (Figure S2A). A bubble chart was created to visualize the top five cell-type markers (Figure 1D). We performed an irGSEA analysis in Figure S2F, in this figure, we demonstrated the situation of the top 50 signaling pathways in different cell clusters.

These major cell types were divided into two subclusters (immune and non-immune cells) to further identify their cell subclusters (Figures S2B, C). In total, 57 different cell clusters were identified, including 41 clusters of immune cells and 16 clusters of non-immune cells in the TME of LUAD. Several points were worth noting in Figure 1D. First, tumor tissues had high levels of $CD4^+FOXP3^+$ Treg cells. Second, $CD8^+$ T (C3) cells were tumor-specific. Additionally, epithelial enriched in several different cell clusters and mainly existed in LUAD tissues (Figures 1A, B, E).

In the comparison of differentially expressed genes (DEGs) between LUAD and normal tissues, three genes (FGFBP2, CRIP1, and PRF1) were mainly expressed in normal tissues but not in tumor-derived cells (Figure 1F). For verification, we conducted immunofluorescence at the protein level (Figure 1F). The results highlighted the upregulation of FGFBP2, CRIP1, and PRF1 for potential clinical application in LUAD.

M2b polarization in the TME of LUAD

We investigated the interaction network among the 214799 cells in the TME of LUAD. To estimate potential ligand-receptor pairs, we adopted the CellChat R package to analyze and visualize cell-cell communication molecules in normal or tumor-derived tissues. Notably, the interaction pairs between macrophages and other cells were significant revealing the macrophages with critical regulatory function in the TME (Figure 2A).

To investigate the heterogeneity of macrophages, we divided 45760 macrophages into four subclusters (Figure 2B). The cluster 1 (C1) and cluster 4 (C4) cells were mainly derived from normal tissue, while cluster 2 (C2) and cluster 3 (C3) were mainly derived from tumor tissue (Figure S3A). TMEs in LUAD were examined for immune checkpoint distribution. Figure 2C showed that the C1 cells expressed a relatively higher CD274 (PD-L1) and PDCD1LG2 (PD-L2) than other clusters. These molecules might bind to PD-1 and inhibit $CD8^+$ T cell activity. Moreover, a major LAG3 ligand, FGL1 (21), was major expressed in C2 macrophages. Since C1 and C2 macrophages were more immunosuppressive than others, the cytotoxic T lymphocyte (CTL) function could be suppressed. Next, we found that cells from C1 ($CD68^+CD163^+FABP4^+$) enriched in the TGF-β pathway from Figure S3D, which was characteristic of the M2a cluster. To determine whether FABP4 was associated with M2-like TAMs, we performed the spearman correlation analysis between

10.3389/fimmu.2022.1046121

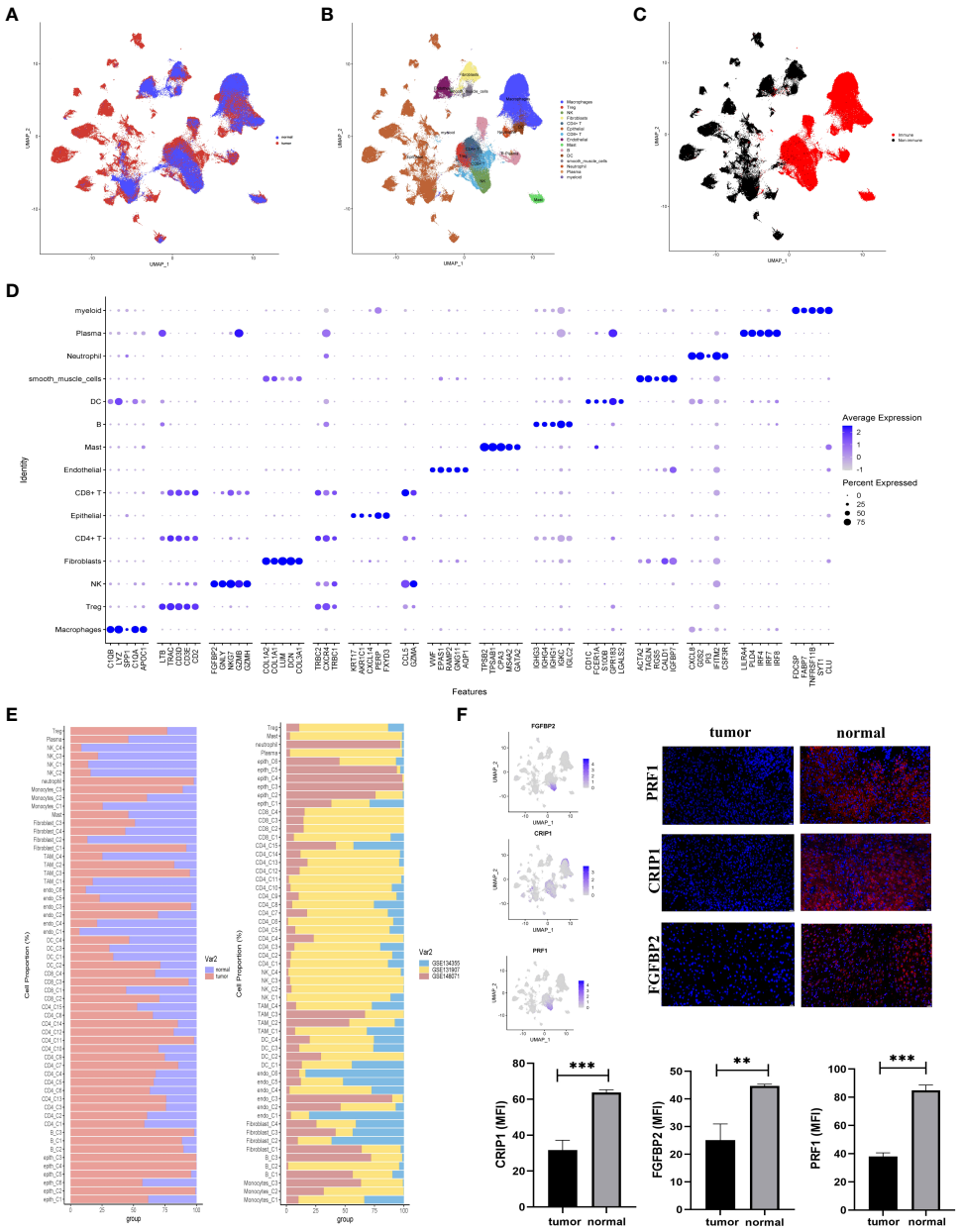

FIGURE 1
Comprehensive scRNA-seq analyses of cells derived from LUAD or normal tissues. **(A–C)** UMAP plot of single-cell transcriptome data with cells colored based on **(A)** tissue type origin (normal or tumor), **(B)** 15 major cell types, and **(C)** the immune cells or the non-immune cells. **(D)** The dot plot showed the top five markers of 15 major cell types. **(E)** The 57 subsets were identified in this study: the relative proportion of cells derived from the normal or tumor specimens (left); and the relative proportion of cells derived from each of the three different datasets (right). **(F)** The expression status of three normal-specific proteins, immunofluorescence and statistical analysis of RPF1, CRIP1, and FGFBP2 in tissue sections. The scale bar represented 20 μm, **p<0.01, ***p<0.001.

FABP4 and other identified markers; all spearman correlation coefficients were higher than 0.3 (Figure S3C). In Figure 2D, the cells from C2 exhibited the $CD68^{+}CD163^{+}ATP5F1E^{+}$ $MMP12^{-}$ phenotype and demonstrated a high IL-10 pathway and low IL-12 pathway. The gene set variation analysis (GSVA) exhibited that the Th2-related inflammation pathways were enriched from C2 (Figure 2E), which were the M2b-like TAMs hallmarks, as depicted according to an earlier study (22). These results indicated that the C2 cells have an M2b-like TAMs phenotype (Figure S3D). In recent studies, a high level of expression of TAM markers was also observed in C2 cells (Figure 2F). To determine the presence of C2 cells, we did immunofluorescence and the

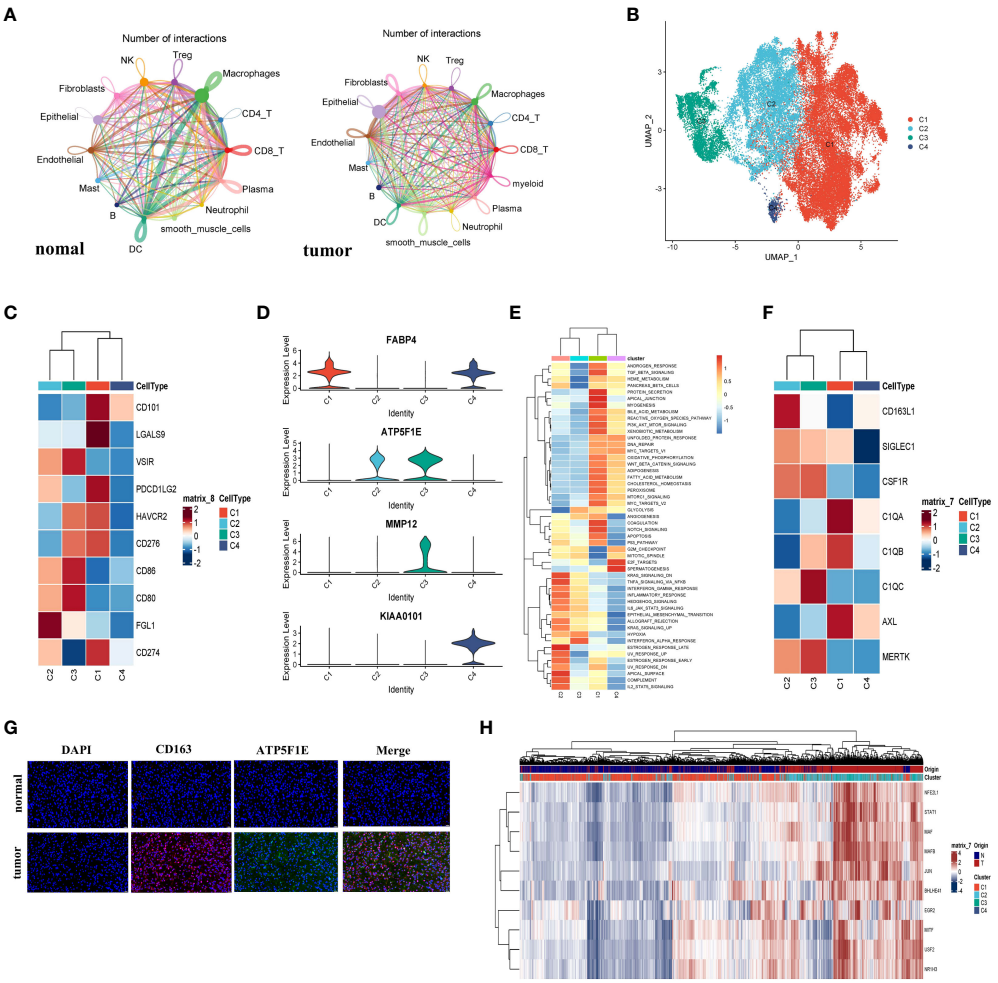

FIGURE 2
The macrophage cells demonstrated M2b polarization in LUAD. **(A)** The cell interaction network generated by CellChat; normal and tumor (left to right); the nodes size and color represented the counts of interaction; the larger size and brighter color correspond to more frequent interactions for different cell types. **(B)** The UMAP plot showed all four types of macrophage cells. **(C)** The heatmap showed the expression level of the immune checkpoint gene on macrophages and represented by a row Z score. **(D)** Violin plots of marker genes for four subgroups. **(E)** The Heatmap demonstrated the expression of the famous M2-like TAM markers. The expression level of the cell cluster was represented by a row Z score. **(F)** Immunofluorescence staining analyzed the expression of CD163 and ATP5F1E in LUAD or normal specimens. The CD163+ ATP5F1E+ macrophages exclusively appeared in tumor specimens. The scale bar represented 20μm. **(G)** The heatmap showed the differences in the activities of 50 hallmark pathways using GSVA. **(H)** The heatmap showed the differences in expression regulation by transcription factors, and the AUC scores were estimated by SCENIC.

result showed that the $CD163^{+}TATP5F1E^{+}$ macrophages were mainly enriched in LUAD tissue (Figure 2G). The ATP5F1E and MMP12 genes involved in the energy metabolism pathway were specifically expressed in the C3 cells (Figure 2D). The GSVA showed that the C3 cells could play a pro-inflammatory and antitumor role in LUAD (Figure 2H). This result revealed that the C3 cells tend to have an M1-like phenotype. The macrophages from C4 showed that KIAA0101 and FABP4 were preferentially upregulated (Figure 2D and Figure S3B). Combining the GSVA analysis and the above results, we inferred that C4 tended to have an M0-like TAMs phenotype. We also performed Psuedotime analysis of the macrophage cluster, and the results showed a population of M2b cells enrichment at a terminal branch of tumor tissue. Taken together, M2b (C2) and M1 (C3) were the main subgroups of macrophages in the TME in LUAD.

The SCENIC analysis demonstrated that the activity of transcription factors including STAT1, NFEIL1, MAF, MAFB, JUN, BHLHE41, EGR2, MITE, USF2, and NR1H3 was upregulated in C2 cells, while the JUND, FOSL1, FOSL2, FOS, and STAT4 transcription factors activity were downregulated (Figure 2H). It was reported that NFE2L1 played a vital role in the carcinogenic process (23), and EGR2 was M2-exclusive (24). Furthermore, a study on murine sarcoma also demonstrated that tumorigenesis and progression were associated with STAT1

pathway activation (22). The results supported the M2b polarization in LUAD, and also shed light on the candidate transcription factors and potential mechanisms.

Exhausted CD8$^+$ T cells enriched in the TME of LUAD

A total of 13670 CD8$^+$ T cells were analyzed in this study. And the CD8$^+$ T cells were the predominant cell type in the LUAD compared with the normal tissue-derived cells. And the CD8$^+$ T cells were then segregated into four subgroups. The cells from C2 (MALAT1^{hi}), C3 (HBB^{hi}), and C4 (IGKC^{hi}) almost specially originated from tumor tissues, while C1 (TMSB4X^{hi}) was almost entirely derived from normal tissue (Figures 3A, B, and Figure S4A). Furthermore, unlike the above groups, we simultaneously divided the T cells into four groups (Tn, Naive T cell; Tcm, Central Memory T cell; Tem, Effective Memory T Cell; Te, Effector T cell) and visualized them. The biomarkers expression by FeaturePlot function (Figure S3D) to represent these four subtype groups CD8+ T situation.

Subsequently, the immune checkpoints were examined in all the cell clusters (Figure 3C). The expressions of checkpoints, CTLA-4, CD27, TIGIT, PDCD1 (PD-1), LAG3, TNFRSF9, and HAVCR2 (TIM3), were upregulated in cells from C2. Based on the knowledge of their role as exhaustion markers of T cells, these data implied that C2 cells tended to be exhausted in the TME of LUAD. We then verified this phenomenon through flow cytometry. As exhibited in Figure 3D, the exhausted molecules were highly enriched in the tumor tissues. Currently, the treatment targets CTLA-4, PD-1, and PD-L1 as the most popular immunotherapy were wildly used in the clinic. Since the expression of CTLA-4 and PD-1 were the highest in the exhausted T cell subgroup (C2) and the C2 cells were mainly of tumor origin. Hence our data further confirmed that CTLA-4 and PD-1/PD-L1 might be significant targets for immune therapies in LUAD.

We inferred cell differentiation trajectory using Monocle 2 pseudotime analysis. And t-Distributed Stochastic Neighbor Embedding (tSNE) plot was utilized to visualize the trajectory (Figure 3F). Interestingly, a subgroup of CD8$^+$ T cells from C1 was obtained from normal tissue and transformed into tumor-infiltrating T cells. At the terminal of the differentiation trajectory was the exhausted T cell cluster (C2) (Figure 3E). In this process, the immune checkpoints of promoting immune cell activation and antitumor immune responses (CD160, TNFRSF14) tended to be downregulated, while the immune checkpoints (TIGIT, TNFRSF9, CTLA-4, LAG3, PD-1) associated with exhausted T cell tended to be upregulated (Figure 3F). A total of three modules of DEGs were identified, and the CD8$^+$ T cells were sorted into three subgroups based on their expression profile (Figure S4B). In exhausted CD8$^+$ T cells, the cell adhesion, the ubiquitin-mediated proteolysis, and the histone modification gene set were highly enriched according to a Metascape enrichment analysis. In addition, we noted that T cell activation and cytokine production existed at the earlier stage of CD8$^+$ T differentiation. These results suggested that the CD8$^+$ T cells were activated in the early stages and then exhausted after continuous antigen stimulation. The TOX was the critical regulator of the differentiation of tumor-specific T cells, which also showed a constant upregulation during this process (Figure S4C) (25).

The SCENIC analysis was conducted to determine transcriptional activity in LUAD-specific T cells (Figures 3G, H). Four members (FLI1, TBX21, XBP1, and MAFF) involved in the inflammatory response, cell proliferation, and activation function were significantly activated in C1 (Figure 3G, H). Furthermore, the CTL pathway also was enriched in C1 (Figure 3I). In contrast, these transcription factors' activity was significantly suppressed in C2, such as TGF- β (Figures 3G–I). Additionally, the STAT3 pathway associated with immunosuppression was upregulated in C2 cells (Figure 3I). These results suggested that the exhausted CD8$^+$ T (C2) was intimately related to an immunosuppressive microenvironment (26). Additionally, these data provided clues for identifying new candidate transcription factors involved in dysfunctional T cells in LUAD patients.

Extremely abnormality in the metabolism of LUAD

The malignant epithelial cells and non-malignant normal epithelial cells were evaluated from scRNA-seq data using the InferCNV algorithm. The DEGs between malignant epithelial cells and non-malignant epithelial cells were identified. There were 89 DEGs, including 29 up-regulated and 60 down-regulated genes (Table S1). Astoundingly, the DEGs were significantly associated with energy metabolic processes, including upregulated and downregulated DEGs (Figure 4A). Therefore, we analyzed the upregulated and downregulated DEGs by Gene Ontology (GO) enrichment. As shown in Figure 4B, catabolism was enriched in malignant cells, while ATP and protein anabolism were suppressed. This result may explain the immunosuppressive properties of LUAD TME.

As we had described in Figure 4C, the GSEA demonstrated that the cell adhesion molecules pathway was enriched in malignant cells. Figures S5A and B showed that three members (CLND1, SDC1, and ALCAM) were upregulated in malignant epithelial cells. At the same time, nearly all CLDN family genes were involved in the cell adhesion molecules pathway and expression in LUAD-derived cells (Figures S5A, B). Notably, malignant cells especially expressed both CLDN1 and CLDN4, while CLDN18 was mainly expressed in the non-malignant epithelial cells (Figures S5A, B). Additionally, samples from the TCGA database showed CLND1 expression relatively

10.3389/fimmu.2022.1046121

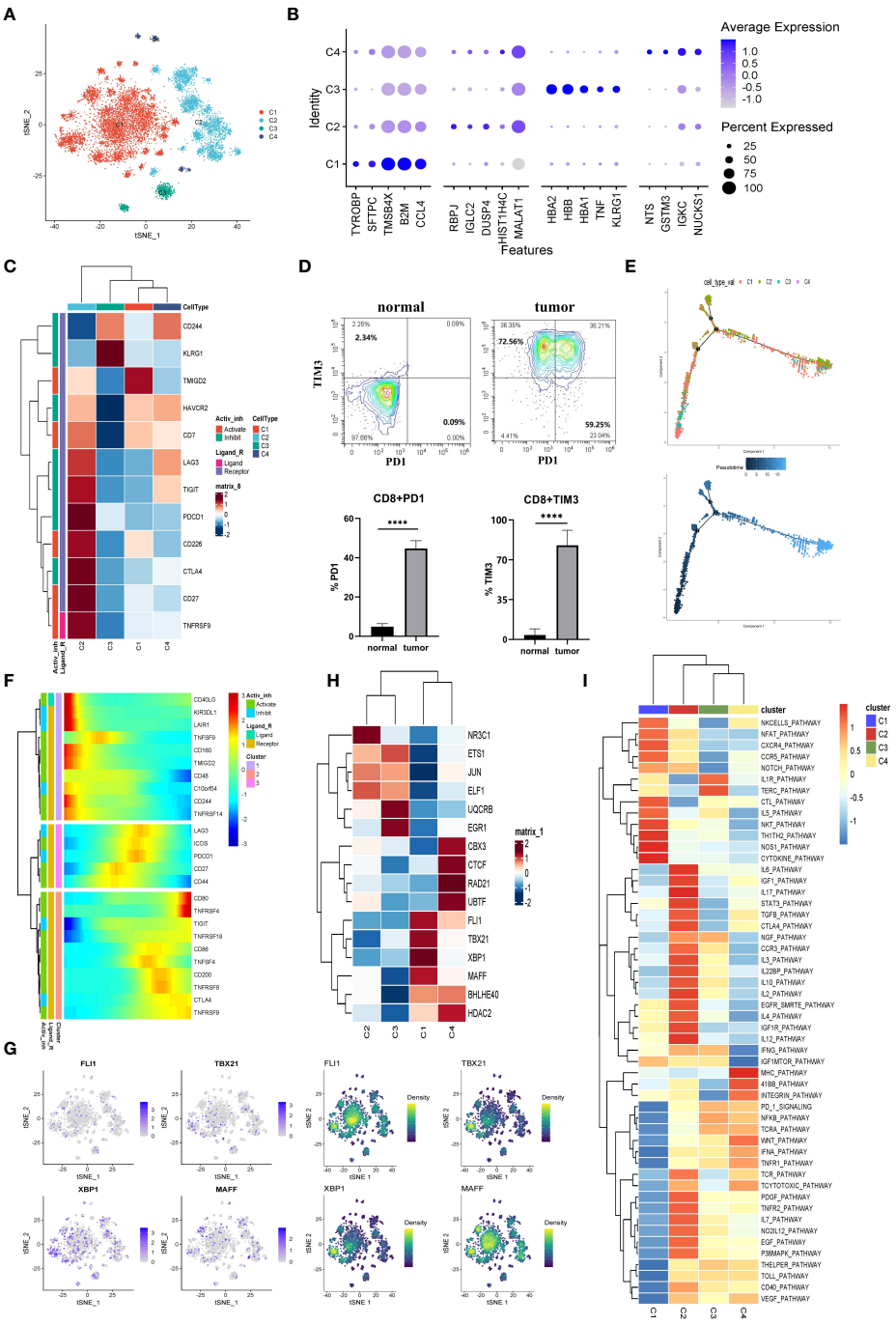

FIGURE 3
The CD8+ T cells in tumor TME preferred to be exhausted state. **(A)** The CD8+ T cells were subdivided into 4 clusters and represented on the tSNE plot. **(B)** The top five markers of the four major cell clusters were shown on the dot plot; the color represented expression level, while the sizes of dots represented abundance. **(C)** The heatmap demonstrated the downregulated or upregulated immune checkpoints in exhausted T cells. The expression level was represented by a row Z score. **(D)** The exhausted T cells in LUAD were analyzed by flow cytometry. The PD1+CD8+ and TIM3 +CD8+ T cells demonstrated specifically enrichment in LUAD specimens. Gate from CD8+T cell, ****p<0.0001.. **(E)** The CD8+ T cells' differentiation trajectory in LUAD and normal tissue and the color represented for clusters (up) or pseudotime (down). **(F)** The pseudo-heatmap showed the variation of immune checkpoint genes expression with the CD8+ T cells differentiation in LUAD, which could be subgrouped into three subcategories. **(G)** The tSNE plot represented the expression level of the indicated transcription factors (left) and the estimated AUC for these transcription factors' activity (right). **(H)** The heatmap showed the transcription factors' activity through SCENIC estimated AUC scores. **(I)** Heatmap of differences in activities of immune-related signaling pathways scored by GSVA.

10.3389/fimmu.2022.1046121

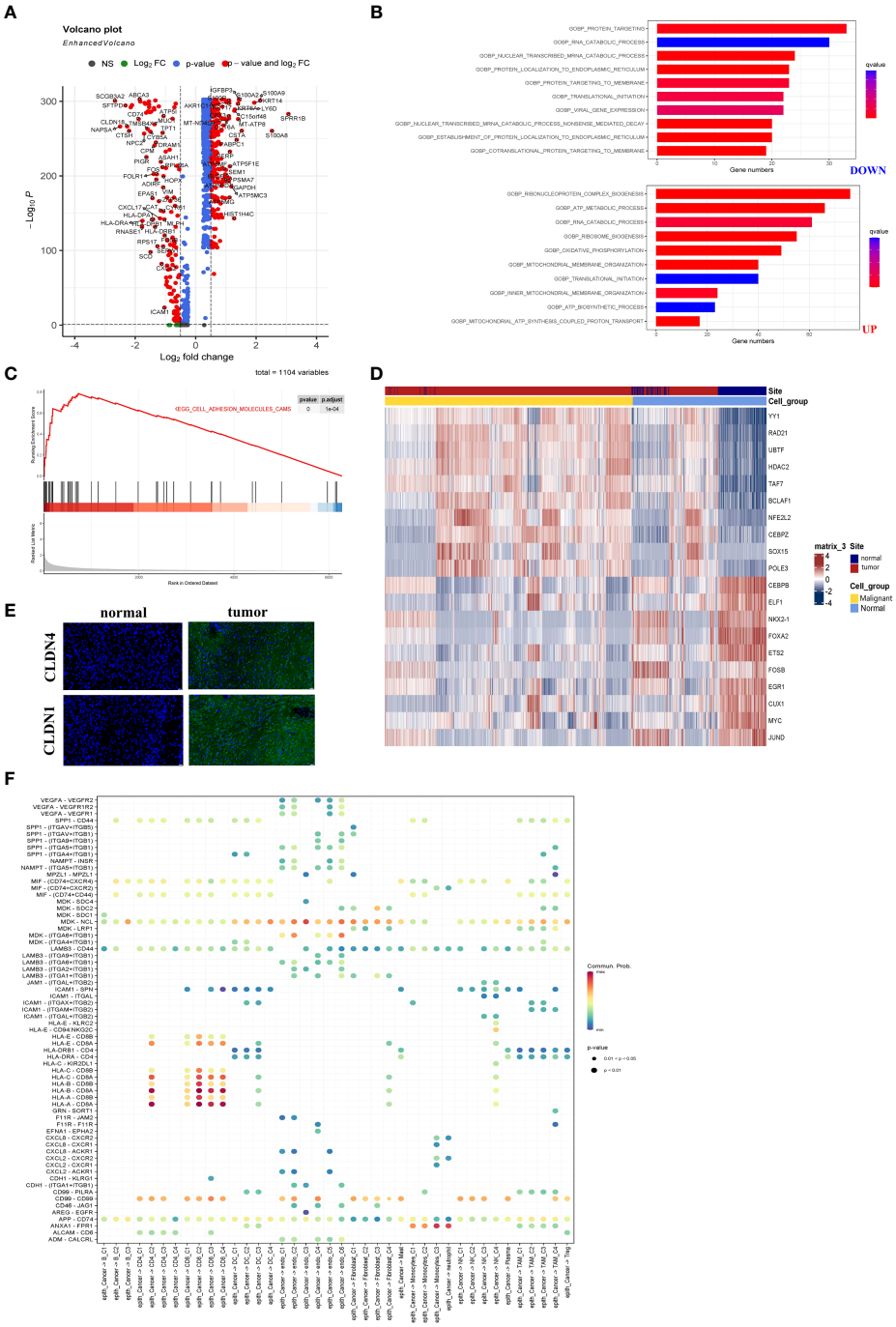

FIGURE 4
The metabolic abnormality was a specific characteristic of LUAD. **(A)** Volcano plot showed DEGs between malignant and non-malignant epithelium. Upregulated and downregulated genes (FC >2 and FDR <0.01) were colored in red. **(B)** Analyzed upregulated and downregulated DEGs using Gene Ontology. The brighter red color was considered a smaller FDR value (FDR <0.01). **(C)** The malignant epithelium was significantly enriched in the ADHESION pathway by GSEA. **(D)** Immunofluorescence staining of CLDN1 and CLDN4 in LUAD or normal tissue. CLDN1 and CLDN4 only emerged in LUAD tissues. The scale bar represented 20 μm. **(E)** The heatmap showed the transcription factors' activity through SCENIC estimated AUC scores. The value was implicated into a row Z score. **(F)** The bubble plot showed selected ligand-receptor pairs. The CellChat R package investigated ligand-receptor interactions between malignant cells and other TME-infiltrated cell clusters.

specific to cancer types (Figure S5C). The results indicated that LUAD was characterized by a unique role in the cell adhesion molecules pathway. To confirm their expression of CLDN4 and CLDN1, immunofluorescence was performed using the laser scanning confocal microscope (Figure 4D). As shown in Figures S5B, CLDN1 and CLDN4 as conventional tumor markers were expressed in malignant epithelial cells, while they were nearly absent in non-malignant epithelial cells. Thus, we recognized that CLDN1 or CLDN4 could be the potential therapeutic targets for LUAD. Malignant LUAD cells were found to have abnormal transcriptional regulatory networks using SCENIC analysis. Notably, some transcriptional factors closely related to LUAD tumorigenesis, such as HDAC2, were upregulated in malignant cells. In comparison, the transcriptional activation factors, such as FOXA2 (inhibiting tumor growth), were downregulated in malignant epithelial cells (Figure 4E). These data revealed the new regulatory networks controlled by transcriptional activation factors and provided novel insights into the mechanism of LUAD.

Finally, we investigated the interaction between cell subgroups in the TME and the cancer cells using CellChat. The LUAD cells demonstrated higher levels of midkine (MDK) interacting with receptors expressed on the other TME cells (Figure 4F). The MDK encoded protein promoted cancer cell growth, metastasis, and angiogenesis. And the MDK interaction with the LRP1 receptor was associated with immunosuppressive macrophage (M2) differentiation (27). These ligand-receptor pairs (including MIF – (CD74 or CXCR4), MIF – (CD74 or CD44), MDK–NCL, and MDK-LRP1) were more frequently occurring in tumors (28). And they served to regulate tumor growth and immunomodulatory processes. These data were similar to previous studies and indicated that abnormal energy metabolism was an important pathway for LUAD progression (29).

Enrichment and heterogeneous expression profile of fibroblasts in LUAD

As demonstrated in Figure 5A, fibroblasts were clustered into four subclusters, and most C1 and half of the C3 fibroblasts originated from tumor tissues. As shown in Figure 5B, the majority of fibroblasts expressed α-SMA (ACTA2), a conventional marker of fibroblasts. Bubble charts were used to visualize the top five markers of the different clusters (Figure 5C). We saw that ACTA2 was highly expressed mainly in C1 and C3. To confirm the phenotype, we stained ACTA2 with immunofluorescence (Figure 5D). In addition, RGS5 was known to promote cancer differentiation and metastasis in NSCLC (30), which was also enhanced in C3.

The SCENIC analysis revealed that the transcriptional activity of TCF12, CREB3L1, and STAT1, which were associated with malignant progression, proliferation, and migration, were upregulated in cells from C1 (Figure 5E). According to our data, tumor-associated fibroblasts exhibited the promoting tumor growth phenotype.

Endothelial cells derived from tumors contributed to the progression of LUAD

According to the present study, 8430 endothelial cells were detected from the tumor or normal tissues. Six clusters were identified among these cells (Figure 5F). Our subsequent analysis identified each cluster's markers and showed that most endothelial cells in LUAD (C2) were blood endothelial cells (FLT1+, Figures 5F, S6A). Four clusters, including C1, C5 ($CCL5^+$), C4 ($CCL21^+$), and C6 ($COX4I2^+$), were enriched in normal tissues, respectively. While C2 ($VWA1^+$) and C3 ($IL13RA2^+$) were nearly derived from tumor tissues (Figures 5F, G). Numerous reports had shown that the $IL13RA2^+$ endothelial subgroup played important roles in immunosuppression in the LUAD TME (31). No marker was detected in C1 cells, which were mainly derived from normal tissues. Nevertheless, their role in the biological process couldn't ignore.

To further identify biomarkers associated with tumors, the endothelial cells' marker genes and the upregulated genes in tumor-derived endothelial cells were overlapped. Then we obtained one gene, RALA (Figure 5H; Figures S6B, C). Almost all cancer types showed an increase in RALA, which was well-known as an endothelial activation marker (32) (Figure 5I). However, the TCGA bulk RNA-seq data showed the expression of RALA to be downregulated in LUAD (Figure S6D). Despite this, our single-cell RNA sequencing analysis further revealed that the RALA was the tumor-derived endothelial cell marker in LUAD. It could serve as a potential therapeutic target for LUAD.

Based on the result of the GSVA pathway analysis on Hallmarker sets, it was found that two endothelial cell clusters (C1 and C3) appeared prominent and significant differences from each other (Figure 5J). Remarkably, C1 cells exhibited an enriched inflammatory response. Instead, C3 exhibited an enriched immune inhibitory pathway, which indicated that a high suppression phenotype was derived from the cells from C3. Furthermore, an increased proliferation phenotype (MYC pathway) was strongly enriched in C3. The above observations confirmed that tumor-derived endothelial cells contributed to the progression of LUAD.

Antitumor immune cells were associated with advanced prognosis in LUAD

As shown in Figure 6A, the two clusters (macrophage C4 and $CD8^+$ T cell C1) were associated with better overall survival (OS), disease-specific survival (DSS), or disease-free interval

10.3389/fimmu.2022.1046121

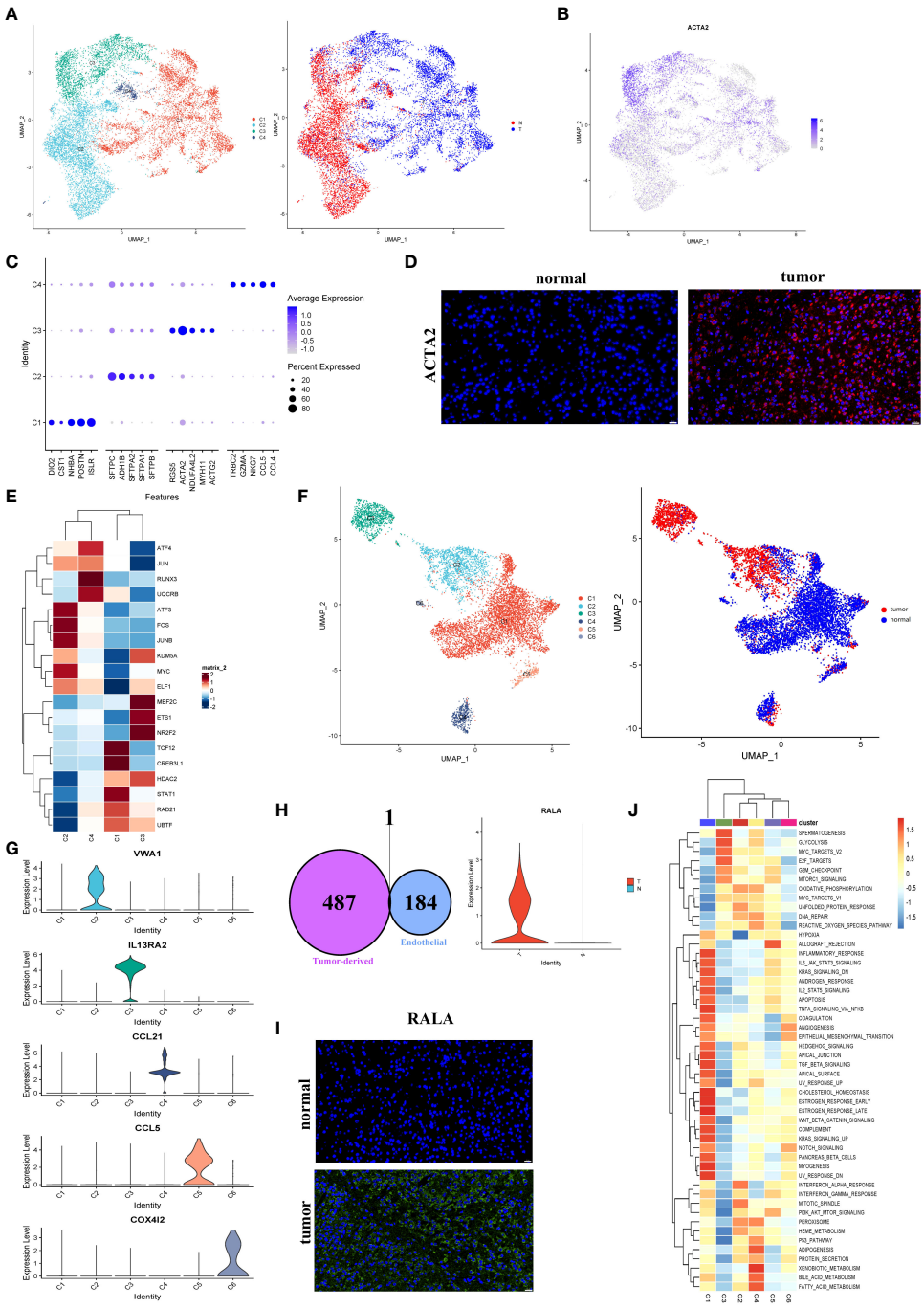

FIGURE 5
Fibroblasts and endothelial cells demonstrated high heterogeneity in LUAD. **(A)** UMAP plot of four fibroblast clusters and tissue type origin (normal or tumor). **(B)** UMAP plot of the expression level of ACTA2. **(C)** The top five markers of four clusters were shown on the dot plot; color represented expression level, and sizes represented abundance. **(D)** Immunofluorescence of ACTA2 in tissue sections. The scale bar represented 20 μm. **(E)** The heatmap showed the transcription factors' activity through SCENIC estimated AUC scores in fibroblast. **(F)** The endothelial cells were color-coded (left) for six endothelial clusters and (right) for tissues of normal or tumor origin. **(G)** The marker gene for different endothelial clusters. **(H)** The Venn diagram intersected the endothelial-specific markers and the DEGs between different endothelial cell types (tumor and normal). One overlapped gene was identified (left). The expression level of RALA was visualized by the violin plots (right). **(I)** The immunofluorescence of RALA in LUAD or normal tissue sections. The RALA was upregulated in LUAD tissue. The scale bar represented 20 μm. **(J)** The GSVA estimated the 50 hallmark pathway activities in the different cell clusters.

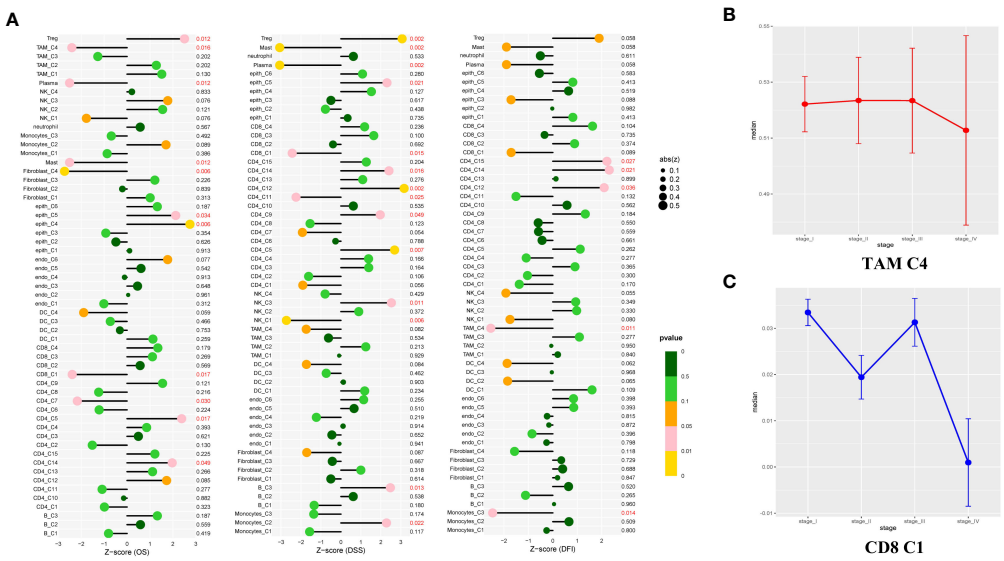

FIGURE 6
Study of the prognostic effect in the TCGA cohort. **(A)** The lollipop plot showed the correlation between the different cell clusters and disease-free interval (DFI), disease-specific survival (DSS), or overall survival (OS). The risk was measured in Z score with a Cox regression model. The clusters with better outcomes ($p < 0.05$). **(B, C)** Line charts showed TAM C4 and CD8 C1 enriched in early-stage LUAD tissues, but showed opposite properties in the late-stage. Measured with the one-way ANOVA test.

(DFI) ($p < 0.05$). The proportion of these cells in the LUAD was significantly lower compared with that of the normal tissue (Figure 1E). Based on these results, we deduced the M0-like macrophages and $CD8^+$ C1 cells with normal functions may be involved in the antitumor function of the TME in LUAD. NK cells C1 and C3 had a better DSS ($p = 0.006$, $p = 0.011$), implying that unidentified mechanisms may contribute to the antitumor process in LUAD *via* NK cells.

Notably, a significant reduction in the proportion of the macrophage C4 and $CD8^+$ T cells was significantly decreased in advanced tumor stage samples (Figures 6B, C). To determine the independent prognosis of macrophage Cluster 4 or CD8+T Cluster 1, we performed multivariate Cox regression analysis for OS, including clinical features (Stage, T, M, N) and the estimated proportion of cell-types (Figure S7). We found only the macrophage Cluster 4 was an independent predictor for better OS. Our research demonstrated that macrophage C4 and CD8+ T cell C1 exerted antitumor activities in LUAD. The number of these two clusters decreased as the LUAD progressed, confirming their antitumor function.

Discussion

Nowadays, the treatment of LUAD is still a challenge to clinicians. Although immunotherapy is considered a first-line treatment for patients with LUAD, the effectiveness and drug resistance of anti-PD-1 treatment remain notable problems despite the possibility of benefit to a few patients. According to a recent study, both the tumor-infiltrating cells and the cancer cells contribute to therapeutic non-response or drug resistance (33), and the underlying mechanisms need to be closely investigated. In the present study, our analysis of multiple LUAD scRNA-seq datasets unveiled an in-depth analysis of immune and unimmune cells, and we also utilized the immunofluorescence technique to identify the markers of the crucial cell subgroups in clinical cohorts. In the present work, the tumor-specific altered pathways, a series of novel cell subgroups, and novel transcriptional activation factors-driven regulatory networks were identified in LUAD. The results would provide novel targets for prognosis and treatment and contribute to better understanding of intratumoral heterogeneity in LUAD.

Although several observations had been reported for intratumoral heterogeneity, much work still needed to be done due to the highly intricated TME in LUAD. Several findings need to note. First, M0-like macrophages (C4) exhibited $KIAA0101^+FABP4^-$ phenotype, M2a-like macrophages (C1) exhibited $KIAA010^-FABP4^+$ phenotype and M2b-like macrophages (C2) exhibited the $ATP5F1E^+MMP12^-$ phenotype, while another $ATP5F1E^+$ $MMP12^+$ (C3) subgroup similar to M1 macrophages exhibited pro-inflammatory properties. Notably, in the TCGA cohort, patients in the M0 subgroup had advanced outcomes, while the $ATP5F1E^+$ subgroup (C2 and C3) showed the opposite. In the analysis of immune checkpoints and pathways, results indicated that the M2b-like TAMs had immunosuppressive properties in the TME *via* downregulation of Th1 cytokines and

upregulation of Th2 cytokines, which could induce a shift from Th1 to Th2 dominance. Through SCENIC analysis, we identified several transcriptional factors (such as JUN) related to the immunosuppressive properties of LUAD, and we firstly found that JUN could be a novel immunotherapy target in LUAD.

Second, we found that the exhausted $CD8^+$ T cells were highly enriched in LUAD (C2, C3, and C4), whereas the C1, mainly derived from normal tissue, showed a better prognosis in the TCGA cohort. This result was consistent with the study that the infiltration of exhausted $CD8^+$ T cells contributed to a worse prognosis in recent studies (34). Pseudotime and differentiation trajectory analysis revealed the T cell exhausted in LUAD and showed the signaling pathways involved in this process. We deduced that it may be possible to reverse T cell dysfunction by intervention in these pathways to revive $CD8^+$ T cells against tumor activity (such as TIGIT, TNFRSF9, CTLA-4, LAG3, PD-1), and this approach maybe represented new strategies for immunotherapy against LUAD. Previous studies had demonstrated that TGF- β was highly expressed in LUAD, which could block the efficacy of PD-1 and promote tumor growth and metastasis, which was associated with poor prognosis (35–37). This was consistent with the high expression of TGF- β in exhausted CD8+ T cells (C2) in our study. Therefore, it was suggested that simultaneous blockade of TGF- β and PD-1 signaling pathways would obtain a better antitumor effect. Furthermore, we discovered novel transcriptional factors alterations FLI1, TBX21, XBP1, and MAFF that may contribute to the exhaustion of T cells. These findings would further enhance our understanding of the LUAD pathological condition Based on our deconvolution results, we found that the patients with a high proportion of macrophage C4 exhibited better clinical outcomes. Meanwhile, $CD8^+$ C1 with the activated T cells enriched was related to a better prognosis. In contrast, the M2b polarization and T cell exhaustion may gradually increase from low to high grades of LUAD, which implied that M2b polarization and T cell exhaustion played a critical role in LUAD progression. Because immune checkpoints mediated M2b polarization and T cell exhaustion, it was confirmed that blocking immune checkpoints provided a credible approach to LUAD intervention. Consequently, we further confirmed the important role of exhausted T cells in LUAD in this study.

Third, we demonstrated abnormal energy metabolism in LUAD malignant cells. We found LUAD tumorigenesis was significantly correlated with the adhesion molecule pathway and abnormal energy metabolism, which had been rarely mentioned before. Notably, the abnormal adhesion molecule pathway was found in malignant epithelial cells, which was poorly reported up to date and worthy of further in-depth study. Therefore, our study proposes a family of adhesion molecules, i.g. CLND1 and CLND4 as novel therapeutic targets in LUAD treatment. Then, we demonstrated the majority of fibroblasts expressed α-SMA (ACTA2) driven from tumor tissues. And, we further found the expression of RALA was specifically upregulated in endothelial cells driven from tumor tissues. It is worth noting that RALA was shown downregulated in LUAD based on the TCGA bulk RNA-seq data, while almost all other cancer types showed an increase in RALA. Hence, it was for the first time revealed that targeting the RALA in tumor endothelial cells maybe a potential therapeutic target for LUAD.

Conclusion

Our study revealed immune and non-immune cell subtypes and type-specific gene expression in TME, and shed light on novel therapeutic strategies *via* multicenter scRNA-seq datasets analysis and verification in our clinical cohorts.

Data availability statement

The original contributions presented in the study are included in the article/Supplementary Material. Further inquiries can be directed to the corresponding authors.

Author contributions

Writing—original draft preparation, TF. Writing—review and editing, ZG and JL. Data curation, LZ. Software, ZG. Resources, TF, ZG, and LZ. Visualization, DN and YZ. Supervision, ZG, BZ, ZZ, and LZ. Funding acquisition, LZ, XH, NP, BL and HF. Providing clinical information, XH. Collection of raw data, NP, BL and HF. All authors had read and agreed to the published version of the manuscript.

Funding

This research was funded by Natural Science Foundation of Shandong Province, China grant number (No. ZR2021MH138), The China Postdoctoral Science Foundation grant number (No. 2016M592142), Wu Jieping Medical Foundation Clinical Research Special Fund (No. 320.6750.2021-2-94), The Scientific Research Fund of Hunan Province Health Commission (No. 202101062143), National Innovation and Entrepreneurship Training Program for College Students (No. S202010545069S) and Innovation and Entrepreneurship Training Program for College Students of Hunan Province (No. 3697).

Acknowledgments

The author thanks ZG, LZ, and all team members for their cooperation and contributions.

Conflict of interest

The authors declare that the research was conducted in the absence of any commercial or financial relationships that could be construed as a potential conflict of interest.

Publisher's note

All claims expressed in this article are solely those of the authors and do not necessarily represent those of their affiliated organizations, or those of the publisher, the editors and the reviewers. Any product that may be evaluated in this article, or claim that may be made by its manufacturer, is not guaranteed or endorsed by the publisher.

Supplementary material

The Supplementary Material for this article can be found online at: https://www.frontiersin.org/articles/10.3389/fimmu.2022.1046121/full#supplementary-material

References

1. Nasim F, Sabath BF, Eapen GA. Lung cancer. *Med Clin North Am* (2019) 103 (3):463–73. doi: 10.1016/j.mcna.2018.12.006

2. Zhang C, Zhang J, Xu FP, Wang YG, Xie Z, Su J, et al. Genomic landscape and immune microenvironment features of preinvasive and early invasive lung adenocarcinoma. *J Thorac Oncol* (2019) 14(11):1912–23. doi: 10.1016/j.jtho.2019.07.031

3. Jurisic V, Vukovic V, Obradovic J, Gulyaeva LF, Kushlinskii NE, Djordjević N. EGFR polymorphism and survival of NSCLC patients treated with TKIs: A systematic review and meta-analysis. *J Oncol* (2020) 2020:1973241. doi: 10.1155/2020/1973241

4. Jahanban-Esfahlan R, Seidi K, Banimohamad-Shotorbani B, Jahanban-Esfahlan A, Yousefi B. Combination of nanotechnology with vascular targeting agents for effective cancer therapy. *J Cell Physiol* (2018) 233(4):2982–92. doi: 10.1002/jcp.26051

5. Jahanban-Esfahlan R, Seidi K, Zarghami N. Tumor vascular infarction: prospects and challenges. *Int J Hematol* (2017) 105(3):244–56. doi: 10.1007/s12185-016-2171-3

6. Mantovani A, Marchesi F, Malesci A, Laghi L, Allavena P. Tumour-associated macrophages as treatment targets in oncology. *Nat Rev Clin Oncol* (2017) 14(7):399–416. doi: 10.1038/nrclinonc.2016.217

7. Hanley CJ, Mellone M, Ford K, Thirdborough SM, Mellows T, Frampton SJ, et al. Targeting the myofibroblastic cancer-associated fibroblast phenotype through inhibition of NOX4. *J Natl Cancer Inst* (2018) 110(1):109–20. doi: 10.1093/jnci/djx121

8. Albini A, Sporn MB. The tumour microenvironment as a target for chemoprevention. *Nat Rev Cancer* (2007) 7(2):139–47. doi: 10.1038/nrc2067

9. Hanahan D, Coussens LM. Accessories to the crime: functions of cells recruited to the tumor microenvironment. *Cancer Cell* (2012) 21(3):309–22. doi: 10.1016/j.ccr.2012.02.022

10. Wang F, Gao X, Wang P, He H, Chen P, Liu Z, et al. Immune subtypes in LUAD identify novel tumor microenvironment profiles with prognostic and therapeutic implications. *Front Immunol* (2022) 13:877896. doi: 10.3389/fimmu.2022.877896

11. Papalexi E, Satija R. Single-cell RNA sequencing to explore immune cell heterogeneity. *Nat Rev Immunol* (2018) 18(1):35–45. doi: 10.1038/nri.2017.76

12. Butler A, Hoffman P, Smibert P, Papalexi E, Satija R. Integrating single-cell transcriptomic data across different conditions, technologies, and species. *Nat Biotechnol* (2018) 36(5):411–20. doi: 10.1038/nbt.4096

13. Becht E, McInnes L, Healy J, Dutertre CA, Kwok IWH, Ng LG, et al. Dimensionality reduction for visualizing single-cell data using UMAP. *Nat Biotechnol* (2018) 37(1):38–44. doi: 10.1038/nbt.4314

14. Zhang X, Lan Y, Xu J, Quan F, Zhao E, Deng C, et al. CellMarker: a manually curated resource of cell markers in human and mouse. *Nucleic Acids Res* (2019) 47 (D1):D721–d728. doi: 10.1093/nar/gky900

15. Aibar S, González-Blas CB, Moerman T, Huynh-Thu VA, Imrichova H, Hulselmans G, et al. SCENIC: single-cell regulatory network inference and clustering. *Nat Methods* (2017) 14(11):1083–6. doi: 10.1038/nmeth.4463

16. Qiu X, Mao Q, Tang Y, Wang L, Chawla R, Pliner HA, et al. Reversed graph embedding resolves complex single-cell trajectories. *Nat Methods* (2017) 14 (10):979–82. doi: 10.1038/nmeth.4402

17. Tirosh I, Izar B, Prakadan SM, Wadsworth MH. 2nd, Treacy D, Trombetta JJ, et al. Dissecting the multicellular ecosystem of metastatic melanoma by single-cell RNA-seq. *Science* (2016) 352(6282):189–96. doi: 10.1126/science.aad0501

18. Wang R, Dang M, Harada K, Han G, Wang F, Pizzi Pool M, et al. Single-cell dissection of intratumoral heterogeneity and lineage diversity in metastatic gastric adenocarcinoma. *Nat Med* (2021) 27(1):141–51. doi: 10.1038/s41591-020-1125-8

19. Yu G, Wang LG, Han Y, He QY. clusterProfiler: an R package for comparing biological themes among gene clusters. *Omics* (2012) 16(5):284–7. doi: 10.1089/omi.2011.0118

20. Jew B, Alvarez M, Rahmani E, Miao Z, Ko A, Garske KM, et al. Accurate estimation of cell composition in bulk expression through robust integration of single-cell information. *Nat Commun* (2020) 11(1):1971. doi: 10.1038/s41467-020-15816-6

21. Wang J, Sanmamed MF, Datar I, Su TT, Ji L, Sun J, et al. Fibrinogen-like protein 1 is a major immune inhibitory ligand of LAG-3. *Cell* (2019) 176(1-2):334–47.e12. doi: 10.1016/j.cell.2018.11.010

22. Biswas SK, Gangi L, Paul S, Schioppa T, Saccani A, Sironi M, et al. A distinct and unique transcriptional program expressed by tumor-associated macrophages (defective NF-kappaB and enhanced IRF-3/STAT1 activation). *Blood* (2006) 107 (5):2112–22. doi: 10.1182/blood-2005-01-0428

23. Fu J, Zheng H, Cui Q, Chen C, Bao S, Sun J, et al. Nfe2l1-silenced insulinoma cells acquire aggressiveness and chemoresistance. *Endocr Relat Cancer* (2018) 25(3):185–200. doi: 10.1530/ERC-17-0458

24. Jablonski KA, Amici SA, Webb LM, Jde Ruiz-Rosado D, Popovich PG, Partida-Sanchez S, et al. Novel markers to delineate murine M1 and M2 macrophages. *PloS One* (2015) 10(12):e0145342. doi: 10.1371/journal.pone.0145342

25. Scott AC, Dündar F, Zumbo P, Chandran SS, Klebanoff CA, Shakiba M, et al. TOX is a critical regulator of tumour-specific T cell differentiation. *Nature* (2019) 571(7764):270–4. doi: 10.1038/s41586-019-1324-y

26. Farhood B, Najafi M, Mortezaee K. CD8(+) cytotoxic T lymphocytes in cancer immunotherapy: A review. *J Cell Physiol* (2019) 234(6):8509–21. doi: 10.1002/jcp.27782

27. Zhang Y, Zuo C, Liu L, Hu Y, Yang B, Qiu S, et al. Single-cell RNA-sequencing atlas reveals an MDK-dependent immunosuppressive environment in ErbB pathway-mutated gallbladder cancer. *J Hepatol* (2021) 75(5):1128–41. doi: 10.1016/j.jhep.2021.06.023

28. Gao Y, Wang H, Chen S, An R, Chu Y, Li G, et al. Single-cell N(6)-methyladenosine regulator patterns guide intercellular communication of tumor microenvironment that contribute to colorectal cancer progression and immunotherapy. *J Transl Med* (2022) 20(1):197. doi: 10.1186/s12967-022-03395-7

29. Zhu M, Zeng Q, Fan T, Lei Y, Wang F, Zheng S, et al. Clinical significance and immunometabolism landscapes of a novel recurrence-associated lipid

metabolism signature in early-stage lung adenocarcinoma: A comprehensive analysis. *Front Immunol* (2022) 13:783495. doi: 10.3389/fimmu.2022.783495

30. Huang G, Song H, Wang R, Han X, Chen L. The relationship between RGS5 expression and cancer differentiation and metastasis in non-small cell lung cancer. *J Surg Oncol* (2012) 105(4):420–4. doi: 10.1002/jso.22033

31. Taguchi A, Taylor AD, Rodriguez J, Celiktaş M, Liu H, Ma X, et al. A search for novel cancer/testis antigens in lung cancer identifies VCX/Y genes, expanding the repertoire of potential immunotherapeutic targets. *Cancer Res* (2014) 74 (17):4694–705. doi: 10.1158/0008-5472.CAN-13-3725

32. Norden PR, Sun Z, Davis GE. Control of endothelial tubulogenesis by rab and ral GTPases, and apical targeting of caveolin-1-labeled vacuoles. *PloS One* (2020) 15(6):e0235116. doi: 10.1371/journal.pone.0235116

33. Wu T, Dai Y. Tumor microenvironment and therapeutic response. *Cancer Lett* (2017) 387:61–8. doi: 10.1016/j.canlet.2016.01.043

34. Guo X, Zhang Y, Zheng L, Zheng C, Song J, Zhang Q, et al. Global characterization of T cells in non-small-cell lung cancer by single-cell sequencing. *Nat Med* (2018) 24(7):978–85. doi: 10.1038/s41591-018-0045-3

35. Yi M, Niu M, Wu Y, Ge H, Jiao D, Zhu S, et al. Combination of oral STING agonist MSA-2 and anti-TGF-β/PD-L1 bispecific antibody YM101: a novel immune cocktail therapy for non-inflamed tumors. *J Hematol Oncol* (2022) 15 (1):142. doi: 10.1186/s13045-022-01363-8

36. Yi M, Zhang J, Li A, Niu M, Yan Y, Jiao Y, et al. The construction, expression, and enhanced anti-tumor activity of YM101: a bispecific antibody simultaneously targeting TGF-β and PD-L1. *J Hematol Oncol* (2021) 14(1):27. doi: 10.1186/s13045-021-01045-x

37. Yi M, Niu M, Zhang J, Li S, Zhu S, Yan Y, et al. Combine and conquer: manganese synergizing anti-TGF-β/PD-L1 bispecific antibody YM101 to overcome immunotherapy resistance in non-inflamed cancers. *J Hematol Oncol* (2021) 14(1):146. doi: 10.1186/s13045-021-01155-6

frontiers | Frontiers in Immunology

TYPE Original Research
PUBLISHED 30 November 2022
DOI 10.3389/fimmu.2022.1077768

OPEN ACCESS

EDITED BY
Yangqiu Li,
Jinan University, China

REVIEWED BY
Wenzhuo Zhuang,
Soochow University, China
Yun Dai,
First Affiliated Hospital of Jilin University, China
Xinliang Mao,
Guangzhou Medical University, China

*CORRESPONDENCE
Mu Hao
haomu@ihcams.ac.cn
Lugui Qiu
qiulg@ihcams.ac.cn

†These authors have contributed equally to this work and share first authorship

SPECIALTY SECTION
This article was submitted to Cancer Immunity and Immunotherapy, a section of the journal Frontiers in Immunology

RECEIVED 23 October 2022
ACCEPTED 14 November 2022
PUBLISHED 30 November 2022

CITATION
Lv J, Sun H, Gong L, Wei X, He Y, Yu Z, Liu L, Yi S, Sui W, Xu Y, Deng S, An G, Yao Z, Qiu L and Hao M (2022) Aberrant metabolic processes promote the immunosuppressive microenvironment in multiple myeloma. *Front. Immunol.* 13:1077768. doi: 10.3389/fimmu.2022.1077768

Aberrant metabolic processes promote the immunosuppressive microenvironment in multiple myeloma

Junqiang Lv[1,2†], Hao Sun[1†], Lixin Gong[1†], Xiaojing Wei[1], Yi He[1], Zhen Yu[1,3], Lanting Liu[1,3], Shuhua Yi[1,3], Weiwei Sui[1], Yan Xu[1,3], Shuhui Deng[1], Gang An[1,3], Zhi Yao[2], Lugui Qiu[1,3*] and Mu Hao[1,3*]

[1]State Key Laboratory of Experimental Hematology, National Clinical Research Center for Blood Diseases, Haihe Laboratory of Cell Ecosystem, Institute of Hematology and Blood Diseases Hospital, Chinese Academy of Medical Sciences and Peking Union Medical College, Tianjin, China, [2]Key Laboratory of Immune Microenvironment and Diseases (Ministry of Education), Department of Immunology, School of Basic Medical Sciences, Tianjin Medical University, Tianjin, China, [3]Tianjin Institutes of Health Science, Tianjin, China

Introduction: Multiple myeloma (MM) is still an incurable plasma cell malignancy. The efficacy of immunotherapy on MM remains unsatisfactory, and the underlying molecular mechanisms still are not fully understood.

Methods: In this study, we delineated the dynamic features of immune cell in MM bone marrow (BM) along with elevated tumor cell infiltration by single-cell RNA sequencing (scRNA-seq), and investigated the underlying mechanisms on dysfunction of immune cells associated with myelomagenesis.

Results: We found that immune cells were activated in those patients with low infiltration of tumor cells, meanwhile suppressed with elevated infiltration of MM cells, which facilitated MM escaping from immune surveillance. Besides PD-1, abnormal expression of *PIM* kinases, *KLRB1* and *KLRC1* were involved in the defect of immune cells in MM patients. Importantly, we found aberrant metabolic processes were associated with the immunosuppressive microenvironment in MM patients. Disordered amino acid metabolism promoted the dysfunction of cytotoxicity CD8 T cells as well as lipid metabolism disorder was associated with the dysregulation of NK and DCs in MM. As metabolic checkpoints, *PIM* kinases would be potential effective strategies for MM immunotherapy.

Discussion: In summary, redressing the disordered metabolism should be the key points to get promising effects in immune-based therapies.

KEYWORDS

multiple myeloma, immune cells, tumor microenvironment, metabolism, PIM kinases

Introduction

Multiple Myeloma (MM) remains an incurable plasma cell malignancy (1–3). The development of MM has been classically viewed as a multistage process (4). However, the common initiating events, including multiple cytogenetic aberrant, with immunoglobulin heavy chain translocation and hyperdiploidy are insufficient to cause MM occurrence, as MGUS/SMM patients commonly harbor these abnormalities and show no clinical symptoms of MM (5, 6). Intra-clonal heterogeneity has been observed at all stages of MM. Mounting evidences suggest that disease occurrence and progression may be induced by inter-subclone competition and external microenvironment of the fittest of these subclones (7).

Avoiding immune destruction is a hallmark of cancer (8). Immunotherapy has proven to be very encouraging in the therapy of cancers especially in hematological malignancy, including MM (9). However, the efficacy of immunotherapy on MM remains far from satisfactory. The immunosuppressive microenvironment interferes the efficacy of immunotherapies, but the underlying molecular mechanisms remain largely unknown. The complicated cell-cell interaction between tumor and immune cells (10–15), as well as cytokines and chemokines by autocrine or paracrine by tumor cells, promotes the immunosuppressive tumor microenvironment (iTME) (16, 17). Recent researches elucidated that the impaired metabolic flexibility associated with tumor cells could result in an ineffective anti-tumor immune response and involved in tumor progression (18–20). The abnormal energy metabolism was also associated with the pathogenesis and outcomes of MM patients (21). However, few study delineated the immune responses, interactions and metabolic states of immune cells at the same space-time dimension in myeloma microenvironment. Further understanding the landscape of the dysfunction of immune cells as well as the underlying molecular mechanisms are necessary for us to identify more efficient therapeutic targets for future clinical intervention. Recently, there were several studies investigated the iTME in MM *via* scRNA-seq (22–25). Most of the reports analyzed the iTME of MM patients based on risk stratification of patients, such as the Revised International Staging System (R-ISS) and the mSMART 3.0 classification. Those data help us to comprehend the effect of genotypic milieu on immune response in MM patients. However, the metabolic restriction in immune cells caused by tumor cells is more relevant to the accumulation of tumor cells but not the genotypic milieu. To investigate the effect of metabolism on immune response in MM patients, we segregated the MM patients enrolled in our study according to the infiltration of MM cells in the bone marrow.

In this study, we utilized single-cell RNA sequencing (scRNA-seq), an unbiased technology to comprehensively categorize cell types for a deeper dissection of immune cell features in newly diagnosed MM (NDMM) patients compared with healthy donors (HDs). The pathophysiology features of immune cell populations in myeloma microenvironment were dissected, and the impact of tumor cells on immunosuppressive microenvironment was investigated as well. Our study proved that the state of immune response was dynamic along with the elevated tumor cells. Such ecosystems were orchestrated by MMs through disordered metabolism induced program.

Abbreviations: MM, Multiple myeloma; BM, bone marrow; scRNA-seq, single-cell RNA sequencing; BMNCs, bone marrow mononuclear cells; HD, healthy donors; NDMM, newly diagnosed MM; SR, standard risk; HR, high risk; UMI, unique molecular identifier; GO, Gene ontology; DCs, dendritic cells; ISS, International Staging System; R-ISS, the Revised International Staging System; PIs, proteasome inhibitor; EDTA, ethylenediaminetetraacetic acid; HSPC, hematopoietic stem and progenitor cells; del, deletion; MHC, major histocompatibility complex; APCs, Professional antigen-presenting cells; cDCs, conventional DCs; pDCs, plasmacytoid DCs; DEGs, differentially expressed genes; mTOR, mammalian target of rapamycin.

Methods

Clinical samples

Bone marrow mononuclear cells (BMNCs) were obtained from 7 HDs and 12 NDMM patients (Figure 1A). The clinical and biological characteristics of 12 NDMM patients are listed in Figure 1B. BMNCs were isolated by Ficoll density-gradient centrifugation. This study was approved by the Institutional Ethics Review Boards from the Institute of Hematology and Blood Diseases Hospital, Chinese Academy of Medical Sciences. Written informed consents were obtained from patients and healthy donors before sample collection.

Single-cell RNA library preparation and sequencing

3'-biased 10× Genomics Chromium was applied (26). The libraries were sequenced on an MGISEQ-2000 sequencer as 150 bp paired-end reads by Novogene Co., Ltd (Novogene, Beijing, China).

scRNA-seq data processing

The Seurat was used for dimension reduction, clustering, and differential gene expression (27). Cell Ranger Software Suite was applied to perform genome alignment, barcode processing, and unique molecular identifier (UMI) counting. The

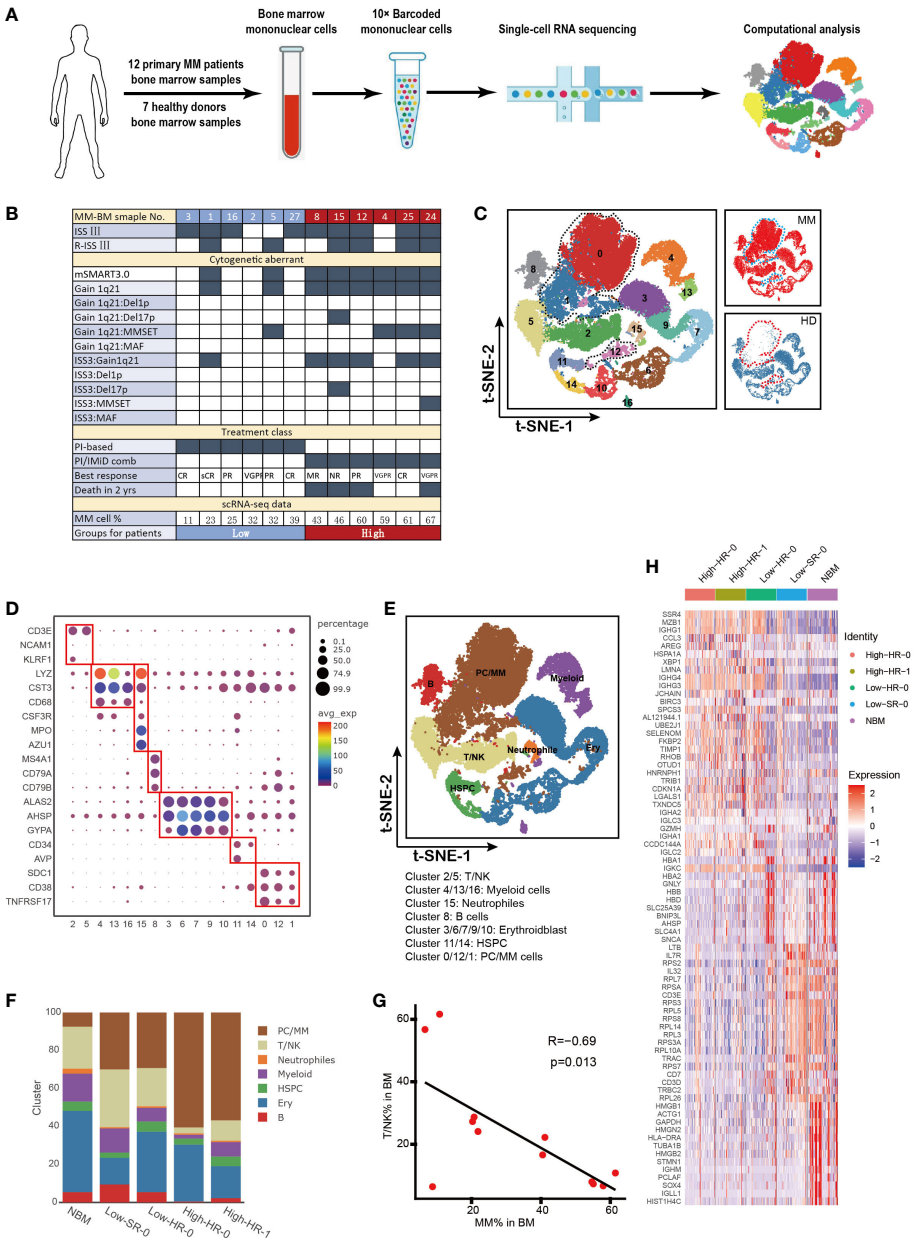

FIGURE 1
Cell identification in myeloma microenvironment at single cell resolution **(A)**. Flow chat of the study. BMNCs from 7 HDs and 12 NDMM patients were subjected to single-cell RNA sequencing on 10× Genomics platform. A total of 42,936 cells were analyzed after quality control. **(B)**. Form shows the detailed characteristics and clinical information of MM patients. **(C)**. Seventeen cell clusters were identified by t-SNE analysis of BMNCs from HD and MM patients. Each dot represents a single cell; colors indicate cell clusters with numbered labels. **(D)**. Bubble chart shows the expression of marker genes of distinctive cell type. The cluster number are presented in the bottom of the figure. **(E)**.t-SNE plot shows the distribution pattern of the BMNCs cell types. Colors represent different cell types. **(F)**. Bar charts show the proportions of distinctive cell type from HD and different MM groups. The cell types in right correspond to the ones in **(E)**. **(G)**. The correlation of proportion of T/NK and MM cells in MM patients. **(H)**. Heatmap shows the expression profile of top 20 signature genes for T/NK clusters from HD and different MM groups. The top bars label the HD and MM groups. tSNE, T-distributed stochastic neighbor embedding; BMNCs, Bone marrow mononuclear cells; MM, multiple myeloma; NDMM, newly diagnosed MM; HD, healthy donors; T/NK, T cells and NK cells; B, B cells; PC/MM, plasma cells and multiple myeloma cells; Ery, erythroidblast; HSPC, hematopoietic stem and progenitor cells.

identification of cell clusters was defined based on marker genes, as described in previous reports (28–31).

Functional enrichment analysis

The metabolic pathways among HD and MM patients were calculated for each cell using the GSVA software package (32). Differential pathway analysis between clusters was done with the limma R software package (33). Gene Ontology (GO) analysis was performed with cluster Profiler4 (34).

Cell function analysis based on scRNA-seq

The cytotoxic score and exhausted score for T cells and active score for dendritic cells (DCs) were defined by AddModuleScore (27). The signature genes for the estimation of cytotoxic/exhausted score and active score were respectively listed in Supplementary Tables 1 and 2. CellPhoneDB was used to estimate cell-cell interactions as described in the previous report (35).

Mouse model and flow cytometry analysis

C57BL/KaLwRij 5TGM1 murine myeloma model (purchased from Harlan Laboratories Inc., Netherlands) were utilized according to the protocol reported (36, 37). BMNCs were collected 5 weeks after 5TGM1 mouse MM cell injection, and flow cytometry was performed to analyze the composition in bone marrow cells. Flow cytometry for BMNCs was performed on Canto flow cytometer, and the data were analyzed by Flowjo V10 software. The detailed information with the antibodies utilized is listed in Supplementary Table 3.

Evaluation to the function of CD8 T cells in MM patients and mouse *in vitro*

BMNCs from MM patients were isolated by Ficoll density-gradient centrifugation. BMNCs were treated with Cell Activation Cocktail (with Brefeldin A) (Biolegend, USA) for 5 hours. Flow cytometry was performed to analyze expression of surface markers and cytokines in T cells.

C57BL/6J mouse (purchased from Vital River Laboratories, Beijing, China) were utilized according to the protocol as follows: Spleens were collected and homogenized using a steel mesh. Red blood cells were lysed using Red Blood Cell Lysis Buffer (Solarbio Science & Technology Co.,Ltd., Beijing, China) for 4 min at room temperature. Washing the splenocytes with PBS for 3 times. Splenocytes were activated by anti-mouse CD3/CD28 (2ug/ml) combined with PIM kinase inhibitor AZD1208 (1ug/ml) or DMSO for 72 hours. Flow cytometry (Canto flow cytometer, BD) was performed to analyze expression of surface markers and cytokines in T cells, and the data were analyzed by Flowjo V10 software. The detailed information with the antibodies utilized was listed in Supplementary Table 3.

Statistical analysis

Data are shown as either mean or median ± SEM or SD. The statistical significance was determined by two-tailed Student's *t*-test, one-way or two-way ANOVA tests. Data analyses were performed with R language and SPSS 18.0. In all instances, $p< 0.05$ was considered significant, * $p < 0.05$, ** $p < 0.01$ and *** $p < 0.001$.

Results

Cell identification in myeloma microenvironment at single cell resolution

Here we utilized scRNA-seq to integrate and delineate the cellular components of BM microenvironment in MM patients compared with HDs. The flowchart of the study was presented in Figure 1A. Twelve NDMM patients and seven 7 HDs were included in this study. Detailed clinical and pathological information, including stage of diseases, cytogenetic aberrant and tumor infiltration, were summarized in Figure 1B. The 9/12 patients were International Staging System (ISS) stage III, and 6/12 patients were Revised ISS (R-ISS) stage III. According to mSMART3.0 (2, 38), 4/12 patients were identified as cytogenetic standard risk, and 8/12 were high risk. 4/12 patients exhibited t (4, 14), and one patient was 17p deletion. Genetic features of five patients (MM4, MM5, MM15, MM24, and MM25) were considered double-hit myeloma. The treatment of the patients grouped: 1) proteasome inhibitor (PIs) based or 2) PIs in combination with immunomodulatory drugs (IMiDs) for those with high-risk MM. Of note, among the eight patients with high-risk genetic features, the overall survival of four cases (MM8, MM12, MM15 and MM24) was inferior with less than 2 years, while other HR patients could benefit from the therapy with favorable outcome.

A total of 42,936 single cells from MM and HDs were included in this analysis after quality control, and an average of 7,939 UMI and 1,243 genes were generated per single cell (Supplementary Figure 1A). t-SNE analysis identified and visualized 17 distinct cellular clusters (Clusters 0-16) according to their transcriptome profile (Figure 1C and Supplementary Figure 1B). Compared to HD, Cluster 0, Cluster 1 and Cluster 12 mainly appear in MM patients, especially Cluster 0 and Cluster 1

(Figure 1C).We annotated seven cell types based on the expression of characteristic genes of these clusters: hematopoietic stem and progenitor cells (HSPC) (*CD34* and *AVP*), T/NK cells (*CD3E* and *KLRF1*), myeloid (*LYZ* and *CST3*), neutrophils (*LYZ, CTS3, CSF3R, AZU1* and *MPO*), plasma/MM cells (*SDC1, TNFRSF17* and *CD38*), B cells (*MA4A1, CD79A* and *CD79B*), Erythroidblast (*ALAS2, AHSP* and *GYPA*) (Figures 1D, E). The characteristic genes for each cluster were referred to previous reports (39–41). In particular, based on high level of *SDC1, TNFRSF17, MZB1, CD38* and low level of *CD19* and *MS4A1*, Cluster 0, Cluster 1 and Cluster 12 were defined as $SDC1^+$ cells, namely plasma cell in HD controls and tumor cells in MM patient (Figure 1E and Supplementary Figure 1B). The BM cellular composition in each MM patients was highly heterogeneous (Supplementary Figure 1C). According to the proportion of MM cells in BM aspiration defined by scRNA-seq (Cluster 0, Cluster1 and Cluster 12), the MM patients could be segregated into two groups, low infiltration group with less MM cells (%MM cells<40%, mean value= 26%, n=6) and high infiltration group (%MM cells>40%, mean value= 56%, n=6) (Figure 1B). Interestingly, we noted that all six patients in high-infiltration group corresponded to the cytogenetic high-risk group according to the criteria of mSMART3.0, whilst two patients with cytogenetic high-risk, MM1 and MM5, belonged to low-infiltration group (Figure 1B). This finding suggests us that except for cytogenetic aberrant of MM cells, tumor-extrinsic local microenvironment was also involved in the determination the tumor cell proliferation and survive. Therefore, it is essential to dig out the underlying mechanisms of the biological heterogeneity resulting in the extremely malignant clinical features of MM.

To further investigate the association between tumor cell infiltration and microenvironment non-malignant cells, the proportion of each type of cells in patients with diverse clinical characteristics were analyzed. As Figure 1F showed, the twelve MM patients were discriminated into four groups with extent of tumor cell infiltration, risk stratification (mSMART3.0) and survival state, as following: High-HR-0 (high tumor infiltration, high risk and survival, including patients MM4 and MM25), High-HR-1 (high tumor infiltration, high risk and death, including patients MM8, MM12, MM15 and MM24), Low-HR-0 (low tumor infiltration, high risk and survival, including patients MM2, MM3, MM16 and MM27), and Low-SR-0 (low tumor infiltration, standard risk and survival, including patients MM1 and MM5). Of note, immune cells, including T and NK cells were decreased in patients with high level tumor cells, including High-HR-0 and High-HR-1, compared with low level ones (Low-SR-0 and Low-HR-0). Among patients with low level infiltration of tumor cells, MM cells with high-risk cytogenetic features (Low-HR-0) did not present superiority in proliferation compared with low-risk ones (Low-SR-0). Moreover, in high level infiltration patients, the immune cells remarkably reduced compared with low level tumor cell infiltration patients. The proportion of T/NK cell was negatively correlated with the proportion of MM cells in BM milieu (R=-0.69, p=0.013, Figure 1G). These findings supported that the proliferation of tumor cells was not only dependent on the characteristics of MM cells, but tumor microenvironment, especially immune microenvironment, which played pivotal roles in the process. Our further analysis confirmed the heterogeneity of T/NK cells among diverse tumor cell infiltration groups of patients. The transcription of T/NK cells was similar in normal BM and Low-SR-0 group patients, and high-HR-0 was similar with high-HR-1. The low-HR-0 fell in between (Figure 1H).

The fluctuation of CD8 T sub-clusters in MM patients with different infiltration of tumor cells

T cells are the major players in anti-tumor immune response. Here we further analyzed the T cells subpopulations in BM of MM patients based on single-cell transcriptome data. tSNE clustering analysis showed that twelve subpopulations of T cells could be further discriminated based on the expression of classical markers (sub-clusters 0 to 11, Figure 2A) including seven sub-clusters of $CD8^+$ T cells and five sub-clusters of $CD4^+$ T cells. All of the T cell subpopulations could be found both in HD and MM patients in different proportions. They were CD8-Naïve (sub-cluster 2), CD8-GNLY (sub-cluster 0), CD8-XCL2 (sub-cluster 6), CD8-S100A8 (sub-cluster 8), CD8-mucosal-associated invariant T cells (CD8-MAIT, sub-cluster 9), CD8-COTL1(sub-cluster10), CD8-MZB1 (sub-cluster 11), CD4-Naïve (sub-cluster 1), CD4-NR4A2 (sub-cluster 3), CD4-GPR183- FOXP1 (sub-cluster 4), CD4-AQP3 (sub-cluster 5) and CD4-Treg (sub-cluster 7) (Figures 2B, C). Based on the description of previous reports (29–31), we further defined the sub-clusters. In detail, sub-cluster 2 was defined as CD8-Naïve T cells with high levels of *CCR7, SELL, LEF1* and low levels of effector genes. CD8-XCL2 was memory $CD8^+$ T cells that characterized by expression *STMN1* and *CD69* (Supplementary Figure 2A). CD8-COTL1 was defined as exhausted CD8 T cell due to the higher level of immune checkpoint TIGIT than other T cell subpopulations (Supplementary Figure 2A). CD8-GNLY T cells were characterized as effector T cells with high expression of cytotoxic genes, including *GNLY, GZMB, TNF* and *IFNG* (Figure 2C and Supplementary Figure 2A). CD8-S100A8 were transitional CD8 effector T cells with expression of GZMK (Supplementary Figure 2A). Sub-cluster 9 was defined as CD8-MAIT with the expression of *SLC4A10*. Within the $CD4^+$ T cell compartment, CD4-Naïve (sub-cluster 1) expressed *SELL, CCR7* and *LEF1*, the common naive cells marker genes. CD4-NR4A2 (sub-cluster 3) was identified as effector CD4 T cells by expressing genes which were induced early after activation, such as *JUNB, FOS, ATF3* and *DNAJB1* (Figure 2C and

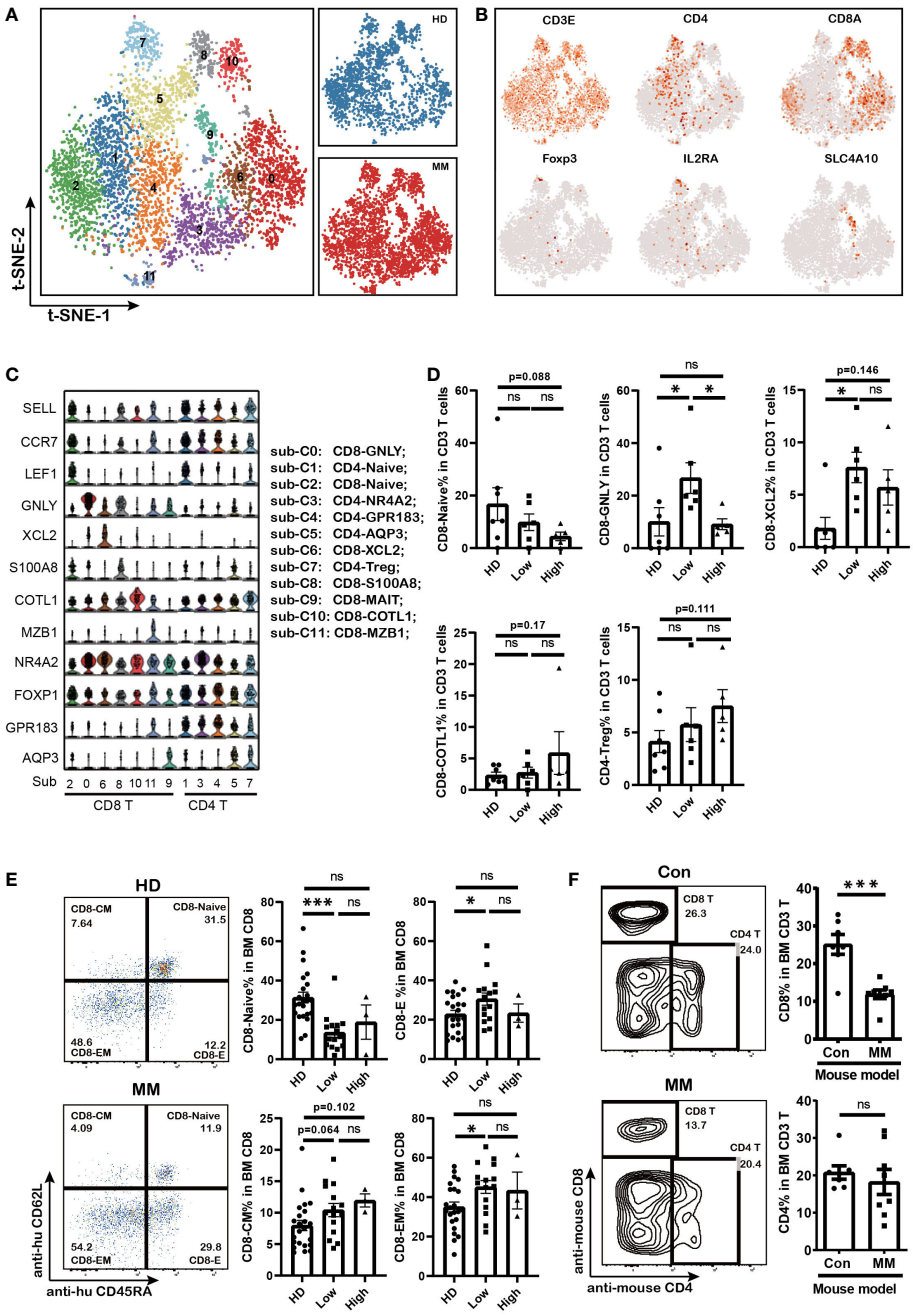

FIGURE 2
The fluctuation of CD8 effector T cells and accumulation of CD8 memory T cells in MM patients with different tumor burden **(A)**. t-SNE shows the T cell sub-clusters in HD and MM patients. Cells with a high level of CD3 (*CD3E*, *CD3G* and *CD3D*) expression were T cells. Each dot represents a single cell; colors indicate cell clusters with numbered labels. **(B)**.t-SNE plot show the expression and distribution of classical cell markers of T cell sub-clusters. Color intensity indicates expression level of selected genes. **(C)**.Violin charts show the expression of classical cell markers of T cell sub-clusters. The sub-cluster numbers in (c) bottom correspond to the ones in **(A)**. Sub-C0: CD8-GNLY (effector T cells); sub-C1: CD4-Naïve; sub-C2: CD8-Naive; sub-C3: CD4-NR4A2; sub-C4: CD4-GPR183_FOXP1; sub-C5: CD4-AQP3; sub-C6: CD8-XCL2 (memory T cells); sub-C7: CD4-Treg; sub-C8: CD8-S100A8; sub-C9: CD8-MALT; sub-C10: CD8-COTL1; sub-C11: CD8-MZB1; **(D)**. Bar charts show the proportions of T cell sub-clusters from HD and different infiltration groups of MM patients. (HD: n=7; Low: n=6; High: n=6) **(E)**. Flow cytometry analysis shows the proportions of CD8+ T cell sub-populations in HD and MM patients. (HD: n=23; Low: n=15; High: n=3) CD8-Naive: $CD3^+CD8^+CD45RA^+CD62L^+$; CD8-Effector: $CD3^+CD8^+CD45RA^+CD62L^-$; CD8-Central memory: $CD3^+CD8^+CD45RA^-CD62L^+$; CD8-Effector memory: $CD3^+CD8^+CD45RA^-CD62L^-$; **(F)**. Flow cytometry analysis and bar charts show the proportion of CD8 T and CD4 T cells in Control and 5TGM1 MM mouse model (Control: n=7; MM: n=8). In all instances, $p < 0.05$ was considered significant, * $p < 0.05$ and *** $p < 0.001$.
ns, no significance.

Supplementary Figure 2A). Sub-Cluster 7 was identified as CD4-Treg by co-expressing *Foxp3* and *CTLA4*.

Notably, the composition of T cell sub-clusters was heterogeneous across the patients with MM (Supplementary Figure 2B). The proportion of effector $CD8^+$ T cells (CD8-GNLY) significantly increased in BM of patients with low MM cell infiltration compared to HD controls and patients with high infiltration ones (Figure 2D). Meanwhile, the fraction of CD8-Naïve cells decreased along with the infiltration extent of MM cells (Figure 2D). CD8-XCL2 cells, as memory CD8 T cells, were increased in BM of all patients whether tumor cell infiltration extent compared with that in HD BM (Figure 2D). In particular, we found a slightly increase of the exhausted T cell cluster (CD8-COTL1) and CD4-Treg in BM of patients with high MM cell infiltration although there was no statistic difference (Figure 2D). We further confirmed the variations in T cell proportions induced by MM cells in BM by flow cytometry using another panel of primary MM patient samples and 5TGM1 murine MM model. Our findings supported that CD8-effector cells increased and CD8-naïve cells decreased in patients with low tumor infiltration (MM %<40%, Figure 2E). In MM mouse model with high tumor infiltration (MM %> 40%), we consistently found that the proportion of $CD8^+$ T cells significantly decreased in their BM, whereas $CD4^+$ T cells remained stable (Figure 2F). These finding indicated that the differentiation of cytotoxicity CD8 T cells from naïve CD8 T cells were interfered by MM cell infiltration, which caused the immunosuppressive microenvironment.

Dysfunction of CD8 T cells associated with aberrant *PIM* kinases and *KLRB1* expression as well as the abnormal metabolism mediated by MM

Except for the amount of immune cell, the dysregulation of immune cells is more important in tumorigenesis. To further investigate the dysfunction of $CD8^+$ T cells in myeloma microenvironment, the cytotoxicity and exhaustion score in each CD8 T cell sub-cluster were evaluated. The cytotoxicity associated genes (*GZMA, GZMB, GZMH, GZMK, GNLY, TYROBP, IFNG, TNF, PRF1, KLRD1, NKG7*, and *FCGR3A*) and classical exhausted marker genes (*PDCD1, CTLA4, VSIR, SLAMF6, CD160, LAG3, TIGIT, HAVCR2*, and *BTLA*) were involved in the calculation. CD8-GNLY, as effector CD8 T cells, exhibited the highest cytotoxicity score among CD8 T cell sub-clusters (Figure 3A). Of note, the cytotoxicity of CD8-GNLY effector T cells in MM patients was lower than that in HD meanwhile it significantly decreased in MM patients in a tumor cell dependent manner (Figure 3A). The differentially expressed genes (DEGs) analysis showed that the cytotoxicity associated genes of CD8-GNLY effector T cells displayed different expression patterns in HD, low infiltration group and high infiltration group. Consistently, CD8-GNLY effector T cells in high infiltration patients expressed low level of *IFNG, GMZB, KLRF1, GZMK, GZMH, GZMM* and *KLRD1* compared to HD and low infiltration group (Figure 3B). Meanwhile this CD8 T cell sub-clusters in low infiltration group expressed high level of *GZMK, GZMH* and *GZMM* and low level of *IFNG, GMZB, KLRF1* and *KLRD1*. However, we did not find variation of exhaustion scores of $CD8^+$ T cell sub-clusters across the groups except to exhaust CD8-COTL1 (Figure 3A). The levels of classical immune checkpoint genes in CD8-GNLY effector T cells were comparable among groups (Figure 3C). The flow cytometry results from MM patients confirmed these findings (Figure 3D and Supplementary Figure 2C). In line with this, we didn't observe the difference on the expression of PD1 and LAG3 in CD8 T cells and CD4 T cells from MM mouse model (Supplementary Figure 2D). CD8-COTL1 exhausted T cell expressed higher immune checkpoint *PDCD1*, especially in myeloma microenvironment with high tumor infiltration (Supplementary Figures 2E, F). These results indicate that the dysfunction of CD8-GNLY effector T cells is associated with tumor infiltration but not classical T cell exhaustion genes.

To clarify the underlying molecular mechanisms of dysfunction of CD8-GNLY effector T cells in myeloma microenvironment, the transcript profile of CD8-GNLY effector T cells was further analyzed. We found that CD8-GNLY effector T cells in high tumor infiltration group displayed increasing level of the serine/threonine kinase PIM family (*PIM2* and *PIM3*), *NR4A2/3, KLF4/6, BCL2, GPR183* and *COTL1* compared to the ones from HD and low tumor infiltration group (Figure 3B). *KLRB1* was notably increased in CD8-GNLY effector T cells both in MM patients with high and low tumor infiltration, which was confirmed by flow cytometry in primary MM patient samples (Figure 3E). We further confirmed that $KLRB1^{high}$ CD8 T cells from MM patients displayed lower IFN-γ abundance than $KLRB1^{low}$ CD8 T cells when they were activated *in vitro*, which supported the weakened cytotoxicity of CD8 T cells high tumor infiltration group (Figure 3F). Moreover, inhibiting PIM kinases by AZD1208, a pan-inhibitor of PIM kinases, could promote the cytotoxicity of CD8 T cells *in vitro* (Supplementary Figure 2G). Of note, GO analysis showed that dysfunction of CD8-GNLY effector T cells in MM accompanied by the cellular response to changes of external environment, evidenced by disturbed biological processes including "response to hydrogen peroxide', "mitochondrial translational termination", "cellular response to hypoxia" and "response to reactive oxygen species" (Figure 3G). Hypoxia and reactive oxygen species are the hallmarks of tumor microenvironment. "Mitochondrial translational termination" indicated the metabolism process of CD8-GNLY effector T cells in MM patients was interfered. PIM kinases *PIM2/3* and *KLRB1* overexpression as well as abnormal metabolism process in BM microenvironment were involved in the dysfunction of CD8-GNLY effector T cells in MM.

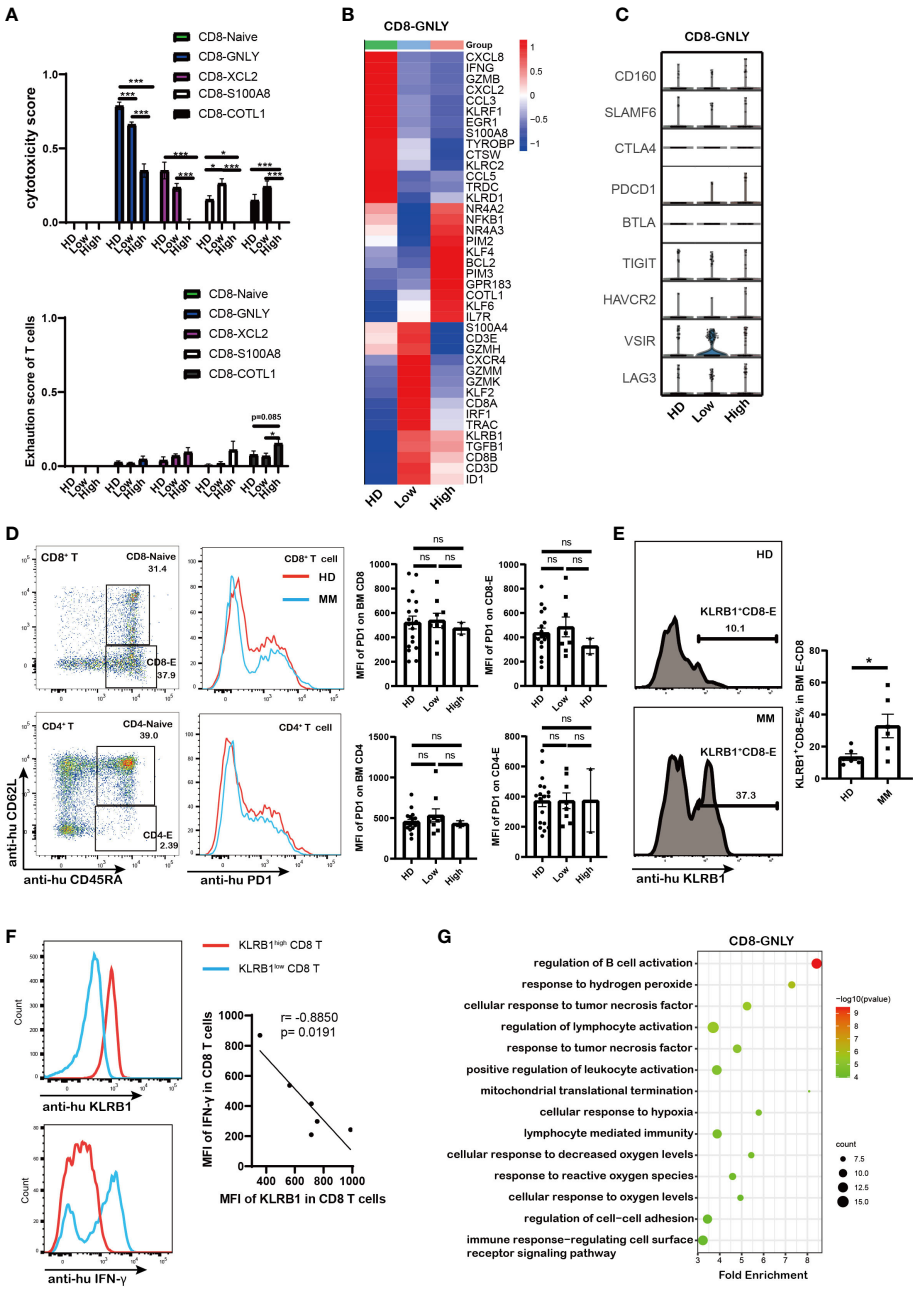

FIGURE 3
Dysfunction of CD8 T cells in high tumor burden group was associated with *PIM* kinases and *KLRB1* as well as the abnormal metabolism mediated by MM **(A)**. Bar charts shows the cytotoxicity scores and exhaustion scores of $CD8^+$ T cells from HD and MM patients in different infiltration groups (HD: n=6; Low: n=6; High: n=6). **(B)**. Heatmap shows the DEGs in CD8-GNLY among HD and MM patients in different infiltration groups (HD: n=6; Low: n=6; High: n=6). **(C)**.Violin plots display gene expression of classical immune checkpoints in CD8-GNLY cell clusters from HD and different MM conditions (HD: n=6; Low: n=6; High: n=6). **(D)**. Flow cytometry analysis shows the expression of PD1 on bone marrow $CD8^+$T cells and $CD4^+$T cells from HD and MM patients (HD: n=18; Low: n=8; High: n=2). **(E)**. Flow cytometry plots and bar chart show the proportion of $KLRB1^+CD8^+$-Effector T cells in CD8-Effector cells from HD and MM patients (HD: n=6; Low: n=6). CD8-Effector: $CD3^+CD8^+CD45RA^+CD62L^-$; **(F)**. Flow cytometry plots and dot plot show the correlation between KLRB1 expression and IFN-γexpression in CD8 T cells from MM patients activated by Cell Activation Cocktail (with Brefeldin A) *in vitro*. (n=6) **(G)**. Scatter plot of Gene Ontology (GO) Enrichment statistics shows the enriched GO terms in DEGs of CD8-GNLY among HD and MM groups. The y-axis indicates different GO terms and the x-axis indicates the Fold Enrichment. The color and size of the dots represent the range of the −log10 (p value) and the number of DEGs mapped to the indicated pathways, respectively. DEGs, Differentially expressed genes. In all instances, $p < 0.05$ was considered significant, * $p < 0.05$ and *** $p < 0.001$. ns, no significance.

PIM1, KLRC1 and abnormal metabolic processes were involved in defective NK cells induced by high tumor infiltration

NK cell is another critical cytotoxicity immune cell population. Here we investigated NK sub-populations in MM patients (except to MM25BM, in which no NK was detected). The *PTPRC*$^{+}$ *KLRF1*$^{+}$ NK cells from HD controls and 11 MM patients were analyzed, and they were divided into six sub-populations by tSNE analysis (Figure 4A and Supplementary Figure 3A). According to the marker gene signature as described in previous reports (29, 42), they were identified as NK-

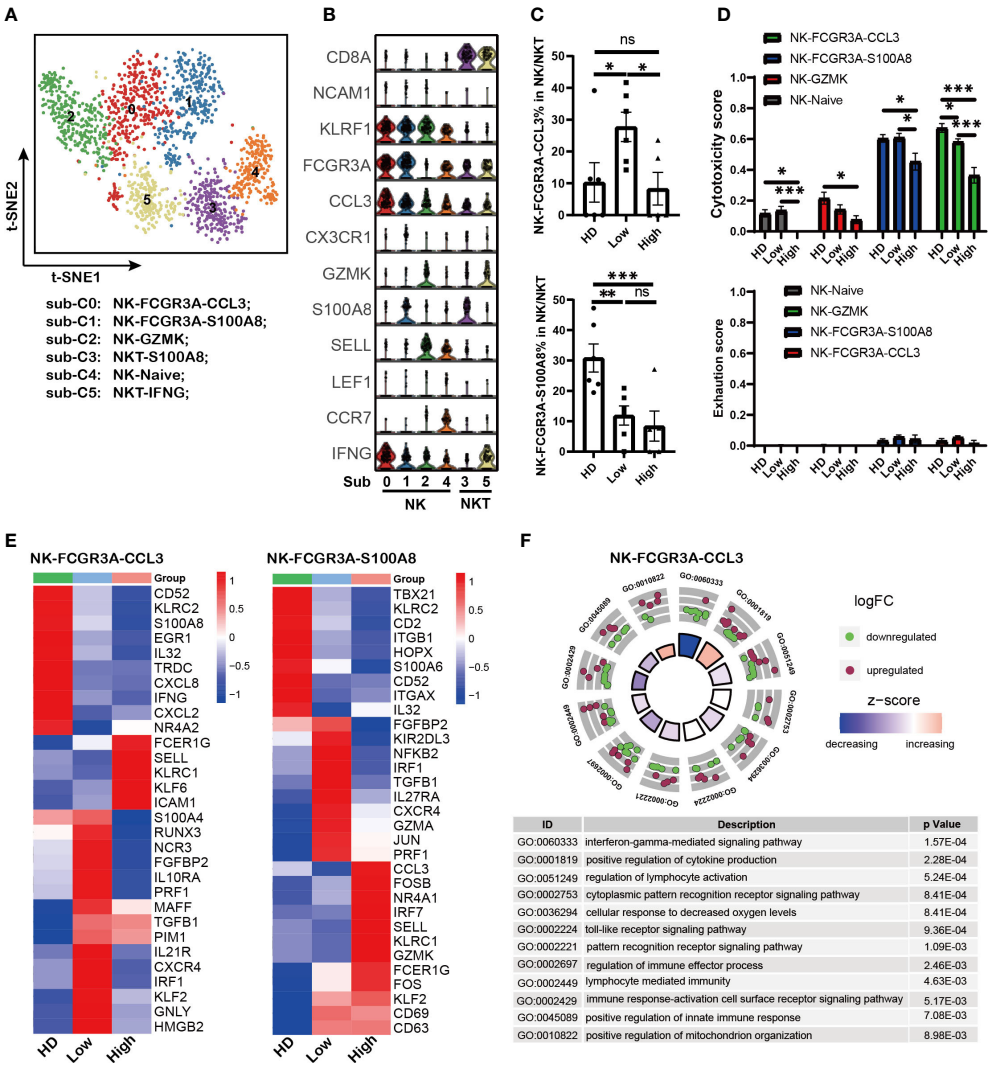

ID	Description	p Value
GO:0060333	interferon-gamma-mediated signaling pathway	1.57E-04
GO:0001819	positive regulation of cytokine production	2.28E-04
GO:0051249	regulation of lymphocyte activation	5.24E-04
GO:0002753	cytoplasmic pattern recognition receptor signaling pathway	8.41E-04
GO:0036294	cellular response to decreased oxygen levels	8.41E-04
GO:0002224	toll-like receptor signaling pathway	9.36E-04
GO:0002221	pattern recognition receptor signaling pathway	1.09E-03
GO:0002697	regulation of immune effector process	2.46E-03
GO:0002449	lymphocyte mediated immunity	4.63E-03
GO:0002429	immune response-activation cell surface receptor signaling pathway	5.17E-03
GO:0045089	positive regulation of innate immune response	7.08E-03
GO:0010822	positive regulation of mitochondrion organization	8.98E-03

FIGURE 4
PIM1, KLRC1 and abnormal metabolism processes were involved in defective NK cells induced by high tumor burden **(A)**. t-SNE shows the NK cell sub-clusters from HD and MM patients. Cells with high expression of PTPRC and KLRF1 were selected as NK/NKT cells. Each dot represents a single cell; colors indicate cell clusters with numbered labels. **(B)**.Violin plots show the expression and distribution of classical cell markers of NK sub-clusters. The sub-cluster numbers in the graph bottom correspond to the ones in (A). Sub-C0: NK-FCGR3A-CCL3; sub-C1: NK-FCGR3A-S100A8; sub-C2; NK-GZMK; sub-C3: NKT-S100A8; sub-C4: NK-NAÏVE; sub-C5; NKT-IFNG-CX3CR1 **(C)**. Bar charts show the proportion of NK cell sub-clusters from HD and MM patients in different infiltration groups (HD: n=7; Low: n=6; High: n=6). **(D)**. Bar charts show the cytotoxicity scores and exhaustion scores of NK cell sub-clusters from HD and MM patients in different infiltration groups (HD: n=7; Low: n=6; High: n=6). **(E)**. Heatmaps shows the DEGs of NK-FCGR3A-CCL3 and NK-S100A8 among HD and MM patients in different infiltration groups. **(F)**. GO Enrichment of DEGs in NK-FCGR3A-CCL3 between MM patients with high tumor burden and low tumor burden. Each dot in the graphs represents a single gene from DEGs. Upregulated genes are indicated as red dots and downregulated genes are indicated as blue dots. The color bar indicates the z-score of each pathway. In all instances, $p < 0.05$ was considered significant, * $p < 0.05$, ** $p < 0.01$ and *** $p < 0.001$. ns, no significance.

FCGR3A-CCL3 (sub-cluster 0), NK-FCGR3A-S100A8 (sub-cluster 1), NK-GZMK (sub-cluster 2), NKT-S100A8 (sub-cluster 3), NK-Naïve (sub-cluster 4) and NKT-IFNG (sub-cluster 5) (Figure 4B). Of note, the sub-population composition of NK cell displayed biological heterogeneity among MM patients (Supplementary Figure 3B). The proportion of NK-FCGR3A-CCL3 cells in MM patients was negatively correlation with tumor infiltration, which was similar to that observed in effector CD8-GNLY T cells as described above. It was the higher extent of tumor infiltration in MM patients, the lower proportion of NK-FCGR3A-CCL3 cells (Figure 4C). The proportion of NK-FCGR3A-S100A8 decreased along with tumor infiltration increase in myeloma microenvironment (Figure 4C). Furthermore, cytotoxicity scores analysis showed that NK-FCGR3A-CCL3 and NK-FCGR3A-S100A8 presented higher cytotoxicity scores (Figure 4D), which could be defined as cytotoxicity NK cells. In patients with high tumor infiltration, the cytotoxicity of NK-FCGR3A-CCL3 and NK-FCGR3A-S100A8 cells significantly decreased. Consistent with cytotoxicity CD8 T cells, we did not observe the significant increase of NK cell exhaustion as well (Figure 4D).

In addition, the transcriptomic profiles showed that both the NK-FCGR3A-CCL3 and NK-FCGR3A-S100A8 in BM with low tumor infiltration expressed high level of CXCR4 compared to the corresponding sub-clusters in HD and high infiltration group (Figure 4E). This data hints us that up-regulation of *CXCR4* should be associated with the higher proportion of NK-FCGR3A-CCL3 and NK-FCGR3A-S100A8 in MM patients with low tumor infiltration. Of note, both of the NK sub-clusters from the high tumor infiltration group expressed high levels of *KLRC1*, a key inhibitory receptor for NK cells (Figure 4E), which suggested that *KLRC1* up-regulation may be a critical factor in the dysfunction of NK cells. Interestingly, the level of *PIM1* significantly increased in NK-FCGR3A-CCL3 from both high infiltration group and low infiltration group compared to HD. These findings further supported that *PIM* family members play key roles in immunosuppression induced by MM cells. GO analysis based on DEGs of NK-FCGR3A-CCL3 across MM patients indicated that NK-FCGR3A-CCL3 from high tumor infiltration group displayed impaired "interferon-gamma mediated signaling pathway", "cellular response to decreased oxygen levels" and "positive regulation of mitochondrion organization" (Figure 4F). Meanwhile, NK-S100A8 from high tumor infiltration group displayed enhanced "hydrogen peroxide metabolic process", "hydrogen peroxide catabolic process" and "reactive oxygen species metabolic process" as well as impaired "response to interferon-gamma" and "regulation of superoxide anion generation" (Supplementary Figure 3C). These results demonstrated that the defective NK sub-clusters in myeloma microenvironment presented aberrant metabolism patterns compared to the corresponding sub-clusters in HD, which should be the results of NK responding to the extracellular environment.

Impaired antigen presentation of DCs contributed to T cell dysfunction in MM

Professional antigen-presenting cells (APCs), including DCs and macrophages, play critical roles in triggering anti-tumor immunity by regulating the activity of T cells. Dysfunction of APCs could result in the reduced anti-tumor activity of T cells. To further clarify the role of APCs in the immunosuppression of MM patients, LYZ^{+} myeloid cells were analyzed based on the description of previous reports (28, 42). Sixteen sub-populations were clustered according to the marker genes expression (Figure 5A and Supplementary Figure 4A). There were four DC sub-clusters with expression of *CD1C, CLEC9A* or *LILRA4*, five monocytes sub-clusters with expression of *LYZ* and *CST3*, and five macrophages sub-clusters with co-expression of *LYZ, CST3, CD68*, and *CD163* (Figure 5B). Interesting, we found that sub-cluster 12 with co-expression of MM marker gene *SDC1* was uniquely found in MM patient samples.

Conventional DC (cDC) plays central roles in the initiation and maintenance of anti-tumor T cell immunity. Firstly, our data showed that cDC-CD1C-AREG (sub-cluster 4) with high level of CD1C was identified as type I cDC (cDC1) and cDC-CD14 (sub-cluster 11) was identified as type II cDC (cDC2) with expression of CLEC9A (Figure 5B), which was referred to previous reports (40, 43). Compared to HD samples, the proportions of cDC-CD14 were reduced in MM patients, meanwhile there was no difference for cDC-AREG across HD and patient groups (Figure 5C). To evaluate the function of DC, the active scores of cDC sub-clusters (44) were calculated. The activity of cDC-CD1C-AREG in low tumor infiltration group was higher than that in HD and high tumor infiltration group (Figure 5D). This was further supported by the high levels of MHC I/II molecules (*HLA–B, HLA-C, HLA-DRB1* and *HLA-DQA1*) expressed in cDC-CD1C-AREG from low tumor infiltration group as well as inflammatory cytokines and chemokines (*IL1B, VEGF and CCL4, etc.*) (Figure 5E). And cDC-CD1C-AREG sub-cluster in high tumor infiltration group expressed low level of genes mentioned above, including *HLA–B, HLA-C, HLA-DRB1, HLA-DQA1, IL1B, VEGF and CCL4*, which like the unstimulated cDC-CD1C-AREG in HD (Figure 5E). These findings suggest that antigen presentation of cDC-CD1C-CD1C-AREG was still efficiently triggered in low tumor infiltration microenvironment, but suppressed along with the increased tumor cells. Notably, the variation pattern of activity of cDC-CD1C-AREG across HD and patient groups was consistent with that in CD8-GNLY cells as we described above. GO analysis revealed the significant variation of

10.3389/fimmu.2022.1077768

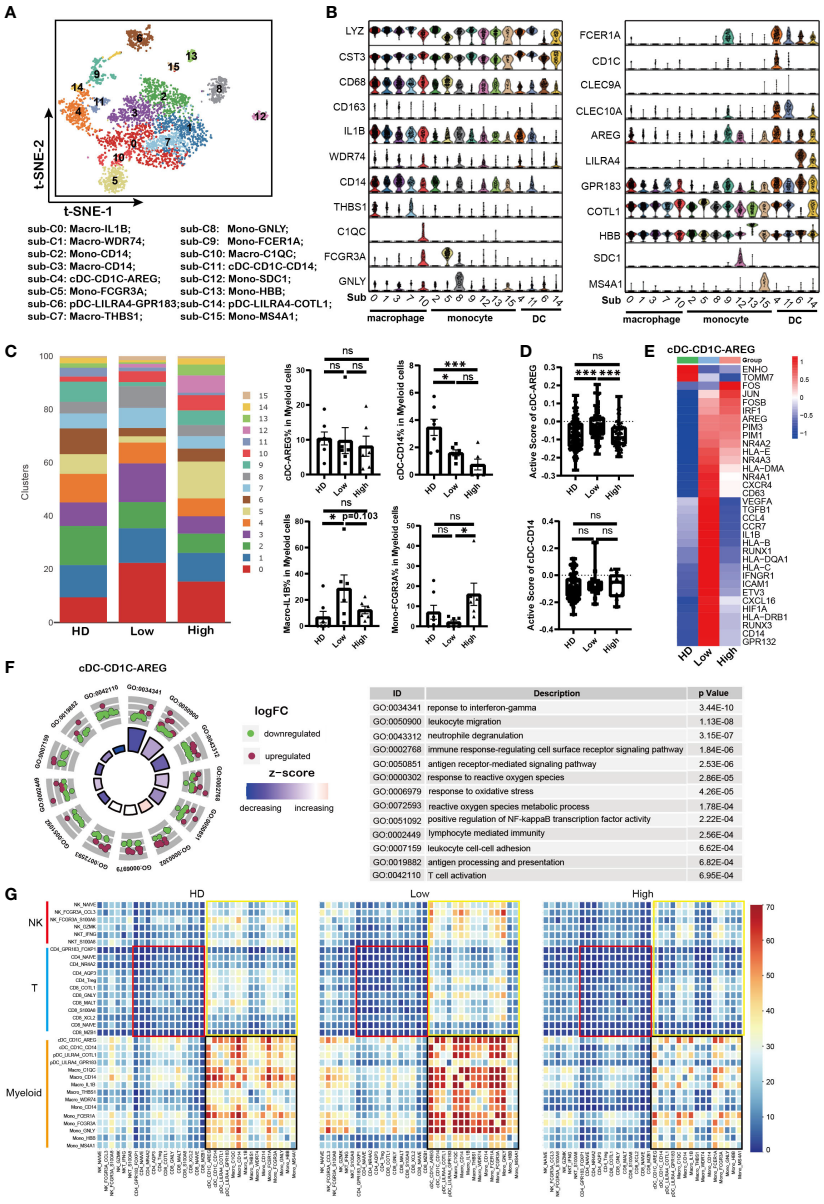

FIGURE 5
Impaired antigen presentation of DCs contributed to T cell dysfunction in MM **(A)**. t-SNE plot shows the sub-clusters of myeloid cells derived from HD and MM cells. Myelocyte (Cluster 4, 13 and 16 identified above) were selected for this analysis. Each dot represents a single cell; colors indicate cell clusters with numbered labels. **(B)**. Violin plots show the expression and distribution of classical cell markers in sub-clusters of myeloid cells from HD and MM patients. The sub-cluster numbers in the graph bottom correspond to the ones in **(A)**. sub-C0: Macro-IL1B; sub-C1: Macro-WDR74; sub-C2: Mono-CD14; sub-C3: Macro-CD14; sub-C4: cDC-CD1C-AREG; sub-C5: Mono-FCGR3A; sub-C6: pDC-LILRA4-GPR83; sub-C7: Macro-THBS1; sub-C8: Mono-GNLY; sub-C9: Mono-FCER1A; sub-C10: Macro-C1QC; sub-C11: cDC-CD1C-CD14; sub-C12: Mono-SDC1; sub-C13: Mono-HBB; sub-C14: pDC-LILRA4-COTL1; sub-C15: Mono-MS4A1; **(C)**. Bar charts show the proportion of myeloid sub-clusters among HD and different groups of MM patients. The sub-cluster numbers in right correspond to the ones in **(A)**. (HD: n=7; Low: n=6; High: n=6). **(D)**. Bar charts show the active scores of cDC among HD and different groups of MM patients (HD: n=7; Low: n=6; High: n=6). **(E)**. Heatmap shows the DEGs in cDC-CD1C-AREG among HD and different infiltration groups of MM patients. **(F)**. GO Enrichment of DEGs in cDC-CD1C-AREG between high-infiltration and low-infiltration groups of MM patients. Each dot in the graphs represents a single gene from DEGs. Upregulated genes are indicated as red dots and downregulated genes are indicated as blue dots. The color bar indicates the z-score of each pathway. **(G)**. Heatmap shows the interaction strength among immune cells across HD and MM groups. The color showed the interaction strength that was calculated by CellPhoneDB. Black box: the interaction among myeloid cells; Yellow box: the interaction among myeloid cells and T/NK cells; Red box: interaction among T cells. In all instances, $p < 0.05$ was considered significant, * $p < 0.05$ and *** $p < 0.001$. ns, no significance.

biological processes in cDC-AREG in high tumor infiltration group, including "response to interferon-gamma", "response to reactive oxygen species" and "reactive oxygen species metabolic process" (Figure 5F). These results demonstrated that the metabolism pattern of cDC-CD1C-AREG was influenced by high level of tumor cells. Moreover, we also found up-regulation of PIM family members (*PIM1*/*PIM3*) in cDC-CD1C-AREG from MM patients compared to HDs (Figure 5E). By contrast, the activity of cDC-CD14 remained stable across HD and patient groups (Figure 5D), though the proportion of the sub-cluster was significantly reduced in MM patients.

Monocytes/Macrophages are another major component of the innate immune system and involved in anti-tumor activity of T cells as APCs. Next, our data showed that macrophage-IL1B (sub-cluster 0) in tumor cell high tumor infiltration group not only displayed a lower proportion (Figure 5C), but also strikingly lacked the expression of MHC molecules, inflammatory cytokines and chemokines compared to the corresponding sub-cluster in low tumor infiltration group (Supplementary Figure 4B). The results demonstrated that macrophage-IL1B and macro-WDR74 were activated in low tumor cell microenvironment, which promoted the anti-MM immunity. However, macrophages became to be in a resting state when MM cells infiltration increased (Supplementary Figure 4B). Conversely, there was a higher proportion of Mono-FCGR3A (sub-cluster 5) in high tumor cell microenvironment compared to low tumor cell group and HDs (Figure 5C). However, Mono-FCGR3A in high tumor infiltration group expressed lower levels of MHC molecules, inflammatory cytokines and chemokines (*HLA-DRB1/HLA-DPB1, TNF, IL1B, CCL3* and *CCL4*), which meant the sub-cluster was less involved in immune responses (Supplementary Figure 4C). Meanwhile, Mono-FCGR3A both in high and low tumor infiltration group expressed high level of *PIM2/PIM3* compared to HDs (Figure 5G). Therefore, the activities of cDC-CD1C-AREG, macrophage-IL1B and Mono-FCGR3A in low tumor infiltration group were elevated as innate immune cells and APCs, but suppressed in high tumor infiltration group.

Repressed crosstalk among immune cells was involved in immunosuppressive microenvironment

Crosstalk among immune cells is necessary in regulating the immune response to tumor or infection. So far, immune cell crosstalk in MM microenvironment has not been fully understood. Here, we investigated the dynamic immune cell crosstalk along with tumor cell infiltration. Our data showed that the interaction among myeloid cells was strongest in each group, including DC, macrophages and monocytes (Figure 5G, black box). Whereas, the interaction among myeloid cells in low tumor infiltration group was significantly strengthened, but weakened in high tumor infiltration group. In addition, myeloid cells kept active communications with T and NK cells (Figure 5G, yellow box). The interaction between T cells and myeloid cells was compromised in high tumor infiltration group (Figure 5G), and the weakest interaction existed among T cells across HD and MM patients (Figure 5G, red box). These results suggest that myeloid cells are the core player in immune cells crosstalk, and the interactions among immune cells in MM were active in low tumor infiltration group, but suppressed in high tumor infiltration group.

Aberrant metabolism of immune cells identified in MM microenvironment with high tumor cell infiltration

Mounting evidence indicates that the aberrant metabolism of immune cells is involved in tumorgenesis (45–47). Here, our analysis showed that effector CD8 T cells and NK cells in high tumor infiltration group displayed unique metabolic features compared to the corresponding sub-clusters in low tumor infiltration group and HDs (Figures 6A, B). Further analysis showed that the immune cell sub-clusters from high tumor infiltration group shared common metabolic pathways. As the key players in anti-tumor immunity, the impaired amino acid metabolism in CD8-GNLY effector T cells and CD8-XCL2 memory T cells was found in high tumor cell microenvironment, including Arginine, Proline, Glycine, Serine, Threonine, Valine, Leucine, Isoleucine and Histidine metabolism shown in Figure 6A. Meanwhile, they displayed enhanced glycolysis/gluconeogenesis, oxidative phosphorylation and lipid metabolism. Besides, CD8-GNLY effector T cells in high tumor infiltration group presented enhanced citrate cycle (TCA cycle), which was different from CD8-XCL2 memory T cells in high tumor infiltration group. Similar to effector CD8 T cells, NK-FCGR3A-CCL3 and NK-FCGR3A-S100A8 in high tumor cell infiltration displayed part of impaired amino acid metabolism as well as enhanced oxidative phosphorylation and lipid metabolism (Figure 6B). Glycolysis/Gluconeogenesis and citrate cycle (TCA cycle) in NK-FCGR3A-CCL3 were enhanced in high tumor cell infiltration group but weakened in NK-FCGR3A-S100A8. Unlike CD8 T and NK cells, the metabolic pattern on myeloid cells in high tumor cell infiltration group was similar to the corresponding one in HD (Figure 6C). This is consistent with the active status of myeloid cells as mentioned above. Further analysis showed that cDC-CD1C-AREG in high tumor cell infiltration group displayed enhanced lipid metabolism, oxidative phosphorylation, glycolysis/gluconeogenesis and citrate cycle (TCA cycle) compared to the one in low tumor cell infiltration group. Macrophages-IL1B in high tumor cell infiltration group

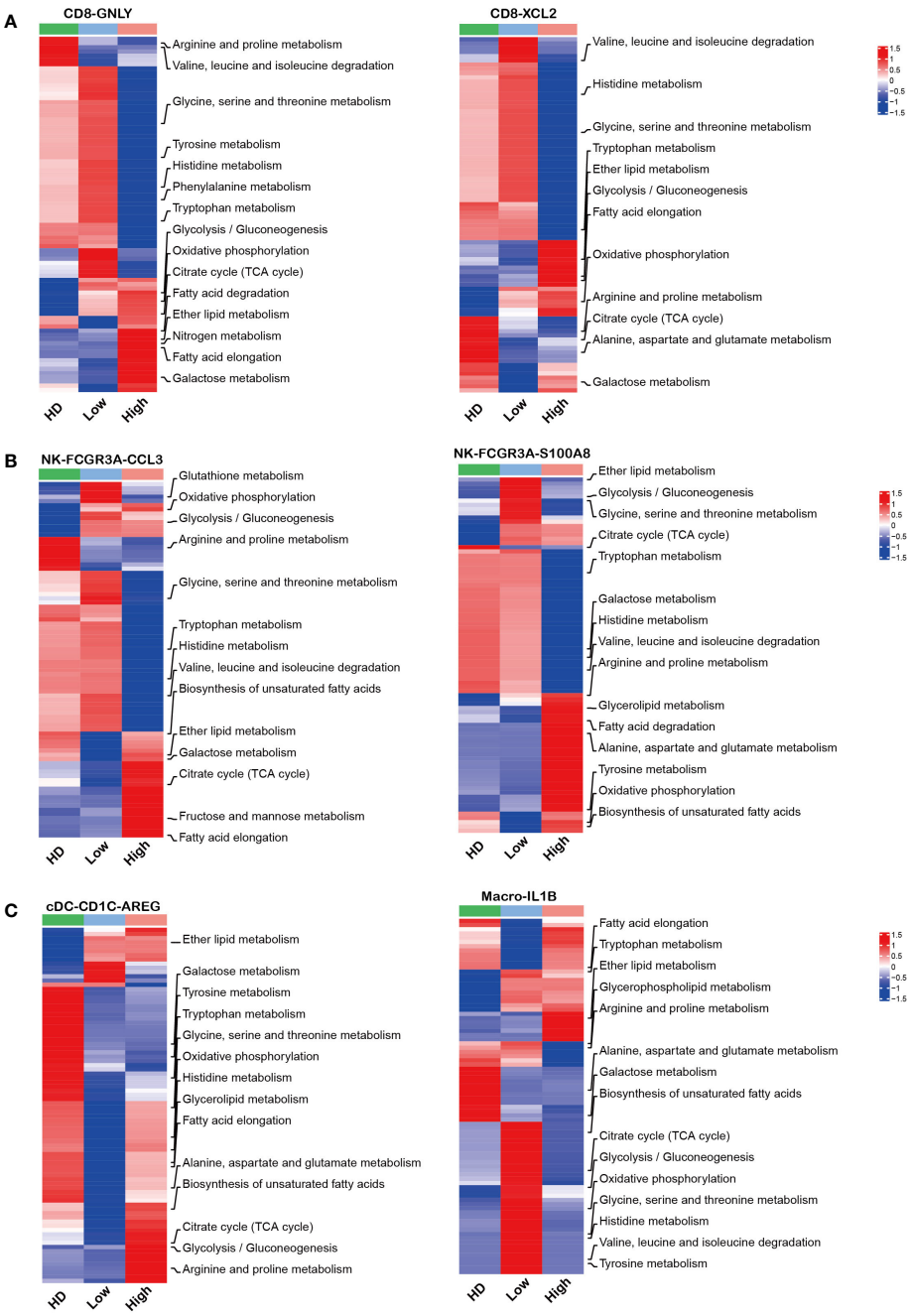

FIGURE 6
Aberrant metabolism of immune cells in MM patients with high tumor burden **(A–C)**: Heatmap charts show the different metabolic pathways in each sub-clusters across HD and MM groups.

exhibited enhanced lipid metabolism and weakened oxidative phosphorylation, glycolysis/gluconeogenesis, citrate cycle (TCA cycle) and amino acid metabolism compared to the corresponding sub-clusters in low tumor cell infiltration group (Figure 6C). The variation of metabolic pathways in immune cells according to diverse tumor cell infiltration suggested that the disordered metabolism also induced the dysfunction of immune cells in MM microenvironment.

Discussion

In this study, we pay close attention to the immune response in MM, and investigated the underlying mechanisms on dysfunction of immune cells associated with tumor infiltration using the unbiased single cell RNA sequencing. Of note, the anti-tumor immune response is active in patients with low tumor cells, but it was notably suppressed with the elevation of tumor cells. The proportion of cytotoxic immune cells (CD8-GNLY effector T cells and NK-FCGR3A-CCL3 cells) increased in myeloma microenvironment when tumor cell infiltration was low, then the activated immune cells were depressed with the growth of tumor cells. This finding is partially supported by the previous reports (22) (48), and indicated the efficient anti-tumor immunity is an external critical factor for tumor cells behavior beside the internal cytogenetic characteristics of MM cells. Intriguingly, we observed a significantly elevation of CD8-XCL2 memory T cells in MM patients compared to HDs. In consideration of the decreased CD8 effector T cells in high tumor infiltration group, we have reason to believe that the differentiation of memory CD8 T cells to effector CD8 T cells was obviously interfered by MM cell. More important, our study demonstrated that the interactions among immune cells were remarkably strengthened at the beginning of disease occurrence with low tumor cells infiltration, but suppressed with the elevation of tumor cell infiltration in BM microenvironment.

Prior studies already demonstrated the immunosuppressive state of BM microenvironment in MM patients, including exhaustion (49, 50) and senescence (10) of T cells and increased Treg (13). However, we did not find significant difference on the proportion of CD8-COTL1 exhaustion T cell among MM groups and HDs, which is in line with the reports by Oksana Zavidij (22) and Carolina (51). Moreover, we did not observe the significant increase of PD1, LAG3, TIGIT, the classic immune checkpoints, on immune cells, which could help us to explain the reason of the unfavorable treatment efficacy of immune checkpoint inhibitors in MM clinic practices. Strikingly, our study identified that serine/threonine kinases *PIM* family (*PIM1/2/3*) would play a pivotal role in myeloma immunosuppression. The up-regulation of *PIM* family member, *PIM1/2/3*, was observed in CD8-GNLY effector T cells, NK-FCGR3A-CCL3, cDC-CD1C-AREG and monocyte-FCGR3A. More and more studies demonstrated *PIM* kinases are constitutively active serine/threonine kinases that play important roles in hematological malignancies (52), including MM (53). Inhibition of PIM kinase displayed significant anti-tumor efficacy in MM (54). Recently, the role of *PIM* family on immune regulation was reported as well. *PIM* kinases were involved in the immunotherapeutic antitumor T-cell response (55, 56). In addition to T and NK cells, the function of DC and MDSC were also regulated by *PIM* kinases (57, 58). Our data also showed that inhibiting PIM kinases could promote the cytotoxicity of $CD8^+$ T cells *in vitro*. These findings by us and other research groups strongly support that *PIM* kinases are more critical in immune suppression mediated by MM cells. Therefore, *PIM* kinases targeted therapy would be an attractive strategy in MM treatment by both inhibiting MM proliferation and activating anti-tumor immunity. In addition, we noted that the overexpression of *KLRB1* (*CD161*) in CD8-GNLY effector T cells and *KLRC1* (*NKG2A*) overexpression in NK-FCGR3A-CCL3 cells. We confirmed the association of KLRB1 with the cytotoxicity of CD8 T from MM patients. Sun et al. reported that $CD8^+KLRB1^+$ T cells displayed weaker cytotoxicity than $CD8^+KLRB1^-$ T cells in hepatocellular carcinoma-infiltrated CD8 T cells (28). Mathewson and colleagues further identified *KLRB1* as an inhibitory receptor for tumor-specific T cells (59). *KLRC1* is an inhibitory receptor for NK cells, which forms a heterodimer with CD94. Preclinical and clinical investigations have provided evidence that CD94/KLRC1 inhibition is a viable therapeutic option for numerous tumors, including chronic lymphoid leukemia and lymphoma (60, 61). All of these findings support that overexpression of *KLRB1* and *KLRC1* in CD8 effector cells and NK cells would be pay more attention in immune cell dysfunction in MM.

Recently, more and more studies elucidate that metabolic plasticity and its ability to adapt to stress conditions play important roles in cancer immunology. The production of immunosuppressive metabolites and the imbalance of nutrient caused by chaotic proliferation of tumor cells could induce dysfunction of immune cells in tumor microenvironment (19, 62–67). PIM kinases are also involved in numerous intercellular metabolic processes of immune cells (56–58). Xin et al. uncovered a previously underappreciated role of PIM1 in regulating lipid oxidative metabolism *via* PPARγ-mediated activities, and sufficiently rescued metabolic and functional defects of $Pim1^{-/-}$ MDSCs (58). In the present study, the impaired amino acid metabolism was observed in CD8-GNLY effector T cell and CD8-XCL2 memory T cells, especially in high tumor cell microenvironment. ntracellular arginine in T cells is important for the promotion of oxidative metabolism, increasing cell viability, persistence, and *in vivo* antitumor response (68, 69). Eric et al. showed that intracellular serine directly modulates adaptive immunity by regulating T cell proliferation and cell viability (70). Consistently, these reports support our results that the impaired amino acid metabolism was involved in the dysfunction of CD8-GNLY effector T cells in MM immune microenvironment. Huang and colleagues reported that amino acid transporter controlled the magnitude of memory T cell generation and persistence by stimulating mTORC1 signaling, which indicates that amino acid is important for memory T cells differentiation (71). Hereby, we speculated the impaired amino acid metabolism resulted in the elevation of CD8 memory T cells in MM microenvironment by hindering differentiation of memory T to effector T cells.

Additionally, our data demonstrated that the notably enhanced lipid metabolism in cytotoxicity NK sub-clusters in high level tumor cell infiltration was involved in the NK cell impairment, which in line with the phenotype in aggressive B-cell lymphoma (72). Accumulation of lipids caused by abnormal fatty acid synthesis is

associated with dendritic cell dysfunction (73). Enhanced biosynthesis of glycosphingolipid, fatty acid and unsaturated fatty acids were observed in our study, which would be associated with the dysfunction of cDC-CD1C-AREG in MM patients with high tumor cell infiltration. Of note, *PIM* kinases up-regulated in immune cells, including effector CD8 T cell, NK cells and DC from MM patients, were also associated with the activity of mammalian target of rapamycin (mTOR) signaling. As metabolic checkpoints, mTOR signaling integrate signals from oxygen, energy and nutrients to regulate protein synthesis and anabolic metabolism. Therefore, our results support that targeting PIM kinases would be a rational strategy to rescue the function of immune cells *via* metabolism regulation. However, more direct evidence is needed to uncover the role of PIM kinases in immune response *via* regulating metabolism and the underlying mechanisms. We will pay more attention to those in the future.

In summary, our present study elucidates the biological heterogeneity of immune microenvironment in MM BM with diverse tumor cell infiltration at single cell resolution. Disordered amino acids and lipid metabolism in immune cells under the microenvironment of MM promote the dysfunction of immune cells and defective immune response in myeloma. Targeting *PIM* kinases could be a promising strategy for MM immunotherapy, and redressing the disordered metabolism would be the key points to get effects in immune-based therapies.

Data availability statement

The data presented in the study are deposited in the Genome Sequence Archive (GSA) repository (https://bigd.big.ac.cn/gsa-human/browse/HRA003504), BioProject ID: PRJCA013382, accession ID: HRA003504.

Ethics statement

The studies involving human participants were reviewed and approved by the Institutional Ethics Review Boards from the Institute of Hematology and Blood Diseases Hospital, Chinese Academy of Medical Sciences and Peking Union Medical College (Protocol code: NSFC-2021012-EC-2). The patients/participants provided their written informed consent to participate in this study. The animal study was reviewed and approved by the Institutional Animal Care and Use committees of the Institute of Hematology and Blood Diseases Hospital, Chinese Academy of Medical Sciences and Peking Union Medical College (Protocol code: KT2020010-EC-2).

Author contributions

Conception and design, LQ and MH. Collection and assembly of data, JL, HS, LG, XW, YH, ZYu, LL, GA, WS, YX, SD, SY, ZYa, and MH. Data analysis and interpretation, JL, HS, LG, and MH. Manuscript writing, JL, HS, LG, LQ, and MH. Final approval for the manuscript submission, LQ and MH. All authors contributed to the article and approved the submitted version.

Funding

This work was supported by the Natural Science Foundation of China (81920108006, 82170194) and CAMS Innovation Fund for Medical Sciences (CIFMS) (2021-I2M-1-040, 2022-I2M-1-022).

Acknowledgments

We sincerely thank the support from Cong Li (BasenByte) for data analysis.

Conflict of interest

The authors declare that the research was conducted in the absence of any commercial or financial relationships that could be construed as a potential conflict of interest.

Publisher's note

Supplementary material

The Supplementary Material for this article can be found online at: https://www.frontiersin.org/articles/10.3389/fimmu.2022.1077768/full#supplementary-material

References

1. Palumbo A, Anderson K. Multiple myeloma. *N Engl J Med* (2011) 364 (11):1046–60. doi: 10.1056/NEJMra1011442

2. Rajkumar SV. Multiple myeloma: 2022 update on diagnosis, risk stratification, and management. *Am J Hematol* (2022) 97(8):1086–107. doi: 10.1002/ajh.26590

3. Yu Z, Wei X, Liu L, Sun H, Fang T, Wang L, et al. Indirubin-3'-Monoxime acts as proteasome inhibitor: Therapeutic application in multiple myeloma. *EBioMedicine* (2022) 78:103950. doi: 10.1016/j.ebiom.2022.103950

4. Manier S, Salem KZ, Park J, Landau DA, Getz G, Ghobrial IM. Genomic complexity of multiple myeloma and its clinical implications. *Nat Rev Clin Oncol* (2017) 14(2):100–13. doi: 10.1038/nrclinonc.2016.122

5. Yan Y, Qin X, Liu J, Fan H, Yan W, Liu L, et al. Clonal phylogeny and evolution of critical cytogenetic aberrations in multiple myeloma at single-cell level by qm-fish. *Blood Adv* (2022) 6(2):441–51. doi: 10.1182/bloodadvances.2021004992

6. Hao M, Franqui-Machin R, Xu H, Shaughnessy JJr., Barlogie B, Roodman D, et al. Nek2 induces osteoclast differentiation and bone destruction *Via* heparanase in multiple myeloma. *Leukemia* (2017) 31(7):1648–50. doi: 10.1038/leu.2017.115

7. Dutta AK, Fink JL, Grady JP, Morgan GJ, Mullighan CG, To LB, et al. Subclonal evolution in disease progression from Mgus/Smm to multiple myeloma is characterised by clonal stability. *Leukemia* (2019) 33(2):457–68. doi: 10.1038/s41375-018-0206-x

8. Nakamura K, Smyth MJ, Martinet L. Cancer immunoediting and immune dysregulation in multiple myeloma. *Blood* (2020) 136(24):2731–40. doi: 10.1182/blood.2020006540

9. Rasche L, Hudecek M, Einsele H. What is the future of immunotherapy in multiple myeloma? *Blood* (2020) 136(22):2491–7. doi: 10.1182/blood.2019004176

10. Suen H, Brown R, Yang S, Weatherburn C, Ho PJ, Woodland N, et al. Multiple myeloma causes clonal T-cell immunosenescence: Identification of potential novel targets for promoting tumour immunity and implications for checkpoint blockade. *Leukemia* (2016) 30(8):1716–24. doi: 10.1038/leu.2016.84

11. von Lilienfeld-Toal M, Frank S, Leyendecker C, Feyler S, Jarmin S, Morgan R, et al. Reduced immune effector cell Nkg2d expression and increased levels of soluble Nkg2d ligands in multiple myeloma may not be causally linked. *Cancer Immunol Immunother* (2010) 59(6):829–39. doi: 10.1007/s00262-009-0807-3

12. Benson DMJr., Bakan CE, Mishra A, Hofmeister CC, Efebera Y, Becknell B, et al. The pd-1/Pd-L1 axis modulates the natural killer cell versus multiple myeloma effect: A therapeutic target for ct-011, a novel monoclonal anti-Pd-1 antibody. *Blood* (2010) 116(13):2286–94. doi: 10.1182/blood-2010-02-271874

13. Feng X, Zhang L, Acharya C, An G, Wen K, Qiu L, et al. Targeting Cd38 suppresses induction and function of T regulatory cells to mitigate immunosuppression in multiple myeloma. *Clin Cancer Res* (2017) 23(15):4290–300. doi: 10.1158/1078-0432.CCR-16-3192

14. Gorgun GT, Whitehill G, Anderson JL, Hideshima T, Maguire C, Laubach J, et al. Tumor-promoting immune-suppressive myeloid-derived suppressor cells in the multiple myeloma microenvironment in humans. *Blood* (2013) 121(15):2975–87. doi: 10.1182/blood-2012-08-448548

15. Leone P, Berardi S, Frassanito MA, Ria R, De Re V, Cicco S, et al. Dendritic cells accumulate in the bone marrow of myeloma patients where they protect tumor plasma cells from Cd8+ T-cell killing. *Blood* (2015) 126(12):1443–51. doi: 10.1182/blood-2015-01-623975

16. Minnie SA, Hill GR. Immunotherapy of multiple myeloma. *J Clin Invest* (2020) 130(4):1565–75. doi: 10.1172/JCI129205

17. Zanwar S, Nandakumar B, Kumar S. Immune-based therapies in the management of multiple myeloma. *Blood Cancer J* (2020) 10(8):84. doi: 10.1038/s41408-020-00350-x

18. Vinay DS, Ryan EP, Pawelec G, Talib WH, Stagg J, Elkord E, et al. Immune evasion in cancer: Mechanistic basis and therapeutic strategies. *Semin Cancer Biol* (2015) 35 Suppl:S185–98. doi: 10.1016/j.semcancer.2015.03.004

19. Reina-Campos M, Moscat J, Diaz-Meco M. Metabolism shapes the tumor microenvironment. *Curr Opin Cell Biol* (2017) 48:47–53. doi: 10.1016/j.ceb.2017.05.006

20. Dey P, Kimmelman AC, DePinho RA. Metabolic codependencies in the tumor microenvironment. *Cancer Discov* (2021) 11(5):1067–81. doi: 10.1158/2159-8290.CD-20-1211

21. Evans LA, Anderson EA, Jessen E, Nandakumar B, Atilgan E, Jevremovic D, et al. Overexpression of the energy metabolism transcriptome within clonal plasma cells is associated with the pathogenesis and outcomes of patients with multiple myeloma. *Am J Hematol* (2022) 97(7):895–902. doi: 10.1002/ajh.26577

22. Zavidij O, Haradhvala NJ, Mouhieddine TH, Sklavenitis-Pistofidis R, Cai S, Reidy M, et al. Single-cell rna sequencing reveals compromised immune microenvironment in precursor stages of multiple myeloma. *Nat Cancer* (2020) 1(5):493–506. doi: 10.1038/s43018-020-0053-3

23. Zhong L, Yang X, Zhou Y, Xiao J, Li H, Tao J, et al. Exploring the r-iss stage-specific regular networks in the progression of multiple myeloma at single-cell resolution. *Sci China Life Sci* (2022) 65(9):1811–23. doi: 10.1007/s11427-021-2097-1

24. Tirier SM, Mallm JP, Steiger S, Poos AM, Awwad MHS, Giesen N, et al. Subclone-specific microenvironmental impact and drug response in refractory multiple myeloma revealed by single-cell transcriptomics. *Nat Commun* (2021) 12 (1):6960. doi: 10.1038/s41467-021-26951-z

25. Liu R, Gao Q, Foltz SM, Fowles JS, Yao L, Wang JT, et al. Co-Evolution of tumor and immune cells during progression of multiple myeloma. *Nat Commun* (2021) 12(1):2559. doi: 10.1038/s41467-021-22804-x

26. Xu C, He J, Wang H, Zhang Y, Wu J, Zhao L, et al. Single-cell transcriptomic analysis identifies an immune-prone population in erythroid precursors during human ontogenesis. *Nat Immunol* (2022) 23(7):1109–20. doi: 10.1038/s41590-022-01245-8

27. Butler A, Hoffman P, Smibert P, Papalexi E, Satija R. Integrating single-cell transcriptomic data across different conditions, technologies, and species. *Nat Biotechnol* (2018) 36(5):411–20. doi: 10.1038/nbt.4096

28. Sun Y, Wu L, Zhong Y, Zhou K, Hou Y, Wang Z, et al. Single-cell landscape of the ecosystem in early-relapse hepatocellular carcinoma. *Cell* (2021) 184(2):404–21.e16. doi: 10.1016/j.cell.2020.11.041

29. Zhang JY, Wang XM, Xing X, Xu Z, Zhang C, Song JW, et al. Single-cell landscape of immunological responses in patients with covid-19. *Nat Immunol* (2020) 21(9):1107–18. doi: 10.1038/s41590-020-0762-x

30. Li H, van der Leun AM, Yofe I, Lubling Y, Gelbard-Solodkin D, van Akkooi ACJ, et al. Dysfunctional Cd8 T cells form a proliferative, dynamically regulated compartment within human melanoma. *Cell* (2019) 176(4):775–89.e18. doi: 10.1016/j.cell.2018.11.043

31. Ren X, Wen W, Fan X, Hou W, Su B, Cai P, et al. Covid-19 immune features revealed by a Large-scale single-cell transcriptome atlas. *Cell* (2021) 184(7):1895–913.e19. doi: 10.1016/j.cell.2021.01.053

32. Hanzelmann S, Castelo R, Guinney J. Gsva: Gene set variation analysis for microarray and rna-seq data. *BMC Bioinf* (2013) 14:7. doi: 10.1186/1471-2105-14-7

33. Ritchie ME, Phipson B, Wu D, Hu Y, Law CW, Shi W, et al. Limma powers differential expression analyses for rna-sequencing and microarray studies. *Nucleic Acids Res* (2015) 43(7):e47. doi: 10.1093/nar/gkv007

34. Wu T, Hu E, Xu S, Chen M, Guo P, Dai Z, et al. Clusterprofiler 4.0: A universal enrichment tool for interpreting omics data. *Innovation (Camb)* (2021) 2 (3):100141. doi: 10.1016/j.xinn.2021.100141

35. Vento-Tormo R, Efremova M, Botting RA, Turco MY, Vento-Tormo M, Meyer KB, et al. Single-cell reconstruction of the early maternal-fetal interface in humans. *Nature* (2018) 563(7731):347–53. doi: 10.1038/s41586-018-0698-6

36. Liu L, Yu Z, Cheng H, Mao X, Sui W, Deng S, et al. Multiple myeloma hinders erythropoiesis and causes anaemia owing to high levels of Ccl3 in the bone marrow microenvironment. *Sci Rep* (2020) 10(1):20508. doi: 10.1038/s41598-020-77450-y

37. Li Z, Liu L, Du C, Yu Z, Yang Y, Xu J, et al. Therapeutic effects of oligo-Single-Stranded DNA mimicking of hsa-Mir-15a-5p on multiple myeloma. *Cancer Gene Ther* (2020) 27(12):869–77. doi: 10.1038/s41417-020-0161-3

38. Walker BA, Mavrommatis K, Wardell CP, Ashby TC, Bauer M, Davies F, et al. A high-risk, double-hit, group of newly diagnosed myeloma identified by genomic analysis. *Leukemia* (2019) 33(1):159–70. doi: 10.1038/s41375-018-0196-8

39. Liao M, Liu Y, Yuan J, Wen Y, Xu G, Zhao J, et al. Single-cell landscape of bronchoalveolar immune cells in patients with covid-19. *Nat Med* (2020) 26 (6):842–4. doi: 10.1038/s41591-020-0901-9

40. Xu G, Qi F, Li H, Yang Q, Wang H, Wang X, et al. The differential immune responses to covid-19 in peripheral and lung revealed by single-cell rna sequencing. *Cell Discovery* (2020) 6:73. doi: 10.1038/s41421-020-00225-2

41. Wang HN, Yang J, Xie DH, Liang Z, Wang Y, Fu RY, et al. Single-cell rna sequencing infers the role of malignant cells in drug-resistant multiple myeloma. *Clin Transl Med* (2021) 11(12):e653. doi: 10.1002/ctm2.653

42. Zhang Q, He Y, Luo N, Patel SJ, Han Y, Gao R, et al. Landscape and dynamics of single immune cells in hepatocellular carcinoma. *Cell* (2019) 179 (4):829–45.e20. doi: 10.1016/j.cell.2019.10.003

43. Chen YP, Yin JH, Li WF, Li HJ, Chen DP, Zhang CJ, et al. Single-cell transcriptomics reveals regulators underlying immune cell diversity and immune subtypes associated with prognosis in nasopharyngeal carcinoma. *Cell Res* (2020) 30(11):1024–42. doi: 10.1038/s41422-020-0374-x

44. Cheng S, Li Z, Gao R, Xing B, Gao Y, Yang Y, et al. A pan-cancer single-cell transcriptional atlas of tumor infiltrating myeloid cells. *Cell* (2021) 184(3):792–809.e23. doi: 10.1016/j.cell.2021.01.010

45. Li S, Yu J, Huber A, Kryczek I, Wang Z, Jiang L, et al. Metabolism drives macrophage heterogeneity in the tumor microenvironment. *Cell Rep* (2022) 39 (1):110609. doi: 10.1016/j.celrep.2022.110609

46. Best SA, Gubser PM, Sethumadhavan S, Kersbergen A, Negron Abril YL, Goldford J, et al. Glutaminase inhibition impairs Cd8 T cell activation in Stk11-/Lkb1-Deficient lung cancer. *Cell Metab* (2022) 34(6):874–87. doi: 10.1016/j.cmet.2022.04.003

47. Giovanelli P, Sandoval TA, Cubillos-Ruiz JR. Dendritic cell metabolism and function in tumors. *Trends Immunol* (2019) 40(8):699–718. doi: 10.1016/j.it.2019.06.004

48. Ryu D, Kim SJ, Hong Y, Jo A, Kim N, Kim HJ, et al. Alterations in the transcriptional programs of myeloma cells and the microenvironment during extramedullary progression affect proliferation and immune evasion. *Clin Cancer Res* (2020) 26(4):935–44. doi: 10.1158/1078-0432.CCR-19-0694

49. Zelle-Rieser C, Thangavadivel S, Biedermann R, Brunner A, Stoitzner P, Willenbacher E, et al. T Cells in multiple myeloma display features of exhaustion and senescence at the tumor site. *J Hematol Oncol* (2016) 9(1):116. doi: 10.1186/s13045-016-0345-3

50. Minnie SA, Kuns RD, Gartlan KH, Zhang P, Wilkinson AN, Samson L, et al. Myeloma escape after stem cell transplantation is a consequence of T-cell exhaustion and is prevented by tigit blockade. *Blood* (2018) 132(16):1675–88. doi: 10.1182/blood-2018-01-825240

51. Schinke C, Poos AM, Bauer MA, John L, Johnson SK, Deshpande S, et al. Characterizing the role of the immune microenvironment in multiple myeloma progression at a single cell level. *Blood Adv* (2022) 6(22):5873–83. doi: 10.1182/bloodadvances.2022007217

52. Cervantes-Gomez F, Chen LS, Orlowski RZ, Gandhi V. Biological effects of the pim kinase inhibitor, sgi-1776, in multiple myeloma. *Clin Lymphoma Myeloma Leuk* (2013) 13 Suppl 2:S317–29. doi: 10.1016/j.clml.2013.05.019

53. Wu J, Chu E, Kang Y. Pim kinases in multiple myeloma. *Cancers (Basel)* (2021) 13(17):4304. doi: 10.3390/cancers13174304

54. Nair JR, Caserta J, Belko K, Howell T, Fetterly G, Baldino C, et al. Novel inhibition of Pim2 kinase has significant anti-tumor efficacy in multiple myeloma. *Leukemia* (2017) 31(8):1715–26. doi: 10.1038/leu.2016.379

55. Daenthanasanmak A, Wu Y, Iamsawat S, Nguyen HD, Bastian D, Zhang M, et al. Pim-2 protein kinase negatively regulates T cell responses in transplantation and tumor immunity. *J Clin Invest* (2018) 128(7):2787–801. doi: 10.1172/JCI95407

56. Chatterjee S, Chakraborty P, Daenthanasanmak A, Iamsawat S, Andrejeva G, Luevano LA, et al. Targeting pim kinase with Pd1 inhibition improves immunotherapeutic antitumor T-cell response. *Clin Cancer Res* (2019) 25 (3):1036–49. doi: 10.1158/1078-0432.CCR-18-0706

57. Liu J, Hu Y, Guo Q, Yu X, Shao L, Zhang C. Enhanced anti-melanoma efficacy of a pim-3-Targeting bifunctional small hairpin rna *Via* single-stranded rna-mediated activation of plasmacytoid dendritic cells. *Front Immunol* (2019) 10:2721. doi: 10.3389/fimmu.2019.02721

58. Xin G, Chen Y, Topchyan P, Kasmani MY, Burns R, Volberding PJ, et al. Targeting Pim1-mediated metabolism in myeloid suppressor cells to treat cancer. *Cancer Immunol Res* (2021) 9(4):454–69. doi: 10.1158/2326-6066.CIR-20-0433

59. Mathewson ND, Ashenberg O, Tirosh I, Gritsch S, Perez EM, Marx S, et al. Inhibitory Cd161 receptor identified in glioma-infiltrating T cells by single-cell analysis. *Cell* (2021) 184(5):1281–98.e26. doi: 10.1016/j.cell.2021.01.022

60. McWilliams EM, Mele JM, Cheney C, Timmerman EA, Fiazuddin F, Strattan EJ, et al. Therapeutic Cd94/Nkg2a blockade improves natural killer cell dysfunction in chronic lymphocytic leukemia. *Oncoimmunology* (2016) 5(10): e1226720. doi: 10.1080/2162402X.2016.1226720

61. Andre P, Denis C, Soulas C, Bourbon-Caillet C, Lopez J, Arnoux T, et al. Anti-Nkg2a mab is a checkpoint inhibitor that promotes anti-tumor immunity by unleashing both T and nk cells. *Cell* (2018) 175(7):1731–43.e13. doi: 10.1016/j.cell.2018.10.014

62. Ocana MC, Martinez-Poveda B, Quesada AR, Medina MA. Metabolism within the tumor microenvironment and its implication on cancer progression: An ongoing therapeutic target. *Med Res Rev* (2019) 39(1):70–113. doi: 10.1002/med.21511

63. Andrejeva G, Rathmell JC. Similarities and distinctions of cancer and immune metabolism in inflammation and tumors. *Cell Metab* (2017) 26(1):49–70. doi: 10.1016/j.cmet.2017.06.004

64. Kishton RJ, Sukumar M, Restifo NP. Metabolic regulation of T cell longevity and function in tumor immunotherapy. *Cell Metab* (2017) 26(1):94–109. doi: 10.1016/j.cmet.2017.06.016

65. Terren I, Orrantia A, Vitalle J, Zenarruzabeitia O, Borrego F. Nk cell metabolism and tumor microenvironment. *Front Immunol* (2019) 10:2278. doi: 10.3389/fimmu.2019.02278

66. LaRue MM, Parker S, Puccini J, Cammer M, Kimmelman AC, Bar-Sagi D. Metabolic reprogramming of tumor-associated macrophages by collagen turnover promotes fibrosis in pancreatic cancer. *Proc Natl Acad Sci USA* (2022) 119(16): e2119168119. doi: 10.1073/pnas.2119168119

67. Peng X, He Y, Huang J, Tao Y, Liu S. Metabolism of dendritic cells in tumor microenvironment: For immunotherapy. *Front Immunol* (2021) 12:613492. doi: 10.3389/fimmu.2021.613492

68. Kishton RJ, Sukumar M, Restifo NP. Arginine arms T cells to thrive and survive. *Cell Metab* (2016) 24(5):647–8. doi: 10.1016/j.cmet.2016.10.019

69. Wang W, Zou W. Amino acids and their transporters in T cell immunity and cancer therapy. *Mol Cell* (2020) 80(3):384–95. doi: 10.1016/j.molcel.2020.09.006

70. Ma EH, Bantug G, Griss T, Condotta S, Johnson RM, Samborska B, et al. Serine is an essential metabolite for effector T cell expansion. *Cell Metab* (2017) 25 (2):345–57. doi: 10.1016/j.cmet.2016.12.011

71. Huang H, Zhou P, Wei J, Long L, Shi H, Dhungana Y, et al. *In vivo* crispr screening reveals nutrient signaling processes underpinning Cd8(+) T cell fate decisions. *Cell* (2021) 184(5):1245–61.e21. doi: 10.1016/j.cell.2021.02.021

72. Kobayashi T, Lam PY, Jiang H, Bednarska K, Gloury R, Murigneux V, et al. Increased lipid metabolism impairs nk cell function and mediates adaptation to the lymphoma environment. *Blood* (2020) 136(26):3004–17. doi: 10.1182/blood.2020005602

73. Herber DL, Cao W, Nefedova Y, Novitskiy SV, Nagaraj S, Tyurin VA, et al. Lipid accumulation and dendritic cell dysfunction in cancer. *Nat Med* (2010) 16 (8):880–6. doi: 10.1038/nm.2172

frontiers | Frontiers in Immunology

TYPE Original Research
PUBLISHED 14 December 2022
DOI 10.3389/fimmu.2022.1060957

OPEN ACCESS

EDITED BY
Andrey Zamyatnin,
I.M. Sechenov First Moscow State Medical University, Russia

REVIEWED BY
Nagaraj Nagathihalli,
University of Miami, United States
Monika Jakubowska,
Jagiellonian University, Poland

*CORRESPONDENCE
Minoti Apte
m.apte@unsw.edu.au

SPECIALTY SECTION
This article was submitted to Cancer Immunity and Immunotherapy, a section of the journal Frontiers in Immunology

RECEIVED 04 October 2022
ACCEPTED 22 November 2022
PUBLISHED 14 December 2022

CITATION
Hosen SMZ, Uddin MN, Xu Z, Buckley BJ, Perera C, Pang TCY, Mekapogu AR, Moni MA, Notta F, Gallinger S, Pirola R, Wilson J, Ranson M, Goldstein D and Apte M (2022) Metastatic phenotype and immunosuppressive tumour microenvironment in pancreatic ductal adenocarcinoma: Key role of the urokinase plasminogen activator (PLAU). *Front. Immunol.* 13:1060957. doi: 10.3389/fimmu.2022.1060957

Metastatic phenotype and immunosuppressive tumour microenvironment in pancreatic ductal adenocarcinoma: Key role of the urokinase plasminogen activator (PLAU)

S. M. Zahid Hosen[1,2], Md. Nazim Uddin[3], Zhihong Xu[1,2], Benjamin J. Buckley[4,5], Chamini Perera[1,2], Tony C. Y. Pang[1,6], Alpha Raj Mekapogu[1,2], Mohammad Ali Moni[7], Faiyaz Notta[8], Steven Gallinger[8], Ron Pirola[1], Jeremy Wilson[1], Marie Ranson[4,5], David Goldstein[9,10] and Minoti Apte[1,2]*

[1]Pancreatic Research Group, SWS Clinical Campus, School of Clinical Medicine, Faculty of Medicine and Health, UNSW Sydney, Sydney, NSW, Australia, [2]Ingham Institute for Applied Medical Research, Liverpool, NSW, Australia, [3]Institute of Food Science and Technology, Bangladesh Council of Scientific and Industrial Research (BCSIR), Dhaka, Bangladesh, [4]Molecular Horizons and School of Chemistry & Molecular Bioscience, Faculty of Science, Medicine and Health, University of Wollongong, Wollongong, NSW, Australia, [5]Illawarra Health and Medical Research Institute, Wollongong, NSW, Australia, [6]Westmead Clinical School, Faculty of Medicine and Health, University of Sydney, The University of Sydney, Sydney, NSW, Australia, [7]School of Health and Rehabilitation Sciences, Faculty of Health and Behavioural Sciences, The University of Queensland, St Lucia, QLD, Australia, [8]PanCuRx Translational Research Initiative, Ontario Institute for Cancer Research, Toronto, ON, Canada, [9]Prince of Wales Clinical School, University of New South Wales, Sydney, NSW, Australia, [10]Department of Medical Oncology, Prince of Wales Hospital, Randwick, NSW, Australia

Background: Previous studies have revealed the role of dysregulated urokinase plasminogen activator (encoded by *PLAU*) expression and activity in several pathways associated with cancer progression. However, systematic investigation into the association of *PLAU* expression with factors that modulate PDAC (pancreatic ductal adenocarcinoma) progression is lacking, such as those affecting stromal (pancreatic stellate cell, PSC)-cancer cell interactions, tumour immunity, PDAC subtypes and clinical outcomes from potential *PLAU* inhibition.

Methods: This study used an integrated bioinformatics approach to identify prognostic markers correlated with PLAU expression using different transcriptomics, proteomics, and clinical data sets. We then determined the association of dysregulated *PLAU* and correlated signatures with oncogenic pathways, metastatic phenotypes, stroma, immunosuppressive tumour microenvironment (TME) and clinical outcome. Finally, using an *in vivo*

orthotopic model of pancreatic cancer, we confirmed the predicted effect of inhibiting PLAU on tumour growth and metastasis.

Results: Our analyses revealed that *PLAU* upregulation is not only associated with numerous other prognostic markers but also associated with the activation of various oncogenic signalling pathways, aggressive phenotypes relevant to PDAC growth and metastasis, such as proliferation, epithelial-mesenchymal transition (EMT), stemness, hypoxia, extracellular cell matrix (ECM) degradation, upregulation of stromal signatures, and immune suppression in the tumour microenvironment (TME). Moreover, the upregulation of *PLAU* was directly connected with signalling pathways known to mediate PSC-cancer cell interactions. Furthermore, *PLAU* upregulation was associated with the aggressive basal/squamous phenotype of PDAC and significantly reduced overall survival, indicating that this subset of patients may benefit from therapeutic interventions to inhibit *PLAU* activity. Our studies with a clinically relevant orthotopic pancreatic model showed that even short-term PLAU inhibition is sufficient to significantly halt tumour growth and, importantly, eliminate visible metastasis.

Conclusion: Elevated *PLAU* correlates with increased aggressive phenotypes, stromal score, and immune suppression in PDAC. *PLAU* upregulation is also closely associated with the basal subtype type of PDAC; patients with this subtype are at high risk of mortality from the disease and may benefit from therapeutic targeting of *PLAU*.

KEYWORDS

***PLAU*, pancreatic stellate cells, proliferation, EMT, stemness, ECM degradation, immune suppression and basal subtype type of PDAC**

1 Introduction

Pancreatic ductal adenocarcinoma (PDAC), the most common subtype of pancreatic cancer (PC), is currently the seventh leading cause of cancer-associated death (1) and has a notoriously dismal prognosis. The incidence of PDAC continues to increase, and it is projected to become the second most common cause of cancer-linked death by 2030 (2). Current treatments have limited impact. The mean overall survival of the current standard treatment of FOLFIRINOX is 12.5 months, and that of Gemcitabine plus Abraxane, 10.3 months, P = 0.05 (3). Immunotherapies, individually or in combination with chemoradiotherapy or targeted therapy, have not made much progress in PDAC (4–7), reflecting an urgent need to identify new biologically driven targets to limit PDAC progression, particularly metastasis, the primary driver of mortality in this disease.

PDAC is no longer considered one disease at the molecular level, with many different molecular subtypes and subtype-specific treatment responses in PDAC (4–6). The two major transcriptomic-based subtypes, which have been confirmed across multiple investigations, are the classical/pancreatic progenitor subtype and the quasi-mesenchymal/basal-like/squamous subtype (4, 5, 8). The basal subtype is over-represented amongst metastatic PDAC tumours, and it is distinguished by ECM-rich activated stroma, the upregulation of expression of laminins and keratins and enriched for genes associated with epithelial-mesenchymal transition (EMT) and TGF-β signalling (9). On the other hand, the classical PDAC signature is characterised by upregulation of a wide range of transcription factors, GATA4, GATA6, NKX2-2 and HNF1A, associated with pancreatic lineage differentiation (4–8). Clinicopathologically, basal-type tumours are poorly differentiated and correlate with a worse prognosis (median OS 10–19.2 months and DFS 4.6–10.9); these tumours are chemoresistant but may have a better response to adjuvant therapy (4–6, 9–13). In contrast, classical type tumours are well-differentiated and are correlated with an overall better prognosis (median OS 19–43.1 months and DFS 13.5–20.6) (4, 6, 8, 10, 14–17).

Histologically, PDAC is well known to be characterised by a prominent stromal reaction comprising non-cellular elements like collagen, fibronectin, glycoproteins, proteoglycans, hyaluronic acid, cytokines, growth factors, and serine protein acidic and rich in cysteine (SPARC), as well as a wide range of cell types including neural, endothelial, immune & pancreatic stellate cells (PSCs). Pancreatic stellate cells (PSCs) are responsible for producing this excessive collagenous stroma in PDAC (18–20). Reciprocal interactions between activated pancreatic stellate and PDAC cells facilitate PDAC development and progression. One of the key pathways that may mediate cancer-stromal interactions is the hepatocyte growth factor (HGF) and its receptor c-MET pathway. Hyperactivity of HGF/c-MET signalling is considered a hallmark of cancer. Further, the serine protease urokinase plasminogen activator (uPA, encoded by *PLAU*) activates pro-HGF (secreted by pancreatic stellate cells) to active HGF, which binds to the c-MET receptor on cancer cells, activating several downstream signalling molecules. In addition, HGF binding to the c-MET receptor induces *PLAU* production by pancreatic and other cancer cells. The increased uPA level further activates pro-HGF, resulting in a feed-forward activation loop to promote cancer progression (21–23).

In normal cells (24–27), *PLAU* expression is very low and tightly controlled (7, 23, 28). However, *PLAU* and subsequently uPA expression is increased several-fold in tumour cells (23, 29–31), which results in catalytic conversion of inactive plasminogen to plasmin. Plasmin degrades extracellular matrix directly or indirectly *via* activation of precursor forms of matrix-degrading enzymes (matrix metalloproteinases) (32). Furthermore, in cancer cells, direct interaction of uPA with its receptor uPAR (encoded by PLAUR) facilitates the activation of multiple intracellular cell-signalling pathways, which regulate proliferation, migration, invasion, epithelial-mesenchymal transition, stem cell-like properties, release from states of dormancy, cell survival, chemoresistance, angiogenesis and vasculogenic mimicry (7, 24–27, 33–41) in cancer. All of which suggests a role as a master regulator in cancer development and progression. Indeed, upregulation of *PLAU* is associated with poor prognosis in several different cancers (33, 42). One study analysed 8 PDAC versus normal tissue gene expression profiles retrieved from the GEO database and found *PLAU* and *PLAU*R to be one of 10 hub genes significantly associated with PDAC pathogenesis (43).

This is the first study to delineate the role of the *PLAU* by integrated publically available transcriptomic, proteomics, and clinical data to 1) further elucidate the mechanisms underlying *PLAU*-related PDAC growth and progression, 2) use this data to undertake analyses of prognostic outcomes (overall survival) and assessment of relationship with clinical attributes, 3) identify the most 'at risk' group based on *PLAU* expression and4) preclinically assess selective uPA inhibition on pancreatic cancer growth and metastasis. To the best of our knowledge, this is the first integrated–omics analysis of the expression of these key components of the uPA system in PDAC.

2 Materials and methods

This study was implemented according to the analytical approach shown in Figure 1. The main steps involved in this task were step 1) identification of differentially expressed *PLAU* mRNA in i) 33 different cancer cohorts in the TCGA database, ii) different cancer cell lines from CCLE and iii) different GEO datasets. Step 2) Kaplan-Meier survival analyses of *PLAU* in PDAC-specific TCGA, ICGC and OICR patient cohorts. Step 3) Identifying other gene signatures correlated with *PLAU* from TCGA, ICGC and OICR patients cohorts. These gene signatures were mainly related to cancer cell functions, immunity and prognosis. A PPI network was constructed based on the gene signatures, and relevant subcellular pathways were identified. Step 4) Assessing the correlation of *PLAU* expression with pathways responsible for PSC-PDAC cell interactions. Step 5) Validation of transcriptome-based prognostic signatures using CPTAC proteomics data and assessing the relationship with clinical attributes. Step 6) Stratifying patient groups according to PLAU protein expression and survival and identifying the most 'at risk' group. Step 7) Further validation of the effect of PLAU inhibition on PDAC tumour growth and metastasis using *in vivo* pancreatic orthotopic model.

2.1 Datasets

We used the GEPIA (Gene Expression Profiling Interactive Analysis) TCGA dataset (http://gepia.cancer-pku.cn/) for comparing the differential mRNA expression of *PLAU* between cancer and normal samples. The Cancer Cell Line Encyclopedia (CCLE) (https://www.broadinstitute.org/ccle) mRNA expression data was used to identify distinctively upregulated *PLAU* in pancreatic cancer cell lines (44, 45). Next, we used different microarray data sets, including GSE16515 (46), GSE58561 (47), GSE71989 (48), GSE62165 (12), GSE71729 (6), and RNAseq GSE119794 (49) from the NCBI-GEO database.

Messenger RNA expression data and associated clinicopathological data were used from The Cancer Genome Atlas (TCGA, http://cancergenome.nih.gov/) and the International Cancer Genome Consortium (ICGC, https://icgc.org/). In particular, normalised gene expression of NGS was downloaded from the cBioPortal, (TCGA, Firehose https://www.cbioportal.org/) (50) on 1st July 2021. For the ICGC-Pancreatic Cancer - Australia (ICGC-PACA-AU) cohort, data were obtained from the Supplementary Material of the corresponding publication (4). In addition, we also used the Ontario Institute for Cancer Research (OICR) PDAC cohort (EGAS00001002543) for gene expression and clinical data through a data access

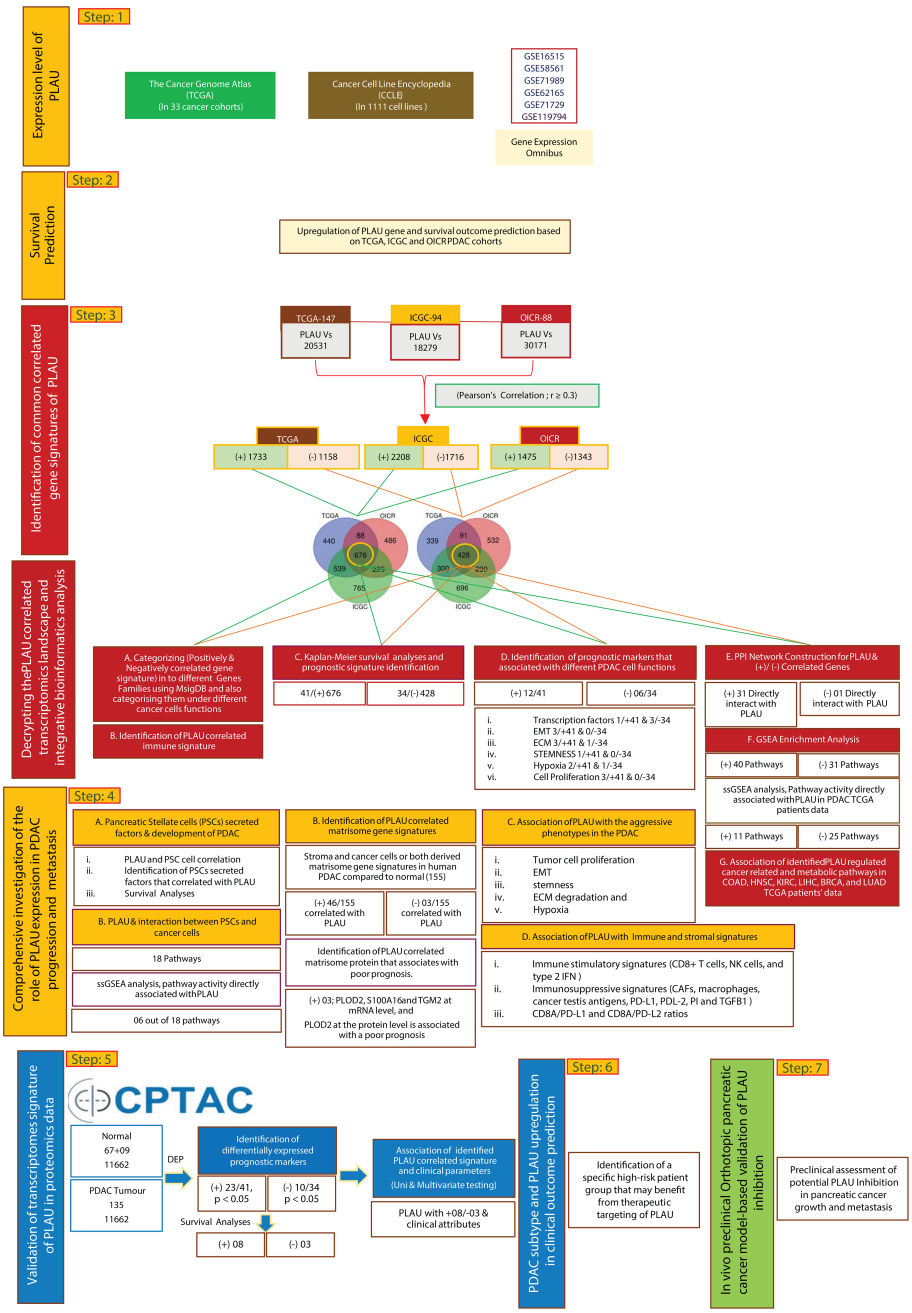

FIGURE 1
An integrative clinical bioinformatics workflow to decipher the role of *PLAU* in PDAC growth and progression, clinical outcome prediction and *in vivo* preclinical method-based validation of *PLAU* inhibition effects in tumour growth and metastasis.

agreement. Likewise, the proteomic and accompanying clinicopathological data from the proteogenomic characterisation of the PDAC study (6) was acquired *via* the Clinical Proteomic Tumor Analysis Consortium (CPTAC, https://cptac-data-portal.georgetown.edu/). Only PDAC cases with matched RNAseq/protein expression and clinical data were included in the analysis for all the cohorts.

2.2 Differential expression analysis

Differential expression analysis was performed using GEO2R (http://www.ncbi.nlm.nih.gov/geo/geo2r) and R packages limma from the Bioconductor project (http://www.bioconductor.org/). The thresholds of P-value < 0.05 and |FC| (fold change) > one was set to determine the significant level.

2.3 Identification of correlated gene signature

We used Pearson's correlation test to identify gene-gene correlation because the expression data is normally distributed. However, we employed Spearman's correlation test between the mRNA expression level of *PLAU* and the ssGSEA score of selected pathways because the data is not normally distributed. The threshold of our correlation analysis was set at greater than 0.30, and FDR ≤0.05. A false discovery rate (FDR) calculated by the Benjamini and Hochberg method (51) was used to adjust for multiple tests.

By comparing annotated gene sets from the Molecular Signatures Database (MSigDB) (52), and using the online tool "Calculate and draw custom Venn diagrams" (http://bioinformatics.psb.ugent.be/webtools/Venn/) we identified common tumour suppressors, oncogenes, translocated cancer genes, transcription factors, cytokines and growth factors, protein kinases, homeodomain proteins, and cell differentiation markers among positive and negatively correlated gene signatures of *PLAU* identified from three PDAC cohorts.

2.4 Gene-set enrichment analysis

We performed gene-set enrichment analysis of the *PLAU*-correlated genes using GSEA (53) with a false discovery rate threshold, FDR < 0.05. The Kyoto Encyclopedia of Genes and Genomes (KEGG) pathways that were significantly associated with the positive and the negatively *PLAU*-correlated genes were also identified (FDR < 0.05).

2.5 Functional analysis

We constructed protein-protein interaction (PPI) networks of the *PLAU*-correlated genes using the STRING (version v11 (54)) and visualised the PPI networks by utilising the Cytoscape 3.9.1 software (55). The rank of genes was identified by the Cytoscape plugin cytoHubba (56). Hub nodes were identified using a threshold of medium interaction score ≥0.40, and we selected the degree of interaction ≥25 for identifying the most closely interacting genes in the PPI.

2.6 Survival analysis

We used the clinical data of TCGA, ICGC, OICR and CPTAC PDAC cohorts for survival analysis. We compared the overall survival (OS) between PDAC patients classified based on gene expression levels (high expression levels >mean > low expression levels). Kaplan-Meier survival curves were used to show the survival time differences, and the log-rank test was utilised to evaluate the significance of survival time differences between both groups. We used the R package "survival" to perform survival analysis (57), and the function "coxph" in the R package "survival" was used for the u*nivariate* and *multivariable Cox regression analyses (*57).

2.7 Evaluation of immune scores, stromal scores, and tumour purity in stromal content

We utilised the "ESTIMATE" R package to calculate an immune score representing the enrichment levels of immune cells and a stromal score representing the content of stromal cells (58) in the TCGA-PDAC cohort. We compared immune and stromal scores between the patients with high expression of *PLAU* and low expression of the *PLAU* group in PDAC (high expression levels >mean > low expression levels). We considered the Wilcoxon sum rank test (P-value ≤0.05) to identify significant differences between both groups.

2.8 Associations of the expression levels of *PLAU* with immune signature, pathway activity, and tumour phenotypes in PDAC

We first identified the *PLAU* correlated cell function and immune gene signatures. Then we used the single-sample gene-set enrichment analysis (ssGSEA) to quantify the enrichment scores of immune and stromal signatures in tumours based on the expression levels of their marker genes (53). We defined the ratio of immune signatures in a tumour sample as the ratio of the average expression levels of their marker genes. The immune and stromal signatures analysed included B cells, CD8+ T cells, CD4+ regulatory T cells, macrophages, neutrophils, natural killer (NK) cells, tumour-infiltrating-lymphocytes (TILs), regulatory T cells (Tregs), cytolytic activity, T cell activation, T cell exhaustion, T follicular helper cells (Tfh), M2 macrophages, tumour-associated macrophage (TAM), T helper 17 cells, myeloid-derived suppressor cell (MDSC), endothelial cell, and cancer-associated fibroblasts (CAFs). Their marker genes are shown in Supplementary Table (ST) B. Moreover, we identified the ssGSEA score of all enriched pathways that directly correlate with *PLAU* and tumour phenotypes (proliferation, EMT, stemness, ECM degradation, and hypoxia). The genes associated with the specific pathways and phenotypes are listed in STB, ST12. Finally, we compared immune signatures and phenotypes of PDAC patients with high expression of *PLAU* with those with low expression of the *PLAU*.

2.9 *In vitro* and *in vivo* study

2.9.1 Isolation and characterisation of cancer-associated hPSCs

Using the outgrowth method (59), CAhPSCs were isolated from surgically removed pancreatic tissue obtained from cancer patients. The characterisation of CAhPSC yield was then assessed by morphology and immunostaining for the selective GFAP and the activation marker αSMA (60).

2.9.2 Cell culture

AsPC-1 cells (American Type Culture Collection, Manassas, VA) and CAhPSCs were cultured according to the supplier's instructions and following previously published protocols by our group (61).

2.9.3 *In vivo* orthotopic model of pancreatic cancer

To validate the outcome of *PLAU* (uPA) inhibition on tumour growth and metastasis *in vivo*, we conducted a pilot study using an orthotopic model of pancreatic cancer as previously established in our laboratory (21, 62, 63). Briefly, 6-8 weeks old female athymic nude mice (BALBc nu/nu) were anaesthetised, and an opening was made in the left flank, followed by exteriorisation of the spleen and tail of the pancreas. Then 1×10^6 human PC cells (AsPC-1) plus 1×10^6 cancer-associated human PSCs (CAhPSCs) in 50μL of PBS were implanted into the tail of the pancreas to replicate early cancer development and progression. Mass Spectrophotometry–Based proteome profiling (ST19) confirmed *PLAU* protein expression in both AsPC1 and CAhPSCs. Seven days after cell implantation, mice were randomised (n=5/group) to receive vehicle control (Ctrl), Gemcitabine (G) 75 mg/kg IP biweekly, uPA small molecule enzymatic inhibitor [5,6-disubstituted amiloride analogue, compound BB2-30F (A26) (64)] 3mg/kg (U3) or 10mg/kg (U10) IP daily. BB230F compounds were formulated for IP injection in 50 mM acetate buffer (pH5.5) + 10% DMSO + 1% Kolliphor HS-15 buffer and filtered through 0.22 μm PVDF syringe-driven filters under sterile conditions (64) The total number of vehicle injections was 28 (daily IP injections), allowing us to control maximally for any effects of IP injections per se in our model. Pancreatic tumour growth was monitored by palpation. At the end of 28 days of treatment, tumours were resected, and tumour volume was determined according to the formula (1/2(length × breadth × width) using digital Vernier callipers (Intech Tools, Thomas Town, VIC, Australia). The abdominal cavity, mesentery, spleen, liver, and lungs were examined, and a metastasis score was calculated based on the presence or absence of visible macrometastatic nodules. Haematoxylin and eosin staining was performed to confirm the presence of such nodules. Primary tumour sections were immunostained for E-cadherin, vimentin and ALDH1A1. Tumour volume data are expressed as mean ± SEM. One-way analysis of variance with Tukey's *post hoc* test was applied. Analyses were performed using GraphPad Prism 9 for Windows 64-bit (GraphPad Software, San Diego, CA, USA).

The animal studies were approved by the University of New South Wales Animal Care and Ethics Committee (Approval Number 18/125B) and accomplished under ARRIVE guidelines.

3 Results

3.1 *PLAU* is significantly differentially expressed in various cancers

Using the GEPIA dataset, it was found that *PLAU* mRNA levels are significantly differentially expressed (compared to relevant normal tissue) in 23 of the 33 different types of cancers assessed (Figure 2A; Red =tumour and Green= normal). In BLCA, BRCA, CESC, COAD, DLBC, ESCA, GBM, HNSC, KICH, KIRC, LGG, LIHC, LUAD, LUSC, OV, PAAD, PRAD, READ, STAD, TGCT, THCA, THYM, and UCEC *PLAU* is significantly upregulated while in KICH, KIRC and PRAD it is downregulated (Figure 2A). In particular, in the PAAD cohort of pancreatic cancer, *PLAU* transcripts were 4.876 (p=1.6e-103) fold elevated compared with normal tissue. In support of the above observations, the Cancer Cell Line Encyclopedia (CCLE) dataset revealed that (https://www.broadinstitute.org/ccle) *PLAU* was also differentially expressed in different cancer cell lines (Figure 2B), including 44 pancreatic cancer cell lines (from primary and metastatic PDAC tumours (ST2 A). Upregulated mRNA and protein expression levels for *PLAU* (relative to normal controls) in 17 PDAC cell lines are depicted in Figure 2C.

The above observations related to PDAC were further confirmed by analysis of several GSE microarrays which showed significant fold increases in *PLAU* mRNA in PDAC vs normal controls as detailed in the following: GSE16515 (logFC 2.73, P=2.32E-07); GSE58561 (logFC 4.94, P = 5.35E-06); GSE71989 (logFC 3.29, P =2.56E-06); GSE62165 (logFC 3.31, P = 1.91E-27); GSE71729 (logFC 1.56, P = 1.98E-09), and RNAseq GSE119794 (logFC 1.256, P= 0.003), ST3. Taken together, the above findings indicate that *PLAU* is significantly upregulated in different tumours and cancer cell lines. Of particular relevance to this study, pancreatic cancer and cell lines, consistently demonstrate upregulation of *PLAU* gene expression, suggesting that *PLAU* may play driver roles in the development and progression of PDAC.

3.2 Upregulated mRNA expression of *PLAU* is associated with poor survival in PDAC patients

Given the significant upregulation of *PLAU* in PDAC patients from distinct datasets, we further investigated the association of *PLAU* with clinical outcomes. TCGA data of 147 PDAC patients from 179 PAAD-TCGA cohorts were

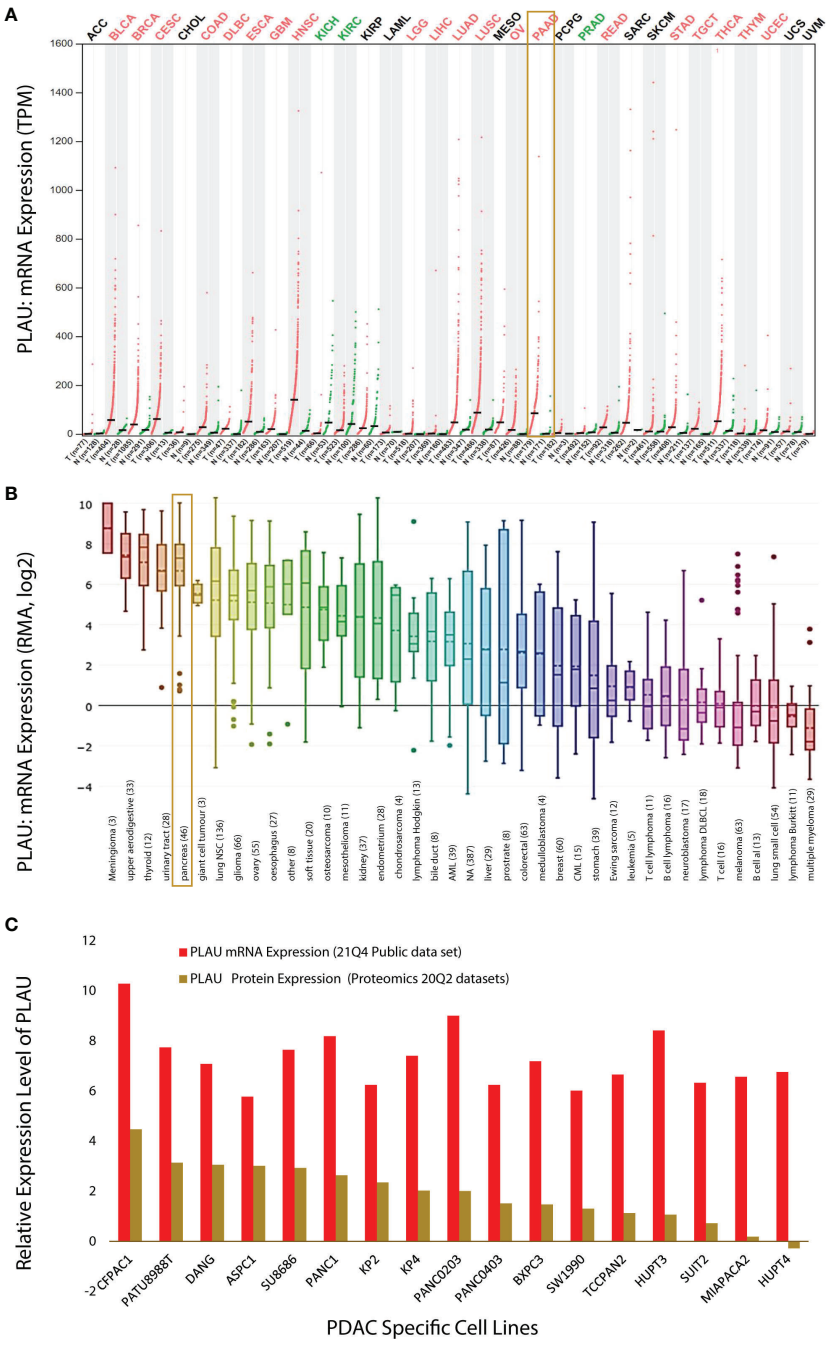

FIGURE 2
PLAU expression in cancers. **(A)** Dot plot depicting *PLAU* gene expression profile across 33 cancer types and paired normal samples (TCGA normal plus GTEx), with each dot representing a distinct tumour or normal sample. The bar height represents the median expression of a certain tumour type or normal tissue. The comparison was performed using GEPIA (Gene Expression Profiling Interactive Analysis). For each TCGA tumour (red), its matched normal and GTEx data (green) are given; T: tumour; N: normal; n: number. Y-axis: transcripts per million log2 (TPM + 1). X-axis: number of tumours and normal samples. **(B)** *PLAU* expression across 1111 human cancer cell lines from the Cancer Cell Line Encyclopedia (CCLE). Box plots showing RNA-seq mRNA expression data from CCLE, with the dashed lines within a box representing the mean. Cell lines derived from the same organ/organ system were grouped, and lineages are indicated at the bottom of the graph, with the number of cell lines per organ/organ system in parenthesis. The "pancreas" group includes the 44 pancreatic cancer cell lines listed in (ST2A). **(C)** Relative expression level of *PLAU* at mRNA and protein level in 17 PDAC cell lines using the depmap portal.

analysed to reveal that patients in the high *PLAU* mRNA expression group had the poorest outcome (high expression group of *PLAU* > mean expression level of *PLAU* > low expression of *PLAU*) (Figure 3A), P=0.042. Similar results were obtained on analysis of the ICGC patient cohort (GSE36924) (Figure 3B), P=0.04 (4). With the third patient cohort in our study (OICR; EGAS00001002543) (65), there was a trend for poorer survival in patients with high *PLAU* mRNA expression, but the difference did not achieve statistical significance P= 0.28 (Figure 3C). Altogether, these data demonstrate that the upregulation of *PLAU* mRNA expression is an adverse prognostic factor in PDAC.

3.3 *PLAU* is significantly correlated with key signal regulatory and tumour immune genes in PDAC

In view of our finding of an association between high *PLAU* gene expression and poor prognosis in PDAC patients, we were interested in analysing other genes that may be correlated with *PLAU* and might influence patient outcomes. Pearson's correlation coefficient test was used to identify gene-gene correlations for all genes in the expression tables of the TCGA, ICGC, and OICR datasets. A Venn diagram was applied to identify *PLAU*-correlated genes common to all three PDAC datasets (ST4, ST5 and Supplementary Figures (SF) 1A, B). The gene signatures were then categorised into different gene families based on annotated gene sets from Molecular Signatures Database (MSigDB). There were 676 genes positively correlated with the *PLAU* that were common to all three datasets. (ST 6A, SF 1A). These included 42 transcription factors (e.g. *FOXC1, HMGA2, RUNX2, SNAI1, SNAI2, TWIST1*, and *WT1*), 16 protein kinases (e.g. *MET, MAPK12*, and *AKT3*), 8 homodomain proteins (including *SIX4, NKX3-2*, and *HLX*);, 27 cell differentiation markers (including *PDL1, CD44, CD70, CDH2*, and *ITGA3)*, 18 oncogenes (e.g. *CDH11, COL1A1*, and *PDGFB)*, 16 translocated cancer genes (*CDH11, CLTCL1, COL1A1, MAF*, and *MAFB)*, one tumour suppressor gene *WT1, and* 38 cytokines and growth factors (including *TGFB2, FGF1, VEGFC, PDGFB, EREG, TGFB1, CCL11, TGFB3, BMP1, IL1,1* and *CCL13)* [Pearson correlation, r>0.3, P> 0.05].

There were 428 genes negatively correlated with the elevated expression levels of *PLAU* that were common to all three datasets (SF 1B). These comprised 31 transcription factors (including *CDX2, FOXA2, GATA6, HNF1A, HNF4A, PDX1, PPARGC1A*, and *TOX3)*, two cell differentiation markers *(FUT4* and *TNFRSF11A)*, 11 protein kinases (e.g. *ACVR1B, ERBB3, FGFR4, HIPK2, KALRN, PKDCC, SCYL3)*, four translocated cancer genes (including *PRDM16* and *TMPRSS2)*, six oncogenes (including *MYCN, CEBPA*, and *MECOM)*, one tumour suppressor gene (*HNF1A)* and four cytokines and growth factors (including *FAM3B, EDN3, SEMA4G*, and *FAM3D*, ST 6A). Several immune-related gene signatures that are positive and negatively associated with *PLAU* were also identified (such as *PDCD1LG2, HAVCR2, ANXA1, TNFRSF12A, PLAT, CD276, PTGES, CD44, MMP9, CT45A3, PIWIL2, METTL7A, IL23R, IL17RB, IL22RA1, TNFRSF11A, BLNK*, and *F5*, ST7).

Further analysis shows that most of the positively correlated gene signatures of *PLAU* in PDAC regulate cancer cell functions such as cell proliferation, stemness and epithelial-mesenchymal transition, and other factors of importance to cancer biologies such as extracellular matrix degradation, hypoxia, endothelialisation, and metastasis promotion. In contrast, negatively correlated gene signatures were largely uninvolved in cancer cell functions (ST 6C, SF 1E and F).

A subanalysis of TCGA transcriptomic and clinical data of PDAC patients revealed specific gene signatures (positively and negatively correlated with *PLAU*) associated with poor survival (ST8, SF 1C and D). Among these prognostic genes, we further identified the following positively correlated *MET*, *ITGA3, EREG, PLOD2, EMP1, CD44 HMGA2, TGM2, GAPDH,*

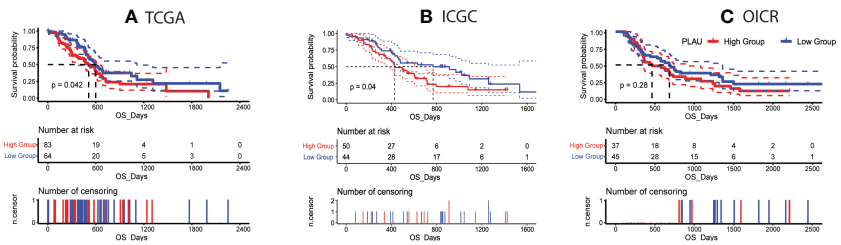

FIGURE 3
Correlation of *PLAU* gene expression with survival in PDAC. **(A, B)** Kaplan-Meier survival curves show that high *PLAU* expression correlated with significantly poorer overall survival (OS) in the TCGA and ICGC PDAC cohorts (log-rank test, P < 0.05), **(C)** but this was not evident with the OICR-PDAC cohort (log-rank test, P = 0.28).

IL31RA, CGB7, CDH3, and negatively correlated *PRDM16, PPARGC1A, CAPN6, SPIB, TOX3*, and *FGFR4* associated with the different cancer cell functions listed in Table 1, while Kaplan Meier curves signifying their prognostic association are presented in Figures 4 and SF 2.

3.4 *PLAU* correlated gene signatures and protein-protein interaction network analysis

The gene analysis described above indicates that upregulated *PLAU* expression is correlated with several key gene signatures that have the potential to influence cancer cell functions and PDAC progression/outcomes. The daunting task is to understand how these positively and negatively *PLAU* correlated genes modulate the PPI network, which can result in dysregulated oncogenic pathways with functional and therapeutic significance. To address this, the 676 positively correlated genes and the 428 negatively correlated genes (common to all three data sets) were entered into the STRING v11 program. 610 of the 676 positively correlated genes and 317 of the 428 negatively correlated genes were involved in the PPI network with PPI enrichment p-value < 1.0e-16 and 3930 edges, and p-value < 1.0e-16 577 edges, respectively. Based on the degree of interactions, some of the top genes within the PPI network were *FN1, GAPDH, COL1A1, CD44, MMP2, COL1A2, MMP9 POSTN, COL5A1, BGN, LOX, COL4A1, MMP14, THBS1*, and *TGFB1* (ST9A). Extracting the *PLAU*-centric PPI network from the original extensive network revealed that *PLAU* interacts with 31 of the positively correlated genes (*FN1, MMP2, GAPDH, CD44, MMP9, MMP14, SERPINE1, TIMP2, TGFB1, THBS1, CAV1, MET, MMP13, TIMP3, VEGFC, IGFBP3, CTSB, ITGA5, SNAI1, PLAT, CTSL, CTSD, MMP11, ITGA3, PDGFC, MRC2, PRSS23, SRPX2, KAL1, MFI2*, and *LYPD3*, SF3 and ST 9C), and interestingly, only one negatively correlated gene *ANG* (ST 9B, D).

3.5 *PLAU* regulates cancer-associated and metabolic pathways in PDAC

To delineate the specific cancer-associated pathways that may be modulated by *PLAU* and its positive/negatively correlated gene signatures, the Functional Class Scoring (FCS) method based on GSEA tool (53) was used (FDR<0.05). Genes that are positively correlated with *PLAU* upregulation were found to be associated with the enrichment of several cancer-associated KEGG pathways (ST 10A). In order to assess whether the expression of *PLAU* was directly associated with the activity of these pathways, correlations between the expression levels of *PLAU* (Log2 normalised) and the specific pathway activity (ssGSEA score of the pathway) were analysed for the TCGA-PDAC cohort (Spearman's correlation test P<0.05). Interestingly, it was found that *PLAU* expression correlated directly with the activity of 11 KEGG pathways, including

TABLE 1 *PLAU* correlated genes and their association with cellular functions in PDAC.

Prognostic genes positively correlated with *PLAU*	**Factors influencing cancer biology**
HMGA2	Stemness, oncogene, Transcription Factor and Translocating cancer gene
TGM2	Endothelialization, Hypoxia and EMT
CD44	ECM degradation, EMT and Cell differential marker
ITGA3	ECM degradation and cell differential marker and Metastasis
MET	Oncogenes and Protein Kinase
EREG	Cell Proliferation, Cytokines and Growth Factor
GAPDH	Hypoxia
PLOD2	ECM degradation and EMT
EMP1	Cell Proliferation
IL31RA	Cell Proliferation
CGB7	Cytokines and Growth factor
CDH3	Metastasis promotion
Prognostic genes negatively correlated with *PLAU*	**Factors influencing cancer biology**
PRDM16	Oncogenes, Transcription Factors, Translocating cancer genes
PPARGC1A	Hypoxia, Transcription Factor
CAPN6	ECM degradation
SPIB	Transcription Factor
TOX3	Transcription Factor
FGFR4	Cytokines and Growth factor and Protein Kinase

ECM, Extracellular matrix; EMT, Epithelial-mesenchymal transitions.

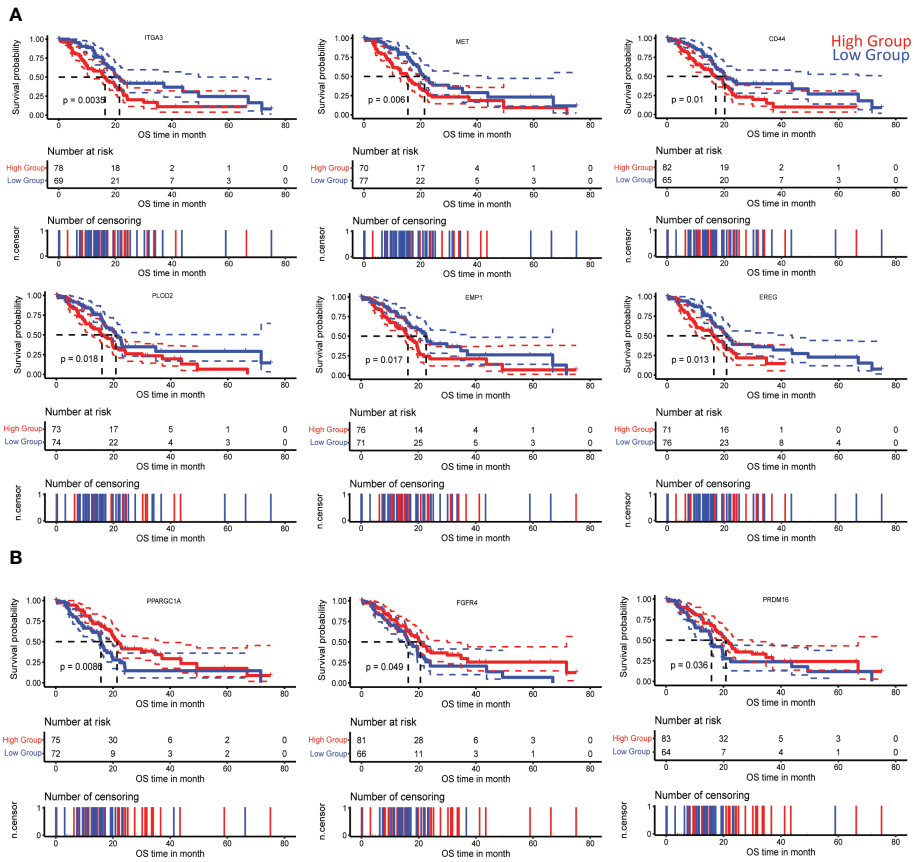

FIGURE 4
Correlation of *PLAU-associated* genes with survival in PDAC. Kaplan-Meier survival curves show that significantly worse overall survival of PDAC patients in the TCGA cohort is correlated with **(A)** increased expression of ITGA3 (log-rank test, P=0.0035), MET (log-rank test, P = 0.006), CD44 (log-rank test, P= 0.01), PLOD2 (log-rank test, P = 0.018), EMP1 (log-rank test, P = 0.017), EREG (log-rank test, P = 0.013) and **(B)** decreased expression of PPARGC1A (log-rank test, P = 0.0086), FGFR4 (log-rank test, P = 0.049), and PRDM16 (log-rank test, P = 0.036).

glycosaminoglycan biosynthesis - chondroitin sulfate, basal cell carcinoma, Hedgehog signalling pathway, axon guidance, pathways in cancer, pancreatic cancer, TGF-beta signalling pathway, arrhythmogenic right ventricular cardiomyopathy (ARVC), wnt signalling pathway, and renal cell carcinoma, FDR<0.01 (Figure 5A and ST 11A).

Genes that were negatively correlated with *PLAU* upregulation were found to be primarily associated with the enrichment of 31 metabolic pathways, covering the metabolism of specific amino acids, carbohydrates, fatty acids and xenobiotics listed in (ST 10B). Interestingly, we discovered that the expression of *PLAU* itself was directly correlated with 25 KEGG pathways (Figure 5B and ST 11B).

A similar observation of *PLAU* association with cancer-associated and metabolic pathways in various cancers, including COAD, HNSC, KIRC, LIHC, BRCA, and LUAD, was revealed in our further analysis (SF 4A, B).

3.6 *PLAU* expression is correlated with pancreatic stellate cell -selective markers & pathways in TME of PDAC

As noted earlier, PSCs facilitate the survival and growth of PDAC cells *via* factors that modulate cancer cell proliferation, invasion, migration, metastasis and chemoresistance. In turn, cancer cells activate PSCs *via* the secretion of growth factors and cytokines (*PDGF, VEGF, bFGF, TGF-ß*), resulting in increased PSC proliferation, migration and production of extracellular matrix proteins (66–69). Given this bidirectional interaction between PSCs and cancer cells, we investigated the association of *PLAU* expression with the abundance of activated PSCs. *PLAU* expression was significantly positively correlated (R= 0.41, P=2.754e-07) with the ssGSEA score of PSC-specific markers in the TCGA-PDAC data set (Figure 6A). Moreover, a significant moderate correlation was found between *PLAU* and all other secreted markers of

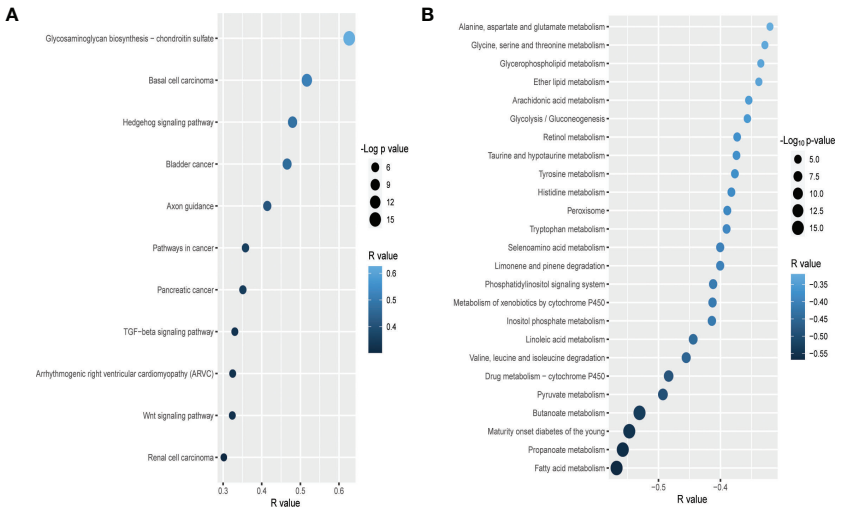

FIGURE 5
Correlation of *PLAU* upregulation with cancer-associated and metabolic pathways in PDAC. In the TCGA PDAC cohort, upregulation of *PLAU* gene expression is **(A)** directly and positively correlated with cancer-associated pathways and **(B)** negatively correlated with metabolic pathways (FDR<0.05).

activated PSCs (ST13), most of which have been shown to play key roles in cancer progression (please see discussion). *PLAU* expression was also correlated with critical pathways known to mediate PSCs-PC interactions (69), including Hedgehog, TGF beta, WNT (Figure 5A), WNT beta-Catenin and hypoxia-inducible factor-1 (Figures 6B, C) signalling pathways.

3.7 Identification of prognostically important *PLAU* correlated matrisome gene in human PDAC

In the tumour microenvironment, *PLAU* is involved in ECM breakdown through activation of plasminogen to plasmin which activates certain pro-matrix metalloproteinases, facilitating local tumour invasion. Dysregulated ECM proteins also influence tumour progress and patient survival by supporting tumour cell proliferation, angiogenesis, inflammation (22, 28), and metastasis (29, 30). However, the association of *PLAU* with the PDAC-specific matrisome gene (produced by tumour cells and stromal pancreatic stellate cells) has not been assessed in the context of PDAC development and progression. In order to systematically examine the correlations of *PLAU* expression with PDAC-specific ECM gene signatures (from TCGA, ICGC and OICR cohorts), 155 PDAC matrisome gene signatures (ST14) were selected (32 secreted by cancer cells, 87 by stromal cells and 36 from both cancer and stromal cells) (70). 49 ECM gene signatures were found to be correlated with *PLAU*, either positively (33) or negatively (3) (Pearson correlation, $r>0.3$; $p< 0.05$). Of the 49 genes, 22 coded for ECM glycoproteins (*EFEMP1, EMILIN1, FBLN2, FBN1, FN1, HMCN1, IGFBP3, LAMA4, LAMC2, LTBP1, LTBP2, MATN2, MFAP2, PCOLCE, POSTN, PXDN, SRPX2, TGFBI, TGM2, THBS1, THBS2* and *TNC*), 12 for ECM regulators (*ADAMTS4, ADAMTSL1, BMP1, CTSB, CTSD, LOX, LOXL1, MMP2, PLOD1, PLOD2, SERPINH1* and *TGM2*), six for collagens (*COL11A1, COL6A1, COL6A2, COL6A3, COL8A1*, and *COL8A2*), four for ECM-affiliated proteins (*ANXA1, ANXA4, LGALS1* and *LGALS4*), three for secreted factors (*S100A16, S100A9*, and *TGFB1*), and two for proteoglycans *BGN* and *VCAN* (ST14, 15A and Figure 7A).

Survival analysis of the TCGA-PDAC cohort revealed that secreted factor *S100A16* (cancer-cell–derived), ECM regulator *PLOD2* (stromal cell-derived) and ECM regulator *TGM2* (derived from both cancer cells and stromal cells) genes were overexpressed in human PDAC and correlated with short patient survival (log-rank test, $P < 0.05$), Figures 7B–D. In contrast, none of the negatively correlated matrisome gene signatures was associated with patient survival. However, at the protein level (using the CPTAC-PDAC cohort), while PLOD2, S100A16 and TGM2 were all significantly differentially overexpressed in tumours compared to the normal adjacent pancreas (ST 15B), only upregulation of PLOD2 (log-rank test, P= 0.05) protein was found to be associated with poor survival (refer to PLOD2).

3.8 Upregulation of the *PLAU* gene is correlated with aggressive phenotypes of PDAC

Aggressive PDAC is characterised by increased cancer cell proliferation, EMT, stemness, active ECM and hypoxia. Using

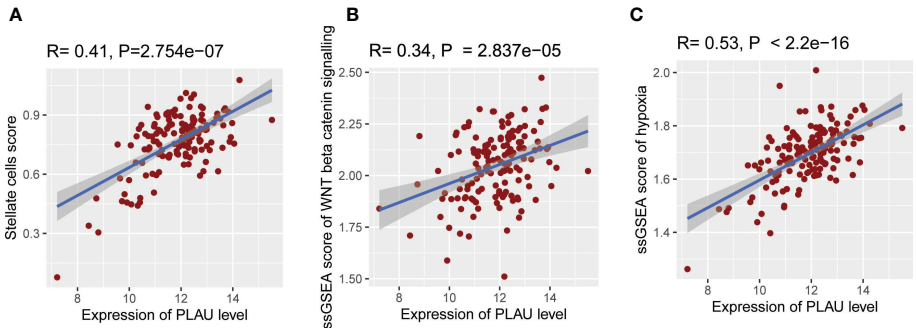

FIGURE 6
Association of *PLAU* gene expression with abundant activated PSCs and pathways responsible for PSC-PC interactions. In the TCGA PDAC cohort, **u**pregulation of *PLAU* gene expression exhibit a significant positive association with **(A)** abundance of activated PSCs in the TME (R= 0.41, P=2.754e−07), **(B)** WNT beta-Catenin pathway activity (R= 0.34, P=2.837e−05), and **(C)** hypoxia score (R= 0.53, P < 2.2e−16).

the TCGA-PDAC cohort to compare the *PLAU* high expressing group (HEG) vs the *PLAU* low expressing group (LEG), scores for each of the above parameters were found to be elevated (Figures 8A–E), and the associated markers significantly correlated (SF 5A–D) with high *PLAU* gene expression.

3.9 Expression of the *PLAU* gene is associated with an immunosuppressive tumour microenvironment in PDAC

Since the infiltration levels of immune cells are an independent predictor of survival in cancers (58), the differences in various immune and stromal signatures between *PLAU*-high and *PLAU*-low patients in the TCGA-PDAC cohort were examined. Stromal and immune scores were calculated (the content of cells) by applying the ESTIMATE (58) algorithm. The stromal score was significantly higher in the HEG of *PLAU* than in the LEG of *PLAU* (Figure 9A, Wilcoxon rank-sum test, p<0.05). In contrast, there was no significant difference in the immune score between the groups. However, the *PLAU*-high group was associated with inhibition of immune stimulatory signatures that included CD8+ T cells, NK cells, and type 2 IFN (Figure 9B) and upregulation of immunosuppressive signatures that included CAFs, macrophages, cancer-testis antigens, PI genes, *PD-L1*, *PDL-2*, and *TGFB1* (Wilcoxon rank-sum test, p<0.05) (Figure 9C). The ratios of CD8+ T cells/CD4+ T cells and pro-/anti-inflammatory cytokines (as assessed by the ratio of average expression levels (log2-transformed) of their marker genes) were significantly lower in the *PLAU* high group (expression levels > average) (Figure 10A, P < 0.05). The pro-inflammatory cytokine genes are immune-stimulatory and include *IFNG*, *IL-1A*, *IL-1B*, and *IL-2*, while the anti-inflammatory cytokine genes *IL-4*, *IL-10*, *IL-11*, and *TGFB1* represent an immune-inhibitory signature. The expression levels of *PLAU* were negatively correlated with CD8A/PD-L1 and CD8A/PD-L2 ratios (Pearson's correlation test, P < 0.05, Figure 10B). Taken together, the above findings indicate that elevated *PLAU* expression has a stronger association with immunosuppressive TME signatures (*PD-L1* and *PD-L2*) than with the anti-tumour immune signature (CD8+ T cells) in the TCGA-PDAC cohort.

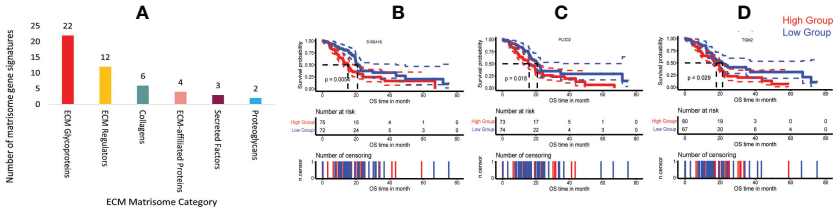

FIGURE 7
Correlation of *PLAU* expression and matrisome gene signatures in human PDAC. **(A)** Upregulation of *PLAU* gene expression was positively correlated with various PDAC ECM matrisome gene signatures. Kaplan Meier survival curves show that in the TCGA-PDAC cohort, poor survival was associated with **(B)** increased expression of *S100A16*, P = 0.0054, **(C)** *PLOD2*, P = 0.018 and **(D)** *TGM2*, P=0.029.

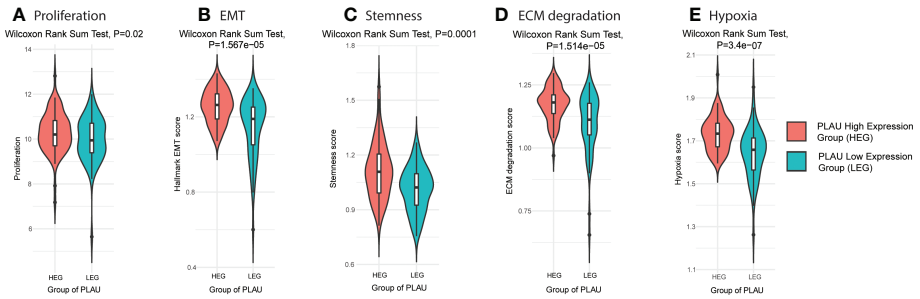

FIGURE 8
PLAU upregulation is associated with aggressive phenotypes of PDAC. Markers of an aggressive phenotype of PDAC were positively correlated with the high *PLAU* expressing group (HEG) compared to the low *PLAU* expression group (LEG), as depicted for **(A)** the tumour cell proliferation and growth index marker, MKI67, Wilcoxon rank-sum test, P= 0.02 **(B)** EMT Wilcoxon rank-sum test, P= 1.567e−05, **(C)** tumour stemness, Wilcoxon Rank Sum Test, P=0.0001, **(D)** ECM degradation, Wilcoxon Rank Sum Test, P= 1.514e−05 **(D, E)** hypoxia, Wilcoxon Rank Sum Test, P= 3.4e−07.

3.10 *PLAU*-correlated prognostic gene markers are also differentially expressed and associated with poor outcomes in PDAC at the protein level

In order to determine whether the identified prognostic gene signatures (*PLAU* correlated 41 positively and 34 negatively in the TCGA-PDAC cohort) translated to protein or not in the PDAC tumour, we performed a differential expression analysis based on the CPTAC-PDAC cohort. 135 patients' tumours proteome profile compared with proteins expression data from 67 normal adjacent and nine normal ducts tissues. The results showed that 23 out of 41 positively correlated prognostics markers were differentially upregulated; out of 34 negatively correlated prognostics markers, 16 were differentially downregulated (ST17).

The correlation of the differentially expressed protein signatures noted above with overall patient survival was also assessed in the CPTAC-PDAC cohort. Upregulated expression of CD44, CDH3, FNDC3B, HMGA2, ITGA3, MET, PPP1R14B, and PLOD2 and downregulation of KIAA0513, OTC, and LYZ were associated with poor survival (Figures 11A, B). Representative immunohistochemistry images from the human proteome atlas further confirmed the level of expression of the above proteins in PDAC tissues (71) (SF6).

3.11 Univariate and multivariate cox regression analysis of *PLAU* correlated (survival-related) proteins and different clinicopathological factors

To rule out the bias caused by the survival-related clinical parameters in the following analysis, we obtained the clinical dataset from CPTAC-PDAC and screened for the survival-related clinical index by univariate and multivariate cox regression analysis. Univariate Cox regression analyses of the CPTAC-PDAC clinical dataset identified eight proteins (out of the 12) and weight, histological grade, distant metastasis, tumour stage, residual tumour, and tobacco smoking history as individual prognostic factors (Figure 12A). Multivariate Cox regression analysis demonstrated that three prognostic proteins (*PLAU*, ITGA3, and PPP1R14B expression) and two clinicopathological factors (tumour stage and tobacco smoking history) were significantly associated with poor survival (Figure 12B).

3.12 *PLAU* and correlated signatures are associated with the basal subtype of PDAC

Identifying the subtypes of pancreatic cancer could assist with providing the patient with a more accurate prognosis prediction and may also allow precise and effective therapy. Therefore, the association of upregulated *PLAU* protein with survival in patients bearing tumours of PDAC basal and classical subtypes was explored (6). The basal/squamous subtype is characterised by mainly low expression of GATA6 with gene signatures enriched for the inflammation, hypoxia response, metabolic reprogramming and TGF-β signalling, and is also characterised by resistance to chemotherapy and poor outcomes. On the other hand, the classical subtype is characterised by high expression of *GATA6*, KRAS dependency, chemoresponsiveness and a better clinical outcome (4, 72). Using the CPTAC-PDAC cohort, we found that upregulation of *PLAU* protein was associated with poor survival (Figure 13A, P=0.0044). Further, a comparison of the survival outcome in basal vs classical clearly shows that the basal group of patients is more at risk of poor prognosis than the classical type (Figure 13B). Assessment of *PLAU* protein expression in basal and classical types

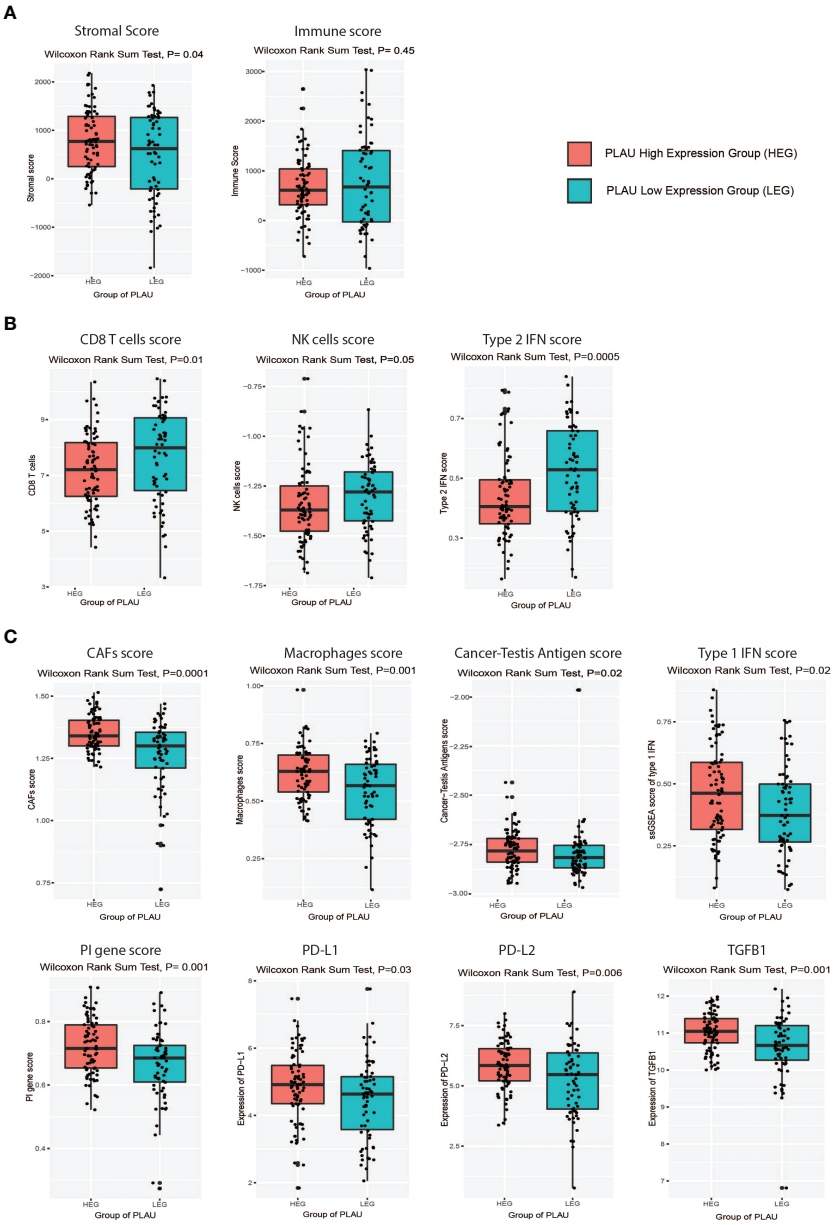

FIGURE 9
Association of *PLAU* upregulation with an immunosuppressive landscape in the TCGA PDAC cohort. Markers of an immunosuppressive landscape in PDAC were positively correlated with the high *PLAU* expressing group (HEG) compared to the low *PLAU* expression group (LEG), as evidenced by **(A)** a high stromal score (Wilcoxon rank-sum test, P=0.04) and a low immune score (Wilcoxon rank-sum test, P=0.45), **(B)** low scores for immune stimulatory signatures CD8+ T cells (Wilcoxon rank-sum test, P=0.01), NK cells (Wilcoxon rank-sum test, P=0.05), and type 2 IFN (Wilcoxon rank-sum test, P=0.0005), **(C)** high scores for immune inhibitory signatures including CAFs (Wilcoxon rank-sum test, P=0.0001), macrophages (Wilcoxon rank-sum test, P=0.001), cancer-testis antigens (Wilcoxon rank-sum test, P=0.02), Type 1 IFN (Wilcoxon rank-sum test, P=0.02), PI genes (Wilcoxon rank-sum test, P=0.001), PD-L1(Wilcoxon rank-sum test, P=0.03), PDL-2(Wilcoxon rank-sum test, P=0.006), and TGFB1 (Wilcoxon rank-sum test, P=0.001).

demonstrated that *PLAU* was significantly more expressed in the basal group than in the classical type (log2FC=0.80, p<0.001, Figure 13C). Furthermore, in all three PDAC cohorts (TCGA, ICGC and OICR PDAC cohorts), high *PLAU* gene expression was positively correlated with basal markers including *S100A2* (R=0.48, p=4.57E-10), *FAM83A* (R=0.55, p= 4.38E-13), *IGTA3* (R=0.45, p= 1.14E-08), *KRT5* (R=0.45, p= 6.81E-09), and *C16orf74* (R=0.64, p= 2.48E-18) and negatively correlated with classical molecular subtype markers including *GATA6* (R=-0.57, p= 2.93E-14) *TFF2* (R=-0.42, p= 1.20E-07), *REG4* (R=-0.40, p=

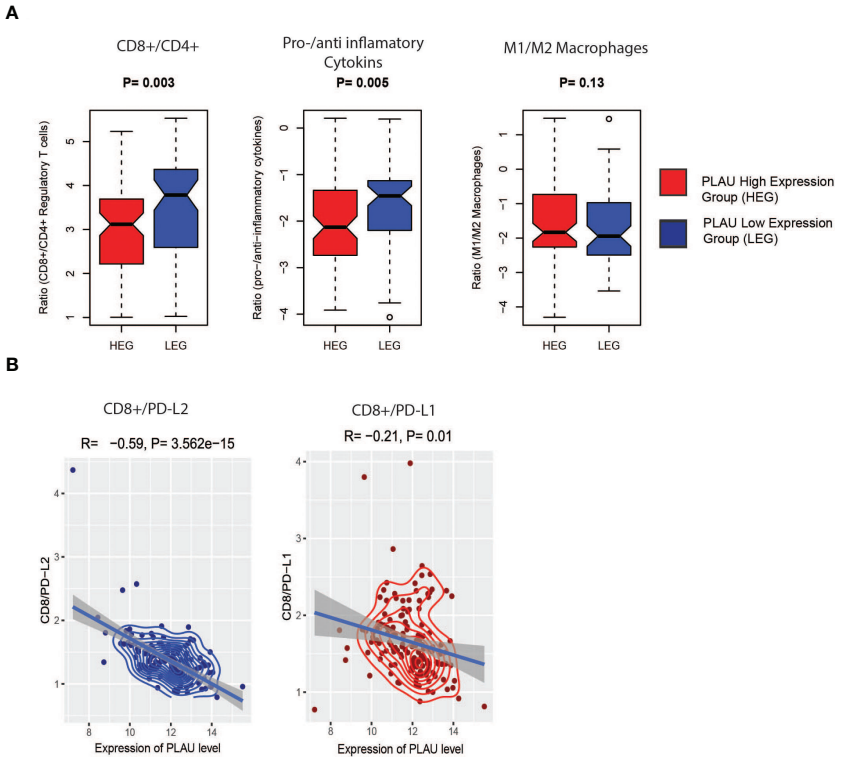

FIGURE 10
Association of *PLAU* upregulation with the immune ratios in the TCGA PDAC cohort. **(A)** CD8+ T cells/CD4+ T cell (P= 0.003) and pro-/anti-inflammatory cytokines (P= 0.005), significantly lower in the high expression group (HEG) of PLAU and **(B)**, the PLAU expression is negatively correlated with CD8A/PD-L1 (Pearson's correlation R=-0.59, P= 3.562e-15) and CD8A/PD-L2 (Pearson's correlation R=-0.21, P= 0.01).

5.98E-07), *LGALS4* (R=-0.39, p= 7.45E-07), and *DDC* (R=-0.44, p= 2.22E-08) (4, 6, 73, 74) (ST 18). Of note, survival analysis in the basal group patients demonstrated poor survival outcomes when stratified into the *PLAU* high group compared to the *PLAU* low group (Figure 13D, P=0.018). Further survival analysis between *PLAU* high basal versus *PLAU* high classical shows that even though upregulation of *PLAU* is found in both basal and classical group patients, *PLAU* high basal is worse than *PLAU* high classical (SF7B, P<0.0001). Consequently, the high and the low in the classical group patients demonstrated no significant association with poor survival (SF7A, P=0.9). These results support the concept that upregulation of *PLAU* protein is clinically associated with the poorest survival outcomes in the basal subtype of PDAC.

3.13 Effect of uPA - inhibition and Gemcitabine on tumour volume and metastasis *in vivo*

Finally, we assessed the effects of uPA inhibition on tumour growth and metastasis using the uPA inhibitor BB230F at 3mg (U3) and 10mg (U10)/kg body weight alongside the standard of care drug gemcitabine in an early intervention orthotopic xenograft mouse model of pancreatic cancer (Figure 14A). In this model, we observed that uPA inhibition (with U10) was comparable to Gemcitabine in reducing primary tumour volume at the endpoint. Importantly, uPA inhibition was significantly superior to Gemcitabine in reducing liver metastasis (key site in this model), with U10-treated mice showing no evidence of metastasis (Figures 14B, C, SF9A-B and ST20) in the liver. The absence of liver metastases in all animals treated with U10 was confirmed by histology. Since one of the main mechanisms underlying metastasis is increased EMT of cancer cells, we measured EMT in the model by assessing the ratio of expression of the mesenchymal marker vimentin to the epithelial marker E-Cadherin. An increase in the vimentin: E-cadherin ratio is an indicator of increased EMT. In the orthotopic tumours in this model, we found that while vimentin expression was unchanged, E-cadherin expression was significantly elevated in U10-treated mice compared to the other groups in Figures 14D-F, suggesting inhibition of cancer cell EMT by *PLAU* inhibition. We support these observations using the CPTAC-PDAC cohort, whereby patients in the upper

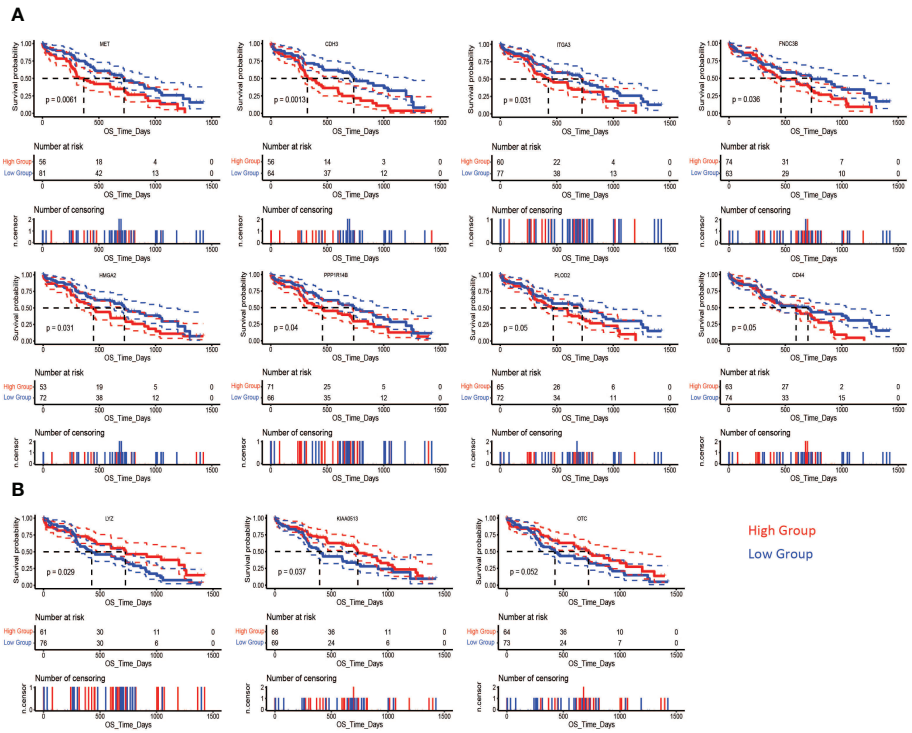

FIGURE 11
Association of differentially expressed proteins and survival in PDAC. In the CPTAC-PDAC cohort, Kaplan-Meier analysis shows that poor overall survival (OS) was correlated **(A)** high expression of MET (log-rank test, P= 0.0061), CDH3 (log-rank test, P= 0.0013), ITGA3 (log-rank test, P= 0.031), FNDC3B (log-rank test, P= 0.036), HMGA2 (log-rank test, P= 0.031), PPP1R14B (log-rank test, P= 0.04), and PLOD2 (log-rank test, P= 0.05) CD44 (log-rank test, P= 0.05), and **(B)** low expression of LYZ (log-rank test, P= 0.029), KIAA0513 (log-rank test, P= 0.037), and OTC (log-rank test, P= 0.05).

quartile of the *PLAU* expression group exhibited a significant decrease in E-cadherin and an increase of vimentin compared to patients in the lower quartile of the *PLAU* expression group (Figures 14G, H). Furthermore, immunostaining for the stem cell marker ALDH1A1, which plays a role in recurrence, metastasis, and treatment resistance, demonstrated that U10 significantly decreased ALDH1A1 expression compared to the mice treated with control and Gemcitabine alone (SF8A, B), suggesting that the uPA inhibition may inhibit cancer stemness.

4 Discussion

Pancreatic ductal adenocarcinoma (PDAC) is an overly aggressive cancer with very high recurrence rates and the poorest prognosis of all solid malignancies. The early and rapid development of metastasis (often seen before the detection of a sizeable pancreatic mass) is the primary driver of the poor clinical outcome of this cancer (75–78).

uPA and its cell surface receptor uPAR play a role in multiple stages of tumorigenesis, especially cancer progression (e.g., ECM degradation and EMT) (7, 24–27, 33–41). Moreover, clinical evidence demonstrates that high *PLAU* mRNA expression is associated with significantly worse clinicopathological characteristics and poor prognosis in PC patients (79, 80). In this study, we have elucidated the key molecular pathways modulated by or associated with *PLAU* upregulation. This will not only enable better prediction of clinical outcomes but importantly may help stratify and identify patients who may best benefit from therapeutic targeting of the uPA.

Using TCGA, CCLE and GEO databases, we have convincingly demonstrated that *PLAU* mRNA levels were significantly upregulated in 44 PDAC cell lines derived from primary or metastatic tumours compared to normal tissues. Importantly, analysis of the TCGA and ICGC PDAC cohorts confirmed the prognostic value of *PLAU* in pancreatic cancer. Validation of this finding at the protein level was obtained by analysis of the CPTAC-PDAC cohort, which demonstrated that high *PLAU* protein expression was significantly correlated with poor survival in PDAC patients.

To help understand the mechanisms mediating *PLAU*-associated poor survival, gene signatures that were commonly positively or negatively correlated with *PLAU* upregulation were identified in the TCGA, ICGC and OICR PDAC-specific

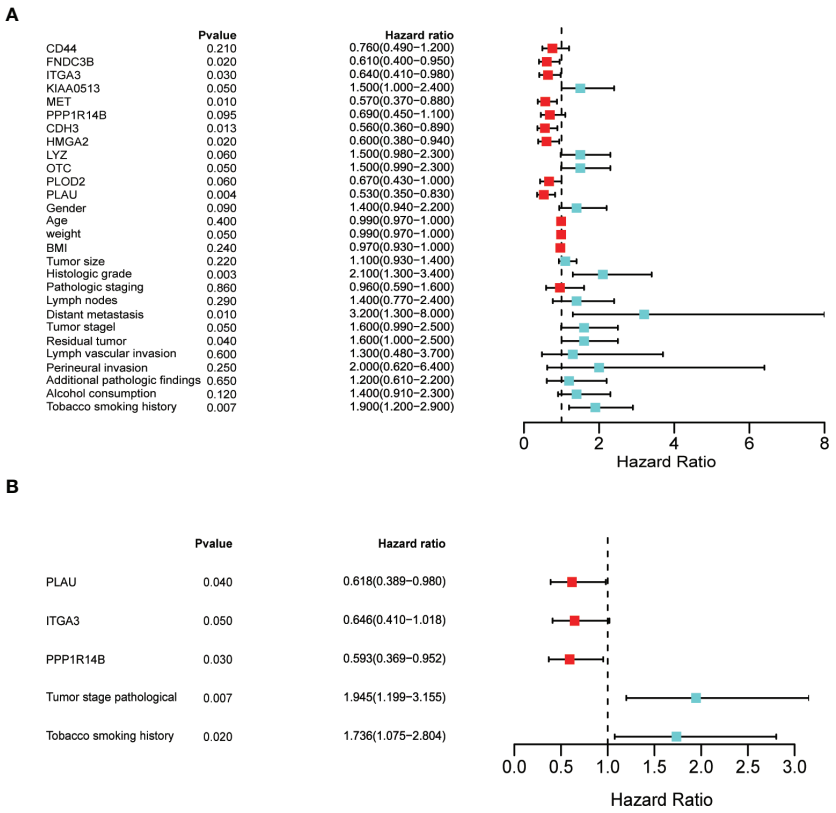

FIGURE 12
Identification of prognostic factors by univariate and multivariate analyses **(A)** Univariate Cox regression analysis of the following as individual prognostic factors: eight proteins (PLAU, MET, ITGA3, CDH3, FNDC3B, HMGA2, KIAA0513, OTC), weight, histological grade, distant metastasis, tumour stage, residual tumour, and tobacco smoking history. **(B)** Multivariate analysis identified three proteins (PLAU, ITGA3, and PPP1R14B), tumour stage and tobacco smoking history as significant prognostic factors.

cohorts. Analysis of these correlated genes revealed that *PLAU* upregulation was associated with gene signatures mainly encoding transcription factors, cytokines, growth factors, protein kinases and oncogene, which are involved with epithelial-mesenchymal transition, ECM degradation, cell proliferation, hypoxia, angiogenesis, stemness and metastasis. Survival analysis revealed that in the TCGA-PDAC cohort, 6% of positive and 7% of negatively correlated gene signatures were associated with poor survival. The key genes and their functions are summarised in Table 1. Of the downregulated genes in colon (81) and ovarian (82) cancer, *PPARGC1A* was reported as a tumour suppressor, and downregulation is associated with poor survival in colon cancer (83). However, the significance of the remaining downregulated genes in PDAC prognosis needs to be explored.

Examination of the protein-protein interaction network revealed that PLAU interacted directly with 31 positively correlated signatures that are active in oncogenesis hypoxia, proliferation, ECM degradation and EMT. On the other hand, PLAU interacted directly with one negatively correlated gene, ANG (angiogenin), the high expression of which is reported to be favourable in pancreatic cancer (84).

Gene set enrichment analysis confirmed that *PLAU* and its positively correlated signatures were involved with pathways that play a role in cancers. In contrast, *PLAU* and its negatively correlated signatures were predominantly related to the downregulation of metabolic pathways. With respect to the former group, 11 main pathways were identified, as depicted in Figure 5. Of particular interest are the following: i) the Hedgehog signalling pathway - known to be involved in early pancreatic cancer tumorigenesis (85). A component of this pathway Sonic HH (SHH), is increased more than 40-fold in pancreatic cancer stem cells responsible for tumour recurrence (86, 87). Li et al. showed that hypoxia-induced ROS production increases the expression of *PLAU* and MMP2 in pancreatic cancer cells through the Hh signalling pathway to facilitate invasion and metastasis (88). ii) the metabolic pathway glycosaminoglycan biosynthesis - chondroitin sulfate that facilitates invasiveness of cancer cells by supporting the adhesion of various cells such as fibroblasts or leukocytes in

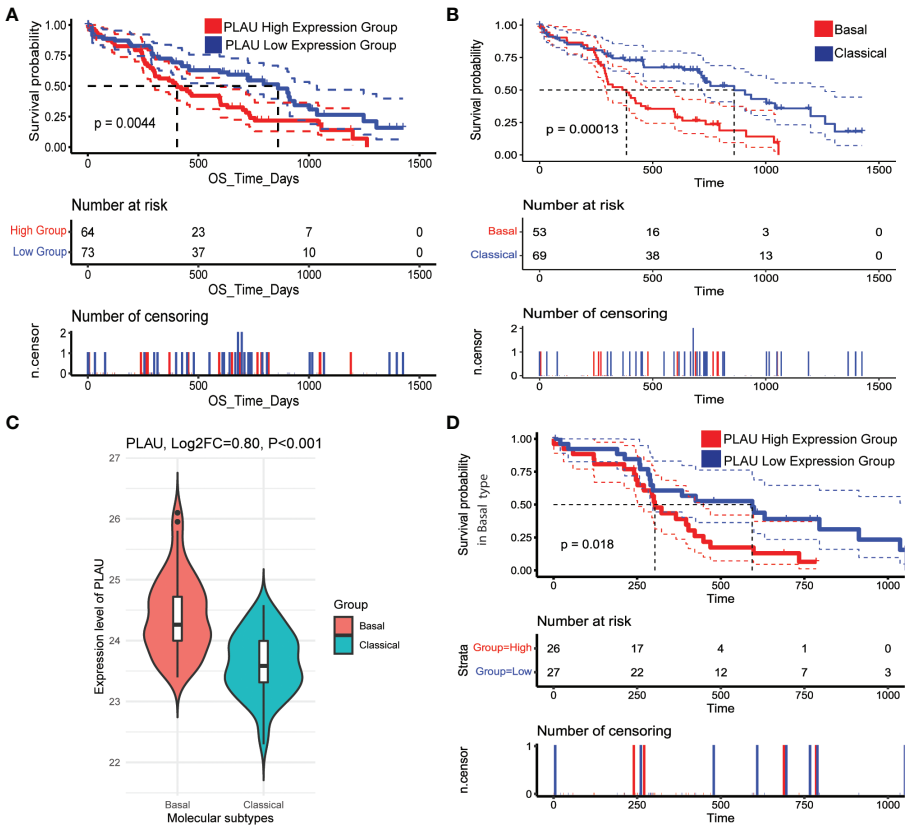

FIGURE 13
PLAU upregulation is associated with the basal type of PDAC. **(A)** In the CPTAC-PDAC cohort, **(A, B)** Kaplan-Meier survival curves show that increased PLAU protein expression is associated with poor prognosis (log-rank test, P=0044), and the basal subtype of PDAC is associated with worse survival than the classical subtype. **(C)** PLAU protein is significantly upregulated in the basal group than classical subtype (Log2FC=0.80, P<0.001); and **(D)** within the basal subtype, the clinical outcome in the high PLAU expression group is significantly worse than the low PLAU expression group (log-rank test, P=0.018).

the TME which are the source of growth factors and ECM-degrading enzymes that enable local migration and dissemination of cancer cells (89, 90). Interestingly, upregulation of components of this pathway, chondroitin and dermatan sulfate, has been reported in pancreatic tumours (91). iii) the Wnt signalling pathway, one of the critical cascades regulating development and stemness in cancer (92). This pathway is known to be critical to the initiation and progression of PDAC (93). iv) the TGF-beta signalling pathway which is most significantly involved in EMT induction in pancreatic cancer cells through activation of ERK/MAPK, PI3K, p38, JNK, RhoA, and other signalling pathways (36–38).

Intriguingly, *PLAU* upregulation and its negatively correlated gene signatures were found to be associated with the downregulation of a large number of metabolic pathways. Such downregulation could be attributed to a severely hypoxic environment in the tumour as a result of pronounced desmoplasia that limits oxygen diffusion (94, 95). Indeed, we found a significant increase in hypoxia in the high expression group of *PLAU* (Figures 6A, C and 8E). Given the central role of PSCs in the production of desmoplasia, it was also of interest that a significant correlation was identified between *PLAU* upregulation and activated PSC abundance (R= 0.41, P=2.754e-07) as well as between *PLAU* upregulation and Hypoxia-inducible factor-1α expression (R= 0.53, P<2.2e-16), a known PSC activation factor.

Moreover, PLAU upregulation is negatively associated with these pathways, suggesting that downregulation of critical metabolic pathways in pancreatic cancer patients may result in worse outcomes. Evidence suggests that metabolic disorders and failure of immunosurveillance to prevent malignancies are key drivers of cancer progression. The tumour immune escape phenomenon can be induced by several factors, including the loss of antigenicity, the loss of immunogenicity, and the immunosuppressive tumour microenvironment (TME), which are orchestrated by nutrient limitation and the build-up of specific metabolites and signalling molecules (96, 97).

10.3389/fimmu.2022.1060957

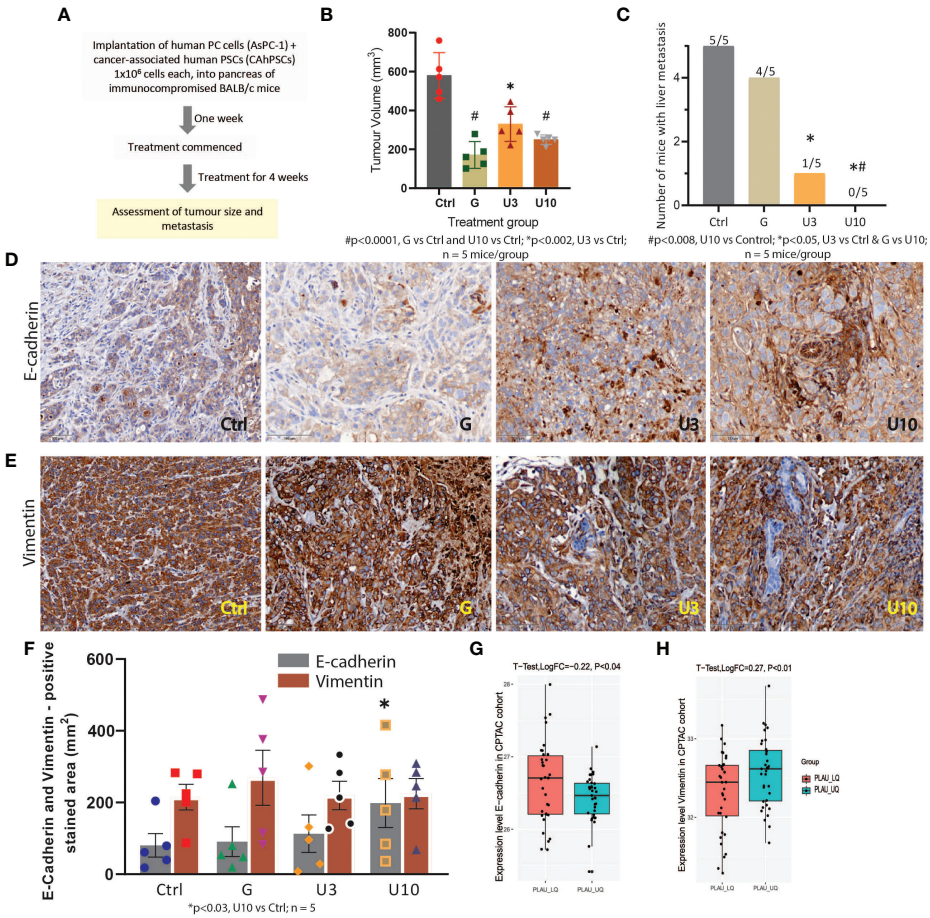

FIGURE 14
In vivo study to assess the effects of PLAU/uPA inhibition and Gemcitabine on tumour progression in an orthotopic model of pancreatic cancer **(A)** Flowchart depicting study design for the orthotopic model. **(B)** Effects of Gemcitabine **(G)**, uPA inhibitor BB230F 3 and 10 mg/kg body weight (U3) (U10), respectively, on endpoint primary tumour volume. Mice bearing orthotopic pancreatic tumours received G, 75 mg/kg body weight twice weekly or U3 or U10 by daily intraperitoneal injections for 28 days. Both gemcitabine and uPA inhibitors significantly reduced tumour volume (n = 5 mice/group). **(C)** uPA inhibition significantly reduced (U3) or completely abolished (U10) liver metastases in mice, while Gemcitabine did not have any effect on metastasis compared to untreated controls. (n = 5 mice/group). **(D, E)** Immunostaining for the mesenchymal marker vimentin and epithelial marker E-Cadherin. Representative photomicrographs depicting staining for E-cadherin and vimentin in mouse pancreas. **(F)** Morphometric analysis shows that while vimentin expression was unchanged by the treatments, E-cadherin expression was significantly increased in U10 compared to controls (n = 5 mice/group). E-cadherin and vimentin (EMT markers), scale bars = 100 µm. **(G, H)** In the CPTAC-PDAC cohort, protein expression analysis of EMT markers indicates that patients in the upper quartile of PLAU expression exhibit low E-cadherin (T-test, LogFC=-0.22 P=0.018) and high vimentin levels (T-test, LogFC=0.27 P<0.01) compared to lower quartile group, suggesting increased EMT in the tumours with upregulated PLAU expression.

The activation of the uPA/uPAR system has been reported to drives aerobic glycolysis (Warburg effect) in melanoma cell lines even in normoxic conditions, and this activation depends on the α5β1-integrin-mediated uPAR connection with EGFR with the engagement of the PI3K-mTOR-HIFα pathway (98). It has been established that the transcription factor HIF-1α promotes aerobic glycolysis and regulates tumour invasion and metabolism (99). Moreover, in this energy-deprived milieu, *PLAU* upregulation was also found to induce more hypoxia and activate the TGF beta pathway, thereby further increasing tumour immune suppression. Based on the above, it would be reasonable to speculate that uPA may participate in altering and/or downregulating metabolic pathways and in facilitating an immunosuppressive environment, thereby ultimately enhancing tumour progression.

PLAU upregulation was also associated with other PSC-derived factors and pathways that are thought to mediate the well-established bidirectional interaction between PSCs and PDAC cells. Activated PSCs markers that were positively correlated with *PLAU* (Pearson correlation test R>0.30, P<0.05), including *CDH11* [Cadherin-11 is elevated in PSCs and is related to PC cells migration (100)), *MME* (or CD10+

PSCs augment the aggressiveness of PDAC (101)], *LGALS1* [Galectin-1 plays role in the development and maintenance of an immunosuppressive microenvironment and promotes PDAC cells metastasis (102–104)], *FERMT2* [progression of pancreatic cancer (105)), *S100A4* (mesenchymal markers increased in activated PSCs (106)], *TGFb1* [TGF-beta signalling in activated PSCs promote ECM accumulation, induced EMT etc. (107, 108)], *POSTN* [promote cancer cell survival, EMT, invasion, and metastasis (109, 110)], *Runx2* [regulate the transcription of extracellular matrix modulators *SPARC* and *MMP1* and impact the tumour microenvironment (111)], *IL-1*[immune suppression (112, 113)], *IL8* (crosstalk with endothelial cells (20)), *PGDF* (proliferation and angiogenesis (20, 114)) and *PLOD2* (creates a permissive microenvironment for migration of cancer cells (115)).

The prominent ECM in PDAC not only supports cancer progression by directly promoting cellular transformation and metastasis but also affects the function of stromal cells to induce angiogenesis and inflammation, thereby resulting in a pro-tumorigenic microenvironment (116, 117). ECM proteins have also been recognised as essential components of the metastatic niche to maintain cancer stem cell properties and enable the outgrowth of metastasis-initiating cells (118–120). Therefore, an analysis of the association of *PLAU* and specific ECM markers and their prognostic significance was also undertaken in this study. 49 ECM gene signatures were found to be correlated with *PLAU*, of which three, namely, secreted factors *S100A16* (cancer-cell–derived), ECM regulator *PLOD2* (PSC-derived) and ECM regulator *TGM2* (cancer and stromal cell-derived) were significantly associated with poor survival in the TCGA-PDAC cohort. However, survival analysis using the CPTAC cohort revealed that only PLOD2 protein upregulation was significantly associated with poor survival (Figure 11A, PLOD2).

The immune system is now recognised to play a central role in cancer biology. There have been no studies to date assessing the association between *PLAU* expression and immune signatures in PDAC. This study has shown for the first time that *PLAU* expression correlates closely with immune gene signatures in three PDAC cohorts. In fact, upregulation of *PLAU* was associated with immune inhibitory rather than immune-stimulatory signatures. This concurs with the observed association of *PLAU* with growth factors and cytokines known to promote an immunosuppressive tumour microenvironment.

In view of the positive association discussed above between *PLAU* and its correlated signatures and factors that signify tumour aggressiveness, high and low *PLAU* groups in the TCGA-PDAC cohort were analysed. The results confirmed that tumours of patients with high *PLAU* gene expression also exhibited significantly increased proliferation, EMT, stemness, ECM degradation, hypoxia and immunosuppressive TME. These results suggest that *PLAU* and its correlated signatures induce an aggressive cancer phenotype leading to poor survival.

As outlined above, this study has clearly established that dysregulated *PLAU* and its correlated gene signatures have the potential to confer a poor prognosis for PDAC. However, without knowledge of related changes in the proteome, the usefulness of prognosis prediction based on only gene expression remains a challenge. Proteins are the key functional drivers of cancer biology, providing a link between genotype and phenotype and are common targets of anticancer drugs. Thus it is important to note that, using the CPTAC-PDAC cohort, most of the *PLAU* correlated prognostic gene markers identified in the TCGA-PDAC cohort were also found to be differentially expressed at the protein level. Eleven proteins were associated with poor survival, including upregulated CD44, CDH3, FNDC3B, HMGA2, ITGA3, MET, PPP1R14B, and PLOD2 and downregulated KIAA0513, OTC, and LYZ. We further confirmed their expression level in HPA. Out of 11 ITGA3, MET, FNDC3B, PPP1R14B and KIAA0513, including *PLAU*, were previously reported as individual prognostic markers in the pancreatic cancer TCGA-PAAD cohort (84). However, we have shown these for the first time in PDAC as prognostic markers in our analysis at the transcriptome and proteome levels.

Univariate analysis showed that *PLAU*, CDH3, FNDC3B, HMGA2, ITGA3, MET, KIAA0513, OTC, weight, histological grade, distant metastasis, tumour stage, residual tumour, and smoking are individual prognostic factors for PDAC. Notably, multivariate analysis revealed that *PLAU* protein upregulation in association with ITGA3, and PPP1R14B expression, tumour stage, and smoking history could predict poor overall survival in PDAC. Overexpression of ITGA3 was confirmed in PDAC clinical specimens and associated with poor prognosis (121). Pan-cancer analysis revealed that increased PPP1R14B expression correlated with poor prognosis and increased immune infiltration levels in myeloid-derived suppressor cells (MDSCs), and PPP1R14B could be used as a prognostic biomarker for pan-cancer (122).

The systematic approach used in this study, based on integrated proteotranscriptomics data, supports a major role for the *PLAU* gene and its corresponding protein (uPA) in driving an aggressive metastatic phenotype of PDAC associated with an immunosuppressed TME. The challenge in using this knowledge to develop *PLAU*-targeted treatment is the well-known heterogeneity of this disease. Therefore, accurate patient stratification is essential to ensure optimal outcomes of targeted therapies. To this end, this study also sought to identify whether specific subtypes of PDAC were associated with *PLAU* upregulation. As noted earlier, the commonest classification of PDAC is based on the morphological features of the tumour, with patients being classified as having classical or basal-like subtypes of PDAC (123). Interestingly, this study found a strong correlation between PLAU upregulation and basal type of PDAC while negatively correlated with classical type gene signatures. Pathway analysis further revealed that *PLAU* upregulation was directly associated with vital oncogenic pathways (WNT, WNT

beta-Catenin (93, 124, 125) and EMT (TGF beta (126) pathways as well as with hypoxia and ECM-rich stroma, all characteristic of basal PDAC (127–129). Finally, the acquisition of all the malignant phenotypes in the high PLAU group supports the basal type PDAC association with *PLAU*. The association of high *PLAU* with the basal PDAC subtype was also validated at the protein level using the CPTAC-PDAC cohort, as was the correlation of the basal subtype with poor survival (Figures 13B-D and SF7).

Importantly, we have validated the concept of a key role for *PLAU*/uPA in cancer progression and its potential as a therapeutic target by performing studies in an orthotopic pancreatic tumour model. Our underlying initial strategy for this study was also to compare a non-chemotherapy targeted approach (uPA inhibitor) with a single agent well-tolerated chemotherapy so as to minimise toxic effects while, at the same time, potentially increasing treatment efficacy. This approach has resulted in very encouraging results where uPA inhibition alone significantly reduced tumour growth to a degree similar to Gemcitabine. Crucially, uPA inhibition was significantly superior to Gemcitabine in reducing metastasis, with U10-treated mice showing no evidence of metastasis. The inhibition of metastasis by uPA inhibition is likely mediated by the decrease in EMT and stemness evident in U10-treated mice. Using uPA knock-out cells Fang et al. has convincingly demonstrated that the knockdown *PLAU* in KYSE-30 cells exhibited significantly reduced tumour growth and weight than the control (normal uPA expression) group, while the *PLAU* overexpression group exhibited increased tumour growth and weight compared with the control group (27). *In vitro* studies using pancreatic cancer cell lines have shown that the knockdown of uPA reduces cancer cell migration, invasion and viability (130).Multiple *in vivo* studies have shown that inhibiting uPA with antibodies, uPA-directed prodrugs or radioisotopes and small molecule inhibitors alone or in combination with other drugs can block cancer growth, invasion and metastasis in prostate and breast cancer (131–135). In addition, uPA inhibitors have also demonstrated very encouraging outcomes in clinical trials for the treatment of different types of solid tumours (136, 137), including using Upamostat (WX-671, Mesupron) in advanced pancreatic cancer patients (138, 139).

This study has yielded novel findings regarding *PLAU* and its role in PDAC tumour progression using comprehensive and integrated transcriptomic/proteomic bioinformatic analyses. Moreover, since upregulation of *PLAU* levels is also frequently observed in a number of malignancies and upregulation of *PLAU* is a prognostic marker not only in pancreatic cancer but also in head and neck, endometrial cancer, renal and lung (42), breast (140) and oesophageal cancer (27). In light of the above, it is highly likely that the approach used in our study for pancreatic cancer could be a promising approach for several other cancers. However, the study does have limitations. All clinical cohorts in this study (with small sample size) primarily comprised Caucasians or Africans; therefore, caution must be exercised to extrapolate the findings to patients of other ethnicities. The orthotopic xenograft model of pancreatic cancer used in this study involved using a mixture of human cancer cells and human pancreatic stellate cells that provided strong support for our concept that uPA drives pancreatic cancer progression. However, the mice were necessarily immunodeficient, and as such, the model did not lend itself to characterise any immune infiltration into the tumours accurately. The findings derived from our *in silico* and *in vivo* analyses need to be validated experimentally in more depth, a step currently being pursued in our laboratory. In this regard, we are evaluating the effects of inhibiting uPA in a clinically representative orthotopic mouse model (early and advanced) of PDAC in both immune-deficient and immune-competent (syngeneic KPC model, where a mixture of mouse cancer cells and mouse pancreatic stellate cells is implanted into the KPC mouse pancreas) settings with more numbers of mice. The immune cell landscape in this model closely resembles that of human pancreatic cancer with infiltration of myeloid-derived suppressor cells (MDSC), Treg cells and a few CD8+ cytotoxic T cells (141–143). Future work will also combine inhibition with multiagent chemotherapy to further optimise outcomes or to demonstrate that single-agent chemotherapy + targeted therapy may be preferred to current multiagent strategies in selected patients. In search of treatment alternatives, we also hypothesise that in basal-like tumours, since upregulation of the PLAU group has higher hypoxia scores and higher immunosuppressive tumour signatures (PD-L1 and PD-L2) than the anti-tumour immune signature (CD8+ T cells), which may be predictive of immunotherapy (in combination with uPA and plus-minus chemotherapy) in this chemo resistant.

5 Conclusion

For the first time, this study has comprehensively revealed the significance of PLAU in PDAC development, metastasis, and immune suppression and has demonstrated the potential translational importance of inhibiting master regulator PLAU protein in basal type PDAC patients. Thus, it would not be unreasonable to hypothesise that selectively inhibiting PLAU (with and without chemo/immune therapy) in patients with basal PDAC may represent a novel and effective therapeutic approach to improve patient outcomes.

Data availability statement

Publicly available datasets were analyzed in this study. This data can be found here: https://www.ncbi.nlm.nih.gov/gds), Cancer Cell Line Encyclopedia (CCLE, https://depmap.org/portal/ccle/), International Cancer Genome Consortium

(ICGC, https://icgc.org/), the Cancer Genome Atlas (TCGA, http://cancergenome.nih.gov/), the National Cancer Institute's Clinical Proteomic Tumor Analysis Consortium (CPTAC, https://pdc.cancer.gov/pdc/) and the Ontario Institute for Cancer Research (OICR) PDAC cohort' gene expression and clinical data are only available upon through a data access agreement with referenced institute.

Ethics statement

The animal study was reviewed and approved by University of New South Wales Animal Care and Ethics Committee (Approval Number 18/125B) and accomplished under ARRIVE guidelines.

Author contributions

SH. designed experiments, acquired and analysed data, interpreted results, and wrote and revised the manuscript. MU helped analysed data and interpret bioinformatics results. ZX acquired data for *in vivo* experiments; BB synthesized and prepared formulation for *in vivo* study. CP acquired data for *in vitro* experiments. TP helped to interpret the results. AM acquired data for *in vivo* experiments. MM helped to interpret the bioinformatics results. FN and SG acquired OICR-cohort data. RP helped to interpret results and revised manuscript. JW helped to interpret results and revised manuscript. MR helped to interpret results and revised manuscript. DG helped to interpret results, and revised manuscript and MA conceived, designed the study and experiments, interpreted results, and revised manuscript. All authors contributed to the article and approved the submitted version.

Funding

This work was supported by a grant from Avner Pancreatic Cancer Foundation (RG172336) and UNSW Scientia Scholarship. This study was also conducted with the support of the Ontario Institute for Cancer Research (PanCuRx Translational Research Initiative) through funding provided by the Government of Ontario, the Wallace McCain Centre for Pancreatic Cancer supported by the Princess Margaret Cancer Foundation, the Terry Fox Research Institute, the Canadian Cancer Society Research Institute, and the Pancreatic Cancer Canada Foundation.

Conflict of interest

The authors declare that the research was conducted in the absence of any commercial or financial relationships that could be construed as a potential conflict of interest.

Publisher's note

Supplementary material

The Supplementary Material for this article can be found online at: https://www.frontiersin.org/articles/10.3389/fimmu.2022.1060957/full#supplementary-material

References

1. Sung H, Ferlay J, Siegel RL, Laversanne M, Soerjomataram I, Jemal A, et al. Global cancer statistics 2020: GLOBOCAN estimates of incidence and mortality worldwide for 36 cancers in 185 countries. *CA: Cancer J Clin* (2021) 71(3):209–49. doi: 10.3322/caac.21660

2. Rahib L, Smith BD, Aizenberg R, Rosenzweig AB, Fleshman JM, Matrisian LM. Projecting cancer incidence and deaths to 2030: The unexpected burden of thyroid, liver, and pancreas cancers in the united states. *Cancer Res* (2014) 74 (11):2913–21. doi: 10.1158/0008-5472.CAN-14-0155

3. Chun JW, Lee SH, Kim JS, Park N, Huh G, Cho IR, et al. Comparison between FOLFIRINOX and gemcitabine plus nab-paclitaxel including sequential treatment for metastatic pancreatic cancer: A propensity score matching approach. *BMC Cancer* (2021) 21(1):537. doi: 10.1186/s12885-021-08277-7

4. Bailey P, Chang DK, Nones K, Johns AL, Patch A-M, Gingras M-C, et al. Genomic analyses identify molecular subtypes of pancreatic cancer. *Nature* (2016) 531(7592):47–52. doi: 10.1038/nature16965

5. Collisson EA, Sadanandam A, Olson P, Gibb WJ, Truitt M, Gu S, et al. Subtypes of pancreatic ductal adenocarcinoma and their differing responses to therapy. *Nat Med* (2011) 17(4):500–3. doi: 10.1038/nm.2344

6. Moffitt RA, Marayati R, Flate EL, Volmar KE, Loeza SGH, Hoadley KA, et al. Virtual microdissection identifies distinct tumor-and stroma-specific subtypes of pancreatic ductal adenocarcinoma. *Nat Genet* (2015) 47(10):1168–78. doi: 10.1038/ng.3398

7. Kumar AA, Buckley BJ, Ranson M. The urokinase plasminogen activation system in pancreatic cancer: Prospective diagnostic and therapeutic targets. *Biomolecules* (2022) 12(2):152. doi: 10.3390/biom12020152

8. Chan-Seng-Yue M, Kim JC, Wilson GW, Ng K, Figueroa EF, O'Kane GM, et al. Transcription phenotypes of pancreatic cancer are driven by genomic events during tumor evolution. *Nat Genet* (2020) 52(2):231–40. doi: 10.1038/s41588-019-0566-9

9. Puleo F, Nicolle R, Blum Y, Cros J, Marisa L, Demetter P, et al. Stratification of pancreatic ductal adenocarcinomas based on tumor and microenvironment features. *Gastroenterology* (2018) 155(6):1999–2013. e3. doi: 10.1053/j.gastro.2018.08.033

10. Kim S, Kang MJ, Lee S, Bae S, Han S, Jang J-Y, et al. Identifying molecular subtypes related to clinicopathologic factors in pancreatic cancer. *Biomed Eng Online* (2014) 13(2):1–11. doi: 10.1186/1475-925X-13-S2-S5

11. Namkung J, Kwon W, Choi Y, Yi SG, Han S, Kang MJ, et al. Molecular subtypes of pancreatic cancer based on miRNA expression profiles have independent prognostic value. *J Gastroenterol Hepatol* (2016) 31(6):1160–7. doi: 10.1111/jgh.13253

12. Janky RS, Binda MM, Allemeersch J, Govaere O, Swinnen JV, Roskams T, et al. Prognostic relevance of molecular subtypes and master regulators in pancreatic ductal adenocarcinoma. *BMC Cancer* (2016) 16(1):1–15. doi: 10.1186/s12885-016-2540-6

13. Birnbaum DJ, Finetti P, Birnbaum D, Mamessier E, Bertucci F. Validation and comparison of the molecular classifications of pancreatic carcinomas. *Mol Cancer* (2017) 16(1):1–7. doi: 10.1186/s12943-017-0739-z

14. Moore MJ, Goldstein D, Hamm J, Figer A, Hecht JR, Gallinger S, et al. Erlotinib plus gemcitabine compared with gemcitabine alone in patients with advanced pancreatic cancer: A phase III trial of the national cancer institute of Canada clinical trials group. *J Clin Oncol* (2007) 25(15):1960–6. doi: 10.1200/JCO.2006.07.9525

15. Royal RE, Levy C, Turner K, Mathur A, Hughes M, Kammula US, et al. Phase 2 trial of single agent ipilimumab (anti-CTLA-4) for locally advanced or metastatic pancreatic adenocarcinoma. *J Immunother (Hagerstown Md: 1997)* (2010) 33(8):828. doi: 10.1097/CJI.0b013e3181eec14c

16. Le DT, Lutz E, Uram JN, Sugar EA, Onners B, Solt S, et al. Evaluation of ipilimumab in combination with allogeneic pancreatic tumor cells transfected with a GM-CSF gene in previously treated pancreatic cancer. *J Immunother (Hagerstown Md: 1997)* (2013) 36(7):382. doi: 10.1097/CJI.0b013e31829fb7a2

17. O'Reilly EM, Oh D-Y, Dhani N, Renouf DJ, Lee MA, Sun W, et al. Durvalumab with or without tremelimumab for patients with metastatic pancreatic ductal adenocarcinoma: A phase 2 randomized clinical trial. *JAMA Oncol* (2019) 5(10):1431–8. doi: 10.1001/jamaoncol.2019.1588

18. Wilson J, Pirola R, Apte M. Stars and stripes in pancreatic cancer: Role of stellate cells and stroma in cancer progression. *Front Physiol* (2014) 5(52). doi: 10.3389/fphys.2014.00052

19. Apte MV, Xu Z, Pothula S, Goldstein D, Pirola RC, Wilson JS. Pancreatic cancer: The microenvironment needs attention too! *Pancreatology* (2015) 15(4 Suppl):S32–8. doi: 10.1016/j.pan.2015.02.013

20. Schnittert J, Bansal R, Prakash J. Targeting pancreatic stellate cells in cancer. *Trends Cancer* (2019) 5(2):128–42. doi: 10.1016/j.trecan.2019.01.001

21. Pothula SP, Xu Z, Goldstein D, Merrett N, Pirola RC, Wilson JS, et al. Targeting the HGF/c-MET pathway: Stromal remodelling in pancreatic cancer. *Oncotarget* (2017) 8(44):76722. doi: 10.18632/oncotarget.20822

22. Bauer TW, Liu W, Fan F, Camp ER, Yang A, Somcio RJ, et al. Targeting of urokinase plasminogen activator receptor in human pancreatic carcinoma cells inhibits c-Met–and insulin-like growth factor-I receptor–mediated migration and invasion and orthotopic tumor growth in mice. *Cancer Res* (2005) 65(17):7775–81. doi: 10.1158/0008-5472.CAN-05-0946

23. Tincknell G, Piper A-K, Aghmesheh M, Becker T, Vine KL, Brungs D, et al. Experimental and clinical evidence supports the use of urokinase plasminogen activation system components as clinically relevant biomarkers in gastroesophageal adenocarcinoma. *Cancers (Basel)* (2021) 13(16):4097. doi: 10.3390/cancers13164097

24. Ranson M, Andronicos NM. Plasminogen binding and cancer: promises and pitfalls. *Front Biosci* (2003) 8:s294–304. doi: 10.2741/1044

25. De Vries T, Van Muijen G, Ruiter D. The plasminogen activation system in tumour invasion and metastasis. *Pathol-Res Prac* (1996) 192(7):718–33. doi: 10.1016/S0344-0338(96)80094-X

26. Chen G, Sun J, Xie M, Yu S, Tang Q, Chen L. PLAU promotes cell proliferation and epithelial-mesenchymal transition in head and neck squamous cell carcinoma. *Front Genet* (2021) 12. doi: 10.3389/fgene.2021.651882

27. Fang L, Che Y, Zhang C, Huang J, Lei Y, Lu Z, et al. PLAU directs conversion of fibroblasts to inflammatory cancer-associated fibroblasts, promoting esophageal squamous cell carcinoma progression *via* uPAR/Akt/NF-κB/IL8 pathway. *Cell Death Discov* (2021) 7(1):1–14. doi: 10.1038/s41420-021-00410-6

28. Bekes EM, Deryugina EI, Kupriyanova TA, Zajac E, Botkjaer KA, Andreasen PA, et al. Activation of pro-uPA is critical for initial escape from the primary tumor and hematogenous dissemination of human carcinoma cells. *Neoplasia* (2011) 13 (9):806–21. doi: 10.1593/neo.11704

29. Irigoyen JP, Munoz-Canoves P, Montero L, Koziczak M, Nagamine Y. The plasminogen activator system: biology and regulation. *Cell Mol Life Sciences: CMLS* (1999) 56(1-2):104–32. doi: 10.1007/PL00000615

30. Montuori N, Rossi G, Ragno P. Post-transcriptional regulation of gene expression in the plasminogen activation system. *Biol Chem* (2002) 383(1):47–53. doi: 10.1515/BC.2002.005

31. Nagamine Y, Medcalf RL, Munoz-Canoves P. Transcriptional and posttranscriptional regulation of the plasminogen activator system. *Thromb Haemostasis* (2005) 93(4):661–75. doi: 10.1160/TH04-12-0814

32. Duffy M, Duggan C. The urokinase plasminogen activator system: a rich source of tumour markers for the individualised management of patients with cancer. *Clin Biochem* (2004) 37(7):541–8. doi: 10.1016/j.clinbiochem.2004.05.013

33. Mahmood N, Mihalcioiu C, Rabbani SA. Multifaceted role of the urokinase-type plasminogen activator (uPA) and its receptor (uPAR): Diagnostic, prognostic, and therapeutic applications. *Front Oncol* (2018) 8(24):. doi: 10.3389/fonc.2018.00024

34. Masucci MT, Minopoli M, Di Carluccio G, Motti ML, Carriero MV. Therapeutic strategies targeting urokinase and its receptor in cancer. *Cancers (Basel)* (2022) 14(3):498. doi: 10.3390/cancers14030498

35. Carriero MV, Stoppelli MP. The urokinase-type plasminogen activator and the generation of inhibitors of urokinase activity and signaling. *Curr Pharm Des* (2011) 17(19):1944–61. doi: 10.2174/138161211796718143

36. Blasi F, Carmeliet P. uPAR: a versatile signalling orchestrator. *Nat Rev Mol Cell Biol* (2002) 3(12):932–43. doi: 10.1038/nrm977

37. Jo M, Thomas KS, Marozkina N, Amin TJ, Silva CM, Parsons SJ, et al. Dynamic assembly of the urokinase-type plasminogen activator signaling receptor complex determines the mitogenic activity of urokinase-type plasminogen activator. *J Biol Chem* (2005) 280(17):17449–57. doi: 10.1074/jbc.M413141200

38. Smith HW, Marshall CJ. Regulation of cell signalling by uPAR. *Nat Rev Mol Cell Biol* (2010) 11(1):23–36. doi: 10.1038/nrm2821

39. Andreucci E, Laurenzana A, Peppicelli S, Biagioni A, Margheri F, Ruzzolini J, et al. uPAR controls vasculogenic mimicry ability expressed by drug-resistant melanoma cells. *Oncol Res Featuring Preclinical Clin Cancer Ther* (2021) 28(7-8):7–8. doi: 10.3727/096504021X16273798026651

40. Laurenzana A, Margheri F, Biagioni A, Chillà A, Pimpinelli N, Ruzzolini J, et al. EGFR/uPAR interaction as druggable target to overcome vemurafenib acquired resistance in melanoma cells. *EBioMedicine* (2019) 39:194–206. doi: 10.1016/j.ebiom.2018.12.024

41. Gonias SL, Hu J. Urokinase receptor and resistance to targeted anticancer agents. *Front Pharmacol* (2015) 6:154. doi: 10.3389/fphar.2015.00154

42. Uhlén M, Fagerberg L, Hallström BM, Lindskog C, Oksvold P, Mardinoglu A, et al. Tissue-based map of the human proteome. *Science* (2015) 347(6220):1–9. doi: 10.1126/science.1260419

43. Ma Y, Pu Y, Peng L, Luo X, Xu J, Peng Y, et al. Identification of potential hub genes associated with the pathogenesis and prognosis of pancreatic duct adenocarcinoma using bioinformatics meta–analysis of multi–platform datasets. *Oncol Letters* (2019) 18(6):6741–51. doi: 10.3892/ol.2019.11042

44. Pacini C, Dempster JM, Boyle I, Gonçalves E, Najgebauer H, Karakoc E, et al. Integrated cross-study datasets of genetic dependencies in cancer. *Nat Commun* (2021) 12(1):1661. doi: 10.1038/s41467-021-21898-7

45. Ghandi M, Huang FW, Jané-Valbuena J, Kryukov GV, Lo CC, McDonald ER, et al. Next-generation characterization of the cancer cell line encyclopedia. *Nature* (2019) 569(7757):503–8. doi: 10.1038/s41586-019-1186-3

46. Pei H, Li L, Fridley BL, Jenkins GD, Kalari KR, Lingle W, et al. FKBP51 affects cancer cell response to chemotherapy by negatively regulating akt. *Cancer Cell* (2009) 16(3):259–66. doi: 10.1016/j.ccr.2009.07.016

47. Wennerström AB, Lothe IM, Sandhu V, Kure EH, Myklebost O, Munthe E. Generation and characterisation of novel pancreatic adenocarcinoma xenograft models and corresponding primary cell lines. *PloS One* (2014) 9(8):e103873. doi: 10.1371/journal.pone.0103873

48. Jiang J, Azevedo-Pouly AC, Redis RS, Lee EJ, Gusev Y, Allard D, et al. Globally increased ultraconserved noncoding RNA expression in pancreatic adenocarcinoma. *Oncotarget* (2016) 7(33):53165–77. doi: 10.18632/oncotarget.10242

49. Lin J, Wu YJ, Liang X, Ji M, Ying HM, Wang XY, et al. Network-based integration of mRNA and miRNA profiles reveals new target genes involved in pancreatic cancer. *Mol Carcinog* (2019) 58(2):206–18. doi: 10.1002/mc.22920

50. Gao J, Aksoy BA, Dogrusoz U, Dresdner G, Gross B, Sumer SO, et al. Integrative analysis of complex cancer genomics and clinical profiles using the cBioPortal. *Sci Signaling* (2013) 6(269):pl1. doi: 10.1126/scisignal.2004088

51. Benjamini Y, Hochberg Y. Controlling the false discovery rate: a practical and powerful approach to multiple testing. *J R Stat Society: Ser B (Methodological)* (1995) 57(1):289–300. doi: 10.1111/j.2517-6161.1995.tb02031.x

52. Liberzon A, Subramanian A, Pinchback R, Thorvaldsdóttir H, Tamayo P, Mesirov JP. Molecular signatures database (MSigDB) 3. *0. Bioinf* (2011) 27 (12):1739–40. doi: 10.1093/bioinformatics/btr260

53. Subramanian A, Tamayo P, Mootha VK, Mukherjee S, Ebert BL, Gillette MA, et al. Gene set enrichment analysis: A knowledge-based approach for interpreting genome-wide expression profiles. *Proc Natl Acad Sci United States America* (2005) 102(43):15545–50. doi: 10.1073/pnas.0506580102

54. Szklarczyk D, Gable AL, Lyon D, Junge A, Wyder S, Huerta-Cepas J, et al. STRING v11: protein–protein association networks with increased coverage,

supporting functional discovery in genome-wide experimental datasets. *Nucleic Acids Res* (2019) 47(D1):D607–13. doi: 10.1093/nar/gky1131

55. Shannon P, Markiel A, Ozier O, Baliga NS, Wang JT, Ramage D, et al. Cytoscape: A software environment for integrated models of biomolecular interaction networks. *Genome Res* (2003) 13(11):2498–504. doi: 10.1101/gr.1239303

56. Chin CH, Chen SH, Wu HH, Ho CW, Ko MT, Lin CY. cytoHubba: Identifying hub objects and sub-networks from complex interactome. *BMC Syst Biol* (2014) 8 Suppl 4(Suppl 4):S11. doi: 10.1186/1752-0509-8-S4-S11

57. Cran, R foundation: Therneau T. M. *A Package for Survival Analysis in R*. (2020). Available at: https://CRAN.R-projectorg/package=survival.

58. Yoshihara K, Shahmoradgoli M, Martínez E, Vegesna R, Kim H, Torres-Garcia W, et al. Inferring tumour purity and stromal and immune cell admixture from expression data. *Nat Commun* (2013) 4(1):2612. doi: 10.1038/ncomms3612

59. Bachem MG, Schneider E, Groß H, Weidenbach H, Schmid RM, Menke A, et al. Identification, culture, and characterization of pancreatic stellate cells in rats and humans. *Gastroenterology* (1998) 115(2):421–32. doi: 10.1016/S0016-5085(98)70209-4

60. Apte M, Haber P, Applegate T, Norton I, McCaughan G, Korsten M, et al. Periacinar stellate shaped cells in rat pancreas: identification, isolation, and culture. *Gut* (1998) 43(1):128–33. doi: 10.1136/gut.43.1.128

61. Pothula SP, Xu Z, Goldstein D, Biankin AV, Pirola RC, Wilson JS, et al. Hepatocyte growth factor inhibition: a novel therapeutic approach in pancreatic cancer. *Br J Cancer* (2016) 114(3):269–80. doi: 10.1038/bjc.2015.478

62. Vonlaufen A, Phillips PA, Xu Z, Goldstein D, Pirola RC, Wilson JS, et al. Pancreatic stellate cells and pancreatic cancer cells: an unholy alliance. *Cancer Res* (2008) 68(19):7707–10. doi: 10.1158/0008-5472.CAN-08-1132

63. Xu Z, Pang TCY, Liu AC, Pothula SP, Mekapogu AR, Perera CJ, et al. Targeting the HGF/c-MET pathway in advanced pancreatic cancer: A key element of treatment that limits primary tumour growth and eliminates metastasis. *Br J Cancer* (2020) 122(10):1486–95. doi: 10.1038/s41416-020-0782-1

64. Buckley BJ, Aboelela A, Minaei E, Jiang LX, Xu Z, Ali U, et al. 6-substituted hexamethylene amiloride (HMA) derivatives as potent and selective inhibitors of the human urokinase plasminogen activator for use in cancer. *J Medicinal Chem* (2018) 61(18):8299–320. doi: 10.1021/acs.jmedchem.8b00838

65. Kalimuthu S N, Wilson GW, Grant RC, Seto M, O'Kane G, Vajpeyi R, et al. Morphological classification of pancreatic ductal adenocarcinoma that predicts molecular subtypes and correlates with clinical outcome. *Gut* (2020) 69(2):317–28. doi: 10.1136/gutjnl-2019-318217

66. Pothula SP, Pirola RC, Wilson JS, Apte MV. Pancreatic stellate cells: Aiding and abetting pancreatic cancer progression. *Pancreatology* (2020) 20(3):409–18. doi: 10.1016/j.pan.2020.01.003

67. Vonlaufen A, Joshi S, Qu C, Phillips PA, Xu Z, Parker NR, et al. Pancreatic stellate cells: partners in crime with pancreatic cancer cells. *Cancer Res* (2008) 68(7):2085–93. doi: 10.1158/0008-5472.CAN-07-2477

68. Xu Z, Vonlaufen A, Phillips PA, Fiala-Beer E, Zhang X, Yang L, et al. Role of pancreatic stellate cells in pancreatic cancer metastasis. *Am J Pathology* (2010) 177(5):2585–96. doi: 10.2353/ajpath.2010.090899

69. Mekapogu A, Pothula S, Pirola R, Wilson J, Apte M. Multifunctional role of pancreatic stellate cells in pancreatic cancer. *Ann Pancreat Cancer* (2019) 2(10):1–15. doi: 10.21037/apc.2019.05.02

70. Tian C, Clauser KR, Öhlund D, Rickelt S, Huang Y, Gupta M, et al. Proteomic analyses of ECM during pancreatic ductal adenocarcinoma progression reveal different contributions by tumor and stromal cells. *Proc Natl Acad Sci* (2019) 116(39):19609–18. doi: 10.1073/pnas.1908626116

71. Deutsch EW, Omenn GS, Sun Z, Maes M, Pernemalm M, Palaniappan KK, et al. Advances and utility of the human plasma proteome. *J Proteome Res* (2021) 20(12):5241–63. doi: 10.1021/acs.jproteome.1c00657

72. Froeling FEM, Casolino R, Pea A, Biankin AV, Chang DK. Precision-panc obo. molecular subtyping and precision medicine for pancreatic cancer. *J Clin Med* (2021) 10(1):149. doi: 10.3390/jcm10010149

73. Rashid NU, Peng XL, Jin C, Moffitt RA, Volmar KE, Belt BA, et al. Purity independent subtyping of tumors (PurIST), a clinically robust, single-sample classifier for tumor subtyping in pancreatic cancer. *Clin Cancer Res* (2020) 26(1):82–92. doi: 10.1158/1078-0432.CCR-19-1467

74. Somerville TD, Xu Y, Miyabayashi K, Tiriac H, Cleary CR, Maia-Silva D, et al. TP63-mediated enhancer reprogramming drives the squamous subtype of pancreatic ductal adenocarcinoma. *Cell Rep* (2018) 25(7):1741–55. e7. doi: 10.1016/j.celrep.2018.10.051

75. Ryan DP, Hong TS, Bardeesy N. Pancreatic adenocarcinoma. *N Engl J Med* (2014) 371(11):1039–49. doi: 10.1056/NEJMra1404198

76. Conroy T, Desseigne F, Ychou M, Bouché O, Guimbaud R, Bécouarn Y, et al. FOLFIRINOX versus gemcitabine for metastatic pancreatic cancer. *New Engl J Med* (2011) 364(19):1817–25. doi: 10.1056/NEJMoa1011923

77. Von Hoff DD, Ervin T, Arena FP, Chiorean EG, Infante J, Moore M, et al. Increased survival in pancreatic cancer with nab-paclitaxel plus gemcitabine. *N Engl J Med* (2013) 369(18):1691–703. doi: 10.1056/NEJMoa1304369

78. Conroy T, Hammel P, Hebbar M, Ben Abdelghani M, Wei AC, Raoul J-L, et al. FOLFIRINOX or gemcitabine as adjuvant therapy for pancreatic cancer. *N Engl J Med* (2018) 379(25):2395–406. doi: 10.1056/NEJMoa1809775

79. Nielsen A, Scarlett CJ, Samra JS, Gill A, Li Y, Allen BJ, et al. Significant overexpression of urokinase-type plasminogen activator in pancreatic adenocarcinoma using real-time quantitative reverse transcription polymerase chain reaction. *J Gastroenterol Hepatol* (2005) 20(2):256–63. doi: 10.1111/j.1440-1746.2004.03531.x

80. Cantero D, Friess H, Deflorin J, Zimmermann A, Bründler M, Riesle E, et al. Enhanced expression of urokinase plasminogen activator and its receptor in pancreatic carcinoma. *Br J Cancer* (1997) 75(3):388–95. doi: 10.1038/bjc.1997.63

81. Feilchenfeldt J, Bründler M-A, Soravia C, Tötsch M, Meier CA. Peroxisome proliferator-activated receptors (PPARs) and associated transcription factors in colon cancer: reduced expression of PPARγ-coactivator 1 (PGC-1). *Cancer Letters* (2004) 203(1):25–33. doi: 10.1016/j.canlet.2003.08.024

82. Zhang Y, Ba Y, Liu C, Sun G, Ding L, Gao S, et al. PGC-1α induces apoptosis in human epithelial ovarian cancer cells through a PPARγ-dependent pathway. *Cell Res* (2007) 17(4):363–73. doi: 10.1038/cr.2007.11

83. Uddin MN, Li M, Wang X. Identification of transcriptional signatures of colon tumor stroma by a meta-analysis. *J Oncol* (2019) 2019:8752862. doi: 10.1155/2019/8752862

84. Uhlén M, Fagerberg L, Hallström BM, Lindskog C, Oksvold P, Mardinoglu A, et al. Proteomics. tissue-based map of the human proteome. *Science* (2015) 347(6220):1260419. doi: 10.1126/science.1260419

85. Thayer SP, di Magliano MP, Heiser PW, Nielsen CM, Roberts DJ, Lauwers GY, et al. Hedgehog is an early and late mediator of pancreatic cancer tumorigenesis. *Nature* (2003) 425(6960):851–6. doi: 10.1038/nature02009

86. Li C, Heidt DG, Dalerba P, Burant CF, Zhang L, Adsay V, et al. Identification of pancreatic cancer stem cells. *Cancer Res* (2007) 67(3):1030–7. doi: 10.1158/0008-5472.CAN-06-2030

87. Lee CJ, Dosch J, Simeone DM. Pancreatic cancer stem cells. *J Clin Oncol* (2008) 26(17):2806–12. doi: 10.1200/JCO.2008.16.6702

88. Li W, Cao L, Chen X, Lei J, Ma Q. Resveratrol inhibits hypoxia-driven ROS-induced invasive and migratory ability of pancreatic cancer cells *via* suppression of the hedgehog signaling pathway. *Oncol Rep* (2016) 35(3):1718–26. doi: 10.3892/or.2015.4504

89. Pudełko A, Wisowski G, Olczyk K, Koźma EM. The dual role of the glycosaminoglycan chondroitin-6-sulfate in the development, progression and metastasis of cancer. *FEBS J* (2019) 286(10):1815–37. doi: 10.1111/febs.14748

90. Ricciardelli C, Mayne K, Sykes PJ, Raymond WA, McCaul K, Marshall VR, et al. Elevated stromal chondroitin sulfate glycosaminoglycan predicts progression in early-stage prostate cancer. *Clin Cancer Res* (1997) 3(6):983–92.

91. Huang Y-F, Mizumoto S, Fujita M. Novel insight into glycosaminoglycan biosynthesis based on gene expression profiles. *Front Cell Dev Biol* (2021) 9. doi: 10.3389/fcell.2021.709018

92. Zhan T, Rindtorff N, Boutros M. Wnt signaling in cancer. *Oncogene* (2017) 36(11):1461–73. doi: 10.1038/onc.2016.304

93. Zhang Y, Morris JP IV, Yan W, Schofield HK, Gurney A, Simeone DM, et al. Canonical wnt signaling is required for pancreatic carcinogenesis. *Cancer Res* (2013) 73(15):4909–22. doi: 10.1158/0008-5472.CAN-12-4384

94. Sousa CM, Kimmelman AC. The complex landscape of pancreatic cancer metabolism. *Carcinogenesis* (2014) 35(7):1441–50. doi: 10.1093/carcin/bgu097

95. Yang J, Ren B, Yang G, Wang H, Chen G, You L, et al. The enhancement of glycolysis regulates pancreatic cancer metastasis. *Cell Mol Life Sci* (2020) 77(2):305–21. doi: 10.1007/s00018-019-03278-z

96. Chang C-H, Qiu J, O'Sullivan D, Buck MD, Noguchi T, Curtis JD, et al. Metabolic competition in the tumor microenvironment is a driver of cancer progression. *Cell* (2015) 162(6):1229–41. doi: 10.1016/j.cell.2015.08.016

97. Wellenstein MD, de Visser KE. Cancer-cell-intrinsic mechanisms shaping the tumor immune landscape. *Immunity* (2018) 48(3):399–416. doi: 10.1016/j.immuni.2018.03.004

98. Laurenzana A, Chillà A, Luciani C, Peppicelli S, Biagioni A, Bianchini F, et al. uPA/uPAR system activation drives a glycolytic phenotype in melanoma cells. *Int J Cancer* (2017) 141(6):1190–200. doi: 10.1002/ijc.30817

99. Kierans SJ, Taylor CT. Regulation of glycolysis by the hypoxia-inducible factor (HIF): implications for cellular physiology. *J Physiol* (2021) 599(1):23–37. doi: 10.1113/JP280572

100. Birtolo C, Pham H, Morvaridi S, Chheda C, Go VL, Ptasznik A, et al. Cadherin-11 is a cell surface marker up-regulated in activated pancreatic stellate cells and is involved in pancreatic cancer cell migration. *Am J Pathol* (2017) 187(1):146–55. doi: 10.1016/j.ajpath.2016.09.012

101. Ikenaga N, Ohuchida K, Mizumoto K, Cui L, Kayashima T, Morimatsu K, et al. CD10+ pancreatic stellate cells enhance the progression of pancreatic cancer. *Gastroenterology* (2010) 139(3):1041–51, 51.e1-8. doi: 10.1053/j.gastro.2010.05.084

102. Tang D, Yuan Z, Xue X, Lu Z, Zhang Y, Wang H, et al. High expression of galectin-1 in pancreatic stellate cells plays a role in the development and maintenance of an immunosuppressive microenvironment in pancreatic cancer. *Int J Cancer* (2012) 130(10):2337–48. doi: 10.1002/ijc.26290

103. Qian D, Lu Z, Xu Q, Wu P, Tian L, Zhao L, et al. Galectin-1-driven upregulation of SDF-1 in pancreatic stellate cells promotes pancreatic cancer metastasis. *Cancer Letters* (2017) 397:43–51. doi: 10.1016/j.canlet.2017.03.024

104. Orozco CA, Martinez-Bosch N, Guerrero PE, Vinaixa J, Dalotto-Moreno T, Iglesias M, et al. Targeting galectin-1 inhibits pancreatic cancer progression by modulating tumor-stroma crosstalk. *Proc Natl Acad Sci United States America* (2018) 115(16):E3769–78. doi: 10.1073/pnas.1722434115

105. Yoshida N, Masamune A, Hamada S, Kikuta K, Takikawa T, Motoi F, et al. Kindlin-2 in pancreatic stellate cells promotes the progression of pancreatic cancer. *Cancer Letters* (2017) 390:103–14. doi: 10.1016/j.canlet.2017.01.008

106. Tian L, Lu ZP, Cai BB, Zhao LT, Qian D, Xu QC, et al. Activation of pancreatic stellate cells involves an EMT-like process. *Int J Oncol* (2016) 48(2):783–92. doi: 10.3892/ijo.2015.3282

107. Lee H, Lim C, Lee J, Kim N, Bang S, Lee H, et al. TGF-beta signaling preserves RECK expression in activated pancreatic stellate cells. *J Cell Biochem* (2008) 104(3):1065–74. doi: 10.1002/jcb.21692

108. Horiguchi K, Shirakihara T, Nakano A, Imamura T, Miyazono K, Saitoh M. Role of ras signaling in the induction of snail by transforming growth factor-beta. *J Biol Chem* (2009) 284(1):245–53. doi: 10.1074/jbc.M804777200

109. Kanno A, Satoh K, Masamune A, Hirota M, Kimura K, Umino J, et al. Periostin, secreted from stromal cells, has biphasic effect on cell migration and correlates with the epithelial to mesenchymal transition of human pancreatic cancer cells. *Int J Cancer* (2008) 122(12):2707–18. doi: 10.1002/ijc.23332

110. Ruan K, Bao S, Ouyang G. The multifaceted role of periostin in tumorigenesis. *Cell Mol Life Sci* (2009) 66(14):2219–30. doi: 10.1007/s00018-009-0013-7

111. Kayed H, Jiang X, Keleg S, Jesnowski R, Giese T, Berger MR, et al. Regulation and functional role of the runt-related transcription factor-2 in pancreatic cancer. *Br J Cancer* (2007) 97(8):1106–15. doi: 10.1038/sj.bjc.6603984

112. Mace TA, Bloomston M, Lesinski GB. Pancreatic cancer-associated stellate cells. *OncoImmunology* (2013) 2(7):e24891. doi: 10.4161/onci.24891

113. Nagathihalli NS, Castellanos JA, VanSaun MN, Dai X, Ambrose M, Guo Q, et al. Pancreatic stellate cell secreted IL-6 stimulates STAT3 dependent invasiveness of pancreatic intraepithelial neoplasia and cancer cells. *Oncotarget* (2016) 7 (40):65982–92. doi: 10.18632/oncotarget.11786

114. Tang D, Wang D, Yuan Z, Xue X, Zhang Y, An Y, et al. Persistent activation of pancreatic stellate cells creates a microenvironment favorable for the malignant behavior of pancreatic ductal adenocarcinoma. *Int J Cancer* (2013) 132 (5):993–1003. doi: 10.1002/ijc.27715

115. Sada M, Ohuchida K, Horioka K, Okumura T, Moriyama T, Miyasaka Y, et al. Hypoxic stellate cells of pancreatic cancer stroma regulate extracellular matrix fiber organization and cancer cell motility. *Cancer Letters* (2016) 372(2):210–8. doi: 10.1016/j.canlet.2016.01.016

116. Physico-mechanical aspects of extracellular matrix influences on tumorigenic behaviors. *Semin Cancer Biol* (2010) 20(3):139-45. doi: 10.1016/j.semcancer.2010.04.004

117. Pickup MW, Mouw JK, Weaver VM. The extracellular matrix modulates the hallmarks of cancer. *EMBO Rep* (2014) 15(12):1243–53. doi: 10.15252/embr.201439246

118. Oskarsson T, Acharyya S, Zhang XH, Vanharanta S, Tavazoie SF, Morris PG, et al. Breast cancer cells produce tenascin c as a metastatic niche component to colonize the lungs. *Nat Med* (2011) 17(7):867–74. doi: 10.1038/nm.2379

119. Oskarsson T, Massagué J. Extracellular matrix players in metastatic niches. *EMBO J* (2012) 31(2):254–6. doi: 10.1038/emboj.2011.469

120. Malanchi I, Santamaria-Martínez A, Susanto E, Peng H, Lehr H-A, Delaloye J-F, et al. Interactions between cancer stem cells and their niche govern metastatic colonization. *Nature* (2012) 481(7379):85–9. doi: 10.1038/nature10694

121. Idichi T, Seki N, Kurahara H, Fukuhisa H, Toda H, Shimonosono M, et al. Involvement of anti-tumor miR-124-3p and its targets in the pathogenesis of pancreatic ductal adenocarcinoma: Direct regulation of ITGA3 and ITGB1 by miR-124-3p. *Oncotarget* (2018) 9(48):28849. doi: 10.18632/oncotarget.25599

122. Deng M, Peng L, Li J, Liu X, Xia X, Li G. PPP1R14B is a prognostic and immunological biomarker in pan-cancer. *Front Genet* (2021) 12:763561. doi: 10.3389/fgene.2021.763561

123. O'Kane GM, Grünwald BT, Jang G-H, Masoomian M, Picardo S, Grant RC, et al. GATA6 expression distinguishes classical and basal-like subtypes in advanced pancreatic cancer. *Clin Cancer Res* (2020) 26(18):4901–10. doi: 10.1158/1078-0432.CCR-19-3724

124. Aguilera KY, Dawson DW. WNT ligand dependencies in pancreatic cancer. *Front Cell Dev Biol* (2021) 9. doi: 10.3389/fcell.2021.671022

125. Khramtsov AI, Khramtsova GF, Tretiakova M, Huo D, Olopade OI, Goss KH. Wnt/β-catenin pathway activation is enriched in basal-like breast cancers and predicts poor outcome. *Am J Pathology* (2010) 176(6):2911–20. doi: 10.2353/ajpath.2010.091125

126. Ellenrieder V, Hendler SF, Boeck W, Seufferlein T, Menke A, Ruhland C, et al. Transforming growth factor β1 treatment leads to an epithelial-mesenchymal transdifferentiation of pancreatic cancer cells requiring extracellular signal-regulated kinase 2 activation. *Cancer Res* (2001) 61(10):4222–8.

127. Brunton H, Caligiuri G, Cunningham R, Upstill-Goddard R, Bailey U-M, Garner IM, et al. HNF4A and GATA6 loss reveals therapeutically actionable subtypes in pancreatic cancer. *Cell Rep* (2020) 31(6):107625. doi: 10.1016/j.celrep.2020.107625

128. Connor AA, Denroche RE, Jang GH, Lemire M, Zhang A, Chan-Seng-Yue M, et al. Integration of genomic and transcriptional features in pancreatic cancer reveals increased cell cycle progression in metastases. *Cancer Cell* (2019) 35(2):267–82. e7. doi: 10.1016/j.ccell.2018.12.010

129. Maurer C, Holmstrom SR, He J, Laise P, Su T, Ahmed A, et al. Experimental microdissection enables functional harmonisation of pancreatic cancer subtypes. *Gut* (2019) 68(6):1034–43. doi: 10.1136/gutjnl-2018-317706

130. Wu C-Z, Chu YC, Lai S-W, Hsieh M-S, Yadav VK, Fong I-H, et al. Urokinase plasminogen activator induces epithelial-mesenchymal and metastasis of pancreatic cancer through plasmin/MMP14/TGF-β axis, which is inhibited by 4-acetyl-antroquinonol b treatment. *Phytomedicine* (2022) 100:154062. doi: 10.1016/j.phymed.2022.154062

131. Ossowski L, Russo-Payne H, Wilson EL. Inhibition of urokinase-type plasminogen activator by antibodies: the effect on dissemination of a human tumor in the nude mouse. *Cancer Res* (1991) 51(1):274–81.

132. Towle MJ, Lee A, Maduakor EC, Schwartz CE, Bridges AJ, Littlefield BA. Inhibition of urokinase by 4-substituted benzo [b] thiophene-2-carboxamidines: An important new class of selective synthetic urokinase inhibitor. *Cancer Res* (1993) 53(11):2553–9.

133. Rabbani S, Harakidas P, Davidson DJ, Henkin J, Mazar AP. Prevention of prostate-cancer metastasis *in vivo* by a novel synthetic inhibitor of urokinase-type plasminogen activator (uPA). *Int J Cancer* (1995) 63(6):840–5. doi: 10.1002/ijc.2910630615

134. Xing RH, Mazar A, Henkin J, Rabbani SA. Prevention of breast cancer growth, invasion, and metastasis by antiestrogen tamoxifen alone or in combination with urokinase inhibitor b-428. *Cancer Res* (1997) 57(16):3585–93.

135. Vine K L, Indira Chandran V M, Locke J, Matesic L, Lee J, Skropeta D, et al. Targeting urokinase and the transferrin receptor with novel, anti-mitotic n-alkylisatin cytotoxin conjugates causes selective cancer cell death and reduces tumor growth. *Curr Cancer Drug Targets* (2012) 12(1):64–73. doi: 10.2174/156800912798888983

136. Meyer JE, Brocks C, Graefe H, Mala C, Thäns N, Bürgle M, et al. The oral serine protease inhibitor WX-671–first experience in patients with advanced head and neck carcinoma. *Breast Care* (2008) 3(Suppl 2):20. doi: 10.1159/000151736

137. Goldstein LJ. Experience in phase I trials and an upcoming phase II study with uPA inhibitors in metastatic breast cancer. *Breast Care* (2008) 3(Suppl 2):25. doi: 10.1159/000151733

138. Schmitt M, Harbeck N, Brünner N, Jänicke F, Meisner C, Mühlenweg B, et al. Cancer therapy trials employing level-of-evidence-1 disease forecast cancer biomarkers uPA and its inhibitor PAI-1. *Expert Rev Mol Diagnostics* (2011) 11 (6):617–34. doi: 10.1586/erm.11.47

139. Heinemann V, Ebert MP, Laubender RP, Bevan P, Mala C, Boeck S. Phase II randomised proof-of-concept study of the urokinase inhibitor upamostat (WX-671) in combination with gemcitabine compared with gemcitabine alone in patients with non-resectable, locally advanced pancreatic cancer. *Br J Cancer* (2013) 108(4):766–70. doi: 10.1038/bjc.2013.62

140. Banys-Paluchowski M, Witzel I, Aktas B, Fasching PA, Hartkopf A, Janni W, et al. The prognostic relevance of urokinase-type plasminogen activator (uPA) in the blood of patients with metastatic breast cancer. *Sci Rep* (2019) 9(1):2318. doi: 10.1038/s41598-018-37259-2

141. Mekapogu AR, Xu Z, Pothula SP, Perera C, Pang T, Hosen S, et al eds. *Hepatocyte growth factor/c-met pathway inhibition combined chemotherapy improves tumor immunity and eliminates metastasis in pancreatic cancer*. MARKET ST, PHILADELPHIA: LIPPINCOTT WILLIAMS & WILKINS TWO COMMERCE SQ (2001). PANCREAS; 2021.

142. Yang J, Zhang Q, Wang J, Lou Y, Hong Z, Wei S, et al. Dynamic profiling of immune microenvironment during pancreatic cancer development suggests early intervention and combination strategy of immunotherapy. *EBioMedicine* (2022) 78:103958. doi: 10.1016/j.ebiom.2022.103958

143. Thyagarajan A, Alshehri MSA, Miller KL, Sherwin CM, Travers JB, Sahu RP. Myeloid-derived suppressor cells and pancreatic cancer: Implications in novel therapeutic approaches. *Cancers (Basel)* (2019) 11(11):1627. doi: 10.3390/cancers11111627

10.3389/fimmu.2022.1060957

Glossary

TCGA	The Cancer Genome Atlas
ICGC	International Cancer Genome Consortium
OICR	Ontario Institute for Cancer Research
CPTAC	Clinical Proteomic Tumor Analysis Consortium
CCLE	Cancer CellLine Encyclopedia
GEPIA	Gene Expression Profiling Interactive Analysis
ACC	adrenocortical carcinoma
BLCA	bladder urothelial carcinoma
BRCA	breast invasive carcinoma
CESC	Cervical squamous cell carcinoma and endocervical adenocarcinoma
CHOL	Cholangiocarcinoma
COAD	colon adenocarcinoma
DLBC	lymphoid neoplasm diffuse large B-cell lymphoma
ESCA	esophageal carcinoma
GBM	glioblastoma multiforme
HNSC	head and neck squamous cell carcinoma
KICH	Kidney chromophobe
KIRC	kidney renal clear cell carcinoma
KIRP	kidney renal papillary cell carcinoma
LAML	acute myeloid leukemia
LGG	brain lower grade glioma
LIHC	Liver hepatocellular carcinoma
LUAD	lung adenocarcinoma
LUSC	lung squamous cell carcinoma
MESO	Mesothelioma
OV	ovarian serous cystadenocarcinoma
PAAD	Pancreatic adenocarcinoma
PCPG	Pheochromocytoma and Paraganglioma
PRAD	prostate adenocarcinoma
READ	rectum adenocarcinoma
SARC	Sarcoma
SKCM	Skin cutaneous melanoma
STAD	stomach adenocarcinoma
TGCT	testicular germ cell tumors
THCA	thyroid carcinoma
THYM	thymoma
UCEC	uterine corpus endometrial carcinoma
UCS	uterine carcinosarcoma
UVM	Uveal Melanoma
HEG	High Expression Group
LEG	Low Expression Group
FDR	false discovery rate
HIF1A	Hypoxia inducible factor 1 subunit alpha
HLAs	human leukocyte antigens
IFN	interferon
MDSCs	myeloid-derived suppressor cells
NK	natural killer
OS	overall survival
PD-1	Programmed cell death protein 1
PDL1	programmed death-ligand 1
PFI	progression-free interval
SGSs	stromal gene signatures
ssGSEA	single-sample gene-set enrichment analysis
TILs	tumor-infiltrating lymphocytes
OG	Oncogenes
TF	Transcription factors
CK and GF	Cytokines and Growth factors
TCG	Translocating cancer genes
CDM	Cell Differential markers
PK	Protein Kinase
HP	Homeodomain Protein
TS	Tumour Suppressor
EA	Endothelial
STM	Stemness
HYPOX	Hypoxia
CP	Cell Proliferation
ECMD	ECM degradation
ECM	Extracellular Matrix
EMT	Epithelial mesenchymal transition
MTGs	Metastasis-related genes/Metastasis-promoting genes
Ctrl	Control
G	Gemcitabine
	uPA inhibitor (BB2-30F) at 3mg (U3) and 10 mg (U10)
PSCs	Pancreatic stellate cells
PC	Pancreatic cancer
CAhPSCs	Cancer associated human pancreatic stellate cells

(Continued)

frontiers | Frontiers in Immunology

TYPE Original Research
PUBLISHED 05 January 2023
DOI 10.3389/fimmu.2022.1051701

OPEN ACCESS

EDITED BY
Mazdak Ganjalikhani Hakemi,
Isfahan University of Medical Sciences, Iran

REVIEWED BY
Paolo Fagone,
University of Catania, Italy
Hanjun Cheng,
Institute for Systems Biology (ISB), United States

*CORRESPONDENCE
Bing Li
libingwxey@126.com

SPECIALTY SECTION
This article was submitted to Cancer Immunity and Immunotherapy, a section of the journal Frontiers in Immunology

RECEIVED 23 September 2022
ACCEPTED 09 December 2022
PUBLISHED 05 January 2023

CITATION
Ni L, Sun P, Zhang S, Qian B, Chen X, Xiong M and Li B (2023) Transcriptome and single-cell analysis reveal the contribution of immunosuppressive microenvironment for promoting glioblastoma progression. *Front. Immunol.* 13:1051701. doi: 10.3389/fimmu.2022.1051701

Transcriptome and single-cell analysis reveal the contribution of immunosuppressive microenvironment for promoting glioblastoma progression

Lulu Ni[1], Ping Sun[2], Sujuan Zhang[3], Bin Qian[4], Xu Chen[1], Mengrui Xiong[1] and Bing Li[5]*

[1]Department of Basic Medicine, Jiangnan University, Wuxi, China, [2]Department of Pathology, The Affiliated Wuxi No. 2 People's Hospital of Nanjing Medical University, Wuxi, China, [3]Institute of Science and Technology Information, Beijing Academy of Science and Technology, Beijing, China, [4]Department of Traditional Chinese Medicine, General Hospital of the Third Division of Xinjiang Production and Construction Corps, Tumushuke, China, [5]Department of Neurosurgery, The Affiliated Wuxi No. 2 People's Hospital of Nanjing Medical University, Wuxi, China

Background and objectives: GBM patients frequently exhibit severe local and systemic immunosuppression, limiting the possible efficacy of immunotherapy strategies. The mechanism through which immunosuppression is established in GBM tumors is the key to successful personalized immunotherapies.

Methods: We divided GBM patients into subtypes according to the expression characteristics of the TME typing-related signature matrix. WGCNA analysis was used to get co-expressed gene modules. The expression activity of hub genes retrieved from co-expressed modules was validated in two single-cell datasets. Then, cell–cell interaction was calculated.

Results: Four subtypes were identified in the TCGA and CGGA RNA-seq datasets simultaneously, one of which was an immunosuppressive subtype rich in immunosuppressive factors with low lymphocyte infiltration and an IDH1 mutation. Three co-expressed gene modules related to the immunosuppressive subtype were identified. These three modules are associated with the inflammatory response, angiogenesis, hypoxia, and carbon metabolism, respectively. The genes of the inflammatory response were mainly related to myeloid cells, especially TAM, angiogenesis was related to blood vessels; hypoxia and glucose metabolism were related to tumors, TAM, and blood vessels. Moreover, there was enhanced interaction between tumor cells and TAM.

Discussion: This research successfully found the immunosuppressive subtype and the major cell types, signal pathways, and molecules involved in the formation of the immunosuppressive subtype and will provide new clues for the improvement of GBM personalized immunotherapy in the future.

KEYWORDS

immunosuppression, GBM, WGCNA, TAM, single-cell, immunotherapy

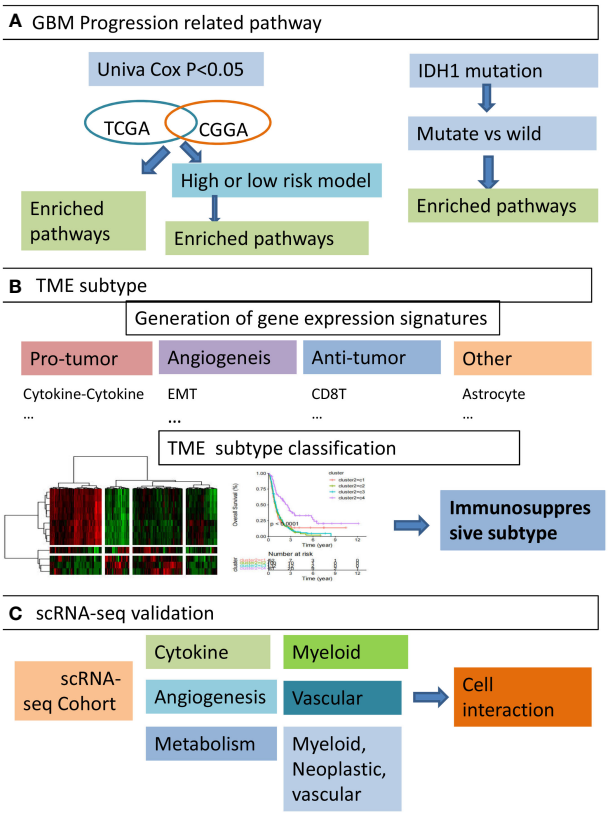

GRAPHICAL ABSTRACT
Overview of the study design. **(A)** We firstly identified five GBM progression related pathways. By performing functional enrichment analysis on gene sets obtained from three perspectives, such as genes co-survival in TCGA–GBM and CGGA cohort, DEGs of high and low risk groups, and DEGs of IDH1 mutation compared with wild type, we identified five pathways significantly associated with poor prognosis in GBM patients. **(B)** Secondly, GBM TME-associated functional gene signatures were constructed. Based on the activity profile of these signatures, GBM patients were classified into four distinct subtypes and immunosuppressive subtypes were found. **(C)** the expression of hub genes from immunosuppressive subtypes were validated in three single-cell RNA-seq datasets, and cell types significantly associated with TME subtypes were identified. The interactions between certain cell types were also elaborated.

Introduction

GBM is the most common primary tumor of the central nervous system (CNS) in adults and is notoriously difficult to treat because of its diffuse nature. The median survival time of GBM patients remains approximately 14–15 months after diagnosis (1, 2). Passage of systemically delivered pharmacological agents into the brain is largely blocked by the blood–brain barrier (BBB) (3). Although recent advances, including the addition of tumor-treating fields (TTF), have shown some modest benefits, the overall survival rate remains effectively unchanged (4). Effective new therapies are urgently required.

Immunotherapy has emerged as a promising treatment for some of the hardest-to-treat tumors, including metastatic melanoma. The general principle of immunotherapy is to fight immune suppression in the tumor microenvironment and activate the patient's own immune system to kill the tumor. Successful cancer immunotherapy depends on the existence of an intact and functional immune system. However, GBM patients frequently exhibit severe local and systemic immunosuppression, which limits the possible efficacy of these therapeutic strategies (5). This apparent immunosuppression is a critical barrier to improving patient survival. Understanding the mechanism of establishing immunosuppression in GBM tumors is the key to successful personalized immunotherapy soon. However, the nature of these mechanisms remains surprisingly elusive.

The implications of specific immune cell types on GBM disease status were unknown. In most cancers, the presence of tumor-infiltrating lymphocytes (TILs) is positively correlated with the improvement of overall survival in patients, but the correlation between the presence of TILs and the improvement of overall survival in GBM patients has not been clearly established (6, 7). Myeloid cells, especially microglia and macrophages, in the tumor microenvironment regulate GBM progression and influence

therapeutic outcomes (8). Besides, resident fibroblasts, endothelial cells, pericytes, and the extracellular matrix also contribute to cancer progression (9). Abnormal cytokine expression was found to be associated with glioma progression. Within the heterogeneous GBM microenvironment, tumor cells, normal brain cells, immune cells, and stem cells interact with each other through the complex cytokine network (10, 11). The formation of the GBM tumor microenvironment has been associated with specific mutations. For example, the IDH mutation has recently been found to be associated with decreased immune cell infiltration (12), whereas inactivated NF1 has been associated with increased macrophage infiltration (13). In addition, several major signaling pathways like NFκB, Wnt, and PI3K–AKT–mTOR are reported to be involved in the pathogenesis of GBM and have been used as therapeutic targets for GBM (14–16).

Based on the above knowledge, we constructed gene signatures that can be used to distinguish GBM samples, including tumor-promoting signaling pathways, angiogenesis-related genes, and various cell-characteristic gene signatures. GBM patients were classified into subtypes by clustering the expression characteristics of these gene signatures in each patient. Also, we found hub genes in each module through WGCNA analysis. Combined with published single-cell data, we identified cell types responsible for the abnormal expression of these hub genes and the pathways involved in this process. At the same time, the interactions between cell types and related ligand–receptor pairs were also studied. These analyses systematically analyzed the formation mechanism of the GBM microenvironment, especially the immunosuppressive microenvironment, and helped to find targets for immunotherapy.

Methods

Publicly available GBM were obtained from The Cancer Genome Atlas (TCGA), and level 3 RNA-seq data for 167 GBM samples were downloaded from the UCSC Xena browser (https://xena.ucsc.edu/) (17). Corresponding clinical characteristics were obtained. Another 345 GBM samples with clinical information were provided by the Chinese Glioma Genome Atlas (CGGA). The detailed clinical and pathological characteristics of the TCGA-GBM and CGGA cohorts were summarized in Supplementary Table 1. Data on RNA-seq were transcripts-per-million (TPM) normalized and log2-transformed. Then, low expressed genes were eliminated.

Three GBM-related scRNA-seq datasets were retrieved from the GEO database (GSE117891 (n = 8), GSE84465 (n = 2), and GSE163120 (n = 12)) (18–20). After removing low-quality cells, followed by normalization and dimension reduction, Louvain clustering was used to group cells. GSE117891 and GSE84465 were integrated. Cell types were annotated using canonical marker genes. Additionally, malignant cells were defined by "InferCNV" (https://github.com/broadinstitute/InferCNV). All these were performed by Seurat (4.0) in the R package (21).

Functional characterization of differential expression analysis (DEGs)

For the RNA-seq data, the DEseq2 R package was used. Genes with an FDR <0.05 and absolute fold change ≥1.5 were considered as differential expressed.

Functional enrichment analysis

Functional annotation of DEGs was performed on the Kyoto Encyclopedia of Genes and Genomes (KEGG) and Gene Ontology (GO) classification databases. Enrichment analysis of GO categories was performed by the R clusterProfiler (v3.14.3) package, and pathway enrichment analysis was tested upon hypergeometric distribution by the R "phyper" function. GO categories with a false detection rate (FDR) of <0.05 were significantly enriched. The pathway with P <0.05 was enriched. Only those go categories or pathways containing ≥5 DEGs were retained.

Weighted gene co-expression network analysis (WGCNA)

WGCNA was performed by the R package WGCNA (V1.69) (22). We use the log2-transformed TPM value as the normalized expression and filter out abnormal samples. According to the principle of scale-free network, coefficient β was set as 14. The parameter of network type was used with "signed" and "bicor" (double weighted correlation) to calculate the correlation adjacency matrix. Co-expression gene modules were identified by using dynamic tree cutting with the following major parameters: The main parameters minModuleSize and deepSplit were 30 and 1, respectively. The highly similar modules with the height of the module eigengene in the clustering lower than 0.2 were merged. A univariate Cox proportional hazard regression was performed on each gene module. Genes in each module with a p-value <0.05 were kept as modules' survival-related genes. Those genes, both survival-related and with kME ≥0.8 and GeneSignificance >0.2 were regarded as hub genes in this study (22). The coexpression of hub genes was plotted by Cytoscape 3.6.0.

Transcriptome deconvolution of the gene signatures

The abundance of infiltrating immune cell populations was estimated by deconvolution methods integrated in the R package "immunedeconv." Other immune- or tumor-associated signatures in each sample were quantified by ssGSEA with the R package "GSVA."

Risk score model

We used univariate Cox regression, LASSO, and stepwise regression successively to screen out candidate mRNAs for construction. In the univariate Cox proportional risk regression analysis, mRNAs with p <0.05 was associated with survival. The criteria for LASSO regression remained in the model more than 900 times out of all 1,000 repetitions. Then step wise were used. The risk scoring model was constructed based on Cox coefficients and mRNAs' expression. Risk score ∑I = 1 = (Coefi × Expri). The Expri represented the expression levels of mRNAs in the gene risk model, K–M survival analyses and ROC curves were performed to evaluate the predictive accuracy of models.

Gene signature activity scores on cells

Specific gene sets' activity scores for each cell type were calculated by AUCell (23). The gene set is the survival-related gene set of modules discussed in the WGCNA section. The scores were plotted as a heatmap and a violinplot.

Cell–cell communication

CellPhoneDB (https://www.cellphonedb.org/) was used to infer the ligand–receptor crosstalk between single cells (24), which interpreted interactions in single cells based on known protein–protein interaction annotations. The number of ligand–receptors at intercellular junctions was calculated. As for the differential cell crosstalk analysis in each group, it was computed separately. The differential crosstalk between cells was visualized. Ligand activity was predicted by NicheNet (V1.1.0) (25).

Statistical analysis

Hierarchical clustering analysis was performed on the R "hclust" function using the "ward.D" method to identify the number of subtypes in TCGA-GBM based on the pattern of signature scores. Univariate and multivariate Cox proportional hazards regression models were used to assess the association between the risk model and overall survival with and without clinical variables. The hazard ratio (HR) and 95% confidence interval (CI) were calculated. Wilcoxon rank sum, or Student tests, were used to compare two groups. For comparisons of more than two groups, one-way ANOVA tests and Kruskal–Wallis tests were utilized as parametric and nonparametric methods, respectively. The Kaplan–Meier method and log-rank test were conducted to compare survival differences between two groups. All statistical analysis was performed using R (version 4.0).

Results

Cytokine–cytokine receptor interaction tops the GBM risk factors

A univariate Cox hazard regression analysis was performed for all expressed genes in the TCGA–GBM cohort. We found 1264 genes as survival related in the TCGA–GBM cohort genes and 2,681 genes in the CGGA cohort (<0.01). There were 86 genes associated with survival in the two datasets (Figure 1A). The enriched KEGG pathways of these 86 genes were shown (Figure 1B). The relationship between these enriched pathways and GBM has been reported in several publications (11, 26, 27).

To further verify the predictive role of these genes in GBM progression, a risk model was constructed. Eight genes met the requirement through the least absolute shrinkage and selector operation (LASSO) regression. After stepwise regression, a model based on the expression of eight genes in the TCGA-GBM cohort was established. Patients in the high-risk group had a worse prognosis than those in the low-risk group (lop-rank test, p <0.001, Figure 1C). The area under the curve (AUC) was higher than 0.75 according to the ROC curves of the 1-, 3-, and 5-year OS predictions (Figure 1D), which means that the risk model has high predictive power. The risk model was validated in the CGGA cohort (Figures S1A, B). Then, the differentially expressed genes (DEGs) between the high- and low-risk groups were calculated in the TCGA–GBM cohort. These DEGs were also enriched in the pathways discussed above, among which cytokine–cytokine receptor interaction was the top one (Figure 1E).

The isocitrate dehydrogenase (IDH1) gene represents a recurrent mutation in GBM patients, which was associated with good prognostic outcomes compared to wild-type counterparts (TCGA-GBM cohort, log-rank p <0.0001, Figure S1C) (12). The enriched, upregulated pathways in the above high-risk patients were downregulated in IDH1 mutation samples, which further validated their pro-tumor characteristics in GBM (Figure 1F). Interestingly, cytokine–cytokine receptor interaction, again, was at the top of enriched pathways between IDH1 mutation and wild-type patients. As reported, within the heterogeneous GBM microenvironment, tumor cells, normal brain cells, immune cells, and stem cells interact with each other through the complex cytokine network (12). Therefore, we included these cell types into consideration next to complicatedly delineate the microenvironment of GBM.

Heterogeneous TME components were associated with tumor-promoting pathways

The tumor microenvironment (TME) is composed of resident fibroblasts, endothelial cells, pericytes, leukocytes,

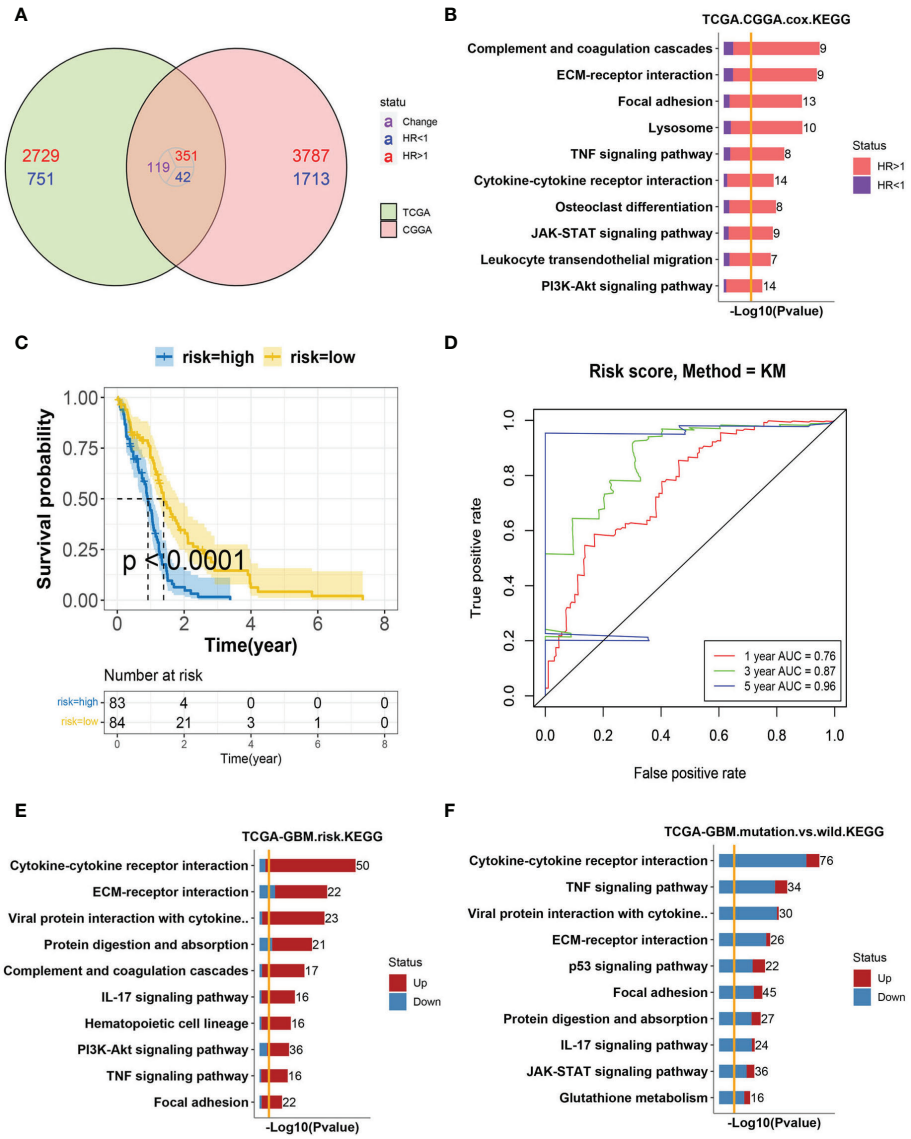

FIGURE 1
Analysis of GBM progression-related pathways **(A)** The Venn diagram of survival-related genes in the TCGA–GBM and CGGA cohorts. A total of 86 genes were found to coexist with diversity, of which 81 genes were associated with a poor prognosis. **(B)** Bar-plot of KEGG enrichment analysis of 86 survival-related genes with x-axis as –log10 transformed P-value. Bars were colored by the ratio of poor and good prognosis-related genes. **(C)** The Kaplan–Meier curves comparing patients with a low- or high-risk score in the TCGA–GBM cohort. Patients were divided into two groups according to the median value of their risk scores. Higher risk scores were correlated with a poorer prognosis. **(D)** ROC curve for the risk model in the TCGA–GBM cohort. **(E)** Bar-plot of KEGG enrichment analysis of DEGs between high- and low-risk groups. Bars were colored by the ratio of up and downregulated genes. Upregulated genes were those with elevated expression in the high-risk group. **(F)** Bar-plot of KEGG enrichment analysis of DEGs between mutant and wild-type patients. Bars were colored by the ratio of up and downregulated genes.

and the extracellular matrix (9). To classify TMEs using a transcriptomic-based analytical platform, gene expression signatures (GES) representing the major functional components and immune, stromal, and other cellular populations of the tumor were constructed (Figure S2A). We selected five tumor-promoting pathways from the above upregulated pathways in high-risk patients according to biological background knowledge. Then we analyzed their correlation with other TME signatures, such as MDSC and monocytes. The five tumor-promoting pathways were significantly positively correlated with other pro-tumor or angiogenesis-related signatures and negatively correlated with anti-tumor-related signatures (Figure S2B). Then, we examined their characteristics in GBM progression by univariate Cox regression analysis on these TME-related characteristics, and we found most signatures were in high HR (Figure S2C). In summary, we comprehensively analyzed TME gene signatures

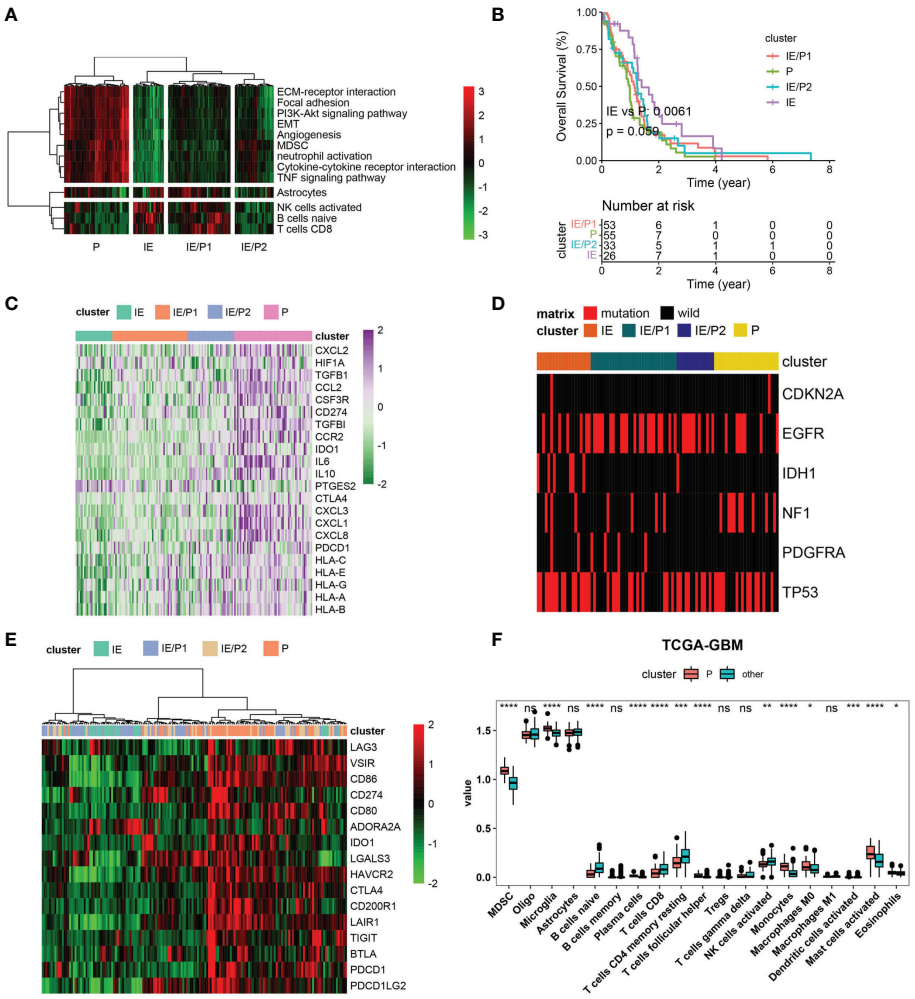

FIGURE 2
Immunosuppressive subtype identification in the TCGA–GBM cohort. **(A)** A heatmap of row-scaled gene signature scores from the cell deconvolution algorithm, with the color ranging from green to red, represents the activity score from low to high. The samples in this column were grouped into four TME subtypes. **(B)** Overall survival of patients stratified by TME subtype classification. The log-rank p-value between subtypes IE and P was 0.0061, and the annova log-rank p-value for four subtypes was 0.059. **(C)** The expression profile of immune suppression-related genes across four TME subtypes, with the color ranging from green to purple, represents the expression value from low to high. **(D)** Mutation frequency of five high-frequency mutant genes across four TME subtypes. Samples were shown in the column. Samples with mutations were color red. **(E)** The expression profile of inhibitory immune checkpoints across four TME subtypes. **(F)** Differential immune cell infiltration level across immunosuppressive subtypes and others. Statistical significance between groups was tested by Wilcox. *P < 0.05, **P < 0.01, ***P < 0.001, ****P < 0.0001, ns > = 0.05.

of GBM and found heterogeneous TME components were associated with tumor-promoting pathways.

Identification of the immunosuppressive subtype of GBM through GES classifier

According to the expression activity of the selected GES in the TCGA–GBM dataset, patients were classified into four subtypes by the hierarchical clustering method. Based on the infiltrating situation of tumor killing cells and tumor progression characteristics, these subtypes were defined as tumor progression (P), immune infiltrating (IE), and expressing both simultaneously (P/IE) (Figure 2A). It was evident that the P subtype had higher tumor progression signatures and lower lymphocyte infiltration. These patients had the worst survival (Figure 2B, log-rank p = 0.0061). Then, we evaluated the differences between IE and P subtypes from several perspectives, such as immunosuppression, ICB, high-frequency mutation distribution, and cell infiltration. The expressions of immunosuppressive factors were plotted as a heat map (28), and it could be seen that subtype P represented higher expression of these genes (Figure 2C). For gene mutations, we plotted the distribution of five high-frequency mutations across the four subtypes (Figure 2D). IDH1 mutations were all of the IE type,

which was consistent with their better outcomes. Tumor cells usually upregulate ICB gene expression to evade the immune system. We evaluated the expression of inhibitory ICBs in P-type cells (Figure 2E). In terms of cell infiltration, the P subtype showed high levels of myeloid cell infiltration and other subtypes showed high levels of lymphocyte infiltration (Figure 2F).

We validated these findings with the CGGA dataset. Four types were also found (Figure S3A). The log-rank p-value between IE and P subtypes was 0.00051 (Figure S3B). The P subtype also showed high expression of immunosuppressive factors and inhibitory ICBs (Figures S3C, E). Myeloid cells were infiltrated in subtype P, and lymphocytes were infiltrated

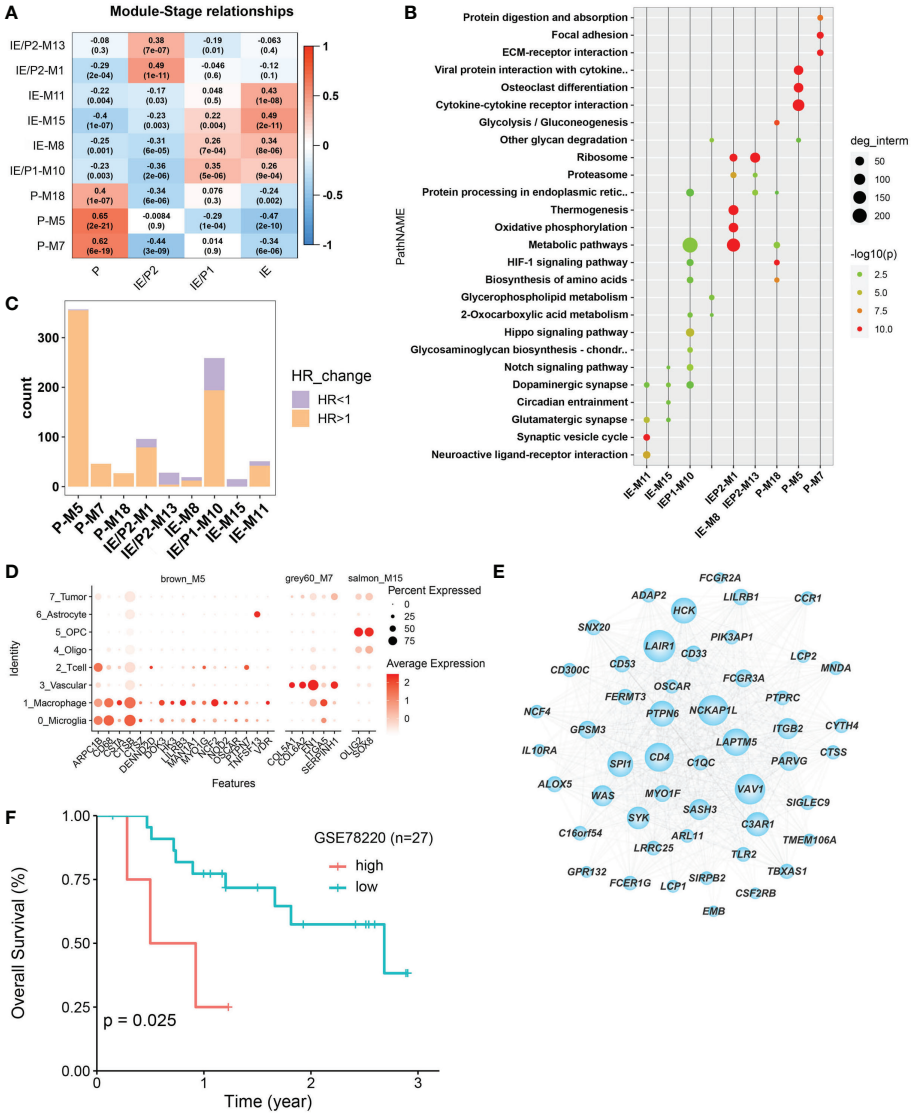

FIGURE 3
Co-expressed gene module detection by WGCNA. **(A)** Correlation between module eigengenes (1st principal component of modules) and TME subtypes in the TCGA–BGM cohort. The correlations were shown as a heatmap, gradually colored lower in blue and higher in red according to the Pearson correlation coefficient. The first line of the value in the heatmap represents the correlation coefficient, and the second line is the p-value from the correlation test. **(B)** Dotplot of the top enriched pathways of each module. Dots were colored gradually by –log10 (p-value), and the size of the dots gradually changed according to the number of genes contained, with the larger the value, the larger the dots. **(C)** Barplot shows the number of molecules that met the requirements of univariate Cox regression p-value <0.05 in each module. Bars were colored with an HR ratio >1 (orange) or <1 (purple). **(D)** The distribution of expression levels of each module's survival-related hub genes across different cell types. The larger the size, the larger the percent of expression. **(E)** Co-expression network between the top 50 hub genes selected according to the kME score. The larger in node size the higher in node degree. The top 15 genes in degree were more important and were defined as Top15_hub. **(F)** Relationship between Top15_hub gene expression and prognosis of immunotherapy samples. The Kaplan–Meier curves comparing Top15_hub gene low and high expressed patients in an immunotherapy dataset (GSE78220).

in subtype IE (Figure S3F). Inconsistent with TCGA-GBM, IDH mutations were not predominantly distributed in the IE type but also in the IE/P type (Figure S3D). In conclusion, we identified immunosuppressive and lymphocyte subtypes both in the TCGA–GBM and CGGA cohorts and found their opposite biological characteristics.

GBM subtypes represented heterogeneous functional gene modules

The WGCNA algorithm was used to construct co-expressed gene modules (22). Twenty co-expressed modules were identified using the "cutreeHybrid" function (Figure S4). To find subtype-specific modules, we calculated the correlation between module genes and subtypes (Figure 3A). Genes in modules 7, 5, and 18 were highly expressed in the P subtype, while modules 1 and 13 were in the IE/P2 subtype, module 10 in the IE/P1 subtype, and modules 15, 8, and 11 were in the IE subtype. Functional enrichment analysis was performed on these subtype-specific modules, and the top 5 pathways with p-values ranking from small to large in each module were plotted (Figure 3B). M5 was enriched with genes participating in inflammatory responses, including cytokine interactions, chemokine signaling, and Th17 cell differentiation (Figure S4C). M7 was enriched with genes related to angiogenesis, including focal adhesion and PI3K/Akt signaling (Figure S4D). M18 was enriched with genes involved in the cellular response to hypoxia and carbon metabolism, including the HIF-1 signaling pathway and glycolysis/gluconeogenesis (Figure S4E). This suggested that these three different functionally related genes were involved in the formation of an immunosuppressive microenvironment. Both the IE/P2 and IE/P1 subtypes were related to metabolism. The IE subtype was mainly enriched in synapse and singling transduction-related pathways (Figure S4F). This indicated that the activity of the nervous system in the IE subtype was high.

The relationship between gene expression and patient survival in each module was analyzed by univariate Cox regression analysis. Genes with P <0.05 and HR >1 were considered pro-tumor-related genes, and genes with HR <1 were considered anti-tumor-related genes. The proportion of pro-tumor genes greater than 0.5 was considered a poor prognosis-related module. Similarly, the proportion of anti-tumor-related genes greater than 0.5 was considered to be prognosis-related. Finally, nine subtype-specific modules were divided into seven poor prognosis and two good prognosis-related modules (Figure 3C), and the survival-related genes of each subtype-specific module were abbreviated as ssMSGs (Supplementary Table 2, hubgene.survival.related.xlsx). A total of 24 hub genes (Supplementary Table 3, module cox logtpm.sel.xlsx) were obtained, which were mainly located in M5 and M7 (P subtype). These genes were mainly located in M5 and M7 (P subtype). Through co-expression analysis of top hub genes in different gene modules, we identified the top 15 hub genes in M5, which represented the top connections with each other (Figure 3E). The top 15 hub genes included LAPTM5, NCKAP1L, PTPN5, SYX, and SIGLEC9, which is consistent with the top risk pathways we concluded above. Further, the signatures of the top 15 hub genes signature were associated with poorer outcomes in immunotherapy cohorts, which is also consistent with the tumor-promoting function of M5 (Figure 3F).

Notably, compared with single-cell datasets, we confirmed that hub genes in M5, M7, and M15 were also marker genes for specific cell types. CSTs (CSTA, CSTB, and CSTZ), CD68, and NOD2 in M5 were markers of macrophages; COL6A2 and ITGA5 in M7 were related to vascular cells; and Oligo2 in M15 was a marker of oligodendrocytes (Figure 3D). This result indicated that specific cell types should represent different functional modules during GBM progression.Therefore, we turned to single-cell datasets in the next part to delineate GBM TME at the single-cell scale.

Macrophages and microglia manipulate tumor-promoting gene modules of GBM

Next, we analyzed the expression activity of ssMSGs from nine subtype-specific modules in two published GBM single-cell datasets (GSE117891, GSE84465, and GSE163120) (18–20). GSE117891 and GSE84465 sequenced 10 patients' single cells from both the tumor core and the peritumoral brain, including tumor cells, vessels, microglia, neurons, and glia. GSE163120 only detected immune cells; myeloid cells accounted for the majority. TAMs, blood vessels, and tumor cells were in the tumor core, while neurons and glial cells were mainly located in peripheral tissues. More immune cells were detected in recurrent samples (Figure S5B).

The "AUCcell" method was used to calculate the expression activity of ssMSGs in single cells (Figures 4A, B). As for the P subtype-related genes, M5 was highly expressed in myeloid cells, including TAMs, microglia, monocytes, and DCs; M7 was mainly expressed in blood vessels; and M18 in blood vessels, myeloid cells, and tumor cells. The IE subtype-related genes were in OPCs and neurons. The expression distribution of 24 hub genes across cells was shown (Figures 4C, D, Figures S5C, D). These genes were expressed in myeloid cells, blood vessels, and OPCs. Combined with these results, we concluded that macrophages manipulated M5, vascular-related cells contributed to M7, and OPC cells regulated M15.

Cell–cell interaction

Considering the significant role of cell–cell interaction during GBM progression, we used cellphoneDB to figure out

10.3389/fimmu.2022.1051701

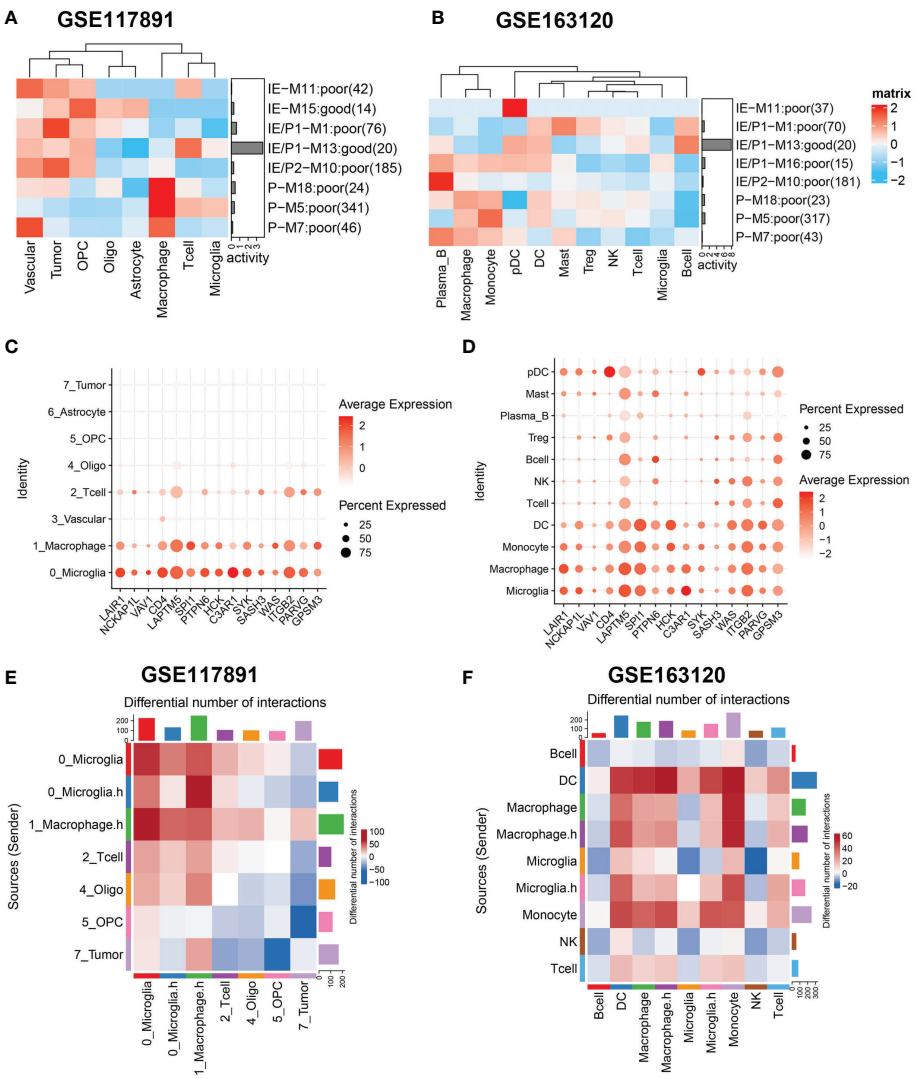

FIGURE 4
Gene sets expression activity and cell-cell interaction in sing-cell RNA-Seq datasets. **(A, B)** Row scaled gene expression activity of ssMSG across cell types in the GSE117891 and GSE163120 datasets, with the color from blue to red representing the activity score from low to high. Cells were clustered by the activity of these gene sets. **(C, D)** The expression level of Top15_hub genes across different cell types in two datasets. The larger the size, the larger the percent of expression. The darker the color, the higher the expression. **(E)** The differential cell–cell interaction weight between the tumor core and peripheral region of GSE117891.Upregulated interactions in tumor core were colored in red, down-regulated in blue. **(F)** The differential cell–cell interaction weight between recurrent and newly diagnosed samples of GSE163120. Upregulated interactions in recurrent samples were colored in red.

the interaction network of GBM (Figures 4E, F). We compared interaction strength in tumor samples with those of normal samples and found that macrophages exhibited high interaction with tumor cells among all cell types. This result was consistent with the characteristics of GBM tumor cells reported by others that they could interact with macrophages and induce their malignant transformation. Then we checked the interaction network among immune cells (Figure 4F). Interestingly, when we divided cells by expression of cytokine-related pathways, we found macrophages expressing higher cytokine pathways represented stronger interaction with DC and T cells, which may underline their pro-tumor mechanism. Similarly, we found microglia cells with higher cytokine pathway expression tend to interact with DC, macrophages, monocytes, and T cells. Specifically, Tregs showed stronger interaction with cytokine-high subtypes

than their counterparts, which could reshape the immunosuppressive microenvironment (Figure S5E).

In summary, we identified specific cell types that manipulate different gene modules in GBM. We then focused on the interactions related to macrophages and microglia with other cell types in the microenvironment.

Macrophage and microglia cells shape an immunosuppressive microenvironment through interaction with Tregs

To further identify the key mediators of macrophage and microglia interaction in GBM patients, we use the R package "NicheNet" based on the expression and downstream targets of ligand–receptor pairs. Based on the above results, we chose Tregs for the following analysis (Figures 5A, B; Figure S6). We found that macrophages and microglia cells could directly contact Tregs through the adhesive ligand–receptor pairs ICAM1-IL2RG and ITGAM-ICAM2. In addition, macrophages and microglia cells enhanced the activation cytokine activity of tregs *via* the expression of EBI3, CD86, and TNF, inducing the expression of IL27RA, CD28, TNFRSF1B, FAS, ICOS, and the immune checkpoint CTLA4 on tregs. Additionally, macrophages and microglia cells enhanced the recruitment of tregs through CXCL16–CXCR6, CCL3–CCR5, CCL2–CCR5 pairs.

Then, we evaluated which ligands on macrophages or microglia cells could most likely regulate Tregs. We merged the GSE163120 and GSE117891 datasets and identified seven ligand genes (Figure 5C). The regulatory network between the top 15 hub genes and these ligands is shown in Figure 5D. SPI1 could be the upstream regulator of TNF, and GPSM3 may

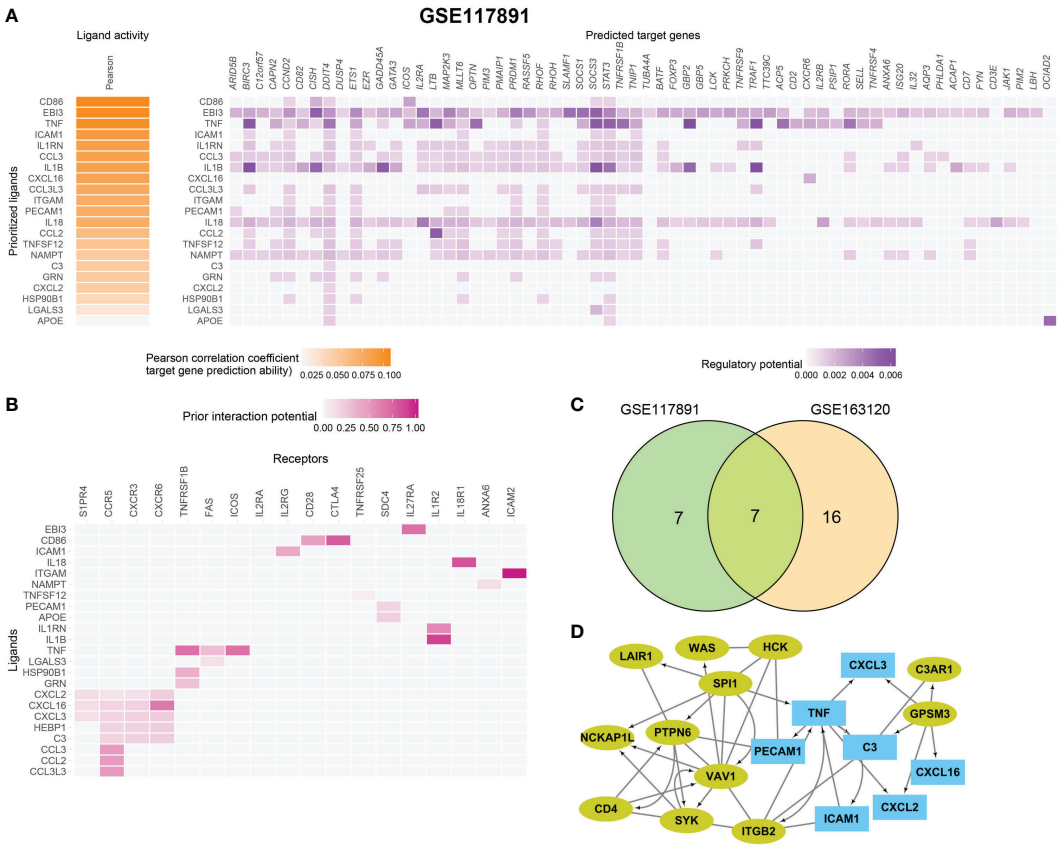

FIGURE 5
Macrophage and microglia cells shape an immunosuppressive microenvironment through interaction with Tregs in GSE163120. **(A)** A heatmap showing the predicted ligand activity by NicheNet on genes highly expressed in Treg. Pearson correlation indicates the ability of each ligand to predict the target genes, and better predictive ligands are thus ranked higher. **(B)** A dot heatmap showing the selected ligand-receptor pairs between macrophages or microglia and Treg cells. Benjamini–Hochberg adjusted permutation test. **(C)** The intersection between top ligands from both datasets, seven ligands in macrophage/microglia were detected. **(D)** protein–protein interaction between Top15_hub genes (colored in yellow green) and seven ligands (colored in sky blue) with both directed and undirected interaction. The directed interaction was shown in arrows. Some Top15_hub genes were involved in the regulation of ligands.

regulate the expression of a series of cytokines and chemokines such as C3, CXCL3, CXCL16, and CXCL2.

In conclusion, we find out how upstream regulators regulate ligand expression on macrophages and microglia cells, how ligands interact with their receptors on tregs, and how these interactions thus shape the immunosuppressive microenvironment of GBM.

Discussion

The characteristics and mechanisms of the tumor microenvironment, especially the immunosuppressive microenvironment, in patients with GBM are still unclear. In addition to immunosuppressive microenvironment, in patients with GBM are still unclear. In addition to various immune cells' infiltration, the tumor microenvironment also contains glial cells, vascular-related cells, fibroblasts, immunosuppressive factors, etc. The major signaling pathways also play a key role in the formation of GBM. On the research of tumor immune microenvironment, previous studies mainly focused on estimating the composition of immune cells or including some immune system-related signatures, while ignoring the role of non-immune factors. In addition, the cell type infiltration and signaling pathways involved were rarely the subjects of deeper discussions in previous studies. In this study, we first collected various functional signatures related to the GBM tumor microenvironment and divided GBM patients into four groups according to the expression profiles of these signatures. The immunosuppressive subtypes were successfully defined and which had elevated expression of immunosuppressive molecules such as IDO1, Il-6, etc. Then we conducted an in-depth study of the cellular composition and interaction of the immunosuppressive subtypes.

As reported, some major pathways played a key role in the tumor progression or influenced the formation of an immunosuppressive microenvironment in GBM (14–16, 29). For example, GBM cancer-related cytokine deregulation might be responsible for the failure of the immune system to recognize malignant tumor cells (11). The increase of pro-angiogenic growth factors, including VEGF, led to a high degree of tumor vascularization (30). In this study, five pathways that were significantly related with the GBM progression were found by analysis from three different perspectives. These three perspectives differed in methodology, but the results were indeed very consistent. This indicated that these pathways were very important in the progression of GBM. They were mainly involved in two directions: inflammatory response related, including TNF-α signaling and cytokine–cytokine interactions and angiogenesis related to ECM, focal adhesion and the PI3K/Akt signaling pathway. The activity of these five signaling pathways was positively correlated with the infiltration of myeloid suppressor cells (MDSCs), which were reported to participate in the immunosuppression of GBM (31). Therefore, we used the genes from these five pathways for further GBM subtyping.

Among the four GBM subtypes we found, these were immune-infiltrating (IE) and immunosuppressive (P). Statistical differences in survival were identified among the types of patients (long-rank p-value <0.01). As expected, the P subtype had high expression of ICB and immunosuppressive factors and no IDH mutation, while the IE subtype had high lymphocyte infiltration. Unexpectedly, in the IE subtype, we did not find the high expression of genes related to lymphocytes activation, but only synapse related genes were detected. It was reported that lymphocytes infiltrated in GBM were rarely activated, which might explain our findings. This suggested that immunotherapy targeting T cells in GBM might not be meaningful.

In addition, we were surprised to find that the three co-expressed gene modules associated with the P subtype differ greatly in enriched pathways according to the following WGCNA analysis. These three gene modules had the functions of inflammatory response (cytokine interaction), angiogenesis, hypoxia, and carbon metabolism, respectively. This indicated that three different functional genes worked together to influence the formation of the P subtype. By verifying the expression of ssMSGs in two publicly available single-cell datasets, we found that three modules corresponded to different types of cells (TAM, blood vessels, tumors). Therefore, we inferred that these types of cells worked together to form the immunosuppressive microenvironment. Also, we found that TAM and tumor had significant interactions in the tumor core through cell interaction analysis. More interestingly, we found novel hub genes from immunosuppressive modules could be the upstream regulators of a series of cytokines and chemokines such as C3, CXCL3, CXCL16, and CXCL2 in macrophages and microglia cell, which further interact with Treg and shape the immunosuppressive microenvironment of GBM.

In conclusion, we combined bulk- and single-cell RNA-seq data to profile the GBM tumor microenvironment using bioinformatics tools, and discovered important cells and pathways involved in the formation of the tumor immunosuppressive microenvironment (Graphic abstract). Future research needs to focus on inhibiting the interference signaling pathways in myeloid cells, especially TAM cells and the interaction between Tregs, which may be a beneficial therapeutic direction for GBM tumors.

Data availability statement

The datasets presented in this study can be found in online repositories. The names of the repository/repositories and accession number(s) can be found in the article/ Supplementary Material.

Author contributions

LN and BL conceived and designed the study. LN, PS, and SZ performed the analysis flowchart and collected the data. BQ, XC, and MX contributed to analyzing the data. LN wrote the manuscript. BL made manuscript revisions. All authors have read and approved the manuscript.

Funding

This study was supported by the National Natural Science Foundation of China (81904171), the Jiangsu Postdoctoral Research Foundation (2020Z388), and the Top Talent Support Program for Young and Middle-Aged People of Wuxi Health Committee, Wuxi Health Commission Scientific Research Project (M202033).

Conflict of interest

The authors declare that the research was conducted in the absence of any commercial or financial relationships that could be construed as a potential conflict of interest.

Publisher's note

Supplementary material

The Supplementary Material for this article can be found online at: https://www.frontiersin.org/articles/10.3389/fimmu.2022.1051701/full#supplementary-material

SUPPLEMENTARY TABLE 1
The detail clinic pathological characteristics for TCGA-GBM and CGGA cohort.

SUPPLEMENTARY TABLE 2
The survival related genes of each subtype specific module; which were mainly located in M5 and M7 (P subtype).

SUPPLEMENTARY FIGURE 1
Risk model in CGGA-cohort **(A)** The Kaplan–Meier curves comparing patients with low or high risk score in CGGA cohort. Patients were divided into two groups according to the median value of risk scores. Higher risk score were correlated to poorer prognosis. **(B)** ROC curve for risk-model in CGGA cohort. **(C)** The Kaplan–Meier curves comparing IDH1 mutation and wild-type patients in TCGA-GBM cohort.

SUPPLEMENTARY FIGURE 2
Generation of the Ges utilized for transcriptomic-based TME classification **(A)** The 13 Gges included in each functional group. **(B)** Correlation analysis between signatures in TCGA-GBM cohort. Positive correlation coefficient was shown in orange and negative correlation coefficient was shown in blue, darker color indicates bigger value. **(C)** Result of univariate Cox regression analysis in TCGA-GBM cohort. HR and p values were displayed.

SUPPLEMENTARY FIGURE 3
Immunosuppressive subtype validation in CGGA cohort **(A)** Heatmap of row scaled gene signature scores from cell deconvolution algorithm with the color from green to red represents the activity score from low to high. Samples in column were grouped into four TME subtypes. **(B)** Overall survival of patients stratified by TME subtype classification. The log-rank p-value between subtype IE and P was 0.0051 and the annova log-rank p-value for four subtypes was 0.0001. **(C)** The expression profile of immune suppression related genes checkpoints across TCGA-GBM four TME subtypes with the color from green to purple represents the expression value from low to high. **(D)** Mutation frequency of five high frequency mutant gene across four TME subtypes. Samples were shown in column. Samples with mutation were colored in red. **(E)** The expression profile of inhibitory immune checkpoints across four TME subtypes. **(F)** Differential immune cell infiltration level across Immunosuppressive subtype and other's. Statistical significance between groups was tested by Wilcox.

SUPPLEMENTARY FIGURE 4
WGCNA construction **(A)** Determine soft-thresholding power in WGCNA. The scale-free fit index for various soft-thresholding powers (β) (Left). The mean connectivity for various softthresholding powers (Right). **(B)** WGCNA cluster dendrogram on TCGA-GBM patients, genes were grouped into several distinct modules. **(C, D, E, F)** Top10 enriched pathways of 4 selected modules, M5 **(C)**, M7 **(D)**, M18 **(E)**, M15 **(F)**.

SUPPLEMENTARY FIGURE 5
Gene expression validation in 2 sing-cell RNA-Seq datasets **(A)** The ratio of cell types between tumor core (T) and peripheral region (N) of GSE117891. **(B)** The ratio of cell types between recurrent (R) and newly diagnosed (ND) samples of GSE163120. **(C, D)** Violin plots of selected pathways' expression activity across cell-types with y-axis as expression activity in two datasets. (E) The interaction weight between Treg and other immune cells in recurrent samples of GSE163120. The thick in line the bigger in weight.

SUPPLEMENTARY FIGURE 6
Cell interaction between macrophage/microglia and T cell in GSE117891 Heatmap showing the predicted ligand activity by NicheNet on genes highly expressed in Treg. Pearson correlation indicates the ability of each ligand to predict the target genes, and better predictive ligands are thus ranked higher.

References

1. Dobes M, Khurana VG, Shadbolt B, Jain S, Smith SF, Smee R, et al. Increasing incidence of glioblastoma multiforme and meningioma, and decreasing incidence of schwannoma (2000-2008): Findings of a multicenter Australian study. *Surg Neurol Int* (2011) 2:176. doi: 10.4103/2152-7806.90696

2. Stupp R, Mason WP, van den Bent MJ, Weller M, Fisher B, Taphoorn MJ, et al. Radiotherapy plus concomitant and adjuvant temozolomide for glioblastoma. *N Engl J Med* (2005) 352:987–96. doi: 10.1056/NEJMoa043330

3. Xie Y, He L, Lugano R, Zhang Y, Cao H, He Q, et al. Key molecular alterations in endothelial cells in human glioblastoma uncovered through single-cell RNA sequencing. *JCI Insight* (2021) 6(15):e150861. doi: 10.1172/jci.insight.150861

4. Stupp R, Wong ET, Kanner AA, Steinberg D, Engelhard H, Heidecke V, et al. NovoTTF-100A versus physician's choice chemotherapy in recurrent glioblastoma: a randomised phase III trial of a novel treatment modality. *Eur J Cancer* (2012) 48:2192–202. doi: 10.1016/j.ejca.2012.04.011

5. Himes BT, Geiger PA, Ayasoufi K, Bhargav AG, Brown DA, Parney IF. Immunosuppression in glioblastoma: Current understanding and therapeutic implications. *Front Oncol* (2021) 11:770561. doi: 10.3389/fonc.2021.770561

6. Buisseret L, Desmedt C, Garaud S, Fornili M, Wang X, Van den Eyden G, et al. Reliability of tumor-infiltrating lymphocyte and tertiary lymphoid structure assessment in human breast cancer. *Mod Pathol* (2017) 30:1204–12. doi: 10.1038/modpathol.2017.43

7. Berghoff AS, Kiesel B, Widhalm G, Rajky O, Ricken G, Wöhrer A, et al. Programmed death ligand 1 expression and tumor-infiltrating lymphocytes in glioblastoma. *Neuro Oncol* (2015) 17:1064–75. doi: 10.1093/neuonc/nou307

8. De Leo A, Ugolini A, Veglia F. Myeloid cells in glioblastoma microenvironment. *Cells* (2020) 10(1):18. doi: 10.3390/cells10010018

9. Hanahan D, Coussens LM. Accessories to the crime: functions of cells recruited to the tumor microenvironment. *Cancer Cell* (2012) 21:309–22. doi: 10.1016/j.ccr.2012.02.022

10. Nengroo MA, Verma A, Datta D. Cytokine chemokine network in tumor microenvironment: Impact on CSC properties and therapeutic applications. *Cytokine* (2022) 156:155916. doi: 10.1016/j.cyto.2022.155916

11. Zhu VF, Yang J, Lebrun DG, Li M. Understanding the role of cytokines in glioblastoma multiforme pathogenesis. *Cancer Lett* (2012) 316:139–50. doi: 10.1016/j.canlet.2011.11.001

12. Amankulor NM, Kim Y, Arora S, Kargl J, Szulzewsky F, Hanke M, et al. Mutant IDH1 regulates the tumor-associated immune system in gliomas. *Genes Dev* (2017) 31:774–86. doi: 10.1101/gad.294991.116

13. Wang Q, Hu B, Hu X, Kim H, Squatrito M, Scarpace L, et al. Tumor evolution of glioma-intrinsic gene expression subtypes associates with immunological changes in the microenvironment. *Cancer Cell* (2017) 32:42–56 e46. doi: 10.1016/j.ccell.2017.06.003

14. Cahill KE, Morshed RA, Yamini B. Nuclear factor-kappaB in glioblastoma: insights into regulators and targeted therapy. *Neuro Oncol* (2016) 18:329–39. doi: 10.1093/neuonc/nov265

15. Lee Y, Lee JK, Ahn SH, Lee J, Nam DH. WNT signaling in glioblastoma and therapeutic opportunities. *Lab Invest* (2016) 96:137–50. doi: 10.1038/labinvest.2015.140

16. Daisy Precilla S, Biswas I, Kuduvalli SS, Anitha TS. Crosstalk between PI3K/AKT/mTOR and WNT/beta-catenin signaling in GBM - could combination therapy checkmate the collusion? *Cell Signal* (2022) 95:110350. doi: 10.1016/j.cellsig.2022.110350

17. Goldman MJ, Craft B, Hastie M, Repecka K, McDade F, Kamath A, et al. Visualizing and interpreting cancer genomics data *via* the xena platform. *Nat Biotechnol* (2020) 38:675–8. doi: 10.1038/s41587-020-0546-8

18. Darmanis S, Sloan SA, Croote D, Mignardi M, Chernikova S, Samghababi P, et al. Single-cell RNA-seq analysis of infiltrating neoplastic cells at the migrating front of human glioblastoma. *Cell Rep* (2017) 21:1399–410. doi: 10.1016/j.celrep.2017.10.030

19. De Vlaminck K, Romao E, Puttemans J, Antunes ARP, Kancheva D, Scheyltjens I, et al. Imaging of glioblastoma tumor-associated myeloid cells using nanobodies targeting signal regulatory protein alpha. *Front Immunol* (2021) 12:777524. doi: 10.3389/fimmu.2021.777524

20. Yu K, Hu Y, Wu F, Guo Q, Qian Z, Hu W, et al. Surveying brain tumor heterogeneity by single-cell RNA-sequencing of multi-sector biopsies. *Natl Sci Rev* (2020) 7:1306–18. doi: 10.1093/nsr/nwaa099

21. Stuart T, Butler A, Hoffman P, Hafemeister C, Papalexi E, Mauck WM 3rd, et al. Comprehensive integration of single-cell data. *Cell* (2019) 177:1888–1902 e1821. doi: 10.1016/j.cell.2019.05.031

22. Zhang B, Horvath S. A general framework for weighted gene co-expression network analysis. *Stat Appl Genet Mol Biol* (2005) 4:Article17. doi: 10.2202/1544-6115.1128

23. Aibar S, Gonzalez-Blas CB, Moerman T, Huynh-Thu VA, Imrichova H, Hulselmans G, et al. SCENIC: single-cell regulatory network inference and clustering. *Nat Methods* (2017) 14:1083–6. doi: 10.1038/nmeth.4463

24. Efremova M, Vento-Tormo M, Teichmann SA, Vento-Tormo R. CellPhoneDB: inferring cell-cell communication from combined expression of multi-subunit ligand-receptor complexes. *Nat Protoc* (2020) 15:1484–506. doi: 10.1038/s41596-020-0292-x

25. Browaeys R, Saelens W, Saeys Y. NicheNet: modeling intercellular communication by linking ligands to target genes. *Nat Methods* (2020) 17:159–62. doi: 10.1038/s41592-019-0667-5

26. Nakada M, Kita D, Watanabe T, Hayashi Y, Teng L, Pyko IV, et al. Aberrant signaling pathways in glioma. *Cancers (Basel)* (2011) 3:3242–78. doi: 10.3390/cancers3033242

27. Piccirillo SGM, Alonso MM, Pasqualetti F. Basic and translational advances in glioblastoma. *BioMed Res Int* (2018) 2018:1820345. doi: 10.1155/2018/1820345

28. Nduom EK, Weller M, Heimberger AB. Immunosuppressive mechanisms in glioblastoma. *Neuro Oncol* (2015) 17 Suppl 7:vii9–vii14. doi: 10.1093/neuonc/nov151

29. He Y, Sun MM, Zhang GG, Yang J, Chen KS, Xu WW, et al. Targeting PI3K/Akt signal transduction for cancer therapy. *Signal Transduct Target Ther* (2021) 6:425. doi: 10.1038/s41392-021-00828-5

30. Khabibov M, Garifullin A, Boumber Y, Khaddour K, Fernandez M, Khamitov F, et al. Signaling pathways and therapeutic approaches in glioblastoma multiforme (Review). *Int J Oncol* (2022) 60(6):69. doi: 10.3892/ijo.2022.5359

31. Raychaudhuri B, Rayman P, Huang P, Grabowski M, Hambardzumyan D, Finke JH, et al. Myeloid derived suppressor cell infiltration of murine and human gliomas is associated with reduction of tumor infiltrating lymphocytes. *J Neurooncol* (2015) 122:293–301. doi: 10.1007/s11060-015-1720-6

frontiers | Frontiers in Immunology

TYPE Original Research
PUBLISHED 09 January 2023
DOI 10.3389/fimmu.2022.997115

OPEN ACCESS

EDITED BY
Gulderen Yanikkaya Demirel,
Yeditepe University, Turkey

REVIEWED BY
Fernando Guimaraes,
Diamantina Institute, The University of Queensland, Australia
Maite Alvarez,
University of Navarra, Spain

*CORRESPONDENCE
Rudolf Schicho
rudolf.schicho@medunigraz.at

SPECIALTY SECTION
This article was submitted to Cancer Immunity and Immunotherapy, a section of the journal Frontiers in Immunology

RECEIVED 18 July 2022
ACCEPTED 07 December 2022
PUBLISHED 09 January 2023

CITATION
Sarsembayeva A, Kienzl M, Gruden E, Ristic D, Maitz K, Valadez-Cosmes P, Santiso A, Hasenoehrl C, Brcic L, Lindenmann J, Kargl J and Schicho R (2023) Cannabinoid receptor 2 plays a pro-tumorigenic role in non-small cell lung cancer by limiting anti-tumor activity of CD8$^+$ T and NK cells. *Front. Immunol.* 13:997115. doi: 10.3389/fimmu.2022.997115

Cannabinoid receptor 2 plays a pro-tumorigenic role in non-small cell lung cancer by limiting anti-tumor activity of CD8$^+$ T and NK cells

Arailym Sarsembayeva [1], Melanie Kienzl [1], Eva Gruden [1], Dusica Ristic [1], Kathrin Maitz [1], Paulina Valadez-Cosmes [1], Ana Santiso [1], Carina Hasenoehrl [1], Luka Brcic [2], Jörg Lindenmann [3], Julia Kargl [1] and Rudolf Schicho [1,4]*

[1]Division of Pharmacology, Otto Loewi Research Center, Medical University of Graz, Graz, Austria, [2]Diagnostic and Research Institute of Pathology, Medical University of Graz, Graz, Austria, [3]Division of Thoracic and Hyperbaric Surgery, Department of Surgery, Medical University of Graz, Graz, Austria, [4]BioTechMed, Graz, Austria

Cannabinoid (CB) receptors (CB_1 and CB_2) are expressed on cancer cells and their expression influences carcinogenesis in various tumor entities. Cells of the tumor microenvironment (TME) also express CB receptors, however, their role in tumor development is still unclear. We, therefore, investigated the role of TME-derived CB_1 and CB_2 receptors in a model of non-small cell lung cancer (NSCLC). Leukocytes in the TME of mouse and human NSCLC express CB receptors, with CB_2 showing higher expression than CB_1. In the tumor model, using CB_1- ($CB_1^{-/-}$) and CB_2-knockout ($CB_2^{-/-}$) mice, only deficiency of CB_2, but not of CB_1, resulted in reduction of tumor burden vs. wild type (WT) littermates. This was accompanied by increased accumulation and tumoricidal activity of CD8$^+$ T and natural killer cells, as well as increased expression of programmed death-1 (PD-1) and its ligand on lymphoid and myeloid cells, respectively. $CB_2^{-/-}$ mice responded significantly better to anti-PD-1 therapy than WT mice. The treatment further increased infiltration of cytotoxic lymphocytes into the TME of $CB_2^{-/-}$ mice. Our findings demonstrate that TME-derived CB_2 dictates the immune cell recruitment into tumors and the responsiveness to anti-PD-1 therapy in a model of NSCLC. CB_2 could serve as an adjuvant target for immunotherapy.

KEYWORDS

CB_1, CB_2, cannabinoid receptors, non-small cell lung cancer, tumor microenvironment, CD8$^+$ T cells, NK cells, immunotherapy

Introduction

Cannabinoid (CB) receptors CB_1 and CB_2 are widely found in human tumor tissue and are well-known to influence the growth of tumor cells (1). However, whether they act as tumor promotors or suppressors, and whether CB receptors located in cancer cells or/and in immune cells of the tumor microenvironment (TME) are involved in tumor progression, is less clear. In particular, CB receptors could significantly influence the development of lung cancer, as suggested by previous studies of non-small cell lung cancer (NSCLC) (2, 3). Some studies show that agonists of CB_1 and/or CB_2 attenuate the carcinogenic potential in lung cancer cells (2, 4–6), and reduce tumor growth in immunodeficient (7) and FVB/N mice (8), however, other studies report the opposite. For instance, CB_1/CB_2 agonist tetrahydrocannabinol (THC) may promote proliferation of lung cancer cells (9) and the growth of breast cancer *in vivo* (10). In addition, silencing of CB_2 in lung cancer cells reportedly decreases their proliferation, migration, and invasion (3). A number of studies on the prognostic value of CB expression revealed discrepant findings based on the cancer type (reviewed in (11)). While some articles described high expression of CB_1/CB_2 receptors in human samples of NSCLC correlating with prolonged survival (2), others described a positive correlation of CB_2 expression with increased tumor size and pathological grading of NSCLC (3), indicating a complex and still unclear role of CB receptors in NSCLC.

CB_1 and CB_2 receptors are part of the endocannabinoid system (ECS), acting in concert with their endogenous ligands (endocannabinoids) and enzymes for synthesis and degradation of these ligands (12, 13). CB_1 is abundantly expressed in the central nervous system (14), but is also detectable in peripheral tissues including the immune system (15, 16). The majority of immune cells express CB_1 at low levels, and its expression is generally affected by the activation status and cell type, as well as the presence of immune stimuli and endocannabinoids (17). In contrast, CB_2 is highly expressed in immune cells, and controls functions such as proliferation, migration, activity, cytokine release, antigen presentation, and antibody production (15, 18). The receptor has previously been described for its immunosuppressive behavior (15, 19). For instance, in plaque-forming cell assays in mouse splenocytes (which measure the capacity of the spleen cells to mount a primary antibody response to sheep red blood cells), THC could directly inhibit the cells *via* CB_2 (20). In addition, the endocannabinoid anandamide suppresses release of pro-inflammatory cytokines like IL-2, TNF-α and IFN-γ from activated human peripheral T-lymphocytes, acting primarily through CB_2 (21). These effects can be mimicked by the CB_2 agonist JWH-015, and blocked by the CB_2 antagonist SR144528 (22). Cannabinoids have been reported to reduce natural killer cell (NK) activity, thus, *in vivo* administration of THC in male Swiss mice results in inhibition of splenic NK cytolytic activity without altering proliferation of splenocytes (23). Also, in human NK cells, THC has been demonstrated to reduce cytolytic activity (reviewed in Braile et al. (24)). CB_2 has previously been suggested to play a key role in suppressing immune activity in cancer, a concept supported by Zhu et al., who showed that CB_2 controls tumor immunity of lung cancer by increasing the levels of Th_2 cytokines like IL-10 and TGF, and by downregulating the Th_1 cytokine IFN-γ (10).

Based on their well-described impact on immune cells, CB receptors could significantly influence immune cell behavior and regulatory components of immune activity, including inhibitory checkpoint proteins like programmed death-1 (PD-1) and its ligand PD-L1, within the TME. PD-1 is an inhibitory receptor expressed on T cells after antigen stimulation, while PD-L1 is found on tumor cells and antigen presenting cells (25). Particularly, in NSCLC, the PD-1/PD-L1 axis has emerged as a successful target for the use of immune checkpoint inhibitors (ICI). However, limited response rates and resistance have hampered their success (26), warranting the discovery of new targets to boost ICI therapy. In this regard, clinical trials using combination therapies of ICIs with anti-angiogenic agents, chemotherapy, ataxia telangiectasia and Rad3-related (ATR) kinase and mitogen-activated protein kinase kinase (MEK) inhibitors, have been conducted or are still ongoing (reviewed in Blach et al. (26)).

In the present study, we investigated whether CB receptors located in the TME control tumor growth and influence susceptibility to ICI treatment. To investigate our hypothesis, we used a mouse model of NSCLC, in which immunocompetent wild type (WT) and CB_1-knockout ($CB_1^{-/-}$) or CB_2-knockout ($CB_2^{-/-}$) mice received a subcutaneous (s.c.) injection of syngeneic lung adenocarcinoma cells (KP cells (27)), thus creating a tumor model with TME cells that either express or lack CB receptor. We report that tumors in $CB_2^{-/-}$ mice are smaller than in their WT littermates, and that $CB_2^{-/-}$ mice respond better to anti-PD-1 therapy, indicating that CB_2 expression in the TME is a critical determinant of immune suppression in this NSCLC model.

Results

Tumor and TME cells express CB receptors *in situ*, and blockade of CB_2, and not CB_1, inhibits tumor growth in a murine NSCLC model

As the role of TME-derived CB receptors in lung cancer has not yet been investigated, we aimed to identify whether TME host cells lacking CB_1 or CB_2 would influence primary tumor growth. After injecting KP cells s.c. into the flanks of $CB_1^{-/-}$, $CB_2^{-/-}$, and WT mice, *ex vivo* measurement of tumor weight and volume demonstrated that tumor burden of $CB_1^{-/-}$ mice did not differ from WTs in our mouse model (Figure 1A). In contrast, mice devoid of CB_2 showed more than 50% reduction in both tumor weight and volume, as compared to WT littermates (Figure 1B). We then investigated whether pharmacological

10.3389/fimmu.2022.997115

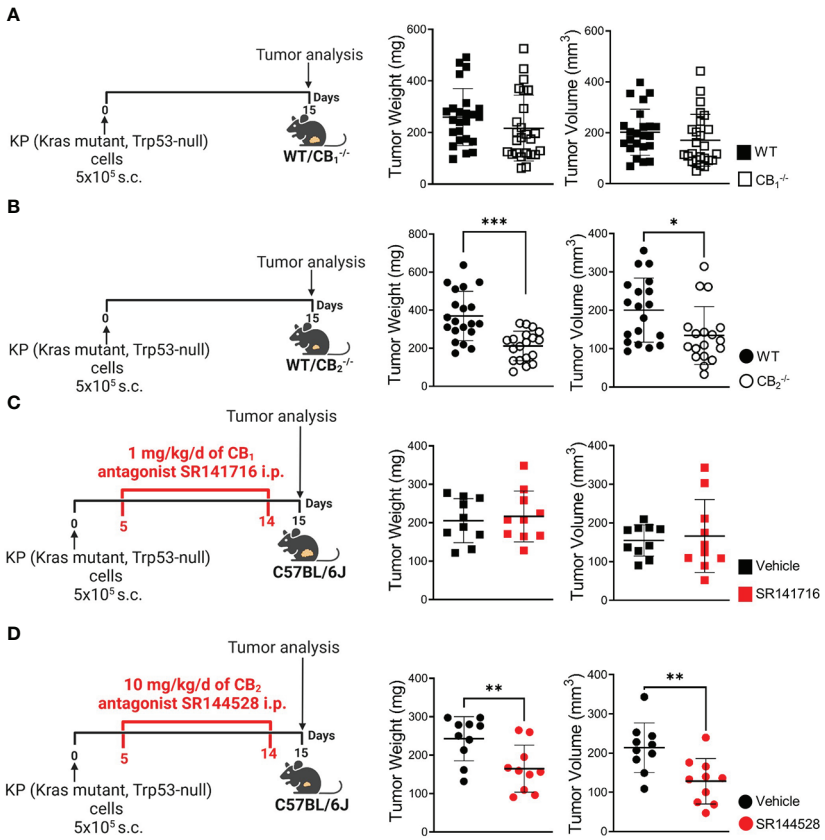

FIGURE 1
Blockade of CB_2, but not CB_1, inhibits tumor growth in a mouse model of NSCLC. **(A)** Experimental design: $CB_1^{-/-}$ mice and wild type (WT) littermates were subcutaneously (s.c.) injected with $5x10^5$ KP (Kras mutant, Trp53-null) lung adenocarcinoma cells on day 0. On day 15, tumors were measured *ex vivo* and harvested for analysis. Data indicate mean values ± SD from three pooled independent experiments. n= 23-25. **(B)** Experimental design: $CB_2^{-/-}$ mice and WT littermates were s.c. injected with $5x10^5$ KP lung adenocarcinoma cells on day 0. On day 15, tumors were measured *ex vivo* and collected for analysis. Data indicate mean values ± SD from two pooled independent experiments. n= 18-20. **(C, D)** Experimental design: C57BL/6J WT mice were s.c. injected with $5x10^5$ KP lung adenocarcinoma cells on day 0. Five-days post-inoculation, KP cell tumor-bearing mice started receiving intraperitoneal (i.p.) injections of either **(C)** 1 mg/kg/d of CB_1 antagonist SR141716 or **(D)** 10 mg/kg/d of CB_2 antagonist SR144528 (or vehicle). On day 15, tumor weight and volume were measured *ex vivo*. One representative experiment is shown. Data indicate mean values ± SD, n= 9-10. All statistical differences were evaluated by using unpaired student`s *t*-test **(A–D)**. *p < .05; **p < .01; ***p < .001. *NSCLC*, non-small cell lung cancer.

blockade of CB receptors in tumor-bearing C57BL/6J mice could replicate findings obtained in knockout mice using previously tested doses of CB_1 antagonist SR141716 (28, 29) and CB_2 antagonist SR144528 (29, 30). As a result, treatment with CB_1 antagonist SR141716 had no effect on both tumor weight and volume (Figure 1C), whereas tumor-bearing C57BL/6J mice treated with CB_2 antagonist SR144528 showed a significant reduction in tumor weight and volume as compared to vehicle-treated animals (Figure 1D).

To further investigate the role of CB receptors in the TME, we identified mRNA expression of these receptors in tumor cells and infiltrating immune cells *in situ*. We used *in situ* hybridization (ISH) technique with specific probes against CB_1 and CB_2 mRNA in combination with immunofluorescence (IF). Dual ISH-IF analysis displayed CB_1 expression in cancer cells as well as immune cells of the TME, but to a far lesser extent than expression of CB_2 (Figure 2A). Around 25% of tumor cells (which positively stained for cytokeratin) co-localized with CB_2 mRNA (Figure 2B). Within the TME, we detected CB_2 mRNA expression in $CD3^+$ T cells, $CD8^+$ T cells, $NKp46/NCR1^+$ cells, $CD163^+$ or $F4/80^+$ macrophages, and $CD11b^+$ cells. Co-localizations ranged between ~20-40% (Figure 2B).

Since several studies described CB receptor expression in tumors of NSCLC patients (2, 3, 7), we stained sections of human lung cancer tissues to assess the distribution of CB_1 and CB_2 receptors in tumor cells and infiltrating immune cells, and also applied flow cytometry in freshly resected NSCLC tissues. In line with our mouse data, CB_1 and CB_2 expression were not only seen in lung cancer cells, but also in infiltrated immune cells, such as $CD3^+$ T and $CD8^+$ T cells, $NKp46/NCR1^+$or $CD56^+$ NK

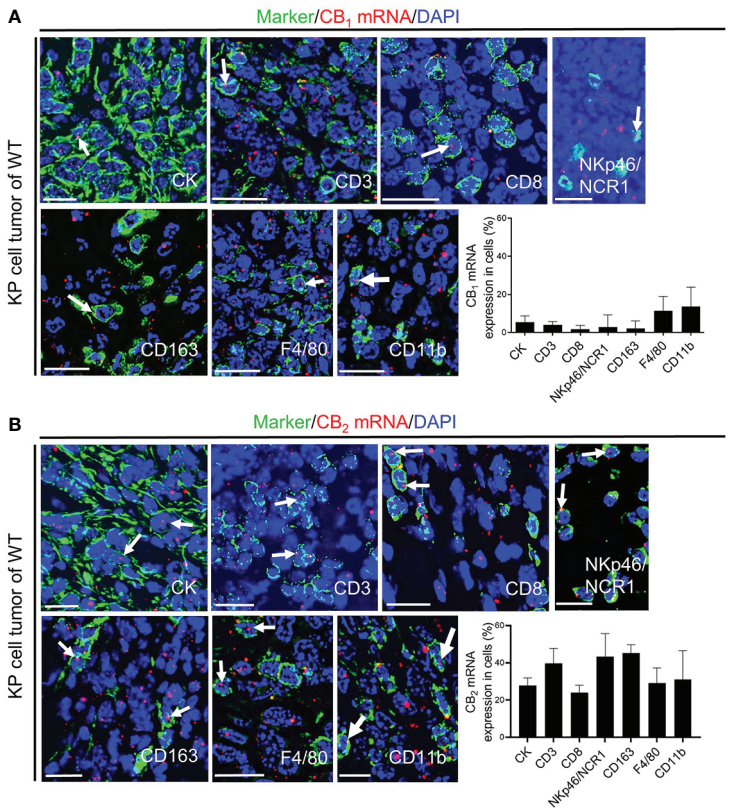

FIGURE 2
CB_1 and CB_2 mRNA in tumor cells and immune cells of the TME. **(A, B)** *In situ* hybridization (ISH)/immunofluorescence (IF) of tumor/immune cells in KP cell tumor sections from wild type mice. **(A)** The graph demonstrates the percentages of co-localization of CB_1 mRNA positive signals with tumor cells (cytokeratin-stained, CK^+ cells; ~ 5%) and leukocytes of the TME, such as $CD3^+$ T cells (~ 4%), $CD8^+$ T cells (~ 3%), $NKp46/NCR1^+$ cells (natural killer, NK cells; ~ 14%), $CD163^+$ M2 macrophages (~ 7%), $F4/80^+$ M1 and M2 macrophages (~ 11%), and $CD11b^+$ myeloid cells (~ 14%). **(B)** The graph shows the percentages of co-localization of CB_2 mRNA signals with tumor cells (~ 25%) and tumor-infiltrating immune cells, including $CD3^+$ T cells (~ 39%), $CD8^+$ T cells (~ 24%), $NKp46/NCR1^+$ NK cells (~ 43%), $CD163^+$ M2 macrophages (~ 43%), $F4/80^+$ M1 and M2 macrophages (~ 29%), and $CD11b^+$ myeloid cells (~ 29%). Arrows denote CB_1 or CB_2 ISH mRNA signals within tumor and immune cells. Calibration bars=20 µm. Data indicate mean values +SD; n=3 (sections from three different tumors, 30-150 cells counted per section). *TME*, tumor microenvironment.

cells, and $CD163^+$ macrophages. Expression of CB_2 was generally higher than that of CB_1 (Figures 3A, B, S2A).

These results indicate that CB_1 and CB_2 is expressed in both tumor and tumor-infiltrated immune cells, however, only deletion of CB_2 on host cells or systemic blockade of CB_2, but not of CB_1, results in a reduction of tumor burden. To validate our results from the KP cell tumor model, we used Lewis lung carcinoma (LLC1) cells in $CB_2^{-/-}$ vs. WT mice and identified that tumor burden was significantly reduced in $CB_2^{-/-}$ mice when compared to WT mice (Figure S2C).

Tumor reduction exclusively relies on deletion of CB_2 in TME host cells

According to dual ISH-IF, we found that besides immune cells, around 20-25% of tumor cells in human NSCLC (Figures 3B, S2A) and mouse tumor (Figures 4A, S2D) tissue co-localized with CB_2 mRNA. According to RT-qPCR, tumors of WT mice showed higher levels of CB_2 mRNA than those from $CB_2^{-/-}$ mice, because host cells, such as immune cells infiltrating the TME in $CB_2^{-/-}$ mice, are devoid of CB_2 expression (Figure 4B). KP cells in culture cells expressed minimal levels of CB_2 (Figures 4B, S2D). We confirmed the specificity of our CB_2 PCR primers by absence of CB_2 mRNA expression in spleen tissue of $CB_2^{-/-}$ mice in comparison to WT mice (Figure S2E).

To address the role of CB_2-expressing KP cells on tumor growth *in situ*, we pharmacologically activated or blocked CB_2 in tumor-bearing $CB_2^{-/-}$ mice using a CB_2 agonist (JWH133) (Figure 4C) or CB_2 antagonist (SR144528) (Figure 4E) at previously published doses (29, 31). The results revealed that activation or inhibition of CB_2 in tumor cells of tumor-bearing $CB_2^{-/-}$ mice had no effect on tumor weight and volume (Figures 4D, F), indicating that the tumor reduction we

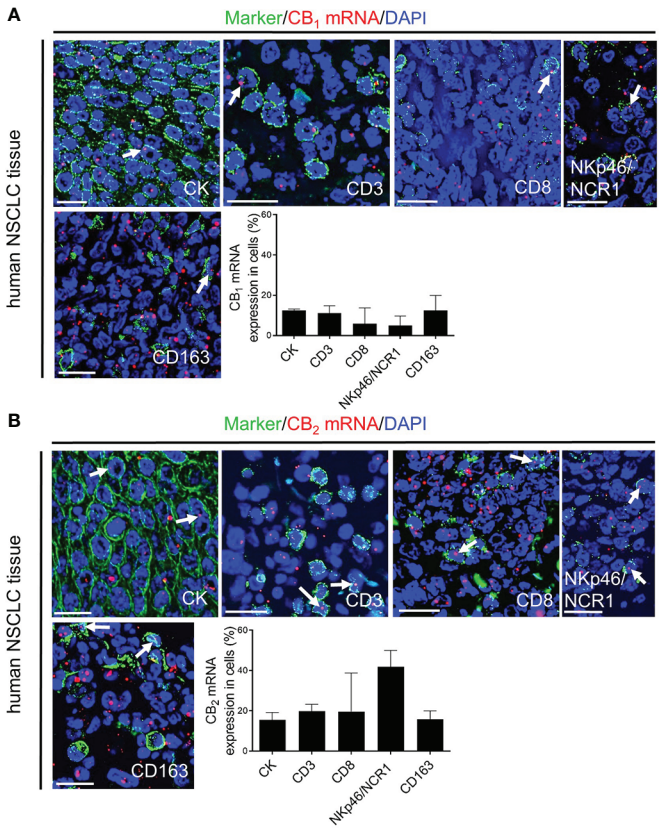

FIGURE 3
In situ hybridization (ISH)/immunofluorescence (IF) of human NSCLC tissue sections **(A, B)** Representative fluorescence microscopy images of human NSCLC tissue sections. The graphs show the percentages of co-localization of CB_1 and CB_2 mRNA signals with tumor cells (cytokeratin-stained, CK^+ cells) as well as tumor-infiltrating immune cells ($CD3^+$ T cells, $CD8^+$ T cells, $NKp46/NCR1^+$ NK cells, and $CD163^+$ M2 macrophages). Arrows indicate CB_1 and CB_2 ISH signals within tumor and immune cells of the TME. Calibration bars = 20 µm. Data indicate mean values +SD. n=3 (tumor sections from three different patients with NSCLC were used for quantification, 30-150 cells counted per section). *NSCLC*, non-small cell lung cancer; *NK*, natural killer cells; *TME*, tumor microenvironment.

observed in the $CB_2^{-/-}$ mice solely depended on CB_2, expressed in cells of the TME.

Knockout of CB_2 in cells of the TME favors an anti-carcinogenic immune cell profile and enhances $CD8^+$ T and NK cell activity

To determine the immune cell profile in tumors of $CB_2^{-/-}$ and WT mice, we used flow cytometry and identified changes in infiltration of immune cells and their subtypes, observing a significant shift of lymphoid cell populations in $CB_2^{-/-}$ as compared to WT mice (gating strategies shown in Figures S1A–C). There were no significant differences in the infiltration of $CD45^+$ leukocytes and myeloid cells between tumors of $CB_2^{-/-}$ and WT mice (Figures 5A, B, S3A). We, however, observed an increased infiltration of T cells ($CD3^+$), NK cells ($NKp46^+$), and $CD8^+$ T cells (Figures 5C, D, S3B–D), but no differences in infiltration of $CD4^+$ T and regulatory T cells (Tregs) into tumors of $CB_2^{-/-}$ mice vs. WTs (Figure 5D). Within the $CD8^+$ T cell population, the number of effector $CD8^+$ T cells increased while naïve $CD8^+$ T cells decreased (Figures 5E, S3E), indicating that $CD8^+$ T cells from $CB_2^{-/-}$, but not from WT mice, were primed to become effector cells. Percentages of infiltrating $CD8^+$ T (Figure 5F) as well as NK cells (Figure 5G) negatively correlated with tumor weight in $CB_2^{-/-}$ mice. Furthermore, no significant changes in lymphoid immune cell composition, including T, B, NK, and NKT cells were seen in the spleens and lungs of healthy $CB_2^{-/-}$ and WT mice (Figures S3F, G).

To identify underlying mechanisms of the tumor reduction in $CB_2^{-/-}$ mice, we checked for apoptosis and proliferation rates of tumor cells ($CD45^-$) and infiltrating immune cells ($CD45^+$). Flow cytometric analysis and cleaved-caspase-3/caspase-3

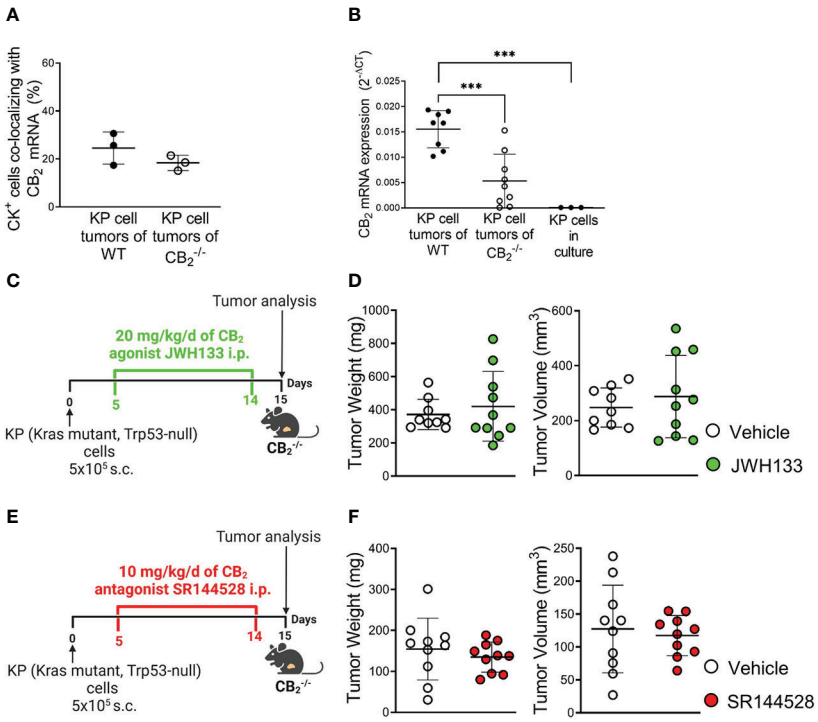

FIGURE 4
Tumor reduction exclusively relies on deletion of CB_2 in TME host cells. **(A)** The graph depicts the percentage of CB_2 mRNA positive cells co-localizing with cytokeratin-stained (CK^+) tumor cells in mouse KP cell tumors, as evaluated by ISH-IF. Data indicate mean values ± SD. n=3/group (sections from three different tumors, 75-150 cells counted per section). **(B)** Relative CB_2 mRNA expression as measured by qPCR in lysates from KP cell tumors from WT and $CB_2^{-/-}$ mice, as well as KP cells in culture. Data indicate mean values ± SD. n≥8/group; n=3 (consecutive passages of KP cells). **(C–F)** Experimental design: $CB_2^{-/-}$ mice were subcutaneously (s.c.) injected with $5x10^5$ KP (Kras mutant, Trp53-null) lung adenocarcinoma cells on day 0. For ten days, $CB_2^{-/-}$ mice were treated intraperitoneally (i.p.) with either **(C)** 20 mg/kg/d of CB_2 agonist JWH133 or **(E)** 10mg/kg/d of CB_2 antagonist SR144528 (or vehicle). Tumor weight and volume were measured at the end of the experiment *ex vivo* on day 15. One representative experiment is shown. Data indicate mean values ± SD. n≥9. Statistical differences were evaluated by using unpaired student`s *t*-test **(A, D, F)** or one-way ANOVA with Tukey's multiple comparison test **(B)**. ***p<.001. *TME*, tumor microenvironment; *ISH/IF*, *in situ* hybridization and immunofluorescence; *WT*, wild type.

immunoblotting of tumors from $CB_2^{-/-}$ and WT mice showed no significant differences in apoptosis rates (Figures S4B–D). Similarly, *in vivo* and *in vitro* cell proliferation in tumor cells and infiltrating immune cells from $CB_2^{-/-}$ mice using bromodeoxyuridine (BrdU) incorporation assay and Ki-67 immunofluorescence did not differ from WT mice (Figures S5B, C). To test whether cytotoxic immune cells were more activated in the $CB_2^{-/-}$ mice, we stimulated tumor-infiltrating $CD8^+$ T and NK cells from $CB_2^{-/-}$ and WT mice *ex vivo* with PMA/Iono and assessed the activity of these cells using flow cytometry. In comparison to WT mice, tumors of $CB_2^{-/-}$ mice showed increased expression levels of IFN-γ on $CD8^+$ T cells (Figure 6A), and CD107a on NK cells (Figures 6B, C), signifying a local activation and enhanced tumoricidal activity of $CD8^+$ T and NK cells. Therefore, a deficiency of CB_2 in the TME leads to a higher number as well as to an increased activity of cytotoxic lymphocytes in the tumor.

A CB_2 deficient TME leads to a higher expression of immune checkpoint proteins and an enhanced responsiveness to PD-1 blocking antibodies

We next aimed to identify possible immune-based therapeutic strategies that could augment tumor reduction and hypothesized that a CB_2 deficiency in the TME would have a favorable effect on immune checkpoint blockade. Thus, we first measured surface expression of different immune checkpoint proteins on immune cells. Results show that PD-1 expression was increased on tumor-infiltrating $CD8^+$ T cells, but not on NK cells in $CB_2^{-/-}$ vs. WT mice. On NK cells, only TIGIT (T cell immunoglobulin and ITIM domain) showed higher expression (Figures 6D, E, S6A). We also detected enhanced expression of

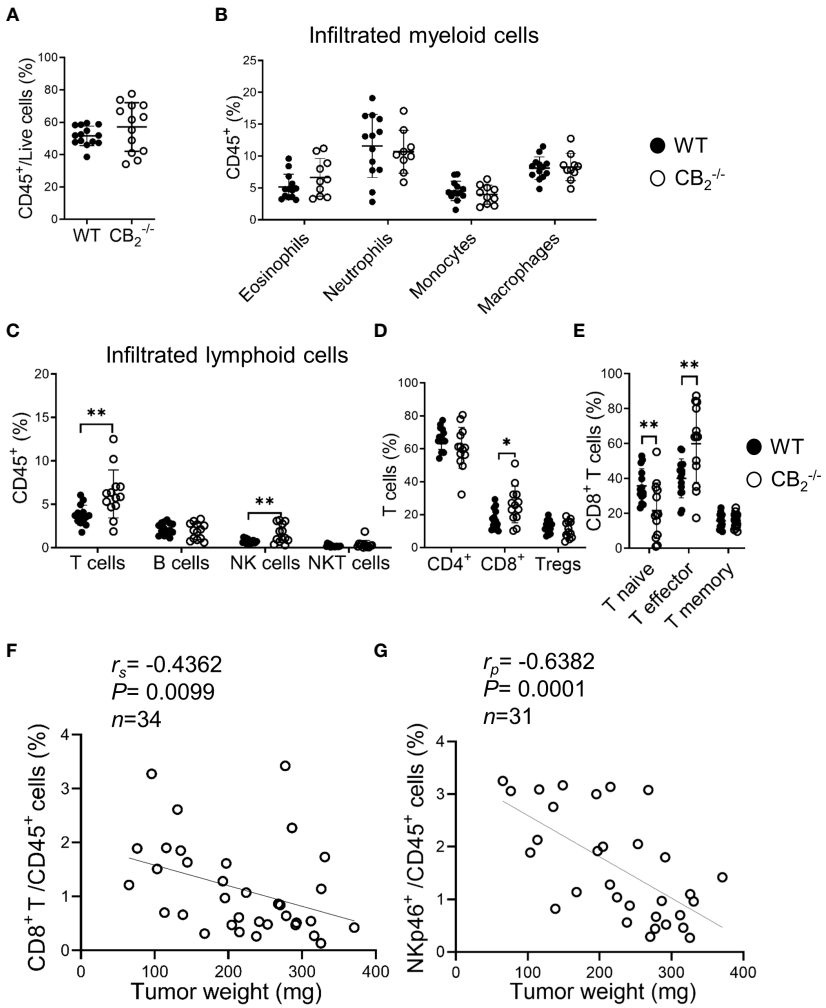

FIGURE 5
Knockout of CB_2 in cells of the TME favors an anti-carcinogenic immune cell profile. **(A–E)** Flow cytometric analysis of single cell suspensions from KP cell tumors. Data indicate mean values ± SD from two pooled independent experiments. n≥10. Detailed information on immune cell markers is provided in Figure S1. Statistical differences were evaluated by using unpaired student`s *t*-test **(A)**, multiple *t*-tests **(B–E)**. **(F, G)** The percentages of tumor-infiltrating $CD8^+$ T ($CD45^+/CD3^+/CD8^+$) and NK ($CD45^+/CD3^-/CD19^-/NKp46^+$) cells (out of $CD45^+$ cells) were plotted against tumor weights from $CB_2^{-/-}$ mice. Data were pooled from four independent experiments. n=31-34. Correlation of samples was assessed using Spearman (r_s) and Pearson (r_p) correlation coefficients after testing for normality. *p < .05; **p < .01. *NK*, natural killer cells, *NKT*, natural killer T cells; *TME*, tumor microenvironment; *Tregs*, regulatory T cells; *WT*, wild type.

PD-L1 on myeloid cells (macrophages and DCs) of $CB_2^{-/-}$ vs. WT mice (Figure 6F). Regarding the other immune checkpoint proteins, no significant differences were detected for CTLA-4 (cytotoxic T-lymphocyte antigen-4), TIM-3 (T cell immunoglobulin and mucin domain-containing protein-3), and LAG-3 (lymphocyte activation gene-3) on NK and $CD8^+$ T cells (Figures S6B–H). Dual ISH-IF revealed that approximately 40% of PD-1^+ and PD-$L1^+$ cells co-localized with CB_2 mRNA in the KP cell tumors (Figure 6G). In human lung cancer, about 20% of PD-1^+ and PD-$L1^+$ cells co-localized with CB_2 mRNA (Figure 6H).

Based on these findings, we treated $CB_2^{-/-}$ mice with anti-PD-1 to boost immune cell activity (Figure 7A). Deficiency of CB_2 on host cells augmented the responsiveness to PD-1 antibody treatment, resulting in an enhanced reduction of tumor growth in the $CB_2^{-/-}$ mice (Figures 7B, C).

Flow cytometric analysis showed that PD-1 antibody therapy potentiated an increase in the number of $CD8^+$ T and NK cells in tumors of $CB_2^{-/-}$ mice (Figures 7H–K), but not in WT (Figures 7D-G), indicating that the deletion of CB_2 in the TME favors an enhanced responsiveness to PD-1 therapy and causes a reduction in tumor burden.

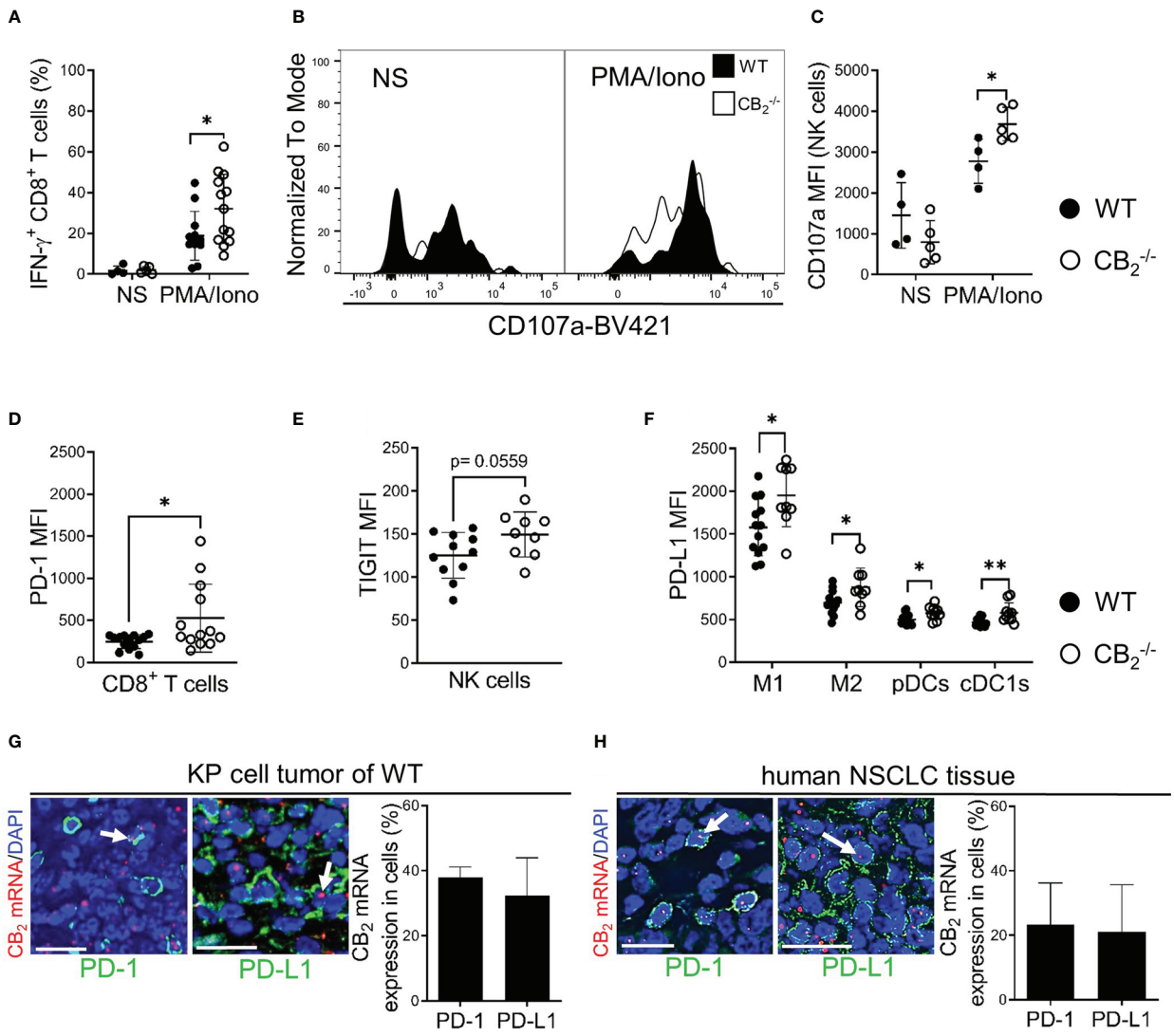

FIGURE 6
A CB_2 deficient TME stimulates activity of $CD8^+$ T and NK cells and alters expression of immune checkpoint proteins. **(A)** IFN-γ production of intratumoral $CD8^+$ T ($CD45^+/CD3^+/CD8^+$) cells prior to (non-stimulated, NS) and after *ex vivo* stimulation with phorbol myristate acetate/ionomycin (PMA/Iono). Data indicate mean values ± SD from two pooled independent experiments. n=4 (for NS); n≥11 (for PMA/Iono). **(B, C)** Degranulation capacity of tumor-infiltrated NK ($CD45^+/CD3^-/NKp46^+$) cells before (NS) and after *ex vivo* stimulation with PMA/Iono. The graph depicts MFI of CD107a on NK cells. One representative experiment is shown. Data indicate mean values ± SD. n≥4. **(D)** MFI of PD-1 on tumor-infiltrated $CD8^+$ T cells is shown. Data indicate mean values ± SD from two pooled independent experiments. n=13-14. **(E)** MFI of TIGIT on tumor-infiltrated NK cells. Data indicate mean values ± SD from two pooled independent experiments. n=13-14. **(F)** MFI of PD-L1 on tumor-infiltrated myeloid cells. Data indicate mean values ± SD from two pooled independent experiments. n=10-13. Detailed information on immune cell markers is provided in Figure S1. **(G)** ISH-IF analysis of KP cell tumors. Co-localization of PD-1/PD-L1 positively stained cells with CB_2 mRNA is shown. Data indicate mean values +SD. n=3 (sections from three different tumors, 30-150 cells counted per section). **(H)** ISH-IF staining of human NSCLC tissue sections. The graph depicts co-localization of $PD\text{-}1^+/PD\text{-}L1^+$ stained cells with CB_2 mRNA. Data indicate mean values +SD. n=3 (tumor sections from three different patients with NSCLC were used for quantification, 30-150 cells counted per section). Arrows indicate co-localization of CB_2 mRNA with cells positive for PD-1/PD-L1. Calibration bars=20 µm. Statistical differences were evaluated by using unpaired student`s *t*-test **(D, E)**, multiple *t*-tests **(A, C, F)**. *p<.05; **p<.01. *IFN-γ*, interferon-gamma; *NK*, natural killer cells; *MFI*, median fluorescence intensity; *PD-1*, programmed death-1; *TIGIT*, T cell immunoglobulin and ITIM domain; *PD-L1*, programmed death-ligand 1; *M1*, M1 macrophages; *M2*, M2 macrophages, *pDCs*, plasmacytoid dendritic cells; *cDC1*, type 1 conventional dendritic cells, *ISH-IF*, *in situ* hybridization and immunofluorescence; *WT*, wild type; *NSCLC*, non-small cell lung cancer.

10.3389/fimmu.2022.997115

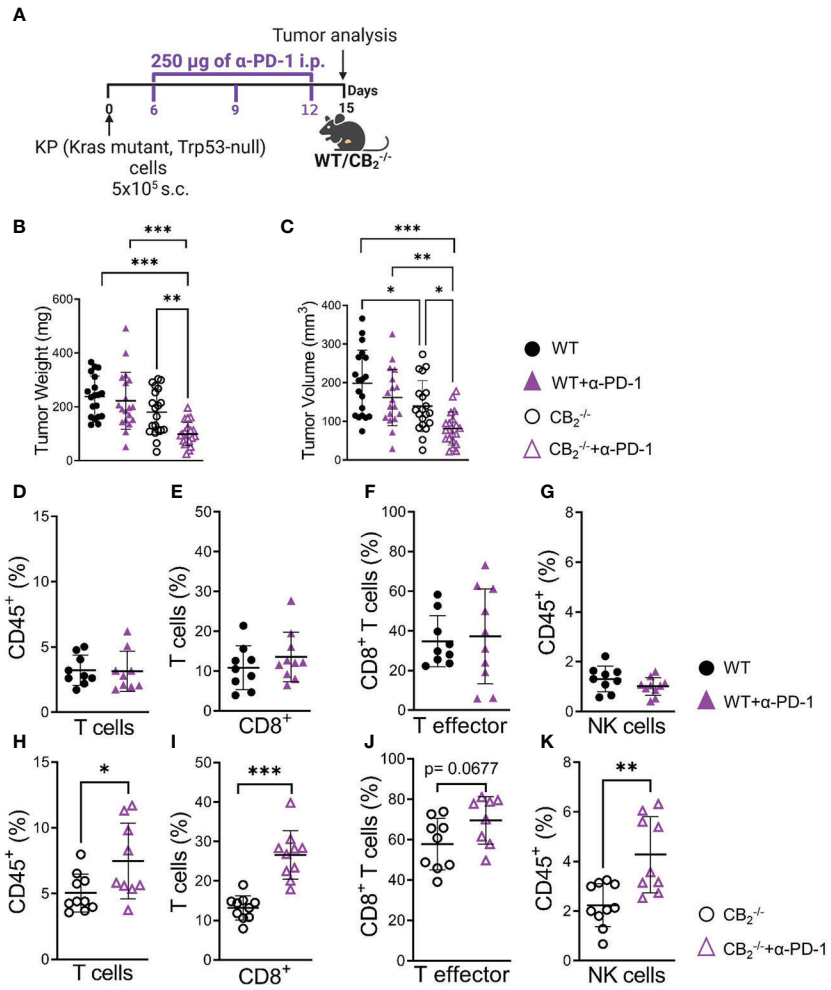

FIGURE 7
$CB_2^{-/-}$ mice are more responsive to anti-PD-1 antibody treatment than their wild type littermates. **(A)** Experimental design: $CB_2^{-/-}$ mice and WT littermates were subcutaneously (s.c.) injected with $5x10^5$ KP (Kras mutant, Trp53-null) lung adenocarcinoma cells on day 0. On days 6, 9, and 12, mice were treated with 250 µg of anti-PD-1 (α-PD-1) antibodies (or isotype control). **(B, C)** Tumor weight and volume were measured at the end of the experiment on day 15 *ex vivo*. Data indicate mean values ± SD from two pooled independent experiments. n=19-21. **(D–K)** Flow cytometric analysis was performed on single cell suspensions from KP cell tumors of $CB_2^{-/-}$ and WT α-PD-1 (or isotype control) treated mice. Detailed information on immune cell markers is provided in Figure S1. Data indicate mean values ± SD. One representative experiment is shown. n≥8. Statistical differences were evaluated by using one-way ANOVA, Tukey's multiple comparison test **(B, C)**, unpaired student`s *t*-test **(D–K)**. *p < .05; **p < .01; ***p < .001; *WT*, wild type; *NK*, natural killer cells.

Discussion

For many decades, the concept that cancer development is mainly driven by genetic mutations within tumor cells, has been studied in detail. However, cancer progression is additionally regulated by the surrounding niche, called the TME, which may deliver vital factors that promote cancer development or escape from host immune surveillance (32). A number of studies have identified the significance of immune cells of the TME in tumor development and as targets in immunotherapy. As such, cytotoxic lymphocytes like $CD8^+$ T and NK cells are important prerequisites for successful immunotherapy (33–37).

CB_1 and CB_2 are over-expressed in various types of cancer, such as skin (38), breast (39) and NSCLC (4), and they have long been implicated in cancer progression (2, 3, 11, 38, 39). However, in addition to tumor cells, CB_1 and CB_2 are expressed in immune cells that can potentially populate the TME, where they could play a pro- or anti-tumorigenic role (27). A number of studies have focused on CB receptor/ligand interactions in tumor cells and how this axis influences tumor growth *in vitro* and *in vivo* (40), including studies in lung cancer cells and models of lung cancer (3, 4, 8). In contrast, little has been described on CB receptors in immune cells of the TME and how TME-derived CB receptors shape the immune cell profile

and the response to immunotherapy. In our current study, we demonstrated that deficiency of CB_2 in the TME host cells contributes to a reduction in tumor burden in a mouse model of NSCLC (summarized in Figure 8).

CB receptors are present in tumor cells and immune cells *in situ*

Using dual ISH-IF analysis of mouse and human lung cancer sections, we revealed that tumor cells as well as tumor-infiltrating immune cells, such as $CD8^+$ T, NK cells, and macrophages express CB_2 at much higher levels than CB_1. ISH-IF showed co-localization of CB_2 mRNA in around 20-40% of immune cells, and 25% in KP tumor cells, suggesting TME cell-mediated and/or possible direct effects on tumor cells by CB_2. Pharmacological activation or inhibition of CB_2 in $CB_2^{-/-}$ mice (i.e., targeting only CB_2-expressing KP tumor cells) revealed no influence of tumor cell-derived CB_2 on tumor growth, indicating that only CB_2 expressed in TME cells was responsible for the diminished tumor growth. The conflicting findings of CB_2 in lung cancer (2–4), therefore, suggest a heterogeneous role for CB_2 in lung carcinogenesis, which most likely depends not only on CB_2 expressing tumor cells, but also on the type of TME-infiltrating immune cells expressing CB_2.

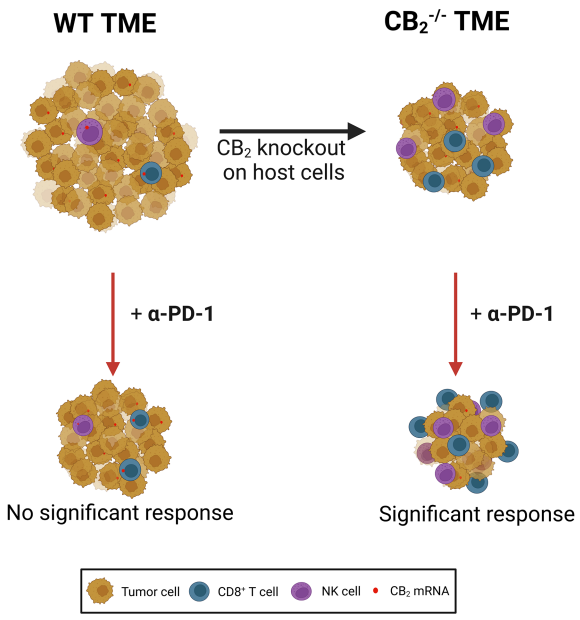

FIGURE 8
CB_2 expressed on tumor microenvironment (TME) cells creates a pro-tumorigenic microenvironment by limiting the activity of cytotoxic lymphocytes in a mouse model of NSCLC. Deletion of the gene encoding CB_2 on host cells results in a reduction of tumor growth as well as increased infiltration and local tumoricidal activity of $CD8^+$ T and natural killer (NK) cells. CB_2 knockout ($CB_2^{-/-}$) mice responded significantly better to anti-PD-1 (α-PD-1) therapy than wild type (WT) mice. α-PD-1 therapy further increased accumulation of $CD8^+$ T and NK cells in the TME of $CB_2^{-/-}$ mice. *NSCLC*, non-small cell lung cancer.

TME-derived CB_2 controls immune cell infiltrates to the tumor

Cannabinoid ligands are known to suppress phagocytosis, antigen presentation, and other features of immune cells that are essential for regulation of immune activity in the TME (16). As we detected widespread CB_2 expression in immune cells of the TME, we assessed the immune cell profile of the tumors.

Our flow cytometric analyses demonstrated that the immune cell landscape was altered in the absence of CB_2 in the TME. Although there was no shift in the myeloid cell profile, we observed a significant infiltration of cytotoxic lymphocytes, mainly of cytotoxic $CD8^+$ T and NK cells into the TME of $CB_2^{-/-}$ as compared to WT mice. We also found a negative correlation between the percentages of infiltrated $CD8^+$ T and NK cells into the TME and the tumor weights in CB_2 deficient mice, suggesting an involvement of $CD8^+$ T and NK cells in the reduction of tumor growth. A more detailed investigation of these cells revealed that tumor-infiltrating $CD8^+$ T and NK cells of $CB_2^{-/-}$ mice possessed higher cytotoxic activity (higher levels of IFN-γ and CD107a). These data are fully consistent with studies describing that an increased infiltration of the cytotoxic lymphocytes into the TME is associated with a good prognosis (41–43). Particularly in NSCLC, activity of $CD8^+$ T and NK cells may be hampered: NK cells can overexpress inhibitory receptors (44), additionally they have been shown to poorly infiltrate NSCLC tumors, and are found more frequently in normal lung than neoplastic tissues (45). Moreover, a reduced number of cytotoxic T cells along with a reduction in IFN-γ expression was observed in NSCLC patients (46, 47). Hence, CB_2 deficiency reversed the low infiltration of NK and $CD8^+$ T cells in our model and boosted their activity, likely contributing to a reduction in tumor size.

$CB_2^{-/-}$ mice are highly susceptible to PD-1 checkpoint inhibitor treatment

Immunotherapies using checkpoint inhibitors have been demonstrated to increase survival of patients in a number of cancer types, including melanoma and lung cancer (48, 49). Among all known checkpoints, the most prominent target for treatment is the PD-1/PD-L1 axis, owing to its proven efficacy in several types of cancers (48–50). Previous studies found that one of the critical requirements for ICIs to work is a sufficient infiltration of lymphocytes, including $CD8^+$ T cells, at tumor sites (33, 51). A major finding of our study is that tumor-bearing $CB_2^{-/-}$ mice responded significantly better to anti-PD-1

treatment than the WT mice (as demonstrated by the significant reduction in tumor burden). In addition, we noticed increased PD-1 expression on $CD8^+$ T cells in tumors of $CB_2^{-/-}$ mice, an indication of high T cell activity against tumor antigens as well as a possible prediction of anti-PD-1 therapy response (25, 34, 52). Our data also revealed increased PD-L1 expression on tumor-infiltrating myeloid cells in $CB_2^{-/-}$ mice, another important finding that the tumor might respond favorably to anti-PD-1 therapy (53–55). Cytotoxic $CD8^+$ T cells are often the main focus of interest in terms of improving immune checkpoint blockade therapies, but other immune cells, such as NK cells may provide an important contribution to the efficacy of checkpoint inhibitors (reviewed in (56)). Thus, the presence of intratumoral cytotoxic NK cells promotes a positive response to immunotherapies, by also targeting the PD-1/PD-L1 axis (35, 36). Recent studies found that the number of NK cells correlated with the responsiveness to anti-PD-1 treatment, and improved overall survival in melanoma and metastatic melanoma patients (37, 43). Zhang et al. identified that the presence of NK cells provided an enhanced clinical benefit of PD-L1 as well as TIGIT-based immunotherapies, as NK cells improved the functional role of $CD8^+$ T cells and/or inhibited their exhaustion (57). The TME of $CB_2^{-/-}$ mice had a significantly higher number of NK cells than WTs, and their presence, therefore, may enhance the susceptibility to immunotherapy with anti-PD-1.

To further assess susceptibility to checkpoint blockade, we determined other proteins that inhibit T and NK cells activity/proliferation, such as CTLA-4, TIM-3, TIGIT, and LAG-3 (58–62). Except for increased expression of TIGIT on NK cells, there were no significant differences between $CB_2^{-/-}$ and WT mice littermates as to the expression rates of these proteins on $CD8^+$ T and NK cells. Collectively, our data suggest that $CD8^+$ T and NK cells in $CB_2^{-/-}$ mice were in an active, non-exhausted state (high levels of IFN-γ and PD-1 on $CD8^+$ T cells, and of CD107a on NK cells).

Deficiency of CB_2 in the TME increases the PD-1 antibody-induced effect on $CD8^+$ T and NK cells

The effect of an anti-PD-1/PD-L1 therapy on the immune cell composition has often been associated with the restoration of effector $CD8^+$ T cell activity to kill tumor cells (63). Other cytotoxic lymphocytes, including NK cells, also contribute to the response to immunotherapy (reviewed in (64)): Lee et al. demonstrated increased frequency of intratumoral and peritumoral NK cells in melanoma patients who responded well to PD-1 blockade (37). Hsu et al. also identified that, in addition to T cells, NK cells can mediate the effect of anti-PD-1/PD-L1 therapy (35). In our study, the anti-PD-1 therapy further increased the number of $CD8^+$ T and NK cells at the tumor site of $CB_2^{-/-}$ as compared to WT mice. This supports the concept that a successful anti-PD-1 therapy is inherently linked to the presence of $CD8^+$ T and NK cells in the TME. It should be mentioned that PD-1 expression in tumor-infiltrating NK cells of $CB_2^{-/-}$ mice was not different from WT mice, and that PD-1 expression was lower on NK than $CD8^+$ T cells. This calls into question whether there is a direct effect of anti-PD-1 antibodies on NK cells, as the checkpoint blockade may have indirectly modulated anti-cancer NK cell functions *via* the crosstalk with other immune cell populations, as previously described (65, 66). While this manuscript was in preparation, a study was published, describing that THC and exogenous cannabinoids (approved for the treatment of chemotherapy-induced nausea) reduced the effect of anti-PD-1 therapy (67), reconfirming our own observations. Cannabis is well-known for its immunosuppressive effects (68), which is also supported by a recent observation that the use of cannabis during treatment with PD-1 checkpoint inhibitor nivolumab in cancer patients lowered their response rate (69). With our study, we highlight a possible mechanism for a lower response, which includes CB_2, $CD8^+$ T and NK cells.

Conclusion

Our results demonstrate that the CB_2 receptor in the TME of NSCLC tumors may act as an immunosuppressor that impedes $CD8^+$ T and NK cell activity, thereby promoting tumor growth. Deletion of CB_2 in the TME releases the immunosuppressive break rendering tumors to be more susceptible to PD-1 inhibitor treatment. The findings also suggest that the use of cannabis or cannabinoid-based medicine during immunotherapy may lead to a low treatment response. Altogether, the CB_2 receptor maybe an interesting adjuvant target for ICI therapy.

Materials and methods

Cancer cell lines and mice

The mouse KP cell line (a generous gift by Dr. McGarry Houghton from the Fred Hutchinson Cancer Center, Seattle, USA) was isolated from a lung adenocarcinoma, grown in a Kras mutant/Trp53-null ($Kras^{LSL\text{-}G12D}/p53^{fl/fl}$) mouse following intratracheal administration of adenoviral Cre recombinase, as described before (70). Briefly, pieces of mechanically disintegrated lung tumor were cultured in Dulbecco's Modified Eagle Medium (DMEM) supplemented with FBS (10%), penicillin (100units/mL) and streptomycin (100µg/mL). Clonal cells were derived by single-cell dilution into 96 well plates (70). Lewis lung carcinoma (LLC1) cell line was purchased from ATCC (Rockville, Maryland, USA). Both cell lines were maintained in DMEM media containing 10% fetal bovine serum (FBS, Life Technologies) and 1% penicillin/streptomycin (P/S, PAA Laboratories) and kept in a

humidified incubator (5% CO_2) at 37°C and passaged every 48 hrs. The cell lines were mycoplasma free.

All animals were bred and maintained in the animal facilities of the Medical University of Graz. Wild type C57BL/6J (B6) mice were purchased from Charles River, Germany. $CB_1^{-/-}$ mice on B6 background were obtained from Dr. Andreas Zimmer, University of Bonn, Germany. $CB_2^{-/-}$ mice (B6.129P2-Cnr2^{tm1Dgen}/J on B6 background) were obtained from Jackson Laboratories (Bar Harbor, ME, USA). Experiments were performed on 6-14-week-old mice. All procedures were granted by the Austrian Federal Ministry of Science and Research (protocol number: BMBWF-66.010/0041-V/3b/2018). Subcutaneous (s.c.) injections of KP or LLC1 cells were performed under inhaled isoflurane anaesthesia. To generate s.c. tumors, KP or LLC1 cells (5×10^5) suspended in 450 µL Dulbecco's Phosphate Buffered Saline (PBS, Gibco) were injected s.c. into the lower flanks of mice on day 0. Tumors were harvested at the experimental endpoint (day 15 for KP cell tumor model; day 21 for LLC1 lung tumor model) and were subsequently weighed, measured with a digital caliper *ex vivo*, and collected for analysis. Tumor volume was calculated based on the following formula: v = length x width x height x π/6 (71).

Pharmacology

To pharmacologically block CB_1 receptors, tumor-bearing C57BL/6J WT mice were intraperitoneally (i.p.) treated with 1 mg/kg/d SR141716 (28, 29) (CB_1 antagonist, Cayman Chemical, Ann Arbor, MI). For pharmacological activation of CB_2 receptors, tumor-bearing $CB_2^{-/-}$ mice were i.p. treated with 20 mg/kg/d JWH-133 (31) (CB_2 agonist, Axon Medchem, Groningen, NL). To pharmacologically block CB_2 receptors, tumor-bearing $CB_2^{-/-}$ mice and C57BL/6J WT mice were i.p. treated with 10 mg/kg/d SR144528 (29, 30) (CB_2 antagonist, Cayman Chemical, Ann Arbor, MI) or vehicle (ethanol). The treatment period for all mentioned interventions was ten days, starting from day 5 when the s.c. tumors were palpable, until day 14. For inhibition of PD-1, tumor-bearing $CB_2^{-/-}$ mice and WT littermates were injected i.p. with 250 µg of rat monoclonal anti-mouse PD-1 antibody (72) (clone 29F.1A12, BioXCell, Lebanon, NH) or rat IgG2a isotype control (clone 2A3, BioXCell, Lebanon, NH) on days 6, 9, and 12.

Single-cell suspensions

Single cell suspensions of dissected mouse KP cell tumors were prepared as previously described (71). Briefly, using surgical scissors, tumors were cut into small pieces, and afterwards digested with DNase I (160 U/ml; Worthington) and collagenase (4.5 U/ml; Worthington) for 20 min at 37°C, while rotating at 800-1000 rpm. The tissue was then passed through a 40 µm cell strainer, washed in staining buffer (SB, PBS +2% FBS), suspended in PBS, counted, and used for surface, intracellular and nuclear antigen staining.

Flow cytometry of dissected KP cell tumors

To exclude dead cells, single cell suspensions were initially incubated for 20 min in Fixable Viability Dye (FVD) eFluor™ 780 (eBioscience) at 4°C in the dark. Prior to staining with surface, intracellular and nuclear antibodies, single cell suspensions were incubated in 1 µg TruStain FcX™ (BioLegend, # 101320) for 10 min at 4°C. Immunostaining was performed for 30 min at 4°C (protected from light) using the pre-mixed antibody panels (Table S1). To detect FoxP3 nuclear antigen within the cells, surface stained cells were permeabilized and fixed with Transcription Factor Buffer Set (BD Biosciences, # 562574) before staining with FoxP3 antibody (Table S1). To detect expression of IFN-γ and CD107a, single-cell suspensions of the tumors (2×10^6 cells per well) were suspended in RPMI media supplemented with 10% FBS, 1% P/S, and GolgiStop (1.5 µl/ml, BD Biosciences), seeded into 96-well U-bottomed plates, and incubated for 4 hrs at 37°C (5% CO_2). During incubation time, CD107a was added, and cells were stimulated with phorbol myristate acetate (PMA) (100 ng/ml, Sigma Aldrich) and ionomycin (Iono) (1 µg/ml, Sigma Aldrich), or used unstimulated (73, 74). Afterwards, surface and intracellular stainings (BD Cytofix/Cytoperm™ Kit) were performed with the pre-mixed antibody panel (Table S1). Cells were then washed and fixed in eBioscience™ IC Fixation Buffer (ThermoFisher Scientific, # 00-8222-49) for 10 min at 4°C. Fixed cells were either acquired on a BD LSR Fortessa™ or a BD Canto™ flow cytometer connected to FACSDiva software (BD Biosciences). FlowJo software (Treestar) was used for analysis and compensation. Fluorescence minus-one-samples were used to define gates (Figures S1A-D).

RNA extraction and RT-qPCR

RNA was extracted from tissue and KP cells using Trizol (Life Technologies) and RNeasy Kit (Qiagen), respectively. Samples were treated either with a DNA-*free*™ DNA Removal Kit (Invitrogen) or RNase-Free DNase set (Qiagen). The quality and concentration of RNA were determined using a NanoDrop ND-1000 spectrophotometer (Thermo Fisher Scientific). Reverse transcription of purified RNA (1 µg) was performed by High-Capacity cDNA Reverse Transcription Kit (Applied Biosystems). Gene expression was assessed by reverse transcription-quantitative polymerase chain reaction (RT-qPCR) using SsoAdvanced Universal SYBR Green Supermix (Bio-Rad). Primers were acquired from Eurofins (Table S2) and

Bio-Rad (Table S3). Relative gene expression was calculated using $2^{-\Delta\Delta CT}$ methods (75).

In situ hybridization and immunofluorescence

Mouse and human NSCLC tissue samples

Tumors from mice were fixed in acid-free phosphate-buffered 10% formaldehyde solution (Roti®- Histofix 10%, pH 7) for 24-48 hrs at room temperature with gentle shaking. Tissue was further processed for paraffin embedding based on standard procedures. Human NSCLC tissue samples (formalin-fixed and paraffin-embedded) were acquired from the Biobank of the Medical University of Graz. Ethical approval was obtained from the Institutional Review Board of the Medical University of Graz (EK-numbers: 30-105 ex 17/18). All procedures involving clinical samples followed the ethical standards of the institutional and/or national research committee and the 1964 Helsinki Declaration and its later amendments or comparable ethical standards. All patients participated in the study gave informed consent.

ISH probes used to detect CB_1 and CB_2 mRNAs in mouse tumor and human NSCLC tissue were purchased from Advanced Cell Diagnostics (ACD, Newark, USA) (Table S4). ISH was performed using RNAscope® 2.5 HD red kit according to manufacturer's instructions. Briefly, tumor tissue sections were first treated with H_2O_2 at room temperature for 10 min and target retrieval was performed using the Brown FS3000 food steamer at 95°C for 15 min. Then, the sections were digested with protease IV in HybEZ™ II oven (ACD, Newark, USA) at 40°C for 20 min, washed in distilled water, followed by incubation with the corresponding probes at 40°C for 2 hrs and stained with Fast Red. To compare tissue samples from $CB_1^{-/-}$ or $CB_2^{-/-}$ and WT mice, sections were placed on a single slide. The specificity of the mouse CB_1 and CB_2 probes was previously verified in $CB_1^{-/-}$ and $CB_2^{-/-}$ mice (76). Immunofluorescence of tumor cells and infiltrated immune cells of the TME was conducted using primary antibodies listed in Table S5. Alexa Fluor® 488-labeled goat anti-rabbit IgG (1:500, Jackson Immuno Research, #111-546-144) and Alexa Fluor® 488-labelled bovine anti-goat IgG (H+L) (1:500, Jackson Immuno Research, # 805-545-180) were used as secondary antibodies. In parallel, sections were processed in the absence of primary antibody as a negative control. Then, sections were mounted with Vectashield® (containing DAPI) (Vector Laboratories) and images were taken using an Olympus IX73 fluorescence microscope (Olympus) connected with a Hamamatsu ORCA-ER digital camera (Hamamatsu Photonics K.K., Japan). Images were processed with an Olympus CellSens® 1.17 imaging software containing a deconvolution program (Olympus). ImageJ software was used to quantify expression and co-localization with the corresponding probes.

Statistical analysis

Data are presented as means ± standard deviation (SD) or standard error of means (SEM) and analyzed using Prism v.9.3.1 (GraphPad Software, La Jolla, CA, USA). Differences between experimental groups were assessed by unpaired student's t-tests, multiple t-tests or two-way analysis of variance (ANOVA) with the indicated *post hoc* test for corrections of multiple comparisons, whereas for multiple comparisons with three or more experimental groups, a one-way ANOVA was applied with the indicated *post hoc* test for corrections of multiple comparisons. Shapiro-Wilk and Kolmogorov-Smirnov tests were used to test a normal distribution. Correlations between tumor weight and infiltration of $CD8^+$ T and NK cells in the TME was determined using Pearson's correlation coefficient (r_p) and Spearman's correlation coefficient *rho* (r_s).

In all cases, a p-value <0.05 was considered significant and represented with one, two or three asterisks when lower than 0.05, 0.01, or 0.001, respectively.

Data availability statement

The original contributions presented in the study are included in the article/Supplementary Material. Further inquiries can be directed to the corresponding author.

Ethics statement

The studies involving human participants were reviewed and approved by the Ethics Committee of the Medical University of Graz. The patients/participants provided their written informed consent to participate in this study. The animal study was reviewed and approved by the Austrian Federal Ministry of Education, Science and Research.

Author contributions

ArS, MK, JK, CH and RS contributed to the conception and design of the study. ArS, MK, EG, DR, CH, KM, AnS and PVC performed experiments and acquired data. ArS, MK, EG, JK and RS contributed to the analysis and interpretation of the data. ArS and RS participated in the writing of the manuscript. LB and JL

provided the human lung cancer samples. All authors contributed to the article and approved the submitted version.

Funding

Ph.D. candidate ArS received funding from the Medical University of Graz (PhD program: *Molecular Medicine*). Work in the lab of JK is funded by the Austrian Science Fund (FWF grant P-35294-B). RS is funded by the Austrian Science Fund (FWF; grants P33325 and KLI887).

Acknowledgments

PhD candidates AnS, DR and PVC were trained within the frame of the PhD programs *Molecular Medicine* and *DK-MOLIN* of the Medical University of Graz and the Austrian Science Fund. We are grateful to Veronika Pommer and Sabine Kern for their excellent technical assistance; we thank Sabine Donner for animal care and Marah Runtsch for carefully reading the manuscript. Experimental design diagrams and the overview of the study were created with BioRender.com.

Conflict of interest

The authors declare that the research was conducted in the absence of any commercial or financial relationships that could be construed as a potential conflict of interest.

Publisher's note

Supplementary material

The Supplementary Material for this article can be found online at: https://www.frontiersin.org/articles/10.3389/fimmu.2022.997115/full#supplementary-material

References

1. Fraguas-Sánchez AI, Martín-Sabroso C, Torres-Suárez AI. Insights into the effects of the endocannabinoid system in cancer: A review. *Br J Pharmacol* (2018) 175:2566–80. doi: 10.1111/bph.14331

2. Milian L, Mata M, Alcacer J, Oliver M, Sancho-Tello M, de Llano JJM, et al. Cannabinoid receptor expression in non-small cell lung cancer. effectiveness of tetrahydrocannabinol and cannabidiol inhibiting cell proliferation and epithelial-mesenchymal transition *in vitro*. *PLoS One* (2020) 15:e0228909. doi: 10.1371/journal.pone.0228909

3. Xu S, Ma H, Bo Y, Shao M. The oncogenic role of CB2 in the progression of non-small-cell lung cancer. *BioMed Pharmacother* (2019) 117:109080. doi: 10.1016/j.biopha.2019.109080

4. Preet A, Qamri Z, Nasser MW, Prasad A, Shilo K, Zou X, et al. Cannabinoid receptors, CB1 and CB2, as novel targets for inhibition of non-small cell lung cancer growth and metastasis. *Cancer Prev Res* (2011) 4:65–75. doi: 10.1158/1940-6207.CAPR-10-0181

5. Boyacıoğlu Ö, Bilgiç E, Varan C, Bilensoy E, Nemutlu E, Sevim D, et al. ACPA decreases non-small cell lung cancer line growth through Akt/PI3K and JNK pathways *in vitro*. *Cell Death Dis* (2021) 12:56. doi: 10.1038/s41419-020-03274-3

6. Vidinský B, Gál P, Pilátová M, Vidová Z, Solár P, Varinská L, et al. Anti-proliferative and anti-angiogenic effects of CB2 r agonist (JWH-133) in non-small lung cancer cells (A549) and human umbilical vein endothelial cells: an in vitro investigation. *CzechRepublic Folia Biol* (2012) 58:75–80.

7. Preet A, Ganju RK, Groopman JE. Δ9-tetrahydrocannabinol inhibits epithelial growth factor-induced lung cancer cell migration *in vitro* as well as its growth and metastasis *in vivo*. *Oncogene* (2008) 27:339–46. doi: 10.1038/sj.onc.1210641

8. Ravi J, Elbaz M, Wani NA, Nasser MW, Ganju RK. Cannabinoid receptor-2 agonist inhibits macrophage induced EMT in non-small cell lung cancer by downregulation of EGFR pathway. *Mol Carcinog* (2016) 55:2063–76. doi: 10.1002/mc.22451

9. Hart S, Fischer OM, Ullrich A. Cannabinoids induce cancer cell proliferation *via* tumor necrosis factor α-converting enzyme (TACE/ADAM17)-mediated transactivation of the epidermal growth factor receptor. *Cancer Res* (2004) 64:1943–50. doi: 10.1158/0008-5472.CAN-03-3720

10. Zhu LX, Sharma S, Stolina M, Gardner B, Roth MD, Tashkin DP, et al. Δ-9-Tetrahydrocannabinol inhibits antitumor immunity by a CB2 receptor-mediated, cytokine-dependent pathway. *J Immunol* (2000) 165:373–80. doi: 10.4049/jimmunol.165.1.373

11. Pyszniak M, Tabarkiewicz J, Łuszczki JJ. Endocannabinoid system as a regulator of tumor cell malignancy – biological pathways and clinical significance. *Onco Targets Ther* (2016) 9:4323–36. doi: 10.2147/OTT.S106944

12. Cristino L, Bisogno T, Di Marzo V. Cannabinoids and the expanded endocannabinoid system in neurological disorders. *Nat Rev Neurol* (2020) 16:9–29. doi: 10.1038/s41582-019-0284-z

13. Lu HC, Mackie K. Review of the endocannabinoid system. *Biol Psychiatry Cognit Neurosci Neuroimaging* (2021) 6:607–15. doi: 10.1016/j.bpsc.2020.07.016

14. Tsou K, Brown S, Sañudo-Peña MC, K Mackie JW. Immunohistochemical distribution of cannabinoid CB1 receptors in the rat central nervous system. *Neuroscience* (1998) 83:393–411. doi: 10.1016/s0306-4522(97)00436-3

15. Basu S, Dittel BN. Unraveling the complexities of cannabinoid receptor 2 (CB2) immune regulation in health and disease. *Immunol Res* (2011) 51:26–38. doi: 10.1007/s12026-011-8210-5

16. Kienzl M, Kargl J, Schicho R. The immune endocannabinoid system of the tumor microenvironment. *Int J Mol Sci* (2020) 21:1–25. doi: 10.3390/ijms21238929

17. Kaplan BLF. The role of CB1 in immune modulation by cannabinoids. *Pharmacol Ther* (2013) 137:365–74. doi: 10.1016/j.pharmthera.2012.12.004

18. Klein TW, Newton C, Friedman H. Cannabinoid receptors and immunity. *Immunol Today* (1998) 19:373–81. doi: 10.1016/S0167-5699(98)01300-0

19. Eisenstein TK, Meissler JJ. Effects of cannabinoids on T-cell function and resistance to infection. *J Neuroimmune Pharmacol* (2015) 10:204–16. doi: 10.1007/s11481-015-9603-3

20. Eisenstein TK, Meissler JJ, Wilson Q, Gaughan JP, Adler MW. Anandamide and Δ9-tetrahydrocannabinol directly inhibit cells of the immune system *via* CB2 receptors. *J Neuroimmunol* (2007) 189:17–22. doi: 10.1016/j.jneuroim.2007.06.001

21. Cencioni MT, Chiurchiù V, Catanzaro G, Borsellino G, Bernardi G, Battistini L, et al. Anandamide suppresses proliferation and cytokine release from primary human T-lymphocytes mainly *via* CB2 receptors. *PloS One* (2010) 5:e8688. doi: 10.1371/journal.pone.0008688

22. Montecucco F, Burger F, Mach F, Steffens S. CB2 cannabinoid receptor agonist JWH-015 modulates human monocyte migration through defined intracellular signaling pathways. *Am J Physiol Hear Circ Physiol* (2008) 294: H1145–55. doi: 10.1152/ajpheart.01328.2007

23. Massi P, Fuzio D, Vigano D, Sacerdote P, Parolaro D. Relative involvement of cannabinoid CB and CB receptors in the Δ9-tetrahydrocannabinol-induced inhibition of natural killer activity. *Eur J Pharmacol* (2000) 387:343–7. doi: 10.1016/S0014-2999(99)00860-2

24. Braile M, Marcella S, Marone G, Galdiero MR, Varricchi G, Loffredo S. The interplay between the immune and the endocannabinoid systems in cancer. *Cells* (2021) 10:1282. doi: 10.3390/cells10061282

25. Simon S, Labarriere N. PD-1 expression on tumor-specific T cells: Friend or foe for immunotherapy? *Oncoimmunology* (2018) 7:e1364828. doi: 10.1080/2162402X.2017.1364828

26. Błach J, Wojas-Krawczyk K, Nicoś M, Krawczyk P. Failure of immunotherapy–the molecular and immunological origin of immunotherapy resistance in lung cancer. *Int J Mol Sci* (2021) 22:9030. doi: 10.3390/ijms22169030

27. Kienzl M, Hasenoehrl C, Maitz K, Sarsembayeva A, Taschler U, Valadez-Cosmes P, et al. Monoacylglycerol lipase deficiency in the tumor microenvironment slows tumor growth in non-small cell lung cancer. *Oncoimmunology* (2021) 10:e1965319. doi: 10.1080/2162402X.2021.1965319

28. Rinaldi-Carmona M, Barth F, Hkaulme M, Shireb D, Calandrab B, Congy C, et al. SR1417 16A, a potent and selective antagonist of the brain cannabinoid receptor. *FEBS Lett* (1994) 350:240–4. doi: 10.1016/0014-5793(94)00773-x

29. Di Marzo V. Targeting the endocannabinoid system: To enhance or reduce? *Nat Rev Drug Discovery* (2008) 7:438–55. doi: 10.1038/nrd2553

30. Rinaldi-Carmona M, Barth F, Millan J, Derocq J-M, Casellas P, Congy C, et al. SR144528, the first potent and selective antagonist of the CB2 cannabinoid receptor. *J Pharmacol Exp Ther* (1998) 284:644–50.

31. Storr MA, Keenan CM, Zhang H, Patel KD, Makriyannis A, Sharkey KA. Activation of the cannabinoid 2 receptor (CB2) protects against experimental colitis. *Inflamm Bowel Dis* (2009) 15:1678–85. doi: 10.1002/ibd.20960

32. Hanahan D. Hallmarks of cancer: New dimensions. *Cancer Discov* (2022) 12:31–46. doi: 10.1158/2159-8290.CD-21-1059

33. Farhood B, Najafi M, Mortezaee K. CD8+ cytotoxic T lymphocytes in cancer immunotherapy: A review. *J Cell Physiol* (2019) 234:8509–21. doi: 10.1002/jcp.27782

34. Thommen DS, Koelzer VH, Herzig P, Roller A, Trefny M, Dimeloe S, et al. A transcriptionally and functionally distinct PD-1+ CD8+ T cell pool with predictive potential in non-small-cell lung cancer treated with PD-1 blockade. *Nat Med* (2018) 24:994–1004. doi: 10.1038/s41591-018-0057-z

35. Hsu J, Hodgins JJ, Marathe M, Nicolai CJ, Bourgeois-Daigneault MC, Trevino TN, et al. Contribution of NK cells to immunotherapy mediated by PD-1/PD-L1 blockade. *J Clin Invest* (2018) 128:4654–68. doi: 10.1172/JCI99317

36. Dong W, Wu X, Ma S, Wang Y, Nalin AP, Zhu Z, et al. The mechanism of anti–PD-L1 antibody efficacy against PD-L1–negative tumors identifies NK cells expressing PD-L1 as a cytolytic effector. *Cancer Discov* (2019) 9:1422–37. doi: 10.1158/2159-8290.CD-18-1259

37. Lee H, Quek C, Silva I, Tasker A, Batten M, Rizos H, et al. Integrated molecular and immunophenotypic analysis of NK cells in anti-PD-1 treated metastatic melanoma patients. *Oncoimmunology* (2019) 8:e1537581. doi: 10.1080/2162402X.2018.1537581

38. Llanos Casanova M, Blázquez C, Martínez-Palacio J, Villanueva C, Fernández-Aceñero MJ, Huffman JW, et al. Inhibition of skin tumor growth and angiogenesis *in vivo* by activation of cannabinoid receptors. *J Clin Invest* (2003) 111:43–50. doi: 10.1172/JCI200316116

39. Caffarel MM, Sarrió D, Palacios J, Guzmán M, Sánchez C. Δ9-tetrahydrocannabinol inhibits cell cycle progression in human breast cancer cells through Cdc2 regulation. *Cancer Res* (2006) 66:6615–21. doi: 10.1158/0008-5472.CAN-05-4566

40. Laezza C, Pagano C, Navarra G, Pastorino O, Proto MC, Fiore D, et al. The endocannabinoid system: A target for cancer treatment. *Int J Mol Sci* (2020) 21:747. doi: 10.3390/ijms21030747

41. Martínez-Lostao L, Anel A, Pardo J. How do cytotoxic lymphocytes kill cancer cells? *Clin Cancer Res* (2015) 21:5047–56. doi: 10.1158/1078-0432.CCR-15-0685

42. Takanami I, Takeuchi K, Giga M. The prognostic value of natural killer cell infiltration in resected pulmonary adenocarcinoma. *J Thorac Cardiovasc Surg* (2001) 121:1058–63. doi: 10.1067/mtc.2001.113026

43. Barry KC, Hsu J, Broz ML, Cueto FJ, Binnewies M, Combes AJ, et al. A natural killer–dendritic cell axis defines checkpoint therapy–responsive tumor microenvironments. *Nat Med* (2018) 24:1178–91. doi: 10.1038/s41591-018-0085-8

44. Jin S, Deng Y, Hao JW, Li Y, Liu B, Yu Y, et al. NK cell phenotypic modulation in lung cancer environment. *PloS One* (2014) 9:e109976. doi: 10.1371/journal.pone.0109976

45. Stankovic B, Bjørhovde HAK, Skarshaug R, Aamodt H, Frafjord A, Müller E, et al. Immune cell composition in human non-small cell lung cancer. *Front Immunol* (2019) 9:3101. doi: 10.3389/fimmu.2018.03101

46. Prado-Garcia H, Romero-Garcia S, Aguilar-Cazares D, Meneses-Flores M, Lopez-Gonzalez JS. Tumor-induced CD8+ T-cell dysfunction in lung cancer patients. *Clin Dev Immunol* (2012) 2012:741741. doi: 10.1155/2012/741741

47. Sheng SY, Gu Y, Lu CG, Zou JY, Hong H, Wang RF. The distribution and function of human memory T cell subsets in lung cancer. *Immunol Res* (2017) 65:639–50. doi: 10.1007/s12026-016-8882-y

48. Amaria RN, Reddy SM, Tawbi HA, Davies MA, Ross MI, Glitza IC, et al. Neoadjuvant immune checkpoint blockade in high-risk resectable melanoma. *Nat Med* (2018) 24:1649–54. doi: 10.1038/s41591-018-0197-1

49. Suresh K, Naidoo J, Lin CT, Danoff S. Immune checkpoint immunotherapy for non-small cell lung cancer: Benefits and pulmonary toxicities. *Chest* (2018) 154:1416–23. doi: 10.1016/j.chest.2018.08.1048

50. Sun C, Mezzadra R, Schumacher TN. Regulation and function of the PD-L1 checkpoint. *Immunity* (2018) 48:434–52. doi: 10.1016/j.immuni.2018.03.014

51. Leclerc M, Voilin E, Gros G, Corgnac S, de Montpréville V, Validire P, et al. Regulation of antitumour CD8 T-cell immunity and checkpoint blockade immunotherapy by neuropilin-1. *Nat Commun* (2019) 10:3345. doi: 10.1038/s41467-019-11280-z

52. Legat A, Speiser DE, Pircher H, Zehn D, Fuertes Marraco SA. Inhibitory receptor expression depends more dominantly on differentiation and activation than "exhaustion" of human CD8 T cells. *Front Immunol* (2013) 4:455. doi: 10.3389/fimmu.2013.00455

53. Topalian SL, Hodi FS, Brahmer JR, Gettinger SN, Smith DC, McDermott DF, et al. Safety, activity, and immune correlates of anti–PD-1 antibody in cancer. *N Engl J Med* (2012) 366:2443–54. doi: 10.1056/nejmoa1200690

54. Herbst RS, Soria JC, Kowanetz M, Fine GD, Hamid O, Gordon MS, et al. Predictive correlates of response to the anti-PD-L1 antibody MPDL3280A in cancer patients. *Nature* (2014) 515:563–7. doi: 10.1038/nature14011

55. Taube JM, Klein A, Brahmer JR, Xu H, Pan X, Kim JH, et al. Association of PD-1, PD-1 ligands, and other features of the tumor immune microenvironment with response to anti-PD-1 therapy. *Clin Cancer Res* (2014) 20:5064–74. doi: 10.1158/1078-0432.CCR-13-3271

56. Shaver KA, Croom-Perez TJ, Copik AJ. Natural killer cells: The linchpin for successful cancer immunotherapy. *Front Immunol* (2021) 12:679117. doi: 10.3389/fimmu.2021.679117

57. Zhang Q, Bi J, Zheng X, Chen Y, Wang H, Wu W, et al. Blockade of the checkpoint receptor TIGIT prevents NK cell exhaustion and elicits potent anti-tumor immunity. *Nat Immunol* (2018) 19:723–32. doi: 10.1038/s41590-018-0132-0

58. Pansy K, Uhl B, Krstic J, Szmyra M, Fechter K, Santiso A, et al. Immune regulatory processes of the tumor microenvironment under malignant conditions. *Int J Mol Sci* (2021) 22:13311. doi: 10.3390/ijms222413311

59. Marin-Acevedo JA, Dholaria B, Soyano AE, Knutson KL, Chumsri S, Lou Y. Next generation of immune checkpoint therapy in cancer: New developments and challenges. *J Hematol Oncol* (2018) 11:39. doi: 10.1186/s13045-018-0582-8

60. Chauvin JM, Pagliano O, Fourcade J, Sun Z, Wang H, Sander C, et al. TIGIT and PD-1 impair tumor antigen-specific CD8+ T cells in melanoma patients. *J Clin Invest* (2015) 125:2046–58. doi: 10.1172/JCI80445

61. Lanitis E, Dangaj D, Irving M, Coukos G. Mechanisms regulating T-cell infiltration and activity in solid tumors. *Ann Oncol* (2017) 28:xii18–32. doi: 10.1093/annonc/mdx238

62. Harjunpää H, Guillerey C. TIGIT as an emerging immune checkpoint. *Clin Exp Immunol* (2020) 200:108–19. doi: 10.1111/cei.13407

63. Huang AC, Postow MA, Orlowski RJ, Mick R, Bengsch B, Manne S, et al. T-Cell invigoration to tumour burden ratio associated with anti-PD-1 response. *Nature* (2017) 545:60–5. doi: 10.1038/nature22079

64. Pesce S, Greppi M, Grossi F, Del Zotto G, Moretta L, Sivori S, et al. PD/1-PD-Ls checkpoint: Insight on the potential role of NK cells. *Front Immunol* (2019) 10:1242. doi: 10.3389/fimmu.2019.01242

65. Alvarez M, Simonetta F, Baker J, Morrison AR, Wenokur AS, Pierini A, et al. Indirect impact of PD-1/PD-L1 blockade on a murine model of NK cell exhaustion. *Front Immunol* (2020) 11:7. doi: 10.3389/fimmu.2020.00007

66. Oyer JL, Gitto SB, Altomare DA, Copik AJ. PD-L1 blockade enhances anti-tumor efficacy of NK cells. *Oncoimmunology* (2018) 7:e1509819. doi: 10.1080/2162402X.2018.1509819

67. Xiong X, Chen S, Shen J, You H, Yang H, Yan C, et al. Cannabis suppresses antitumor immunity by inhibiting JAK/STAT signaling in T cells through CNR2. *Signal Transduct Target Ther* (2022) 7:99. doi: 10.1038/s41392-022-00918-y

68. Danial Yahyal M, Watson RR. Immunomodulation by morphine and marijuana. *Life Sci* (1987) 41:2503–10. doi: 10.1016/0024-3205(87)90434-6

69. Taha T, Meiri D, Talhamy S, Wollner M, Peer A, Bar-Sela G. Cannabis impacts tumor response rate to nivolumab in patients with advanced malignancies. *Oncologist* (2019) 24:549–54. doi: 10.1634/theoncologist.2018-0383

70. Mathsyaraja H, Catchpole J, Freie B, Eastwood E, Babaeva E, Geuenich M, et al. Loss of MGA repression mediated by an atypical polycomb complex promotes tumor progression and invasiveness. *Elife* (2021) 10:e64212. doi: 10.7554/eLife.64212

71. Kienzl M, Hasenoehrl C, Valadez-Cosmes P, Maitz K, Sarsembayeva A, Sturm E, et al. IL-33 reduces tumor growth in models of colorectal cancer with the help of eosinophils. *Oncoimmunology* (2020) 9:1–12. doi: 10.1080/2162402X.2020.1776059

72. Strauss L, Mahmoud MAA, Weaver JD, Tijaro-Ovalle NM, Christofides A, Wang Q, et al. Targeted deletion of PD-1 in myeloid cells induces antitumor immunity. *Sci Immunol* (2020) 5:1–27. doi: 10.1126/sciimmunol.aay1863

73. Lucarini V, Zicchedda G, Macchia I, La Sorsa V, Peschiaroli F, Buccione C, et al. IL-33 restricts tumor growth and inhibits pulmonary metastasis in melanoma-bearing mice through eosinophils. *Oncoimmunology* (2017) 6:e1317420. doi: 10.1080/2162402X.2017.1317420

74. Alter G, Malenfant JM, Altfeld M. CD107a as a functional marker for the identification of natural killer cell activity. *J Immunol Methods* (2004) 294:15–22. doi: 10.1016/j.jim.2004.08.008

75. Pfaffl MW. A new mathematical model for relative quantification in real-time RT-PCR. *Nucleic Acids Res* (2001) 29:e45. doi: 10.1093/nar/29.9.e45

76. Grill M, Hasenoehrl C, Kienzl M, Kargl J, Schicho R. Cellular localization and regulation of receptors and enzymes of the endocannabinoid system in intestinal and systemic inflammation. *Histochem Cell Biol* (2019) 151:5–20. doi: 10.1007/s00418-018-1719-0

Glossary

ANOVA	Analysis of variance
ATR	Ataxia telangiectasia and Rad3-related
BrdU	Bromodeoxyuridine
CB	Cannabinoid
$CB_1^{-/-}$	CB_1 knockout
$CB_2^{-/-}$	CB_2 knockout
cDC1	Type 1 conventional dendritic cells
CK	Cytokeratin
CTLA-4	Cytotoxic T-lymphocyte antigen-4
DC	Dendritic cell
DMEM	Dulbecco's Modified Eagle Medium
ECS	Endocannabinoid system
EGF	Epidermal growth factor
EPCAM	Epithelial cell adhesion molecule
FBS	Fetal bovine serum
FVD	Fixable Viability Dye
i.p.	Intraperitoneal
ICI	Immune checkpoint inhibitor
IFN-γ	Interferon-gamma
IL-10	Interleukin-10
IL-2	Interleukin-2
ISH-IF	In situ hybridization and immunofluorescence
LAG-3	Lymphocyte activation gene-3
LLC1	Lewis lung carcinoma
M1	M1 macrophages
M2	M2 macrophages
MEK	Mitogen-activated protein kinase kinase
MFI	Median fluorescence intensity
NK	Natural killer cells
NKT	Natural killer T cells
NS	Non-stimulated
NSCLC	Non-small cell lung cancer
P/S	Penicillin/streptomycin
PBS	Phosphate Buffered Saline
PD-1	Programmed death-1
pDC	Plasmacytoid dendritic cells
PD-L1	Programmed death-ligand 1
PMA/Iono	Phorbol myristate acetate/Ionomycin
PVDF	Polyvinylidene difluoride
RBC	Red blood cell
RT-qPCR	Reverse transcription-quantitative polymerase chain reaction
s.c.	Subcutaneous
SB	Staining buffer
SD	Standard deviation
SEM	Standard error of mean
TBST	Tris-buffered saline with 0.1% Tween® 20 Detergent
TGF	Transforming growth factor
Th_1	T helper 1
Th_2	T helper 2
THC	Tetrahydrocannabinol
TIGIT	T cell immunoglobulin and ITIM domain
TIM-3	T cell immunoglobulin and mucin domain-containing protein-3
TME	Tumor microenvironment
TNF-α	Tumor necrosis factor-alpha
Tregs	Regulatory T
WB	Western blotting
WT	Wild type

frontiers | Frontiers in Immunology

TYPE Original Research
PUBLISHED 18 January 2023
DOI 10.3389/fimmu.2023.1078705

OPEN ACCESS

EDITED BY
Gulderen Yanikkaya Demirel,
Yeditepe University, Turkey

REVIEWED BY
Mario Leonardo Squadrito,
Vita-Salute San Raffaele University, Italy
Chiara Bresesti,
San Raffaele Telethon Institute for Gene Therapy, Italy, in collaboration with reviewer MS
Ferdinando Pucci,
Oregon Health and Science University, United States

*CORRESPONDENCE
Xiaojiang Zhou
yfyzxj1970@163.com
Yong Xie
xieyong_tfahoncu@163.com

SPECIALTY SECTION
This article was submitted to Cancer Immunity and Immunotherapy, a section of the journal Frontiers in Immunology

RECEIVED 24 October 2022
ACCEPTED 03 January 2023
PUBLISHED 18 January 2023

CITATION
Zhou F, Liu Y, Liu C, Wang F, Peng J, Xie Y and Zhou X (2023) Knowledge landscape of tumor-associated macrophage research: A bibliometric and visual analysis.
Front. Immunol. 14:1078705.
doi: 10.3389/fimmu.2023.1078705

Knowledge landscape of tumor-associated macrophage research: A bibliometric and visual analysis

Feng Zhou[1,2,3,4], Yang Liu[1,2,3,4], Cong Liu[1,2,3,4], Fangfei Wang[1,2,3,4], Jianxiang Peng[1,2,3,4], Yong Xie[1,2,3,4]* and Xiaojiang Zhou[1,2,3,4]*

[1]Department of Gastroenterology, Digestive Disease Hospital, The First Affiliated Hospital of Nanchang University, Nanchang, Jiangxi, China, [2]Department of Gastroenterology, Gastroenterology Institute of Jiangxi Province, Nanchang, Jiangxi, China, [3]Key Laboratory of Digestive Diseases of Jiangxi Province, The First Affiliated Hospital of Nanchang University, Nanchang, Jiangxi, China, [4]Department of Gastroenterology, Jiangxi Clinical Research Center for Gastroenterology, Nanchang, Jiangxi, China

Background and aims: Tumor-associated macrophage (TAM) is a highly abundant immune population in tumor microenvironment, which plays an important role in tumor growth and progression. The aim of our study was to explore the development trends and research hotspots of TAM by bibliometric method.

Methods: The publications related to TAM were obtained from the Web of Science Core Collection database. Bibliometric analysis and visualization were conducted using VOSviewer, CiteSpace and R software.

Results: A total of 6,405 articles published between 2001 and 2021 were included. The United States and China received the most citations, whereas the University of Milan, the university of California San Francisco and Sun Yat-sen University were the main research institutions. Mantovani, Alberto from Humanitas University was the most productive authors with the most citations. Cancer Research published the most articles and received the most co-citations. Activation, angiogenesis, breast cancer, NF-κB and endothelial growth factor were important keywords in TAM research. Among them, PD-1/L1, nanoparticle, PI3Kγ, resistance and immune microenvironment have become the focus of attention in more recent research.

Conclusions: The research on TAM is rapidly evolving with active cooperation worldwide. Anticancer therapy targeting TAM is emerging and promising area of future research, especially in translational application. This may provide guidance and new insights for further research in the field of TAM.

KEYWORDS

tumor-associated macrophage, cancer, bibliometrics, visualization, hotspots

Introduction

Macrophages has long been considered to be an evolutionarily ancient cell type involved in tissue homeostasis and immune defense. Recently, macrophages were discovered to regulate a variety of diseases depending on the surrounding tissue microenvironment, especially for cancer (1–3). Tumor-associated macrophage (TAM) is a highly abundant immune population in tumors, which plays an important role in cancer progression, metastasis and treatment resistance.

The ability of macrophages to adapt to subtle changes in external stimuli results in the diversity of TAM between different types of cancer or within the same tumor. Macrophages are generally divided into classically activated M1 phenotypes and alternately activated M2 phenotypes to reflect the Th1/Th2 immune response. Although TAM often shows more similar patterns to M2- polarized macrophages that suppresses immune responses and promotes tumor progression, the simplified M1/M2 definition might not be sufficient to cover the full complexity of TAMs (4). In fact, TAM rarely completely follow the true M1 and M2 phenotypes, and even some macrophages can share both M1 and M2 signatures (5–7). In addition, the cell subsets do not exist at a steady stage and changes as the tumor progresses. Each population has a unique landscape based on the type, stage and immune composition of the infiltrated tumors. The plasticity and heterogeneity allow TAM to promote or suppress tumor growth and progression through multiple pathways. Therefore, there is great significance to quantitatively evaluate the research status, focus area and development trend of TAM.

Bibliometrics is an interdisciplinary science that provides a comprehensive and objective assessment of knowledge carriers by mathematics and statistics (8–10). The bibliographic analysis helps scholars understand the development of specific topic and reveals the evolution trend of this field. This study aimed to explore the landscape of tumor-associated macrophages, hoping to provide new clues and ideas for future research in the field of TAM.

Methods

Search strategies

Scientific output data was extracted from the Web of Science Core Collection (WoSCC) database, which is one of the most widely used source for academic and bibliometric analysis. The search formula was presented as follows: TS = ("tumor associated macrophage*") OR ("tumor-associated macrophage*") OR ("tumour associated macrophage*") OR ("tumour-associated macrophage*") OR ("cancer associated macrophage*") OR ("cancer-associated macrophage*"). The publication period was limited to between 2001 and 2021, and the publication type was limited to original articles written in English. Moreover, we also used broader terms as a benchmark dataset to better evaluate the overall trend of immune cell research in cancer such as "tumor OR tumour OR cancer" and "T cell OR macrophage OR neutrophil*". The literature search and data collection were performed independently by two researchers to ensure the reliability of the results.

Data collection

Original data was extracted from selected publications, including titles, abstracts, authors, affiliations, countries/regions, journals, publication years, references and keywords. The H-index of scholars, impact factor (IF) and Journal citation reports (JCR) division of journals were obtained from the Web of Science. Productivity of activities is measured by the number of citations. Overlapping items were merged into a single element and misspelled words were corrected artificially. The cleaned data were exported for further analysis.

Bibliometric analysis

Bibliometric indicators are used to quantitatively describe and evaluate the characteristics of literature and its trends. We used R software to conduct Lotka's Law analysis (11). VOSviewer is a bibliometric tool for developing scientometric network and knowledge visualization (12). The network graph generated by VOSviewer displays the size of nodes according to the number of publications, where closely related nodes are grouped into the same cluster. The connection indicates the association of different nodes, and the thickness of the connection depends on the strength of the association. Centrality is used to measure the importance of a node's location in the network, and nodes with centrality greater than 0.1 are generally considered as critical nodes. CiteSapce software provides new angle for the bursts of research hotspots in the field of TAM (13).

Results

A total of 9,694 literatures were published in the field between 2001 and 2021. According to the exclusion criteria, we finally included 6,405 eligible original articles in our study. The specific flow diagram was illustrated in Figure 1.

Growth trend of publication

The overall growth trend of immune cell research in cancer were showed in Figure 2A. Although T cell is the most heavily studied immune population, the field of macrophage showed similar increase rate of up to three times. For tumor-associated macrophage research, the number of articles published exhibited a steady increase from 2001 to 2021 (Figure 2B). The output of publications from 2001 to 2008 was low, with less than 100 articles per year. With the fast increase in the number of annual publications, there were 6,028 articles on TAM published between 2009 and 2021, accounting for 94.1% in the past two decades. These findings indicated that TAM has gained great interest and entered the phase of rapid development.

Distribution of countries/regions and institutions

The publications on TAM were conducted by 5,294 institutions in 99 countries/regions (Table 1). The United States received the highest

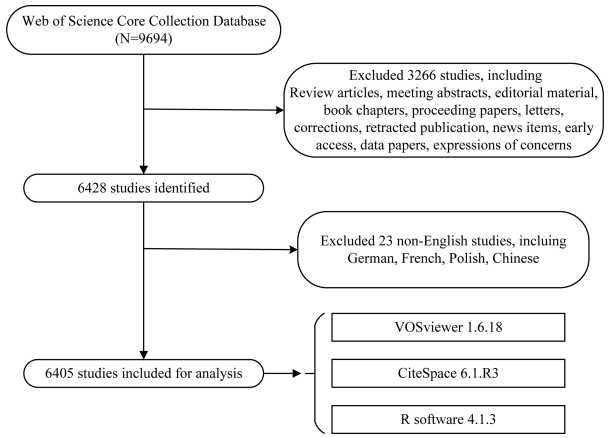

FIGURE 1
Flowchart of literature screening.

citations (N=123799), followed by China (N=71126) and Italy (N=28368). Annual citations per publication peaked in the middle of the study period in most countries/regions, especially for Italy (Figure 3A). Although China carried out the most publications, the average number of citations is lower than other countries/regions. The bibliometric map revealed the tight communications between countries/regions (Figure 3B). Intense collaborations between countries/regions resulted in thicker connecting lines between nodes. Of them, the centrality of the United States is as high as 0.37, suggesting that it plays a strong bridge role between the cooperations. In addition, China, Italy, Germany, Japan and United Kingdom are also important nodes among clusters, with centrality greater than 0.1.

The 5,294 institutions constituted seven main clusters (Figure 3C). The University of Milan, the university of California San Francisco and Sun Yat-sen University were the most productive institutions, with centrality ranged from 0.02 to 0.12. The University of Texas MD Anderson Cancer Center and Memorial Sloan-Kettering Cancer Center also had a centrality of more than 0.1 and belonged to a key node of the network.

Author and co-author analysis

There were 41,399 authors involved in the study of tumor-associated macrophages. Scientific productivity based on Lotka's law shows that 73.1% of authors contributed only one publication (Figure 4A). Mantovani, Alberto from Humanitas University received the most citations (N=10675) with the most publications (Table 2). The next productive authors were Sica, Antonio from University of Eastern Piedmont Amedeo Avogadro (N=9344) and Coussens, Lisa M from University of California San Francisco (N=5745). There were active collaborations among the author clusters of seven different colors (Figure 4B). A certain degree of collaborations existed between two linked nodes in different clusters, such as Pollard, Jeffrey W and De Palma, Michele.

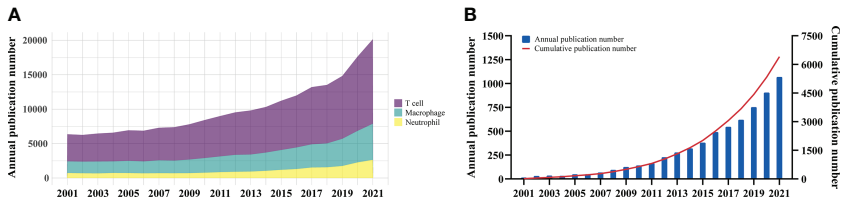

FIGURE 2
(A) The overall growth trend of annual immune cell research in cancer. **(B)** Annual and cumulative growth trend of TAM publications.

TABLE 1 The top 10 countries/regions and institutions that have contributed to publications on tumor-associated macrophage research.

Country	Centrality	Count	Citation	Institution	Centrality	Count	Citation
United States	0.37	1947	123799	Univ Milan	0.12	67	12892
China	0.13	2157	71126	Univ Calif San Francisco	0.02	55	8971
Italy	0.14	369	28368	Sun Yat Sen Univ	0.05	165	7727
Germany	0.20	469	25772	Univ Texas Md Anderson Canc Ctr	0.12	107	6741
Japan	0.17	599	22314	Harvard Univ	0.08	55	6529
United Kingdom	0.15	253	15545	Mem Sloan Kettering Canc Ctr	0.11	73	6436
France	0.05	199	13833	Fudan Univ	0.01	152	6425
Switzerland	0.06	135	11200	Shanghai Jiao Tong Univ	0.07	149	6397
Netherlands	0.06	170	10305	Stanford Univ	0.04	74	6335
Spain	0.04	157	9849	Massachusetts Gen Hosp	0.04	55	5708

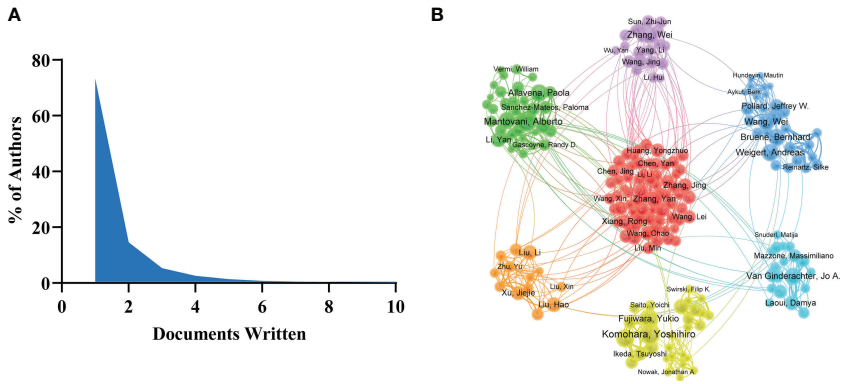

FIGURE 3
(A) Scientific productivity of authors based on Lotka's Law. **(B)** The network map of authors on tumor-associated macrophage research.

Journals and cited academic journals

A total of 1,201 journals were identified in this research field. The journal with the most publications was Cancer Research (N=173), followed by Plos One (N=152) and Oncotarget (N=148). Among the top ten journals related to TAM, 7 journals have an impact factor greater than 5, and 5 journals were at the Q1 JCR division (Table 3). At the same time, Cancer Research generated the most co-citations (N=18479). Figure 5A showed Scientific Reports, Cancers and Frontiers in Oncology were relatively new to this field, but developed rapidly.

The cited journals network indicated the association between two journals. Journals are divided into four clusters, and the size of nodes represented the number of co-citations (Figure 5B). There was similar theme between journals of the same color, especially for red cluster.

Keywords co-occurrence, clusters and bursts

Keywords were extracted from the 6,405 published articles. As shown in Table 4, NF-κB (N=336), endothelial growth factor (N=204)

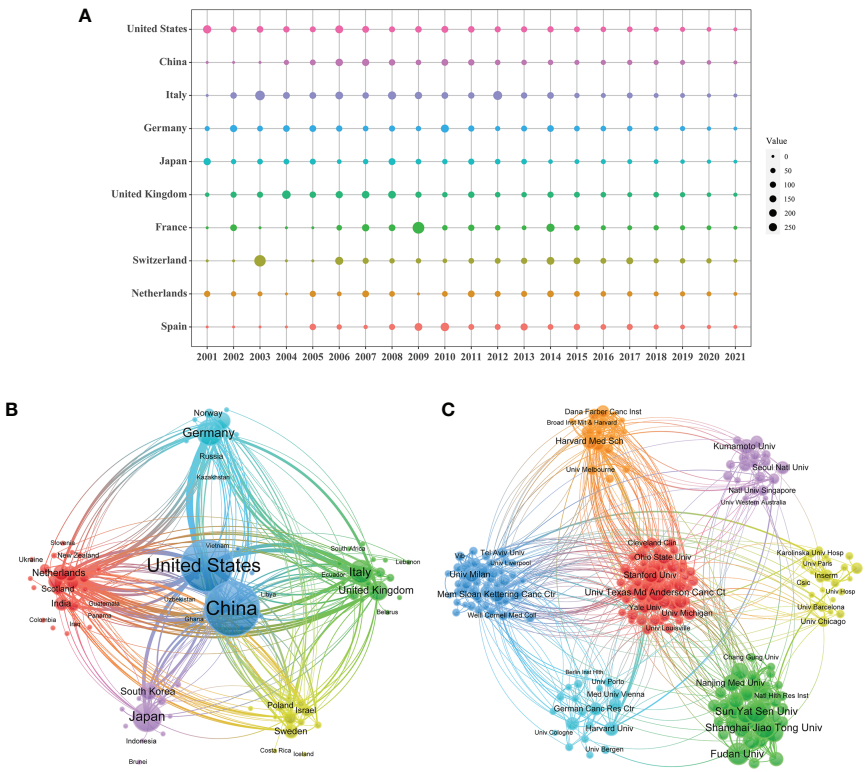

FIGURE 4
(A) Annual citations per publication for the top 10 countries. The network map of countries/regions **(B)** and institutions **(C)** on tumor-associated macrophage research.

TABLE 2 The top 10 productive authors and cited authors in the field of tumor-associated macrophages.

Authors	Count	H-index	Cited author	Count	H-index
Mantovani, Alberto	39	182	Mantovani, Alberto	10675	182
Komohara, Yoshihiro	36	45	Sica, Antonio	9344	72
Fujiwara, Yukio	33	32	Coussens, Lisa M	5745	81
Bruene, Bernhard	30	73	DeNardo, David G	4519	40
Weigert, Andreas	27	40	Lawrence, Toby	3909	40
Sica, Antonio	26	72	Ruffell, brian	3848	29
Aiba, Setsuya	24	40	Van Ginderachter, Jo A	3702	62
Takeya, Motohiro	23	62	Weissleder, Ralph	3337	168
Van Ginderachter, Jo A	22	45	Pollard, Jeffrey W	3246	30
Van Ginderachter, Jo A	22	62	Pittet, Mikael	3187	72

and PD-L1 (N=170) were the most commonly involved molecules. Activation (N=1002), polarization (N=903) and angiogenesis (N=806) appeared more frequently for pathological processes. As for specific diseases, breast cancer (N=840), colorectal cancer (N=287) and lung cancer (N=251) received the most attention.

Clustering keywords help to identify the distribution of research content on a specific topic (Figure 6). The largest blue cluster consisted of keywords was associated with the pathological processes and molecules of macrophages, including angiogenesis, NF-Kappa B and oxidative stress. Red cluster involved the cancer treatment, including immunotherapy, resistance and nanoparticle. Yellow cluster mainly explored the factors associated with tumor prognosis.

A visual map was constructed to show the trend of keywords bursts, where the red part represented the duration of citation burst (Figure 7). The early burst keywords included angiogenesis, epithelial growth factor, and colony stimulating factor. Citation bursts in the middle period (2011-2016) were significantly attenuated with a decrease in hotspot keywords such as NF-κB, Hodgkin lymphoma and scavenger receptor. In recent years (2018-2020), the treatment of cancer received increasing attention from researchers. PD-1/L1, PI3Kγ, resistance, nanoparticle and immune microenvironment has become the focus of attention of current research.

Discussion

Tumor-associated macrophage is an important part of the tumor microenvironment and interacts with cancer cells to maintain the most of characteristics of tumors. The diversity of TAM forms a complex communication network between cancer and immune cells (14). In this study, we extracted TAM studies from public databases for bibliometric analysis to identify its hotspots and development trends. The increasing trend in annual publication volume demonstrated the significant potential of TAM in cancers.

The United States and China were the countries with the most citations. The distribution of institutions is consistent with countries/

TABLE 3 The top 10 journals and cited journals related to tumor associated macrophages.

Journal	Count	IF (2021)	JCR (2021)	Cited journal	Citation	IF (2021)	JCR (2021)
Cancer Research	173	13.312	Q1	Cancer Research	18479	13.312	Q1
Plos One	152	3.752	Q2	Cancer Cell	9039	38.585	Q1
Oncotarget	148	–	–	Clinical Cancer Research	8991	13.801	Q1
Oncoimmunology	110	7.723	Q1	Proceedings of the National Academy of Sciences of the United States of America	8035	12.779	Q1
Scientific Reports	104	4.996	Q2	Plos One	7910	3.752	Q2
Clinical Cancer Research	95	13.801	Q1	Journal of Experimental Medicine	7358	17.579	Q1
Cancers	90	6.575	Q1	Journal of Immunology	8030	5.426	Q2
Cancer Letters	86	9.756	Q1	Journal of Clinical Investigation	6982	19.456	Q1
Journal of Immunology	85	5.426	Q2	Blood	6437	25.476	Q1
Frontiers in Oncology	83	5.738	Q2	Nature Communication	3943	17.694	Q1

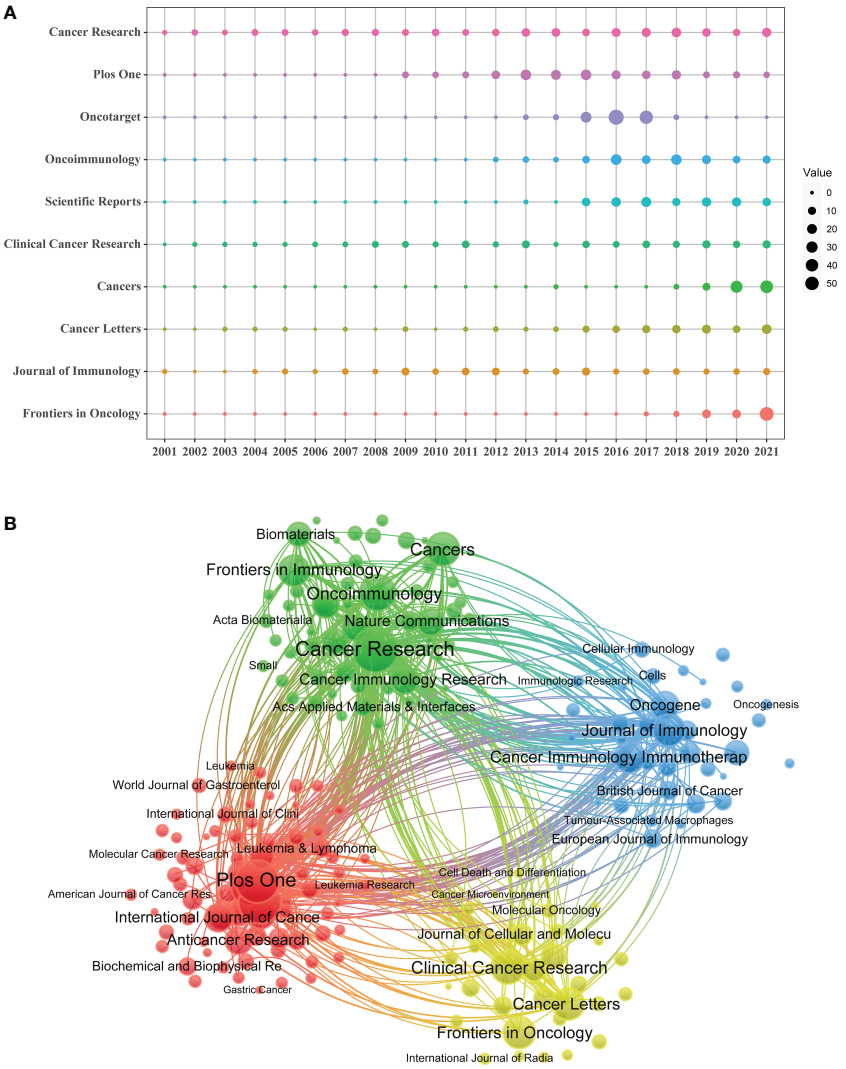

FIGURE 5
(A) Annual number of publications for the top 10 journals. **(B)** The network map of journals on tumor-associated macrophage research.

TABLE 4 The top 10 molecules, pathological process and disease related to tumor associated macrophages research.

Molecules	Count	Pathological processes	Count	Diseases	Count
NF-Kappa B	336	Activation	1002	Breast cancer	840
Endothelial growth factor	204	Polarization	903	Colorectal cancer	287
PD-L1	170	Angiogenesis	806	Lung cancer	251
CD163	149	Infiltration	341	Hepatocellular carcinoma	240
Colony stimulating factor	146	Differentiation	291	Glioblastoma	164
INF-gamma	141	Proliferation	255	Gastric cancer	164
TGF-β	118	Epithelial mesenchymal transition	219	Ovarian cancer	148
STAT3	116	Apoptosis	206	Pancreatic cancer	141
Nitric Oxide	107	Metabolism	99	Melanoma	137
CD68	93	Recruitment	97	Prostate cancer	136

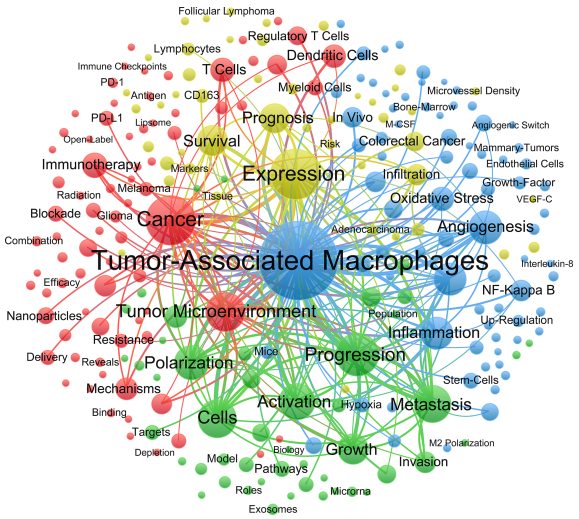

FIGURE 6
The network map of keywords on tumor-associated macrophage research.

Top 50 Keywords with the Strongest Citation Bursts

Keywords	Year	Strength	Begin	End	2001 - 2021
Angiogenesis	2001	31.36	2001	2012	
Endothelial Growth Factor	2001	23.6	2001	2014	
Colony-Stimulating Factor	2001	16.45	2001	2013	
Infiltration	2001	12.8	2001	2013	
Breast Carcinoma	2001	12.54	2001	2011	
Endothelial Cell	2001	12.57	2002	2012	
Microvessel Density	2001	9.67	2002	2012	
Nitric Oxide Synthase	2001	9.46	2002	2010	
Messenger RNA	2001	7.38	2002	2010	
Cytokine	2001	5.85	2002	2011	
In Vivo	2001	23.91	2003	2013	
Necrosis Factor Alpha	2001	17.74	2003	2014	
Nitric Oxide	2001	11.78	2003	2012	
Monocyte Chemoattractant Protein 1	2001	9.34	2003	2012	
Gene Expression	2001	20.58	2004	2012	
Dendritic Cell	2001	16.44	2004	2013	
Immune Reponse	2001	5.72	2004	2011	
Human Monocyte	2001	9.79	2005	2013	
Mast Cell	2001	7.24	2005	2011	
IFN Gamma	2001	9.61	2006	2015	
Population	2001	5.36	2007	2012	
VEGF	2001	5.26	2007	2013	
Mammary Tumor	2001	12.99	2008	2014	
Lymphangiogenesis	2001	8.38	2008	2015	
Innate Immunity	2001	7.08	2008	2011	
Epithelial Cell	2001	5.59	2008	2012	
Tumor Growth	2001	5.09	2008	2015	
NF-Kappa B	2001	21.52	2009	2014	
Alternative Activation	2001	13.68	2009	2015	
Follicular Lymphoma	2001	6.49	2009	2015	
Angiogenic Switch	2001	6.29	2009	2013	
IL-10	2001	5.05	2009	2013	
Suppressor Cell	2001	7.32	2010	2011	
Scavenger receptor	2001	5.42	2011	2016	
Hodgkin Lymphoma	2001	6.91	2012	2014	
Epstein Barr Virus	2001	7.72	2013	2015	
Tumorigenesis	2001	6.74	2013	2017	
Inflammatory Response	2001	4.84	2015	2018	
Anticancer Therapy	2001	5.94	2016	2018	
Nivolumab	2001	6.58	2017	2021	
Solid Tumor	2001	5.54	2017	2018	
PD-L1	2001	6.53	2018	2021	
PD-1	2001	5.74	2018	2021	
Transcription	2001	5.08	2018	2021	
Blockade	2001	17.45	2019	2021	
Resistance	2001	12.67	2019	2021	
Nanoparticle	2001	10.08	2019	2021	
PI3K-Gamma	2001	6.58	2019	2021	
Immune microenvironment	2001	5.44	2019	2021	
Efficacy	2001	5.02	2019	2021	

FIGURE 7
The top 50 keywords with the strongest citation bursts on tumor-associated macrophage research.

regions based on geographical location. However, the average citations for most countries/regions and institutions did not correspond well to the number of publications in this field. More robust efforts may be required to deeply clarify the role and mechanism of TAM in tumor. Meanwhile, the United States achieves a maximum level of cooperation in TAM research with a centrality of 0.37. Compared with other countries, it constitutes several cooperative subnetworks to better promote the development of the field, such as the University of Texas MD Anderson Cancer Center, Memorial Sloan-Kettering Cancer Center and University of Chicago.

Regarding the productivity of authors, Alberto Mantovani received the most citations in the TAM field. Mantovani mainly focused on the regulatory effect of chemokines on TAM (15–17) and some related anticancer drugs such as trabectedin (18, 19). Given the limitation of the binary M1-M2 classification of macrophage, Mantovani also attempted to divide macrophages into additional subsets (M2a, M2b and M2c) (20) or used looser terms (M1-like and M2-like) (21). Besides the collaborations with Mantovani, Antonio Sica made efforts to link inflammatory reaction to cancer through NF-κB (22–24). Coussens's group from University of California San Francisco focused more on the immune cell crosstalk in breast cancer (25–27).

Cancer research published the most articles and received the highest number of co-citations. Scientific Reports, Cancers and Frontiers in Oncology were emerging journals spreading macrophage research. Papers published in highly cited journals such as Nature, Blood and Cell were more likely to be reviewed by scholars and have more access to citations.

The clustering analysis of keywords indicated that TAM research ranged from the biological properties of macrophages to the targeted therapy of cancer. TAM is highly related to specific pathological context, and its complex mechanism in tumors has attracted extensive attention. Angiogenesis is the initial research focus, which provides basic condition for tumor growth and dissemination. Angiogenesis is the initial research focus, which provides basic condition for tumor progression. Studies have shown that TAM can promote angiogenesis through the release of cytokines, growth factors and matrix metalloproteinases or the expression of TIE2 receptors (28–32). NF-κB is considered to be a molecular link between the inflammation and cancer. In the middle period, it gradually presented the highest citation burst strength. NF-κB activation in macrophages is essential for tumor growth. Inhibition of IKKβ leads to a significant reduction in tumor onset and load of several inflammation-induced cancer models (33–35). However, TAM often shows alternative immunosuppressive M2-like phenotype, which is not easily reconciled with the proinflammatory function of NF-κB in TAM. The scavenger receptor MARCO expressed on the surface of macrophages is able to regulate macrophage polarization and enhance tumor killing (36, 37).

Recently, anticancer therapy targeting TAM has generated the most research enthusiasm. Immunosuppression microenvironment limits the efficacy of checkpoint block and adoptive cell therapy, particularly in solid tumors (38). TAMs can suppress immunotherapy efficacy by inhibiting T-cell activity and enhancing the expression of PD-L1 in the TME. In addition to inhibiting T cell activation, a study from Sydney et al. showed that immune checkpoint inhibitor PD-1/L1 also inhibited TAM phagocytosis, which may be associated with M2 polarization (39). In-depth inquiry of PD-1/L1 expanded the knowledge of PD-1/L1 from its role in T cells to many other cell types, including macrophages.

PI3K/Akt is also an important signaling pathway participating in macrophages survival, proliferation and cytoskeleton rearrangement. PI3K induces TAMs into M2-like phenotype and is closely correlated with poor clinical outcomes of cancers (40). Inhibition of PI3Kγ make tumors sensitive to immune checkpoint inhibitors by reprogramming TAM, demonstrating the importance of macrophage-mediated immune microenvironment for optimal immunotherapy efficacy (41–43). CSF-1R expressed on TAMs is involved in the activation of PI3K signaling pathway, and regulate the immune inhibition in macrophages. Blockade of CSF1 has been shown to deplete TAM and prevent TAM recruitment to the tumor (44, 45). Targeting TAM can play its unique regulatory function in promoting the antitumor effects of current immunotherapy.

Due to the unique biophysical properties, nanoparticles show greater advantages and potentials in cancer treatment. Compared with traditional drugs, nanoparticles can extend retention time and achieve targeted delivery with a decreased toxicity. Some studies have reported that nanoparticles specifically enhance anticancer immune responses by targeting TAM (46–50). The rich blood circulation and strong phagocytosis ability also make macrophages themselves become the optimal carrier of drug delivery. TAM allows the delivery of nanotherapeutic drugs to tumor cells and alters the spatial diffusion of drugs within the tumor (51, 52). Imaging the response between tumors and nanomaterials provide a reliable basis for the development of highly effective targeted therapies.

The bibliometric study reflected the development trend and research hotspots in this field to a certain extent. At the same time, this study has several limitations. The included literatures were collected from WOSCC database, which caused the omission of some information. Furthermore, there were potential biases in bibliometric method based on natural language processing. Excessive adjustments for inaccurate elements may reduce the credibility of the results.

In conclusion, the research on TAM is rapidly evolving with active cooperation worldwide. And anticancer therapy targeting TAM is emerging and promising area of future research, especially in translational application. This may provide guidance and new insights for further research in the field of TAM.

Data availability statement

The raw data supporting the conclusions of this article will be made available by the authors, without undue reservation.

Author contributions

XZ and YX designed the study. YL, CL and FW conducted data extraction. FZ, YX and JP performed data analysis. FZ drafted the manuscript. XZ interpreted the data and revised the manuscript. All authors contributed to the article and approved the submitted version.

Conflict of interest

The authors declare that the research was conducted in the absence of any commercial or financial relationships that could be construed as a potential conflict of interest.

Publisher's note

References

1. Pittet MJ, Michielin O, Migliorini D. Clinical relevance of tumour-associated macrophages. *Nat Rev Clin Oncol* (2022) 19(6):402–21. doi: 10.1038/s41571-022-00620-6

2. Mehla K, Singh PK. Metabolic regulation of macrophage polarization in cancer. *Trends Cancer* (2019) 5(12):822–34. doi: 10.1016/j.trecan.2019.10.007

3. Wynn TA, Chawla A, Pollard JW. Macrophage biology in development, homeostasis and disease. *Nature* (2013) 496(7446):445–55. doi: 10.1038/nature12034

4. Christofides A, Strauss L, Yeo A, Cao C, Charest A, Boussiotis VA. The complex role of tumor-infiltrating macrophages. *Nat Immunol* (2022) 23(8):1148–56. doi: 10.1038/s41590-022-01267-2

5. Locati M, Curtale G, Mantovani A. Diversity, mechanisms, and significance of macrophage plasticity. *Annu Rev Pathol* (2020) 15:123–47. doi: 10.1146/annurev-pathmechdis-012418-012718

6. Yang M, McKay D, Pollard JW, Lewis CE. Diverse functions of macrophages in different tumor microenvironments. *Cancer Res* (2018) 78(19):5492–503. doi: 10.1158/0008-5472.Can-18-1367

7. Orecchioni M, Ghosheh Y, Pramod AB, Ley K. Macrophage polarization: Different gene signatures in M1(Lps+) vs. classically and M2(Lps-) vs. alternatively activated macrophages. *Front Immunol* (2019) 10:1084. doi: 10.3389/fimmu.2019.01084

8. Agarwal A, Durairajanayagam D, Tatagari S, Esteves SC, Harlev A, Henkel R, et al. Bibliometrics: Tracking research impact by selecting the appropriate metrics. *Asian J Androl* (2016) 18(2):296–309. doi: 10.4103/1008-682x.171582

9. Chen C, Song M. Visualizing a field of research: A methodology of systematic scientometric reviews. *PloS One* (2019) 14(10):e0223994. doi: 10.1371/journal.pone.0223994

10. Chen C. Searching for intellectual turning points: Progressive knowledge domain visualization. *Proc Natl Acad Sci U.S.A.* (2004) 101 Suppl 1(Suppl 1):5303–10. doi: 10.1073/pnas.0307513100

11. Aria M, Cuccurullo C. Bibliometrix: An r-tool for comprehensive science mapping analysis. *J Informetrics* (2017) 11(4):959–75. doi: 10.1016/j.joi.2017.08.007

12. van Eck NJ, Waltman L. Software survey: Vosviewer, a computer program for bibliometric mapping. *Scientometrics* (2010) 84(2):523–38. doi: 10.1007/s11192-009-0146-3

13. Chen C. Science mapping: A systematic review of the literature. *J Data Inf Sci* (2017) 2(2):1–40. doi: 10.1515/jdis-2017-0006

14. Li MO, Wolf N, Raulet DH, Akkari L, Pittet MJ, Rodriguez PC, et al. Innate immune cells in the tumor microenvironment. *Cancer Cell* (2021) 39(6):725–9. doi: 10.1016/j.ccell.2021.05.016

15. Marelli G, Erreni M, Anselmo A, Taverniti V, Guglielmetti S, Mantovani A, et al. Heme-Oxygenase-1 production by intestinal Cx3cr1(+) macrophages helps to resolve inflammation and prevents carcinogenesis. *Cancer Res* (2017) 77(16):4472–85. doi: 10.1158/0008-5472.Can-16-2501

16. Savino B, Caronni N, Anselmo A, Pasqualini F, Borroni EM, Basso G, et al. Erk-dependent downregulation of the atypical chemokine receptor D6 drives tumor aggressiveness in kaposi sarcoma. *Cancer Immunol Res* (2014) 2(7):679–89. doi: 10.1158/2326-6066.Cir-13-0202

17. Schioppa T, Uranchimeg B, Saccani A, Biswas SK, Doni A, Rapisarda A, et al. Regulation of the chemokine receptor Cxcr4 by hypoxia. *J Exp Med* (2003) 198(9):1391–402. doi: 10.1084/jem.20030267

18. Germano G, Frapolli R, Simone M, Tavecchio M, Erba E, Pesce S, et al. Antitumor and anti-inflammatory effects of trabectedin on human myxoid liposarcoma cells. *Cancer Res* (2010) 70(6):2235–44. doi: 10.1158/0008-5472.Can-09-2335

19. Belgiovine C, Bello E, Liguori M, Craparotta I, Mannarino L, Paracchini L, et al. Lurbinectedin reduces tumour-associated macrophages and the inflammatory tumour microenvironment in preclinical models. *Br J Cancer* (2017) 117(5):628–38. doi: 10.1038/bjc.2017.205

20. Mantovani A, Sica A, Sozzani S, Allavena P, Vecchi A, Locati M. The chemokine system in diverse forms of macrophage activation and polarization. *Trends Immunol* (2004) 25(12):677–86. doi: 10.1016/j.it.2004.09.015

21. Biswas SK, Mantovani A. Macrophage plasticity and interaction with lymphocyte subsets: Cancer as a paradigm. *Nat Immunol* (2010) 11(10):889–96. doi: 10.1038/ni.1937

22. Porta C, Ippolito A, Consonni FM, Carraro L, Celesti G, Correale C, et al. Protumor steering of cancer inflammation by P50 nf-κb enhances colorectal cancer progression. *Cancer Immunol Res* (2018) 6(5):578–93. doi: 10.1158/2326-6066.Cir-17-0036

23. Biswas SK, Gangi L, Paul S, Schioppa T, Saccani A, Sironi M, et al. A distinct and unique transcriptional program expressed by tumor-associated macrophages (Defective nf-kappab and enhanced irf-3/Stat1 activation). *Blood* (2006) 107(5):2112–22. doi: 10.1182/blood-2005-01-0428

24. Saccani A, Schioppa T, Porta C, Biswas SK, Nebuloni M, Vago L, et al. P50 nuclear factor-kappab overexpression in tumor-associated macrophages inhibits M1 inflammatory responses and antitumor resistance. *Cancer Res* (2006) 66(23):11432–40. doi: 10.1158/0008-5472.Can-06-1867

25. Ruffell B, Chang-Strachan D, Chan V, Rosenbusch A, Ho CM, Pryer N, et al. Macrophage il-10 blocks Cd8+ t cell-dependent responses to chemotherapy by suppressing il-12 expression in intratumoral dendritic cells. *Cancer Cell* (2014) 26 (5):623–37. doi: 10.1016/j.ccell.2014.09.006

26. DeNardo DG, Barreto JB, Andreu P, Vasquez L, Tawfik D, Kolhatkar N, et al. Cd4(+) t cells regulate pulmonary metastasis of mammary carcinomas by enhancing protumor properties of macrophages. *Cancer Cell* (2009) 16(2):91–102. doi: 10.1016/j.ccr.2009.06.018

27. Shiao SL, Ruffell B, DeNardo DG, Faddegon BA, Park CC, Coussens LM. Th2-polarized Cd4(+) t cells and macrophages limit efficacy of radiotherapy. *Cancer Immunol Res* (2015) 3(5):518–25. doi: 10.1158/2326-6066.Cir-14-0232

28. Fu LQ, Du WL, Cai MH, Yao JY, Zhao YY, Mou XZ. The roles of tumor-associated macrophages in tumor angiogenesis and metastasis. *Cell Immunol* (2020) 353:104119. doi: 10.1016/j.cellimm.2020.104119

29. Larionova I, Kazakova E, Gerashchenko T, Kzhyshkowska J. New angiogenic regulators produced by tams: Perspective for targeting tumor angiogenesis. *Cancers (Basel)* (2021) 13(13). doi: 10.3390/cancers13133253

30. Deryugina EI, Quigley JP. Tumor angiogenesis: Mmp-mediated induction of intravasation- and metastasis-sustaining neovasculature. *Matrix Biol* (2015) 44-46:94–112. doi: 10.1016/j.matbio.2015.04.004

31. Duran CL, Borriello L, Karagiannis GS, Entenberg D, Oktay MH, Condeelis JS. Targeting Tie2 in the tumor microenvironment: From angiogenesis to dissemination. *Cancers (Basel)* (2021) 13(22). doi: 10.3390/cancers13225730

32. Casazza A, Laoui D, Wenes M, Rizzolio S, Bassani N, Mambretti M, et al. Impeding macrophage entry into hypoxic tumor areas by Sema3a/Nrp1 signaling blockade inhibits angiogenesis and restores antitumor immunity. *Cancer Cell* (2013) 24(6):695–709. doi: 10.1016/j.ccr.2013.11.007

33. Hagemann T, Lawrence T, McNeish I, Charles KA, Kulbe H, Thompson RG, et al. "Re-educating" tumor-associated macrophages by targeting nf-kappab. *J Exp Med* (2008) 205(6):1261–8. doi: 10.1084/jem.20080108

34. Greten FR, Eckmann L, Greten TF, Park JM, Li ZW, Egan LJ, et al. Ikkbeta links inflammation and tumorigenesis in a mouse model of colitis-associated cancer. *Cell* (2004) 118(3):285–96. doi: 10.1016/j.cell.2004.07.013

35. Luedde T, Beraza N, Kotsikoris V, van Loo G, Nenci A, De Vos R, et al. Deletion of Nemo/Ikkgamma in liver parenchymal cells causes steatohepatitis and hepatocellular carcinoma. *Cancer Cell* (2007) 11(2):119–32. doi: 10.1016/j.ccr.2006.12.016

36. La Fleur L, Boura VF, Alexeyenko A, Berglund A, Pontén V, Mattsson JSM, et al. Expression of scavenger receptor marco defines a targetable tumor-associated macrophage subset in non-small cell lung cancer. *Int J Cancer* (2018) 143(7):1741–52. doi: 10.1002/ijc.31545

37. Georgoudaki AM, Prokopec KE, Boura VF, Hellqvist E, Sohn S, Östling J, et al. Reprogramming tumor-associated macrophages by antibody targeting inhibits cancer progression and metastasis. *Cell Rep* (2016) 15(9):2000–11. doi: 10.1016/j.celrep.2016.04.084

38. Li X, Shao C, Shi Y, Han W. Lessons learned from the blockade of immune checkpoints in cancer immunotherapy. *J Hematol Oncol* (2018) 11(1):31. doi: 10.1186/s13045-018-0578-4

39. Gordon SR, Maute RL, Dulken BW, Hutter G, George BM, McCracken MN, et al. Pd-1 expression by tumour-associated macrophages inhibits phagocytosis and tumour immunity. *Nature* (2017) 545(7655):495–9. doi: 10.1038/nature22396

40. Yang D, Yang L, Cai J, Li H, Xing Z, Hou Y. Phosphoinositide 3-Kinase/Akt and its related signaling pathways in the regulation of tumor-associated macrophages polarization. *Mol Cell Biochem* (2022) 477(10):2469–80. doi: 10.1007/s11010-022-04461-w

41. De Henau O, Rausch M, Winkler D, Campesato LF, Liu C, Cymerman DH, et al. Overcoming resistance to checkpoint blockade therapy by targeting Pi3kγ in myeloid cells. *Nature* (2016) 539(7629):443–7. doi: 10.1038/nature20554

42. Kaneda MM, Cappello P, Nguyen AV, Ralainirina N, Hardamon CR, Foubert P, et al. Macrophage Pi3kγ drives pancreatic ductal adenocarcinoma progression. *Cancer Discovery* (2016) 6(8):870–85. doi: 10.1158/2159-8290.Cd-15-1346

43. Han MG, Jang BS, Kang MH, Na D, Kim IA. Pi3kγδ inhibitor plus radiation enhances the antitumour immune effect of pd-1 blockade in syngenic murine breast cancer and humanised patient-derived xenograft model. *Eur J Cancer* (2021) 157:450–63. doi: 10.1016/j.ejca.2021.08.029

44. Ries CH, Cannarile MA, Hoves S, Benz J, Wartha K, Runza V, et al. Targeting tumor-associated macrophages with anti-Csf-1r antibody reveals a strategy for cancer therapy. *Cancer Cell* (2014) 25(6):846–59. doi: 10.1016/j.ccr.2014.05.016

45. Pyonteck SM, Akkari L, Schuhmacher AJ, Bowman RL, Sevenich L, Quail DF, et al. Csf-1r inhibition alters macrophage polarization and blocks glioma progression. *Nat Med* (2013) 19(10):1264–72. doi: 10.1038/nm.3337

46. Trac N, Chen LY, Zhang A, Liao CP, Poon C, Wang J, et al. Ccr2-targeted micelles for anti-cancer peptide delivery and immune stimulation. *J Control Release* (2021) 329:614–23. doi: 10.1016/j.jconrel.2020.09.054

47. Liu Y, Wang J, Zhang J, Marbach S, Xu W, Zhu L. Targeting tumor-associated macrophages by Mmp2-sensitive apoptotic body-mimicking nanoparticles. *ACS Appl Mater Interfaces* (2020) 12(47):52402–14. doi: 10.1021/acsami.0c15983

48. Zhang Y, Chen Y, Li J, Zhu X, Liu Y, Wang X, et al. Development of toll-like receptor agonist-loaded nanoparticles as precision immunotherapy for reprogramming tumor-associated macrophages. *ACS Appl Mater Interfaces* (2021) 13(21):24442–52. doi: 10.1021/acsami.1c01453

49. Nie W, Wu G, Zhang J, Huang LL, Ding J, Jiang A, et al. Responsive exosome nano-bioconjugates for synergistic cancer therapy. *Angew Chem Int Ed Engl* (2020) 59 (5):2018–22. doi: 10.1002/anie.201912524

50. Li H, Somiya M, Kuroda S. Enhancing antibody-dependent cellular phagocytosis by re-education of tumor-associated macrophages with resiquimod-encapsulated liposomes. *Biomaterials* (2021) 268:120601. doi: 10.1016/j.biomaterials.2020.120601

51. Xia Y, Rao L, Yao H, Wang Z, Ning P, Chen X. Engineering macrophages for cancer immunotherapy and drug delivery. *Adv Mater* (2020) 32(40):e2002054. doi: 10.1002/adma.202002054

52. Cheng Y, Song S, Wu P, Lyu B, Qin M, Sun Y, et al. Tumor associated macrophages and tams-based anti-tumor nanomedicines. *Adv Healthc Mater* (2021) 10(18):e2100590. doi: 10.1002/adhm.202100590

frontiers | Frontiers in Immunology

TYPE Original Research
PUBLISHED 19 January 2023
DOI 10.3389/fimmu.2023.1078118

OPEN ACCESS

EDITED BY
Loredana Ruggeri,
University of Perugia, Italy

REVIEWED BY
Minoru Kanaya,
Aiiku Hospital, Japan
Ibrahim C. Haznedaroglu,
Hacettepe University Hospital, Türkiye
Ahmet Emre Eskazan,
Istanbul University-Cerrahpasa, Türkiye

*CORRESPONDENCE
Yangqiu Li
yangqiuli@hotmail.com
Ling Xu
lingxu114@163.com

SPECIALTY SECTION
This article was submitted to Cancer Immunity and Immunotherapy, a section of the journal Frontiers in Immunology

RECEIVED 24 October 2022
ACCEPTED 03 January 2023
PUBLISHED 19 January 2023

CITATION
Yao D, Lai J, Lu Y, Zhong J, Zha X, Huang X, Liu L, Zeng X, Chen S, Weng J, Du X, Li Y and Xu L (2023) Comprehensive analysis of the immune pattern of T cell subsets in chronic myeloid leukemia before and after TKI treatment. *Front. Immunol.* 14:1078118. doi: 10.3389/fimmu.2023.1078118

Comprehensive analysis of the immune pattern of T cell subsets in chronic myeloid leukemia before and after TKI treatment

Danlin Yao [1,2], Jing Lai [3], Yuhong Lu [3], Jun Zhong [3], Xianfeng Zha [4], Xin Huang [5], Lian Liu [1], Xiangbo Zeng [1], Shaohua Chen [1], Jianyu Weng [5], Xin Du [5], Yangqiu Li [1*] and Ling Xu [1*]

[1]Key Laboratory for Regenerative Medicine of Ministry of Education, Institute of Hematology, School of Medicine, Jinan University, Guangzhou, China, [2]Department of Hematology, The Second Affiliated Hospital, Guangzhou Medical University, Guangzhou, China, [3]Department of Hematology, First Affiliated Hospital, Jinan University, Guangzhou, China, [4]Department of Clinical Laboratory, First Affiliated Hospital, Jinan University, Guangzhou, China, [5]Department of Hematology, Guangdong Provincial People's Hospital, Guangdong Academy of Medical Sciences, Guangzhou, China

Background: Immunological phenotypes and differentiation statuses commonly decide the T cell function and anti-tumor ability. However, little is known about these alterations in CML patients.

Method: Here, we investigated the immunologic phenotypes (CD38/CD69/HLA-DR/CD28/CD57/BTLA/TIGIT/PD-1) of T subsets (TN, TCM, TEM, and TEMRA) in peripheral blood (PB) and bone marrow (BM) from de novo CML patients (DN-CML), patients who achieved a molecular response (MR) and those who failed to achieve an MR (TKI-F) after tyrosine kinase inhibitor (TKI) treatment using multicolor flow cytometry.

Results: CD38 or HLA-DR positive PB CD8+TN and TCM cells decreased in the DN-CML patients and this was further decreased in TKI-F patients. Meanwhile, the level of PD-1 elevated in CD8+ TEM and TEMRA cells from PB in all groups. Among BM sample, the level of HLA-DR+CD8+TCM cells significantly decreased in all groups and CD8+TEMRA cells from TKI-F patients exhibited increased level of TIGIT and CD8+ tissue-residual T cells (TRM) from DN-CML patients expressed a higher level of PD-1 and TIGIT. Lastly, we found a significantly decreased proportion of CD86+ dendritic cells (DCs) and an imbalanced CD80/CD86 in the PB and BM of DN-CML patients, which may impair the activation of T cells.

Conclusion: In summary, early differentiated TN and TCM cells from CML patients may remain in an inadequate activation state, particularly for TKI-F patients. And effector T cells (TEM, TEMRA and TRM) may be dysfunctional due to the expression of PD-1 and TIGIT in CML patients. Meanwhile, DCs cells exhibited the impairment of costimulatory molecule expression in DN-CML patients. Those factors may jointly contribute to the immune escape in CML patients.

KEYWORDS

T cell subsets, CML, bone marrow microenvironment, immunological phenotypes, tyrosine kinase inhibitor

Introduction

Chronic myeloid leukemia (CML) is a hematological tumor driven by the BCR-ABL1 fusion protein, which constitutively activates tyrosine kinases. This activation leads to the accumulation of immature granulocytes and their progenitors in peripheral blood (PB) and bone marrow (BM). The advent of tyrosine kinase inhibitors (TKIs) has transformed CML into a chronic disease. Most patients achieve a life expectancy close to that of the general population (1–5). However, some patients do not have an optimal response in the initial stage of TKI treatment or lose a previously achieved hematological, cytogenetic, or molecular response during TKI treatment. These patients are identified as failing response to TKIs (TKI-F) and frequently develop into the accelerated phase (AP) or blast crisis (BC) phase, leading to poor prognosis (6–8). Additionally, due to the side effects and costs of TKIs, many CML patients who achieve major molecular remission (MMR) are eager to withdraw from the drug. Currently, studying the immune system changes in those patients before and after TKI treatment may provide more information for solving their problems.

T cells play an integral role against pathogens and clear tumor cells. During the immune process, naïve T (T_N) cells recognize pathogens presented by dendritic cells (DCs) and accept activation signals by binding the costimulatory ligand CD80 or CD86 on DCs. T_N cells further differentiate into effector memory T cells (T_{EM})/ $CD45RA^+$ effector memory T cells (T_{EMRA}) to clear antigens. Once pathogens were cleared, most activated T cells experienced apoptosis and a minority of survival effector T cells becomes central memory T cells (T_{CM}) cells. Afterward, T_{CM} cells provide immediate protection when re-infected and ultimately persist for a lifetime (9–13). Thus, the different differentiated status of the T cell subsets partially indicates the function of T cells. Recently, increasing evidence has indicated that the immunological status of T cell subsets provides better prognostication than $CD4^+$ or $CD8^+$ T cells in cancer patients, e.g., AML patients who express a higher percentage of $PD\text{-}1^+Tim3^+CD8^+$ T_{CM} cells are prone to relapse, and the prognosis of breast cancer patient with a higher number of $CD8^+$ tissue residual memory T (T_{RM}) cells was better (14, 15).

Indeed, accumulating evidence has proven that CML patients undergo several phenotypic and functional aberrations in the immune system, and this phenomenon is applicable to CML patients who at diagnosis, achieve MMR on TKI therapy and even at treatment-free remission (16–20). It's well known that the activation and proliferation of T cells are impaired due to the lower expression of CD3ζ and higher expression of immune checkpoints (ICs) (18, 21, 22). However, most studies only focused on total $CD8^+$ or $CD4^+$ T cells, and exploration of the immunophenotypes of T cell subsets remains limited for CML patients, particularly TKI-F patients. Additionally, BM is the origin and natural shelter for leukemia cells. Moreover, the BM accumulates immunosuppressive cells, including regulatory T (Treg) cells, myeloid-derived suppressor cells (MDSCs), and plasmacytoid DC that inhibit the anti-tumor response of T cells (23–27). These characteristics make the BM microenvironment (BMM) similar to the immunologic microenvironment of solid tumors. Hence, intensive study of the immunophenotypic characteristics of the T cell subsets driven by the leukemia BMM is critical for providing effective immunotherapy for CML patients.

Here, we used flow cytometry to assay the expression of the activation markers CD38, CD69, and human leukocyte antigen – DR isotype (HLA-DR), the IC molecules programmed death-1 (PD-1), B, and T lymphocyte attenuator (BTLA), and T cell immunoglobulin and ITIM domain (TIGIT), the co-stimulation marker CD28, and the immune senescence marker CD57 on different T cell subsets in PB and BM from CML patients. We categorized CML patients into different statuses according to the level of BCR-ABL1 and TKI-treatment response: *de novo* CML (DN-CML: BCR-ABL1 > 10%), molecular remission (MR: BCR-ABL1 < 10%), and TKI-F. The TKI-F patients were identified as CML patients who failed to achieve a molecular response (TKI-F, BCR-ABL1 > 10%) with regular oral administration of first or second-generation TKIs after 3 months. Finally, we describe the T cell costimulatory molecules CD80 and CD86 on DCs in the CML groups.

Materials and methods

Patient samples

PB samples were obtained from DN-CML (n = 16), TKI-F (n = 9), and MR (n = 20) patients. BM aspirate samples were extracted from 23 cases, including 11 newly diagnosed patients, 6 at MR, and 6 at TKI-F. PB samples were obtained from healthy individuals (HIs; n =12), BM aspirate samples from hematopoietic stem cell transplantation (HSCT) donors (n = 6) and patients with iron-deficiency anemia (n = 3) were collected as control. All MR patients achieved complete hematologic response (CHR) with BCR/ABL < 10% after TKI treatment. In addition, previous studies have found that the immunologic characteristics of T cells in CML patients varied with different molecular remission levels (18). The MR patients were further divided into 2 groups according to the BCR/ABL1 level. MMR patients (n = 10) with a level ≤ 0.1% and pre-MMR (n = 10) representing the period before MMR was achieved with a BCR-ABL1 transcript level > 0.1% and < 10%. The TKI-F were patients with BCR/ABL1 > 10% consistently after regular 12-month TKI treatment. Sample data are shown in Tables 1, 2. Detailed sample information of TKI-F patients are shown in Table 3.

Flow cytometry analysis

PB and BM samples were collected in EDTA tubes. First, 150 μl of PB or BM aspirate was incubated with CCR7-BV421 for 15 min in the dark at 37°C. Then, the samples were incubated with multiple premixed fluorescence antibodies for 20 min in the dark at room temperature. The final volume was 200 μl. T cells subsets and surface antibodies staining were performed in two 11-color panels including the following antibodies. CD45-BUV395 (clone HI30, BD) was used

TABLE 1 Peripheral blood sample characteristics.

	DN-CML	TKI-F	Pre-MMR	MMR	HI
Cases	16	9	10	10	12
Status	CP/BC(14/2)	CP/AP/BC (4/3/2)	CHR	CHR	_
Age (median; range)	45.5 (32-74)	48 (35-68)	39.5 (28-79)	40.5 (21-79)	42.5 (21-74)
Gender (male/female)	9/7	7/2	6/3	3/6	6/6
Diagnosis data (median, range)					
BCR-ABL1 (IS)%	95.6 (13.4-240.0)	32 (11.8-194.4)	2.35 (0.005-9.1)	0.029 (0.028-0.09)	
TKI duration (median, range) months	_	28 (14-120)	7 (1-83)	47 (5-108)	

DN, de novo; CP, chronic phase; AP, acceleration phase; BC, blast crisis; CHR, clinical hematologic remission; IS, international standard.

to identify $CD45^{high}$ cells which can rule out tumor cells. CD3-AF700 (clone UCHT1, BD), CD4-APC-H7 (clone RPA-T4, BD), CD8-APC-H7 (clone SK1, BD), CD45RA-Percp-cy5 (clone HI100, Biolegend), CCR7-BV605 (clone 3D12, BD) and CD69-PE-cy7 (clone FN50, BD) were used to identify $CD4^+$ or $CD8^+$ T subsets. CD38-APC (clone HIT2, BD), BTLA-PE-CF594 (clone J168-540, BD), TIGIT-BV421 (clone A15153G, Biolegend) and CD28-BB515 (clone CD28.2, BD) were used in Tube 1, CD57-APC (clone NK-1, BD), PD-1-BV421 (clone EH12.2H7, Biolegend), and HLA-DR-PE-CF594 (clone G46-6, BD) were used in Tube 2. DCs cells and surface antibodies staining were performed in 5-color panels including the following antibodies. CD45-BUV395 (clone HI30, BD), HLA-DR-PE-CF594 (clone G46-6, BD), Lin-FITC (CD3, CD14, CD16, CD20, CD56, cat:340546, BD), CD80-PE (clone L307.4, BD), CD86-PE-cy7 (clone FUN-1, BD). The samples were lysed using lysis buffer (BD; Cat: 555899) for 15-20 min and washed and suspended in phosphate buffer saline (PBS). Finally, 20 µl of absolute count microsphere (Thermos; Cat: C36950) were added to the samples to calculate the absolute number of cells. A minimum of 20,000 $CD3^+$ T cells and 2000 DC cells were acquired by flow cytometry (FACS Fortessa, BD Bioscience) and analyzed using Flowjo 10.6. FCS.

Statistical analysis

All data were represented as medians, and differences between every two groups were analyzed by the Mann-Whitney U test. The statistical analysis and figure generation were performed using GraphPad Prism version 8.02 software. Significance is indicated as $P < 0.05$.

Results

A higher percentage of PD-1^+CD8^+ T cells in the PB of CML patients of different statuses

The gating strategy for identifying the CD4+ and CD8+ T cells and their phenotypic characteristics was shown in Figure 1A. We first identified the absolute number of $CD3^+$, $CD4^+$, and $CD8^+$ T cells in PB and BM in each CML group and found that there was a slightly increased trend for $CD3^+$ T cells (1,133 cells/µl vs 2,064 cells/µl, $P = 0.0883$) and a significant increase in $CD8^+$ T cells in the PB of DN-CML patients compared with HIs (368 cells/µl vs 1,581 cells/µl, $P = 0.0178$) (Figure 1B). In the BM, $CD3^+$ (616 cells/µl vs 1320 cells/µl $P = 0.0015$), $CD4^+$ (301 cells/µl vs 671 cells/µl, $P = 0.0117$), and $CD8^+$ (210 cells/µl vs 507 cells/µl, $P = 0.0005$) T cells were all significantly increased in DN-CML patients compared with HIs (Figure 1C). No significant differences were observed between other CML groups and HIs.

Next, we compared the expression of CD38, CD69, HLA-DR, CD28, CD57, BTLA, TIGIT, and PD-1 on the $CD4^+$ and $CD8^+$ T subsets in PB for each CML group. The results demonstrated that the expression of the activation marker CD38 on the $CD4^+$ T subset was significantly decreased in TKI-F patients compared with HIs (19.6% vs 10.5%, $P = 0.0020$) (Figures 1D and F), while the level of CD69 and HLA-DR also showed a decreasing trend on the $CD4^+$ and $CD8^+$ T subset respectively (Figure 1F). These alterations suggest that the activation capacity of $CD4^+$ and $CD8^+$ T cells from TKI-F patients may be impaired. In addition, a lower level of $CD69^+CD4^+$ T cells (5.46% vs 1.89%, $P < 0.0001$) was found in MR patients compared to

TABLE 2 Bone marrow sample characteristics.

	DN-CML	TKI-F	MR	HI
Cases	11	6	6	9
Status	CP/AP (10/1)	CP/AP/CHR (1/2/3)	CHR	CHR
Age (median; range)	45 (32-74)	42.5 (35-68)	43 (25-79)	35.5 (19-62)
Gender (male/female)	7/4	4/2	3/3	4/5

DN, de novo; CP, chronic phase; AP, acceleration phase; BC, blast crisis; CHR, clinical hematologic remission; IS, international standard.

TABLE 3 TKI-F PB sample characteristics.

	Age/ Gender	Status	BCR-ABL 1 (IS) %	Mutation in ABL1 kinase region	TKI-Duration(months)	TKI-drug
P1	46/M	BC	89.723	N	14	Imatinib
P2	50/M	AP	124.154	T315I	50	Nilotinib
P3	48/M	AP	118.073	N	26	Dasatinib
P4	35/M	BC	45.931	N	20	Dasatinib
P5	51/M	AP	49.931	F317I	96	Imatinib
P6	56/F	CP	13.732	c.1423_1424ins35 (p.Cys475fs*11)	28	Nilotinib
P7	35/M	CP	194.110	N	17	Imatinib
P8	39/F	CP	58.121	T315I	40	Imatinib
P9	68/M	CP	11.843	N	120	Imatinib

CP, chronic phase; AP, acceleration phase; BC, blast crisis; IS, international standard.

HIs (Figures 1D, F). For the exhausted and senescent molecular expression pattern, we found that the level of PD-1$^+$CD8$^+$ T cells was significantly increased in DN-CML (25.3% vs 16.5%, P = 0.0231), TKI-F (24.6% vs 16.5%, P = 0.0076), and MR (23.8% vs 16.5%, P = 0.0016) patients when compared with HIs (Figure 1F).

An increased PD-1 level in the CD8$^+$ T_{EM} and T_{EMRA} subsets in PB from CML patients

To further understand the immunophenotypic alterations in each T cell subset. We divided the CD4$^+$ and CD8$^+$ T cells into T_N (CD45RA$^+$CCR7$^+$), T_{CM} (CD45RA$^-$CCR7$^+$), T_{EM} (CD45RA$^+$CCR7$^-$), and T_{EMRA} (CD45RA$^-$CCR7$^-$) subsets based on CD45RA and CCR7 expression. We compared activated/inhibitory/senescent phenotypic characteristics of each subset in the PB of the patient groups and HIs. The gating strategy is shown in Figure 2A. To exhibit the differences of a single marker in the T cell subsets, the fold change (FC) of the mean value between each CML group and HIs was shown in volcano figures (Figures 2B-E). We found that the expression of the activation markers CD38, CD69, and HLA-DR decreased on T_N and T_{CM} subsets in DN-CML patients and further decreased in TKI-F patients. Moreover, these abnormalities gradually restored to normal levels at the time of remission. The detailed expression characteristics of each group were shown in Supplementary Figure 1. Unlike T_N and T_{CM}, which exhibit a lower level of activation markers, the T_{EM} and T_{EMRA} subsets mainly demonstrate increased expression of PD-1 in the PB of the CML patient groups. (Figures 2B-E). We further compared PD-1 expression on T_{EM} and T_{EMRA} cells between the CML patients and HIs. The percentage of PD-1$^+$CD4$^+$ T_{EM} cells significantly increased in DN-CML (31.54%, P = 0.0032), TKI-F (35.47%, P = 0.0026), and Pre-MMR (31.7%, P = 0.0044) patients compared to HIs (21.2%). No significant difference was observed in the CD4$^+$ T_{EMRA} subset between CML patients and HIs. Similarly, the proportion of PD1$^+$CD8$^+$ T_{EM} cells increased in DN-CML (41.90%, P = 0.0006), TKI-F (33.28%, P = 0.0101), Pre-MMR (33.75%, P = 0.0039), and even MMR (29.56%, P = 0.0101) patients compared with HIs (20.08%). In addition, the level of PD-1$^+$CD8$^+$ T_{EMRA} significantly increased in DN-CML (16.57%, P = 0.0083), TKI-F (18.73%, P = 0.0019), and Pre-MMR (17.32%, P = 0.0052) patients but returned to a normal level in some MMR patients (15.27%, P = 0.3686) when compared with HIs (7.94%) (Figure 2F).

Increased PD-1$^+$/TIGIT$^+$CD8$^+$ T_{RM} cells in BM of DN-CML patients

The immunosuppressive BMM protects malignant hematopoietic stem cells from immunological surveillance, which may contribute to leukemia relapse (23). We examined the expression of each marker on BM CD8$^+$ T cells and subsets. The results revealed no significant difference in the expression of each of the above markers on total CD8$^+$ T cells between each CML group and HIs. However, when looking at the subset level, we found a significantly decreased level of HLA-DR$^+$CD8$^+$$T_{CM}$ in DN-CML (36.75% vs 12.40%, P = 0.0462) and a further decrease in TKI-F (36.75% vs 6.71%, P = 0.0087) and MR (37.75% vs 5.20%, P = 0.0082) patients compared to the control group. For other markers, only an increased percentage of TIGIT$^+$CD8$^+$ T_{EMRA} (42.60% vs 75.45%, P = 0.0256) was observed in TKI-F patients (Supplementary Figure 2).

With the exception of the classic memory T cell subsets, we also examined the expression of the above markers on T_{RM} cells, which are abundant in non-lymphoid tissues, such as skin, lung, and BM (28). T_{RM} cells express a low level of CD45RA and lack CCR7, and CD69 is a key marker to identify T_{RM} (CD45RA$^+$CCR7$^-$CD69$^+$) from T_{EM} cells (29). Detailed gating strategies are shown in Figure 3A and the expression of PD-1 and TIGIT in the BM of HI and CML patients were shown in Figure 3C. These results demonstrated that the number of CD8$^+$ T_{RM} cells increased in DN-CML patients but there was no difference in the TKI-F and MR groups compared to HIs (Figure 3B). Further, we also found a significantly increased percentage of PD-1$^+$CD8$^+$ T_{RM} cells (53.50% vs 73.30%, P = 0.0409) and TIGIT$^+$CD8$^+$ T_{RM} (61.40% vs 77.00%, P = 0.0465) cells in DN-CML patients compared with HIs (Figure 3D).

10.3389/fimmu.2023.1078118

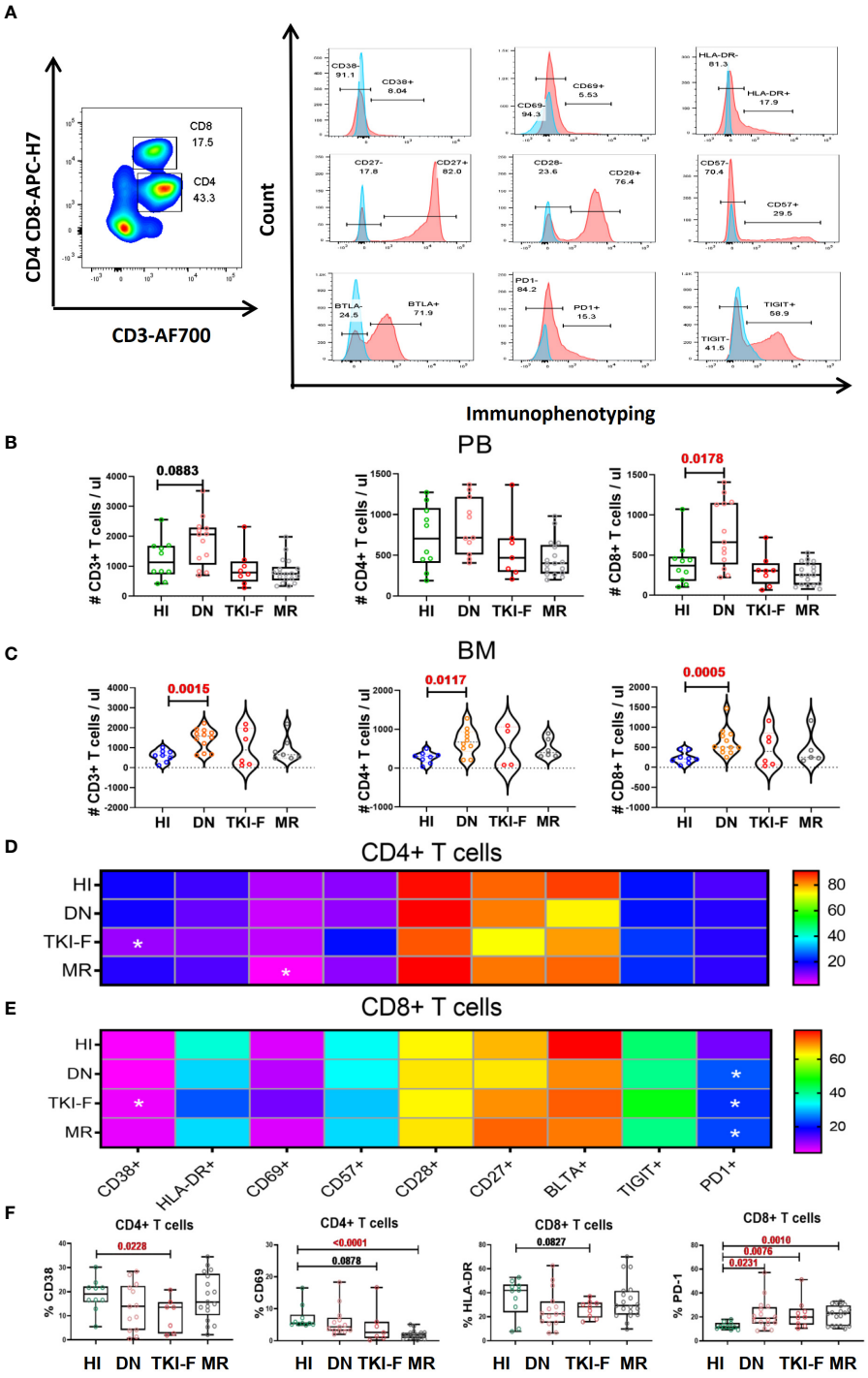

FIGURE 1
TKI-F patients exhibit a lower level of the activation markers CD38 and CD69 on $CD4^+$ T cells and HLA-DR on $CD8^+$ T cells, and the exhaustion marker PD-1 increased on PB-$CD8^+$ T cells in all CML groups. **(A)** The top figure shows the gating strategy for CD38, CD69, HLA-DR, CD28, CD57 BTLA, TIGIT, and PD-1 in the $CD4^+$ and $CD8^+$ populations by flow cytometry. The absolute number of $CD3^+$, $CD4^+$, and $CD8^+$ T cells in the PB and BM **(B, C)** The darkness of the color represents the mean frequency of a single immune marker on $CD4^+$ **(D)** and $CD8^+$ **(E)** T cells in PB from HIs and DN-CML, TKI-F, and MR patients. The asterisk (*) represents a significant alteration in CML patients compared with HIs. **(F)** The proportion of $CD38^+CD4^+$, $CD69^+CD4^+$, $HLA\text{-}DR^+CD8^+$, and $PD\text{-}1^+CD8^+$ in PB from HIs and DN-CML, TKI-F, and MR patients. HIs-PB (CD4, n = 12, CD8, n = 12), DN-CML-PB (CD4, n = 12, CD8, n = 16), TKI-F-PB (CD4, n = 7, CD8, n = 9), and MR-PB (CD4, n = 17, CD8, n = 20). The *P* values shown are from the Mann-Whitney U test between groups.

10.3389/fimmu.2023.1078118

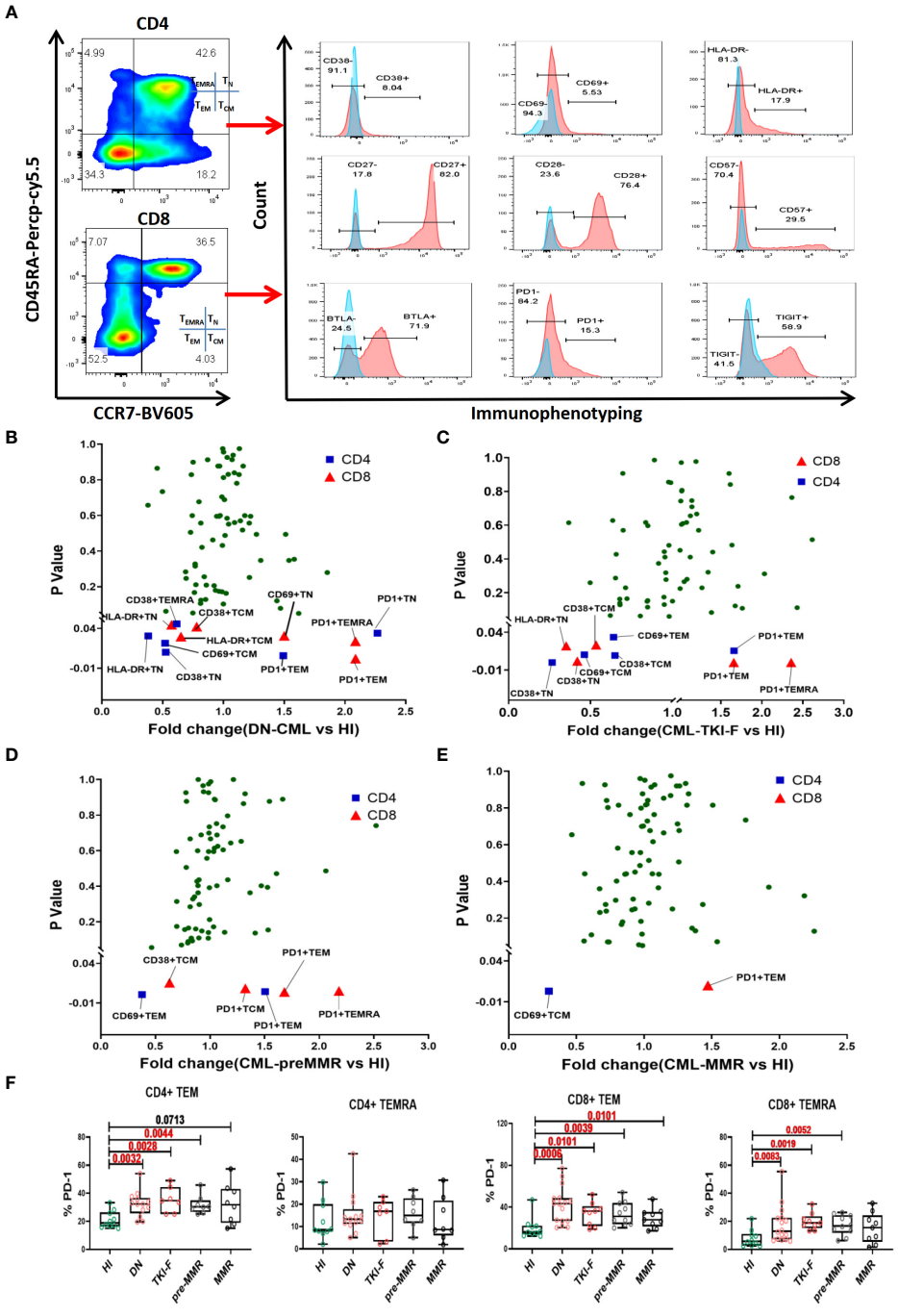

FIGURE 2
The abnormal immunophenotype of PB T cell subsets distributed in DN-CML and TKI-F patients gradually returning to normal in pre-MMR and MMR groups. **(A)** Gating strategy for the $CD4^+$ and $CD8^+$ T cells subsets in one HI. CD45RA and CCR7 were used to divide the T cells into T_N ($CD45RA^+CCR7^+$), T_{CM} ($CD45RA^-CCR7^+$), T_{EM} ($CD45RA^-CCR7^-$), and T_{EMRA} ($CD45RA^+CCR7^-$) cells. The proportion of the T cell subset single-marker immunophenotypes in HIs and DN-CML **(B)**, TKI-F **(C)**, pre-MMR **(D)**, and MMR **(E)** patients were compared (Mann-Whitney U test). The *P-value* plotted on the vertical axis of volcano figure. Immunologic characteristics with the mean percentage of fold change (FC) > 1 are enriched in CML patients, and FC < 1 was more frequent in HIs. The blue and red points respectively represent $CD4^+$ and $CD8^+$ T cells. **(F)** The frequency of PD-1 on $CD4^+$ T_{EM}, $CD4^+$ T_{EMRA}, $CD8^+$ T_{EM}, and $CD8^+$ T_{EMRA} cells in PB from HIs and DN-CML, TKI-F, pre-MMR, and MMR patients. HIs-PB (CD4, n = 10, CD8, n = 10), DN-CML-PB (CD4, n = 13, CD8, n = 16), TKI-F-PB (CD4, n = 7, CD8, n = 9) and MR-PB (CD4, n = 18, CD8, n = 20). The *P* values shown are from the Mann-Whitney U test between groups.

Decreased expression of CD86 on DC cells in PB and BM from DN-CML patients

DCs can provide costimulatory signals driven by the molecules CD80 and CD86 to induce T cell activation and functional differentiation. Here, we identified DCs ($HLA\text{-}DR^+Lin^-$) from the $CD45^{high}$ population aiming to eliminate the interference from leukemia cells. Next, we analyzed the expression of CD80 and CD86 on DCs, and detailed gating strategies are presented in Figure 4A. The results show that the percentage of $CD86^+$ DCs

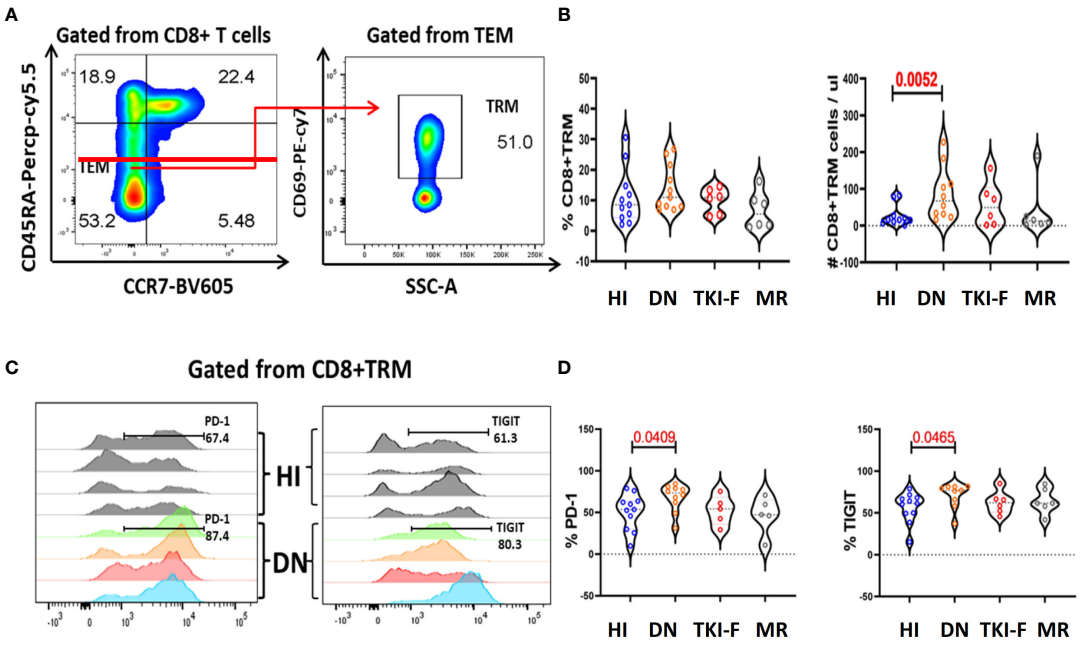

FIGURE 3
The absolute numbers of $CD8^+T_{RM}$ cells increased in the BM of DN-CML patients while accompanied by an elevated expression of PD-1 and TIGIT. **(A)** Gating strategies to indicate the T_{RM} cells. $CD45RA^-$ and $CCR7^-$ were used to identify the T_{EM} subsets and then T_{RM} cells were further gated by CD69 expression. **(B)** The percentage and absolute number of $CD8^+T_{RM}$ cells in HIs, DN-CML, TKI-F, and MR patients. **(C)** Flow-cytometry analysis detected the frequency of $PD\text{-}1^+CD8^+$ T_{RM} (left) and $TIGIT^+CD8^+$ T_{RM} (right) in HIs (top: n = 4) and DN-CML (below: n = 4). **(D)** Increased proportion of PD-1 (left) and TIGIT (right) on $CD8^+$ T_{RM} cells in BM from HIs (n = 10) and DN-CML (n = 10), TKI-F (n = 6), and MR (n = 6) patients. The *P* values shown are from the Mann-Whitney U test between groups.

decreased in PB (41.2% vs 21.5%, $P = 0.0011$) and BM (30.9% vs 12.45%, $P = 0.0207$) of DN-CML patients compared to controls. Previous studies have reported that DCs expressing a normal level of CD80 and lower CD86 act as immature DCs. We further assayed CD80 and CD86 on T cells in the CML groups and HIs. The result demonstrated a significantly decreased ratio of CD80/CD86 both in the PB (0.42 vs 0.90, $P = 0.0173$) and BM (0.19 vs 0.36, $P = 0.0650$) of DN-CML patients, and 5 patients had an inverse ratio. Additionally, the CD86 expression and CD80/CD86 ratio could return to a normal level after TKI treatment (Figures 4B, C).

Discussion

Our previous study found that memory T cell subset distribution skewed toward a terminally differentiated status in DN-CML patients and restore in MR-CML patients, suggesting that the T cell subset distribution might be important for inducing and maintaining remission in CML patients (30). In this study, we further found that the immunophenotype of the T cell subsets (T_N, T_{CM}, T_{EM}, T_{EMRA}, T_{RM}) was associated with the disease status and location. On the level of the total $CD4^+$ and $CD8^+$ population, we only found a few function markers or even no markers were changed in the PB and BM of patients respectively, however, further analysis of the T cell subsets revealed that the markers representing the activation and proliferation (CD38, HLA-DR, and CD69) (31, 32) were decreased in the less differentiated T_N and T_{CM} subsets in the DN-CML and TKI-F patients, while gradually recovered in the pre-MMR and MMR patients. In addition, the higher expression of PD-1 on peripheral $CD8^+$ T cells detected in all the patients treated with TKI, especially for TKI-F patients, this consistent with recent research that a higher percentage of PD-1 detected on $CD4^+$, $CD8^+$ and Treg cells in CML patients resistant to TKI (33), however, on the level of T cell subsets, we can see that the percentage of PD-1 high expression T cell subsets mainly decreased in the patients who achieved MMR but not in TKI-F and Pre-MMR patients. Those results indicated that dynamic monitoring of the changes of these immune phenotypes in the level of T cell subsets may help to predict the effects and outcomes after TKI treatment.

PD-1 and TIGIT are two classic IC receptors that negatively modulate T-cell responsiveness and limit T-cell activation during antigen exposure (34–36). Consistent with previous studies, our results also demonstrated that the level of $PD\text{-}1^+CD8^+$ T cells increased in the PB but not BM of DN-CML patients (18, 37), but taking a close look at the subsets, we found that $CD8^+$ T_{EM} and T_{EMRA} subsets were mainly impaired, while the $CD4^+$ T_{EM} also affected. In the BM T cell subsets, the higher TIGIT expression was only found in the $CD8^+$ T_{EMRA} subset in the TKI-F group but not in the total $CD8^+$ level. T_{EM} and T_{EMRA} are the main effector subsets contributing to quickly clearing pathogens. The increased expression of PD-1 and TIGIT on these two subsets may attenuate their anti-leukemia function. A clinical trial aiming to improve the MMR ratio for TKI-F patients by adding anti-PD-1 nivolumab/pembrolizumab to TKI inhibitors has been completed, however, approximately 40% of the patients still were TKI treatment failed (NCT#02011945). Our data may help to discover more precise anti-leukemia immune therapy by focusing on studying the pathologic mechanism of the dysfunction of T_{EM} and T_{EMRA} subsets in the future.

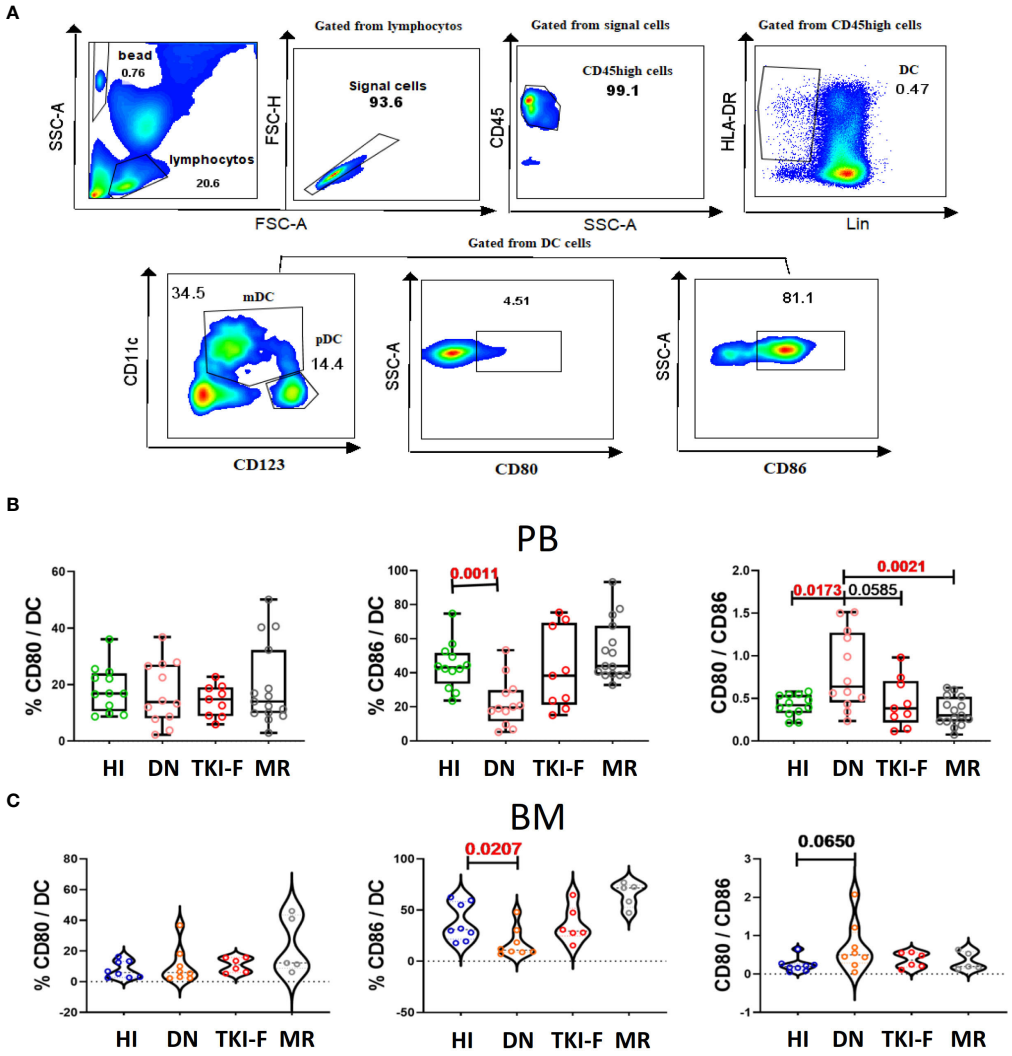

FIGURE 4
PB and BM DCs cells from DN-CML patients express a lower percentage of CD86 and with an unbalance CD80/CD86 ratio. **(A)** Gating strategy to identify DCs cells and the expression of CD80/CD86 on DCs cells. The $CD45^{high}$ population was used to eliminate immature cells, and then $HLA\text{-}DR^{+}$ and Lin^{-} (CD3, CD19, CD56, CD14 and CD16) was used to identify that DCs. $CD80^{+}$ and $CD86^{+}$ were further used to gate $CD80^{+}$ DCs and $CD86^{+}$ DCs cells. **(B)** The frequency of $CD80^{+}$ DC, $CD86^{+}$ DC, and CD80/CD86 ratio in PB **(B)** and BM **(C)** of HIs (PB, n = 12, BM, n = 8) and DN-CML (PB, n = 12, BM, n = 8), TKI-F (PB, n = 9, BM, n = 6), and MR (PB, n = 17, BM, n = 5) patients. The *P* values shown are from the Mann-Whitney U test between groups.

Except for the classical memory T cell subsets, T_{RM} is a specific memory T cell located in unique tissue and organs, which provides a lifelong immune protective effect to the regional tissue (28, 38, 39). Increasingly studies have found that the quantity and quality of T_{RM} cells are critical targets for immunotherapeutic modulation and prognostic outcomes in tumor (14). However, there are still no reports that describe $CD8^{+}$ T_{RM} alterations in the BM of CML patients. Here, we first time found that the number of $CD8^{+}$ T_{RM} cells is significantly increased in the BM of DN-CML patients accompanied by a higher expression of TIGIT and PD-1, however, patients who received TKI treatment not shown the same pattern. This result indicates that BM T_{RM} cells from DN-CML patients may be impaired by the leukemia cell. Further study of the function of $CD8^{+}$ T_{RM} cells from the BM of DN-CML patients and looking for the BM microenvironment mechanisms which lead to this result may help to understand more immune dysfunction mechanisms during the development of CML.

For the proper functioning of T cells, the co-stimulatory signal provided by DCs is an essential determinant. Through interaction with CD80 and CD86 on the DC surface, CD28 modulates T cell proliferation, differentiation, survival, and cytokine secretion (40, 41). Indeed, previous studies have found that CD80 may prefer to combine with PD-L1 and CTLA-4 if CD80 had an advantage in expression (42). Several studies have found that CTLA4 expression regulatory T cells accumulated in the leukemia environment of DN-CML patients, while CML cells increased the expression of PD-L1 (18, 33, 43). Therefore, though the expression of $CD28^{+}$ T cells remains at a normal level, the decreased level of $CD86^{+}$ DCs and the unbalanced ratio of CD80/CD86 may also prevent the activation of T cells in DN-CML patients. Further explore the mechanism of the downregulation

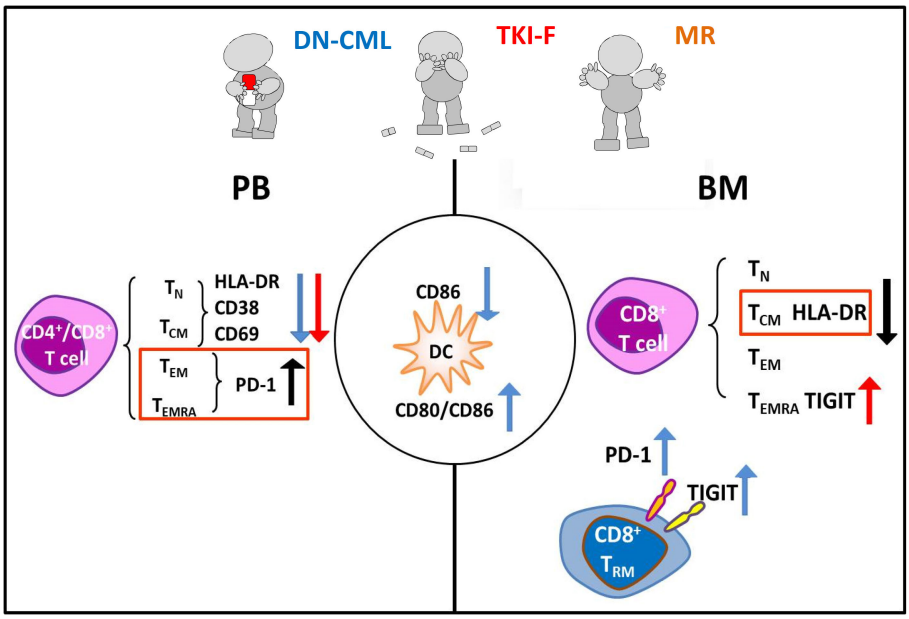

FIGURE 5
Model illustrating the immunophenotypic differences of the T cells subsets in PB and BM in HIs and CML groups. The left and right of the figure respectively show the alterations of PB and BM, and the center represents the common change in PB and BM. Blue, red, and black respectively represent alterations in DN-CML, TKI-F, and MR.

of CD86 on DCs cells using RNA sequencing and other methods is necessary for developing DCs related immune treatment strategies.

Here, we further observed that the early differentiated T cell subsets (T_N, T_{CM}) were inadequate activation and effector T cell subsets (T_{EM}, T_{EMRA}, T_{RM}) exhibited diverse exhausted phenotypes in the PB and BM of CML patients with different disease statuses, which may impair T cells' long-term immunological surveillance and simultaneously attenuate their ability to remove leukemia cells. Meanwhile, the DCs cells may be unable to valid stimulate T activation due to the decreased expression of CD86 and unbalanced CD80/CD86 ratio in DN-CML patients (Figure 5). These complex immune defects are worth further immune therapy strategy development. For example, immunotherapeutic methods not only need to inhibit PD-1 expression on effector T cells but also need to enhance the activation T_N and T_{CM} cells, as well as increase the co-stimulate function of DCs cells synergistically.

Data availability statement

The original contributions presented in the study are included in the article further inquiries can be directed to the corresponding authors.

Ethics statement

The studies involving human participants were reviewed and approved by Ethics Committee of the Medical School of Jinan University. The patients/participants provided their written informed consent to participate in this study. Written informed consent was obtained from the individual(s) for the publication of any potentially identifiable images or data included in this article.

Author contributions

LX and YQL contributed to the concept development and study design. DY, LX, LL, and XBZ performed the laboratory studies. YHL, JZ, XFZ, XH, JW and XD collected the clinical information of patients. DY and LX drafted the manuscript. SC managed the laboratory reagents and financial affairs. DY, LX and YQL helped modify the manuscript. All authors contributed to the article and approved the submitted version.

Funding

This work was supported by the [National Natural Science Foundation of China] under Grant [Nos. 82000108, 82070152, 91642111, 82293630, 82293632, 81890991], [China postdoctoral science foundation] under Grant [No. 2018M640884], [Guangdong Province Science and Technology Project] under Grant [2020A1515110310], [Guangzhou Science and Technology Project] under Grant [201803040017], and [Key Laboratory for Regenerative Medicine of Ministry of Education Project] under Grant [ZSYXM202001].

Acknowledgments

We thank the flow facility of the Biological Translational Research Institute of Jinan University as well as Yuanqing Tu, a research

assistant from the Translational Research Institute of Jinan University. We also would like to thank the volunteers who donated blood to this project.

Conflict of interest

The authors declare that the research was conducted in the absence of any commercial or financial relationships that could be construed as a potential conflict of interest.

Publisher's note

Supplementary material

The Supplementary Material for this article can be found online at: https://www.frontiersin.org/articles/10.3389/fimmu.2023.1078118/full#supplementary-material

SUPPLEMENTARY FIGURE 1
$CD4^+$ or $CD8^+$ T_N and T_{CM} cells from the PB of DN-CML patients have a lower percentage of the activation markers CD38 and HLA-DR, and this is further decreased in TKI-F patients. The frequency of CD38, CD69, and HLA-DR on $CD4^+$ T_N **(A)**, $CD4^+$ T_{CM} **(B)**, $CD8^+$ T_N **(C)** and $CD8^+$ T_{CM} **(D)** in the PB of HIs (PB, n = 12, BM, n = 8) and DN-CML (PB, n = 12, BM, n = 8), TKI-F (PB, n = 9, BM, n = 6) pre-MMR (CD4, n = 9, CD8, n = 9), and MMR (CD4, n = 8, CD8, n = 8) patients. The *P* values shown are from the Mann-Whitney U test between groups. Significance is indicated as *, $P < 0.05$ in red.

SUPPLEMENTARY FIGURE 2
A decreased level of $HLA\text{-}DR^+CD8^+$ T_{CM} cells exists in all CML groups, and TKI-F patients have increased expression of the exhaustion marker TIGIT on BM $CD8^+$ T_{EMRA} cells. The frequency of CD38, CD69, HLA-DR, CD57, CD28, BTLA, TIGIT, and PD-1 in $CD8^+$ T cells **(A)**, $CD8^+T_N$ **(B)**, $CD8^+T_{CM}$ **(C)**, $CD8^+T_{EM}$ and $CD8^+T_{EMRA}$ among HIs (n = 8) and DN-CML (n = 11), TKI-F (n = 6) and MR (n = 6) patients. The *P* values shown are derived from the Mann-Whitney U test between groups.

References

1. Ross DM, Branford S, Seymour JF, Schwarer AP, Arthur C, Yeung DT, et al. Safety and efficacy of imatinib cessation for CML patients with stable undetectable minimal residual disease: results from the TWISTER study. *Blood* (2013) 122(4):515–22. doi: 10.1182/blood-2013-02-483750

2. Minciacchi VR, Kumar R, Krause DS. Chronic myeloid leukemia: A model disease of the past, present and future. *Cells* (2021) 10(1):117. doi: 10.3390/cells10010117

3. Ning L, Hu C, Lu P, Que Y, Zhu X, Li D. Trends in disease burden of chronic myeloid leukemia at the global, regional, and national levels: a population-based epidemiologic study. *Exp Hematol Oncol* (2020) 9(1):29. doi: 10.1186/s40164-020-00185-z

4. Hou JZ, Ye JC, Pu JJ, Liu H, Ding W, Zheng H, et al. Novel agents and regimens for hematological malignancies: recent updates from 2020 ASH annual meeting. *J Hematol Oncol* (2021) 14(1):66. doi: 10.1186/s13045-021-01077-3

5. Ciftciler R, Haznedaroglu IC. Tailored tyrosine kinase inhibitor (TKI) treatment of chronic myeloid leukemia (CML) based on current evidence. *Eur Rev Med Pharmacol Sci* (2021) 25(24):7787–98. doi: 10.26355/eurrev_202112_27625

6. Baccarani M, Gugliotta G, Castagnetti F, Soverini S, Rosti G. A review and an update of European LeukemiaNet recommendations for the management of chronic myeloid leukemia. *Chronic Myeloid Leuk* (2016), 55–69. doi: 10.1007/978-3-319-33198-0_4

7. Bachireddy P, Hainz U, Rooney M, Pozdnyakova O, Aldridge J, Zhang W, et al. : Reversal of *in situ* T-cell exhaustion during effective human antileukemia responses to donor lymphocyte infusion. *Blood* (2014) 123(9):1412–21. doi: 10.1182/blood-2013-08-523001

8. Cortes J, Lang F. Third-line therapy for chronic myeloid leukemia: current status and future directions. *J Hematol Oncol* (2021) 14(1):44. doi: 10.1186/s13045-021-01055-9

9. Sallusto F, Geginat J, Lanzavecchia A. Central memory and effector memory T cell subsets: function, generation, and maintenance. *Annu Rev Immunol* (2004) 22:745–63. doi: 10.1146/annurev.immunol.22.012703.104702

10. Cavanagh LL, Bonasio R, Mazo IB, Halin C, Cheng G, van der Velden AW, et al. Activation of bone marrow-resident memory T cells by circulating, antigen-bearing dendritic cells. *Nat Immunol* (2005) 6(10):1029–37. doi: 10.1038/ni1249

11. Surh CD, Sprent J. Homeostasis of naive and memory T cells. *Immunity* (2008) 29 (6):848–62. doi: 10.1016/j.immuni.2008.11.002

12. van den Broek T, Borghans JAM, van Wijk F. The full spectrum of human naive T cells. *Nat Rev Immunol* (2018) 18(6):363–73. doi: 10.1038/s41577-018-0001-y

13. Zhang Y, Liu Z, Wei W, Li Y. TCR engineered T cells for solid tumor immunotherapy. *Exp Hematol Oncol* (2022) 11(1):38. doi: 10.1186/s40164-022-00291-0

14. Noviello M, Manfredi F, Ruggiero E, Perini T, Oliveira G, Cortesi F, et al. Bone marrow central memory and memory stem T-cell exhaustion in AML patients relapsing after HSCT. *Nat Commun* (2019) 10(1):1065. doi: 10.1038/s41467-019-08871-1

15. Savas P, Virassamy B, Ye C, Salim A, Mintoff CP, Caramia F, et al. Single-cell profiling of breast cancer T cells reveals a tissue-resident memory subset associated with improved prognosis. *Nat Med* (2018) 24(7):986–93. doi: 10.1038/s41591-018-0078-7

16. Rohon P, Porkka K, Mustjoki S. Immunoprofiling of patients with chronic myeloid leukemia at diagnosis and during tyrosine kinase inhibitor therapy. *Eur J Haematol* (2010) 85(5):387–98. doi: 10.1111/j.1600-0609.2010.01501.x

17. Humlova Z, Klamova H, Janatkova I, Malickova K, Kralikova P, Sterzl I, et al. Changes of immunological profiles in patients with chronic myeloid leukemia in the course of treatment. *Clin Dev Immunol* (2010) 2010:137320. doi: 10.1155/2010/137320

18. Hughes A, Clarson J, Tang C, Vidovic L, White DL, Hughes TP, et al. CML patients with deep molecular responses to TKI have restored immune effectors and decreased PD-1 and immune suppressors. *Blood* (2017) 129(9):1166–76. doi: 10.1182/blood-2016-10-745992

19. Boddu P, Kantarjian H, Garcia-Manero G, Allison J, Sharma P, Daver N. The emerging role of immune checkpoint based approaches in AML and MDS. *Leuk Lymphoma* (2018) 59(4):790–802. doi: 10.1080/10428194.2017.1344905

20. Bruck O, Blom S, Dufva O, Turkki R, Chheda H, Ribeiro A, et al. Immune cell contexture in the bone marrow tumor microenvironment impacts therapy response in CML. *Leukemia* (2018) 32(7):1643–56. doi: 10.1038/s41375-018-0175-0

21. Chen S, Yang L, Chen S, Li Y. TCR zeta chain expression in T cells from patients with CML. *Hematology* (2009) 14(2):95–100. doi: 10.1179/102453309X385241

22. Chen X, Woiciechowsky A, Raffegerst S, Schendel D, Kolb HJ, Roskrow M. Impaired expression of the CD3-zeta chain in peripheral blood T cells of patients with chronic myeloid leukaemia results in an increased susceptibility to apoptosis. *Br J Haematol* (2000) 111(3):817–25. doi: 10.1111/j.1365-2141.2000.02415.x

23. Shafat MS, Gnaneswaran B, Bowles KM, Rushworth SA. The bone marrow microenvironment - home of the leukemic blasts. *Blood Rev* (2017) 31(5):277–86. doi: 10.1016/j.blre.2017.03.004

24. Mendez-Ferrer S, Bonnet D, Steensma DP, Hasserjian RP, Ghobrial IM, Gribben JG, et al. Bone marrow niches in haematological malignancies. *Nat Rev Cancer* (2020) 20 (5):285–98. doi: 10.1038/s41568-020-0245-2

25. Swatler J, Turos-Korgul L, Kozlowska E, Piwocka K. Immunosuppressive cell subsets and factors in myeloid leukemias. *Cancers (Basel)* (2021) 13(6):1203. doi: 10.3390/cancers13061203

26. Anderson NM, Simon MC. The tumor microenvironment. *Curr Biol* (2020) 30 (16):R921–5. doi: 10.1016/j.cub.2020.06.081

27. Yu S, Ren X, Li L. Myeloid-derived suppressor cells in hematologic malignancies: two sides of the same coin. *Exp Hematol Oncol* (2022) 11(1):43. doi: 10.1186/s40164-022-00296-9

28. Mueller SN, Mackay LK. Tissue-resident memory T cells: local specialists in immune defence. *Nat Rev Immunol* (2016) 16(2):79–89. doi: 10.1038/nri.2015.3

29. Cibrian D, Sanchez-Madrid F. CD69: from activation marker to metabolic gatekeeper. *Eur J Immunol* (2017) 47(6):946–53. doi: 10.1002/eji.201646837

30. Yao D, Xu L, Tan J, Zhang Y, Lu S, Li M, et al. Re-balance of memory T cell subsets in peripheral blood from patients with CML after TKI treatment. *Oncotarget* (2017) 8 (47):81852–9. doi: 10.18632/oncotarget.20965

31. Cesano A, Visonneau S, Deaglio S, Malavasi F, Santoli D. Role of CD38 and its ligand in the regulation of MHC-nonrestricted cytotoxic T cells. *J Immunol* (1998) 160 (3):1106–15. doi: 10.4049/jimmunol.160.3.1106

32. Palacios R, Moller G, Claesson L, Peterson PA. HLA-DR antigens induce proliferation and cytotoxicity of T cells against haptenated (TNP and FITC) self structures. *Immunogenetics* (1981) 14(5):367–82. doi: 10.1007/BF00373317

33. Harrington P, Dillon R, Radia D, McLornan D, Woodley C, Asirvatham S, et al. Chronic myeloid leukaemia patients at diagnosis and resistant to tyrosine kinase inhibitor therapy display exhausted T-cell phenotype. *Br J Haematol* (2022) 198(6):1011–5. doi: 10.1111/bjh.18302

34. Dong H, Strome SE, Salomao DR, Tamura H, Hirano F, Flies DB, et al. Tumor-associated B7-H1 promotes T-cell apoptosis: a potential mechanism of immune evasion. *Nat Med* (2002) 8(8):793–800. doi: 10.1038/nm730

35. Iwai Y, Ishida M, Tanaka Y, Okazaki T, Honjo T, Minato N. Involvement of PD-L1 on tumor cells in the escape from host immune system and tumor immunotherapy by PD-L1 blockade. *Proc Natl Acad Sci U.S.A.* (2002) 99(19):12293–7. doi: 10.1073/pnas.192461099

36. Harjunpaa H, Guillerey C. TIGIT as an emerging immune checkpoint. *Clin Exp Immunol* (2020) 200(2):108–19. doi: 10.1111/cei.13407

37. Lee MY, Park CJ, Cho YU, You E, Jang S, Seol CA, et al. Differences in PD-1 expression on CD8+ T-cells in chronic myeloid leukemia patients according to disease phase and TKI medication. *Cancer Immunol Immunother* (2020) 69(11):2223–32. doi: 10.1007/s00262-020-02617-5

38. Di Rosa F, Pabst R. The bone marrow: a nest for migratory memory T cells. *Trends Immunol* (2005) 26(7):360–6. doi: 10.1016/j.it.2005.04.011

39. Amsen D, van Gisbergen K, Hombrink P, van Lier RAW. Tissue-resident memory T cells at the center of immunity to solid tumors. *Nat Immunol* (2018) 19(6):538–46. doi: 10.1038/s41590-018-0114-2

40. June CH, Ledbetter JA, Linsley PS, Thompson CB. Role of the CD28 receptor in T-cell activation. *Immunol Today* (1990) 11(6):211–6. doi: 10.1016/0167-5699(90)90085-N

41. Slavik JM, Hutchcroft JE, Bierer BE. CD28/CTLA-4 and CD80/CD86 families: signaling and function. *Immunol Res* (1999) 19(1):1–24. doi: 10.1007/BF02786473

42. Ke N, Su A, Huang W, Szatmary P, Zhang Z. Regulating the expression of CD80/CD86 on dendritic cells to induce immune tolerance after xeno-islet transplantation. *Immunobiology* (2016) 221(7):803–12. doi: 10.1016/j.imbio.2016.02.002

43. Mumprecht S, Schurch C, Schwaller J, Solenthaler M, Ochsenbein AF. Programmed death 1 signaling on chronic myeloid leukemia-specific T cells results in T-cell exhaustion and disease progression. *Blood* (2009) 114(8):1528–36. doi: 10.1182/blood-2008-09-179697

frontiers | Frontiers in Immunology

TYPE Review
PUBLISHED 20 January 2023
DOI 10.3389/fimmu.2023.1108200

OPEN ACCESS

EDITED BY
Giovanna Schiavoni,
National Institute of Health (ISS), Italy

REVIEWED BY
Stuart Rushworth,
University of East Anglia, United Kingdom
Chunyan Ji,
Shandong University, China

*CORRESPONDENCE
Gülderen Yanıkkaya-Demirel
gulderen.ydemirel@yeditepe.edu.tr

†These authors have contributed equally to this work and share the first authorship

SPECIALTY SECTION
This article was submitted to Cancer Immunity and Immunotherapy, a section of the journal Frontiers in Immunology

RECEIVED 25 November 2022
ACCEPTED 03 January 2023
PUBLISHED 20 January 2023

CITATION
Aru B, Pehlivanoğlu C, Dal Z, Dereli-Çalışkan NN, Gürlü E and Yanıkkaya-Demirel G (2023) A potential area of use for immune checkpoint inhibitors: Targeting bone marrow microenvironment in acute myeloid leukemia. *Front. Immunol.* 14:1108200. doi: 10.3389/fimmu.2023.1108200

A potential area of use for immune checkpoint inhibitors: Targeting bone marrow microenvironment in acute myeloid leukemia

Başak Aru[1†], Cemil Pehlivanoğlu[1†], Zeynep Dal[2], Nida Nur Dereli-Çalışkan[1], Ege Gürlü[2] and Gülderen Yanıkkaya-Demirel[1*]

[1]Immunology Department, Faculty of Medicine, Yeditepe University, Istanbul, Türkiye, [2]School of Medicine, Yeditepe University, Istanbul, Türkiye

Acute myeloid leukemia (AML) arises from the cells of myeloid lineage and is the most frequent leukemia type in adulthood accounting for about 80% of all cases. The most common treatment strategy for the treatment of AML includes chemotherapy, in rare cases radiotherapy and stem cell and bone marrow transplantation are considered. Immune checkpoint proteins involve in the negative regulation of immune cells, leading to an escape from immune surveillance, in turn, causing failure of tumor cell elimination. Immune checkpoint inhibitors (ICIs) target the negative regulation of the immune cells and support the immune system in terms of anti-tumor immunity. Bone marrow microenvironment (BMM) bears various blood cell lineages and the interactions between these lineages and the noncellular components of BMM are considered important for AML development and progression. Administration of ICIs for the AML treatment may be a promising option by regulating BMM. In this review, we summarize the current treatment options in AML treatment and discuss the possible application of ICIs in AML treatment from the perspective of the regulation of BMM.

KEYWORDS

bone marrow microenvironment, immune checkpoint inhibitors (ICI), immune checkpoint proteins (ICP), acute myeloid leukemia, tumor microenvironment

1 Acute myeloid leukemia

Acute myeloid leukemia (AML) stems from the myeloid cell lineage and is defined as the presence of immature myeloid precursors (blast cells) in bone marrow or peripheral blood (1). Although it mostly affects adults, its clinical presentation and features vary among individuals. The latest WHO classification considers AML in 25 subtypes. Even though AML

is mostly seen in blood and bone marrow, extramedullary manifestations can also be seen with certain types. AML manifests with aggressive progression, with an overall 5-year survival rate of approximately 25% (2, 3).

In AML, nonfunctional abnormally proliferated blast cells dominate the bone marrow and thus impair normal hematopoiesis that may result in pancytopenia which will further demonstrate itself with manifestations such as anemia, clotting disorders, and immunosuppression, where the latter increases vulnerability to infections (4–6). In some cases, exceedingly high leukocyte count can increase the risk of disseminated intravascular coagulation and leukostasis of which the latter leads to lethal manifestations related to the central nervous system (CNS) and lungs (7, 8). Patients may experience weakness, fatigue, pulmonary leukostasis and some abnormal bleeding, along with bruising resulting from minor traumas (9–11). Coagulation disorders are considered the most severe presentations of AML and they account for death in 7% of all cases (12).

Diagnosis of AML is made by the presence of 20% blast count in peripheral blood or bone marrow aspirate. Subtypes of the disease is assessed by flow cytometry to define the subtype of the disease, while chromosomal alterations are investigated using cytogenetic approaches, morphological changes in cells can be observed by bone marrow smears, and oncogenic mutations can be detected by genomic sequencing (1, 13).

2 Current treatment strategies in acute myeloid leukemia

Treatment strategies in AML depend on prior toxic exposure, precursor myelodysplasia, karyotypic and molecular abnormalities and patient-specific factors, including assessment of comorbid conditions, age, risk status, or disease situation such as relapsed or refractory. National Comprehensive Cancer Network (NCCN) Clinical Practice Guidelines in Oncology offer annually updated recommendations for the diagnosis and treatment of AML in adults, based on the reviews of recently published clinical trials which have led to significant improvements in treatment. Although details of treatment strategies are not a focus of this review, we will summarize the current therapeutic opportunities to provide a general perspective based on the NHHC 2022 guidelines (14, 15).

The European LeukemiaNet (ELN) risk stratification and the National Comprehensive Cancer Network (NCCN) guidelines classify AML patients into three groups that are associated with specific prognoses and may guide medical decision-making: favorable, intermediate, and poor (16). The classification is based on chromosomal and genetic abnormalities that certainly may have therapeutic significance, and likely to be changed as newer strategies become available. These markers include nucleophosmin 1 (NPM1), FLT3, CCAAT/enhancer-binding protein alpha (CEBPA), IDH1/2, DNA (cytosine-5)-methyltransferase 3A (DNMT3A), KIT, tumor suppressor protein 53 (TP53), Runt-related transcription factor 1 (RUNX1), and additional sex combs like-1 (ASXL1) gene mutations. FLT3 inhibitors (midostaurin, gilteritinib, quizartinib) are effective against FLT3-mutated AML, while IDH inhibitors (ivosidenib, enasidenib) are active against IDH1 or IDH2 mutated AML, respectively, and TP53 inhibitors (eprenetapopt) are effective against secondary AML and therapy-related leukemia. Other targeted therapy options include B-cell lymphoma 2 (Bcl2) inhibitors such as venetoclax; Hedgehog signaling pathway inhibitors such as glasdegib and hypomethylating agents (HMAs: azacytidine, decitabine) (17). Some patients admitted with isolated extramedullary disease may be eligible for systemic radiation therapy. In rare cases, local radiotherapy or surgery may be used for residual disease (18).

Currently, the main treatment for most types of AML is cytotoxic chemotherapy that consists of two phases: remission induction and post-remission consolidation treatments. Although patients are managed according to the same general therapeutic principles, chemotherapy regimens may vary depending on whether the patient is a candidate for intensive or non-intensive therapeutic regimens. In patients eligible for high intensity induction chemotherapy, the "7+3 regimen" of cytarabine plus anthracycline is commonly used (19). Other alternatives include fludarabine + cytarabine + granulocyte colony-stimulating factor + andidarubicin regimens (FLAG-IDA) and mitoxantrone-based cytarabine regimens (20). In addition to these regimens, addition of the kinase inhibitor midostaurin to induction therapy for FLT3-mutant AML patients has become standard (21). For remission consolidation therapies, regimens containing moderate doses of cytarabine are widely used and may improve blood count recovery. Despite the lack of a consensus, in patients who are not considered candidates for intensive therapy, following regimens are often used in the context of clinical trials: Azacitidine or decitabine + venetoclax combination, low dose cytarabine + venetoclax combination, azacitidine + ivosidenib combination (AML with IDH1 mutation), ivosidenib monotherapy for very frail patients (AML with IDH1 mutation) or best supportive care including hydroxyurea for patients who cannot tolerate or refuse any anti-leukemic therapy (20). To be considered in remission, bone marrow biopsy should show normocellular bone marrow while blasts should not exceed 5%; yet many patients develop relapsed and refractory diseases despite therapeutic options (22). Stem cell transplantations are reported to decrease the risk of leukemia relapse more than the standard chemotherapeutic approaches, yet they are also likely to lead to severe complications (23). Another approach in AML treatment is the administration of high doses of chemotherapeutics followed by either an allogeneic or autologous hematopoietic stem cell transplantation (HSCT). Currently, HSCT is the most recognized and frequently used cellular therapeutic option (24).

Antibody–Drug Conjugates (ADC), monoclonal antibodies that are linked to cytotoxic agents are novel treatment options in AML (25). The antibody targets a cell surface antigen that is exclusively expressed on tumor cells, the linker provides stability and enable selective intracellular release, and cytotoxic compound exerts DNA-damaging or microtubule-inhibitory activities (26). Contrary to conventional monoclonal antibodies, antibody conjugates in ADC do not induce any biological response. These antibodies should remain intact in the circulation, they have high target affinity while

exerting limited immunogenicity and cross-reactivity. In 2017, Gemtuzumab ozogamicin (GO) became the first clinically approved ADC for the treatment of CD33-positive AML, and remains as the only FDA approved ADC for AML treatment (26). IMGN632 which combines an anti-CD123 antibody with a unique DNA-alkylating agent is another ADC that revealed promising results when tested in cell lines and animal models of AML as well as primary patient samples, and currently being tested in AML treatment either as monotherapy or in combination with venetoclax and/or azacytidine (27, 28).

Besides the abovementioned therapeutic interventions, other immunotherapeutic strategies in AML include immune checkpoint blockade, bispecific T cell engagers (BiTE), chimeric antigen receptor T cells (CAR-T) and tissue infiltrating lymphocytes (TIL) are under investigation (19, 22). As extensively described in the literature, the expression of inhibitory checkpoint proteins on AML blasts has been recognized as an important immune escape mechanism (29). Immune checkpoint inhibitors are under investigation for treatment of AML in many experimental and clinical studies.

3 Immune checkpoint inhibitors in treatment of acute myeloid leukemia

Immune checkpoints are receptor-based signal cascades that lead to negative regulation of immune cells, enabling escape from immune surveillance that eventually results in failure of tumor cell elimination favoring tumor progression. Immune checkpoint blockade exerts its' anti-cancer effect by promoting the immune response through administration of monoclonal antibodies that target immune checkpoint proteins present on immune cells or tumor cells. Inhibition of immune checkpoints such as cytotoxic T lymphocyte antigen 4 (CTLA-4), programmed death-1 (PD-1), and programmed death-ligand 1 (PD-L1) enhances immune responses by inhibiting negative signaling receptors and supporting immune activation, where, in turn, elimination of the tumor promotes cancer regression. Currently, three different classes of Immune Checkpoint Inhibitors (ICIs); PD-1 inhibitors (cemiplimab, nivolumab, pembrolizumab, dostarlimab), PD-L1 inhibitors (avelumab, atezolimumab, durvalumab), and one CTLA-4 inhibitor (ipilimumab) have been approved by the US Food and Drug Administration (FDA) for the treatment of various malignancies while others targeting T cell immunoglobulin and mucin domain 3 (TIM3) and lymphocyte activating-3 (LAG-3) are still under investigation (30–32). All checkpoint pathways differ from each other according to the stages they involve the in the immune responses as well as their signaling mechanisms; however, the common purpose of ICIs is to observe similar impact on T-cell activity and clinical regression of cancer.

Although ICIs are already being used in the treatment of various malignancies, studies on AML are still ongoing. There are many completed and ongoing experimental studies and clinical trials in distinct phases evaluating ICIs in treatment of AML either as monotherapy or part of a combinational therapy with other agents including chemotherapeutics, HMAs or other immunotherapies. Experimental studies and clinical trials regarding ICIs, either in combination with other therapeutic interventions or alone are summarized below.

3.1 Experimental studies on immune checkpoint inhibitor therapy in acute myeloid leukemia

Importance of IC pathways in immune evasion of AML as well as their blockade with specific agents in AML treatment has been underlined in several experimental studies which involved AML cell lines and murine models.

Constitutive expression of regulatory cell surface antigen CTLA-4 expression in more than 80% of AML samples was first reported two decades ago (33) and in 2006, its' blockade with monoclonal antibodies were reported to enhance T cell responses in AML *in-vitro* (34). In a study involving a DA1-3b mouse model of AML, leukemic cells were reported to be present months despite the presence of an effective antileukemic immune response. Persistent leukemic cells were reported to have enhanced B7-H1 (PD-L1) and B7.1 expressions and resistant to cytotoxic T cell (CTL) mediated killing (35). The authors stated that an effective immunotherapeutic intervention should facilitate leukemia rejection and targeting overcoming the mechanisms that lie behind tumor dormancy and revealed that inhibition of B7-H1 (PD-L1) and B7.1/CTLA-4 interactions augmented CTL-mediated killing of the persistent cells as well as prolonging survival of naive mice injected with persistent leukemic cells. However, it should be noted that targeting B7.1/CTLA-4 and PD-1/PD-L1 axes may target different mechanisms compared to monotherapies (36), and elucidating such pathways in leukemias may pave the way for novel combinatorial therapies.

In terms of PD-1/PD-L1 axis, numerous experiments revealed upregulated expressions of both proteins in murine leukemia cells while demonstrating that genetic ablation or pharmacological inhibition of PD-1 can suppress leukemic cell proliferation and enhance survival in AML bearing mice (37). Combinatorial administration of innate immune agonists along with an ICI has revealed promising results by enhancing anti-tumor activity in a preclinical AML model: an innate immune agonist 5,6-dimethylxanthenone-4-acetic acid (DMXAA) activated the stimulator of interferon genes (STING) pathway that promoted dendritic cell maturation and in turn, maturation of leukemia-specific T-cells, resulting in a prolonged overall survival in leukemic mice (38). In anti-tumor responses, type I interferons (IFN) promotes the infiltration of CD8+ T cells, hence acts as a bridge between the innate and adaptive immunity (39, 40). This pathway also activates STAT6 and nuclear factor kappa B (NF-κB) pathways that result in the production of inflammatory mediators including TNF-α, IL-6 and CCL2/MCP-1 (41, 42). Unlike solid tumors, type I IFN response is shown not to be activated in hematological malignancies and activating STING pathway to promote anti-leukemic T cell responses stands out as a promising strategy (43). However, expression of immunosuppressive indolamine-2,3-dioxygenase (IDO) and upregulation of PD-L1 as a response to IFN-γ may be the restricting factors for the administration of STING agonists as a single agent in AML treatment. Thus, determination and inhibition of

immune escape pathways induced by STING activation may enable STING agonists' administration in the clinical setting. In line with this hypothesis, DMXAA inhibited the growth of murine AML cell line C1498 and increased PD-L1 expression while combination of PD-1 inhibition along with DMXAA therapy boosted activated host T cell numbers and bone marrow PD-1/L1/L2 expression, reducing disease burden and prolonging overall survival *in-vivo* (44). In an *in-vitro* study, DMXAA exposure promoted PD-L1 expression while leading to a slight increase in apoptosis and IL-6 and IFN-b production in C1498 AML cell line while coupling DMXAA with an anti-PD-1 antibody significantly reduced disease burden and extended general survival in C1498 grafted leukemic mice (45). Mice receiving combinatorial treatment exhibited boosted memory T-cells and mature dendritic cells along with lesser numbers of regulatory T-cells, proving apoptosis of leukemic cells. These findings were further supported by increased serum levels of type I interferons (IFN) and IFN-γ. These studies suggest that STING agonists can be used in combination with ICI for enhanced anti-tumor efficacy. Besides DMXAA, other STING agonists include GSK3745417 that has been shown promising anti-cancer activity on AML cell lines as well as primary AML cell cultures and MIW815 (ADU-S100) which recently have been reported to induce systemic immune activation while being well tolerated in patients with advanced/metastatic cancers, though AML was not investigated in the latter (46, 47). A recent study revealed that a novel STING agonist SHR1032 enhanced anti-tumor immunity and induced AML apoptosis under *in-vitro* and *in-vivo* settings (48). Besides AML, STING agonists have been under evaluation for the treatment of other solid and hematological malignancies: Ulevostinag (MK-1454) has been tested in combination with pembrolizumab in participants with advanced/metastatic solid tumors or lymphomas (49), while GSK3745417 is currently being tested either alone or in combination with PD-1 inhibitor dostarlimab (50), and BMS-98630 is being tested alone or in combination with nivolumab and ipilimumab in patients with advanced solid tumors (51). However, there are certain questions to be addressed before the implementation of STING agonists in the field of immune oncology, including whether the overstimulation of the pathway can induce autoimmune conditions, or if the pathway is a valid target in case of epigenetic silencing of STING (52).

Recent findings suggest that AML cells express high levels of TIM-3 and release galectin-9 (Gal-9) that impair activity of cytotoxic T cells and NK cells (53). The association between PI3K/Akt/mTOR signaling pathways and the regulation of immune checkpoint ligands including PD-L1, Galectin-9 (Gal-9), and CD155 was investigated in human AML cell line HL-60 *in-vitro*. For this purpose, cells were treated with idelalisib as PI3K inhibitor, MK-2206 as Akt inhibitor, and everolimus as mTOR inhibitor either in a single or combined format (54). Combinatorial treatment of HL-60 cells with two or three inhibitors diminished the expression levels of PD-L1, Gal-9, and CD155 checkpoint ligands, decreased proliferation and enhanced apoptosis. This study revealed that besides their cytotoxic properties, drugs targeting the PI3K/Akt/mTOR pathway play role in the regulation of ICP expression and interfere with immune evasion mechanisms of AML cells.

Recently, Xu et al. reported co-expression of PD-1 along with TIGIT on CD8+ T cells of AML patients' bone marrow samples, moreover PD-1 and TIGIT positivity on CD8+ T cells showed positive correlation with age, suggesting greater T cell dysfunction in elderly patients. This study also revealed the increased frequency of PD-1+ and TIGIT+ CD8+ T cells in bone marrow samples compared to peripheral blood, a finding that indicates the importance of targeting immunosuppressive bone marrow microenvironment (BMM) in AML treatment (55). In another study aiming to characterize NK cell subsets of AML patients in bone marrow and peripheral blood, Brauneck et al. revealed TIGIT and poliovirus receptor-related immunoglobulin domain-containing (PVRIG) co-expression on NK cells of AML patients, and their simultaneous blockade enhanced the NK cell mediated killing *in-vitro* (56). In another study, Li et al. reported PVRIG ligand (poliovirus receptor-related 2, PVRL2) on AML patient blasts, and proven that blocking the PVRIG/PVRL2 axis enhanced NK cell activation and in turn, promoted killing of patient derived primary AML blasts (57).

CD47 is a macrophage ICP that is particularly involved in myeloid malignancies and has been identified as a leukemic stem cell marker in AML. Blockade of CD47-SIRPα pathway has been shown to increase several therapeutics in pre-clinical studies (58). Similarly, CD200 plays role in the formation of T regulatory cells (Tregs) is commonly overexpressed in AML blasts and shown to be associated with poor outcome (59). Along with CD200 on AML blasts, TIM-3 expression on peripheral blood T cells was proven to be involved in AML development, and these proteins hold the potential to serve as prognostic markers (60).

Programmed Death-1 Homolog (V-domain Ig suppressor of T cell activation, VISTA) is a novel co-inhibitory molecule that promotes immune evasion in solid tumors, and an *in-vivo* study revealed the connection between PD-1H and epigenetic modifications as well as their role in immune evasion in AML where DNA methyl transferase inhibition by 5-aza-2'-deoxycytidine (Decitabine) increased T cell infiltration that potentiated the anti-leukemic effect of the PD-1H blockade and significantly prolonged survival (61). VISTA has also been shown to be expressed on myeloid-derived suppressor cells (MDSCs) present in the peripheral blood of AML patients and contribute to the inhibition of T cell responses in AML (62). Moreover, authors reported a positive correlation between VISTA expression on MDSCs and PD-1 expression on T cells of AML patients, highlighting the potential of combinatorial VISTA and PD-1 inhibition in leukemia treatment. In an *in-vitro* study, both CTLA-4 and LAG-3 expression levels were reported higher in comparison with healthy controls in AML, and the receiver-operating characteristic (ROC) curve analysis suggested that CTLA-4 and LAG-3 co-positivity can be used as a diagnostic criteria for the disease (63).

It should be noted that even if the ICIs are promising in the cancer treatment, the broadly distributed immune-related adverse events (irAEs) may not be tolerable in some cases. To overcome this, some experimental studies focus on restricted immune checkpoint blockade such as α-PD-1 × α-CD3 × α-CD33, a bifunctional checkpoint inhibitory T cell–engaging antibody (CiTE) that directs T-cells to CD33 on AML cells with locally restricted immune checkpoint blockade (64). By the synergistic effect of ICI and avidity-dependent binding, PD-1 attachment improved T-cell activation (3.3-fold elevation of IFN-γ) and led to efficient and highly selective

cytotoxicity against CD33+ PD-L1+ cell lines as well as patient-derived AML cells. In a murine xenograft model, CiTE induced complete AML eradication without initial signs of irAEs.

3.2 Clinical trials on immune checkpoint inhibitor therapy in acute myeloid leukemia

HMAs have been approved by FDA, and they are being used as epigenetic modifiers for the treatment of myelodysplastic syndromes (MDS) and acute AML patients, who are not eligible for induction chemotherapy (65, 66). It is reported that in these patients who underwent the treatment with HMAs, surface expression of ICPs (PD-L1, PD-L2, PD-1, and to a lesser extent, CTLA-4) increased in a dose-dependent matter. For the patients for whom the up-regulation of PD-L1 was to the greatest extent, it is reported that the response to HMA therapy was the shortest, and it was associated with a lower survival (67). Concerning these observations, clinicians suggested that HMA therapies lead to immune checkpoint activation and up-regulation, indicating that this resistance may be overcome by combining HMA with ICIs (68, 69).

In a phase 2 clinical trial, nivolumab was administered with azacitidine to a high-risk population of relapsed or refractory (R/R) AML patients. Among 70 patients, the response rate to therapy was 33%, with 22% being in complete remission or incomplete hematologic recovery. Grade 3/4 irAEs were reported in 11% of patients, the most frequent one being pneumonitis. For all 70 patients, the median survival was 6.3 months, while for 32 salvage-1 patients (the first therapy administered after all standard treatments proved ineffective), it was 10.5 months. This finding indicates a promising response rate for the combination therapy, as also stated by the authors. A greater response rate was recorded in patients with higher CD3+CD8+ T cell infiltration pre-therapy. Thus, it was reported that pre-therapy T cell infiltration can be considered an inflamed tumor marker and a biomarker that can be used in deciding which patient group would benefit from ICI-based treatments (70). In an expanded cohort study as a follow-up study to the clinical trial, the anti-CTLA-4 antibody ipilimumab was added to azacitidine and nivolumab regimen and administered to 24 R/R AML patients. The study has reported a 1-year overall survival of 45% in R/R AML patients. When this new triple combination treatment is compared in the aspect of the median overall survival, with the previous azacytidine and nivolumab double treatment and with the current treatment with hypomethylating agents, the results were respectively 10.5, 6.4 and 4.6 months. These findings demonstrate an encouraging and promising efficacy. Although regarding its safety, it is worth mentioning that in 6 patients (25%), grade 3/4 immune-related toxicity, including rash, pneumonitis, and colitis was reported (71). In another phase 2 study, the anti-PD-1 antibody pembrolizumab was administered to recently diagnosed R/R AML patients in combination with azacitidine. In this cohort, out of 29 eligible patients, 4 (14%) achieved complete remission or incomplete hematologic recovery, while 1 patient (4%) had partial remission. The median overall survival was 10.8 months. After 22 newly diagnosed older AML patients not eligible for intensive chemotherapy joined the study, out of 17 of whom were evaluable, 47% achieved complete remission or incomplete hematologic recovery, while 12% had partial remission. The new median survival was 13.1 months. These two cohorts display that azacitidine and pembrolizumab combination therapy proved beneficial in both R/R and recently diagnosed older patient groups. Grade 3/4 irAEs were observed in both patient groups, the ratios being more frequent (24%) in the first cohort and less (14%) in the second. Although at this point this treatment combination looks more suitable to newly diagnosed older patient groups, more specifically directed research is still needed (72).

A phase 1b/2 study reported that azacytidine leads to PD-1 and PD-L1 upregulation in AML which causes drug resistance that may be overcome by including the PD-1 inhibitor nivolumab. In a study, azacitidine was combined with nivolumab and administered to 35 relapsed AML patients. Out of 35 patients evaluated, the preliminary data from this study showed that 6 (18%) were in complete remission (CR) or CR with incomplete count recovery (CRi) and 5 (15%) were in hematologic improvement. A decrease in blast count greater than 50% was observed in 14 patients (26%), and the median overall survival was reported as 9.3 months (range, 1.8 - 14.3). Patients with CR/CRi, higher levels of pre-treatment CD3+ and CD8+T-cell infiltration were detected in bone marrow aspirates (73). In conclusion, azacytidine in combination with nivolumab yielded a promising and durable response in relapsed AML, and irAEs may be managed with systemic steroid administration.

In another multi-centered, randomized, international phase 2 clinical trial, azacitidine was administered to high-risk MDS or AML patients in combination with the anti-PD-L1 antibody durvalumab or as a single agent. In this study with 129 AML patients older than 65 years old who were not eligible for chemotherapy; a comparison between the azacitidine and Durvalumab combination therapy and azacitidine as a single agent therapy showed no statistically significant difference in total response rate (31.3% vs. 35.4%) or complete remission rate (17.2% vs. 21.5%). The overall survival rate was 13.0 and 14.4 months, respectively, with no unexpected side effects. Although this study portrays an important role regarding its comparatively larger sample size, it is worth considering that more than half of the patients did not continue with the study regimens, which might be taken into account in interpreting the results (74).

The resistance mechanisms and biomarkers playing role in processes that play role in treatment response are not yet fully explained, but a study from Herbrich et al. puts forth a possible explanation. In their study, Herbrich et al. evaluated the bone marrow and peripheral blood samples taken from nine relapsed or refractory AML patients who received azacitidine and anti-PD-L1 antibody avelumab using single-cell mass cytometry. Out of nine evaluable patients, four had an initial decrease in blast count, and seven showed a fast progression subsequently. Authors reported that in AML bone marrow, CD4+ and CD8+ T cells had a significantly lower proportion of naïve T cells at baseline, along with a smaller ratio of terminally differentiated CD8+ cells. Contrarily, the largest portion of T-cells in AML bone marrow consisted of the effector memory CD4 and CD8 cells. In these patients, a high PD-L2 protein expression was observed in AML cells, and PD-L1 expression was low in the samples taken at both baseline and during therapy. PD-L2 was also frequently expressed in the newly formed clones which were not present at baseline. These findings may indicate a possible explanation for the different response rates to PD-1 and PD-L1 inhibition observed

during AML treatment. These findings also indicate that the immune cell distribution is significantly affected in AML patients' bone marrow. The T cell distribution ratio and the different checkpoints that are expressed on AML cells, such as PD-L2, may pose a key in the consideration of the approach and response of the treatment (75, 76).

In their study, Berger et al. administered anti-PD-1 monoclonal antibody CT-011 (pidilizumab) to patients with advanced hematologic malignities in a phase 1 clinical trial, where pidilizumab was administered to 17 patients (8 being diagnosed with AML) in doses between 0.2 and 0.6 mg/kg. Complete remission was observed in one patient, while clinical benefit is reported in 33%. Although serious adverse events were reported in 4 patients, who were all diagnosed with AML and passed away later, the study reported that none of these were related to the treatment but to fulminate-resistant leukemia and that the dose aforementioned can be considered safe (77, 78). Currently, pidilizumab is also being investigated in combination with a dendritic cell vaccine on AML patients in complete remission (79). In a phase 1/1b multi-centered study performed with hematologic cancer patients who were in relapse following post-allogenic HSCT, the anti-CTLA-4 antibody ipilimumab was administered to the patients. In 22 patients who were receiving 10 mg/kg, four were diagnosed with extramedullary AML, and one was diagnosed with MDS which progressed to AML; five patients (23%) were in complete remission, 2 (9%) showed partial response and 6 (27%) had a decreased tumor burden. A sustained response for longer than a year was reported in four patients. Although this study was noted to be attainable in patients with AML post-allogenic HSCT; the irAEs were reported in 6 patients (21%) including one death reported. Graft versus host disease (GvHD) is also reported in 4 (14%), which resulted in the conclusion of further application of ipilimumab. Altogether, these data revealed promising results regarding ipilimumab administration in patients with post-allogenic HSCT relapsed AML (65, 80). In a phase 2 study evaluating the effect of PD-1 inhibition after cytotoxic chemotherapy on clinical response, 37 patients diagnosed with relapsed or refractory AML were administered high-dose cytarabine followed by IV 200 mg pembrolizumab on the 14^{th} day. The patients who responded to the treatment continued to receive pembrolizumab for two years. The overall response rate was 46%, the composite complete remission was 38%, and the median overall survival was 11.1 months. For refractory or early relapsed patients, and for patients who received the treatment as the first salvage, the median overall survival was 13.2 and 11.3 months, respectively, which was considered promising by the authors. Grade 3 and higher irAEs were reported to be rare and self-limiting, with 14% which is promising when treatment feasibility is considered (81). In another phase 2 study, a patient group of nine who received pembrolizumab following high dose cytarabine was compared with a control group of 18 who underwent allogeneic HSCT and didn't receive ICI. According to the one-year survival data, no significant difference was reported between the two groups (67% vs. 78%; p=0.34). For the group that received ICI, the 100-day mortality rate was 0%, while in the control group, it was 17%. Grade 3/4 acute GVHD risk didn't increase in patients who received pembrolizumab prior to allogeneic HSCT while no indicator of chronic GVHD was reported (82). These findings support the aforementioned phase 2 study, in reflecting both the clinical activity and safety profile of cytarabine and pembrolizumab combination. Besides agents targeting PD-1/PD-L1 axis, anti-leukemic potential of humanized anti-TIM-3 antibody sabatolimab in combination with HMAs was investigated in 48 patients who were newly diagnosed with AML and ineligible for intensive chemotherapy (83). The overall response rate was reported as 40% while 30% of these patients achieved CR/CRi.

When ICIs' role in maintenance is considered, preclinical studies indicate that ICIs can prevent leukemic cells' evasion of the immune system and, thus, overcome tumor persistence. Another phase 2 study investigating efficacy of nivolumab on 14 high-risk AML patients in complete remission who were not eligible for allogeneic HSCT indicated that by the end of the year, 71% of patients were in complete remission, indicating the drug's safety and feasibility in high-risk AML (84).

In brief, numerous recent clinical studies involving ICI as a single agent or combined with other treatments demonstrated promising results regarding clinical efficacy and safety profile. However, it is early to draw distinct conclusions about ICIs' use in AML and further research is needed. It should be noted that currently, there is no ICI approved by the FDA in the treatment of AML, and the clinical trials regarding ICI in AML treatment are still at the early stages with results revealing modest efficacy, especially for monotherapy the refractory settings (85).

As mentioned earlier, chemotherapy in AML is divided into two phases; induction therapy and consolidation therapies which both vary according to the patient's age, presence of co-morbidities and genetic alterations. Induction therapy aims to eliminate the blasts in the peripheral blood and to restore normal hematopoiesis while consolidation therapy is administered to remove residual leukemic cells (86). In clinical trials, efficacy of ICIs is mainly investigated in combination with chemotherapy agents and HMA (87). intervention in AML remains as allogeneic HSCT while the clinical trials involving ICI are ongoing and up-and-coming.

4 The interaction between bone marrow microenvironment and cancer cells in AML

Bone marrow is an extraordinary tissue where various cells from lineages reside. BMM is a substantial gatekeeper in maintenance of the blood cell formation and is a complex structure which is composed of cellular and noncellular elements (88). The cellular elements consist of hematopoietic cells, stromal cells (fibroblasts, endothelial cells, endothelial progenitor cells, osteoblasts, osteoclasts, adipocytes) and noncellular elements consists of ECM components, autonomic nervous system and soluble factors such as cytokines (89). BMM is usually divided into two different anatomical locations as endosteal niche and perivascular niche (90); the main function of endosteal niche and perivascular niche is to aid long term storage of HSCs by providing a hypoxic environment and to support the proliferation and differentiation of HSCs by maintaining a more oxygenated environment, respectively. Based on their different functions and structural features, these niches have been divided

into various subgroups; endosteal niche mainly comprise of osteolineage cells while the perivascular niche consists of different subtypes associated with endothelial and perivascular cells (91) (Figure 1). Various cellular or non-cellular components of BM is critical for maintenance of physiological conditions of microenvironments (92). In addition, in some sources, a third bone marrow niche called reticular niche, a transitional zone of endosteal and perivascular niches is described (117).

In leukemia, a growing body of evidence indicates leukemic cells' involvement in malignant transformation, disease progression, treatment resistance, and relapse as the interplay between leukemic stem cells and the microenvironment alters the hemostasis in a way to support leukemic cells' survival and proliferation, suggesting a bidirectional interaction between HSCs and BMM (118, 119). AML cells mainly bind to the BM fibroblast, fibronectin and laminin (120); SCF exposure enhances these cells' adhesion to fibronectin (121). Both SCF and fibronectin are found in the BMM at high levels, and together they protect AML cells from apoptosis (121). These cells also remodel the BMM *via* secreting matrix metalloproteinases (MMPs) (122, 123). MMP-2 and -9 have been indicated to be secreted by leukemic blasts and involved in dissemination of myeloproliferative malignancies including AML. Thus, it can be concluded that the mediators released by the BMM play role in survival of the leukemic cells as well as regulating their mobilization, and in leukemia treatment, targeting BMM-related signaling pathways has been shown to enhance the therapeutic efficacy (124). Moreover, various BM-derived populations including myeloid cell–derived suppressor cells, mesenchymal stem cells, and tumor-associated macrophages are shown to be involved in escaping anti-tumor immune responses by suppressing anti-tumor responses (125). Angiogenesis enhances leukemogenesis by providing necessary factors that favor malignancy as certain angiogenic cytokines and factors were reported to be increased in AML patients and it was associated with poor prognosis (126). Lipolysis and remodeling of BMAT are induced in the setting of AML, and free fatty acids yielded by lipolysis are used as nutrient by leukemic cells (127). Sympathetic neuropathy may be seen due to bone marrow infiltration of malignant cells, and it was associated with AML progression (128). Along with chronic myeloid leukemia (CML), the niche microenvironment of acute myeloid leukemia (AML) is well established: with the help of recent studies, significant progress has been made in understanding the impact of genetic mutations or functional alterations in the BM on leukemia. Examples include the deletion of Dicer1 in osteoprogenitors, which leads to the development of myelodysplastic syndrome (MDS) with

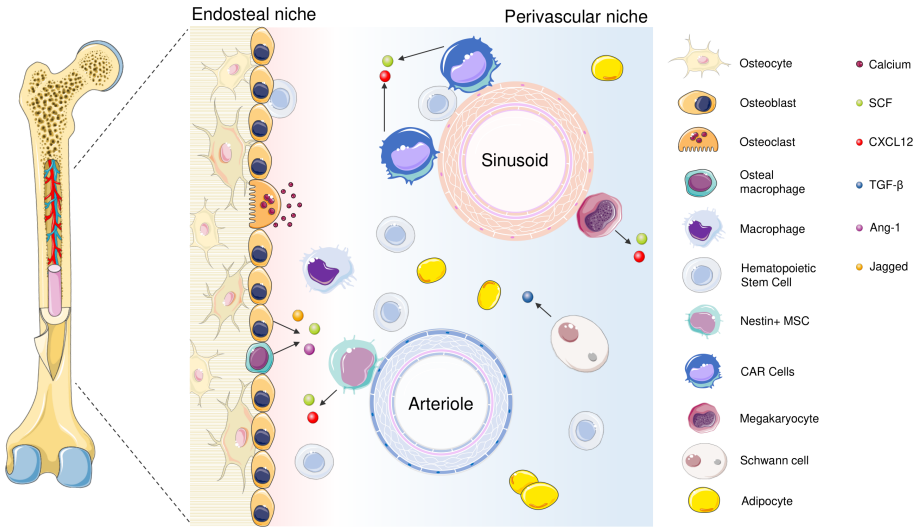

FIGURE 1
The cellular components of the BM niches include endothelial cells, HSCs, megakaryocytes, osteoblasts, osteoclasts, adipocytes, sympathetic neurons that are related to Schwann's cells, bone macrophages and reticular cells (90, 92). Both soluble factors and direct contact between cells regulate HSC maintenance. Quiescent HSCs are kept in contact with osteoblasts and Nestin+ MSCs as well as CXCL12 - abundant reticular (CAR) cells in the perivascular niche; both secrete soluble factors such as Stem Cell Factor (SCF), CXCL12 (CXC motif chemokine ligand 12) and Ang-1 (Angiopoietin-1) while in the perivascular niche, secrete (93). Osteomacs, the bone-marrow-resident macrophages are also found in the endosteal niche and facilitate colonization; in the absence of osteomacs, HSCs are shown to leave BM and join circulation (92, 94). Jagged-1 is released from cells of osteocyte lineage, and responsible for the activation of Notch pathway (95). Organized as a monolayer in the internal compartment of blood vessels, ECs take part in various physiological processes including facilitating blood flow, contributing coagulation, nutrient exchange and regulate hematopoiesis (96). According to their localization in the BM, they are divided into two categories: sinusoid endothelial cells (SECs) which have low CD31 and Endomucin expression (type L), or arteriolar endothelial cells (AECs) with CD31 and Endomucin expression (type H). Both cell types play different roles in the modulation of BM niche (97). SECs are the compartments of more permeable sinusoidal vessels and secrete high levels of CXCL12 as well as E-selectin that regulate HSC homing (96, 98). On the contrary, AECs are the compartments of arteriolar vessels which have low penetration and ensure a relatively hypoxic environment (99, 100). AECs generate SCF which play a fundamental role in maintaining HSCs and express CXCL12. In addition, they produce Netrin-1 that retains HSCs' quiescence and self-renewal (101). Megakaryocytes are the basic subunit in the perisinusoidal area and regulate HSC quiescence (102–104). In the endosteal niche, osteoblasts stabilize bone formation and produce mediators which are essential for HSC maintenance; and CXCL12, granulocyte colony-stimulating factor (G-CSF), SCF, Annexin 2 (ANXA2), Ang-1, Thrombopoietin (TPO) that are required for the regulation of HSC homing, quiescence and mobilization (105–113). Schwann cells are found in the perivascular niche and protect the quiescent HSCs through transforming growth factor-β (TGF-β) (114). Bone marrow adipocytes were also reported to support HSC proliferation through secreting adiponectin and contribute to energy metabolism (115, 116).

sporadic transformation to AML (129), or overexpression of β-catenin in osteoblasts as observed in 38% of the patients diagnosed with MDS or AML (130). Similarly, activation of the parathyroid hormone receptor in osteoblasts is shown to promote KMT2A-MLLT3 oncogene-induced AML (131). AML cells are also capable of modulating the BMM as cells harboring BCR-ABL1 and Nup98/HoxA9 fusion gene are indicated to inhibit mature osteoblasts and disrupt bone homeostasis by secreting CCL3 (132). Likewise, KMT2A-MLLT3 AML cells have been shown to inhibit terminal differentiation of bone marrow mesenchymal stromal cells to mature osteoblasts, which eventually results in decreased bone mineralization (128).

Recently, upregulated ICP expressions including PD-1, TIM-3, LAG-3 in addition to expansion of myeloid-derived suppressor cells and increased Treg frequency in the BMM of AML patients were reported, which highlights the importance of IC blockade as a novel therapeutic strategy in the treatment of the disease (133).

4.1 Targeting bone marrow microenvironment in acute myeloid leukemia – existing strategies

When considering treatments targeting BM microenvironment, CXCL12 (C-X-C motif chemokine ligand 12)/CXCR4 (C-X-C chemokine receptor 4) axis is the most studied pathway in AML treatment; as reported, inhibition of this pathway leads to mobilization of leukemic cells, sensitizes them to chemotherapy and promotes apoptosis (134–138). The anti-CXCR4 antibody ulocuplumab has shown to inhibit CXCL12-mediated cell migration and promote apoptosis in *in vivo* murine AML models as well as promoting chemosensitivity *via* mobilizing AML cells to circulation in clinical studies (139–141). Another common strategy is inhibiting the Wnt/β-catenin pathway to diminish the protection provided by BMM: β-catenin is highly expressed in unfavorable and relapsed AML patients, and Wnt/β-catenin inhibitor PRI-724 was shown to suppress cell growth while promoting apoptosis in AML blasts and stem/progenitors (142). Wnt/β-catenin/FLT3 inhibitor SKLB-677 promoted apoptosis in FLT3-driven AML both *in-vitro*, *in-vivo* and *exvivo* (143). Another Wnt/β-catenin inhibitor, BC2059 has shown promising results in treatment of AML stem or blast progenitor cells with FLT3 internal tandem duplication expression in combination with receptor tyrosine kinase inhibitors quizartinib and crenolanib (144).

Targeting adhesion molecules which support the leukemic cells is another approach in AML treatment. Being the receptor of vascular cell adhesion molecule (VCAM-1), integrin α4β1 (very late antigen 4 – VLA 4) plays role in the adhesion of leukemic myeloblasts to BMM (145). Humanized VLA-4 monoclonal antibody natalizumab has been reported to induce mobilization and sensitize leukemic cells to chemotherapy (146). In combination with cytarabine, VLA-4 inhibitor FNIII14 has shown to eradicate minimal residual disease in a murine AML model, underlining the importance of inhibiting cell adhesion-mediated drug resistance (147). By regulating VLA-4 avidity, adhesion molecule CD44 was shown to strengthen the connection between AML cells and BMM, thus, contributing to the supportive BMM (148). In a phase I study, humanized anti-CD44 monoclonal antibody RG7356 was found to be safe and well tolerated though it is not suitable as a monotherapy due to its' limited clinical activity in AML treatment (149).

The endothelial cell adhesion molecule E-selectin is another important component of the vascular niche that regulates the balance between HSC renewal and commitment. However, the inflammatory mediators secreted by AML blasts increase the expression of endothelial niche E-selectin, which, in turn, promotes their survival and chemoresistance through AKT/NF-κB/mTOR signaling pathways (150). In an AML murine model bearing the human KMT2A-MLLT3 oncogene, the small molecule E-selectin mimetic GMI-1271/Uproleselan has enhanced the efficacy of AML treatment by overcoming vascular niche-mediated chemoresistance, indicating E-selectin blockade alleviates pro-survival signaling and improving therapeutic efficacy (150).

4.2 Targeting bone marrow microenvironment in acute myeloid leukemia with an emphasis on immune checkpoint proteins

AML blasts modulate TME to enable disease progression, provide protection against therapeutic interventions and contribute to recurrence (151). In terms of ICPs, AML blasts can alter the T cell immunological synapses, promote inhibitory soluble factors to hamper T cell responses, and promote activity of MDSCs as well as promoting polarization of tumor associated macrophages (TAMs) to immunomodulatory M2 phenotype (151, 152). The interaction between AML cells and immune cells are visualized in Figure 2.

4.2.1 Leukemic cells

PD-1/PD-L1 axis is the most studied IC pathway in AML (153), and PD-L1 expression on AML blasts were reported to be linked with the inflamed tumor microenvironment, highlighting the potential of targeting BMM in disease management (154, 155). In addition, AML cells also secrete soluble ICPs to the microenvironment to create an immunosuppressive milieu as human AML cells including leukemic stem cells have higher TIM-3 and its' ligand Gal-9 expression levels compared to healthy HSCs. By binding TIM-3 expressed on NK cells, Gal-9 can inhibit granzyme B transfer, and in turn, NK-mediated cell lysis while soluble TIM-3 can suppress IL-2 production by T cells, hampering NK and CTL activation (156).

4.2.2 Endothelial cells

Bone marrow endothelial cells are an important part of the BMM; by secreting growth factors along with certain cytokines and forming physical contact with hematopoietic progenitors, they take part in the regulation of hematopoiesis (157). In cancer, tumor vessels are highly abnormal, and they favor immune suppression (158). T cells can remodel the ECM by downregulating adhesion molecules to prevent infiltration and recruitment of effector immune cells to the cancer milieu; the production of immunosuppressive metabolites, chemokines and cytokines inhibit CTL function while promoting M2 macrophages and MDSCs (159, 160). Thus, normalization of the

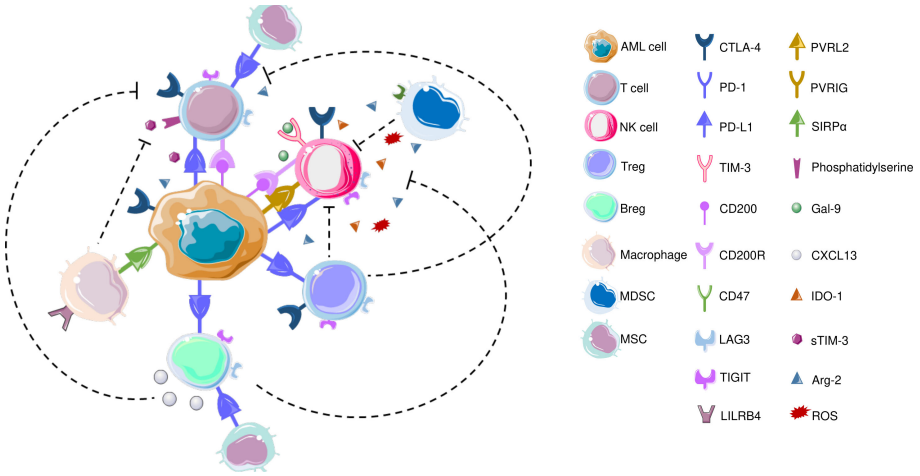

FIGURE 2
CTLA-4, which is also expressed on T cells and NK cells is the first ICP that is reported to be commonly overexpressed in AML to inhibit T cell responses. In terms of T cells, increased frequency of PD-1+CD4+ T cells as well as PD-1+/CD8+ cells co-expressing TIM3 or LAG3 were reported in AML patients' bone marrow samples. LSCs also secrete Gal-9 that leads to the elimination Th1 effector cells. LILRB4 is expressed on monocytic leukemic cells and interact with T cells to alter their function. CD200 is also expressed on AML cells that engage in CD200R on T cells and NK cells. Similar to T cells, PD-L1 expression has been detected on Bregs in AML patients. Recently, blocking PD1/PD-L1 axis along with inhibiting CXCL13 has been increased chemotherapeutic efficacy, and CXCL13 has been suggested as a novel ICP; TIGIT is also expressed on BREGs, though both these findings are yet to be confirmed in AML BM samples. TAMs express CD47 that protects phagocytosis of AML LSCs. AML: acute myeloid leukemia; Arg-2: Arginase 2; Breg: B regulatory cell; CTLA-4: Cytotoxic T-lymphocyte antigen-4; CXCL-13: CXC chemokine ligand 13; Gal-9: Galectin-9; IDO-1: Indoleamine 2,3-dioxygenase; LAG3: Lymphocyte-activation gene 3; LILRB4: Leukocyte immunoglobulin like receptor B4; MDSC: myeloid-derived suppressor cell; MSC: Mesenchymal stem cell; NK cell: Natural killer cell; PD-1: Programmed death – 1; PD-L1: Programmed death ligand 1; PVRIG: Poliovirus receptor related immunoglobulin domain containing; PVRL2: Poliovirus receptor-related 2 (Nectin-2); ROS: Reactive oxygen species; SIRPα: Signal regulatory protein α; sTIM-3: soluble TIM-3; TIGIT: T cell immunoreceptor with Ig and ITIM domains; TIM-3: T-cell immunoglobulin and mucin domain 3; Treg: T regulatory cell; VISTA: V-domain Ig suppressor of T cell activation.

cancer vasculature would improve immune cell infiltration, promote the immune reactivity, and hamper immune suppressive microenvironment: inhibition of angiogenesis by drugs targeting VEGF-dependent signaling pathways were suggested to improve immunotherapy outcomes (161).

4.2.3 T cells

T cell function holds great importance in IC blockade since they are the main targets of ICIs which are interfered by MDSCs that lead to poor clinical outcome in ICI treatment (162). In AML, certain clinical studies have revealed disruptions in T cell immunity such as increased Treg frequency, reduced T helper cells, increased T cell exhaustion (19). Resident T cells from AML bone marrow samples of AML patients were reported to have altered transcription profiles expressing genes related stemness and myeloid priming (163). Increased frequency of PD-1+CD4+ and ICOS+/CD4+ effector T cells were reported in the BM samples of AML patients (164, 165). In terms of Tregs, their proportion in the BMM was reported to be higher compared to healthy controls, and a higher frequency of PD-1^+/$CD8^+$ cells co-expressing TIM3 or LAG3 was detected, especially in patients who had multiply relapsed AML. Secreted by LSCs, Gal-9 promotes apoptosis of Th1 effector cells and CTLs expressing TIM-3 that eventually leads to T cell exhaustion and immune evasion (166, 167). In TP53-mutated AML patients, leukemia blasts from BMM were more frequently positive for PD-L1 (164). Even after allogeneic HSCT, T cells infiltrating the bone marrow were reported to have early differentiated memory stem (TSCM) and central memory bone marrow-T cell features with multiple IC receptor expressions (168). Another mechanism that inhibit T cell growth is the expression of immunoglobulin-like receptor B4 (LILRB4) which is exclusively expressed on monocytic leukemic cells (M4 and M5 subtypes) that interact with T cells to alter their function *via* releasing arginase-1 to suppress T cell proliferation (169). The immune-suppressive molecule, CD200 is also increased on AML cells to interact with CD200 receptor (CD200R) on T cells to inhibit memory T cell function and increase Treg populations (170).

4.2.4 B cells

Regulatory B cells (Bregs), immunomodulatory B cells that exert immunomodulatory effects mainly *via* secreting various soluble mediators including IL-10 are reported to increase in peripheral blood as well as bone marrow samples in AML patients, highlighting their role in the AML pathogenesis (171). Recently, PD-L1 expression has been reported on Bregs in AML patients and is associated with a worse prognosis (165). According to an *in-vivo* study, CXCL13 has been suggested as a novel IC regulating Breg activity where ablation of CXCL13 increased the efficacy of chemotherapy and PD-1 blockade, though this study did not involve an AML model (172). Other ICPs involved in Bregs' involve TIGIT, although its' mechanism of action in AML is yet to be elucidated (173).

4.2.5 Myeloid-derived suppressor cells

Myeloid-derived suppressor cells (MDSCs) are a heterogenous group of CD11b+ CD33+ HLA-$DR^{lo/neg}$ immature myeloid cells that consist of three major groups: monocytic MDSCs (M-MDSCs, CD11b +CD14+HLA-DR^{lo}) that resemble monocytes in terms of their phenotypes and morphologies, polymorphonuclear MDSCs (PMN-

MDSCs, CD11b+CD15+CD14^{neg}) that are similar to neutrophils and early-stage MDSC (eMDSC, CD11b+CD33+CD14^{neg}CD15^{neg}HLA-DR^{neg}) (174–176). All subsets of MDSCs are known to exert immunosuppressive effects, both at a systemic and at the tumor level which led to the investigations questioning their potential for being biomarkers in response to ICI (176). In pathological conditions including cancer, MDSCs expand in response to inflammatory mediators as well as growth factors released, and they undergo expansion to participate in disease development. The presence of circulating M-MDSCs may correlate with response to anti-PD-1 treatments: advanced melanoma patients with lower circulating M-MDSCs levels prior to nivolumab treatment had shown better response to treatment, and Gal-9 expression of M-MDSCs is shown to be associated with TIM-3 expression on lymphocytes which contributes to nivolumab resistance in non-small cell lung carcinoma. In AML, expansion of MDSCs were shown to suppress T-cell proliferation and T-cell responses while MDSC expansion was reported to be Muc-1 mediated c-myc expression dependent, which has shown to be associated with PD-L1 expression in AML cases with TP53 mutations (177). VISTA has been found to be highly expressed on MDSCs, and knockdown of this ICP reduced MDSC-mediated CD8+ T cell inhibition (62). Previously, cytarabine in combination with CXCR4 inhibitor plerixafor and anti-PD-L1 monoclonal antibody have successfully decreased Tregs and MDSCs in the peripheral blood and leukemic cells in the bone marrow (178).

4.2.6 Tumor associated macrophages

Polarization of TAMs to anti-inflammatory M2 phenotype has been well documented in AML, which hampers anti-tumor immunity and promotes cancer progression (179, 180). A study published by Al-Matary et al. revealed that AML increases invasion of TAMs in the BM and spleen in mice as well as leukemic patients, and Growth factor independence-1 is the main regulator of M2 polarization (181). Novel macrophage ICP, CD47 plays important role in various cancers, mainly in myeloid malignancies and it is recognized as an LSC marker in AML (58). CD47 prevents phagocytosis of AML leukemic stem cells by interacting with SIRPα, and inhibition of this pathway replenishes the phagocytosis ability of TAMs to engulf AML LSCs (182). In line with these findings, the anti-CD47 antibody magrolimab was revealed to show promising results when combined with azacitidine in AML and MDS patients (58), and a phase 3 study evaluating the efficacy of magrolimab in combination with venetoclax and azacytidine has been ongoing (183). As magrolimab promotes phagocytosis by interacting Fc gamma receptors on macrophages, the mechanism of action of the monoclonal antibody raised questions in terms of its' toxicity as CD47 is also expressed on healthy cells (58, 184). However, inhibition of CD47 only promoted phagocytosis if prophagocytic signals are present, which are normally absent on healthy cells (184).

4.2.7 Natural killer cells

Along with T cells, NK cells target AML blasts *via* MHC molecules, leukemia-associated antigens (LAAs), or NK cell activating ligands (185), and ratio of NK cells in the BM samples of the patients has been shown to be correlated with better prognosis (186). However, AML can modulate NK cell activity to eliminate anti-leukemic responses by altering expression of ligands and receptors (187), and studies revealed a correlation between AML blast ligand repertoire and NK receptor expression in patients receiving chemotherapy (188, 189). Recently, NK cells are reported to express PD-1, and inhibiting the PD-1/PD-L1 axis has been shown to activate these cells, suggesting NK activation as another result of ICI administration (190). However, it should be noted that this study did not involve AML patients but murine cancer models, and the functional effects of PD-1 engagement on NK cells was investigated *in-vitro*. Another recent study highlighted the involvement of PVRIG/PVRL2 axis in AML and suggested that PVRIG blockade may be a novel approach to enhance NK cell activity in PVRL2+ AML (57). Besides PD-1 and PVRIG, expression of TIM-3, LAG3, TIGIT, Siglec-7/9, CD200R, CTLA-4, or B7H3 were also reported on NK cells, though in a lesser extent in comparison with T cells (191, 192). It should be noted that none of these studies focus on the activity of NK cells with an emphasis on AML, indicating the requirement of further analyses regarding the NK cell-mediated anti-leukemic mechanisms of ICI in AML.

4.2.8 Mesenchymal stem cells

MSCs influence their microenvironment by interacting with neighboring cells *via* direct contact or secreting various mediators that regulate innate and adaptive immune cells (193). MSCs inhibit the function of T cells, NK cells; suppress dendritic cells' maturation, and promote Tregs' proliferation (194). MSCs also support hematopoiesis and promote HSCs' colonization, and sharing the same microenvironment with HSCs, leukemic stem cells can modulate MSCs immunomodulatory actions: in AML, Nestin+ BM-MSCs were reported to have altered properties that contribute to disease development and chemoresistance (119). Under inflammatory conditions, MSCs are reported to produce PD-L1 and PD-L2 which bind to PD-1 on T cells to inhibit their activation and contribute to immune escape (195). However, our current knowledge regarding ICP expression on MSCs are limited, and further studies on ICI-mediated anti-leukemic effects of MSCs are required.

4.2.9 Adipocytes

Bone marrow adipocytes (BMAs) are thought to be differentiated from Sca1+ CD45− CD31− or LepR+ CD45− CD31− MSCs (196, 197). These small adipocytes secrete high levels of adipokines but have lower CD36 and triglyceride levels compared to white adipose tissue, and they do not share the same progenitors with brown adipose tissue and contribute to inflammation by secreting high levels of proinflammatory cytokines (198, 199). In 2018, Wu et al. demonstrated PD-L1 gene expression in murine adipose tissue and indicated that inducing adipogenesis in mouse cell lines *in vitro* enhanced its' expression up to 100-fold (200). Recently, Picarda et al. reported that ICP B7-H3 is expressed on both mouse and human adipocyte progenitors and involve in the glycolytic and mitochondrial activity while its' loss upon adipocytic differentiation results in impaired oxidative metabolism and increased lipid accumulation (201). However, none of these studies involve BMAs; when considering their unique properties, expression levels of ICPs and

their involvement in the regulation of hematopoiesis as well as leukemia initiation and progression all require further studies.

5 Conclusions and future perspectives

Today it is widely known that the structure and the function of BMM is altered to facilitate AML progression, dissemination and escape immune surveillance (202). Manipulation of the CXCL12/CXCR4 pathway is the key player in AML blasts' growth, survival, and chemotherapy resistance: CXCR4 expression on AML blasts that is involved in trafficking of malignant LSCs within BM while the migration of healthy stem cells in BM is prohibited (22). Regulation of tumor immune microenvironment stands out as a promising strategy in cancer treatment; in AML, inhibitors of several pathways are currently being investigated, either alone or in combination (203). When considering the therapeutic interventions targeting tumor microenvironment can alter ICP expression in tumor microenvironment, inhibiting ICPs on AML blasts and stem cells may be regarded as a combinatorial treatment strategy. In colorectal cancer, HMA decitabine enhanced the therapeutic efficacy of PD-L1 blockade and in ovarian cancer, dual inhibition of CXCL12-CXCR4 and PD-1-PD-L1 axes alleviated the immunosuppressive tumor microenvironment (204, 205). While these data underline the potential of ICP blockade in AML treatment *via* BMM modulation, it should be noted that our current knowledge regarding ICIs mainly relies on studies with solid tumors, and more data involving larger patient cohorts are needed to determine whether they will be integrated into therapeutic routines in hematological malignancies, and the impact of tumor immune microenvironment on the success of ICIs require more investigation.

Author contributions

Drafting manuscript: BA, CP, ZD, NND-C and EG. Preparing the figures: BA and NND-C. Editing and revising the manuscript: GY-D. All authors contributed to the article and approved the submitted version.

Acknowledgments

We sincerely thank Ayşe Nur Çaldıran and Özlem Deniz Çulcu for their valuable contributions to drafting, and Pervin Yanıkkaya Aydemir for carefully reading and editing the manuscript. We thank to Yeditepe University Rectorate for supporting us with the article processing fee.

Conflict of interest

The authors declare that the research was conducted in the absence of any commercial or financial relationships that could be construed as a potential conflict of interest.

Publisher's note

References

1. Arber DA, Orazi A, Hasserjian R, Thiele J, Borowitz MJ, Le Beau MM, et al. The 2016 revision to the world health organization classification of myeloid neoplasms and acute leukemia. *Blood* (2016) 127(20):2391–405. doi: 10.1182/blood-2016-03-643544

2. Jaffe E, Arber D, Campo E, Harris N, Quintanilla-Fend L. *Hematopathology. 2nd ed.* New York: Elsevier (2016).

3. Narayanan D, Weinberg OK. How I investigate acute myeloid leukemia. *Int J Lab Hematol* (2020) 42(1):3–15. doi: 10.1111/ijlh.13135

4. Jalaeikhoo H, Kashfi SMH, Azimzadeh P, Narimani A, Gouhari Moghadam K, Rajaienejad M, et al. Acute myeloid leukemia as the main cause of pancytopenia in Iranian population. *Iran J Pathol* (2017) 12(3):265–71. doi: 10.30699/ijp.2017.25647

5. Lad D, Jain A, Varma S. Complications and management of coagulation disorders in leukemia patients. *Blood Lymphat Cancer* (2017) 7:61–72. doi: 10.2147/blctt.S125121

6. Ferraro F, Miller CA, Christensen KA, Helton NM, O'Laughlin M, Fronick CC, et al. Immunosuppression and outcomes in adult patients with *De novo* acute myeloid leukemia with normal karyotypes. *Proc Natl Acad Sci U.S.A.* (2021) 118(49): e2116427118. doi: 10.1073/pnas.2116427118

7. Uchiumi H, Matsushima T, Yamane A, Doki N, Irisawa H, Saitoh T, et al. Prevalence and clinical characteristics of acute myeloid leukemia associated with disseminated intravascular coagulation. *Int J Hematol* (2007) 86(2):137–42. doi: 10.1532/ijh97.06173

8. Stahl M, Shallis RM, Wei W, Montesinos P, Lengline E, Neukirchen J, et al. Management of hyperleukocytosis and impact of leukapheresis among patients with acute myeloid leukemia (Aml) on short- and long-term clinical outcomes: A Large, retrospective, multicenter, international study. *Leukemia* (2020) 34(12):3149–60. doi: 10.1038/s41375-020-0783-3

9. Rico-Rodríguez J, Villanueva-Ortiz Á, Santana-Cabrera L, Rodríguez-Pérez H. Pulmonary leukostasis with severe respiratory impairment as a debut of acute myeloid leukemia. *Int J Crit Illn Inj Sci* (2015) 5(2):125–6. doi: 10.4103/2229-5151.158423

10. Nabhan C, Kamat S, Karl Kish J. Acute myeloid leukemia in the elderly: What constitutes treatment value? *Leuk Lymphoma* (2019) 60(5):1164–70. doi: 10.1080/10428194.2018.1520992

11. Weinberg OK, Hasserjian RP, Baraban E, Ok CY, Geyer JT, Philip J, et al. Clinical, immunophenotypic, and genomic findings of acute undifferentiated leukemia and comparison to acute myeloid leukemia with minimal differentiation: A study from the bone marrow pathology group. *Mod Pathol* (2019) 32(9):1373–85. doi: 10.1038/s41379-019-0263-3

12. Franchini M, Frattini F, Crestani S, Bonfanti C. Bleeding complications in patients with hematologic malignancies. *Semin Thromb Hemost* (2013) 39(1):94–100. doi: 10.1055/s-0032-1331154

13. Jongen-Lavrencic M, Grob T, Hanekamp D, Kavelaars FG, Al Hinai A, Zeilemaker A, et al. Molecular minimal residual disease in acute myeloid leukemia. *N Engl J Med* (2018) 378(13):1189–99. doi: 10.1056/NEJMoa1716863

14. National Comprehensive Cancer Network. *Nccn clinical practice guidelines in oncology: Acute myeloid leukemia* (2022). Available at: https://www.nccn.org/login?ReturnURL=https://www.nccn.org/professionals/physician_gls/pdf/aml.pdf.

15. National Comprehensive Cancer Network. *Nccn clinical practice guidelines in oncology (Nccn guidelines®): Acut myeloid leukemia nccn evidence blocks* (2022). Available at: https://www.nccn.org/professionals/physician_gls/pdf/aml_blocks.pdf.

16. Ishii H, Yano S. New therapeutic strategies for adult acute myeloid leukemia. *Cancers (Basel)* (2022) 14(11):2806. doi: 10.3390/cancers14112806

17. Ball B, Mei M, Otoukesh S, Stein A. Current and emerging therapies for acute myeloid leukemia. In: Pullarkat V, Marcucci G, editors. *Biology and treatment of leukemia and bone marrow neoplasms*. Cham: Springer International Publishing (2021). p. 57–73.

18. Bakst RL, Dabaja BS, Specht LK, Yahalom J. Use of radiation in extramedullary Leukemia/Chloroma: Guidelines from the international lymphoma radiation oncology group. *Int J Radiat Oncol Biol Phys* (2018) 102(2):314–9. doi: 10.1016/j.ijrobp.2018.05.045

19. Hao F, Sholy C, Wang C, Cao M, Kang X. The role of T cell immunotherapy in acute myeloid leukemia. *Cells* (2021) 10(12):3376. doi: 10.3390/cells10123376

20. Döhner H, Wei AH, Appelbaum FR, Craddock C, DiNardo CD, Dombret H, et al. Diagnosis and management of aml in adults: 2022 recommendations from an international expert panel on behalf of the eln. *Blood* (2022) 140(12):1345–77. doi: 10.1182/blood.2022016867

21. Stubbins RJ, Francis A, Kuchenbauer F, Sanford D. Management of acute myeloid leukemia: A review for general practitioners in oncology. *Curr Oncol* (2022) 29(9):6245–59. doi: 10.3390/curroncol29090491

22. Hino C, Pham B, Park D, Yang C, Nguyen MHK, Kaur S, et al. Targeting the tumor microenvironment in acute myeloid leukemia: The future of immunotherapy and natural products. *Biomedicines* (2022) 10(6):1410. doi: 10.3390/biomedicines10061410

23. Reis M, Ogonek J, Qesari M, Borges NM, Nicholson L, Preußner L, et al. Recent developments in cellular immunotherapy for hsct-associated complications. *Front Immunol* (2016) 7:500. doi: 10.3389/fimmu.2016.00500

24. Dessie G, Derbew Molla M, Shibabaw T, Ayelign B. Role of stem-cell transplantation in leukemia treatment. *Stem Cells Cloning* (2020) 13:67–77. doi: 10.2147/sccaa.S262880

25. Fathi AT. Antibody-based therapy in aml: Antibody–drug conjugates and bispecific agents. *Clin Lymphoma Myeloma Leukemia* (2021) 21:S112–S3. doi: 10.1016/S2152-2650(21)01231-3

26. Jabbour E, Paul S, Kantarjian H. The clinical development of antibody-drug conjugates - lessons from leukaemia. *Nat Rev Clin Oncol* (2021) 18(7):418–33. doi: 10.1038/s41571-021-00484-2

27. Kovtun Y, Jones GE, Adams S, Harvey L, Audette CA, Wilhelm A, et al. A Cd123-targeting antibody-drug conjugate, Imgn632, designed to eradicate aml while sparing normal bone marrow cells. *Blood Adv* (2018) 2(8):848–58. doi: 10.1182/bloodadvances.2018017517

28. *Imgn632 as monotherapy or with venetoclax and/or azacitidine for patients with Cd123-positive acute myeloid leukemia* . Available at: https://clinicaltrials.gov/ct2/show/NCT04086264.

29. Taghiloo S, Asgarian-Omran H. Immune evasion mechanisms in acute myeloid leukemia: A focus on immune checkpoint pathways. *Crit Rev Oncol Hematol* (2021) 157:103164. doi: 10.1016/j.critrevonc.2020.103164

30. Aru B, Soltani M, Pehlivanoglu C, Gurlu E, Ganjalikhani-Hakemi M, Yanikkaya Demirel G. Comparison of laboratory methods for the clinical follow up of checkpoint blockade therapies in leukemia: Current status and challenges ahead. *Front Oncol* (2022) 12:789728. doi: 10.3389/fonc.2022.789728

31. Shiravand Y, Khodadadi F, Kashani SMA, Hosseini-Fard SR, Hosseini S, Sadeghirad H, et al. Immune checkpoint inhibitors in cancer therapy. *Curr Oncol* (2022) 29(5):3044–60. doi: 10.3390/curroncol29050247

32. Costa B, Vale N. Dostarlimab: A review. *Biomolecules* (2022) 12(8):1031. doi: 10.3390/biom12081031

33. Pistillo MP, Tazzari PL, Palmisano GL, Pierri I, Bolognesi A, Ferlito F, et al. Ctla-4 is not restricted to the lymphoid cell lineage and can function as a target molecule for apoptosis induction of leukemic cells. *Blood* (2003) 101(1):202–9. doi: 10.1182/blood-2002-06-1668

34. Zhong RK, Loken M, Lane TA, Ball ED. Ctla-4 blockade by a human mab enhances the capacity of aml-derived dc to induce T-cell responses against aml cells in an autologous culture system. *Cytotherapy* (2006) 8(1):3–12. doi: 10.1080/14653240500499507

35. Saudemont A, Quesnel B. In a model of tumor dormancy, long-term persistent leukemic cells have increased B7-H1 and B7.1 expression and resist ctl-mediated lysis. *Blood* (2004) 104(7):2124–33. doi: 10.1182/blood-2004-01-0064

36. Wei SC, Anang NAS, Sharma R, Andrews MC, Reuben A, Levine JH, et al. Combination anti-Ctla-4 plus anti-Pd-1 checkpoint blockade utilizes cellular mechanisms partially distinct from monotherapies. *Proc Natl Acad Sci U.S.A.* (2019) 116(45):22699–709. doi: 10.1073/pnas.1821218116

37. Zhang L, Gajewski TF, Kline J. Pd-1/Pd-L1 interactions inhibit antitumor immune responses in a murine acute myeloid leukemia model. *Blood* (2009) 114(8):1545–52. doi: 10.1182/blood-2009-03-206672

38. Curran E, Chen X, Corrales L, Kline DE, Dubensky TWJr., Duttagupta P, et al. Sting pathway activation stimulates potent immunity against acute myeloid leukemia. *Cell Rep* (2016) 15(11):2357–66. doi: 10.1016/j.celrep.2016.05.023

39. Gajewski TF. Failure at the effector phase: Immune barriers at the level of the melanoma tumor microenvironment. *Clin Cancer Res* (2007) 13(18 Pt 1):5256–61. doi: 10.1158/1078-0432.Ccr-07-0892

40. Fuertes MB, Kacha AK, Kline J, Woo SR, Kranz DM, Murphy KM, et al. Host type I ifn signals are required for antitumor Cd8+ T cell responses through Cd8α+ dendritic cells. *J Exp Med* (2011) 208(10):2005–16. doi: 10.1084/jem.20101159

41. Chen H, Sun H, You F, Sun W, Zhou X, Chen L, et al. Activation of Stat6 by sting is critical for antiviral innate immunity. *Cell* (2011) 147(2):436–46. doi: 10.1016/j.cell.2011.09.022

42. Fu J, Kanne DB, Leong M, Glickman LH, McWhirter SM, Lemmens E, et al. Sting agonist formulated cancer vaccines can cure established tumors resistant to pd-1 blockade. *Sci Transl Med* (2015) 7(283):283ra52. doi: 10.1126/scitranslmed.aaa4306

43. Zhang L, Chen X, Liu X, Kline DE, Teague RM, Gajewski TF, et al. Cd40 ligation reverses T cell tolerance in acute myeloid leukemia. *J Clin Invest* (2013) 123(5):1999–2010. doi: 10.1172/jci63980

44. Przespolewski A, Portwood S, Den Haese J, Lewis D, Wang ES. Targeting innate and adaptive immune responses for the treatment of acute myeloid leukemia. *Blood* (2016) 128(22):2833–. doi: 10.1182/blood.V128.22.2833.2833

45. Przespolewski AC, Portwood S, Wang ES. Targeting acute myeloid leukemia through multimodal immunotherapeutic approaches. *Leuk Lymphoma* (2022) 63(4):918–27. doi: 10.1080/10428194.2021.1992614

46. Adam M, Yu J, Plant R, Shelton C, Schmidt H, Yang J. Sting agonist Gsk3745417 induces apoptosis, antiproliferation, and cell death in a panel of human aml cell lines and patient samples. *Blood* (2022) 140(Supplement 1):11829–. doi: 10.1182/blood-2022-167652

47. Meric-Bernstam F, Sweis RF, Hodi FS, Messersmith WA, Andtbacka RHI, Ingham M, et al. Phase I dose-escalation trial of Miw815 (Adu-S100), an intratumoral sting agonist, in patients with Advanced/Metastatic solid tumors or lymphomas. *Clin Cancer Res* (2022) 28(4):677–88. doi: 10.1158/1078-0432.Ccr-21-1963

48. Song C, Liu D, Liu S, Li D, Horecny I, Zhang X, et al. Shr1032, a novel sting agonist, stimulates anti-tumor immunity and directly induces aml apoptosis. *Sci Rep* (2022) 12(1):8579. doi: 10.1038/s41598-022-12449-1

49. *Study of ulevostinag (Mk-1454) alone or in combination with pembrolizumab (Mk-3475) in participants with Advanced/Metastatic solid tumors or lymphomas (Mk-1454-001)* (2022). Available at: https://clinicaltrials.gov/ct2/show/NCT03010176.

50. *Phase 1 first time in human (Ftih), open label study of Gsk3745417 administered to participants with advanced solid tumors* (2022). Available at: https://clinicaltrials.gov/ct2/show/NCT03843359.

51. *An investigational immunotherapy study of bms-986301 alone or in combination with nivolumab, and ipilimumab in participants with advanced solid cancers* (2022). Available at: https://clinicaltrials.gov/ct2/show/NCT03956680.

52. Motedayen Aval L, Pease JE, Sharma R, Pinato DJ. Challenges and opportunities in the clinical development of sting agonists for cancer immunotherapy. *J Clin Med* (2020) 9(10):3323. doi: 10.3390/jcm9103323

53. Gonçalves Silva I, Rüegg L, Gibbs BF, Bardelli M, Fruehwirth A, Varani L, et al. The immune receptor Tim-3 acts as a trafficker in a Tim-3/Galectin-9 autocrine loop in human myeloid leukemia cells. *Oncoimmunology* (2016) 5(7):e1195535. doi: 10.1080/2162402x.2016.1195535

54. Taghiloo S, Norozi S, Asgarian-Omran H. The effects of Pi3k/Akt/Mtor signaling pathway inhibitors on the expression of immune checkpoint ligands in acute myeloid leukemia cell line. *Iran J Allergy Asthma Immunol* (2022) 21(2):178–88. doi: 10.18502/ijaai.v21i2.9225

55. Xu L, Liu L, Yao D, Zeng X, Zhang Y, Lai J, et al. Pd-1 and tigit are highly Co-expressed on Cd8(+) T cells in aml patient bone marrow. *Front Oncol* (2021) 11:686156. doi: 10.3389/fonc.2021.686156

56. Brauneck F, Seubert E, Wellbrock J, Schulze Zur Wiesch J, Duan Y, Magnus T, et al. Combined blockade of tigit and Cd39 or A2ar enhances nk-92 cell-mediated cytotoxicity in aml. *Int J Mol Sci* (2021) 22(23):12919. doi: 10.3390/ijms222312919

57. Li J, Whelan S, Kotturi MF, Meyran D, D'Souza C, Hansen K, et al. Pvrig is a novel natural killer cell immune checkpoint receptor in acute myeloid leukemia. *Haematologica* (2021) 106(12):3115–24. doi: 10.3324/haematol.2020.258574

58. Chao MP, Takimoto CH, Feng DD, McKenna K, Gip P, Liu J, et al. Therapeutic targeting of the macrophage immune checkpoint Cd47 in myeloid malignancies. *Front Oncol* (2019) 9:1380. doi: 10.3389/fonc.2019.01380

59. Tonks A, Hills R, White P, Rosie B, Mills KI, Burnett AK, et al. Cd200 as a prognostic factor in acute myeloid leukaemia. *Leukemia* (2007) 21(3):566–8. doi: 10.1038/sj.leu.2404559

60. Zahran AM, Mohammed Saleh MF, Sayed MM, Rayan A, Ali AM, Hetta HF. Up-regulation of regulatory T cells, Cd200 and Tim3 expression in cytogenetically normal acute myeloid leukemia. *Cancer biomark* (2018) 22(3):587–95. doi: 10.3233/cbm-181368

61. Kim TK, Han X, Wang J, Sanmamed M, Zhang T, Halene S, et al. Pd-1h (Vista) induces immune evasion in acute myeloid leukemia. *Blood* (2017) 130(Supplement 1):2658–. doi: 10.1182/blood.V130.Suppl_1.2658.2658

62. Wang L, Jia B, Claxton DF, Ehmann WC, Rybka WB, Mineishi S, et al. Vista is highly expressed on mdscs and mediates an inhibition of T cell response in patients with aml. *Oncoimmunology* (2018) 7(9):e1469594. doi: 10.1080/2162402x.2018.1469594

63. Radwan SM, Elleboudy NS, Nabih NA, Kamal AM. The immune checkpoints cytotoxic T lymphocyte antigen-4 and lymphocyte activation gene-3 expression is up-regulated in acute myeloid leukemia. *Hla* (2020) 96(1):3–12. doi: 10.1111/tan.13872

64. Herrmann M, Krupka C, Deiser K, Brauchle B, Marcinek A, Ogrinc Wagner A, et al. Bifunctional pd-1 × Acd3 × Acd33 fusion protein reverses adaptive immune escape in acute myeloid leukemia. *Blood* (2018) 132(23):2484–94. doi: 10.1182/blood-2018-05-849802

65. Assi R, Kantarjian H, Ravandi F, Daver N. Immune therapies in acute myeloid leukemia: A focus on monoclonal antibodies and immune checkpoint inhibitors. *Curr Opin Hematol* (2018) 25(2):136–45. doi: 10.1097/moh.0000000000000401

66. Daver N, Alotaibi AS, Bücklein V, Subklewe M. T-Cell-Based immunotherapy of acute myeloid leukemia: Current concepts and future developments. *Leukemia* (2021) 35(7):1843–63. doi: 10.1038/s41375-021-01253-x

67. Yang H, Bueso-Ramos C, DiNardo C, Estecio MR, Davanlou M, Geng QR, et al. Expression of pd-L1, pd-L2, pd-1 and Ctla4 in myelodysplastic syndromes is enhanced by treatment with hypomethylating agents. *Leukemia* (2014) 28(6):1280–8. doi: 10.1038/leu.2013.355

68. Ørskov AD, Treppendahl MB, Skovbo A, Holm MS, Friis LS, Hokland M, et al. Hypomethylation and up-regulation of pd-1 in T cells by azacytidine in Mds/Aml patients: A rationale for combined targeting of pd-1 and DNA methylation. *Oncotarget* (2015) 6(11):9612–26. doi: 10.18632/oncotarget.3324

69. Daver N, Boddu P, Garcia-Manero G, Yadav SS, Sharma P, Allison J, et al. Hypomethylating agents in combination with immune checkpoint inhibitors in acute myeloid leukemia and myelodysplastic syndromes. *Leukemia* (2018) 32(5):1094–105. doi: 10.1038/s41375-018-0070-8

70. Daver N, Garcia-Manero G, Basu S, Boddu PC, Alfayez M, Cortes JE, et al. Efficacy, safety, and biomarkers of response to azacitidine and nivolumab in Relapsed/Refractory acute myeloid leukemia: A nonrandomized, open-label, phase ii study. *Cancer Discovery* (2019) 9(3):370–83. doi: 10.1158/2159-8290.Cd-18-0774

71. Daver NG, Garcia-Manero G, Konopleva MY, Alfayez M, Pemmaraju N, Kadia TM, et al. Azacitidine (Aza) with nivolumab (Nivo), and aza with nivo + ipilimumab (Ipi) in Relapsed/Refractory acute myeloid leukemia: A non-randomized, prospective, phase 2 study. *Blood* (2019) 134(Supplement_1):830–. doi: 10.1182/blood-2019-131494

72. Gojo I, Stuart RK, Webster J, Blackford A, Varela JC, Morrow J, et al. Multi-center phase 2 study of pembroluzimab (Pembro) and azacitidine (Aza) in patients with Relapsed/Refractory acute myeloid leukemia (Aml) and in newly diagnosed (≥65 years) aml patients. *Blood* (2019) 134(Supplement_1):832–. doi: 10.1182/blood-2019-127345

73. Daver N, Basu S, Garcia-Manero G, Cortes JE, Ravandi F, Jabbour EJ, et al. Phase Ib/Ii study of nivolumab in combination with azacytidine (Aza) in patients (Pts) with relapsed acute myeloid leukemia (Aml). *Blood* (2016) 128(22):763–. doi: 10.1182/blood.V128.22.763.763

74. Zeidan AM, Cavenagh J, Voso MT, Taussig D, Tormo M, Boss I, et al. Efficacy and safety of azacitidine (Aza) in combination with the anti-Pd-L1 durvalumab (Durva) for the front-line treatment of older patients (Pts) with acute myeloid leukemia (Aml) who are unfit for intensive chemotherapy (Ic) and pts with higher-risk myelodysplastic syndromes (Hr-mds): Results from a Large, international, randomized phase 2 study. *Blood* (2019) 134(Supplement_1):829–. doi: 10.1182/blood-2019-122896

75. Duan J, Cui L, Zhao X, Bai H, Cai S, Wang G, et al. Use of immunotherapy with programmed cell death 1 vs programmed cell death ligand 1 inhibitors in patients with cancer: A systematic review and meta-analysis. *JAMA Oncol* (2020) 6(3):375–84. doi: 10.1001/jamaoncol.2019.5367

76. Herbrich S, Cavazos A, Cheung CMC, Alexander-Williams L, Short NJ, Matthews J, et al. Single-cell mass cytometry identifies mechanisms of resistance to immunotherapy in aml. *Blood* (2019) 134(Supplement_1):1428–. doi: 10.1182/blood-2019-128601

77. Berger R, Rotem-Yehudar R, Slama G, Landes S, Kneller A, Leiba M, et al. Phase I safety and pharmacokinetic study of ct-011, a humanized antibody interacting with pd-1, in patients with advanced hematologic malignancies. *Clin Cancer Res* (2008) 14(10):3044–51. doi: 10.1158/1078-0432.Ccr-07-4079

78. Boddu P, Kantarjian H, Garcia-Manero G, Allison J, Sharma P, Daver N. The emerging role of immune checkpoint based approaches in aml and mds. *Leuk Lymphoma* (2018) 59(4):790–802. doi: 10.1080/10428194.2017.1344905

79. *Blockade of pd-1 in conjunction with the dendritic Cell/Aml vaccine following chemotherapy induced remission* (2022). Available at: https://clinicaltrials.gov/ct2/show/NCT01096602.

80. Davids MS, Kim HT, Bachireddy P, Costello C, Liguori R, Savell A, et al. Ipilimumab for patients with relapse after allogeneic transplantation. *N Engl J Med* (2016) 375(2):143–53. doi: 10.1056/NEJMoa1601202

81. Zeidner JF, Vincent BG, Ivanova A, Moore D, McKinnon KP, Wilkinson AD, et al. Phase ii trial of pembrolizumab after high-dose cytarabine in Relapsed/Refractory acute myeloid leukemia. *Blood Cancer Discovery* (2021) 2(6):616–29. doi: 10.1158/2643-3230.Bcd-21-0070

82. Tschernia NP, Kumar V, Moore DT, Vincent BG, Coombs CC, Van Deventer H, et al. Safety and efficacy of pembrolizumab prior to allogeneic stem cell transplantation for acute myelogenous leukemia. *Transplant Cell Ther* (2021) 27(12):1021.e1–.e5. doi: 10.1016/j.jtct.2021.08.022

83. Brunner AM, Esteve J, Porkka K, Knapper S, Traer E, Scholl S, et al. Efficacy and safety of sabatolimab (Mbg453) in combination with hypomethylating agents (Hmas) in patients (Pts) with very High/High-risk myelodysplastic syndrome (Vhr/Hr-mds) and acute myeloid leukemia (Aml): Final analysis from a phase ib study. *Blood* (2021) 138 (Supplement 1):244–. doi: 10.1182/blood-2021-146039

84. Kadia TM, Cortes JE, Ghorab A, Ravandi F, Jabbour E, Daver NG, et al. Nivolumab (Nivo) maintenance (Maint) in high-risk (Hr) acute myeloid leukemia (Aml) patients. *J Clin Oncol* (2018) 36(15_suppl):7014–. doi: 10.1200/JCO.2018.36.15_suppl.7014

85. Bewersdorf JP, Stahl M, Zeidan AM. Immune checkpoint-based therapy in myeloid malignancies: A promise yet to be fulfilled. *Expert Rev Anticancer Ther* (2019) 19(5):393–404. doi: 10.1080/14737140.2019.1589374

86. Silva M, Martins D, Mendes F. The role of immune checkpoint blockade in acute myeloid leukemia. *Onco* (2022) 2(3):164–80. doi: 10.3390/onco2030011

87. Thummalapalli R, Knaus HA, Gojo I, Zeidner JF. Immune checkpoint inhibitors in aml-a new frontier. *Curr Cancer Drug Targets* (2020) 20(7):545–57. doi: 10.2174/1568009620666200421081455

88. Fröbel J, Landspersky T, Percin G, Schreck C, Rahmig S, Ori A, et al. The hematopoietic bone marrow niche ecosystem. *Front Cell Dev Biol* (2021) 9:705410. doi: 10.3389/fcell.2021.705410

89. Dammacco F, Leone P, Silvestris F, Racanelli V, Vacca A. Chapter 9 - cancer stem cells in multiple myeloma and the development of novel therapeutic strategies. In: Dammacco F, Silvestris F, editors. *Oncogenomics*. (USA: Academic Press) (2019). p. 121–37.

90. Sendker S, Waack K, Reinhardt D. Far from health: The bone marrow microenvironment in aml, a leukemia supportive shelter. *Children (Basel)* (2021) 8 (5):371. doi: 10.3390/children8050371

91. Lo Celso C, Fleming HE, Wu JW, Zhao CX, Miake-Lye S, Fujisaki J, et al. Live-animal tracking of individual haematopoietic Stem/Progenitor cells in their niche. *Nature* (2009) 457(7225):92–6. doi: 10.1038/nature07434

92. Reagan MR, Rosen CJ. Navigating the bone marrow niche: Translational insights and cancer-driven dysfunction. *Nat Rev Rheumatol* (2016) 12(3):154–68. doi: 10.1038/nrrheum.2015.160

93. Ehninger A, Trumpp A. The bone marrow stem cell niche grows up: Mesenchymal stem cells and macrophages move in. *J Exp Med* (2011) 208(3):421–8. doi: 10.1084/jem.20110132

94. Winkler IG, Sims NA, Pettit AR, Barbier V, Nowlan B, Helwani F, et al. Bone marrow macrophages maintain hematopoietic stem cell (Hsc) niches and their depletion mobilizes hscs. *Blood* (2010) 116(23):4815–28. doi: 10.1182/blood-2009-11-253534

95. Canalis E. Notch signaling in skeletal diseases. In: Zaidi M, editor. *Encyclopedia of bone biology*. Oxford: Academic Press (2020). p. 130–40.

96. Peci F, Dekker L, Pagliaro A, van Boxtel R, Nierkens S, Belderbos M. The cellular composition and function of the bone marrow niche after allogeneic hematopoietic cell transplantation. *Bone Marrow Transplant* (2022) 57(9):1357–64. doi: 10.1038/s41409-022-01728-0

97. Itkin T, Gur-Cohen S, Spencer JA, Schajnovitz A, Ramasamy SK, Kusumbe AP, et al. Distinct bone marrow blood vessels differentially regulate haematopoiesis. *Nature* (2016) 532(7599):323–8. doi: 10.1038/nature17624

98. Winkler IG, Barbier V, Nowlan B, Jacobsen RN, Forristal CE, Patton JT, et al. Vascular niche e-selectin regulates hematopoietic stem cell dormancy, self renewal and chemoresistance. *Nat Med* (2012) 18(11):1651–7. doi: 10.1038/nm.2969

99. Kenswil KJG, Jaramillo AC, Ping Z, Chen S, Hoogenboezem RM, Mylona MA, et al. Characterization of endothelial cells associated with hematopoietic niche formation in humans identifies il-33 as an anabolic factor. *Cell Rep* (2018) 22(3):666–78. doi: 10.1016/j.celrep.2017.12.070

100. Ding L, Saunders TL, Enikolopov G, Morrison SJ. Endothelial and perivascular cells maintain haematopoietic stem cells. *Nature* (2012) 481(7382):457–62. doi: 10.1038/nature10783

101. Renders S, Svendsen AF, Panten J, Rama N, Maryanovich M, Sommerkamp P, et al. Niche derived netrin-1 regulates hematopoietic stem cell dormancy *Via* its receptor neogenin-1. *Nat Commun* (2021) 12(1):608. doi: 10.1038/s41467-020-20801-0

102. Bruns I, Lucas D, Pinho S, Ahmed J, Lambert MP, Kunisaki Y, et al. Megakaryocytes regulate hematopoietic stem cell quiescence through Cxcl4 secretion. *Nat Med* (2014) 20(11):1315–20. doi: 10.1038/nm.3707

103. Nakamura-Ishizu A, Takubo K, Fujioka M, Suda T. Megakaryocytes are essential for hsc quiescence through the production of thrombopoietin. *Biochem Biophys Res Commun* (2014) 454(2):353–7. doi: 10.1016/j.bbrc.2014.10.095

104. Zhao M, Perry JM, Marshall H, Venkatraman A, Qian P, He XC, et al. Megakaryocytes maintain homeostatic quiescence and promote post-injury regeneration of hematopoietic stem cells. *Nat Med* (2014) 20(11):1321–6. doi: 10.1038/nm.3706

105. Rankin EB, Wu C, Khatri R, Wilson TL, Andersen R, Araldi E, et al. The hif signaling pathway in osteoblasts directly modulates erythropoiesis through the production of epo. *Cell* (2012) 149(1):63–74. doi: 10.1016/j.cell.2012.01.051

106. Stier S, Ko Y, Forkert R, Lutz C, Neuhaus T, Grünewald E, et al. Osteopontin is a hematopoietic stem cell niche component that negatively regulates stem cell pool size. *J Exp Med* (2005) 201(11):1781–91. doi: 10.1084/jem.20041992

107. Taichman RS, Emerson SG. Human osteoblasts support hematopoiesis through the production of granulocyte colony-stimulating factor. *J Exp Med* (1994) 179(5):1677–82. doi: 10.1084/jem.179.5.1677

108. Jung Y, Wang J, Song J, Shiozawa Y, Wang J, Havens A, et al. Annexin ii expressed by osteoblasts and endothelial cells regulates stem cell adhesion, homing, and engraftment following transplantation. *Blood* (2007) 110(1):82–90. doi: 10.1182/blood-2006-05-021352

109. Nakamura Y, Arai F, Iwasaki H, Hosokawa K, Kobayashi I, Gomei Y, et al. Isolation and characterization of endosteal niche cell populations that regulate hematopoietic stem cells. *Blood* (2010) 116(9):1422–32. doi: 10.1182/blood-2009-08-239194

110. Arai F, Hirao A, Ohmura M, Sato H, Matsuoka S, Takubo K, et al. Tie2/Angiopoietin-1 signaling regulates hematopoietic stem cell quiescence in the bone marrow niche. *Cell* (2004) 118(2):149–61. doi: 10.1016/j.cell.2004.07.004

111. Yoshihara H, Arai F, Hosokawa K, Hagiwara T, Takubo K, Nakamura Y, et al. Thrombopoietin/Mpl signaling regulates hematopoietic stem cell quiescence and interaction with the osteoblastic niche. *Cell Stem Cell* (2007) 1(6):685–97. doi: 10.1016/j.stem.2007.10.020

112. Jung Y, Wang J, Schneider A, Sun YX, Koh-Paige AJ, Osman NI, et al. Regulation of sdf-1 (Cxcl12) production by osteoblasts; a possible mechanism for stem cell homing. *Bone* (2006) 38(4):497–508. doi: 10.1016/j.bone.2005.10.003

113. Asada N, Katayama Y, Sato M, Minagawa K, Wakahashi K, Kawano H, et al. Matrix-embedded osteocytes regulate mobilization of hematopoietic Stem/Progenitor cells. *Cell Stem Cell* (2013) 12(6):737–47. doi: 10.1016/j.stem.2013.05.001

114. Yamazaki S, Ema H, Karlsson G, Yamaguchi T, Miyoshi H, Shioda S, et al. Nonmyelinating schwann cells maintain hematopoietic stem cell hibernation in the bone marrow niche. *Cell* (2011) 147(5):1146–58. doi: 10.1016/j.cell.2011.09.053

115. Fallati A, Di Marzo N, D'Amico G, Dander E. Mesenchymal stromal cells (Mscs): An ally of b-cell acute lymphoblastic leukemia (B-all) cells in disease maintenance and progression within the bone marrow hematopoietic niche. *Cancers (Basel)* (2022) 14 (14):3303. doi: 10.3390/cancers14143303

116. DiMascio L, Voermans C, Uqoezwa M, Duncan A, Lu D, Wu J, et al. Identification of adiponectin as a novel hemopoietic stem cell growth factor. *J Immunol* (2007) 178(6):3511–20. doi: 10.4049/jimmunol.178.6.3511

117. Hoffman R, Marcellino BK. Bone marrow microenvironment in health and disease. In: Zaidi M, editor. *Encyclopedia of bone biology*, vol. . p . Oxford: Academic Press (2020). p. 1–11.

118. Yao Y, Li F, Huang J, Jin J, Wang H. Leukemia stem cell-bone marrow microenvironment interplay in acute myeloid leukemia development. *Exp Hematol Oncol* (2021) 10(1):39. doi: 10.1186/s40164-021-00233-2

119. Forte D, García-Fernández M, Sánchez-Aguilera A, Stavropoulou V, Fielding C, Martín-Pérez D, et al. Bone marrow mesenchymal stem cells support acute myeloid leukemia bioenergetics and enhance antioxidant defense and escape from chemotherapy. *Cell Metab* (2020) 32(5):829–43.e9. doi: 10.1016/j.cmet.2020.09.001

120. Bendall LJ, Kortlepel K, Gottlieb DJ. Human acute myeloid leukemia cells bind to bone marrow stroma *Via* a combination of beta-1 and beta-2 integrin mechanisms. *Blood* (1993) 82(10):3125–32. doi: 10.1182/blood.V82.10.3125.3125

121. Bendall LJ, Makrynikola V, Hutchinson A, Bianchi AC, Bradstock KF, Gottlieb DJ. Stem cell factor enhances the adhesion of aml cells to fibronectin and augments fibronectin-mediated anti-apoptotic and proliferative signals. *Leukemia* (1998) 12 (9):1375–82. doi: 10.1038/sj.leu.2401136

122. Ries C, Loher F, Zang C, Ismair MG, Petrides PE. Matrix metalloproteinase production by bone marrow mononuclear cells from normal individuals and patients with acute and chronic myeloid leukemia or myelodysplastic syndromes. *Clin Cancer Res* (1999) 5(5):1115–24.

123. Lin LI, Lin DT, Chang CJ, Lee CY, Tang JL, Tien HF. Marrow matrix metalloproteinases (Mmps) and tissue inhibitors of mmp in acute leukaemia: Potential role of mmp-9 as a surrogate marker to monitor leukaemic status in patients with acute myelogenous leukaemia. *Br J Haematol* (2002) 117(4):835–41. doi: 10.1046/j.1365-2141.2002.03510.x

124. Kuek V, Hughes AM, Kotecha RS, Cheung LC. Therapeutic targeting of the leukaemia microenvironment. *Int J Mol Sci* (2021) 22(13):6888. doi: 10.3390/ijms22136888

125. Noh H, Hu J, Wang X, Xia X, Satelli A, Li S. Immune checkpoint regulator pd-L1 expression on tumor cells by contacting Cd11b positive bone marrow derived stromal cells. *Cell Commun Signal* (2015) 13:14. doi: 10.1186/s12964-015-0093-y

126. Dias S, Shmelkov SV, Lam G, Rafii S. Vegf(165) promotes survival of leukemic cells by Hsp90-mediated induction of bcl-2 expression and apoptosis inhibition. *Blood* (2002) 99(7):2532–40. doi: 10.1182/blood.v99.7.2532

127. Lu W, Weng W, Zhu Q, Zhai Y, Wan Y, Liu H, et al. Small bone marrow adipocytes predict poor prognosis in acute myeloid leukemia. *Haematologica* (2018) 103 (1):e21–e4. doi: 10.3324/haematol.2017.173492

128. Hanoun M, Zhang D, Mizoguchi T, Pinho S, Pierce H, Kunisaki Y, et al. Acute myelogenous leukemia-induced sympathetic neuropathy promotes malignancy in an altered hematopoietic stem cell niche. *Cell Stem Cell* (2014) 15(3):365–75. doi: 10.1016/j.stem.2014.06.020

129. Raaijmakers MH, Mukherjee S, Guo S, Zhang S, Kobayashi T, Schoonmaker JA, et al. Bone progenitor dysfunction induces myelodysplasia and secondary leukaemia. *Nature* (2010) 464(7290):852–7. doi: 10.1038/nature08851

130. Kode A, Manavalan JS, Mosialou I, Bhagat G, Rathinam CV, Luo N, et al. Leukaemogenesis induced by an activating B-catenin mutation in osteoblasts. *Nature* (2014) 506(7487):240–4. doi: 10.1038/nature12883

131. Krause DS, Fulzele K, Catic A, Sun CC, Dombkowski D, Hurley MP, et al. Differential regulation of myeloid leukemias by the bone marrow microenvironment. *Nat Med* (2013) 19(11):1513–7. doi: 10.1038/nm.3364

132. Frisch BJ, Ashton JM, Xing L, Becker MW, Jordan CT, Calvi LM. Functional inhibition of osteoblastic cells in an in vivo mouse model of myeloid leukemia. *Blood* (2012) 119(2):540–50. doi: 10.1182/blood-2011-04-348151

133. Bewersdorf JP, Zeidan AM. Myeloid-derived suppressor cells: A grey eminence in the aml tumor microenvironment? *Expert Rev Anticancer Ther* (2022) 22(3):239–41. doi: 10.1080/14737140.2022.2030227

134. Zeng Z, Xi Shi Y, Samudio IJ, Wang R-Y, Ling X, Frolova O, et al. Targeting the leukemia microenvironment by Cxcr4 inhibition overcomes resistance to kinase inhibitors and chemotherapy in aml. *Blood* (2009) 113(24):6215–24. doi: 10.1182/blood-2008-05-158311

135. Abraham M, Klein S, Bulvik B, Wald H, Weiss ID, Olam D, et al. The Cxcr4 inhibitor bl-8040 induces the apoptosis of aml blasts by downregulating erk, bcl-2, mcl-1 and cyclin-D1 *Via* altered mir-15a/16-1 expression. *Leukemia* (2017) 31(11):2336–46. doi: 10.1038/leu.2017.82

136. Cho B-S, Zeng Z, Mu H, Wang Z, Konoplev S, McQueen T, et al. Antileukemia activity of the novel peptidic Cxcr4 antagonist Ly2510924 as monotherapy and in combination with chemotherapy. *Blood* (2015) 126(2):222–32. doi: 10.1182/blood-2015-02-628677

137. Chen Y, Zeng Z, Shi Y, Jacamo R, Ludin C, Dembowsky K, et al. Targeting Cxcr4, Sdf1 and beta-adrenergic receptors in the aml microenvironment by novel antagonist Pol6326, G-csf and isoproterenol. *Blood* (2010) 116(21):2179–. doi: 10.1182/blood.V116.21.2179.2179

138. Kovacsovics TJ, Mims A, Salama ME, Pantin J, Rao N, Kosak KM, et al. Combination of the low anticoagulant heparin cx-01 with chemotherapy for the treatment of acute myeloid leukemia. *Blood Adv* (2018) 2(4):381–9. doi: 10.1182/bloodadvances.2017013391

139. Kuhne MR, Mulvey T, Belanger B, Chen S, Pan C, Chong C, et al. Bms-936564/Mdx-1338: A fully human anti-Cxcr4 antibody induces apoptosis in vitro and shows antitumor activity in vivo in hematologic malignancies. *Clin Cancer Res* (2013) 19(2):357–66. doi: 10.1158/1078-0432.Ccr-12-2333

140. Chien S, Beyerle LE, Wood BL, Estey EH, Appelbaum FR, Cardarelli PM, et al. Mobilization of blasts and leukemia stem cells by anti-Cxcr4 antibody bms-936564 (Mdx 1338) in patients with Relapsed/Refractory acute myeloid leukemia. *Blood* (2013) 122 (21):3882–. doi: 10.1182/blood.V122.21.3882.3882

141. Becker PS, Foran JM, Altman JK, Yacoub A, Castro JE, Sabbatini P, et al. Targeting the Cxcr4 pathway: Safety, tolerability and clinical activity of ulocuplumab (Bms-936564), an anti-Cxcr4 antibody, in Relapsed/Refractory acute myeloid leukemia. *Blood* (2014) 124(21):386–. doi: 10.1182/blood.V124.21.386.386

142. Jiang X, Mak PY, Mu H, Tao W, Mak DH, Kornblau S, et al. Disruption of Wnt/B-catenin exerts antileukemia activity and synergizes with Flt3 inhibition in Flt3-mutant acute myeloid leukemia. *Clin Cancer Res* (2018) 24(10):2417–29. doi: 10.1158/1078-0432.Ccr-17-1556

143. Ma S, Yang LL, Niu T, Cheng C, Zhong L, Zheng MW, et al. Sklb-677, an Flt3 and Wnt/B-catenin signaling inhibitor, displays potent activity in models of Flt3-driven aml. *Sci Rep* (2015) 5:15646. doi: 10.1038/srep15646

144. Fiskus W, Sharma S, Saha S, Shah B, Devaraj SG, Sun B, et al. Pre-clinical efficacy of combined therapy with novel B-catenin antagonist Bc2059 and histone deacetylase inhibitor against aml cells. *Leukemia* (2015) 29(6):1267–78. doi: 10.1038/leu.2014.340

145. Bae MH, Oh SH, Park CJ, Lee BR, Kim YJ, Cho YU, et al. Vla-4 and Cxcr4 expression levels show contrasting prognostic impact (Favorable and unfavorable, respectively) in acute myeloid leukemia. *Ann Hematol* (2015) 94(10):1631–8. doi: 10.1007/s00277-015-2442-8

146. Hsieh Y-T, Jiang E, Pham J, Kim H-N, Abdel-Azim H, Khazal S, et al. Vla4 blockade in acute myeloid leukemia. *Blood* (2013) 122(21):3944–. doi: 10.1182/blood.V122.21.3944.3944

147. Matsunaga T, Fukai F, Miura S, Nakane Y, Owaki T, Kodama H, et al. Combination therapy of an anticancer drug with the Fniii14 peptide of fibronectin effectively overcomes cell adhesion-mediated drug resistance of acute myelogenous leukemia. *Leukemia* (2008) 22(2):353–60. doi: 10.1038/sj.leu.2405017

148. Gutjahr JC, Bayer E, Yu X, Laufer JM, Höpner JP, Tesanovic S, et al. Cd44 engagement enhances acute myeloid leukemia cell adhesion to the bone marrow microenvironment by increasing vla-4 avidity. *Haematologica* (2021) 106(8):2102–13. doi: 10.3324/haematol.2019.231944

149. Vey N, Delaunay J, Martinelli G, Fiedler W, Raffoux E, Prebet T, et al. Phase I clinical study of Rg7356, an anti-Cd44 humanized antibody, in patients with acute myeloid leukemia. *Oncotarget* (2016) 7(22):32532–42. doi: 10.18632/oncotarget.8687

150. Barbier V, Erbani J, Fiveash C, Davies JM, Tay J, Tallack MR, et al. Endothelial e-selectin inhibition improves acute myeloid leukaemia therapy by disrupting vascular niche-mediated chemoresistance. *Nat Commun* (2020) 11(1):2042. doi: 10.1038/s41467-020-15817-5

151. Tettamanti S, Pievani A, Biondi A, Dotti G, Serafini M. Catch me if you can: How aml and its niche escape immunotherapy. *Leukemia* (2022) 36(1):13–22. doi: 10.1038/s41375-021-01350-x

152. Lopez-Yrigoyen M, Cassetta L, Pollard JW. Macrophage targeting in cancer. *Ann N Y Acad Sci* (2021) 1499(1):18–41. doi: 10.1111/nyas.14377

153. Lamble AJ, Lind EF. Targeting the immune microenvironment in acute myeloid leukemia: A focus on T cell immunity. *Front Oncol* (2018) 8:213. doi: 10.3389/fonc.2018.00213

154. Tamura H, Dan K, Tamada K, Nakamura K, Shioi Y, Hyodo H, et al. Expression of functional B7-H2 and B7.2 costimulatory molecules and their prognostic implications in *De novo* acute myeloid leukemia. *Clin Cancer Res* (2005) 11(16):5708–17. doi: 10.1158/1078-0432.Ccr-04-2672

155. Krönig H, Kremmler L, Haller B, Englert C, Peschel C, Andreesen R, et al. Interferon-induced programmed death-ligand 1 (Pd-L1/B7-H1) expression increases on human acute myeloid leukemia blast cells during treatment. *Eur J Haematol* (2014) 92 (3):195–203. doi: 10.1111/ejh.12228

156. Gonçalves Silva I, Yasinska IM, Sakhnevych SS, Fiedler W, Wellbrock J, Bardelli M, et al. The Tim-3-Galectin-9 secretory pathway is involved in the immune escape of human acute myeloid leukemia cells. *EBioMedicine* (2017) 22:44–57. doi: 10.1016/j.ebiom.2017.07.018

157. Almeida-Porada G, Ascensão JL. Isolation, characterization, and biologic features of bone marrow endothelial cells. *J Lab Clin Med* (1996) 128(4):399–407. doi: 10.1016/S0022-2143(96)80012-6

158. Balamurugan K. Hif-1 at the crossroads of hypoxia, inflammation, and cancer. *Int J Cancer* (2016) 138(5):1058–66. doi: 10.1002/ijc.29519

159. Liu Y, Shaw SK, Ma S, Yang L, Luscinskas FW, Parkos CA. Regulation of leukocyte transmigration: Cell surface interactions and signaling events. *J Immunol* (2004) 172(1):7–13. doi: 10.4049/jimmunol.172.1.7

160. Huang Y, Kim BYS, Chan CK, Hahn SM, Weissman IL, Jiang W. Improving immune-vascular crosstalk for cancer immunotherapy. *Nat Rev Immunol* (2018) 18 (3):195–203. doi: 10.1038/nri.2017.145

161. Khan KA, Kerbel RS. Improving immunotherapy outcomes with anti-angiogenic treatments and vice versa. *Nat Rev Clin Oncol* (2018) 15(5):310–24. doi: 10.1038/nrclinonc.2018.9

162. Limagne E, Richard C, Thibaudin M, Fumet JD, Truntzer C, Lagrange A, et al. Tim-3/Galectin-9 pathway and mmdsc control primary and secondary resistances to pd-1 blockade in lung cancer patients. *Oncoimmunology* (2019) 8(4):e1564505. doi: 10.1080/2162402x.2018.1564505

163. van Galen P, Hovestadt V, Wadsworth Ii MH, Hughes TK, Griffin GK, Battaglia S, et al. Single-cell rna-seq reveals aml hierarchies relevant to disease progression and immunity. *Cell* (2019) 176(6):1265–81.e24. doi: 10.1016/j.cell.2019.01.031

164. Williams P, Basu S, Garcia-Manero G, Hourigan CS, Oetjen KA, Cortes JE, et al. The distribution of T-cell subsets and the expression of immune checkpoint receptors and ligands in patients with newly diagnosed and relapsed acute myeloid leukemia. *Cancer* (2019) 125(9):1470–81. doi: 10.1002/cncr.31896

165. Shi Y, Liu Z, Wang H. Expression of pd-L1 on regulatory b cells in patients with acute myeloid leukaemia and its effect on prognosis. *J Cell Mol Med* (2022) 26(12):3506–12. doi: 10.1111/jcmm.17390

166. Kang CW, Dutta A, Chang LY, Mahalingam J, Lin YC, Chiang JM, et al. Apoptosis of tumor infiltrating effector Tim-3+Cd8+ T cells in colon cancer. *Sci Rep* (2015) 5:15659. doi: 10.1038/srep15659

167. Zhu C, Anderson AC, Schubart A, Xiong H, Imitola J, Khoury SJ, et al. The Tim-3 ligand galectin-9 negatively regulates T helper type 1 immunity. *Nat Immunol* (2005) 6 (12):1245–52. doi: 10.1038/ni1271

168. Noviello M, Manfredi F, Ruggiero E, Perini T, Oliveira G, Cortesi F, et al. Bone marrow central memory and memory stem T-cell exhaustion in aml patients relapsing after hsct. *Nat Commun* (2019) 10(1):1065. doi: 10.1038/s41467-019-08871-1

169. Deng M, Gui X, Kim J, Xie L, Chen W, Li Z, et al. Lilrb4 signalling in leukaemia cells mediates T cell suppression and tumour infiltration. *Nature* (2018) 562(7728):605–9. doi: 10.1038/s41586-018-0615-z

170. Coles SJ, Hills RK, Wang EC, Burnett AK, Man S, Darley RL, et al. Increased Cd200 expression in acute myeloid leukemia is linked with an increased frequency of Foxp3+ regulatory T cells. *Leukemia* (2012) 26(9):2146–8. doi: 10.1038/leu.2012.75

171. Lv Y, Wang H, Liu Z. The role of regulatory b cells in patients with acute myeloid leukemia. *Med Sci Monit* (2019) 25:3026–31. doi: 10.12659/msm.915556

172. Ren J, Lan T, Liu T, Liu Y, Shao B, Men K, et al. Cxcl13 as a novel immune checkpoint for regulatory b cells and its role in tumor metastasis. *J Immunol* (2022) 208 (10):2425–35. doi: 10.4049/jimmunol.2100341

173. Hasan MM, Nair SS, O'Leary JG, Thompson-Snipes L, Nyarige V, Wang J, et al. Implication of tigit(+) human memory b cells in immune regulation. *Nat Commun* (2021) 12(1):1534. doi: 10.1038/s41467-021-21413-y

174. Sun H, Li Y, Zhang ZF, Ju Y, Li L, Zhang BC, et al. Increase in myeloid-derived suppressor cells (Mdscs) associated with minimal residual disease (Mrd) detection in adult acute myeloid leukemia. *Int J Hematol* (2015) 102(5):579–86. doi: 10.1007/s12185-015-1865-2

175. Yu S, Ren X, Li L. Myeloid-derived suppressor cells in hematologic malignancies: Two sides of the same coin. *Exp Hematol Oncol* (2022) 11(1):43. doi: 10.1186/s40164-022-00296-9

176. Peranzoni E, Ingangi V, Masetto E, Pinton L, Marigo I. Myeloid cells as clinical biomarkers for immune checkpoint blockade. *Front Immunol* (2020) 11:1590. doi: 10.3389/fimmu.2020.01590

177. Pyzer AR, Stroopinsky D, Rajabi H, Washington A, Tagde A, Coll M, et al. Muc1-mediated induction of myeloid-derived suppressor cells in patients with acute myeloid leukemia. *Blood* (2017) 129(13):1791–801. doi: 10.1182/blood-2016-07-730614

178. Hwang HS, Han AR, Lee JY, Park GS, Min WS, Kim HJ. Enhanced anti-leukemic effects through induction of immunomodulating microenvironment by blocking Cxcr4 and pd-L1 in an aml mouse model. *Immunol Invest* (2019) 48(1):96–105. doi: 10.1080/08820139.2018.1497057

179. Mantovani A, Sozzani S, Locati M, Allavena P, Sica A. Macrophage polarization: Tumor-associated macrophages as a paradigm for polarized M2 mononuclear phagocytes. *Trends Immunol* (2002) 23(11):549–55. doi: 10.1016/s1471-4906(02)02302-5

180. Miari KE, Guzman ML, Wheadon H, Williams MTS. Macrophages in acute myeloid leukaemia: Significant players in therapy resistance and patient outcomes. *Front Cell Dev Biol* (2021) 9:692800. doi: 10.3389/fcell.2021.692800

181. Al-Matary YS, Botezatu L, Opalka B, Hönes JM, Lams RF, Thivakaran A, et al. Acute myeloid leukemia cells polarize macrophages towards a leukemia supporting state in a growth factor independence 1 dependent manner. *Haematologica* (2016) 101 (10):1216–27. doi: 10.3324/haematol.2016.143180

182. Majeti R, Chao MP, Alizadeh AA, Pang WW, Jaiswal S, Gibbs KDJr., et al. Cd47 is an adverse prognostic factor and therapeutic antibody target on human acute myeloid leukemia stem cells. *Cell* (2009) 138(2):286–99. doi: 10.1016/j.cell.2009.05.045

183. *Study evaluating the safety and effectiveness magrolimab versus placebo in combination with venetoclax and azacitidine in participants with acute myeloid leukemia (Aml) (Enhance-3)* (2022). Available at: https://clinicaltrials.gov/ct2/show/NCT05079230.

184. Liu J, Wang L, Zhao F, Tseng S, Narayanan C, Shura L, et al. Pre-clinical development of a humanized anti-Cd47 antibody with anti-cancer therapeutic potential. *PloS One* (2015) 10(9):e0137345. doi: 10.1371/journal.pone.0137345

185. Barrett AJ, Le Blanc K. Immunotherapy prospects for acute myeloid leukaemia. *Clin Exp Immunol* (2010) 161(2):223–32. doi: 10.1111/j.1365-2249.2010.04197.x

186. Dai YJ, He SY, Hu F, Li XP, Zhang JM, Chen SL, et al. Bone marrow infiltrated natural killer cells predicted the anti-leukemia activity of Mcl1 or Bcl2 inhibitors in acute myeloid leukemia. *Mol Cancer* (2021) 20(1):8. doi: 10.1186/s12943-020-01302-6

187. Rahmani S, Yazdanpanah N, Rezaei N. Natural killer cells and acute myeloid leukemia: Promises and challenges. *Cancer Immunol Immunother* (2022) 71(12):2849–67. doi: 10.1007/s00262-022-03217-1

188. Fauriat C, Just-Landi S, Mallet F, Arnoulet C, Sainty D, Olive D, et al. Deficient expression of ncr in nk cells from acute myeloid leukemia: Evolution during leukemia treatment and impact of leukemia cells in ncrdull phenotype induction. *Blood* (2007) 109 (1):323–30. doi: 10.1182/blood-2005-08-027979

189. Mastaglio S, Wong E, Perera T, Ripley J, Blombery P, Smyth MJ, et al. Natural killer receptor ligand expression on acute myeloid leukemia impacts survival and relapse after chemotherapy. *Blood Adv* (2018) 2(4):335–46. doi: 10.1182/bloodadvances.2017015230

190. Hsu J, Hodgins JJ, Marathe M, Nicolai CJ, Bourgeois-Daigneault MC, Trevino TN, et al. Contribution of nk cells to immunotherapy mediated by pd-1/Pd-L1 blockade. *J Clin Invest* (2018) 128(10):4654–68. doi: 10.1172/jci99317

191. Lanuza PM, Pesini C, Arias MA, Calvo C, Ramirez-Labrada A, Pardo J. Recalling the biological significance of immune checkpoints on nk cells: A chance to overcome Lag3, Pd1, and Ctla4 inhibitory pathways by adoptive nk cell transfer? *Front Immunol* (2019) 10:3010. doi: 10.3389/fimmu.2019.03010

192. Khan M, Arooj S, Wang H. Nk cell-based immune checkpoint inhibition. *Front Immunol* (2020) 11:167. doi: 10.3389/fimmu.2020.00167

193. Razazian M, Khosravi M, Bahiraii S, Uzan G, Shamdani S, Naserian S. Differences and similarities between mesenchymal stem cell and endothelial progenitor cell immunoregulatory properties against T cells. *World J Stem Cells* (2021) 13(8):971–84. doi: 10.4252/wjsc.v13.i8.971

194. Tan Z, Kan C, Wong M, Sun M, Liu Y, Yang F, et al. Regulation of malignant myeloid leukemia by mesenchymal stem cells. *Front Cell Dev Biol* (2022) 10:857045. doi: 10.3389/fcell.2022.857045

195. Davies LC, Heldring N, Kadri N, Le Blanc K. Mesenchymal stromal cell secretion of programmed death-1 ligands regulates T cell mediated immunosuppression. *Stem Cells* (2017) 35(3):766–76. doi: 10.1002/stem.2509

196. Ambrosi TH, Scialdone A, Graja A, Gohlke S, Jank AM, Bocian C, et al. Adipocyte accumulation in the bone marrow during obesity and aging impairs stem cell-based hematopoietic and bone regeneration. *Cell Stem Cell* (2017) 20(6):771–84.e6. doi: 10.1016/j.stem.2017.02.009

197. Yue R, Zhou BO, Shimada IS, Zhao Z, Morrison SJ. Leptin receptor promotes adipogenesis and reduces osteogenesis by regulating mesenchymal stromal cells in adult bone marrow. *Cell Stem Cell* (2016) 18(6):782–96. doi: 10.1016/j.stem.2016.02.015

198. Miggitsch C, Meryk A, Naismith E, Pangrazzi L, Ejaz A, Jenewein B, et al. Human bone marrow adipocytes display distinct immune regulatory properties. *EBioMedicine* (2019) 46:387–98. doi: 10.1016/j.ebiom.2019.07.023

199. Horowitz MC, Berry R, Holtrup B, Sebo Z, Nelson T, Fretz JA, et al. Bone marrow adipocytes. *Adipocyte* (2017) 6(3):193–204. doi: 10.1080/21623945.2017.1367881

200. Wu B, Sun X, Gupta HB, Yuan B, Li J, Ge F, et al. Adipose pd-L1 modulates pd-1/Pd-L1 checkpoint blockade immunotherapy efficacy in breast cancer. *Oncoimmunology* (2018) 7(11):e1500107. doi: 10.1080/2162402x.2018.1500107

201. Picarda E, Galbo PMJr., Zong H, Rajan MR, Wallenius V, Zheng D, et al. The immune checkpoint B7-H3 (Cd276) regulates adipocyte progenitor metabolism and obesity development. *Sci Adv* (2022) 8(17):eabm7012. doi: 10.1126/sciadv.abm7012

202. Menter T, Tzankov A. Tumor microenvironment in acute myeloid leukemia: Adjusting niches. *Front Immunol* (2022) 13:811144. doi: 10.3389/fimmu.2022.811144

203. Tang T, Huang X, Zhang G, Hong Z, Bai X, Liang T. Advantages of targeting the tumor immune microenvironment over blocking immune checkpoint in cancer immunotherapy. *Signal Transduct Target Ther* (2021) 6(1):72. doi: 10.1038/s41392-020-00449-4

204. Zeng Y, Li B, Liang Y, Reeves PM, Qu X, Ran C, et al. Dual blockade of Cxcl12-Cxcr4 and pd-1-Pd-L1 pathways prolongs survival of ovarian tumor-bearing mice by prevention of immunosuppression in the tumor microenvironment. *FASEB J* (2019) 33 (5):6596–608. doi: 10.1096/fj.201802067RR

205. Huang KC, Chiang SF, Chen WT, Chen TW, Hu CH, Yang PC, et al. Decitabine augments chemotherapy-induced pd-L1 upregulation for pd-L1 blockade in colorectal cancer. *Cancers (Basel)* (2020) 12(2):462. doi: 10.3390/cancers12020462

frontiers | Frontiers in Immunology

TYPE Review
PUBLISHED 27 January 2023
DOI 10.3389/fimmu.2023.1110325

OPEN ACCESS

EDITED BY
Mazdak Ganjalikhani Hakemi,
Isfahan University of Medical Sciences,
Isfahan, Iran

REVIEWED BY
Yishan Ye,
Zhejiang University, China
Jean-René Pallandre,
INSERM U1098 Interactions Hôte-Greffon-Tumeur &Ingénierie Cellulaire et Génique, France

*CORRESPONDENCE
Xiuli Wu
siulier@163.com
Zhenyi Jin
jinzhenyijnu@163.com

SPECIALTY SECTION
This article was submitted to Cancer Immunity and Immunotherapy, a section of the journal Frontiers in Immunology

RECEIVED 28 November 2022
ACCEPTED 12 January 2023
PUBLISHED 27 January 2023

CITATION
Jiang X, Wu X, Xiao Y, Wang P, Zheng J, Wu X and Jin Z (2023) The ectonucleotidases CD39 and CD73 on T cells: The new pillar of hematological malignancy. *Front. Immunol.* 14:1110325. doi: 10.3389/fimmu.2023.1110325

The ectonucleotidases CD39 and CD73 on T cells: The new pillar of hematological malignancy

Xuan Jiang[1], Xiaofang Wu[1], Yuxi Xiao[1], Penglin Wang[1], Jiamian Zheng[1], Xiuli Wu[1*] and Zhenyi Jin[2*]

[1]Key Laboratory for Regenerative Medicine of Ministry of Education, Institute of Hematology, School of Medicine, Jinan University, Guangzhou, China, [2]Department of Pathology, School of Medicine, Jinan University, Guangzhou, China

Hematological malignancy develops and applies various mechanisms to induce immune escape, in part through an immunosuppressive microenvironment. Adenosine is an immunosuppressive metabolite produced at high levels within the tumor microenvironment (TME). Adenosine signaling through the A_{2A} receptor expressed on immune cells, such as T cells, potently dampens immune responses. Extracellular adenosine generated by ectonucleoside triphosphate diphosphohydrolase-1 (CD39) and ecto-5′-nucleotidase (CD73) molecules is a newly recognized 'immune checkpoint mediator' and leads to the identification of immunosuppressive adenosine as an essential regulator in hematological malignancies. In this Review, we provide an overview of the detailed distribution and function of CD39 and CD73 ectoenzymes in the TME and the effects of CD39 and CD73 inhibition on preclinical hematological malignancy data, which provides insights into the potential clinical applications for immunotherapy.

KEYWORDS
CD39, CD73, T cells, hematological malignancy, immunotherapy

1 Introduction

In the tumor microenvironment (TME), unusually high extracellular adenosine concentrations promote tumor proliferation through various immunosuppressive mechanisms. Adenosine triphosphate (ATP) represents the currency for energy metabolism inside the cell. By contrast, extracellular space usually derives from passive leakage from necrotic or injured cells, enhancing inflammation, hypoxia, and cancer (1, 2). High extracellular ATP (eATP) concentrations influence cell metabolism, adhesion, and migration in acute inflammation, in which the ectonucleotidases CD39 and CD73 take part in catabolizing nucleotides and producing immunosuppressant adenosine (ADO), which are devoted to restoring homeostasis. The ATP degradation pathway proceeds through CD39, which converts eATP or ADP to AMP, and CD73, which hydrolyzes and converts AMP to ADO (3) (Figure 1). Although ectonucleotidases help prevent excessive inflammation and tissue damage, their contribution to generating an immunosuppressive microenvironment in tumor biology is more worrying. In hematological malignancies, the overexpression of CD39 and CD73 has been linked to increased homing to

protected niches, increased survival, proliferation, and modulation of immune responses toward tolerance (4, 5). In some instances, ectonucleotidases have become reliable markers for monitoring disease and stratifying patient subsets or molecular targets for novel treatment strategies.

In this review, we discuss the structure and function of CD39 and CD73 in physiological conditions and then focus on their expression and roles in the TME of several hematological malignancies. In addition, we illustrate their potential as new targets in hematological malignancies, and the experimental findings and clinical trials of CD39 or CD73 therapies are extensively discussed.

2 Classic features of CD39 and CD73

The cascade starting with ATP and leading to ADO production is governed by CD39 and CD73, which affect purinergic signaling by modulating ligand availability (6). CD39 is an extracellular enzyme known as ecto-nucleotide triphosphate diphosphohydrolase 1 (ENTPDase1), which belongs to the membrane-bound extracellular nucleoside triphosphate diphosphate hydrolase family. It is an integral membrane protein depending on Ca^{2+} and Mg^{2+}. Human CD39, encoded by the *ENTPD1* gene on the 10q24.1 chromosome, is a protein composed of 510 amino acids, and its molecular weight is approximately 78 kDa. CD39 contains seven heavily glycosylated N-linked glycosylation sites, 11 cysteine residues, and two transmembrane regions. These two transmembrane regions include a small cytoplasmic domain containing NH_2- and COOH-terminal segments and a large extracellular hydrophobic domain containing five highly conserved domains known as apyrase conserved domains (ACRs) 1-5. This structure is significant for the catabolic activity of the enzyme and the maintenance of molecular structural integrity and contributes to nucleotide binding (7).

CD73, also known as ecto-5'-nucleotidase (ecto-5'-NT), is a membrane-bound glycoprotein connected by glycosylphosphatidylinositols (GPI) (8). Encoded by the *NT5E* gene located on human chromosome 6q14-21, CD73 is a protein molecule composed of 574 amino acids (according to its cDNA sequence), the molecular weight of which in its naturally purified form is 70 kDa (9). CD73 consists of three domains: the N-terminal domain with a metal binding site, the C-terminal domain in which the catalytic site is located, and the bridged α-helix domain (10). The non-covalent hydrophobic interaction at the C terminus and the binding of two zinc ions can stabilize the homodimerization of CD73 and achieve complete catalytic activity. CD73 homodimer can effectively hydrolyze AMP and convert it into ADO by opening and closing conformational cycles.

For this reason, it is also called the rate-limiting enzyme of the second step of purine nucleotide metabolism (11). ADO is a nucleoside molecule produced by the hydrolysis of ATP and is a critical signal molecule in the ATP-adenosine pathway. ADO can bind to four adenosine receptors belonging to the same G protein-coupled receptor (GPCR) family: A_1R, $A_{2A}R$, $A_{2B}R$, and A_3R. Among these, A_1R and A_3R are preferentially coupled to Gi protein to inhibit the action of adenylate cyclase and reduce the production of cyclic adenosine monophosphate (cAMP). However, $A_{2A}R$ and $A_{2B}R$ are generally Gs-coupled and trigger the action of adenylate cyclase and subsequently promote the production and accumulation of intracellular cAMP (12, 13). cAMP accumulation can activate both the canonical protein kinase A (PKA) and the non-canonical EPAC pathways (5). Additionally, all four adenosine receptors have been shown to induce the mitogen-activated protein kinase (MAPK) and JUN N-terminal kinase (JNK) pathways (14) (Figure 1).

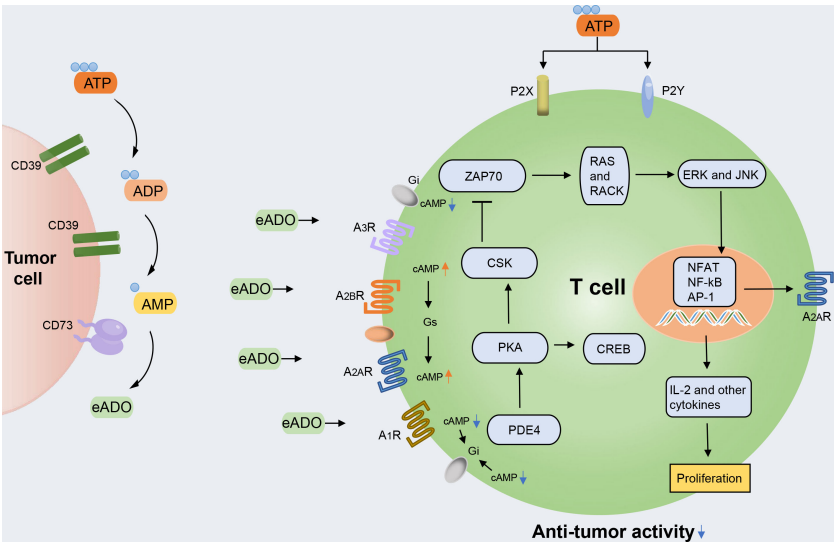

FIGURE 1
The ATP-adenosine pathway regulates immune response in the tumor microenvironment (TME). The accumulated extracellular ATP (eATP) can activate immune cell inflammation activity by stimulating type 2 purinergic receptors (P2XR and P2YR). The accumulated extracellular ADO (eADO) can bind to the downstream purinergic receptors (A_1R, $A_{2A}R$, $A_{2B}R$, and A_3R), resulting in the accumulation of cAMP. cAMP accumulation leads to protein kinase A (PKA) phosphorylation and the activation of C-terminal Src kinase (CSK), which reduces downstream LCK-dependent activation of ZAP70, extracellular signal-regulated kinase 1 (ERK1), and JNK and protein kinase C (PKC). PKA activation also activates cAMP-responsive element-binding protein 1 (CREB), which contributes to the inhibition of the major pro-inflammatory transcription factor nuclear factor-κB (NF-κB). Through this intracellular signaling pathway, the TCR-mediated activation of immune cells is counteracted.

3 CD39 and CD73 in the TME

3.1 CD39 and CD73 expressed on immune cells

Interactions between tumor cells and their immunological microenvironment are essential for the pathophysiology of lymphocytes, myeloid-derived suppressor cells (MDSCs), dendritic cells (DCs), and macrophages, which can co-express CD39 and CD73 (15) (Figure 2). Human B cells co-express CD39 and CD73 while the former was initially described as a B cell activation marker and expresses A_1, A_2, and A_3 adenosine receptors (16, 17). It has been characterized that the phenotype and functionality of $CD39^+$ human regulatory B cell (Breg) promotes Breg functions and shows high proliferative capacity while acting through adenosine generation and interleukin-10 (IL-10) secretion to immunosuppress T cells (18). CD73 is broadly expressed in human peripheral blood (PB) B cells and can also be expressed in memory B cells that develop outside of the germinal center, such as in the context of an extrafollicular reaction (19). Notably, adenosine-producing B cells produce significantly more interleukin-6 (IL-6) and IL-10, and activation of A_1 and A_{2A} receptors promote expansion and increase the differentiation of B cells toward class-switched B cells (20). Natural killer (NK) cells belonging to the innate immune subset are involved in anti-tumor immunity and contribute to the effects of ATP through type 2 purinergic receptors (P2XR and P2YR). CD39 and CD73 expression levels in NK cells are low but increase under specific conditions. CD39 can inhibit NK cell-mediated damage and decrease interferon-γ (IFN-γ) secretion (21). Additionally, CD73 expression is virtually absent in NK cells in healthy individuals but significant in tumor-infiltrating tissues, which suggests that NK cells can exert immunosuppressive function through the production of adenosine, environmental factors permitting (22).

CD39 and CD73 also exert their pro-tolerogenic effects on myeloid compartments. CD39 and CD73 levels of MDSCs are higher in tumor patients than in healthy controls (23). A positive correlation between intratumor CD39- and CD73-expressing MDSCs and tumor stage, node involvement, and metastasis status in non-small cell lung cancer has been reported (24). In further research, MDSCs expressing high levels of CD39 and CD73 increased immunosuppressive activity *ex vivo* compared with myeloid cells present in colorectal cancer (25). Thus, MDSCs that infiltrate tumors are probably an important source of extracellular adenosine, which contributes to tumor immune escape. eATP can activate the immune system through the stimulation of P2XR7 on DCs and promote an increase of interleukin-1β (IL-1β) and interleukin-18 (IL-18) secretion (26). Furthermore, IL-1β facilitates macrophage maturation and increases cytokine production (27). Additionally, CD39 is expressed on DCs, affecting DC-driven $CD4^+$ T cell activation and differentiation through NLRP3 inflammasome, which is activated by the ATP-adenosine pathway (15, 28). NLRP3 is a prerequisite for IL-1β and IL-18 production (29). Furthermore, the accumulation of adenosine can impair the normal function of DCs, the so-called immune-suppressive regulatory DCs (30). Tumor-associated macrophages co-express CD39 and the eATP receptor. Inhibiting CD39 on macrophages significantly increases their

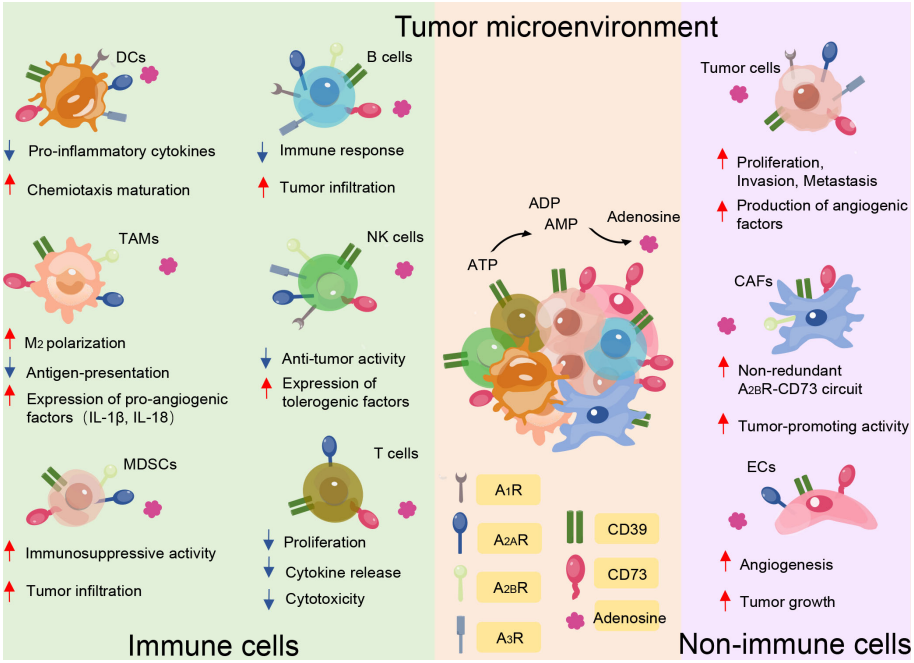

FIGURE 2
CD39 and CD73 serve as major immune suppressive mediators in the tumor microenvironment mainly through the generation of eADO. Besides the effect of ectonucleotidases on tumor cell proliferation, angiogenesis, infiltration, and metastasis, CD39 and CD73 expression by immune cells and non-immune cells impairs anti-tumor immunity by suppressing the function of protective immune cells, including T cells, B cells, natural killer (NK) cells, dendritic cells (DCs), myeloid derived suppressor cells (MDSCs), and tumor-associated macrophages, while maintaining the function of non-immune cells, including tumor cells, cancer-associated fibroblasts (CAFs), and endothelial cells (ECs). The red and blue arrows indicate whether functions are enhanced or reduced by adenosine binding to the different receptor subtypes.

production of tumor necrosis factor-α (TNF) and interleukin-12 (IL-12), while decreasing IL-10 secretion, thus inhibiting tumor growth (31, 32). It has been suggested that these macrophages that produce ADO suppress the activation of $CD4^+$ T cells *in vitro* (33). In the context of a subgroup, the classification of immune cells based on CD39 and CD73 better reflects their function.

3.2 CD39 and CD73 are expressed on non-immune cells

Increasing evidence has also verified that CD39 and CD73 are the key regulatory molecules in tumor development, including tumor growth, metastasis, and angiogenesis, and their suppressive effects on the immune system in the TME (15). A high density of angiogenesis can support the sustenance of tumor cell growth, and angiogenesis is also an important pathway for the distant invasion of tumor cells.

CD39 is highly expressed on cancer-associated fibroblasts (CAFs) in ovarian cancer and pancreatic cancer (34). In a mouse model of chronic pancreatitis and fibrosis, it was shown that CD39-deficient mice develop significantly limited fibrosis. Additionally, tissue and plasma levels of anti-fibrotic IFN-γ significantly increased (35). These results suggest a role for $CD39^+$ CAFs in promoting parenchymal fibrosis in pancreatic tissue (34). Elevated CD73 activity correlates strongly with high CAF abundance in colorectal cancer tissues (36). Furthermore, in a mouse model with ovarian cancer, a previous study demonstrated that CD73 on CAFs promotes tumor immune escape (37). ATP is well known to modulate a variety of processes linked to endothelial cell activation and increase the intracellular levels of Ca^{2+}, which induces cytoskeletal rearrangements. In addition, ATP is released by endothelial cells during changes in flow or after exposure to hypoxic conditions, activating P2YR and promoting the release of vessel relaxation (38). In the TME, the expression of CD39 in the vascular system, especially endothelial cells, can promote tumor growth by scavenging eATP and promoting angiogenesis (39). In melanoma, lung carcinoma, and colon tumors, suppressed tumor growth in CD39-deficient mice has been associated with decreased angiogenesis; CD39 co-expression with CD73 in endothelial cells will ultimately generate adenosine, which promotes angiogenesis (34). Indeed, CD73-mediated adenosine and A_{2A} signaling in endothelial cells have been shown to promote angiogenesis in a variety of experimental conditions, including during tumorigenesis (40) (Figure 2).

4 CD39 and CD73 are expressed on different T cell populations in the TME

The immortality of malignant cells demonstrates the host anti-tumor immune responses' failure and induces an immunosuppressive microenvironment in which they can freely grow and expand. It has been shown that adenosine concentration is significantly increased in the TME, and a variety of immune cells, especially T cell subsets, are involved in the immunosuppression process (Figure 3). In effector T cells, after adenosine receptor activation, type I protein kinase A (PKA) and its C-terminal Src kinase (CSK) phosphorylation are activated to inhibit SRC family tyrosine kinases LCK and FYN. This attenuates the activation of transcription factors that are downstream of T cell receptor (TCR) activation, including NFAT, nuclear factor-κB (NF-κB), and AP-1. TCR activation increases A_{2A}Rs through NF-κB-dependent induction (41). The generation of

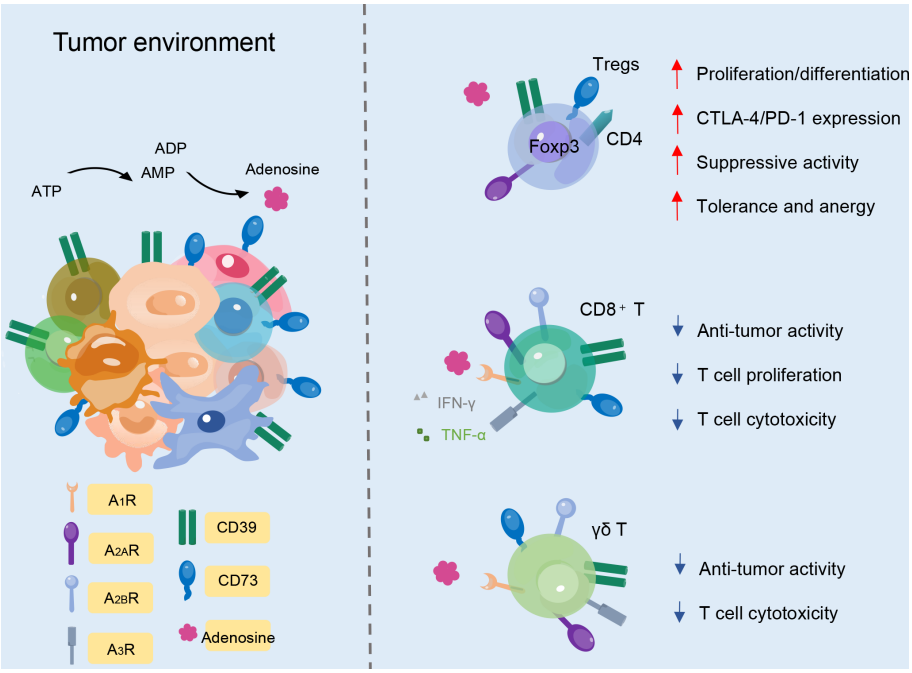

FIGURE 3
CD39 and CD73 expression on different T cell subtypes. In $Foxp3^+CD4^+$ Treg cells, CD39 and CD73 improve immunosuppressive activity. In $CD8^+$ T cells, ectonucleotidases decrease cytotoxicity, proliferation, and anti-tumor activity. Likewise, CD39 and CD73 expression on γδ T cells can also decrease anti-tumor activity and T cell cytotoxicity.

high local concentrations of adenosine by CD39 and CD73 leads to potent immunosuppression *via* the impairment of T cell activation and function, with simultaneous enhancement of regulatory T cells (Tregs) (42). Hence, the ability to block adenosine generation by inhibiting the enzymatic activity of CD39 and CD73 provides a direct line of attack on adenosine-mediated immunosuppression, and the ATP-adenosine pathway functions as a critical modulator of innate and adaptive immunity with the TME.

4.1 CD39 and CD73 are expressed on Treg cells

In human PB, approximately one-third of $CD4^+$ T cells and a small proportion of $CD8^+$ T cells express CD39 (15). On the contrary, CD73 is expressed by less than 50% of $CD8^+$ T cells and by less than 10% of $CD4^+$ T cells (15). Adenosine in turn modulates Treg function. Tregs play an indispensable role in maintaining immunological unresponsiveness to self-antigens, and counteraction of the immunosuppressive features of the TME is an attractive strategy for cancer treatment. ADO produced by CD39 and CD73 through the ATP-adenosine pathway can regulate the function of Tregs, activate receptors on Tregs to promote proliferation, and increase the expression of immunosuppressive receptors to enhance immunosuppressive function (43). In the TME, the aggregation of Tregs is associated with high CD39 expression, which promotes adenosine accumulation, tumor growth, and angiogenesis (44, 45). Compared with traditional Tregs, $CD39^+$ Tregs show more vital inhibitory ability (46). Studies also have shown that $CD39^+$ Tregs specifically suppress Interleukin-17 (IL-17) production to some extent, preventing the transdifferentiation of Tregs into T helper 17 (Th17) cells or endowing already differentiated Th17 cells with an immunosuppressive phenotype. Additionally, inhibition of human CD73 can reduce immunosuppression mediated by Tregs (47).

4.2 CD39 and CD73 are expressed on $CD8^+$ T cells

Some studies have suggested that $CD8^+$ T cells expressing CD39 and CD73 also show regulatory characteristics. Meanwhile, CD39 is potentially involved in mediating the suppressive abilities of tumor-infiltrating $CD8^+$ Tregs (48). The isolated $CD39^+CD8^+$ T cells from tumor-infiltrating lymphocytes (TILs) can inhibit T cell proliferation *in vitro*, which mediates tumor invasion, and display a gene signature of exhaustion (49). $CD8^+$ T cells express a high frequency of CD39 in solid tumors and non-solid tumors, which affects their normal cytotoxicity and ability to secrete cytokines (50). The phenotypes of exhaustion mean that the production of TNF-α, IFN-γ, and interleukin-2 (IL-2) cytokines decreases, accompanied by the upregulation of co-inhibitory receptors, including programmed cell death 1 (PD-1), cytotoxic T-lymphocyte-associated protein 4 (CTLA4), lymphocyte-activation gene 3 (LAG3), T cell immunoreceptor with Ig and ITIM domains (TIGIT), and T-cell immunoglobulin mucin-3 (TIM-3) (48, 51, 52). IL-6 and transforming growth factor-β (TGF-β) are additional factors that contribute to the upregulation of CD39 on $CD8^+$ T cells and subsequently potentiate the immunosuppressive activity in the TME. Beyond the TME, $CD39^+CD8^+$ T cells are also abundant in invaded lymph nodes and metastases and in the peripheral circulation lymphoid organs (51, 53). Interestingly, the expansion of the $CD39^+CD8^+$ T cell population in the blood is associated with clinical responses to anti-PD-1 therapy (53).

4.3 CD39 and CD73 are Expressed on γδ T Cells

Human γδ TCR-expressing cells constitute 1–5% of total T cells in the PB and play an indispensable role in the immune system. γδ T cells belong to the non-conventional lymphocyte family though they can produce many cytokines, such as IFN-γ, and act cytotoxically (54). γδ T cells are composed of different subpopulations with different functions. Recent research has shown that activated murine γδ T cells co-express CD73 and CD39 and display immunosuppressive functions, while most resting γδ τ cells do not constitutively express CD39 (55). CD39 has been identified as a marker of regulatory γδ T cells (15, 55). In murine lymph nodes, the $CD25^+CD39^+$ γδ T cell population can suppress the proliferation of αβ T cells *in vitro* (55). In the TME, $CD39^+$ γδ T cells of invasive mouse pancreatic tumors are upregulated, together with other immunosuppressive factors, and support tumorigenesis by inhibiting αβ T cell proliferation (56). Vγ9Vδ2 T cells are a subset of γδ T cells in the peripheral circulation and function by detecting self and pathogen-associated phosphoantigens (pAgs). Normally, these cells do not express CD39 or CD73 but can upregulate CD39 upon TCR stimulation. Gruenbacher et al. proved that CD39 dephosphorylates pAgs, which specifically activate Vγ9Vδ2 T cells, rendering them inactivate at stimulating γδ T cells, and thus revealed a previously unrecognized immunoregulatory role of CD39 (57). CD73 is expressed in more than 90% of peripheral γδ T cells (58). In a study of CD73 deficient mice, CD73 proved essential for γδ T cell development and might participate in its regulatory function (58). γδ T cells express different levels of CD73 before and after their activation, and the level of CD73 expression correlates with the pro- and anti-inflammatory activities of γδ T cells in Th17 autoimmune responses (59). Researchers have found that CD73-expressing γδ T cells are much more potent at converting AMP to adenosine than all other $CD73^+$ immune cell types (59).

5 The role of ectonucleotidases CD39 and CD73 in hematological malignancy

5.1 Acute myeloid leukemia

Acute myeloid leukemia (AML) is a progressive myeloproliferative malignant tumor, which is mainly characterized by abnormal proliferation of primitive and immature myeloid cells in the bone marrow (BM) and PB (60). It has been shown that there is an abnormally high CD39 expression in Treg cells in patients with AML (35). Nicolas Dulphy et al. found that compared with healthy people, the proportion of Tregs in the circulation of AML patients increased,

and the frequency of CD39 decreased (36). However, the percentage of $CD39^+$ Tregs did not decrease, which suggests that the function of CD39 in Tregs of AML patients could be maintained. At the same time, only a few patients and healthy people expressed CD73 in the Tregs, and the frequency was deficient. The increase of Treg subsets indicated that there is an overall immunosuppressive environment in tissues and BM in patients with AML (61, 62).

It has been suggested that $CD39^+CD8^+$ T cells can be used as a potential marker of exhaustion in patients with AML (63). In a study by Brauneck et al., $TIGIT^+CD73^-CD8^+$ from AML patients showed a distinct characteristic, both in PB and BM. These cells were divided into $PD1^+TIGIT^+CD73^-CD8^+$ T and $CD39^+TIGIT^+CD73^-CD8^+$ T cell subsets. As the disease progressed, the proportion of $PD1^+TIGIT^+CD73^-CD8^+$ T cells gradually increased, and this was maintained in remission (63). The latest study suggested CD39 could be used as a marker of poor treatment response and prognosis in patients with AML. Aroua et al. graded the fold enrichment of the CD39 expression cells in AML patients after chemotherapy and found that the disease-free survival rate of the 'high CD39 ratio' group was significantly worse than that of the 'low CD39 ratio' group (64). Moreover, when the focus was on patients under 60, this survival disadvantage was more significant, indicating that CD39 could be used as a prognostic marker of adverse response to chemotherapy in AML (64). The drug blocking the inhibition of CD39 activity can not only block the mitochondrial metabolic reprogramming related to AraC resistance but also significantly enhance its cytotoxicity and sensitivity to AML cells *in vivo* and *in vitro* (64, 65). Additionally, Franziska Brauneck et al. found that γδ T cells in patients with AML expresses high levels of CD39 and PD-1, TIM-3, TIGIT, and other immunosuppressive receptors, which is similar to that of $CD8^+$ T cells but higher than that of $CD4^+$ T cells (66). In further analysis, the researchers found that CD39 expression on Vδ1 T cells is significantly increased and significantly co-expressed with PD-1, TIM-3, and TIGIT, which shows further depletion characteristics (66).

Similarly, CD73 is also closely related to T-cell depletion in patients with AML and can be used as an essential target (67). The frequency of CD73 expression in $CD8^+$ T cells of newly diagnosed AML patients is significantly lower than that of healthy controls. This suggests that the downregulation of CD73 expression is phenotypically related to T cell depletion, and the expression of CD73 on $CD8^+$ T cells is increased significantly after complete remission. Therefore, the low expression of CD73 on $CD8^+$ T cells is associated with a high burden of leukemia (67). Contrary to the long-recognized negative immune regulation of ATP-adenosine signal in tumor tissue and the increase of CD73 associated with poor prognosis, the researchers found that the expression of CD73 on $CD8^+$ T cells in patients with AML is related to the enhancement of immune response and has a higher function (67). On the other hand, $CD73^-CD8^+$ T cells express high levels of inhibitory receptors, such as PD-1, TIGIT, and immunosuppressive molecules, and have the ability to produce cytokines, including IL-2, TNF-α, and IFN-γ, is decreased, thus increasing the likelihood of apoptosis (67). Therefore, understanding the specific distribution pattern of CD73 in each cancer type or disease state is very important for the optimal design of clinical studies of cancer treatment of CD73 (67, 68).

5.2 Chronic lymphocytic leukemia

Chronic lymphocytic leukemia (CLL) is the most common type of leukemia in adults and is characterized by the proliferation and progressive accumulation of functionally deficient B cells in PB, BM, and lymphoid tissues (69). The clinical course of the disease is highly variable, and some patients have a good prognosis and a long survival time, while others can rapidly develop invasive lymphoma or leukemia (70). To better differentiate prognostic subsets, novel biological parameters have been added to clinical staging systems, and TME appears to play a critical role in genesis and progression. The expression level of CD39 on CLL cells is significantly higher than that of normal lymphocytes, and the levels of $CD39^+CD4^+$ T and $CD39^+CD8^+$ T cells in PB are also significantly higher (71). Compared with $CD39^{low}$ T cells, the time-to-first treatment of CLL patients with $CD39^{high}$ T cells is significantly shorter, which indicates that the expression of CD39 on $CD4^+$ T cells is closely related to the more advanced stage of the disease and that CD39 plays a role in the invasion of the disease (71, 72). In addition, the number of $CD39^+CD4^+$ T cells increases in CLL patients with poor prognostic markers, which is associated with a shorter initial treatment time. In addition, the frequency of $CD39^+CD4^+$ T cells in CLL patients with cytogenetic abnormalities with poor prognosis is also similar to that in patients with normal- or low- or moderate-risk cytogenetic abnormalities (73). Above all, the data suggest that $CD39^+CD4^+$ T cells are associated with a poor prognosis in patients with CLL (73). In patients with CLL, the increase of Tregs has also been associated with disease progression, and the unique proportion of $CD39^+$ Tregs subsets is related to the disease stage of CLL (74). However, compared with healthy controls, $Foxp3^+$ and $Foxp3^-CD39^+CD4^+$ T cells in CLL are increased, and the levels of these two subsets are related to the severity of CLL. This suggests that the expression of Foxp3 on $CD39^+CD4^+$ T cells has no additional predictive value for the prognosis of CLL patients (73). The results referred to above were obtained from a cross-sectional study, so it is not clear whether CD39 expression on T cells increases with the deterioration of the disease.

CD73 expression may also be related to the prognosis of CLL. M. Kicova et al. showed that high CD73 expression is related to the significant shortening of the overall survival time of CLL patients (75). This was the first time that researchers have directly proven the effect of CD73 expression on the survival of patients with CLL. In addition, CD73 expression has been found on B cells in CLL patients, and Serra et al. found that high CD73 expression is associated with more aggressive clinical behavior, which is characterized by large CLL clones and poor prognosis (75, 76). Therefore, further research is needed to determine the effect of CD73 expression in patients with progressive disease.

5.3 Multiple myeloma

Multiple myeloma (MM) is the second most common hematological malignancy and is characterized by abnormal proliferation of clonal and terminally differentiated B cells in the BM. Owing to the heterogeneity of its disease progression and the

changes in the bone marrow microenvironment, most patients have a recurrence, and the prognosis of different patients is very different (77, 78). Therefore, individualized treatment of MM is critical. In patients with malignant MM, the number of $CD39^+$ Tregs is increased and they participate in the inhibition of the Th17 response. Additionally, they are used as a myeloma cell promoter that produces IL-17, especially in myeloma-permitted BM environments (79, 80). The appearance of activated $CD39^+$ Treg cells and BM resident $CD39^+$ Tregs may represent the early changes caused by malignant MM cells, thus promoting the clinical progress of MM (79).

In addition, Rui Yang et al. detected the expression of CD39 on $CD8^+$ T cells of MM patients. Interestingly, similar to $CD8^+$ TIL cells related to antigen-specific depletion, these $CD39^+CD8^+$T cells can also co-express PD-1 (81). In addition, Arghya Ray et al. found that targeted CD73 therapy, alone or in combination with an immune stimulant TLR-7 agonist, can enhance the activity of MM-specific $CD8^+$ cytotoxic T cells, which is a promising new strategy to restore patients' anti-MM immunity (23, 82). In the BM of patients with MM, the expression of CD39 on γδ T cells is significantly increased, especially on Vδ1 T cell subsets (66). Moreover, CD39 is often co-expressed with inhibitory receptors, such as TIGIT, PD-1, and TIM-3 on γδ T cells, which suggests that γδ T cells may be in a state of depletion. Therefore, targeted CD39 has potential application value in activating and enhancing the cytotoxicity of γδ T cells.

5.4 Diffuse large B-cell lymphoma

Diffuse large B-cell lymphoma (DLBCL) is the most common subtype of aggressive non-Hodgkin's lymphoma and can occur *de novo* or as a result of the transformation of indolent lymphoma (83). Owing to the heterogeneity of DLBCL, approximately one-third of patients still have a poor prognosis. The latest study found that the ATP-adenosine axis can inhibit the activity of $CD8^+$ T cells, and the combination of PD-1 and CD73 can define more dysfunctional $CD8^+$ T cell subsets (84). Targeting of the PD-1/PD-L1 (programmed cell death-ligand 1) immunosuppressive pathway combined with CD73 inhibitors may provide additional clinical benefits and partially overcome primary and secondary drug resistance to PD-1/PD-L1 blockade, as well as put forward a strong theoretical basis for precise immunotherapy and further the development of CD73 immunotherapy strategies for DLBCL patients.

6 Clinical study of the ectonucleotidases CD39 and CD73 in tumor immunity

The specific expression pattern of the ectonucleotidases CD39 and CD73 make them capable of serving as markers to selectively tag leukemia cells and deliver therapeutic agents while limiting off-targets. Additionally, as they operate in a coordinated cascade of events, the inhibition of one of them is sufficient to block the downstream processes. Hence, their intervention opens the possibility of modulating immunosuppression.

Recent studies have shown that blocking CD39 and CD73 can not only prevent the accumulation of adenosine but also restore anti-tumor immunity by stabilizing extracellular pro-inflammatory ATP (23). As a drug target for cancer, various drugs against CD39 have entered clinical trials (Table 1). CD39 inhibitors, including ARL67156 and POM-1, are effective in animal models of follicular lymphoma,

TABLE 1 Antagonists of CD39 currently in clinical trials.

Clinical trial identifier	Phase	Start date	Status	Cancer type (population, N)	Interventions and combination	Primary outcome measures	Secondary outcome measures
NCT00002652	II	November 01, 1999	Completed	MM, Plasma cell tumor (N≈unknown)	Suramin	Not provided	Not provided
NCT02724163	III	January 8, 2016	Recruiting	AML (N≈700)	Mitoxantrone, fludarabine, gemtuzumab ozogamicin	DLTs, EFS, RFS	AEs, PK, CR, CIR, DCR, EFS, OS
NCT03829254	I/II	January 30, 2019	Recruiting	Advanced cancer, lymphoma, solid tumor (N≈94)	NUC-7738	DLTs, MTD, ORR, DoR, DCR, DoSD, PFS	ORR, DoR, DCR, DoSD, PFS
NCT02514083	II	July 31, 2015	Active, not recruiting	CLL, SLL (N≈29)	Fludarabine	Safety, efficacy	Not provided
NCT03884556	I/Ib	March 16, 2019	Active, not recruiting	Solid tumor, lymphoma (N≈56)	TTX-030, pembrolizumab	Safety, DLTs, MTD, RP2D	Anti-tumor activity, Cmax, PK, CD39 expression
NCT04425655	II	June 3, 2020	Recruiting	AML (N≈27)	Fludarabine	ORR, CR, CRi	Safety, CR rate, OS, LFS, EFS
NCT04261075	I	January 7, 2020	Active, not recruiting	Advanced solid tumors (N≈57)	IPH5201 (alone), durvalumab, oleclumab	Safety, ECG	DC, Cmax

ADAs, anti-drug antibodies; AEs, adverse events; ALL, acute lymphoblastic leukemia; AML, acute myelocytic leukemia; CIR, cumulative incidence of relapse; Cmax, maximum concentration; CR, complete response; CRi, incomplete count recovery; DC, disease control; DCR, disease control rate; DLTs, dose-limiting toxicity; DoR, duration of response; DoSD, duration of stable disease; ECG, electrocardiogram; EFS, event-free survival; LFS, leukemia-free survival; MM, multiple myeloma; MTD, maximum tolerated dose; ORR, objective response rate; OS, overall survival; PFS, progression-free survival; PK, pharmacokinetics; RFS, relapse-free survival; RP2D, recommended phase 2 dose.
Durvalumab, humanized anti-human PD-L1 monoclonal antibody; fludarabine, CD39 antagonist; gemtuzumab ozogamicin, CD33 Inhibitor; IPH5201, CD39 antagonist; mitoxantrone, CD39 antagonist; NUC-7738, CD39 antagonist; oleclumab, anti-CD73 monoclonal antibody; pembrolizumab, humanized anti-human PD-1 monoclonal antibody; suramin, CD39 antagonist; TTX-030, CD39 antagonist.

sarcoma, or mouse melanoma, resulting in the partial overcoming of poor T cell response to stimulation, enhanced response to chemotherapeutic drugs, and inhibition of tumor growth, respectively (47). After administration of CD39 inhibitor ARL67156, eATP in tumors increases, which promotes the recruitment of dendritic cells and $CD4^+$ and $CD8^+$ cells producing IFN-γ and simultaneously promotes the immune control of autophagy-deficient tumors (85). Considering the delicate balance between eATP and extracellular adenosine in regulating the immune response in TME, CD39-guided therapy may affect tumor-immune interaction in other aspects (23). In addition to monotherapy, some preclinical studies have shown that there is a synergistic blocking effect between the release of immunosuppressive tumor microenvironment and anti-PD-1/PD-L1 resulting from targeting of the ATP-adenosine pathway (including CD39 and CD73) (85). Preclinical studies have also shown that the synergistic effect of targeted CD39 antagonist IPH5201 and PD-L1 checkpoint inhibitors have better complete regression and improved survival than PD-L1 inhibitors alone (86).

CD73 can also be expressed in normal cells, and for this reason, therapy targeting CD73 (such as an anti-CD73 monoclonal antibody) is often considered a non-specific therapy (87). Interestingly, studies have proved that CD73 is highly effective in targeted therapy for cancer (Table 2). Antagonists targeting CD73 often combine with other immune checkpoint blockers to improve the prognosis for cancer patients. Tests of CD73 small molecule inhibitor AB680 in pancreatic cancer patients have shown that it can effectively restore T cell proliferation, cytokine secretion, and suppressed cytotoxicity (88).

TABLE 2 Antagonists of CD73 currently in clinical trials.

Clinical trial identifier	Phase	Start date	Status	Cancer type (population, N)	Interventions and combination	Primary outcome measures	Secondary outcome measures
NCT03249636	Not provided	August 9, 2017	Not provided	ALL (N≈50)	Flow cytometric analysis	Expression of markers in ALL	Not provided
NCT03454451	I	April 25, 2018	Recruiting	NHL, solid tumor (N≈378)	CPI-006, ciforadenant/ pembrolizumab	DLTs, MDL	AUC, Cmax
NCT04668300	II	November 26, 2020	Recruiting	Sarcoma (N≈75)	Oleclumab, durvalumab	RR, EFS	PFS, RR, OS, AEs
NCT05227144	I	January 6, 2022	Recruiting	R/R MM (N≈48)	ORIC-533	RP2D, safety, tolerability	Cmax, AUClast, PK
NCT02503774	I	July 24, 2015	Active, not recruiting	Solid tumor (N≈190)	MEDI9447, MEDI4736	Safety, SAEs	OR, DoR, DC, PFS, OS
NCT02754141	I/II	June 21, 2016	Completed	Solid tumor (N≈234)	BMS-986179, nivolumab	AEs, SAEs	ORR, DoR, PFSR, ADAs, DF, etc.
NCT03381274	I/II	May 8, 2018	Active, not recruiting	NSCLC (N≈43)	MEDI9447, AZD4635	Safety, RR	DoR, DC, PFS, OS, OR, etc.
NCT03267589	II	June 16, 2018	Completed	Ovarian cancer (N≈25)	MEDI9447, durvalumab, tremelilumab	DCR	PFS, OS, RR, DoR
NCT03835949	I	July 16, 2019	Active, not recruiting	Solid tumor (N≈36)	TJ004309, atezolizumab	MTD	II agent, Antitumor activity, etc.
NCT04672434	I	November 19, 2020	Recruiting	Solid tumor (N≈100)	Sym024, Sym021	AEs, MTD/MAD	OR, SD, TTP, AUC, Cmax, Tmax, etc.
NCT05174585	I/II	August, 2022	Not yet recruiting	Solid tumor (N≈62)	JAB-BX102, pembrolizumab	DLTs, AEs, ORR, DOR	PK, ORR, DoR, DCR, PFS
NCT04572152	I	January 18, 2021	Recruiting	Solid tumor (N≈195)	AK119, AK104	AEs, DLTs	ORR, DCR, Cmax, Cmin, ADAs
NCT04940286	II	September 28, 2021	Recruiting	Solid tumor (N≈30)	Oleclumab, durvalumab	RR, AEs	Not provided
NCT04989387	I	October 4, 2021	Recruiting	Solid tumor (N≈230)	INCA00186, retifanlimab, INCB106385	Safety, tolerability, DLTs, RDE	ORR, DCR, DoR, Cmax, CL, etc.
NCT05431270	I	June 23, 2022	Recruiting	Solid tumor (N≈38)	PT199, anti-PD-1 monoclonal antibody	MTD	RR, PK

ADAs, anti-drug antibodies; AEs, adverse events; AUC, area under the curve; CL, clearance; CLL, chronic lymphocytic leukemia; Cmax, maximum concentration; Cmin, minimum observed concentration; DC, disease control; DCR, disease control rate; DF, degree of fluctuation or fluctuation index; DLTs, dose-limiting toxicity; DoR, duration of response; EFS, event-free survival; MDL, maximum dose level; MTD, maximum tolerated dose; MM, multiple myeloma; NHL, non-Hodgkin lymphoma; NSCLC, non-small-cell lung cancer; OR, objective response; ORR, objective response rate; OS, overall survival; PK, pharmacokinetics; PFS, progression-free survival; PFSR, progression-free survival rate; RDE, recommended dose for expansion; RP2D, recommended phase 2 dose; RR, relative risk; SAEs, serious adverse events; SD, stable disease; Tmax, time to reach maximum concentration; TTP, time to progression.

AK104, anti-PD-1/CTLA-4 bispecific antibody; AK119, CD73 antagonist; atezolizumab, PD-1/PD-L1 inhibitor; AZD4635, A2AR antagonist; BMS-986179, CD73 antagonist; ciforadenant, A2A antagonist; CPI-006, CD73 antagonist; durvalumab, humanized anti-human PD-L1 monoclonal antibody; INCA00186, CD73 antagonist; INCB106385, anti-A2AR/A2BR bispecific antibody; JAB-BX102, CD73 antagonist; MEDI4736, humanized anti-human PD-L1 monoclonal antibody; MEDI9447, CD73 antagonist; nivolumab, PD-1 inhibitor; oleclumab, CD73 antagonist; ORIC-533, CD73 antagonist; pembrolizumab, humanized anti-human PD-1 monoclonal antibody; PT199, CD73 antagonist; retifanlimab, PD-1 inhibitor; Sym021, humanized anti-human PD-1 monoclonal antibody; Sym024, CD73 antagonist; TJ004309, CD73 antagonist; tremelilumab, anti-CTLA-4 monoclonal antibody.

Consistent with the previously reported anti-tumor effect of immune checkpoint blockers combined with CD73 targeted drugs, the use of AB680 combined with PD-1 blocking *in vitro* can overcome the inhibitory effect of adenosine on human T cells and enhance the anti-tumor activity of drugs and the anti-tumor effect *in vivo* (88). In addition, in the breast cancer model, anti-CD73 antibodies partially prevent lung metastasis in mice (89). Currently, a therapeutic anti-CD73 antibody MEDI9447 is also in clinical trials with patients with solid cancer (NCT02503774; NCT03611556) (90).

7 Conclusion

Although ectonucleotidases CD39 and CD73 represent promising targets for novel therapeutic strategies, most current therapeutic strategies come from solid tumors. They involve hematological malignancies in which they can act as disease and prognostic markers and, to some extent, directly contribute to leukemia progress and expansion. The proper design of clinical trials incorporating a comprehensive biomarker strategy will be paramount for robustly impacting tumor-immune interactions and regulating the suppressive TME. As discussed previously, there are additional combination regimens that can synergize with CD39 or CD73 blockade to provide potential benefits to patients. It is worth noting that some key issues remain unaddressed, including determining the consequences of targeting CD39, CD73, and adenosine receptors on extracellular ATP levels, evaluating the activity of the dual targeting of CD39 and CD73, and developing reliable methods to measure extracellular adenosine levels in the TME.

Author contributions

XLW and ZYJ contributed to the outline and revision of the manuscript; XJ wrote the initial manuscript draft; XFW prepared the figure; JMZ and YXX organized the literature for the manuscript; PLW and XJ revised the final draft. All authors read and approved the submitted manuscript.

Funding

This study was supported by grants from the Science and Technology Program of Guangzhou City (202201010164), the National Natural Science Foundation of China (81800143, 81770150, 81200388, and 82170220), the Natural Science Foundation of Guangdong Province (2020A1515010817 and 2022A1515010313), the National Innovation and Entrepreneurship Training Program for Undergraduates (202010559081), Guangdong's Innovation and Entrepreneurship Training Program for Undergraduates (202010559081 and 202210559083), the "Challenge Cup" National Undergraduate curricular academic science and technology works by race (21112027), and Guangdong College Students' Scientific and Technological Innovation (CX22438, CX22446, and CX21285).

Conflict of interest

The authors declare that the research was conducted in the absence of any commercial or financial relationships that could be construed as a potential conflict of interest.

Publisher's note

References

1. Kepp O, Loos F, Liu P, Kroemer G. Extracellular nucleosides and nucleotides as immunomodulators. *Immunol Rev* (2017) 280(1):83–92. doi: 10.1111/imr.12571

2. Dosch M, Gerber J, Jebbawi F, Beldi G. Mechanisms of Atp release by inflammatory cells. *Int J Mol Sci* (2018) 19(4):1-16. doi: 10.3390/ijms19041222

3. Longhi MS, Robson SC, Bernstein SH, Serra S, Deaglio S. Biological functions of ecto-enzymes in regulating extracellular adenosine levels in neoplastic and inflammatory disease states. *J Mol Med (Berl)* (2013) 91(2):165–72. doi: 10.1007/s00109-012-0991-z

4. Vaisitti T, Arruga F, Deaglio S. Targeting the adenosinergic axis in chronic lymphocytic leukemia: A way to disrupt the tumor niche? *Int J Mol Sci* (2018) 19(4):1-21. doi: 10.3390/ijms19041167

5. Antonioli L, Blandizzi C, Pacher P, Hasko G. Immunity, inflammation and cancer: A leading role for adenosine. *Nat Rev Cancer* (2013) 13(12):842–57. doi: 10.1038/nrc3613

6. Vaisitti T, Arruga F, Guerra G, Deaglio S. Ectonucleotidases in blood malignancies: A tale of surface markers and therapeutic targets. *Front Immunol* (2019) 10:2301. doi: 10.3389/fimmu.2019.02301

7. Heine P, Braun N, Sévigny J, Robson SC, Servos J, Zimmermann H. The c-terminal cysteine-rich region dictates specific catalytic properties in chimeras of the ectonucleotidases Ntpdase1 and Ntpdase2. *Eur J Biochem* (2001) 268(2):364–73. doi: 10.1046/j.1432-1033.2001.01896.x

8. Colgan SP, Eltzschig HK, Eckle T, Thompson LF. Physiological roles for ecto-5'-Nucleotidase (Cd73). *Purinergic Signal* (2006) 2(2):351–60. doi: 10.1007/s11302-005-5302-5

9. Resta R, Yamashita Y, Thompson LF. Ecto-enzyme and signaling functions of lymphocyte Cd73. *Immunol Rev* (1998) 161:95–109. doi: 10.1111/j.1600-065x.1998.tb01574.x

10. Fini C, Talamo F, Cherri S, Coli M, Floridi A, Ferrara L, et al. Biochemical and mass spectrometric characterization of soluble ecto-5'-Nucleotidase from bull seminal plasma. *Biochem J* (2003) 372(2):443–51. doi: 10.1042/bj20021687

11. Knapp K, Zebisch M, Pippel J, El-Tayeb A, Muller CE, Strater N. Crystal structure of the human ecto-5'-Nucleotidase (Cd73): Insights into the regulation of purinergic signaling. *Structure* (2012) 20(12):2161–73. doi: 10.1016/j.str.2012.10.001

12. Mosenden R, Tasken K. Cyclic amp-mediated immune regulation–overview of mechanisms of action in T cells. *Cell Signal* (2011) 23(6):1009–16. doi: 10.1016/j.cellsig.2010.11.018

13. Young A, Ngiow SF, Barkauskas DS, Sult E, Hay C, Blake SJ, et al. Co-Inhibition of Cd73 and A2ar adenosine signaling improves anti-tumor immune responses. *Cancer Cell* (2016) 30(3):391–403. doi: 10.1016/j.ccell.2016.06.025

14. Schulte G, Fredholm BB. Signalling from adenosine receptors to mitogen-activated protein kinases. *Cell Signal* (2003) 15(9):813–27. doi: 10.1016/s0898-6568(03)00058-5

15. Allard B, Longhi MS, Robson SC, Stagg J. The ectonucleotidases Cd39 and Cd73: Novel checkpoint inhibitor targets. *Immunol Rev* (2017) 276(1):121–44. doi: 10.1111/imr.12528

16. Zacca ER, Amezcua Vesely MC, Ferrero PV, Acosta CDV, Ponce NE, Bossio SN, et al. B Cells from patients with rheumatoid arthritis show conserved Cd39-mediated

regulatory function and increased Cd39 expression after positive response to therapy. *J Mol Biol* (2021) 433(1):166687. doi: 10.1016/j.jmb.2020.10.021

17. Saze Z, Schuler PJ, Hong CS, Cheng D, Jackson EK, Whiteside TL. Adenosine production by human b cells and b cell-mediated suppression of activated T cells. *Blood* (2013) 122(1):9–18. doi: 10.1182/blood-2013-02-482406

18. Figueiro F, Muller L, Funk S, Jackson EK, Battastini AM, Whiteside TL. Phenotypic and functional characteristics of Cd39(High) human regulatory b cells (Breg). *Oncoimmunology* (2016) 5(2):e1082703. doi: 10.1080/2162402X.2015.1082703

19. Sweet RA, Cullen JL, Shlomchik MJ. Rheumatoid factor b cell memory leads to rapid, switched antibody-forming cell responses. *J Immunol* (2013) 190(5):1974–81. doi: 10.4049/jimmunol.1202816

20. Kaku H, Cheng KF, Al-Abed Y, Rothstein TL. A novel mechanism of b cell-mediated immune suppression through Cd73 expression and adenosine production. *J Immunol* (2014) 193(12):5904–13. doi: 10.4049/jimmunol.1400336

21. Hu G, Wu P, Cheng P, Zhang Z, Wang Z, Yu X, et al. Tumor-infiltrating Cd39(+) Gammadeltatregs are novel immunosuppressive T cells in human colorectal cancer. *Oncoimmunology* (2017) 6(2):e1277305. doi: 10.1080/2162402X.2016.1277305

22. Chatterjee D, Tufa DM, Baehre H, Hass R, Schmidt RE, Jacobs R. Natural killer cells acquire Cd73 expression upon exposure to mesenchymal stem cells. *Blood* (2014) 123 (4):594–5. doi: 10.1182/blood-2013-09-524827

23. Moesta AK, Li XY, Smyth MJ. Targeting Cd39 in cancer. *Nat Rev Immunol* (2020) 20(12):739–55. doi: 10.1038/s41577-020-0376-4

24. Li J, Wang L, Chen X, Li L, Li Y, Ping Y, et al. Cd39/Cd73 upregulation on myeloid-derived suppressor cells *Via* tgf-Beta-Mtor-Hif-1 signaling in patients with non-small cell lung cancer. *Oncoimmunology* (2017) 6(6):e1320011. doi: 10.1080/2162402X.2017.1320011

25. Limagne E, Euvrard R, Thibaudin M, Rebe C, Derangere V, Chevriaux A, et al. Accumulation of mdsc and Th17 cells in patients with metastatic colorectal cancer predicts the efficacy of a folfox-bevacizumab drug treatment regimen. *Cancer Res* (2016) 76(18):5241–52. doi: 10.1158/0008-5472.CAN-15-3164

26. Mariathasan S, Weiss DS, Newton K, McBride J, O'Rourke K, Roose-Girma M, et al. Cryopyrin activates the inflammasome in response to toxins and atp. *Nature* (2006) 440(7081):228–32. doi: 10.1038/nature04515

27. Pan MH, Maresz K, Lee PS, Wu JC, Ho CT, Popko J, et al. Inhibition of tnf-alpha, il-1alpha, and il-1beta by pretreatment of human monocyte-derived macrophages with menaquinone-7 and cell activation with tlr agonists in vitro. *J Med Food* (2016) 19 (7):663–9. doi: 10.1089/jmf.2016.0030

28. Mascanfroni ID, Yeste A, Vieira SM, Burns EJ, Patel B, Sloma I, et al. Il-27 acts on dcs to suppress the T cell response and autoimmunity by inducing expression of the immunoregulatory molecule Cd39. *Nat Immunol* (2013) 14(10):1054–63. doi: 10.1038/ni.2695

29. Zhao H, Bo C, Kang Y, Li H. What else can Cd39 tell us? *Front Immunol* (2017) 8:727. doi: 10.3389/fimmu.2017.00727

30. Veglia F, Gabrilovich DI. Dendritic cells in cancer: The role revisited. *Curr Opin Immunol* (2017) 45:43–51. doi: 10.1016/j.coi.2017.01.002

31. Savio LEB, de Andrade Mello P, Figliuolo VR, de Avelar Almeida TF, Santana PT, Oliveira SDS, et al. Cd39 limits P2x7 receptor inflammatory signaling and attenuates sepsis-induced liver injury. *J Hepatol* (2017) 67(4):716–26. doi: 10.1016/j.jhep.2017.05.021

32. Cohen HB, Ward A, Hamidzadeh K, Ravid K, Mosser DM. Ifn-gamma prevents adenosine receptor (A2br) upregulation to sustain the macrophage activation response. *J Immunol* (2015) 195(8):3828–37. doi: 10.4049/jimmunol.1501139

33. Montalban Del Barrio I, Penski C, Schlahsa L, Stein RG, Diessner J, Wockel A, et al. Adenosine-generating ovarian cancer cells attract myeloid cells which differentiate into adenosine-generating tumor associated macrophages - a self-amplifying, Cd39- and Cd73-dependent mechanism for tumor immune escape. *J Immunother Cancer* (2016) 4:49. doi: 10.1186/s40425-016-0154-9

34. Allard D, Allard B, Stagg J. On the mechanism of anti-Cd39 immune checkpoint therapy. *J Immunother Cancer* (2020) 8(1):1-11. doi: 10.1136/jitc-2019-000186

35. Kunzli BM, Nuhn P, Enjyoji K, Banz Y, Smith RN, Csizmadia E, et al. Disordered pancreatic inflammatory responses and inhibition of fibrosis in Cd39-null mice. *Gastroenterology* (2008) 134(1):292–305. doi: 10.1053/j.gastro.2007.10.030

36. Yu M, Guo G, Huang L, Deng L, Chang CS, Achyut BR, et al. Cd73 on cancer-associated fibroblasts enhanced by the a(2b)-mediated feedforward circuit enforces an immune checkpoint. *Nat Commun* (2020) 11(1):515. doi: 10.1038/s41467-019-14060-x

37. Turcotte M, Spring K, Pommey S, Chouinard G, Cousineau I, George J, et al. Cd73 is associated with poor prognosis in high-grade serous ovarian cancer. *Cancer Res* (2015) 75(21):4494–503. doi: 10.1158/0008-5472.CAN-14-3569

38. Lohman AW, Billaud M, Isakson BE. Mechanisms of atp release and signalling in the blood vessel wall. *Cardiovasc Res* (2012) 95(3):269–80. doi: 10.1093/cvr/cvs187

39. Kunzli BM, Bernlochner MI, Rath S, Kaser S, Csizmadia E, Enjyoji K, et al. Impact of Cd39 and purinergic signalling on the growth and metastasis of colorectal cancer. *Purinergic Signal* (2011) 7(2):231–41. doi: 10.1007/s11302-011-9228-9

40. Allard B, Turcotte M, Spring K, Pommey S, Royal I, Stagg J. Anti-Cd73 therapy impairs tumor angiogenesis. *Int J Cancer* (2014) 134(6):1466–73. doi: 10.1002/ijc.28456

41. Cekic C, Linden J. Purinergic regulation of the immune system. *Nat Rev Immunol* (2016) 16(3):177–92. doi: 10.1038/nri.2016.4

42. Verma NK, Wong BHS, Poh ZS, Udayakumar A, Verma R, Goh RKJ, et al. Obstacles for T-lymphocytes in the tumour microenvironment: Therapeutic challenges, advances and opportunities beyond immune checkpoint. *EBioMedicine* (2022) 83:104216. doi: 10.1016/j.ebiom.2022.104216

43. Ohta A, Kini R, Ohta A, Subramanian M, Madasu M, Sitkovsky M. The development and immunosuppressive functions of Cd4(+) Cd25(+) Foxp3(+) regulatory T cells are under influence of the adenosine-A2a adenosine receptor pathway. *Front Immunol* (2012) 3:190. doi: 10.3389/fimmu.2012.00190

44. Borsellino G, Kleinewietfeld M, Di Mitri D, Sternjak A, Diamantini A, Giometto R, et al. Expression of ectonucleotidase Cd39 by Foxp3+ treg cells: Hydrolysis of extracellular atp and immune suppression. *Blood* (2007) 110(4):1225–32. doi: 10.1182/blood-2006-12-064527

45. Peres RS, Donate PB, Talbot J, Cecilio NT, Lobo PR, Machado CC, et al. Tgf-beta signalling defect is linked to low Cd39 expression on regulatory T cells and methotrexate resistance in rheumatoid arthritis. *J Autoimmun* (2018) 90:49–58. doi: 10.1016/j.jaut.2018.01.004

46. Lu Y, Wang X, Gu J, Lu H, Zhang F, Li X, et al. Itreg induced from Cd39(+) naive T cells demonstrate enhanced proliferate and suppressive ability. *Int Immunopharmacol* (2015) 28(2):925–30. doi: 10.1016/j.intimp.2015.03.039

47. Mandapathil M, Hilldorfer B, Szczepanski MJ, Czystowska M, Szajnik M, Ren J, et al. Generation and accumulation of immunosuppressive adenosine by human Cd4 +Cd25highfoxp3+ regulatory T cells. *J Biol Chem* (2010) 285(10):7176–86. doi: 10.1074/jbc.M109.047423

48. Vieyra-Lobato MR, Vela-Ojeda J, Montiel-Cervantes L, Lopez-Santiago R, Moreno-Lafont MC. Description of Cd8(+) regulatory T lymphocytes and their specific intervention in graft-Versus-Host and infectious diseases, autoimmunity, and cancer. *J Immunol Res* (2018) 2018:3758713. doi: 10.1155/2018/3758713

49. Gallerano D, Ciminati S, Grimaldi A, Piconese S, Cammarata I, Focaccetti C, et al. Genetically driven Cd39 expression shapes human tumor-infiltrating Cd8(+) T-cell functions. *Int J Cancer* (2020) 147(9):2597–610. doi: 10.1002/ijc.33131

50. Timperi E, Barnaba V. Cd39 regulation and functions in T cells. *Int J Mol Sci* (2021) 22(15):1-13. doi: 10.3390/ijms22158068

51. Canale FP, Ramello MC, Nunez N, Araujo Furlan CL, Bossio SN, Gorosito Serran M, et al. Cd39 expression defines cell exhaustion in tumor-infiltrating Cd8(+) T cells. *Cancer Res* (2018) 78(1):115–28. doi: 10.1158/0008-5472.CAN-16-2684

52. Noble A, Mehta H, Lovell A, Papaioannou E, Fairbanks L. Il-12 and il-4 activate a Cd39-dependent intrinsic peripheral tolerance mechanism in Cd8(+) T cells. *Eur J Immunol* (2016) 46(6):1438–48. doi: 10.1002/eji.201545939

53. Simoni Y, Becht E, Fehlings M, Loh CY, Koo SL, Teng KWW, et al. Bystander Cd8 (+) T cells are abundant and phenotypically distinct in human tumour infiltrates. *Nature* (2018) 557(7706):575–9. doi: 10.1038/s41586-018-0130-2

54. Kalyan S, Kabelitz D. Defining the nature of human gammadelta T cells: A biographical sketch of the highly empathetic. *Cell Mol Immunol* (2013) 10(1):21–9. doi: 10.1038/cmi.2012.44

55. Otsuka A, Hanakawa S, Miyachi Y, Kabashima K. Cd39: A new surface marker of mouse regulatory gammadelta T cells. *J Allergy Clin Immunol* (2013) 132(6):1448–51. doi: 10.1016/j.jaci.2013.05.037

56. Daley D, Zambirinis CP, Seifert L, Akkad N, Mohan N, Werba G, et al. Gammadelta T cells support pancreatic oncogenesis by restraining alphabeta T cell activation. *Cell* (2016) 166(6):1485–99 e15. doi: 10.1016/j.cell.2016.07.046

57. Gruenbacher G, Gander H, Rahm A, Idzko M, Nussbaumer O, Thurnher M. Ecto-atpase Cd39 inactivates isoprenoid-derived Vgamma9vdelta2 T cell phosphoantigens. *Cell Rep* (2016) 16(2):444–56. doi: 10.1016/j.celrep.2016.06.009

58. Coffey F, Lee SY, Buus TB, Lauritsen JP, Wong GW, Joachims ML, et al. The tcr ligand-inducible expression of Cd73 marks gammadelta lineage commitment and a metastable intermediate in effector specification. *J Exp Med* (2014) 211(2):329–43. doi: 10.1084/jem.20131540

59. Li X, Liang D, Shao H, Born WK, Kaplan HJ, Sun D. Adenosine receptor activation in the Th17 autoimmune responses of experimental autoimmune uveitis. *Cell Immunol* (2019) 339:24–8. doi: 10.1016/j.cellimm.2018.09.004

60. Weigert N, Rowe JM, Lazarus HM, Salman MY. Consolidation in aml: Abundant opinion and much unknown. *Blood Rev* (2022) 51:100873. doi: 10.1016/j.blre.2021.100873

61. Schick J, Vogt V, Zerwes M, Kroell T, Kraemer D, Kohne CH, et al. Antileukemic T-cell responses can be predicted by the composition of specific regulatory T-cell subpopulations. *J Immunother* (2013) 36(4):223–37. doi: 10.1097/CJI.0b013e31829180e7

62. Dulphy N, Henry G, Hemon P, Khaznadar Z, Dombret H, Boissel N, et al. Contribution of Cd39 to the immunosuppressive microenvironment of acute myeloid leukaemia at diagnosis. *Br J Haematol* (2014) 165(5):722–5. doi: 10.1111/bjh.12774

63. Brauneck F, Haag F, Woost R, Wildner N, Tolosa E, Rissiek A, et al. Increased frequency of Tigit(+)Cd73-Cd8(+) T cells with a tox(+) tcf-1low profile in patients with newly diagnosed and relapsed aml. *Oncoimmunology* (2021) 10(1):1930391. doi: 10.1080/2162402X.2021.1930391

64. Aroua N, Boet E, Ghisi M, Nicolau-Travers ML, Saland E, Gwilliam R, et al. Extracellular atp and Cd39 activate camp-mediated mitochondrial stress response to promote cytarabine resistance in acute myeloid leukemia. *Cancer Discovery* (2020) 10 (10):1544–65. doi: 10.1158/2159-8290.CD-19-1008

65. Luna-Yolba R, Marmoiton J, Gigo V, Marechal X, Boet E, Sahal A, et al. Disrupting mitochondrial electron transfer chain complex I decreases immune checkpoints in murine and human acute myeloid leukemic cells. *Cancers (Basel)* (2021) 13(14):1-18. doi: 10.3390/cancers13143499

66. Brauneck F, Weimer P, Schulze Zur Wiesch J, Weisel K, Leypoldt L, Vohwinkel G, et al. Bone marrow-resident Vdelta1 T cells Co-express tigit with pd-1, Tim-3 or Cd39 in

aml and myeloma. *Front Med (Lausanne)* (2021) 8:763773. doi: 10.3389/fmed.2021.763773

67. Kong Y, Jia B, Zhao C, Claxton DF, Sharma A, Annageldiyev C, et al. Downregulation of Cd73 associates with T cell exhaustion in aml patients. *J Hematol Oncol* (2019) 12(1):40. doi: 10.1186/s13045-019-0728-3

68. Jia B, Zhao C, Rakszawski KL, Claxton DF, Ehmann WC, Rybka WB, et al. Eomes (+)T-Bet(Low) Cd8(+) T cells are functionally impaired and are associated with poor clinical outcome in patients with acute myeloid leukemia. *Cancer Res* (2019) 79(7):1635–45. doi: 10.1158/0008-5472.CAN-18-3107

69. Hallek M, Shanafelt TD, Eichhorst B. Chronic lymphocytic leukaemia. *Lancet* (2018) 391(10129):1524–37. doi: 10.1016/S0140-6736(18)30422-7

70. Ciszak L, Frydecka I, Wolowiec D, Szteblich A, Kosmaczewska A. Patients with chronic lymphocytic leukaemia (Cll) differ in the pattern of ctla-4 expression on cll cells: The possible implications for immunotherapy with ctla-4 blocking antibody. *Tumour Biol* (2016) 37(3):4143–57. doi: 10.1007/s13277-015-4217-1

71. Mosaad Zaki E, Mohamed Zahran A, Abdelazeem Metwaly A, Hafez R, Hussein S, Elaiw Mohammed A. Impact of Cd39 expression on Cd4+ T lymphocytes and 6q deletion on outcome of patients with chronic lymphocytic leukemia. *Hematol/Oncol Stem Cell Ther* (2019) 12(1):26–31. doi: 10.1016/j.hemonc.2018.09.002

72. Abousamra NK, Salah El-Din M, Hamza Elzahaf E, Esmael ME. Ectonucleoside triphosphate diphosphohydrolase-1 (E-Ntpdase1/Cd39) as a new prognostic marker in chronic lymphocytic leukemia. *Leuk Lymphoma* (2015) 56(1):113–9. doi: 10.3109/10428194.2014.907893

73. Perry C, Hazan-Halevy I, Kay S, Cipok M, Grisaru D, Deutsch V, et al. Increased Cd39 expression on Cd4(+) T lymphocytes has clinical and prognostic significance in chronic lymphocytic leukemia. *Ann Hematol* (2012) 91(8):1271–9. doi: 10.1007/s00277-012-1425-2

74. D'Arena G, Laurenti L, Minervini MM, Deaglio S, Bonello L, De Martino L, et al. Regulatory T-cell number is increased in chronic lymphocytic leukemia patients and correlates with progressive disease. *Leuk Res* (2011) 35(3):363–8. doi: 10.1016/j.leukres.2010.08.010

75. Kicova M, Michalova Z, Coma M, Gabzdilova J, Dedinska K, Guman T, et al. The expression of Cd73 on pathological b-cells is associated with shorter overall survival of patients with cll. *Neoplasma* (2020) 67(4):933–8. doi: 10.4149/neo_2020_190826N822

76. Serra S, Horenstein AL, Vaisitti T, Brusa D, Rossi D, Laurenti L, et al. Cd73-generated extracellular adenosine in chronic lymphocytic leukemia creates local conditions counteracting drug-induced cell death. *Blood* (2011) 118(23):6141–52. doi: 10.1182/blood-2011-08-374728

77. Premkumar V, Bhutani D, Lentzsch S. Modern treatments and future directions for Relapsed/Refractory multiple myeloma patients. *Clin Lymphoma Myeloma Leuk* (2020) 20(11):736–43. doi: 10.1016/j.clml.2020.06.023

78. Casey M, Nakamura K. The cancer-immunity cycle in multiple myeloma. *Immunotargets Ther* (2021) 10:247–60. doi: 10.2147/ITT.S305432

79. Marsh-Wakefield F, Kruzins A, McGuire HM, Yang S, Bryant C, Fazekas de St Groth B, et al. Mass cytometry discovers two discrete subsets of Cd39(-)Treg which discriminate mgus from multiple myeloma. *Front Immunol* (2019) 10:1596. doi: 10.3389/fimmu.2019.01596

80. Fletcher JM, Lonergan R, Costelloe L, Kinsella K, Moran B, O'Farrelly C, et al. Cd39+Foxp3+ regulatory T cells suppress pathogenic Th17 cells and are impaired in multiple sclerosis. *J Immunol* (2009) 183(11):7602–10. doi: 10.4049/jimmunol.0901881

81. Yang R, Elsaadi S, Misund K, Abdollahi P, Vandsemb EN, Moen SH, et al. Conversion of Atp to adenosine by Cd39 and Cd73 in multiple myeloma can be successfully targeted together with adenosine receptor A2a blockade. *J Immunother Cancer* (2020) 8(1):1-14. doi: 10.1136/jitc-2020-000610

82. Ray A, Song Y, Du T, Buon L, Tai YT, Chauhan D, et al. Identification and validation of ecto-5' nucleotidase as an immunotherapeutic target in multiple myeloma. *Blood Cancer J* (2022) 12(4):50. doi: 10.1038/s41408-022-00635-3

83. Wang X, Zhang T, Song Z, Li L, Zhang X, Liu J, et al. Tumor Cd73/A2ar adenosine immunosuppressive axis and tumor-infiltrating lymphocytes in diffuse Large b-cell lymphoma: Correlations with clinicopathological characteristics and clinical outcome. *Int J Cancer* (2019) 145(5):1414–22. doi: 10.1002/ijc.32144

84. Zhang T, Liu H, Jiao L, Zhang Z, He J, Li L, et al. Genetic characteristics involving the Pd-1/Pd-L1/L2 and Cd73/A2ar axes and the immunosuppressive microenvironment in Dlbcl. *J Immunother Cancer* (2022) 10(4):1-13. doi: 10.1136/jitc-2021-004114

85. Guo S, Han F, Zhu W. Cd39 - a bright target for cancer immunotherapy. *BioMed Pharmacother* (2022) 151:113066. doi: 10.1016/j.biopha.2022.113066

86. Perrot I, Michaud HA, Giraudon-Paoli M, Augier S, Docquier A, Gros L, et al. Blocking antibodies targeting the Cd39/Cd73 immunosuppressive pathway unleash immune responses in combination cancer therapies. *Cell Rep* (2019) 27(8):2411–25 e9. doi: 10.1016/j.celrep.2019.04.091

87. Ghalamfarsa G, Kazemi MH, Raoofi Mohseni S, Masjedi A, Hojjat-Farsangi M, Azizi G, et al. Cd73 as a potential opportunity for cancer immunotherapy. *Expert Opin Ther Targets* (2019) 23(2):127–42. doi: 10.1080/14728222.2019.1559829

88. Jeffrey JL, Lawson KV, Powers JP. Targeting metabolism of extracellular nucleotides *Via* inhibition of ectonucleotidases Cd73 and Cd39. *J Med Chem* (2020) 63(22):13444–65. doi: 10.1021/acs.jmedchem.0c01044

89. Stagg J, Divisekera U, McLaughlin N, Sharkey J, Pommey S, Denoyer D, et al. Anti-Cd73 antibody therapy inhibits breast tumor growth and metastasis. *Proc Natl Acad Sci U.S.A.* (2010) 107(4):1547–52. doi: 10.1073/pnas.0908801107

90. Hay CM, Sult E, Huang Q, Mulgrew K, Fuhrmann SR, McGlinchey KA, et al. Targeting Cd73 in the tumor microenvironment with Medi9447. *Oncoimmunology* (2016) 5(8):e1208875. doi: 10.1080/2162402X.2016.1208875

frontiers | Frontiers in Immunology

TYPE Original Research
PUBLISHED 01 February 2023
DOI 10.3389/fimmu.2023.1070679

OPEN ACCESS

EDITED BY
Gulderen Yanikkaya Demirel,
Yeditepe University, Türkiye

REVIEWED BY
Ana Vuletić,
Institute of Oncology and Radiology of Serbia, Serbia
Weisheng Guo,
Guangzhou Medical University, China

*CORRESPONDENCE
Xin Huang
smaraxinxinhuang@163.com
Bingdi Chen
inanochen@tongji.edu.cn

SPECIALTY SECTION
This article was submitted to Cancer Immunity and Immunotherapy, a section of the journal Frontiers in Immunology

RECEIVED 15 October 2022
ACCEPTED 16 January 2023
PUBLISHED 01 February 2023

CITATION
Zhu Y, Chen J, Li J, Zhou C, Huang X and Chen B (2023) Ginsenoside Rg1 as a promising adjuvant agent for enhancing the anti-cancer functions of granulocytes inhibited by noradrenaline.
Front. Immunol. 14:1070679.
doi: 10.3389/fimmu.2023.1070679

Ginsenoside Rg1 as a promising adjuvant agent for enhancing the anti-cancer functions of granulocytes inhibited by noradrenaline

Yuqian Zhu, Jingyao Chen, Jun Li, Chenqi Zhou, Xin Huang* and Bingdi Chen*

Shanghai East Hospital, The Institute for Biomedical Engineering & Nano Science, Tongji University School of Medicine, Shanghai, China

Introduction: In recent years, numerous studies have confirmed that chronic stress is closely related to the development of cancer. Our previous research showed that high levels of stress hormones secreted in the body during chronic stress could inhibit the cancer-killing activity of granulocytes, which could further promote the development of cancer. Therefore, reversing the immunosuppressive effect of stress hormones on granulocytes is an urgent problem in clinical cancer treatment. Here, we selected noradrenaline (NA) as a representative stress hormone.

Methods and results: After screening many traditional Chinese herbal medicine active ingredients, a promising compound, ginsenoside Rg1, attracted our attention. We verified the immunoprotective effect of ginsenoside Rg1 on granulocytes *in vitro* and *ex vivo*, and attempted to understand its potential immunoprotective mechanism. We confirmed the immunoprotective effect of ginsenoside Rg1 on granulocytes using cell and animal experiments. Cell counting kit-8 (CCK-8) and *ex vivo* experiments were performed to investigate the immunoprotective effects of ginsenoside Rg1 on the anti-cancer function of granulocytes inhibited by NA. Transcriptome sequencing analysis and qRT-PCR showed that NA elevated the mRNA expression of *ARG2*, *MMP1*, *S100A4*, and *RAPSN* in granulocytes, thereby reducing the anti-cancer function of granulocytes. In contrast, ginsenoside Rg1 downregulated the mRNA expression of *ARG2*, *MMP1*, *S100A4*, and *RAPSN*, and upregulated the mRNA expression of *LAMC2*, *DSC2*, *KRT6A*, and *FOSB*, thereby enhancing the anti-cancer function of granulocytes inhibited by NA. Transwell cell migration experiments were performed to verify that ginsenoside Rg1 significantly enhanced the migration capability of granulocytes inhibited by NA. Tumor-bearing model mice were used to verify the significant immunoprotective effects *in vivo*. Finally, CCK-8 and hematoxylin and eosin staining experiments indicated that ginsenoside Rg1 exhibited high biosafety *in vitro* and *in vivo*.

Discussion: In future clinical treatments, ginsenoside Rg1 may be used as an adjuvant agent for cancer treatment to alleviate chronic stress-induced adverse events in cancer patients.

KEYWORDS

granulocytes, cancer, ginsenoside Rg1, noradrenaline, stress

1 Introduction

In recent years, increasing evidence has shown that chronic stress is closely related to the development of cancer (1–7). During chronic stress, the dysregulation of the hypothalamic-pituitary-adrenal axis could further lead to the persistent abnormal secretion of stress hormones [hydrocortisone, adrenaline, and noradrenaline (NA)] in the body (8). The long-term dysregulation of neuroendocrine hormones could lead to a series of health problems, including cancer development (9–11). Thus far, numerous studies have confirmed that high stress hormone levels over a prolonged period of time can inhibit immune system function (12–14). Data showed that chronic stress could promote the proliferation and migration of tumor cells by inhibiting different functional stages of the immune system (such as antigen presentation, humoral immunity, and cellular immunity) (15–21).

Neutrophils are the primary responders to infections that display potent antimicrobial functions including phagocytosis, degranulation, and neutrophil extracelluar trap (NET) production (22, 23). Meanwhile, the results and clinical correlative evidence have revealed that neutrophil subpopulations have distinct functions under the tumour microenvironment (24, 25). Tumor-associated neutrophils (TANs) have differential states of activation: N1 antitumorigenic phenotype and N2 protumorigenic phenotype. N1 neutrophils can directly kill tumour cells through the release of ROS and RNS. They also promote T cell activation and recruitment of pro-inflammatory macrophages. N2 neutrophils promote tumor angiogenesis and inhibit NK cell function *via* the release of MMP9. In addition, they recruit anti-inflammatory macrophages and Treg cells (24, 26, 27). The results discussed above suggest that neutrophils have high heterogeneity and plasticity. Our previous study suggested that stress hormones secreted in the body during chronic stress could alter neutrophil cell function and phenotype.

In 2020, our research group reported that the high levels of stress hormones secreted in the body during chronic stress could inhibit the cancer-killing activity (CKA) of granulocytes, which could further reduce the anti-cancer function of the immune system and thus promote the occurrence and development of cancer (28). Our findings provided strong evidence to support the view that chronic stress promotes the occurrence and development of cancer.

Patients often develop chronic mental stress after the diagnosis of cancer (8, 9, 29, 30). The prolonged maintenance of elevated stress hormone levels in these patients further inhibits the CKA of granulocytes and ultimately promotes the development of cancer (8, 9). Therefore, it is necessary to develop an agent that can effectively reverse the immunosuppressive effects of stress hormones and ensure its biosafety. To address this issue, we screened a variety of bioactive components in Chinese traditional herbs during our preliminary exploration experiments. Among them, ginsenoside Rg1 attracted our attention because of its excellent immunoprotective function.

Ginsenoside Rg1 is an extract of ginseng (31). Previous reports showed that ginsenoside Rg1 can improve immunity and enhance anti-tumor activity, and exhibits broad application prospects in high-end health care and other fields (32, 33). However, no study has reported the potential application of ginsenoside Rg1 in anti-tumor therapy for patients with cancer suffering from stress. In the present study, we investigated whether ginsenoside Rg1 could enhance the CKA of stress-hormone-inhibited granulocytes. This study will also provide a new direction for the clinical application of ginsenoside Rg1 in the future.

In a previous report, we investigated the immunosuppressive effects of three stress hormones (hydrocortisone, adrenaline, and NA). Among the three stress hormones, NA exhibited the strongest immunosuppressive effect *in vivo* (28). Therefore, in this study, NA was selected as a representative stress hormone to explore the protective effect of ginsenoside Rg1 on the CKA of stress hormone-inhibited granulocytes. Here, the biosafety of ginsenoside Rg1 was investigated *via* cytotoxicity experiments; the immunoprotective effects of ginsenoside Rg1 *in vitro* were investigated using cell counting kit-8 (CCK-8) and transwell cell migration tests; the immunoprotective mechanism of ginsenoside Rg1 was investigated by transcriptome sequencing analysis and qRT-PCR; the immunoprotective function of ginsenoside Rg1 *in vivo* was verified using tumor-bearing model mice. The results of this study showed that ginsenoside Rg1 could enhance the CKA of granulocytes inhibited by NA. Ginsenoside Rg1 may find application as an immunoprotective agent to alleviate the immunosuppressive effect of chronic stress in future clinical treatments.

2 Materials and methods

2.1 Reagents

All reagents were commercially available. Ultrapure water was obtained from Millipore machines (Billerica, MA, USA). CCK-8 and Annexin V-fluorescein isothiocyanate (FITC)/propidium iodide (PI) apoptosis detection kit were purchased from Dojindo (Tokyo, Japan); Dulbecco's Modified Eagle's Medium (DMEM), fetal bovine serum (FBS), and phosphate-buffered saline (PBS) were purchased from Biological Industries (Kibbutz Beit Haemek, Israel); diff-quik staining solution and 4', 6-diamidino-2-phenylindole (DAPI) were purchased from Solarbio (Beijing, China); red cells lysis bAuffer was purchased from BioGems (CA, USA); percoll was purchased from GE Healthcare Life Sciences (MA, USA); cytokeratin 19 antibody and cluster of differentiation 66 antibody were purchased from Abcam (Cambridge, UK); ginsenoside Rg1 was purchased from MACKLIN (Shanghai, China); and NA was purchased from AMQUAR (Shanghai, China).

2.2 Instrumentation

An HT7700 120KV electron microscope (Hitachi, Tokyo, Japan) was used for transmission electron microscopy (TEM); an ECLIPSE 80i fluorescence microscope (Nikon, Tokyo, Japan) was used for fluorescence imaging; a MULTISKAN MK3 Microplate Reader (Thermo Scientific, MA, USA) was used for cell viability tests; a BD

Abbreviations: NA, noradrenaline; CKA, cancer killing activity; CCK-8, cell counting kit-8; FITC, fluorescein isothiocyanate; PI, propidium iodide; DMEM, Dulbecco's Modified Eagle's Medium; FBS, fetal bovine serum; PBS, phosphate buffer saline; DAPI, 4', 6-diamidino-2-phenylindole; CK, cytokeratin; CD, cluster of differentiation; E, effector cells; T, target cells; OD, optical density; KEGG, Kyoto Encyclopedia of Gene and Genomes; GO, gene ontology; FC, foldchange; *P*, probability; RT, reverse transcription; TEM, transmission electron microscopy; i.p., intraperitoneally.

FACSVerse (NJ, USA) was used for flow cytometry; and a Leica TCS SP5 II (Hesse, Germany) was used for confocal microscope imaging.

2.3 Cells

A549 and S180 cell lines were purchased from Shanghai Institute of Cell Biology (Shanghai, China).

2.4 Animals

In this study, 27 adult male SD rats (clean grade, weight ~160 g) and 24 adult male nude mice (SPF grade, weight ~20 g) were purchased from Shanghai SLAC Laboratory Animal Co., Ltd (Shanghai, China). Production license number: SCXK (Shanghai) 2017-0005; use license number: SYXK (Shanghai) 2017-0008. This study was approved by the Tongji University Institutional Review Board (Grant No. TJAA07221402).

2.5 Donors

A total of 50 healthy donors (18–25 years) from Tongji University (Shanghai, China) who consented were recruited as the study participants. Volunteers were required to fill in informed consent before donating blood. None of the participants consumed alcohol, smoked, or took any medication during the study period. This study was approved by the Tongji University Institutional Review Board (Grant No. 2019tjdx282).

2.6 Granulocyte isolation

From each participant, 10 mL of blood was collected by heparinized venipuncture (Yu Li, Jiangsu, China) on the day of use. Granulocytes were isolated from human whole blood *via* percoll gradient separation (28, 34).

2.7 CKA assay

A549 cells (8×10^3 cells/well) were incubated with DMEM supplemented with 10% FBS at 37°C for 24 h. CKA was tested as described previously (28, 34). Briefly, granulocytes were added to A549 cells as effector cells: target cells (E: T) ratio of 10: 1 and incubated at 37°C for 24 h. After thorough removal of non-adherent cells, the viable target cells were determined by CCK-8 assay according to the manufacturers' instruction. Each data point was the average of the triplicates.

2.8 Cytotoxicity test

2.8.1 Effects of ginsenoside Rg1 on A549 cell viability

A549 cells were seeded in 96 wells plate at a concentration of 8×10^3 cells/well and incubated at 37°C for 24 h. After discarding the culture medium, different concentrations of ginsenoside Rg1 (0, 0.1, 1, 10, and 100 mg/L) were added to A549 and incubated at 37°C for additional 24 h. After discarding the culture medium, CCK-8 reagent diluted with DMEM containing 10% FBS (110 μL) was added into each well and incubated at 37°C for 1–2 h. Optical density (OD) values were measured using a microtiter plate reader at 450 nm (35).

2.8.2 Effects of ginsenoside Rg1 on granulocyte viability

Granulocytes were first seeded in 96-well plates at a concentration of 3×10^5 cells/well. Subsequently, different concentrations of ginsenoside Rg1 (0, 0.1, 1, 10, and 100 mg/L) were added to granulocytes and incubated at 37°C for 24 h. CCK-8 reagent was then added into each well and incubated at 37°C for an additional 12 h. OD values were measured using a microtiter plate reader at 450 nm (35).

2.9 RNA isolation and library preparation

Total RNA was isolated from the granulocytes of healthy volunteers. The granulocytes were divided into four groups (Control group, NA group, Rg1 group, and NA + Rg1 group). Each group contained three biological duplicate samples (Control 1, Control 2, Control 3, NA 1, NA 2, NA 3, Rg1 1, Rg1 2, Rg1 3, NA + Rg1 1, NA + Rg1 2, and NA + Rg1 3). The total RNA was isolated using TRIzol reagent (Invitrogen, CA, USA). The quality and purity of the isolated RNA were assessed using a NanoDrop 2000 spectrophotometer (Thermo Scientific). The cDNA libraries were constructed using a TruSeq Stranded mRNA LT Sample Prep Kit (Illumina, CA, USA).

2.10 RNA sequencing and analysis of differentially expressed genes

Transcriptome sequencing and analysis were conducted by OE Biotech Co., Ltd. (Shanghai, China). The cDNA libraries were sequenced on an Illumina HiSeq X Ten platform (Illumina). Differentially expressed genes were analyzed using the DESeq (2012) R package. Kyoto Encyclopedia of Gene and Genomes (KEGG) and Gene Ontology (GO) enrichment analysis were performed using R based on the hypergeometric distribution (36). We used the STRING database to predict protein-protein interaction networks (37). The threshold of significantly differential expression was: probability (P) < 0.05 and foldchange (FC) > 2 or (FC) < 0.5.

2.11 qRT-PCR

Total RNA was extracted from cells using TRIzol reagent. Quantification was conducted through a two-step reaction process: reverse transcription (RT) and PCR. RT reactions were performed in a GeneAmp PCR System 9700 (Applied Biosystems, USA). Real-time PCR was performed using a LightCycler 480 II Real-time PCR

Instrument (Roche, Swiss). At the end of the PCR cycles, melting curve analysis was performed to validate the specific generation of the expected PCR product. *ACTB* was used as the housekeeping gene. Relative expression quantification analysis was performed using the $2^{-\Delta\Delta Ct}$ method (38). The following are the details of the primers used:

ARG2 forward: 5'- ACAACAACCTGATAGTGAATCC-3', *ARG2* reverse: 5'- TCTGACACAGCTCTGCTAAC-3';

MMP1 forward: 5'-GAGGAAATCTTGCTCATGCTT-3', *MMP1* reverse: 5'- CTCTCTGAAATTGTTGGTCCAC-3';

S100A4 forward: 5'- TTGGACAGCAACAGGGACAA-3', *S100A4* reverse: 5'- AGAATTCGTTACACATCATGGC-3';

RAPSN forward: 5'- TTGTGAGGTTCCACGAGT-3', *RAPSN* reverse: 5'- GGCTGTTCTTCTCGCCTAT-3';

LAMC2 forward: 5'-CCCTGGGTTGAACAGTGTAT-3', *LAMC2* reverse: 5'- AGTCTCGCTGAATCTCTCTT-3';

DSC2 forward: 5'- ACACGGCCCAAAACTATACCA-3', *DSC2* reverse: 5'- TTTCCAGTGTCTCTCTCCACATA-3';

KRT6A forward: 5'- CTTTCCACTGGCTCTCAAAC-3', *KRT6A* reverse: 5'- GTCACTTGTGCTTTCATGGAT-3';

FOSB forward: 5'- ACCTGACGGCTTCTCTCTTTA-3', *FOSB* reverse: 5'- GGACAAACGAAGAAGTGTACG-3';

ACTB forward: 5'- CATTCCAAATATGAGATGCGTT-3', *ACTB* reverse: 5'- TACACGAAAGCAATGCTATCAC-3'.

2.12 Cell migration assay

Five healthy volunteers were recruited and 10 mL of peripheral blood was collected from each volunteer. The granulocytes were separated from whole blood *via* percoll gradient separation and divided into four groups (groups A, B, C, and E) and added into non-adherent 24-well plates. Granulocytes in group A and E were incubated at 37°C for 24 h. Those in group B were first incubated at 37°C for 12 h. Subsequently, NA (50 μg/mL) was added and the granulocytes were further incubated at 37°C for an additional 12 h. Granulocytes in group C were first incubated with ginsenoside Rg1 (100 mg/L) at 37°C for 12 h. Subsequently, NA (50 μg/mL) was added and the granulocytes were further incubated at 37°C for an additional 12 h. The granulocytes in the above four groups were then collected and centrifuged at 1000 rpm for 5 min. After discarding the culture medium, granulocytes were dispersed in DMEM and counted using Countstar (ALIT Life Science, Shanghai, China). Transwell chambers were placed in a 24-well plate inoculated with or without A549 cells (600 μL, 2.5×10^5 cells/well). Granulocyte suspension (100 μL, E: T = 10: 1) was added to the upper chambers and incubated at 37°C for 3 h (A549 cells were pre-inoculated in the lower chambers of group A, B, and C; no cells were pre-inoculated in the lower chambers of group E). Subsequently, cells in the upper chambers were wiped off with cotton swabs. Cells in the lower chambers were digested with trypsin and resuspended in PBS solution. Cells were counted using Countstar (cell numbers in the lower chambers of groups A, B, C, and E were recorded as A, B, C, and E, respectively). The number of A549 cells inoculated was recorded as D. The chemotactic index of granulocytes in group A = (A - D)/E; chemotactic index of granulocytes in group B = (B - D)/E; chemotactic index of granulocytes in group C = (C - D)/E (39).

2.13 *In vivo* immunoprotective evaluation of ginsenoside Rg1

On day 0, 24 healthy nude mice were randomly divided into four groups: Control group, NA group, NA + Rg1 group, and Rg1 group. On day 1, mice in the Control group were intraperitoneally (i.p.) injected with 100 μL PBS per day for 24 consecutive days; mice in the NA group were i.p. injected with NA (100 μL, 2 mg/kg) per day for 24 consecutive days; mice in NA + Rg1 group were i.p. injected with NA (100 μL, 2 mg/kg) and ginsenoside Rg1 (100 μL, 50 mg/kg) per day for 24 consecutive days; mice in Rg1 group were i.p. injected with ginsenoside Rg1 (100 μL, 50 mg/kg) per day for 24 consecutive days. On day 8, ascites tumor S180 cells (500 μL, 2×10^6 cells/mL) were inoculated into the abdominal cavity of the mice in the 4 groups. The body weight, abdominal circumference, average food consumption, and survival rate were recorded daily for 24 days.

2.14 Statistic analysis

Three biological replicates were performed for all experiments in this study, unless otherwise indicated. Statistical analyses were performed using GraphPad Prism software, version 7.01 (GraphPad Software, San Diego, CA, USA). One-way analysis of variance with Dunnett post-test was used to analyze the differences between multiple groups. Two-tailed Student's t-test was used to analyze the differences between the two groups. Log-rank test was used to analyze the survival curve. Statistical significance was set at a P value of less than 0.05, 0.01, or 0.001, indicated by *, **, and ***, respectively.

3 Results

3.1 Granulocytes from the peripheral blood of healthy humans exhibited anticancer function

We recruited five healthy volunteers and collected 10 mL of peripheral blood from each volunteer. We separated granulocytes from whole blood *via* percoll gradient separation and tested the CKA of granulocytes. Firstly, we tested the cancer-killing efficiency of granulocytes from five healthy volunteers by CCK-8 (target cells: A549; E: T = 10: 1) (28). The results showed that the granulocytes from the five healthy volunteers exhibited significant cancer-killing efficiency in the range of 35–73%, which was consistent with the result of our previous report (Figure 1A) (28). Next, we further verified the anti-cancer function of granulocytes by flow cytometry. Granulocytes were added to A549 cells (E: T = 10: 1) and incubated at 37°C for 24 h. After thoroughly discarding non-adherent cells and washing A549 with PBS three times, A549 cells were harvested and stained with Annexin V-FITC and PI. In the detection results, the cells divided into the first quadrant were mechanically damaged cells, those in the second quadrant were non-viable apoptotic cells or cells that experienced secondary cell death, those in the third quadrant were normal living cells, and those in the fourth quadrant were viable apoptotic cells (40). The flow cytometry results showed that 99.1% of

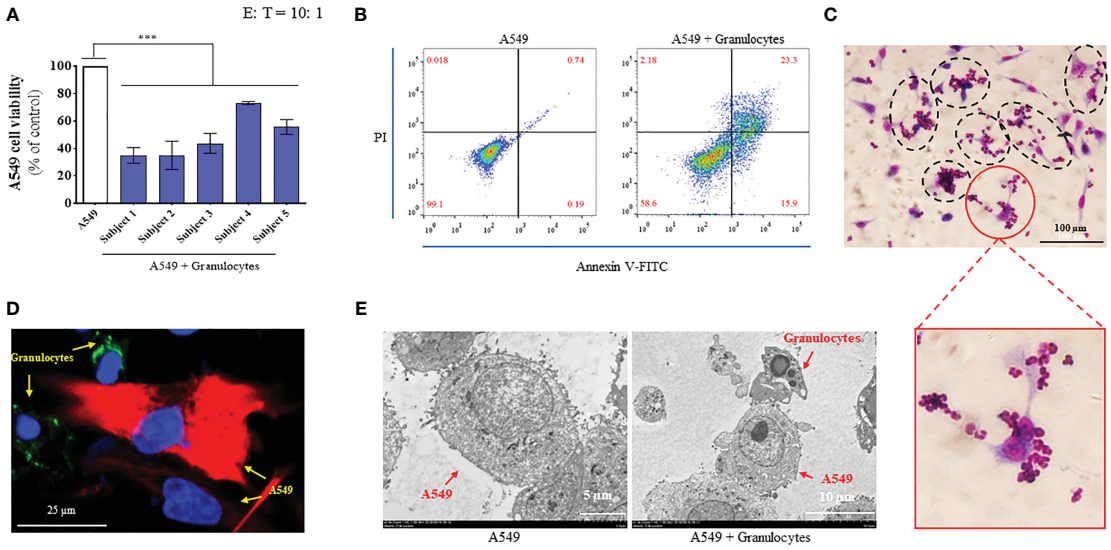

FIGURE 1
Granulocytes collected from the peripheral blood of healthy humans exhibited significant anticancer function. **(A)** Cancer-killing activity of granulocytes from 5 healthy volunteers tested using cell counting kit-8 (CCK-8) reagent (n = 3; mean ± SD; one-way analysis of variance with Dunnett post-test; ***, P < 0.001). **(B)** Cancer-killing efficiency of human granulocytes against A549 tested by flow cytometry (Annexin V-FITC/PI). **(C)** Images of granulocytes attacking A549 by diff-quik staining (magnification: 20 ×). **(D)** Confocal microscope image of granulocytes attacking A549 (magnification: 60 ×). Here, A549 cells were marked by CK19 (red), granulocyte cells were marked by CD66 (green), and the nuclei were marked by DAPI (blue). **(E)** Transmission electron microscopy (TEM) images of A549 (left, magnification: 2000 ×) and granulocyte attacking A549 (right, magnification: 1500 ×).

the A549 group were normal living cells, 0.018% were mechanically damaged cells, 0.19% were viable apoptotic cells, and 0.74% were non-viable apoptotic cells or cells that experienced secondary cell death. While 58.6% of the A549 + granulocyte group were normal living cells, 2.18% were mechanically damaged cells, 15.9% were viable apoptotic cells, and 23.3% were non-viable apoptotic cells or cells that experienced secondary cell death. Compared with the A549 group, the percentage of normal living A549 cells decreased from 99.1% to 58.6% in the A549 + granulocytes group. Moreover, the percentage of apoptotic cells (including viable apoptotic cells and non-viable apoptotic cells) in the A549 + granulocytes group increased from 0.93% to 39.2% (Figure 1B). The above results indicated that the A549 cells were mainly killed by granulocytes *via* the apoptosis pathway. Furthermore, diff-quik staining, confocal microscopy, and TEM images showed that when granulocytes attacked A549 cells, the A549 cells were surrounded by granulocytes to form a "rosette" structure (Figures 1C-E), which was consistent with our previous report (41). Simultaneously, A549 cells exhibited apoptotic characteristics (Figure 1E), which was consistent with the results of flow cytometry.

3.2 Ginsenoside Rg1 enhanced the anti-cancer function of granulocytes inhibited by NA *in vitro*

Our previous study showed that stress hormones (hydrocortisone, adrenaline, and NA) were secreted under conditions of stress, which could inhibit the function of the immune system and reduce the CKA efficiency of granulocytes (28). Additionally, among the three stress hormones mentioned above, NA may be the strongest inhibitor of CKA of granulocytes *in vivo* (28). This raised the question as to whether ginsenoside Rg1 could enhance the anti-cancer function of stress hormone-inhibited granulocytes. The present study focused on NA.

First, we explored the cytotoxicity of ginsenoside Rg1. Ginsenoside Rg1 was added to human granulocytes or A549 human lung cancer cells at concentrations of 0, 0.1, 1, 10, and 100 mg/L and incubated at 37°C for 24 h. Cell survival rate was measured using CCK-8. The experiment results are shown in Figures 2D-E. Data showed that 0–100 mg/L ginsenoside Rg1 exhibited no significant inhibitory effect on the survival rate of human granulocytes and A549 cells, indicating that ginsenoside Rg1 was biologically safe. These results were consistent with those of previous reports (42).

Subsequently, different concentrations of ginsenoside Rg1 (0, 10, and 100 mg/L) were added to human whole blood and incubated at 37°C for 12 h. NA (50 μg/L) was then added to the whole blood and incubated at 37°C for an additional 12 h. After isolating granulocytes from the whole blood, cancer cell viability was measured using CCK-8 (Figure 2A). The experiment results are shown in Figure 2B. The data showed that 1) NA inhibited the CKA of human granulocytes, which is consistent with the results of our previous study (28); 2) ginsenoside Rg1 significantly enhanced the cancer-killing efficiency of granulocytes immunosuppressed by NA; 3) ginsenoside Rg1 exhibited dose-dependent immunoprotective effects. At the concentration range explored in this study, the CKA of granulocytes increased with increasing Rg1 concentration.

Finally, we investigated the effects of ginsenoside Rg1 on the CKA of granulocytes in healthy humans. In this experiment, different concentrations of ginsenoside Rg1 were added to human whole blood and incubated at 37°C. After 24 h, the CKA of human granulocytes was measured using CCK-8. The results were shown in Figure 2C. The data showed that 1) ginsenoside Rg1 improved the

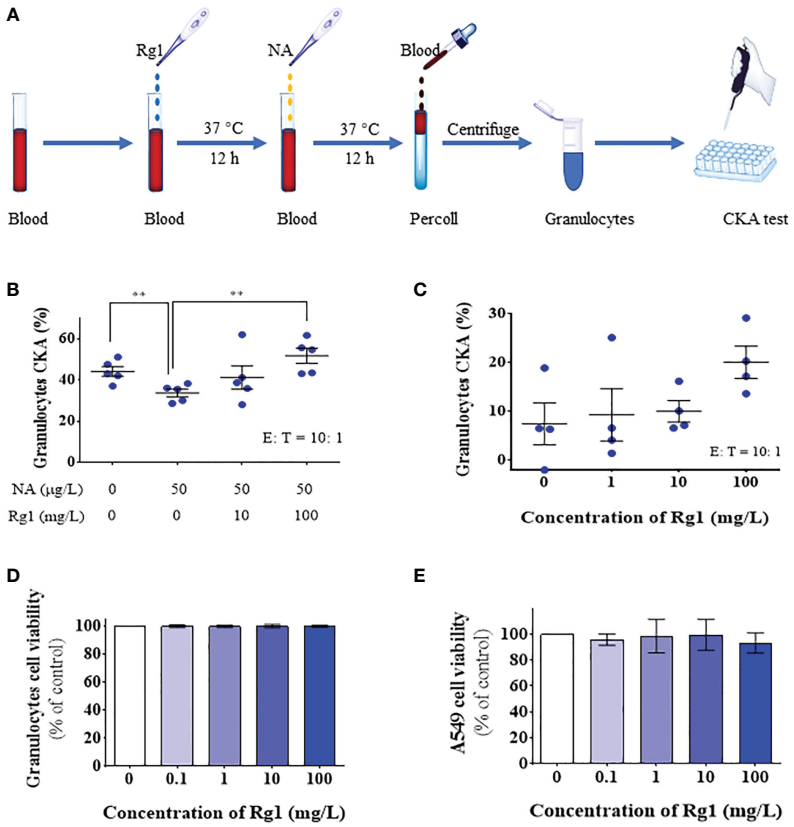

FIGURE 2
In vitro, ginsenoside Rg1 could enhance the anti-cancer function of granulocytes inhibited by noradrenaline (NA). **(A)** Detection of the effects of ginsenoside Rg1 on the anti-cancer function of granulocytes inhibited by NA. **(B)** The effects of ginsenoside Rg1 on granulocyte cancer-killing activity **(CKA)** immunosuppressed by NA at different concentrations (n = 5; mean ± SD; two-tailed student's t-test; **, P < 0.01). **(C)** The effects of ginsenoside Rg1 on granulocyte CKA at different concentrations. **(D)** The effects of ginsenoside Rg1 on granulocyte cell viability at different concentrations. **(E)** The effects of ginsenoside Rg1 on A549 cell viability at different concentrations.

CKA of human granulocytes to a certain extent, but the improvement showed no statistical significance; 2) ginsenoside Rg1 showed a concentration-dependent enhancement effect on the CKA of human granulocytes. At the concentration range explored in this study, the CKA of granulocytes increased with increasing Rg1 concentration.

3.3 Ginsenoside Rg1 could enhance the cancer-killing efficiency of granulocytes immunosuppressed by NA in healthy rats *ex vivo*

We investigated the immunoprotective effects of ginsenoside Rg1 in an *ex vivo* test. In this experiment, rats in the Control group were i.p. injected with 1.5 mL saline per day for 10 days; rats in the NA group were first i.p. injected with 1.5 mL saline per day for 3 days, then i.p. injected with 50 μg/kg NA per day for 7 days; rats in the NA + Rg1 group were first i.p. injected with 20 mg/kg ginsenoside Rg1 per day for 3 days, then i.p. injected with 20 mg/kg ginsenoside Rg1 and NA (50 μg/kg) per day for 7 days. On the 10th day, blood was collected 2 h after injection, and the CKA of granulocytes was detected (Figures 3A-C). The results are shown in Figure 3D. The results showed that 1) NA inhibited the CKA of granulocytes in healthy rats to a certain extent, but the inhibitory effect was not statistically significant; 2) ginsenoside Rg1 significantly enhanced the cancer-killing efficiency of granulocytes immunosuppressed by NA in healthy rats, which was consistent with the *in vitro* results.

Furthermore, we investigated the effects of ginsenoside Rg1 on the CKA of granulocytes in healthy rats. In this experiment, rats in the Control group were i.p. injected with 1.5 mL saline per day for 10 days; rats in the Rg1 group were i.p. injected with 20 mg/kg ginsenoside Rg1 per day for 10 days. Blood was collected on the 10th day and the CKA of granulocytes was tested using CCK-8 (Figure S1A–B). The results showed that ginsenoside Rg1 had no significant effect on the CKA of the granulocytes of healthy rats, indicating that ginsenoside Rg1 has no significant toxic effect on the CKA of granulocytes in healthy rats (Figure S1C).

3.4 Transcriptome analysis

We performed transcriptome analysis to explore the immunoprotective mechanism of ginsenoside Rg1 on the anti-cancer functions of granulocytes inhibited by NA (43). In this study, we performed a comparative RNA-seq analysis on four groups (NA group vs Control group, NA + Rg1 group vs NA group, and Rg1 group vs Control group) including 12 samples (Control 1, Control 2, Control 3,

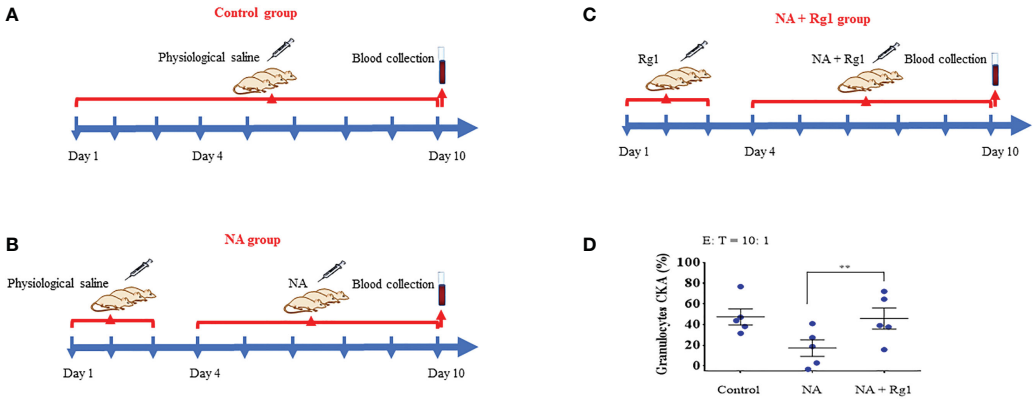

FIGURE 3
In the *ex vivo* test, ginsenoside Rg1 could improve the cancer-killing efficiency of rats granulocytes immunosuppressed by noradrenaline (NA). **(A - C)** Detection of the effect of ginsenoside Rg1 on the cancer-killing efficiency of granulocytes in rats immunosuppressed by NA. **(D)** Effect of ginsenoside Rg1 (20 mg/kg) on the cancer-killing efficiency of granulocytes immunosuppressed by NA in rats (n = 5; mean ± SD; two-tailed student's t-test; **, P < 0.01).

NA 1, NA 2, NA 3, Rg1 1, Rg1 2, Rg1 3, NA + Rg1 1, NA + Rg1 2, and NA + Rg1 3). Here, granulocytes in the Control group were not treated. Granulocytes in the NA group were treated with NA (50 μg/L) at 37°C for 12 h. Granulocytes in NA + Rg1 group were first treated with ginsenoside Rg1 (100 mg/L) for 12 h, then treated with ginsenoside Rg1 (100 mg/L) and NA (50 μg/L) for an additional 12 h at 37°C. Granulocytes in the Rg1 group were treated with ginsenoside Rg1 (100 mg/L) at 37°C for 24 h. The analysis results are shown in Figure 4. The screening conditions for differentially expressed genes are as follows: FC ≥ 2 and P < 0.05. Figure 4A shows the volcano plot of data comparison between different groups, which demonstrated the overall distribution of differentially expressed genes. In the NA group vs Control group, a total of 11 differentially expressed genes, namely 3 upregulated and 8 downregulated genes, were found. In the NA + Rg1 group vs NA group, a total of 87 differentially expressed genes, namely 62 upregulated and 25 downregulated genes, were found. In the Rg1 group vs Control group, a total of 123 differentially expressed genes, namely 56 upregulated and 67 downregulated genes, were found. Figure 4B shows the cluster analysis of differentially expressed genes between different groups. The result shows that the trend of differentially expressed genes was consistent among different samples in the same group, while there were significant differences among different treatment groups.

3.5 Predicted mechanism whereby ginsenoside Rg1 enhances the anti-cancer function of NA-inhibited granulocytes

We focused on the analysis of differentially expressed genes between the NA + Rg1 group and NA group to discuss the possible molecular mechanisms by which ginsenoside Rg1 enhanced the anti-cancer function of granulocytes inhibited by NA. First, we performed GO enrichment analysis of differentially expressed genes between the NA + Rg1 group and the NA group (Figure 5A). The analysis showed a total of 87 differentially expressed genes between the NA + Rg1 group and the NA group, which could be divided into three main GO categories: biological processes, cellular components, and molecular functions. Among them, the 62 upregulated differentially expressed genes were assigned to 43 GO terms, including 21 biological processes, 13 cellular components, and 9 molecular functions. The 25 downregulated differentially expressed genes were assigned to 39 GO terms, including 20 biological processes, 13 cellular components, and 6 molecular functions. Moreover, we performed a signaling pathway analysis of differentially expressed genes between the NA + Rg1 group and the NA group using the KEGG database (Figure 5B). The result showed that a total of 56 upregulated and 32 downregulated differentially expressed genes between the NA + Rg1 group and the NA group were categorized into known KEGG pathways. Among the 56 upregulated genes, 2 genes were distributed in cellular processes, 10 genes in environmental information processing, 3 genes in genetic information processing, 16 genes in human diseases, 7 genes in metabolism, and 18 genes in organic systems. Among the 32 downregulated genes, 8 genes were distributed in environmental information processing, 10 genes in human diseases, 4 genes in metabolism, and 10 genes in organismal systems. In our previous studies, the granulocyte-mediated killing of cancer cells was roughly divided into 3 stages: chemotaxis, recognition, and killing (28, 44). Therefore, we considered that factors related to cell migration, cell adhesion, cytoskeleton composition, cell proliferation and apoptosis, and immune response may all be associated with the immunoprotective effect of ginsenoside Rg1 on granulocytes inhibited by NA. Therefore, among the 87 differentially expressed genes between the NA + Rg1 group and the NA group, we screened 15 genes that might be related to the immunoprotective effects of ginsenoside Rg1 on granulocytes inhibited by NA (Table 1). Furthermore, we predicted the protein-protein interaction networks for these 15 genes using the STRING database (Figure 5C). The prediction results showed a possible association among the 15 genes.

3.6 Verification of the immunoprotective mechanism of ginsenoside Rg1

Among the 15 genes screened above (Table 1), we selected 8 genes of interest (*ARG2*, *MMP1*, *S100A4*, *RAPSN*, *LAMC2*, *DSC2*, *KRT6A*, and

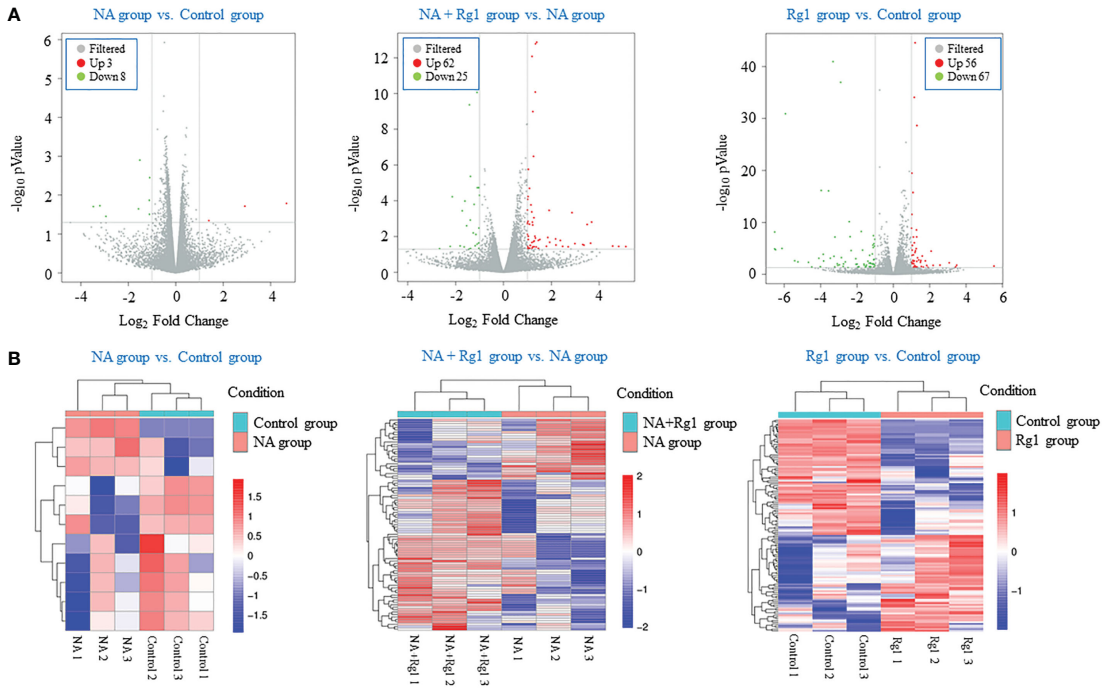

FIGURE 4
Transcriptome analysis of the effects of noradrenaline (NA) and ginsenoside Rg1 on the gene expression of granulocyte from healthy humans. **(A)** Volcano plot of data comparison between different groups. Every dot represents a differentially expressed gene. Gray represents no significant difference in gene expression between the two groups. Red represents significantly upregulated gene expression. Green represents significantly downregulated gene expression. **(B)** Clustering analysis of differentially expressed genes between different groups. Red represents upregulated genes. Blue represents downregulated genes. The depth of different colors represents different levels of gene expression.

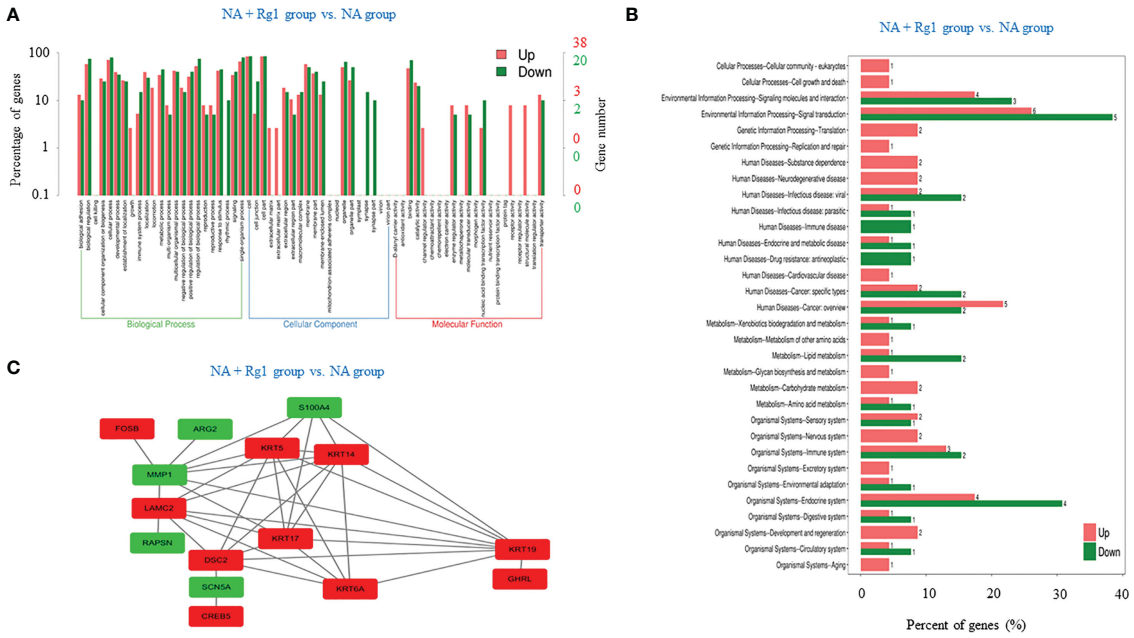

FIGURE 5
Correlation analysis of differentially expressed genes between the noradrenaline (NA) + Rg1 group and NA group. **(A)** Gene ontology (GO) enrichment of differentially expressed genes between the NA + Rg1 group and NA group. Three GO categories include biological process, cell component, and molecular function. Red represented upregulated genes, and green represented downregulated genes. **(B)** Kyoto Encyclopedia of Gene and Genomes **(KEGG)** analysis of differentially expressed genes between the NA + Rg1 group and NA group. Red represented upregulated genes, and green represented downregulated genes. **(C)** Predicted protein-protein interaction networks. Protein interaction networks that predicted 15 differential genes using the STRING database. Red represented upregulated genes, and green represented downregulated genes.

TABLE 1 15 genes that may be associated with increased granulocytes cancer-killing efficiency (NA + Rg1 group vs NA group).

Gene symbol	Description	Function	Fold change (log_2)
LAMC2	Laminin subunit gamma 2	Cell adhesion, positive regulation of cell migration	2.86
DSC2	Desmocollin 2	Cell adhesion	1.06
KRT5	Keratin 5	Cytoskeleton organization	1.28
KRT6A	Keratin 6A	Cytoskeleton organization	4.81
KRT14	Keratin 14	Structural constituent of cytoskeleton	3.50
KRT17	Keratin 17	Enables structural molecule activity, intermediate filament organization, positive regulation of cell growth, positive regulation of translation	2.38
KRT19	Keratin 19	Structural constituent of cytoskeleton	5.11
GHRL	Ghrelin and obestatin prepropeptide	Actin polymerization or depolymerization, negative regulation of apoptotic process	1.33
CREB5	cAMP responsive element binding protein 5	Enables cAMP response element binding	1.00
FOSB	FosB proto-oncogene, AP-1 transcription factor subunit	Regulators of cell proliferation, differentiation, and transformation	1.02
SCN5A	Sodium voltage-gated channel alpha subunit 5	Tetrodotoxin-resistant voltage-gated sodium channel subunit	-2.22
RAPSN	Receptor associated protein of the synapse	Enables acetylcholine receptor binding, enables ionotropic glutamate receptor binding, enables metal ion binding, enables protein-membrane adaptor activity	-1.09
MMP1	Matrix metallopeptidase 1	Breakdown of extracellular matrix in normal physiological processes, as well as in disease processes	-1.54
S100A4	S100 calcium binding protein A4	This protein may function in motility, invasion, and tubulin polymerization.	-1.10
ARG2	Arginase 2	Enables arginase activity, involved in adaptive immune response, involved in innate immune response	-1.61

FOSB), and measured the mRNA expression of these genes using qRT-PCR. The results showed that, compared with the Control group, the mRNA expression levels of *ARG2*, *MMP1*, *S100A4*, and *RAPSN* were significantly elevated in NA group. However, the mRNA expression level of these four genes was significantly reduced in the NA + Rg1 group (Figures 6A-D). These results were consistent with the results of transcriptome analysis (Table 1). In addition, compared with the Control group, the mRNA expression levels of *LAMC2*, *DSC2*, *KRT6A*, and *FOSB* showed no statistically significant difference in the NA group. Compared with the NA group, the mRNA expression level of these four genes was significantly elevated in the NA + Rg1 group (Figures 6E-H). These results were consistent with the results of transcriptome analysis (Table 1). These results suggested that NA inhibited granulocyte CKA by elevating the expression of *ARG2*, *MMP1*, *S100A4*, and *RAPSN*. Moreover, ginsenoside Rg1 could enhance granulocyte CKA (which was inhibited by NA) by inhibiting the expression of *ARG2, MMP1, S100A4*, and *RAPSN* while simultaneously elevating the expression of *LAMC2, DSC2, KRT6A*, and *FOSB* (Figure 7).

Previous research reported that the high expression of *ARG2* was related to immunosuppressive microenvironments (45, 46); The high expression of *MMPs* was associated with N2 tumor-associated neutrophils (47); and the overexpression of *S100A4* would promote the metastasis, invasion, and angiogenesis of cancer cells, which are related to poor prognosis in patients with cancer (48–50). The decreased methylation of *RAPSN* would upregulate the function of *RAPSN* and further accelerate downstream pathways, which was positively correlated with the development of lung cancer (51, 52). The above analysis indicated that the mRNA expression of *ARG2, MMP1, S100A4*, and *RAPSN* in neutrophils was significantly increased after the regulation of NA. These changes could inhibit the anti-cancer function of granulocytes and promote the development of cancer.

Additionally, *LAMC2* promotes the chemotactic function of granulocytes (53, 54); *DSC2* correlates positively with adhesion, migration, and infiltration of granulocytes (55, 56); and *KRT6A* protein inhibits the proliferation, migration and invasion abilities of lung cancer cells. The high expression of *KRT6A* protein is related to good prognosis in patients with lung adenocarcinoma (57); *FOSB* protein plays an anti-tumor role in lung cancer (58). These results indicated that ginsenoside Rg1 significantly inhibited the mRNA expression of *ARG2, MMP1, S100A4*, and *RAPSN* in granulocytes inhibited by NA and, simultaneously, significantly elevated the mRNA expression of *LAMC2, DSC2, KRT6A*, and *FOSB*. These changes could enhance the anti-cancer function of granulocytes and inhibit cancer cell development and progression.

3.7 Verification of the immunoprotective effects of ginsenoside Rg1 on granulocytes *in vitro*

We validated the *in vitro* immunoprotective effects of ginsenoside Rg1 using cell migration assays. The data showed that NA inhibited

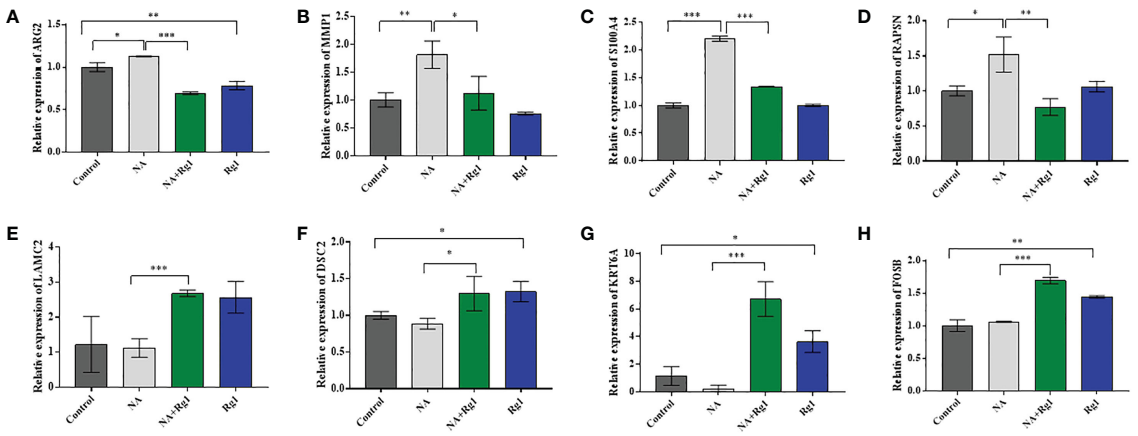

FIGURE 6
mRNA expression of *ARG2* **(A)**, *MMP1* **(B)**, *S100A4* **(C)**, *RAPSN* **(D)**, *LAMC2* **(E)**, *DSC2* **(F)**, *KRT6A* **(G)**, and *FOSB* **(H)** (n = 3; mean ± SD; two-tailed student's *t*-test; *, $P < 0.05$; **, $P < 0.01$; ***, $P < 0.001$).

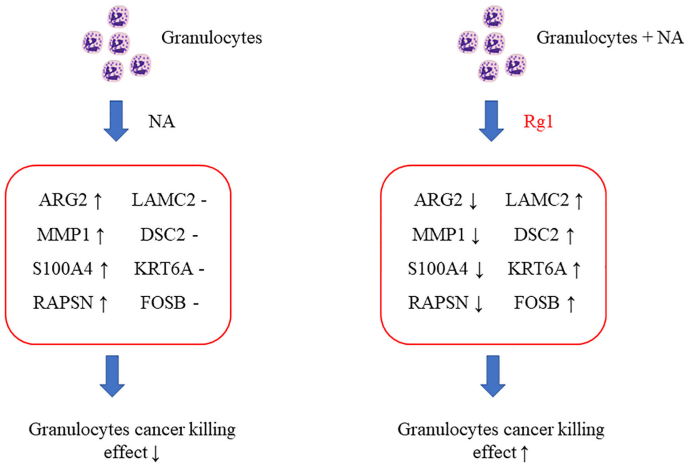

FIGURE 7
Schematic diagram about the mechanism of ginsenoside Rg1 promoting the anti-cancer function of granulocytes immunosuppressed by noradrenaline (NA).

the migration capability of granulocytes and that ginsenoside Rg1 significantly enhanced the migration capability of granulocytes inhibited by NA (Figure S2). The data above was consistent with the changing trend of *LAMC2* and *DSC2* in Figures 6–7.

3.8 Verification of the immunoprotective effects of ginsenoside Rg1 on granulocytes *in vivo*

We validated the *in vivo* immunoprotective effects of ginsenoside Rg1 in tumor-bearing model mice. On day 0, healthy nude mice were randomly divided into 4 groups: Control group, NA group, NA + Rg1 group, and Rg1 group. From day 1 to day 24, mice in the Control group were i.p. injected with PBS (100 μL) per day; mice in NA group were i.p. injected with NA (2 mg/kg, 100 μL) per day; mice in NA + Rg1 group were i.p. injected with NA (2 mg/kg, 100 μL) and ginsenoside Rg1 (50 mg/kg, 100 μL) per day; mice in Rg1 group were i.p. injected with ginsenoside Rg1 (50 mg/kg, 100 μL) per day. On day 9, we inoculated S180 cells into the abdominal cavity of healthy nude mice to establish the ascites tumor model mice. For 24 days, the body weight, abdominal circumference, average food consumption, and survival rate of the mice were recorded daily. The results are shown in Figure 8.

The data showed that there was no significant difference in mouse body weight among the four experimental groups before inoculation with S180 cells. After inoculation with S180 cells, the mouse body weight in the Control group and NA group increased rapidly; the mouse body weight in the NA + Rg1 group increased at a slower rate than that in the Control group and NA group; while the mouse body weight in the Rg1 group had the slowest rate of increase among the four groups (Figure 8A). The abdominal circumference data showed that there was no significant difference among the four experimental groups before inoculation with S180 cells. After inoculation with S180 cells, the mouse abdominal circumference in the Control group and NA group increased rapidly; mouse abdominal circumference in the NA + Rg1 group increased at a slower rate than that in the Control group and NA

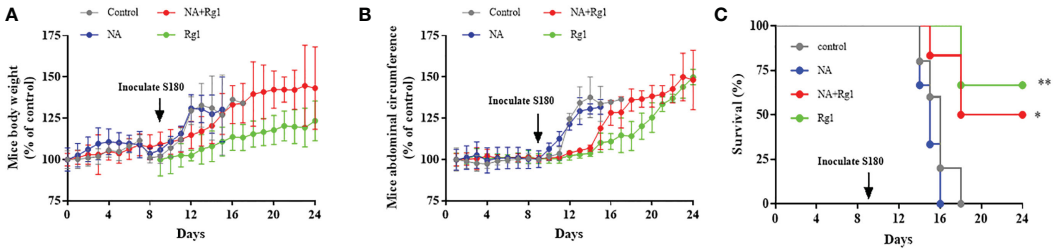

FIGURE 8
Immunoprotective effects of ginsenoside Rg1 *in vivo*. **(A)** Data of mouse body weight. **(B)** Data of mice abdominal circumference. **(C)** Data of survival rate. (n ≥ 5; log-rank test; *, $P < 0.01$; **, $P < 0.001$).

group, while the mouse abdominal circumference in the Rg1 group had the slowest increase (Figure 8B). Before inoculation with S180 cells, the mice average food consumption in the NA group and the NA + Rg1 group decreased rapidly; while the mouse average food consumption in the Control group and Rg1 group did not change significantly. After inoculation with S180 cells, the mouse average food consumption in the Control group and NA group decreased rapidly; while the mouse average food consumption in the NA + Rg1 group and Rg1 group decreased relatively slowly (Figure S3). In addition, before inoculation with S180 cells, the mouse survival rate in the four groups was 100%. After inoculation with S180 cells, mice in the NA group died the fastest, with a median survival time of 15 days. On day 16, all mice in the NA group had died; mice in the Control group also died quickly, with a median survival time of 16 days. On day 18, mice in the Control group were all dead; in contrast, mice in the NA + Rg1 group died slower than those in the Control group and NA group, with a median survival time of 18 days. On day 24, 50% of the mice were still alive; mice in the Rg1 group died the slowest, with a median survival time longer than 24 days. On day 24, 67% of the mice in this group still survived (Figure 8C). Data above indicated that ginsenoside Rg1 showed significant immunoprotective effects *in vivo*, which prolonged the survival time and slowed the growth of ascites tumors in tumor-bearing mice immunosuppressed by NA.

3.9 Toxicity test of ginsenoside Rg1 *in vivo*

We assessed the *in vivo* toxicity of ginsenoside Rg1 by hematoxylin and eosin (H&E) staining. In this test, ginsenoside Rg1 (50 mg/kg, 100 μL, Rg1 group) and PBS (100 μL, Control group) were i.p. injected into healthy nude mice. After 24 h, the mice were anesthetized with isoflurane and euthanized by cervical dislocation. Hearts, livers, spleens, lungs, and kidneys were collected and stained with H&E staining reagents. The results are shown in Figure 9. No significant difference was observed in the pathology images of important organs between the Control group and the Rg1 group. The data above also indicated that ginsenoside Rg1 exhibited high biosafety *in vivo*, which is desirable for application in future anti-cancer clinical adjuvant therapy.

4 Discussion

In the clinic, cancer patients often experience strong, stressful emotions upon being diagnosed with cancer. In 2020, our research group published an article that revealed the inhibitory effects of mental stress on the anti-cancer function of human granulocytes (28). Data showed that stress hormones (hydrocortisone, adrenaline, and NA) are released into the peripheral blood under mentally stressful conditions. These stress hormones could further inhibit the anti-cancer function of human granulocytes and promote the occurrence and development of cancer.

Granulocytes include neutrophils, eosinophils and basophils (59). Neutrophil are the most abundant leukocytes in peripheral blood of healthy human (60). Eosinophils account for 0~3% of the total leukocyte count (59). The number of basophils in peripheral blood is extremely low, less than 1% of total leukocytes (59). In the study, we separated granulocytes from human blood by Percoll density gradient centrifugation. Neutrophils account for more than 95% of granulocytes obtained by this method. Therefore, the results of granulocytes in the study also mainly reflect changes of the anti-cancer function of neutrophils.

This raises the question as to how stress-induced suppression of the immune system of patients with cancer can be eliminated or relieved. To address this issue, in our previous research, NA was selected as a representative stress hormone to screen herbal extracts, which could effectively reverse the immunosuppressive effects of NA.

Ginsenoside Rg1 is the most active and abundant components of ginseng (61). Ginsenoside Rg1 has medicinal value due to their steroidal structure and exert pharmacological effects against a variety of diseases. Research shows that ginsenoside Rg1 has neuroprotective activity through inhibition of oxidative stress and neuroinflammation (62). In the cardiac-cerebral vascular disease field, ginsenoside Rg1 effectively promotes angiogenesis and attenuates myocardial fibrosis, leading to improved left ventricular function (63). Meanwhile, the great potential of ginsenoside Rg1 has been reported in clinical research against cancer. It inhibits breast cancer cell migration and invasion by suppressing MMP-9 expression and induces apoptotic cell death in triple-negative breast cancer cell lines (32, 64). Ginsenoside Rg1 also can increase the immune activity of CD4(+) T cells. However, the anti-cancer immunoprotective effect of ginsenoside Rg1 on neutrophils has not been reported. We found that ginsenoside Rg1 could effectively enhance the anti-cancer function of granulocytes inhibited by NA, which showed potential for clinical application.

In this study, CCK-8 and *ex vivo* experiments were performed to investigate the immunoprotective effects of ginsenoside Rg1 on the anti-cancer function of granulocytes inhibited by NA *in vitro* and *ex*

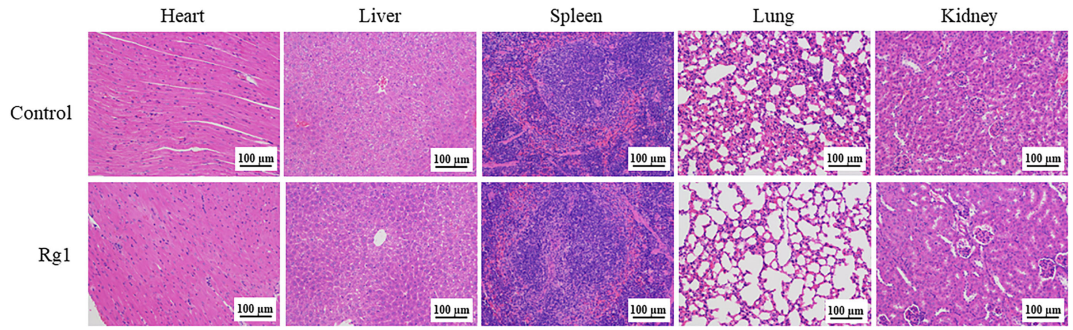

FIGURE 9
Healthy nude mice were intraperitoneally (i.p.) injected with phosphate-buffered saline (PBS; 100 μL, Control group) and ginsenoside Rg1 (50 mg/kg, 100 μL, Rg1 group), respectively. After 24 h, the heart, liver, spleen, lung, and kidney were stained with hematoxylin and eosin (H&E) staining reagents.

vivo. Transcriptome sequencing analysis and qRT-PCR were used to investigate the immunoprotective mechanism of ginsenoside Rg1. Transwell cell migration experiments were performed to verify the immunoprotective effects of ginsenoside Rg1 *in vitro*. Tumor-bearing model mice were used to verify the immunoprotective effects of ginsenoside Rg1 *in vivo*. CCK-8 and H&E staining tests were performed to investigate the biosafety of ginsenoside Rg1 *in vitro* and *in vivo*. The obtained data indicated that NA exhibited significant inhibitory effects on the anti-cancer function of granulocytes, while ginsenoside Rg1 exhibited significant immunoprotective effects on the anti-cancer function of granulocytes inhibited by NA.

The immunosuppressive mechanism of NA can be described as follows: NA elevated the mRNA expression of *ARG2*, *MMP1*, *S100A4*, and *RAPSN* in granulocytes, thereby inhibiting the CKA of granulocytes and promoting cancer development. The study showed that overexpression of *ARG2* could cause immune cell dysfunction (65). *ARG2* expression was increased in prostate cancer (66, 67), breast cancer (68) and glioblastoma (69). Overexpression of *ARG2* promoted the *MMP2/9* expression, further enhancing tumor cell proliferation, migration, invasion and angiogenesis (69). *MMP1* was also overexpressed in a variety of cancers (70–72). Because of its role in extracellular matrix degradation in tumor invasion, dysregulation of *MMP1* transcription promotes tumor metastasis (73–75). Overexpression of *S100A4* promoted metastasis of non-metastatic human breast cancer cells to the lung and lymph nodes (76). The study demonstrated that macrophages, fibroblasts, and tumor cells all could release *S100A4* into the tumor microenvironment (77), and its elevated concentration promoted the formation of a pre-metastatic niche (78, 79). Several studies revealed an association between RAPSNT hypomethylation in the peripheral blood of different populations and breast and lung cancer (51, 52, 80).

The immunoprotective mechanism of ginsenoside Rg1 can be described as follows: ginsenoside Rg1 inhibits the mRNA expression of *ARG2*, *MMP1*, *S100A4*, and *RAPSN* and elevates the mRNA expression of *LAMC2, DSC2, KRT6A*, and *FOSB*, which enhance the CKA of granulocytes (which was inhibited by NA) and inhibit the development of cancer. Mature neutrophils entered the circulation from the bone marrow and migrated along a chemotactic gradient in the interstitium to perform their immune function (81). *LAMC2* could promote neutrophil chemotaxis and stimulate their motility (53, 54). Moreover, *DSC2* was an important member of the desmosomal cadherin family and served as a vital regulator in signaling processes such as migration, differentiation, and cell apoptosis (55). It was found that desmosomes are important for maintaining cell migration ability (82). *DSC2* also inhibited the metastasis of gastric cancer by inhibiting the BRD4/Snail signaling pathway and the transcriptional activity of β-catenin (83). Moreover, the loss of *DSC2* promoted the proliferation of colon cancer cells (56). The upregulation of *LAMC2* and *DSC2* expression improved the migration ability of granulocytes, which is consistent with the results of the cell migration assay in this study. The protein encoded by *KRT6A* is a member of the keratin gene family. The peptides from the C-terminal region of the protein show antimicrobial activity against bacterial pathogens. *KRT6A* protein inhibits the proliferation, migration and invasion abilities of lung adenocarcinoma cells, and high expression of *KRT6A* protein is a predictor of good prognosis in patients with lung adenocarcinoma (57). Neutrophils could directly kill tumor cells by releasing NO (84). *FosB* was a transcription factor involved in NO production through modulation of iNOS expression (58).

In summary, NA contributed to the proliferation and invasion of tumor cells, while ginsenoside Rg1 enhanced the migration capability and anti-cancer activity of granulocytes, thus inhibiting the proliferation and invasion of tumor cells.

This study highlights a new direction for the clinical application of ginsenoside Rg1 in the future. Ginsenoside Rg1 is expected to be used as an adjuvant drug treatment for patients with cancer suffering from mental stress in the future.

Data availability statement

The transcriptome sequencing and analysis data that support the findings of this study are openly available in NCBI SRA, accession number: PRJNA929088. Other raw data that support the findings of this study are available from the corresponding author upon reasonable request.

Ethics statement

The studies involving human participants were reviewed and approved by Tongji University Institutional Review Board (Grant No. 2019tjdx282). The patients/participants provided their written informed consent to participate in this study. The animal study was reviewed and approved by Tongji University Institutional Review Board (Grant No. TJAA07221402).

Author contributions

BC and XH: Conceptualization, Methodology, Writing - Reviewing and Editing. YZ and XH: Investigation, Data curation, Writing - Original draft preparation. JC, JL and CZ: Software, Validation. All authors contributed to the article and approved the submitted version.

Funding

This work was supported by Natural Science Foundation of China [grant numbers 82102232]; Shanghai Health and Family Planning Commission Project [grant numbers 2017YQ051, 202240009]; Shanghai Science and Technology Commission Project [grant number 17411968700, 18441900300]; Shanghai Municipal Commission of Health Project [grant number 20194Y0394]; China Postdoctoral Science Foundation [grant number 2020M681402]; Independent original basic research projects of Tongji University [grant number 22120220646].

Conflict of interest

The authors declare that the research was conducted in the absence of any commercial or financial relationships that could be construed as a potential conflict of interest.

Publisher's note

Supplementary material

The Supplementary Material for this article can be found online at: https://www.frontiersin.org/articles/10.3389/fimmu.2023.1070679/full#supplementary-material

References

1. Kennedy B, Fang F, Valdimarsdottir U, Udumyan R, Montgomery S, Fall K. Stress resilience and cancer risk: A nationwide cohort study. *J Epidemiol Community Health* (2017) 71(10):947–53. doi: 10.1136/jech-2016-208706

2. Al-Wadei HA, Al-Wadei MH, Ullah MF, Schuller HM. Celecoxib and gaba cooperatively prevent the progression of pancreatic cancer in vitro and in xenograft models of stress-free and stress-exposed mice. *PloS One* (2012) 7(8):e43376. doi: 10.1371/journal.pone.0043376

3. Al-Wadei HA, Plummer HK3rd, Ullah MF, Unger B, Brody JR, Schuller HM. Social stress promotes and gamma-aminobutyric acid inhibits tumor growth in mouse models of non-small cell lung cancer. *Cancer Prev Res (Philadelphia Pa)* (2012) 5(2):189–96. doi: 10.1158/1940-6207.capr-11-0177

4. Flint MS, Baum A, Episcopo B, Knickelbein KZ, Liegey Dougall AJ, Chambers WH, et al. Chronic exposure to stress hormones promotes transformation and tumorigenicity of 3t3 mouse fibroblasts. *Stress (Amsterdam Netherlands)* (2013) 16(1):114–21. doi: 10.3109/10253890.2012.686075

5. Schuller HM, Al-Wadei HA, Ullah MF, Plummer HK3rd. Regulation of pancreatic cancer by neuropsychological stress responses: A novel target for intervention. *Carcinogenesis* (2012) 33(1):191–6. doi: 10.1093/carcin/bgr251

6. Shin KJ, Lee YJ, Yang YR, Park S, Suh PG, Follo MY, et al. Molecular mechanisms underlying psychological stress and cancer. *Curr Pharm design* (2016) 22(16):2389–402. doi: 10.2174/1381612822666160226144025

7. Chida Y, Hamer M, Wardle J, Steptoe A. Do stress-related psychosocial factors contribute to cancer incidence and survival? *Nat Clin Pract Oncol* (2008) 5(8):466–75. doi: 10.1038/ncponc1134

8. Krizanova O, Babula P, Pacak K. Stress, catecholaminergic system and cancer. *Stress (Amsterdam Netherlands)* (2016) 19(4):419–28. doi: 10.1080/10253890.2016.1203415

9. Surman M, Janik ME. Stress and its molecular consequences in cancer progression. *Postepy higieny i medycyny doswiadczalnej (Online)* (2017) 71(0):485–99. doi: 10.5604/01.3001.0010.3830

10. Kruk J, Aboul-Enein BH, Bernstein J, Gronostaj M. Psychological stress and cellular aging in cancer: A meta-analysis. *Oxid Med Cell Longevity* (2019) 2019:1270397. doi: 10.1155/2019/1270397

11. Moreno-Villanueva M, Burkle A. Stress hormone-mediated DNA damage response–implications for cellular senescence and tumour progression. *Curr Drug Targets* (2016) 17(4):398–404. doi: 10.2174/1389450116666151001113720

12. Oppong E, Cato AC. Effects of glucocorticoids in the immune system. *Adv Exp Med Biol* (2015) 872:217–33. doi: 10.1007/978-1-4939-2895-8_9

13. Colon-Echevarria CB, Lamboy-Caraballo R, Aquino-Acevedo AN, Armaiz-Pena GN. Neuroendocrine regulation of tumor-associated immune cells. *Front Oncol* (2019) 9:1077. doi: 10.3389/fonc.2019.01077

14. Reiske L, Schmucker S, Steuber J. Glucocorticoids and catecholamines affect in vitro functionality of porcine blood immune cells. *Animals (Basel)* (2019) 9(8):545. doi: 10.3390/ani9080545

15. Costanzo ES, Sood AK, Lutgendorf SK. Biobehavioral influences on cancer progression. *Immunol Allergy Clinics North America* (2011) 31(1):109–32. doi: 10.1016/j.iac.2010.09.001

16. Xiang Y, Yan H, Zhou J, Zhang Q, Hanley G, Caudle Y, et al. The role of toll-like receptor 9 in chronic stress-induced apoptosis in macrophage. *PloS One* (2015) 10(4):e0123447. doi: 10.1371/journal.pone.0123447

17. Gurfein BT, Hasdemir B, Milush JM, Touma C, Palme R, Nixon DF, et al. Enriched environment and stress exposure influence splenic B lymphocyte composition. *PLoS One* (2017) 12(7):e0180771. doi: 10.1371/journal.pone.0180771

18. McGregor BA, Murphy KM, Albano DL, Ceballos RM. Stress, cortisol, and b lymphocytes: A novel approach to understanding academic stress and immune function. *Stress (Amsterdam Netherlands)* (2016) 19(2):185–91. doi: 10.3109/10253890.2015.1127913

19. Harle G, Kaminski S, Dubayle D, Frippiat JP, Ropars A. Murine splenic b cells express corticotropin-releasing hormone receptor 2 that affect their viability during a stress response. *Sci Rep* (2018) 8(1):143. doi: 10.1038/s41598-017-18401-y

20. Rudak PT, Gangireddy R, Choi J, Burhan AM, Summers KL, Jackson DN, et al. Stress-elicited glucocorticoid receptor signaling upregulates tigit in innate-like invariant T lymphocytes. *Brain behavior Immun* (2019) 80:793–804. doi: 10.1016/j.bbi.2019.05.027

21. Prather AA, Epel ES, Portela Parra E, Coccia M, Puterman E, Aiello AE, et al. Associations between chronic caregiving stress and T cell markers implicated in immunosenescence. *Brain behavior Immun* (2018) 73:546–9. doi: 10.1016/j.bbi.2018.06.019

22. Silvestre-Roig C, Fridlender ZG, Glogauer M, Scapini P. Neutrophil diversity in health and disease. *Trends Immunol* (2019) 40(7):565–83. doi: 10.1016/j.it.2019.04.012

23. Jaillon S, Ponzetta A, Di Mitri D, Santoni A, Bonecchi R, Mantovani A. Neutrophil diversity and plasticity in tumour progression and therapy. *Nat Rev Cancer* (2020) 20(9):485–503. doi: 10.1038/s41568-020-0281-y

24. Fridlender ZG, Sun J, Kim S, Kapoor V, Cheng G, Ling L, et al. Polarization of tumor-associated neutrophil phenotype by tgf-beta: "N1" versus "N2" tan. *Cancer Cell* (2009) 16(3):183–94. doi: 10.1016/j.ccr.2009.06.017

25. Que H, Fu Q, Lan T, Tian X, Wei X. Tumor-associated neutrophils and neutrophil-targeted cancer therapies. *Biochim Biophys Acta Rev Cancer* (2022) 1877(5):188762. doi: 10.1016/j.bbcan.2022.188762

26. Giese MA, Hind LE, Huttenlocher A. Neutrophil plasticity in the tumor microenvironment. *Blood* (2019) 133(20):2159–67. doi: 10.1182/blood-2018-11-844548

27. Nolan E, Bridgeman VL, Ombrato L, Karoutas A, Rabas N, Sewnath CAN, et al. Radiation exposure elicits a neutrophil-driven response in healthy lung tissue that enhances metastatic colonization. *Nat Cancer* (2022) 3(2):173–87. doi: 10.1038/s43018-022-00336-7

28. Huang X, Le W, Chen Q, Chen J, Zhu Y, Shi D, et al. Suppression of the innate cancer-killing activity in human granulocytes by stress reaction as a possible mechanism for affecting cancer development. *Stress* (2019) 23(1):87–96. doi: 10.1080/10253890.2019.1645112

29. Sharpley CF, Christie DRH, Bitsika V, Andronicos NM, Agnew LL, Richards TM, et al. Comparing a genetic and a psychological factor as correlates of anxiety, depression, and chronic stress in men with prostate cancer. *Supportive Care Cancer Off J Multinational Assoc Supportive Care Cancer* (2018) 26(9):3195–200. doi: 10.1007/s00520-018-4183-4

30. Lantheaume S, Montagne M, Shankland R. Intervention focused on resources to reduce anxiety and depression disorders in cancer patients: A pilot study. *Encephale* (2020) 46(1):13–22. doi: 10.1016/j.encep.2019.07.005

31. Luo M, Yan D, Sun Q, Tao J, Xu L, Sun H, et al. Ginsenoside Rg1 attenuates cardiomyocyte apoptosis and inflammation *Via* the Tlr4/Nf-Kb/Nlrp3 pathway. *J Cell Biochem* (2020) 121(4):2994–3004. doi: 10.1002/jcb.29556

32. Chu Y, Zhang W, Kanimozhi G, Brindha GR, Tian D. Ginsenoside Rg1 induces apoptotic cell death in triple-negative breast cancer cell lines and prevents carcinogen-induced breast tumorigenesis in sprague dawley rats. *Evid Based Complement Alternat Med* (2020) 2020:8886955. doi: 10.1155/2020/8886955

33. Li QF, Shi SL, Liu QR, Tang J, Song J, Liang Y. Anticancer effects of ginsenoside Rg1, cinnamic acid, and tanshinone iia in osteosarcoma mg-63 cells: Nuclear matrix downregulation and cytoplasmic trafficking of nucleophosmin. *Int J Biochem Cell Biol* (2008) 40(9):1918–29. doi: 10.1016/j.biocel.2008.01.031

34. Blanks MJ, Stehle JRJr., Du W, Adams JM, Willingham MC, Allen GO, et al. Novel innate cancer killing activity in humans. *Cancer Cell Int* (2011) 11:26. doi: 10.1186/1475-2867-11-26

35. Bhuyan DJ, Sakoff J, Bond DR, Predebon M, Vuong QV, Chalmers AC, et al. *In vitro* anticancer properties of selected eucalyptus species. *In Vitro Cell Dev Biol Anim* (2017) 53(7):604–15. doi: 10.1007/s11626-017-0149-y

36. Kanehisa M, Araki M, Goto S, Hattori M, Hirakawa M, Itoh M, et al. Kegg for linking genomes to life and the environment. *Nucleic Acids Res* (2008) 36(Database issue): D480–4. doi: 10.1093/nar/gkm882

37. Szklarczyk D, Gable AL, Lyon D, Junge A, Wyder S, Huerta-Cepas J, et al. String V11: Protein-protein association networks with increased coverage, supporting functional discovery in genome-wide experimental datasets. *Nucleic Acids Res* (2019) 47(D1):D607–d13. doi: 10.1093/nar/gky1131

38. Livak KJ, Schmittgen TD. Analysis of relative gene expression data using real-time quantitative pcr and the 2(-delta delta C(T)) method. *Methods* (2001) 25(4):402–8. doi: 10.1006/meth.2001.1262

39. Bai M, Grieshaber-Bouyer R, Wang J, Schmider AB, Wilson ZS, Zeng L, et al. Cd177 modulates human neutrophil migration through activation-mediated integrin and chemoreceptor regulation. *Blood* (2017) 130(19):2092–100. doi: 10.1182/blood-2017-03-768507

40. Rieger AM, Barreda DR. Accurate assessment of cell death by imaging flow cytometry. *Methods Mol Biol* (2016) 1389:209–20. doi: 10.1007/978-1-4939-3302-0_15

41. Hicks AM, Riedlinger G, Willingham MC, Alexander-Miller MA, Von Kap-Herr C, Pettenati MJ, et al. Transferable anticancer innate immunity in spontaneous Regression/Complete resistance mice. *Proc Natl Acad Sci United States America* (2006) 103(20):7753–8. doi: 10.1073/pnas.0602382103

42. Wang Y, Liu Y, Zhang X-Y, Xu L-H, Ouyang D-Y, Liu K-P, et al. Ginsenoside Rg1 regulates innate immune responses in macrophages through differentially modulating the nf-κb and Pi3k/Akt/Mtor pathways. *Int Immunopharmacol* (2014) 23(1):77–84. doi: 10.1016/j.intimp.2014.07.028

43. Zhou W, Li X, Lin Y, Yan W, Jiang S, Huang X, et al. A comparative transcriptome between anti-drug sensitive and resistant candida auris in China. *Front Microbiol* (2021) 12:708009. doi: 10.3389/fmicb.2021.708009

44. Le W, Chen B, Maharaj D, Cui Z. Natural cancer-killing activity of human granulocytes. *Integr Cancer Sci Ther* (2018) 5(1):1–7. doi: 10.15761/ICST.1000263

45. Murray PJ. Amino acid auxotrophy as a system of immunological control nodes. *Nat Immunol* (2016) 17(2):132–9. doi: 10.1038/ni.3323

46. McGovern N, Shin A, Low G, Low D, Duan K, Yao LJ, et al. Human fetal dendritic cells promote prenatal T-cell immune suppression through arginase-2. *Nature* (2017) 546 (7660):662–6. doi: 10.1038/nature22795

47. Zhao S, Yu M. Identification of Mmp1 as a potential prognostic biomarker and correlating with immune infiltrates in cervical squamous cell carcinoma. *DNA Cell Biol* (2020) 39(2):255–72. doi: 10.1089/dna.2019.5129

48. Zhang J, Gu Y, Liu X, Rao X, Huang G, Ouyang Y. Clinicopathological and prognostic value of S100a4 expression in non-small cell lung cancer: A meta-analysis. *Biosci Rep* (2020) 40(7):BSR20201710. doi: 10.1042/bsr20201710

49. Jia F, Liu M, Li X, Zhang F, Yue S, Liu J. Relationship between S100a4 protein expression and pre-operative serum Ca19.9 levels in pancreatic carcinoma and its prognostic significance. *World J Surg Oncol* (2019) 17(1):163. doi: 10.1186/s12957-019-1707-4

50. Domenis R, Pilutti D, Orsaria M, Marzinotto S, Candotti V, Bosisio G, et al. Expression and modulation of S100a4 protein by human mast cells. *Cell Immunol* (2018) 332:85–93. doi: 10.1016/j.cellimm.2018.08.001

51. Tang Q, Holland-Letz T, Slynko A, Cuk K, Marme F, Schott S, et al. DNA Methylation array analysis identifies breast cancer associated rptor, Mgrn1 and rapsn hypomethylation in peripheral blood DNA. *Oncotarget* (2016) 7(39):64191–202. doi: 10.18632/oncotarget.11640

52. Qiao R, Di F, Wang J, Wei Y, Zhang Y, Xu T, et al. The association between rapsn methylation in peripheral blood and early stage lung cancer detected in case-control cohort. *Cancer Manag Res* (2020) 12:11063–75. doi: 10.2147/cmar.S275321

53. Mydel P, Shipley JM, Adair-Kirk TL, Kelley DG, Broekelmann TJ, Mecham RP, et al. Neutrophil elastase cleaves laminin-332 (Laminin-5) generating peptides that are chemotactic for neutrophils. *J Biol Chem* (2008) 283(15):9513–22. doi: 10.1074/jbc.M706239200

54. Harvath L, Brownson NE, Fields GB, Skubitz AP. Laminin peptides stimulate human neutrophil motility. *J Immunol* (1994) 152(11):5447–56. doi: 10.4049/jimmunol.152.11.5447

55. Sun C, Wang L, Yang XX, Jiang YH, Guo XL. The aberrant expression or disruption of Desmocollin2 in human diseases. *Int J Biol Macromol* (2019) 131:378–86. doi: 10.1016/j.ijbiomac.2019.03.041

56. Kamekura R, Kolegraff KN, Nava P, Hilgarth RS, Feng M, Parkos CA, et al. Loss of the desmosomal cadherin desmoglein-2 suppresses colon cancer cell proliferation through egfr signaling. *Oncogene* (2014) 33(36):4531–6. doi: 10.1038/onc.2013.442

57. Xiao J, Kuang X, Dai L, Zhang L, He B. Anti-tumour effects of keratin 6a in lung adenocarcinoma. *Clin Respir J* (2020) 14(7):667–74. doi: 10.1111/crj.13182

58. Ratajczak-Wrona W, Jablonska E, Garley M, Jablonski J, Radziwon P, Iwaniuk A, et al. Pi3k-Akt/Pkb signaling pathway in neutrophils and mononuclear cells exposed to n-nitrosodimethylamine. *J Immunotoxicol* (2014) 11(3):231–7. doi: 10.3109/1547691x.2013.826307

59. Carrick JB, Begg AP. Peripheral blood leukocytes. *Vet Clin North Am Equine Pract* (2008) 24(2):239–59. doi: 10.1016/j.cveq.2008.05.003

60. Hidalgo A, Casanova-Acebes M. Dimensions of neutrophil life and fate. *Semin Immunol* (2021) 57:101506. doi: 10.1016/j.smim.2021.101506

61. Shi ZY, Zeng JZ, Wong AST. Chemical structures and pharmacological profiles of ginseng saponins. *Molecules* (2019) 24(13):2443. doi: 10.3390/molecules24132443

62. González-Burgos E, Fernandez-Moriano C, Gómez-Serranillos MP. Potential neuroprotective activity of ginseng in parkinson's disease: A review. *J Neuroimmune Pharmacol* (2015) 10(1):14–29. doi: 10.1007/s11481-014-9569-6

63. Yin H, Liu Z, Li F, Ni M, Wang B, Qiao Y, et al. Ginsenoside-Rg1 enhances angiogenesis and ameliorates ventricular remodeling in a rat model of myocardial infarction. *J Mol Med (Berl)* (2011) 89(4):363–75. doi: 10.1007/s00109-011-0723-9

64. Li L, Wang Y, Qi B, Yuan D, Dong S, Guo D, et al. Suppression of pma-induced tumor cell invasion and migration by ginsenoside Rg1 *Via* the inhibition of nf-κb-Dependent mmp-9 expression. *Oncol Rep* (2014) 32(5):1779–86. doi: 10.3892/or.2014.3422

65. Yang Z, Ming XF. Functions of arginase isoforms in macrophage inflammatory responses: Impact on cardiovascular diseases and metabolic disorders. *Front Immunol* (2014) 5:533. doi: 10.3389/fimmu.2014.00533

66. Mumenthaler SM, Yu H, Tze S, Cederbaum SD, Pegg AE, Seligson DB, et al. Expression of arginase ii in prostate cancer. *Int J Oncol* (2008) 32(2):357–65. doi: 10.3892/ijo.32.2.357

67. Gannon PO, Godin-Ethier J, Hassler M, Delvoye N, Aversa M, Poisson AO, et al. Androgen-regulated expression of arginase 1, arginase 2 and interleukin-8 in human prostate cancer. *PloS One* (2010) 5(8):e12107. doi: 10.1371/journal.pone.0012107

68. Perez G, Olivares IM, Rodriguez MG, Ceballos GM, Garcia Sanchez JR. Arginase activity in patients with breast cancer: An analysis of plasma, tumors, and its relationship with the presence of the estrogen receptor. *Onkologie* (2012) 35(10):570–4. doi: 10.1159/000343005

69. Costa H, Xu X, Overbeek G, Vasaikar S, Patro CP, Kostopoulou ON, et al. Human cytomegalovirus may promote tumour progression by upregulating arginase-2. *Oncotarget* (2016) 7(30):47221–31. doi: 10.18632/oncotarget.9722

70. Murray GI, Duncan ME, O'Neil P, McKay JA, Melvin WT, Fothergill JE. Matrix metalloproteinase-1 is associated with poor prognosis in oesophageal cancer. *J Pathol* (1998) 185(3):256–61. doi: 10.1002/(SICI)1096-9896(199807)185:3<256::AID-PATH115>3.0.CO;2-A

71. Ito T, Ito M, Shiozawa J, Naito S, Kanematsu T, Sekine I. Expression of the mmp-1 in human pancreatic carcinoma: Relationship with prognostic factor. *Mod Pathol* (1999) 12(7):669–74.

72. Inoue T, Yashiro M, Nishimura S, Maeda K, Sawada T, Ogawa Y, et al. Matrix metalloproteinase-1 expression is a prognostic factor for patients with advanced gastric cancer. *Int J Mol Med* (1999) 4(1):73–7. doi: 10.3892/ijmm.4.1.73

73. Kurnia I, Rauf S, Hatta M, Arifuddin S, Hidayat YM, Natzir R, et al. Molecular patho-mechanisms of cervical cancer (Mmp1). *Ann Med Surg (Lond)* (2022) 77:103415. doi: 10.1016/j.amsu.2022.103415

74. Wu YH, Wu TC, Liao JW, Yeh KT, Chen CY, Lee H. P53 dysfunction by xeroderma pigmentosum group c defects enhance lung adenocarcinoma metastasis *Via* increased Mmp1 expression. *Cancer Res* (2010) 70(24):10422–32. doi: 10.1158/0008-5472.Can-10-2615

75. Visse R, Nagase H. Matrix metalloproteinases and tissue inhibitors of metalloproteinases: Structure, function, and biochemistry. *Circ Res* (2003) 92(8):827–39. doi: 10.1161/01.Res.0000070112.80711.3d

76. Grigorian M, Ambartsumian N, Lykkesfeldt AE, Bastholm L, Elling F, Georgiev G, et al. Effect of Mts1 (S100a4) expression on the progression of human breast cancer cells. *Int J Cancer* (1996) 67(6):831–41. doi: 10.1002/(SICI)1097-0215(19960917)67:6<831::AID-IJC13>3.0.CO;2-4

77. Cabezón T, Celis JE, Skibshøj I, Klingelhöfer J, Grigorian M, Gromov P, et al. Expression of S100a4 by a variety of cell types present in the tumor microenvironment of human breast cancer. *Int J Cancer* (2007) 121(7):1433–44. doi: 10.1002/ijc.22850

78. Peinado H, Zhang H, Matei IR, Costa-Silva B, Hoshino A, Rodrigues G, et al. Pre-metastatic niches: Organ-specific homes for metastases. *Nat Rev Cancer* (2017) 17(5):302–17. doi: 10.1038/nrc.2017.6

79. Ambartsumian N, Klingelhöfer J, Grigorian M, Christensen C, Kriajevska M, Tulchinsky E, et al. The metastasis-associated Mts1(S100a4) protein could act as an angiogenic factor. *Oncogene* (2001) 20(34):4685–95. doi: 10.1038/sj.onc.1204636

80. Lei S, Li L, Yang X, Yin Q, Xu T, Zhou W, et al. The association between rapsn methylation in peripheral blood and breast cancer in the Chinese population. *J Hum Genet* (2021) 66(11):1069–78. doi: 10.1038/s10038-021-00933-x

81. Kraus RF, Gruber MA. Neutrophils-from bone marrow to first-line defense of the innate immune system. *Front Immunol* (2021) 12:767175. doi: 10.3389/fimmu.2021.767175

82. Loschke F, Homberg M, Magin TM. Keratin isotypes control desmosome stability and dynamics through pkcα. *J Invest Dermatol* (2016) 136(1):202–13. doi: 10.1038/jid.2015.403

83. Sun C, Wang L, Du DD, Ji JB, Yang XX, Yu BF, et al. Dsc2 suppresses the metastasis of gastric cancer through inhibiting the Brd4/Snail signaling pathway and the transcriptional activity of β-catenin. *Oxid Med Cell Longev* (2022) 2022:4813571. doi: 10.1155/2022/4813571

84. Hedrick CC, Malanchi I. Neutrophils in cancer: Heterogeneous and multifaceted. *Nat Rev Immunol* (2022) 22(3):173–87. doi: 10.1038/s41577-021-00571-6

frontiers | Frontiers in Immunology

TYPE Review
PUBLISHED 06 February 2023
DOI 10.3389/fimmu.2023.1086803

OPEN ACCESS

EDITED BY
Mazdak Ganjalikhani Hakemi,
Isfahan University of Medical Sciences, Iran

REVIEWED BY
Lionel Franz Poulin,
INSERM U1003 Laboratoire de Physiologie Cellulaire, France
Nahid Eskandari,
Isfahan University of Medical Sciences, Iran

*CORRESPONDENCE
Qingsong Yin
jnyinqingsong@163.com

SPECIALTY SECTION
This article was submitted to Cancer Immunity and Immunotherapy, a section of the journal Frontiers in Immunology

RECEIVED 01 November 2022
ACCEPTED 18 January 2023
PUBLISHED 06 February 2023

CITATION
Lu J, Liang T, Li P and Yin Q (2023) Regulatory effects of IRF4 on immune cells in the tumor microenvironment. *Front. Immunol.* 14:1086803. doi: 10.3389/fimmu.2023.1086803

Regulatory effects of IRF4 on immune cells in the tumor microenvironment

Jing Lu[1], Taotao Liang[1], Ping Li[2] and Qingsong Yin[1*]

[1]Department of Hematology, The Affiliated Cancer Hospital of Zhengzhou University and Henan Cancer Hospital, Zhengzhou, Henan, China, [2]Department of Hematology, The University of Texas MD Anderson Cancer Center, Houston, TX, United States

The tumor microenvironment (TME) is implicated in tumorigenesis, chemoresistance, immunotherapy failure and tumor recurrence. Multiple immunosuppressive cells and soluble secreted cytokines together drive and accelerate TME disorders, T cell immunodeficiency and tumor growth. Thus, it is essential to comprehensively understand the TME status, immune cells involved and key transcriptional factors, and extend this knowledge to therapies that target dysfunctional T cells in the TME. Interferon regulatory factor 4 (IRF4) is a unique IRF family member that is not regulated by interferons, instead, is mainly induced upon T-cell receptor signaling, Toll-like receptors and tumor necrosis factor receptors. IRF4 is largely restricted to immune cells and plays critical roles in the differentiation and function of effector cells and immunosuppressive cells, particularly during clonal expansion and the effector function of T cells. However, in a specific biological context, it is also involved in the transcriptional process of T cell exhaustion with its binding partners. Given the multiple effects of IRF4 on immune cells, especially T cells, manipulating IRF4 may be an important therapeutic target for reversing T cell exhaustion and TME disorders, thus promoting anti-tumor immunity. This study reviews the regulatory effects of IRF4 on various immune cells in the TME, and reveals its potential mechanisms, providing a novel direction for clinical immune intervention.

KEYWORDS

IRF4, tumor microenvironment, immunosuppressive cells, T cell exhaustion, immunoregulation

Introduction

The occurrence and development of tumors highly depend on the surrounding matrix environment, called the tumor microenvironment (TME). The oncogene proteins expressed by tumor cells stimulate and induce the abnormal activation of effector T cells (1, 2). Multiple soluble tumor-derived products, such as the chemokines CCL2, CCL5 and the cytokines IL10 and TGFβ, etc., recruit tumor-associated macrophages (TAMs) (3–6) and myeloid-derived suppressor cells (MDSCs) (7) into the TME, and lead to the impairment of differentiation, maturation and function of dendritic cells (DCs) (8, 9). These factors in turn jointly aggravates TME disorders, inhibits the anti-tumor immunity of effector T cells, and

induces T cell exhaustion and the development of regulatory T (Treg) cells (2). As a result, apart from genetic deficiencies, the immunosuppressive TME is considered to be involved in tumorigenesis (10), chemoresistance, immunotherapy failure and even tumor recurrence (2, 6).

Given this reliance on the TME, there is an opportunity for anti-tumor immunotherapies that work by targeting TME components and their signaling pathways (11, 12). Although tremendous progress has been made in the past few years, including immune checkpoint inhibitors (13), bispecific antibodies (14) and chimeric antigen receptor (CAR) T cells (15), many studies focusing on elements of the TME have failed to show promising efficacy in patients, particularly with sustainable efficacy (16–18). Therefore, the development of new immunotherapies may also require consideration of the key transcription regulatory factors involved in multiple components and processes in the TME.

Interferon regulatory factor 4 (IRF4) is a member of the interferon regulatory factor (IRF) family, and its unique characteristics and the importance in multiple biological processes have been highlighted by oncology and immunology. It first serves as an oncogene or a tumor suppressor in multiple types of lymphoid neoplasms (19–21). In addition, intriguingly, accumulating studies have demonstrated that IRF4 is a central determinant of differentiation, activation and effector function for various immune cells (22, 23). IRF4 is essential for the sustained differentiation and proliferation of CD8+ cytotoxic T cells (CTLs) and T helper 1 (Th1) cells, promoting anti-tumor immunity. In parallel, IRF4 is also involved in T cell exhaustion in specific biological contexts (24, 25). In contrast, it plays an important role in the differentiation and function of various immunosuppressive cells, such as Th2 cells, Treg cells, TAMs and MDSCs, establishing an immunosuppressive TME to inhibit anti-tumor immunity and favor the immune escape and survival of tumor cells (3–5, 7) (Figure 1). Thus, an in-depth understanding of the effects and potential mechanisms of IRF4 in a variety of immune cells and a disordered TME may provide new directions for clinical immune intervention.

Structure and function of IRF4

The IRF family consists of nine members (IRF1-IRF9) in mammals that play important roles in regulating innate and adaptive immune responses. Unlike other IRFs, IRF4 is a unique family member that is not regulated by interferons (IFNs) (22), instead, is mainly induced upon T-cell receptor (TCR) signaling, Toll-like receptors (TLRs; such as TLR4 and TLR9) and tumor necrosis factor receptors. The expression of IRF4 is restricted to immune cells, including T and B cells, macrophages and DCs (19, 22). In naïve T cells, IRF4 is expressed at low levels (23); however,

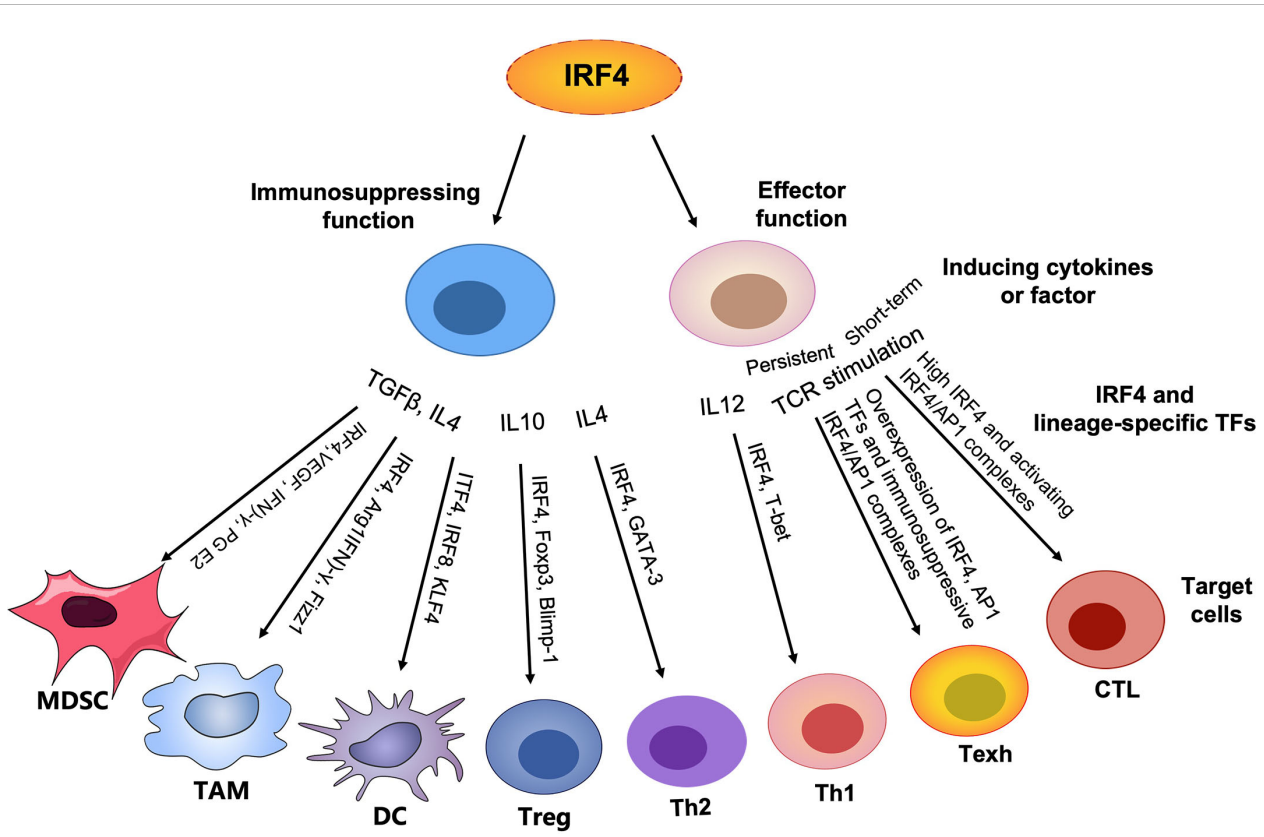

FIGURE 1
Graphical abstract. In contrast to lineage-specific TFs, IRF4 plays an important role in T cell differentiation and function by regulating the expression of corresponding transcription factors (TFs) to control the generation of other lineages, particularly the differentiation and proliferation of effector T cells, promoting anti-tumor immunity. However, persistently high expression of IRF4 and AP1 family members leads to overabundance of IRF4/AP1 complexes to drive T cell exhaustion. In addition, IRF4 plays an important role in the development and function of a series of immunosuppressive cells, such as MDSCs, TAMs, immature DCs, Treg cells and Th2 cells, maintaining immune homeostasis and in parallel establishing an immunosuppressive TME and inhibiting anti-tumor immunity.

following TCR signaling it is immediately induced and mediates critical immune responses by interacting with upstream signaling pathways, such as the TCR signaling, and its diverse binding partners (26).

IRF4 is composed of three structural domains: a variable C-terminal functional regulatory domain, a highly conserved N-terminal DNA-binding domain and an intermediate compact linker domain (22, 27, 28) (Figure 2). IRF4 interacts with numerous DNA-binding domains to play corresponding functions as a homodimer or heterodimer (29). IRF4 binds to interferon-stimulated response elements (ISREs) to regulate the activation of interferon-stimulated genes (ISGs) as a homodimer. However, the formation of heterodimeric complexes containing IRF4 depends largely on the target cell type. For instance, IRF4 engages activator protein 1 (AP1)-IRF composite elements (AICE) as a heterodimer mainly in T cells, germinal center B cells and plasma cells (23, 28). Whereas the binding of IRF4 with erythroblast transformation (ET)-specific transcription factors (TFs) is largely restricted to B cells and DCs. Of note, the binding of IRF4 to AICE requires AP1 family TFs, including basic leucine zipper transcription factor ATF-like (BATF), BATF3 and Jun family members, such as JunB, c-Jun, for high-affinity interaction (23, 30–33). These TFs form ternary complexes through physical interaction to coordinately regulate the differentiation and function of T cells, as well as T cell exhaustion, in a special microenvironment (24, 33–35).

Collectively, IRF4 can signal to regulate diverse transcriptional programs through complexes containing ET or AP1 TF motifs in different cell types depending on the corresponding cellular context, particularly T cell exhaustion in the TME, thus suggesting new directions for improving anti-tumor immunity by modulating IRF4-dependent transcription.

Roles of IRF4 in the differentiation and function OF CD4+ T cells

According to different functions, CD4+ T cells can be divided into CD4+ effector T cells, including Th1, Th2 and Th17 cells, which predominantly promote the immune response, T follicular helper cells (Tfh), which orchestrate antibody responses (26), and Treg cells, which are characterized by their inhibition of the immune response and maintenance of immune tolerance (26, 36, 37). In contrast to lineage-specific TFs (e.g., T-bet for Th1, GATA3 for Th2, RORγt for Th17, B-cell lymphoma 6 (Bcl6) for Tfh and Foxp3 for Treg), TCR signaling-induced IRF4 plays an important role in Th cell differentiation and function by regulating the expression of corresponding TFs to control the generation of other lineages, thus determining the fate of Th cells (23, 26, 29, 38).

IRF4 determines the fate of Th1, Th2, Th17 and Tfh

Th cell differentiation is regulated by the coordinated functions of distinct cytokines and transcription factors. A recent study has demonstrated that increased IRF4 promotes the differentiation of CD4+ $CD25^{low}$ Teff cells, including Th1, Th2 and Th17 cells, at the expense of Tfh cells (26). In fact, the development and differentiation of Tfh cells only needs an appropriate amount IRF4 in addition to specific TFs, including Bcl-6 and signal transducer and activator of transcription 3 (STAT3) (26, 39). B-lymphocyte-induced maturation protein 1 (Blimp1) is a critical antagonist for Tfh cell differentiation, but it is an important TF for other Th cells, including Th1, Th2, Th17 and Treg cells (40). It has been found that IRF4 cooperates with STAT3 to activate Blimp1 (41), and lack of IRF4 in CD4+ T cells reduces binding to STAT3, resulting in Tfh deficiency (41, 42).

Increasing studies have shown that IRF4 regulates Th17 cell development (43–45). IRF4 knockout decreases the expression of RORγt, a specific TF in Th17 cells (45, 46), which leads to a decrease in Th17 counts, in line with a reduction in serum IL17 and IL21 (47). Likewise, IRF4 deficiency also results in the impairment of Th2 cell differentiation and function by reducing GATA3 and IL4, as well as growth factor independence 1 (Gfi1), a transcriptional repressor required by Th2 cells (48, 49), instead, can promote the T-bet expression and skew toward Th1 cells (48), suggesting that IRF4 plays a pivotal role in the development of Th2 cells rather than Th1 cells. Additionally, IRF4 deficiency inevitably impairs the development of Th2 cells (49). Collectively, IRF4 regulates the differentiation and function of diverse Th subsets that mainly depend on its expression level as well as lineage-specific TFs (26).

IRF4 favors the development and suppressive activity of Tregs

Treg cells are indispensable for maintaining immune tolerance (37, 50); nevertheless, they also impair anti-tumor capability and promote tumor growth, particularly tumor-infiltrating Treg cells (51).

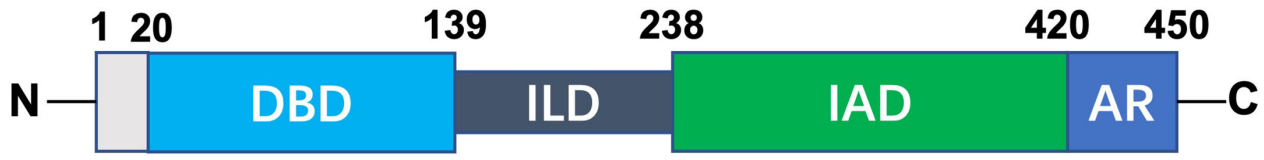

FIGURE 2
Schematic diagram of IRF4 structure. IRF4 consists of three structural domains: a highly conserved N-terminal DNA-binding domain (DBD), a variable C-terminal IRF association domain (IAD) and an intermediate linker domain (ILD). The DBD is characterized by five conserved tryptophans enabling it to form a helix–loop–helix motif that facilitates DNA binding. IAD is a protein–protein interaction domain that mediates the interaction of IRF4 with itself or multiple distinct transcription factors. IAD also contains a C-terminal auto-inhibitory region (AR) which physically interacts with DBD and results in low DNA binding affinity.

Foxp3 is a lineage-defining TF for Tregs and the key regulator of its development and function (52, 53). IRF4, which acts downstream of Foxp3, can physically and functionally interact with Foxp3 and cooperate with BATF3 to regulate Foxp3 expression (54, 55), which instructs effector Treg cell differentiation and immune suppression (56). Moreover, Blimp1 is a target of Foxp3 in Treg cells, and it is directly induced by IRF4 (57, 58). Accordingly, lack of IRF4 in Treg cells suppresses Blimp1 expression, and more intriguingly, leads to decreases in multiple Treg-related molecules, such as inducible T cell costimulatory (ICOS), IL10 and IL1 receptor 11 (IL1RL1), confirming that IRF4 cooperates with Blimp1 to regulate the differentiation and function of Treg cells (56, 58).

Additionally, compared with IRF4-deficient Treg cells, IRF4+ Treg cells overexpress BATF, IKAROS family zinc finger 2 (IKZF2), Ki67, ICOS and inhibitory molecules, such as programmed cell death protein 1 (PD1) and T cell immunoreceptor with immunoglobulin and ITIM domain (TIGIT) (38), exhibiting a highly activated phenotype and strong inhibitory effects in several tumors (59–61). In particular, an increase in intratumoral IRF4+ Treg cells with superior suppressive activity was significantly correlated with early tumor recurrence and poor disease-free survival (DFS) and overall survival (OS) (38). Accordingly, inhibition of IRF4 severely impaired the development and function of Treg cells at the tumor-infiltrating sites and significantly repressed tumor growth in a mouse model (38, 51). Collectively, growing evidence implicates IRF4 plays a central role in the differentiation and immunosuppressive activity of Treg cells in the TME, and IRF4+ Treg cells definitely inhibit anti-tumor immunity. Therefore, specifically targeting IRF4 in Treg cells may reverse the tumor microenvironment from immunosuppression to immune activation against tumor cells, which may become an effective anti-tumor therapeutic strategy.

Effect of IRF4 on the differentiation and function of CD8+ T cells

CD8+ T cells play critical roles in adaptive immunity. Antigen stimulation drives naïve CD8+ T cells to rapidly undergo a step-by-step process of early activation, clonal expansion and differentiation (62–65). In addition to early activation, IRF4 participates in the entire process of differentiation and function of effector CD8+ T cells (66, 67). Intriguingly, the amount and duration of IRF4 expression determine the fate of CD8+ T cells, which are differentiated into CD8+ effector T cells or exhausted T cells (24, 67–69).

High IRF4 promotes the expansion and sustained differentiation of CD8+ T cells

Following antigen stimulation, naïve CD8+ T cells are differentiated into a large number of antigen-specific short-lived effector cells (SLECs) (62, 63), exerting cytotoxic activity (Figure 3A). Mechanically, antigen stimulation drives the expression of TCR responsive factor IRF4 (68). Next, IRF4 combined with AP1 family TFs form an activating IRF4/AP1 complex, which integrates TCR and costimulatory signals to induce the production of a series of effector cytokines. After antigen clearance, the expression of IRF4 decreased, followed by an increase in expression of stemness-like gene T cell factor 7 (*Tcf7*; encoding TCF1) (Figure 3B), and further producing memory precursor cells (MPECs) and TCF1+ memory-like T cells to rapidly function in the secondary response (64, 65) (Figure 3A).

The intensity of TCR signaling regulates the expression of IRF4 (66, 70). High levels of IRF4 in CD8+ T cells contribute to the clonal expansion of SLECs, which are critical for maintaining effective anti-tumor immunity (71) and acute pathogen control (64). Interestingly, ectopic expression of IRF4 remarkably enhances the clonal expansion and effector cytokine production of T cells induced by low-intensity TCR signaling (69). Conversely, selective knockout of IRF4 in peripheral CD8+ T cells leads to progressive loss of the effector function of CD8+ T cells (72–74). The RNA-binding protein Roquin1, a key target upstream of IRF4, can effectively inhibit the expansion of CD8+ T cells (75). Accordingly, lack of Roquin1 can significantly promote the proliferation of CD8+ T cells by upregulating IRF4 (71). However, if IRF4 is also deficient, the expansion-promoting effects caused by Roquin1 deficiency is completely abolished (71). Therefore, the Roquin-IRF4 axis may also serve as a potential target for enhancing anti-tumor immunity.

IRF4 also converts TCR affinity into appropriate transcriptional programs, linking metabolic function to T cell clone expansion and effector differentiation (76) by regulating the expression of key molecules required for aerobic glycolysis on effector T cells, including hypoxia inducible factor1 α (HIF1α) and forkhead box protein o1 (Foxo1) (77). Compared with weak or low-affinity TCR stimulation, strong or high-affinity TCR stimulation contributes to increased glucose uptake in an IRF4-dependent manner (78). Taken together, IRF4 regulates the expansion and differentiation of effector CD8+ T cells by translating the TCR signal and converting it to metabolic function.

IRF4 maintains the effector function of CD8+ memory T cells

Not surprisingly, similar to initial antigen stimulation, IRF4 overexpression significantly induces an increase in the cytotoxicity of memory CD8+ T cells (32, 68, 79). By contrast, IRF4 deficiency may cause memory CD8+ T cells to produce but not proliferate (68), which results in impairment of the effector function (32, 72, 79). So far, at least three types of memory CD8+ T cells have been defined: central memory T (T_{CM}) cells, effector memory T (T_{EM}) cells and tissue-resident memory T (T_{RM}) cells (80). Compared with T_{EM} cells, T_{RM} cells express higher levels of IRF4, and their formation and maintenance are IRF4 dependent (32). IRF4 deletion leads to an increase in T_{EM} cells and a decrease in T_{RM} cells, but it does not affect the total number of memory T cells (32). Thus, targeting IRF4 may strongly reduce the number of T_{RM} cells, thus substantially weakening transplant rejection (81).

In addition, recent studies have shown that TCF1 is essential for maintaining CD8+ T_{CM} cells and serves as a positive biomarker for prolonged survival and effective responses to PD1 inhibitors in various solid tumors and hematological malignancies (82–85). Undoubtedly, high-level IRF4 is beneficial to the initial effector function, but sustained overexpression of IRF4 inhibits the expression of TCF1, which further damages the production of antigen-specific T_{CM} cells and is not conductive to the rapid effect function in recall responses (24). Collectively, accumulating studies

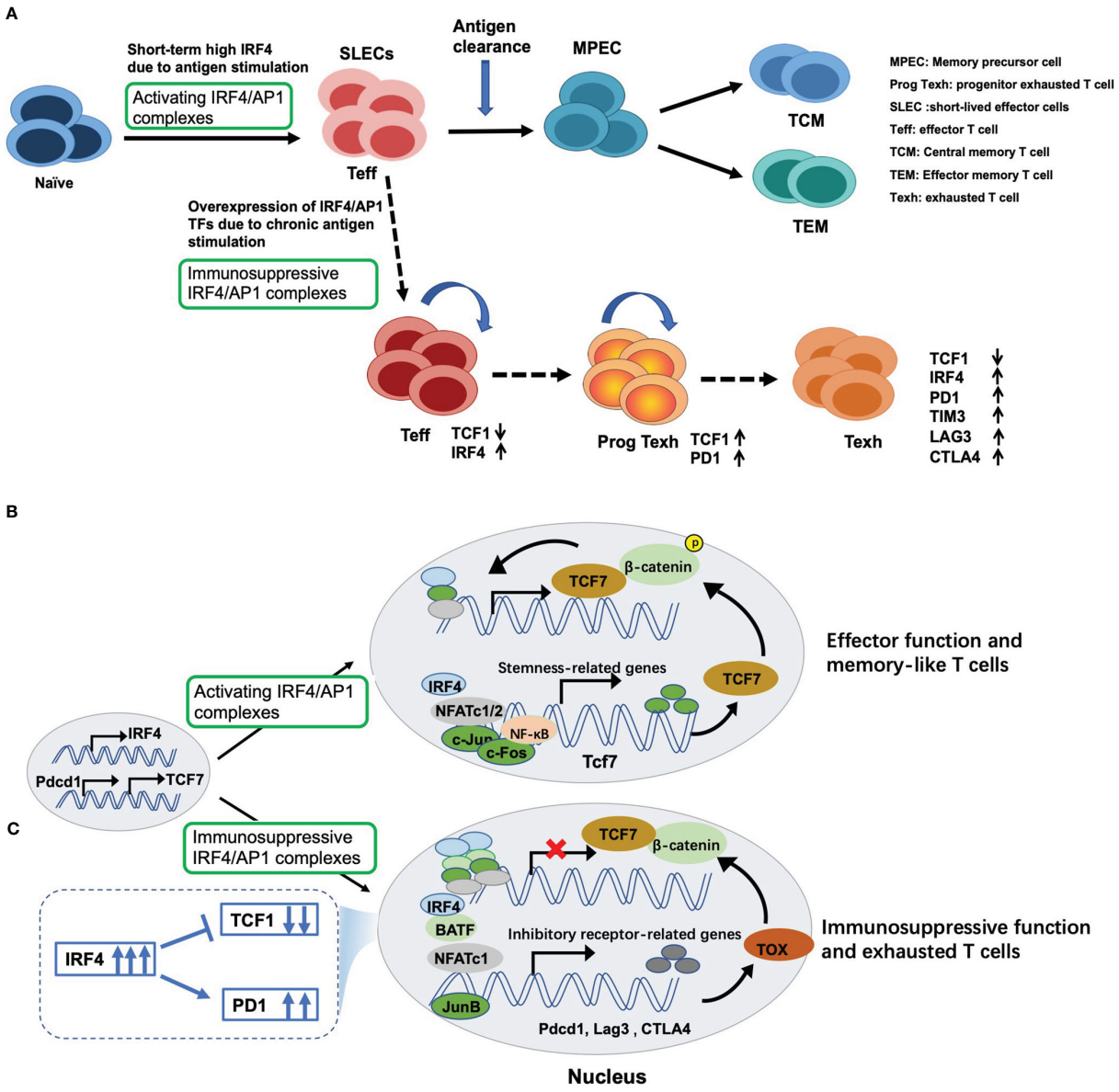

FIGURE 3
Dual regulatory effects of IRF4 on T cell immunity and underlying mechanisms. **(A)** Antigen stimulation drives and induces the expression of IRF4, which contributes to maintaining the expansion and sustained differentiation of effector CD8+ T cells. However, sustained overexpression of IRF4 due to chronic antigen stimulation drives CD8+ T cell exhaustion. Mechanically, **(B)** once antigen stimulation, IRF4 is induced and combined with its binding partners to form activating IRF4/AP1 complexes, thus inducing the production of effector cytokines and exerting cytotoxic activity. Once antigen clearance, the expression of IRF4 decreases, followed by an increase in expression of stemness-like gene TCF7 expression, thus producing TCF1+ memory-like T cells; **(C)** however, persistent overexpression of IRF4 and AP1 family members, such as BATF, BATF3 and JunB, leads to the formation of immunosuppressive IRF4/AP1 complexes, which opens multiple exhaustion-related chromatin regions, promoting the expression of inhibitory receptors and NR4A and TOX family members, which inhibits TCF7 expression and eventually drives CD8+ T cell exhaustion.

have demonstrated that IRF4 is indispensable for robust proliferation and the effector function of memory T cells in recall responses.

Persistently high IRF4-driven the exhaustion of CD8+ T cells and how to revert the exhaustion

High IRF4 is essential for maintaining the differentiation and expansion of effector CD8+ T cells (68, 72). However, too much is as bad as too little. Persistent antigen stimulation due to tumor or chronic viral infection can cause constitutively high expression of IRF4, which in turn induces CD8+ T cell exhaustion (24). There are several characteristics of exhausted CD8+ T cells (Figures 3A, 4): (1) up-regulation of multiple inhibitory receptors (86), (2) progressive loss of effector function and impaired differentiation of potential memory T cells (85, 87), (3) decreased production of cytokines involved in chemotaxis, adhesion and migration, and (4) metabolic deficiency (88). Thus, functional exhaustion is probably due to both active suppression and passive defects in signaling and metabolism.

Studies have demonstrated that the epigenetic and transcriptional programs driving CD8+ T cell exhaustion are triggered by sustained

antigen-dependent activation of TCR signaling, leading to two events: (1) the sustained overexpression of TCR-responsive IRF4 and its binding partners, mainly AP1 family members, including BATF, BATF3, JunB and JunD (24, 35, 89–92), as well as nuclear factor of activated T cells (NFAT), a key regulator of T cell activation (93), followed by (2) sustained expression of multiple exhaustion-related molecules (24). Specifically, overexpressed IRF4 binding with AP1 family members or NFAT leads to an overabundance of IRF4/AP1 complexes or NFAT homodimers that are recruited to specific DNA sites to open multiple exhaustion-related chromatin regions, including inhibitory receptors, such as PD1, T-cell immunoglobulin and mucin domain 3 (TIM3) and cytotoxic T lymphocyte antigen 4 (CTLA4) (24, 35, 94, 95), as well as orphan nuclear receptor 4A (NR4A) and thymocyte selection-associated high mobility group box (TOX) family members, which act to impose exhaustion (96, 97), further inhibiting TCF1 expression (Figure 3C) (24, 35). These events eventually drive CD8+ T cell exhaustion and limit the development of TCF1+ memory-like T cells and anti-tumor activity (Figure 3A). This chromatin binding imbalance due to the accumulation of IRF4/AP1 TF complexes was also found in CAR-T cell therapy (89).

Fortunately, Lynn et al. (89) found that ectopic overexpression of c-Jun in exhausted CAR-T cells can effectively rescue exhaustion and restore anti-tumor activity by disrupting and/or displacing immunosuppressive transcriptional complexes containing IRF4 and AP1 family members (89). Moreover, based on the overexpression of BATF and IRF4 in exhausted T cells (89, 98), knockdown of BATF or IRF4 could remarkably enhance the tumor-killing ability of CAR-T cells by reversing their exhaustion and prolonging their persistence (89, 90). Likewise, Seo et al. (25) found that overexpressed BATF in BATF-transduced CAR-T cells could cooperate with appropriate amount of IRF4 to counteract exhaustion, promoting the expansion of CD8+ CAR-T cells and increasing their effector cytokine production. Nevertheless, inhibiting the interaction between BATF and IRF4 will greatly weaken the tumor control ability of BATF-overexpressing CAR-T cells (25).

Collectively, these findings show that persistent overexpression of IRF4 drives T cell exhaustion depending on the specific microenvironment and the amount and functional status of its binding partners. Therefore, manipulating the formation of IRF4/AP1 complexes may be an inspiring therapeutic strategy to overcome T cell exhaustion. Yet, the core transcriptional network of IRF4 involved in these two opposing programs still needs to be further elucidated.

Regulation of IRF4 in immunosuppressive cells in the TME

Various immunosuppressive cells and multiple soluble chemokines and cytokines in the TME interact to not only establish an immunosuppressive TME but also directly or indirectly inhibit the proliferation and activation of CD8+ T cells (99, 100), which may cause chemoresistance and failure of immunotherapy and facilitate tumor growth and metastasis (101–103). IRF4 plays important and complicated roles in the development and function of immunosuppressive cells and their interaction with T cells (Figure 4) (104, 105).

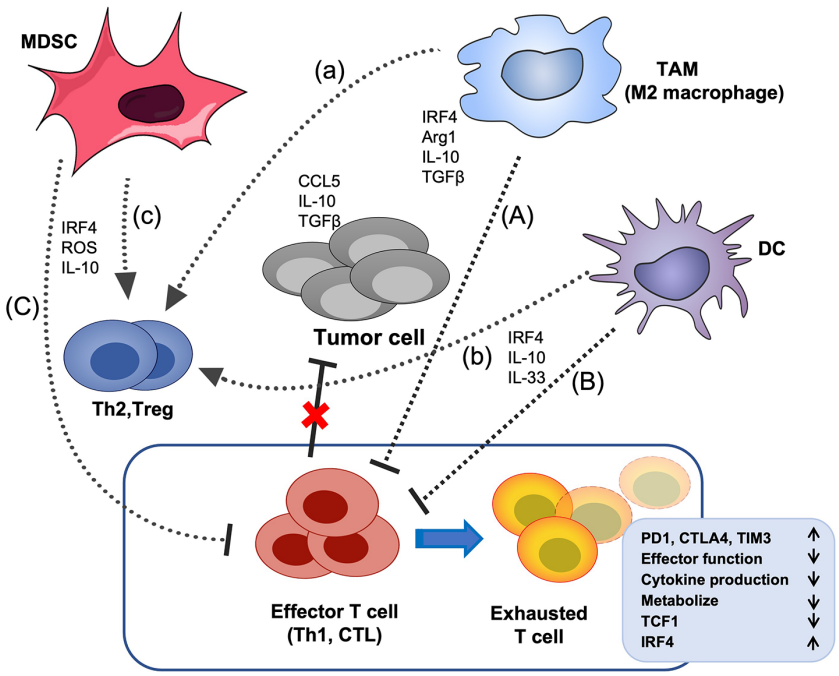

FIGURE 4
The effects of IRF4 on the crosstalk between immunosuppressive cells and T cells in the TME. Tumor cells and multiple soluble chemokines and cytokines recruit and induced various immunosuppressive cells, such as MDSCs, TAMs and DCs to the TME, which further aggravate the TME disorder and promote tumor growth. These myeloid derived immunosuppressive cells can suppress the effector function of CTL and Th1 cells and promote the differentiation of Treg cells and Th2 cells. In addition, tumor-related antigens stimulate the abnormal activation of effector T cells, ultimately, lead to the CD8+ T cell exhaustion, characterized by up-regulation of multiple inhibitory receptors, progressive loss of effector function and impaired differentiation of memory T cells, etc. IRF4 plays critical roles in the generation of various immunosuppressive cells, and the above crosstalk between myeloid derived immunosuppressive cells and effector T cells **(A–C)** and Treg cells **(a-c)** in the TME. The black arrow indicates promotion, the black horizontal line indicates inhibition, and the red cross indicates that the anti-tumor activity of effector T cells is impaired.

IRF4 promotes the polarization of M2 macrophages in the TME

There are two types of macrophages: M1 (anti-tumor activity) (106, 107) and M2 (pro-tumor activity) (108). Generally, TAMs mainly refer to M2 macrophages, which are characterized by high expression of arginase1 (Arg1), chitinase-like 3 (Ym1/Chil3), found in inflammatory zone 1 (Fizz1) and mannose receptor (MR) (109, 110). IRFs play a key role in macrophage maturation and phenotypic polarization. Of the nine IRFs, IRF1, IRF5 and IRF8 are involved in the commitment of M1 macrophages, whereas IRF3 and IRF4 are crucial for M2 macrophage polarization through regulating the expression of Arg1 and Ym1, which further sufficiently produces Th2 and directly suppresses effector T cell proliferation (111–113).

In addition, it has been reported that Jumonji domain containing 3 (Jmjd3) is essential for M2 macrophage polarization, and IRF4 is a Jmjd3 target gene (110, 114). Phosphatidylserine released by apoptotic tumor cells could induce the polarization and accumulation of M2 macrophages *via* a STAT3-Jmjd3-IRF4 signaling axis (115); therefore, down-regulation of Jmjd3 by targeting the STAT3-Jmjd3-IRF4 axis may be a candidate approach for inhibiting the accumulation of M2 macrophages in tumor sites and remodeling the TME. Moreover, some miRNAs have been found to promote the transformation of macrophages from M2 to M1 by targeting IRF4 to activate IRF5 (116, 117). Given that IRF4 promotes the polarization of M2 macrophages, targeting IRF4 to reprogram TAM polarization in the TME appears to be a promising therapy for tumors.

IRF4 is beneficial to DC differentiation in the TME

DCs, known as professional antigen presenting cells, play a major role in orchestrating immune responses, and can be mainly divided into three subtypes: plasmacytoid DCs (pDCs), classical DCs (cDCs, including cDC1 and cDC2), and monocyte-derived DCs (mo-DCs) (9, 118, 119). However, the differentiation and maturation of DCs are often impaired by the immunosuppressive TME, which leads to DC dysfunction and induces tolerance to tumor cells (8, 9, 118, 119). For instance, mature pDCs exert immunostimulatory function, which is characterized by the production of large amounts of type I IFNs. Whereas, in the TME, pDCs with reduced production of type I IFNs favor the development of Treg cell, exert immunosuppressive effects on CTLs and promote tumor progression (8, 9, 120, 121). Several studies have indicated a role for IRF4 in development of monocytes, pDCs, and cDCs (122–124). IRF4 contributes to the differentiation of pDCs (122). In addition, IRF4 plays a key role in the development of cDC2 and promotes their survival and migration to lymph nodes and is essential TF for cDC2-mediated Th2 induction (122). By contrast, inhibition of IRF4 in DCs represses Th2 and promotes Th17 responses (123).

The monocytes in the TME can prioritize differentiation into monocyte-derived macrophages (mo-Macs) rather than mo-DCs (3, 105). The presence of mo-DCs has been correlated with CD8+ T cell activation and successful anti-tumor therapy (125). IRF4 is essential for human mo-DC differentiation and efficient antigen cross-presentation, whereas IRF4-deficent monocytes are phone to differentiation into mo-Macs (124). Devalaraja et al. found that the TME induces tumor cells to produce retinoic acid (RA) in murine sarcoma models, which drives intratumor monocyte polarization to mo-Macs instead of mo-DCs by inhibiting IRF4 (3). Interestingly, overexpression of IRF4 in human monocytes can sufficiently block RA-mediated mo-Mac differentiation (3, 124). Collectively, these results suggest that IRF4 plays critical and complicated roles in the maturation and differentiation of DCs in the TME.

Tumor and MDSC-restricted IRF4 expression enhances the suppressive activity of MDSCs and promotes the immunosuppressive TME

MDSCs are immature myeloid cells that do not differentiate into mature myeloid cells, and this is a major obstacle to achieving successful immunotherapy in tumors (126, 127). Two major subpopulations, monocytic (M) MDSCs and polymorphonuclear (PMN)-MDSCs, have an immune suppressive function. IRF4 plays a role in the lymphoid cell development. However, IRF4 expression is decreased in immature myeloid cells, such as MDSCs in tumor-bearing mice and chronic myeloid leukemia cells (104, 128). Accordingly, IRF4 deficiency further favors the generation of MDSCs in the TME, and increases the expansion of M-MDSCs and the infiltration of PMN-MDSCs with a strong suppressive capacity, which inhibits the proliferation of CD8+ T cells through IL10 and ROS generation and promotes tumor growth (104, 129). By contrast, an increase in the IRF4 expression in MDSCs from bone marrow cells inhibits the numbers of MDSCs through induction differentiation, and further damages the immunosuppressive function of MDSCs (104). Unfortunately, IRF4 expression is remarkably suppressed during the development of MDSCs and tumor formation in the TME (104).

Altogether, these data show that IRF4 plays a critical role in preventing the generation of MDSCs; nevertheless, IRF4 expression is limited by tumors and MDSCs, which may in turn boost the accumulation and suppressive activity of MDSCs to accelerate the generation of an immunosuppressive TME. Thus far, the exact mechanisms regulating IRF4 in the differentiation of MDSCs remains largely unknown.

Conclusion and future prospects

IRF4 plays key roles in the development of various immunosuppressive cells in the TME. More importantly, this TF is also indispensable in the differentiation and function of effector T cells, particularly memory T cells in the secondary response (32, 64, 78). Notably, the amount and duration of IRF4 expression determines CD8+ T cell differentiation into effector T cells or exhausted T cells, depending on the specific microenvironment and states of its binding partners (24, 34, 35, 91). Thus far, the dual regulatory mechanism of IRF4 in T cell immunity is not completely clear. Given the imbalance between the activating and immunoregulatory IRF4/AP1 complexes

induced by persistent high expression of IRF4 and AP1 family members in specific contexts, manipulating the composition of the IRF4/AP1 complexes may be a novel therapeutic strategy for overcoming T cell exhaustion and improving anti-tumor potency.

Recently, several studies have reported exciting findings, including the regulation of the physical interaction between IRF4 and its binding partners, the formation of ternary complexes through overexpression of BATF or c-Jun, and the regulation of the amount of IRF4 or BATF, which are essential for rescuing exhaustion and improving anti-tumor potency in tumor-specific CAR-T cells (25, 89, 90). In addition, several recent studies have focused on targeting Roquin and Regnase1, negative regulators of T cell activation and differentiation, to enhance the proliferation and persistence of tumor-antigen-specific CD8+ T cells or CAR-T cells and effectively inhibit tumor growth (71, 130–132). In fact, the beneficial effects of the regulation of these targets are caused not only by loss of function of a single gene, but likely also caused by the cooperative regulation of multiple targets. For instance, the promotion of the survival and proliferation of tumor-antigen-specific CD8+ T cells by inactivating Roquin1 is highly dependent on the expression of IRF4 (71). Similarly, Regnase1 deficiency contributed to CAR-T cell survival and proliferation, which also specifically required BATF (130), further enhancing recall responses by increasing TCF1+ CAR-T cell population (131). By coincidence, proper reduction of IRF4 contributes to the generation of TCF1+ memory T cells that control tumor recurrence (25). Together, these findings point to promising new targets for improving immunotherapy.

Taken together, based on the close cooperation and regulatory relationships between IRF4, BATF, TCF1 and Roquin or Regnase1, targeting IRF4 or IRF4-based multi-target combination is an important direction for regulating human anti-tumor T cell immunity and the TME to improve therapeutic efficacy in the future.

Author contributions

JL reviewed the literature and wrote the manuscript. TL and PL contributed to literature collection and manuscript revision. QY designed the review, and wrote and revised the manuscript. All authors contributed to the article and approved the submitted version.

Funding

This study was supported by Bethune · Blood Scientific Research Capacity Building Project (J202201E023), the Medical Science and Technology Research Project of Henan Province (LHGJ20220185) and National Natural Science Foundation of China (82200222).

Conflict of interest

The authors declare that the research was conducted in the absence of any commercial or financial relationships that could be construed as a potential conflict of interest.

Publisher's note

References

1. Fu C, Jiang A. Dendritic cells and CD8 T cell immunity in tumor microenvironment. *Front Immunol* (2018) 9:3059. doi: 10.3389/fimmu.2018.03059

2. Nakamura K, Smyth MJ. Myeloid immunosuppression and immune checkpoints in the tumor microenvironment. *Cell Mol Immunol* (2020) 17(1):1–12. doi: 10.1038/s41423-019-0306-1

3. Devalaraja S, To TKJ, Folkert IW, Natesan R, Alam MZ, Li M, et al. Tumor-derived retinoic acid regulates intratumoral monocyte differentiation to promote immune suppression. *Cell* (2020) 180(6):1098–114.e16. doi: 10.1016/j.cell.2020.02.042

4. Mougiakakos D, Bach C, Bottcher M, Beier F, Röhner L, Stoll A, et al. The IKZF1-IRF4/IRF5 axis controls polarization of myeloma-associated macrophages. *Cancer Immunol Res* (2021) 9(3):265–78. doi: 10.1158/2326-6066.CIR-20-0555

5. Carbó JM, León TE, Font-Díaz J, de la Rosa JV, Castrillo A, Picard FR, et al. Pharmacologic activation of LXR alters the expression profile of tumor-associated macrophages and the abundance of regulatory T cells in the tumor microenvironment. *Cancer Res* (2021) 81(4):968–85. doi: 10.1158/0008-5472.CAN-19-3360

6. Li K, Shi H, Zhang B, Ou X, Ma Q, Chen Y, et al. Myeloid-derived suppressor cells as immunosuppressive regulators and therapeutic targets in cancer. *Signal Transd Target Ther* (2021) 6(1):362. doi: 10.1038/s41392-021-00670-9

7. Yang Q, Xie H, Li X, Feng Y, Xie S, Qu J, et al. Interferon regulatory factor 4 regulates the development of polymorphonuclear myeloid-derived suppressor cells through the transcription of c-myc in cancer. *Front Immunol* (2021) 12:627072. doi: 10.3389/fimmu.2021.627072

8. Verneau J, Sautés-Fridman C, Sun CM. Dendritic cells in the tumor microenvironment: Prognostic and theranostic impact. *Semin Immunol* (2020) 48:101410. doi: 10.1016/j.smim.2020.101410

9. Subtil B, Cambi A, Tauriello DVF, de Vries IJM. The therapeutic potential of tackling tumor-induced dendritic cell dysfunction in colorectal cancer. *Front Immunol* (2021) 12:724883. doi: 10.3389/fimmu.2021.724883

10. Lu C, Rong D, Zhang B, Zheng W, Wang X, Chen Z, et al. Current perspectives on the immunosuppressive tumor microenvironment in hepatocellular carcinoma: Challenges and opportunities. *Mol Cancer* (2019) 18(1):130. doi: 10.1186/s12943-019-1047-6

11. Xiao Y, Yu D. Tumor microenvironment as a therapeutic target in cancer. *Pharmacol Ther* (2021) 221:107753. doi: 10.1016/j.pharmthera.2020.107753

12. Liu Y, Song Y, Yin Q. Effects of ibrutinib on T-cell immunity in patients with chronic lymphocytic leukemia. *Front Immunol* (2022) 13:962552. doi: 10.3389/fimmu.2022.962552

13. Hanna BS, Yazdanparast H, Demerdash Y, Roessner PM, Schulz R, Lichter P, et al. Combining ibrutinib and checkpoint blockade improves CD8+ T-cell function and control of chronic lymphocytic leukemia in em-TCL1 mice. *Haematologica* (2021) 106(4):968–77. doi: 10.3324/haematol.2019.238154

14. Lejeune M, Köse MC, Duray E, Einsele H, Beguin Y, Caers J. Bispecific, T-cell-recruiting antibodies in b-cell malignancies. *Front Immunol* (2020) 11:762. doi: 10.3389/fimmu.2020.00762

15. Mehta PH, Fiorenza S, Koldej RM, Jaworowski A, Ritchie DS, Quinn KM. T Cell fitness and autologous CAR T cell therapy in haematologic malignancy. *Front Immunol* (2021) 12:780442. doi: 10.3389/fimmu.2021.780442

16. Zhang ZZ, Wang T, Wang XF, Zhang YQ, Song SX, Ma CQ. Improving the ability of CAR-T cells to hit solid tumors: Challenges and strategies. *Pharmacol Res* (2022) 175:106036. doi: 10.1016/j.phrs.2021.106036

17. Zhang M, Kim JA, Huang AY. Optimizing tumor microenvironment for cancer immunotherapy: Beta-glucan-based nanoparticles. *Front Immunol* (2018) 9:341. doi: 10.3389/fimmu.2018.00341

18. Barnestein R, Galland L, Kalfeist L, Ghiringhelli F, Ladoire S, Limagne E. Immunosuppressive tumor microenvironment modulation by chemotherapies and targeted therapies to enhance immunotherapy effectiveness. *Oncoimmunology* (2022) 11(1):2120676. doi: 10.1080/2162402X.2022.2120676

19. Wong RWJ, Ong JZL, Theardy MS, Sanda T. IRF4 as an oncogenic master transcription factor. *Cancers* (2022) 14(17):4314. doi: 10.3390/cancers14174314

20. Sundararaj S, Seneviratne S, Williams SJ, Enders A, Casarotto MG. The molecular basis for the development of adult T-cell leukemia/lymphoma in patients with an IRF4 (K59R) mutation. *Protein Sci* (2022) 31(4):787–96. doi: 10.1002/pro.4260

21. Maffei R, Fiorcari S, Benatti S, Atene CG, Martinelli S, Zucchini P, et al. IRF4 modulates the response to BCR activation in chronic lymphocytic leukemia regulating IKAROS and SYK. *Leukemia* (2021) 35(5):1330–43. doi: 10.1038/s41375-021-01178-5

22. Nam S, Lim JS. Essential role of interferon regulatory factor 4 (IRF4) in immune cell development. *Arch Pharm Res* (2016) 39(11):1548–55. doi: 10.1007/s12272-016-0854-1

23. Huber M, Lohoff M. IRF4 at the crossroads of effector T-cell fate decision. *Eur J Immunol* (2014) 44(7):1886–95. doi: 10.1002/eji.201344279

24. Man K, Gabriel SS, Liao Y, Gloury R, Preston S, Henstridge DC, et al. Transcription factor IRF4 promotes CD8(+) T cell exhaustion and limits the development of memory-like T cells during chronic infection. *Immunity* (2017) 47 (6):1129–41.e5. doi: 10.1016/j.immuni.2017.11.021

25. Seo H, González-Avalos E, Zhang W, Ramchandani P, Yang C, Lio CJ, et al. BATF and IRF4 cooperate to counter exhaustion in tumor-infiltrating CAR T cells. *Nat Immunol* (2021) 22(8):983–95. doi: 10.1038/s41590-021-00964-8

26. Krishnamoorthy V, Kannanganat S, Maienschein-Cline M, Cook SL, Chen J, Bahroos N, et al. The IRF4 gene regulatory module functions as a read-write integrator to dynamically coordinate T helper cell fate. *Immunity* (2017) 47(3):481–97.e7. doi: 10.1016/j.immuni.2017.09.001

27. Sundararaj S, Seneviratne S, Williams SJ, Enders A, Casarotto MG. Structural determinants of the IRF4/DNA homodimeric complex. *Nucleic Acids Res* (2021) 49 (4):2255–65. doi: 10.1093/nar/gkaa1287

28. Remesh SG, Santosh V, Escalante CR. Structural studies of IRF4 reveal a flexible autoinhibitory region and a compact linker domain. *J Biol Chem* (2015) 290(46):27779–90. doi: 10.1074/jbc.M115.678789

29. Li P, Spolski R, Liao W, Leonard WJ. Complex interactions of transcription factors in mediating cytokine biology in T cells. *Immunol Rev* (2014) 261(1):141–56. doi: 10.1111/imr.12199

30. Li P, Spolski R, Liao W, Wang L, Murphy TL, Murphy KM, et al. BATF-JUN is critical for IRF4-mediated transcription in T cells. *Nature* (2012) 490(7421):543–6. doi: 10.1038/nature11530

31. Murphy TL, Tussiwand R, Murphy KM. Specificity through cooperation: BATF-IRF interactions control immune-regulatory networks. *Nat Rev Immunol* (2013) 13 (7):499–509. doi: 10.1038/nri3470

32. Harberts A, Schmidt C, Schmid J, Reimers D, Koch-Nolte F, Mittrücker HW, et al. Interferon regulatory factor 4 controls effector functions of CD8(+) memory T cells. *Proc Natl Acad Sci U.S.A.* (2021) 118(16):e2014553118. doi: 10.1073/pnas.2014553118

33. Glasmacher E, Agrawal S, Chang AB, Murphy TL, Zeng W, Vander Lugt B, et al. A genomic regulatory element that directs assembly and function of immune-specific AP-1-IRF complexes. *Science* (2012) 338(6109):975–80. doi: 10.1126/science.1228309

34. Papavassiliou AG, Musti AM. The multifaceted output of c-jun biological activity: Focus at the junction of CD8 T cell activation and exhaustion. *Cells* (2020) 9(11):2470. doi: 10.3390/cells9112470

35. Seo W, Jerin C, Nishikawa H. Transcriptional regulatory network for the establishment of CD8(+) T cell exhaustion. *Exp Mol Med* (2021) 53(2):202–9. doi: 10.1038/s12276-021-00568-0

36. Hombach AA, Abken H. Most do, but some do not: CD4(+)CD25(-) T cells, but not CD4(+)CD25(+) treg cells, are cytolytic when redirected by a chimeric antigen receptor (CAR). *Cancers* (2017) 9(9):112. doi: 10.3390/cancers9090112

37. Brown CY, Sadlon T, Hope CM, Wong YY, Wong S, Liu N, et al. Molecular insights into regulatory T-cell adaptation to self, environment, and host tissues: Plasticity or loss of function in autoimmune disease. *Front Immunol* (2020) 11:1269. doi: 10.3389/fimmu.2020.01269

38. Alvisi G, Brummelman J, Puccio S, Mazza EM, Tomada EP, Losurdo A, et al. IRF4 instructs effector treg differentiation and immune suppression in human cancer. *J Clin Invest* (2020) 130(6):3137–50. doi: 10.1172/JCI130426

39. Bollig N, Brüstle A, Kellner K, Ackermann W, Abass E, Raifer H, et al. Transcription factor IRF4 determines germinal center formation through follicular T-helper cell differentiation. *Proc Natl Acad Sci U.S.A.* (2012) 109(22):8664–9. doi: 10.1073/pnas.1205834109

40. Johnston RJ, Poholek AC, DiToro D, Yusuf I, Eto D, Barnett B, et al. Bcl6 and blimp-1 are reciprocal and antagonistic regulators of T follicular helper cell differentiation. *Science* (2009) 325(5943):1006–10. doi: 10.1126/science.1175870

41. Kwon H, Thierry-Mieg D, Thierry-Mieg J, Kim HP, Oh J, Tunyaplin C, et al. Analysis of interleukin-21-induced Prdm1 gene regulation reveals functional cooperation of STAT3 and IRF4 transcription factors. *Immunity* (2009) 31(6):941–52. doi: 10.1016/j.immuni.2009.10.008

42. Wu H, Deng Y, Zhao M, Zhang J, Zheng M, Chen G, et al. Molecular control of follicular helper T cell development and differentiation. *Front Immunol* (2018) 9:2470. doi: 10.3389/fimmu.2018.02470

43. Capone A, Volpe E. Transcriptional regulators of T helper 17 cell differentiation in health and autoimmune diseases. *Front Immunol* (2020) 11:348. doi: 10.3389/fimmu.2020.00348

44. Bunte K, Beikler T. Th17 cells and the IL-23/IL-17 axis in the pathogenesis of periodontitis and immune-mediated inflammatory diseases. *Int J Mol Sci* (2019) 20 (14):3394. doi: 10.3390/ijms20143394

45. Brüstle A, Heink S, Huber M, Rosenplänter C, Stadelmann C, Yu P, et al. The development of inflammatory T(H)-17 cells requires interferon-regulatory factor 4. *Nat Immunol* (2007) 8(9):958–66. doi: 10.1038/ni1500

46. Sha Y, Markovic-Plese S. Activated IL-1RI signaling pathway induces Th17 cell differentiation *via* interferon regulatory factor 4 signaling in patients with relapsing-remitting multiple sclerosis. *Front Immunol* (2016) 7:543. doi: 10.3389/fimmu.2016.00543

47. Lorenz G, Moschovaki-Filippidou F, Würf V, Metzger P, Steiger S, Batz F, et al. IFN regulatory factor 4 controls post-ischemic inflammation and prevents chronic kidney disease. *Front Immunol* (2019) 10:2162. doi: 10.3389/fimmu.2019.02162

48. Tominaga N, Ohkusu-Tsukada K, Udono H, Abe R, Matsuyama T, Yui K. Development of Th1 and not Th2 immune responses in mice lacking IFN-regulatory factor-4. *Int Immunol* (2003) 15(1):1–10. doi: 10.1093/intimm/dxg001

49. Xu WD, Pan HF, Ye DQ, Xu Y. Targeting IRF4 in autoimmune diseases. *Autoimmun Rev* (2012) 11(12):918–24. doi: 10.1016/j.autrev.2012.08.011

50. Schumann K, Raju SS, Lauber M, Kolb S, Shifrut E, Cortez JT, et al. Functional CRISPR dissection of gene networks controlling human regulatory T cell identity. *Nat Immunol* (2020) 21(11):1456–66. doi: 10.1038/s41590-020-0784-4

51. Aramini B, Masciale V, Samarelli AV, Dubini A, Gaudio M, Stella F, et al. Phenotypic, functional, and metabolic heterogeneity of immune cells infiltrating non-small cell lung cancer. *Front Immunol* (2022) 13:959114. doi: 10.3389/fimmu.2022.959114

52. Saleh R, Elkord E. FoxP3(+) T regulatory cells in cancer: Prognostic biomarkers and therapeutic targets. *Cancer Lett* (2020) 490:174–85. doi: 10.1016/j.canlet.2020.07.022

53. van der Veeken J, Glasner A, Zhong Y, Hu W, Wang ZM, Bou-Puerto R, et al. The transcription factor Foxp3 shapes regulatory T cell identity by tuning the activity of trans-acting intermediaries. *Immunity* (2020) 53(5):971–84.e5. doi: 10.1016/j.immuni.2020.10.010

54. Arnold PR, Wen M, Zhang L, Ying Y, Xiao X, Chu X, et al. Suppression of FOXP3 expression by the AP-1 family transcription factor BATF3 requires partnering with IRF4. *Front Immunol* (2022) 13:966364. doi: 10.3389/fimmu.2022.966364

55. Zheng Y, Chaudhry A, Kas A, deRoos P, Kim JM, Chu TT, et al. Regulatory T-cell suppressor program co-opts transcription factor IRF4 to control T(H)2 responses. *Nature* (2009) 458(7236):351–6. doi: 10.1038/nature07674

56. Koizumi SI, Ishikawa H. Transcriptional regulation of differentiation and functions of effector T regulatory cells. *Cells* (2019) 8(8):939. doi: 10.3390/cells8080939

57. Cretney E, Leung PS, Trezise S, Newman DM, Rankin LC, Teh CE, et al. Characterization of blimp-1 function in effector regulatory T cells. *J Autoimmun* (2018) 91:73–82. doi: 10.1016/j.jaut.2018.04.003

58. Cretney E, Xin A, Shi W, Minnich M, Masson F, Miasari M, et al. The transcription factors blimp-1 and IRF4 jointly control the differentiation and function of effector regulatory T cells. *Nat Immunol* (2011) 12(4):304–11. doi: 10.1038/ni.2006

59. Van Damme H, Dombrecht B, Kiss M, Roose H, Allen E, Van Overmeire E, et al. Therapeutic depletion of CCR8(+) tumor-infiltrating regulatory T cells elicits antitumor immunity and synergizes with anti-PD-1 therapy. *J Immunother Cancer* (2021) 9(2): e001749. doi: 10.1136/jitc-2020-001749

60. Stéphan P, Lautraite R, Voisin A, Grinberg-Bleyer Y. Transcriptional control of regulatory T cells in cancer: Toward therapeutic targeting? *Cancers* (2020) 12(11):3194. doi: 10.3390/cancers12113194

61. Swatler J, Turos-Korgul L, Kozlowska E, Piwocka K. Immunosuppressive cell subsets and factors in myeloid leukemias. *Cancers* (2021) 13(6):1203. doi: 10.3390/cancers13061203

62. Kavazović I, Polić B, Wensveen FM. Cheating the hunger games; mechanisms controlling clonal diversity of CD8 effector and memory populations. *Front Immunol* (2018) 9:2831. doi: 10.3389/fimmu.2018.02831

63. Reina-Campos M, Scharping NE, Goldrath AW. CD8(+) T cell metabolism in infection and cancer. *Nat Rev Immunol* (2021) 21(11):718–38. doi: 10.1038/s41577-021-00537-8

64. Nayar R, Schutten E, Bautista B, Daniels K, Prince AL, Enos M, et al. Graded levels of IRF4 regulate CD8+ T cell differentiation and expansion, but not attrition, in response to acute virus infection. *J Immunol* (2014) 192(12):5881–93. doi: 10.4049/jimmunol.1303187

65. Richard AC. Divide and conquer: Phenotypic and temporal heterogeneity within CD8(+) T cell responses. *Front Immunol* (2022) 13:949423. doi: 10.3389/fimmu.2022.949423

66. Gallagher MP, Conley JM, Vangala P, Garber M, Reboldi A, Berg LJ. Hierarchy of signaling thresholds downstream of the T cell receptor and the tec kinase ITK. *Proc Natl Acad Sci U.S.A.* (2021) 118(35):e2025825118. doi: 10.1073/pnas.2025825118

67. Pritzl CJ, Daniels MA, Teixeiro E. Interplay of inflammatory, antigen and tissue-derived signals in the development of resident CD8 memory T cells. *Front Immunol* (2021) 12:636240. doi: 10.3389/fimmu.2021.636240

68. Miyakoda M, Honma K, Kimura D, Akbari M, Kimura K, Matsuyama T, et al. Differential requirements for IRF4 in the clonal expansion and homeostatic proliferation of naive and memory murine CD8(+) T cells. *Eur J Immunol* (2018) 48(8):1319–28. doi: 10.1002/eji.201747120

69. Yao S, Buzo BF, Pham D, Jiang L, Taparowsky EJ, Kaplan MH, et al. Interferon regulatory factor 4 sustains CD8(+) T cell expansion and effector differentiation. *Immunity* (2013) 39(5):833–45. doi: 10.1016/j.immuni.2013.10.007

70. Wu H, Witzl A, Ueno H. Assessment of TCR signal strength of antigen-specific memory CD8(+) T cells in human blood. *Blood Adv* (2019) 3(14):2153–63. doi: 10.1182/bloodadvances.2019000292

71. Zhao H, Liu Y, Wang L, Jin G, Zhao X, Xu J, et al. Genome-wide fitness gene identification reveals roquin as a potent suppressor of CD8 T cell expansion and anti-tumor immunity. *Cell Rep* (2021) 37(10):110083. doi: 10.1016/j.celrep.2021.110083

72. Grusdat M, McIlwain DR, Xu HC, Pozdeev VI, Knievel J, Crome SQ, et al. IRF4 and BATF are critical for CD8(+) T-cell function following infection with LCMV. *Cell Death Differ* (2014) 21(7):1050–60. doi: 10.1038/cdd.2014.19

73. Raczkowski F, Ritter J, Heesch K, Schumacher V, Guralnik A, Höcker L, et al. The transcription factor interferon regulatory factor 4 is required for the generation of protective effector CD8+ T cells. *Proc Natl Acad Sci U.S.A.* (2013) 110(37):15019–24. doi: 10.1073/pnas.1309378110

74. Zou D, Fu J, Guo Z, Chen W. Interferon regulatory factor 4 deficiency in CD8(+) T cells abrogates terminal effector differentiation and promotes transplant acceptance. *Immunology* (2020) 161(4):364–79. doi: 10.1111/imm.13258

75. Behrens G, Heissmeyer V. Cooperation of RNA-binding proteins - a focus on roquin function in T cells. *Front Immunol* (2022) 13:839762. doi: 10.3389/fimmu.2022.839762

76. Finlay D. IRF4 links antigen affinity to CD8+ T-cell metabolism. *Immunol Cell Biol* (2014) 92(1):6–7. doi: 10.1038/icb.2013.72

77. Man K, Miasari M, Shi W, Xin A, Henstridge DC, Preston S, et al. The transcription factor IRF4 is essential for TCR affinity-mediated metabolic programming and clonal expansion of T cells. *Nat Immunol* (2013) 14(11):1155–65. doi: 10.1038/ni.2710

78. Man K, Kallies A. Synchronizing transcriptional control of T cell metabolism and function. *Nat Rev Immunol* (2015) 15(9):574–84. doi: 10.1038/nri3874

79. Lugli E, Brummelman J, Pilipow K, Roychoudhuri R. Paths to expansion: Differential requirements of IRF4 in CD8(+) T-cell expansion driven by antigen and homeostatic cytokines. *Eur J Immunol* (2018) 48(8):1281–4. doi: 10.1002/eji.201847727

80. Parga-Vidal L, van Gisbergen KPJM. Area under immunosurveillance: Dedicated roles of memory CD8 T-cell subsets. *Cold Spring Harb Perspect Biol* (2020) 12(11): a037796. doi: 10.1101/cshperspect.a037796

81. Abou-Daya KI, Tieu R, Zhao D, Rammal R, Sacirbegovic F, Williams AL, et al. Resident memory T cells form during persistent antigen exposure leading to allograft rejection. *Sci Immunol* (2021) 6(57):eabc8122. doi: 10.1126/sciimmunol.abc8122

82. Siddiqui I, Schaeuble K, Chennupati V, Fuertes Marraco SA, Calderon-Copete S, Pais Ferreira D, et al. Intratumoral Tcf1(+)PD-1(+)CD8(+) T cells with stem-like properties promote tumor control in response to vaccination and checkpoint blockade immunotherapy. *Immunity* (2019) 50(1):195–211.e10. doi: 10.1016/j.immuni.2018.12.021

83. Pagliarulo F, Cheng PF, Brugger L, van Dijk N, van den Heijden M, Levesque MP, et al. Molecular, immunological, and clinical features associated with lymphoid neogenesis in muscle invasive bladder cancer. *Front Immunol* (2022) 12:793992. doi: 10.3389/fimmu.2021.793992

84. Liang T, Wang X, Liu Y, Ai H, Wang Q, Wang X, et al. Decreased TCF1 and BCL11B expression predicts poor prognosis for patients with chronic lymphocytic leukemia. *Front Immunol* (2022) 13:985280. doi: 10.3389/fimmu.2022.985280

85. Zhang J, Lyu T, Cao Y, Feng H. Role of TCF-1 in differentiation, exhaustion, and memory of CD8(+) T cells: A review. *FASEB J* (2021) 35(5):e21549. doi: 10.1096/fj.202002566R

86. Jiang W, He Y, He W, Wu G, Zhou X, Sheng Q, et al. Exhausted CD8+T cells in the tumor immune microenvironment: New pathways to therapy. *Front Immunol* (2021) 11:622509. doi: 10.3389/fimmu.2020.622509

87. Kim C, Jin J, Weyand CM, Goronzy JJ. The transcription factor TCF1 in T cell differentiation and aging. *Int J Mol Sci* (2020) 21(18):6497. doi: 10.3390/ijms21186497

88. Wherry EJ, Ha SJ, Kaech SM, Haining WN, Sarkar S, Kalia V, et al. Molecular signature of CD8+ T cell exhaustion during chronic viral infection. *Immunity* (2007) 27 (4):670–84. doi: 10.1016/j.immuni.2007.09.006

89. Lynn RC, Weber EW, Sotillo E, Gennert D, Xu P, Good Z, et al. C-jun overexpression in CAR T cells induces exhaustion resistance. *Nature* (2019) 576 (7786):293–300. doi: 10.1038/s41586-019-1805-z

90. Jiang P, Zhang Z, Hu Y, Liang Z, Han Y, Li X, et al. Single-cell ATAC-seq maps the comprehensive and dynamic chromatin accessibility landscape of CAR-T cell dysfunction. *Leukemia* (2022) 36(11):2656–68. doi: 10.1038/s41375-022-01676-0

91. Kurachi M, Barnitz RA, Yosef N, Odorizzi PM, DiIorio MA, Lemieux ME, et al. The transcription factor BATF operates as an essential differentiation checkpoint in early effector CD8+ T cells. *Nat Immunol* (2014) 15(4):373–83. doi: 10.1038/ni.2834

92. Chennupati V, Held W. Feeling exhausted? tuning Irf4 energizes dysfunctional T cells. *Immunity* (2017) 47(6):1009–11. doi: 10.1016/j.immuni.2017.11.028

93. Martinez GJ, Pereira RM, Äijö T, Kim EY, Marangoni F, Pipkin ME, et al. The transcription factor NFAT promotes exhaustion of activated CD8(+) T cells. *Immunity* (2015) 42(2):265–78. doi: 10.1016/j.immuni.2015.01.006

94. Mognol GP, Spreafico R, Wong V, Scott-Browne JP, Togher S, Hoffmann A, et al. Exhaustion-associated regulatory regions in CD8(+) tumor-infiltrating T cells. *Proc Natl Acad Sci U.S.A.* (2017) 114(13):E2776–85. doi: 10.1073/pnas.1620498114

95. Chen J, López-Moyado IF, Seo H, Lio CJ, Hempleman LJ, Sekiya T, et al. NR4A transcription factors limit CAR T cell function in solid tumours. *Nature* (2019) 567 (7749):530–4. doi: 10.1038/s41586-019-0985-x

96. Seo H, Chen J, González-Avalos E, Samaniego-Castruita D, Das A, Wang YH, et al. TOX and TOX2 transcription factors cooperate with NR4A transcription factors to impose CD8(+) T cell exhaustion. *Proc Natl Acad Sci U.S.A.* (2019) 116(25):12410–5. doi: 10.1073/pnas.1905675116

97. Scott AC, Dündar F, Zumbo P, Chandran SS, Klebanoff CA, Shakiba M, et al. TOX is a critical regulator of tumour-specific T cell differentiation. *Nature* (2019) 571 (7764):270–4. doi: 10.1038/s41586-019-1324-y

98. Doering TA, Crawford A, Angelosanto JM, Paley MA, Ziegler CG, Wherry EJ. Network analysis reveals centrally connected genes and pathways involved in CD8+ T cell exhaustion versus memory. *Immunity* (2012) 37(6):1130–44. doi: 10.1016/j.immuni.2012.08.021

99. Takahashi K, Kurashina K, Yamaguchi H, Kanamaru R, Ohzawa H, Miyato H, et al. Altered intraperitoneal immune microenvironment in patients with peritoneal metastases from gastric cancer. *Front Immunol* (2022) 13:969468. doi: 10.3389/fimmu.2022.969468

100. Almeida-Nunes DL, Mendes-Frias A, Silvestre R, Dinis-Oliveira RJ, Ricardo S. Immune tumor microenvironment in ovarian cancer ascites. *Int J Mol Sci* (2022) 23 (18):10692. doi: 10.3390/ijms231810692

101. Salmaninejad A, Valilou SF, Soltani A, Ahmadi S, Abarghan YJ, Rosengren RJ, et al. Tumor-associated macrophages: role in cancer development and therapeutic implications. *Cell Oncol (Dordr)* (2019) 42(5):591–608. doi: 10.1007/s13402-019-00453-z

102. Wu Y, Yi M, Niu M, Mei Q, Wu K. Myeloid-derived suppressor cells: an emerging target for anticancer immunotherapy. *Mol Cancer* (2022) 21(1):184. doi: 10.1186/s12943-022-01657-y

103. Fujimura T, Aiba S. Significance of immunosuppressive cells as a target for immunotherapies in melanoma and non-melanoma skin cancers. *Biomolecules* (2020) 10 (8):1087. doi: 10.3390/biom10081087

104. Nam S, Kang K, Cha JS, Kim JW, Lee HG, Kim Y, et al. Interferon regulatory factor 4 (IRF4) controls myeloid-derived suppressor cell (MDSC) differentiation and function. *J Leukoc Biol* (2016) 100(6):1273–84. doi: 10.1189/jlb.1A0215-068RR

105. Jahchan NS, Mujal AM, Pollack JL, Binnewies M, Sriram V, Reyno L, et al. Tuning the tumor myeloid microenvironment to fight cancer. *Front Immunol* (2019) 10:1611. doi: 10.3389/fimmu.2019.01611

106. Wang C, Lin Y, Zhu H, Zhou Y, Mao F, Huang X, et al. The prognostic and clinical value of tumor-associated macrophages in patients with breast cancer: A systematic review and meta-analysis. *Front Oncol* (2022) 12:905846. doi: 10.3389/fonc.2022.905846

107. Zhang SY, Song XY, Li Y, Ye LL, Zhou Q, Yang WB. Tumor-associated macrophages: A promising target for a cancer immunotherapeutic strategy. *Pharmacol Res* (2020) 161:105111. doi: 10.1016/j.phrs.2020.105111

108. Cao H, Huang T, Dai M, Kong X, Liu H, Zheng Z, et al. Tumor microenvironment and its implications for antitumor immunity in cholangiocarcinoma: Future perspectives for novel therapies. *Int J Biol Sci* (2022) 18(14):5369–90. doi: 10.7150/ijbs.73949

109. Wang LX, Zhang SX, Wu HJ, Rong XL, Guo J. M2b macrophage polarization and its roles in diseases. *J Leukoc Biol* (2019) 106(2):345–58. doi: 10.1002/JLB.3RU1018-378RR

110. Satoh T, Takeuchi O, Vandenbon A, Yasuda K, Tanaka Y, Kumagai Y, et al. The Jmjd3-Irf4 axis regulates M2 macrophage polarization and host responses against helminth infection. *Nat Immunol* (2010) 11(10):936–44. doi: 10.1038/ni.1920

111. El Chartouni C, Schwarzfischer L, Rehli M. Interleukin-4 induced interferon regulatory factor (Irf) 4 participates in the regulation of alternative macrophage priming. *Immunobiology* (2010) 215(9–10):821–5. doi: 10.1016/j.imbio.2010.05.031

112. Oishi S, Takano R, Tamura S, Tani S, Iwaizumi M, Hamaya Y, et al. M2 polarization of murine peritoneal macrophages induces regulatory cytokine production and suppresses T-cell proliferation. *Immunology* (2016) 149(3):320–8. doi: 10.1111/imm.12647

113. Al Mamun A, Chauhan A, Qi S, Ngwa C, Xu Y, Sharmeen R, et al. Microglial IRF5-IRF4 regulatory axis regulates neuroinflammation after cerebral ischemia and impacts stroke outcomes. *Proc Natl Acad Sci U.S.A.* (2020) 117(3):1742–52. doi: 10.1073/pnas.1914742117

114. Liang H, Liu B, Gao Y, Nie J, Feng S, Yu W, et al. Jmjd3/IRF4 axis aggravates myeloid fibroblast activation and M2 macrophage to myofibroblast transition in renal fibrosis. *Front Immunol* (2022) 13:978262. doi: 10.3389/fimmu.2022.978262

115. Liang X, Luo M, Shao B, Yang JY, Tong A, Wang RB, et al. Phosphatidylserine released from apoptotic cells in tumor induces M2-like macrophage polarization through the PSR-STAT3-JMJD3 axis. *Cancer Commun* (2022) 42(3):205–22. doi: 10.1002/cac2.12272

116. Xing Y, Ruan G, Ni H, Qin H, Chen S, Gu X, et al. Tumor immune microenvironment and its related miRNAs in tumor progression. *Front Immunol* (2021) 12:624725. doi: 10.3389/fimmu.2021.624725

117. Hu A, Chen X, Bi Q, Xiang Y, Jin R, Ai H, et al. A parallel and cascade control system: magnetofection of miR125b for synergistic tumor-association macrophage polarization regulation and tumor cell suppression in breast cancer treatment. *Nanoscale* (2020) 12(44):22615–27. doi: 10.1039/d0nr06060g

118. Gardner A, Ruffell B. Dendritic cells and cancer immunity. *Trends Immunol* (2016) 37(12):855–65. doi: 10.1016/j.it.2016.09.006

119. Laoui D, Keirsse J, Morias Y, Van Overmeire E, Geeraerts X, Elkrim Y, et al. The tumour microenvironment harbours ontogenically distinct dendritic cell populations with opposing effects on tumour immunity. *Nat Commun* (2016) 7:13720. doi: 10.1038/ncomms13720

120. Conrad C, Gregorio J, Wang YH, Ito T, Meller S, Hanabuchi S, et al. Plasmacytoid dendritic cells promote immunosuppression in ovarian cancer *via* ICOS costimulation of Foxp3(+) T-regulatory cells. *Cancer Res* (2012) 72(20):5240–9. doi: 10.1158/0008-5472.CAN-12-2271

121. Caro AA, Deschoemaeker S, Allonsius L, Coosemans A, Laoui D. Dendritic cell vaccines: A promising approach in the fight against ovarian cancer. *Cancers* (2022) 14 (16):4037. doi: 10.3390/cancers14164037

122. Sichien D, Scott CL, Martens L, Vanderkerken M, Van Gassen S, Plantinga M, et al. IRF8 transcription factor controls survival and function of terminally differentiated conventional and plasmacytoid dendritic cells, respectively. *Immunity* (2016) 45(3):626–40. doi: 10.1016/j.immuni.2016.08.013

123. Lee J, Zhang J, Chung YJ, Kim JH, Kook CM, González-Navajas JM, et al. Inhibition of IRF4 in dendritic cells by PRR-independent and -dependent signals inhibit Th2 and promote Th17 responses. *Elife* (2020) 9:e49416. doi: 10.7554/eLife.49416

124. Briseño CG, Haldar M, Kretzer NM, Wu X, Theisen DJ, Kc W, et al. Distinct transcriptional programs control cross-priming in classical and monocyte-derived dendritic cells. *Cell Rep* (2016) 15(11):2462–74. doi: 10.1016/j.celrep.2016.05.025

125. Kuhn S, Yang J, Ronchese F. Monocyte-derived dendritic cells are essential for CD8(+) T cell activation and antitumor responses after local immunotherapy. *Front Immunol* (2015) 6:584. doi: 10.3389/fimmu.2015.00584

126. Bruger AM, Dorhoi A, Esendagli G, Barczyk-Kahlert K, van der Bruggen P, Lipoldova M, et al. How to measure the immunosuppressive activity of MDSC: Assays, problems and potential solutions. *Cancer Immunol Immunother* (2019) 68(4):631–44. doi: 10.1007/s00262-018-2170-8

127. Sanaei MJ, Salimzadeh L, Bagheri N. Crosstalk between myeloid-derived suppressor cells and the immune system in prostate cancer: MDSCs and immune system in prostate cancer. *J Leukoc Biol* (2020) 107(1):43–56. doi: 10.1002/JLB.4RU0819-150RR

128. Cumbo C, Tarantini F, Anelli L, Zagaria A, Redavid I, Minervini CF, et al. IRF4 expression is low in Philadelphia negative myeloproliferative neoplasms and is associated with a worse prognosis. *Exp Hematol Oncol* (2021) 10(1):58. doi: 10.1186/s40164-021-00253-y

129. Metzger P, Kirchleitner SV, Boehmer DFR, Hörth C, Eisele A, Ormanns S, et al. Systemic but not MDSC-specific IRF4 deficiency promotes an immunosuppressed tumor microenvironment in a murine pancreatic cancer model. *Cancer Immunol Immunother* (2020) 69(10):2101–12. doi: 10.1007/s00262-020-02605-9

130. Wei J, Long L, Zheng W, Dhungana Y, Lim SA, Guy C, et al. Targeting REGNASE-1 programs long-lived effector T cells for cancer therapy. *Nature* (2019) 576 (7787):471–6. doi: 10.1038/s41586-019-1821-z

131. Zheng W, Wei J, Zebley CC, Jones LL, Dhungana Y, Wang YD, et al. Regnase-1 suppresses TCF-1+ precursor exhausted T-cell formation to limit CAR-t-cell responses against ALL. *Blood* (2021) 138(2):122–35. doi: 10.1182/blood.2020009309

132. Behrens G, Edelmann SL, Raj T, Kronbeck N, Monecke T, Davydova E, et al. Disrupting roquin-1 interaction with regnase-1 induces autoimmunity and enhances antitumor responses. *Nat Immunol* (2021) 22(12):1563–76. doi: 10.1038/s41590-021-01064-3

frontiers | Frontiers in Immunology

TYPE Review
PUBLISHED 24 March 2023
DOI 10.3389/fimmu.2023.1110522

OPEN ACCESS

EDITED BY
Jayakumar Nair,
National Institutes of Health (NIH),
United States

REVIEWED BY
Toshana Foster,
University of Nottingham, United Kingdom
Peter James Mullen,
University of Southern California,
United States

*CORRESPONDENCE
Aleksandra A. Pandyra
aleksandra.pandyra@uni-duesseldorf.de

SPECIALTY SECTION
This article was submitted to Cancer Immunity and Immunotherapy, a section of the journal Frontiers in Immunology

RECEIVED 28 November 2022
ACCEPTED 13 March 2023
PUBLISHED 24 March 2023

CITATION
Stachura P, Stencel O, Lu Z, Borkhardt A and Pandyra AA (2023) Arenaviruses: Old viruses present new solutions for cancer therapy.
Front. Immunol. 14:1110522.
doi: 10.3389/fimmu.2023.1110522

Arenaviruses: Old viruses present new solutions for cancer therapy

Paweł Stachura[1,2], Olivia Stencel[1], Zhe Lu[1], Arndt Borkhardt[1] and Aleksandra A. Pandyra[1*]

[1]Department of Pediatric Oncology, Hematology and Clinical Immunology, Medical Faculty, Heinrich-Heine-University, Düsseldorf, Germany, [2]Department of Molecular Medicine II, Medical Faculty, Heinrich Heine University, Düsseldorf, Germany

Viral-based cancer therapies have tremendous potential, especially in the context of treating poorly infiltrated cold tumors. However, in tumors with intact anti-viral interferon (IFN) pathways, while some oncolytic viruses induce strong innate and adaptive immune responses, they are neutralized before exerting their therapeutic effect. Arenaviruses, particularly the lymphocytic choriomeningitis virus (LCMV) is a noncytopathic virus with preferential cancer tropism and evolutionary mechanisms to escape the immune system for longer and to block early clearance. These escape mechanisms include inhibition of the MAVS dependent IFN pathway and spike protein antigen masking. Regarding its potential for cancer treatment, LCMV is therefore able to elicit long-term responses within the tumor microenvironment (TME), boost anti-tumor immune responses and polarize poorly infiltrating tumors towards a hot phenotype. Other arenaviruses including the attenuated Junin virus vaccine also have anti-tumor effects. Furthermore, the LCMV and Pichinde arenaviruses are currently being used to create vector-based vaccines with attenuated but replicating virus. This review focuses on highlighting the potential of arenaviruses as anti-cancer therapies. This includes providing a molecular understanding of its tropism as well as highlighting past and present preclinical and clinical applications of noncytophatic arenavirus therapies and their potential in bridging the gap in the treatment of cancers weakly responsive or unresponsive to oncolytic viruses. In summary, arenaviruses represent promising new therapies to broaden the arsenal of anti-tumor therapies for generating an immunogenic tumor microenvironment

KEYWORDS

virotherapy, arenaviruses, LCMV (lymphocytic choriomeningitis virus), immunomodualtors, cold tumors, noncytopathic virus

Introduction

Recognition of the importance of the immune system in tumor surveillance has revolutionized the therapeutic landscape with the advent of immunotherapies such as checkpoint inhibitors (CI) (1). Despite some breakthroughs, tumor immune evasion provides obstacles to effective CI and/or other immunotherapeutic treatments focused

on T cells and based on enhancing adaptive immune responses. These obstacles are commonly driven by an unfavourable tumor microenvironment (TME) milieu. Specifically, exhausted/dysfunctional T cells, an abundance of immunosuppressive tumor-associated macrophages (TAMs), monocytes and regulatory T cells (Treg's), ineffective innate immune responses, poor immune cell infiltration and downregulated antigen presenting machinery within the TME contribute not only to CI unresponsiveness/resistance but generally immune evasion (2). Therefore, to elicit responsiveness to immunotherapies, the conversion of poorly inflamed cold tumors into hot tumors is therapeutically attractive and an area of active research (3). Strategies to induce this cold to hot conversion within the TME are numerous and can include innate immune activation (4), increasing MHC-I expression in tumor cells (3) and the use of viruses as anti-cancer agents (5).

The use of viruses as anti-cancer agents has been particularly relevant in recent decades as viruses are ideal vectors for gene therapy approaches and have been successfully applied in virus-based therapeutic vaccines as well as cell-based vaccines (6). Virus-based anti-tumor vaccines involve a combination of tumor-specific antigens, co-stimulatory proteins and immunomodulating molecules which boost the immune system to elicit anti-tumor responses (6). Examples in clinical development include the TG4001 modified vaccinia virus Ankara (MVA) vaccine encoding the HPV16 antigens and the interleukin 2 (IL-2) gene (7). Virus engineered cell based vaccines are centred on more personalized approaches and modify a patient's immune cells *ex vivo* using viral vectors. Notable examples include the recently approved YESCARTA and KYMRIAH both of which target a patient's T cells with a retrovirally inserted anti-CD19 Chimeric Antigen Receptor (CAR) for the treatment of non-Hodgkin lymphomas and acute lymphoblastic leukemia, respectively (8, 9). There are currently over three hundred clinical trials testing the efficacy of CAR-T cell therapy (6). The use of oncolytic viruses that preferentially replicate within the TME causing subsequent tumor cell lysis (10) and anti-tumoral activation of the adaptive immune system is another promising approach. Rigvir, the first approved oncolytic virus (in Latvia since 2014), is a genetically unmodified enteric cytopathic human orphan virus type 7 (ECHO-7) strain selected for melanoma (11). Another virus, Oncorine, is a modified adenovirus, approved in China for head and neck cancer (12) while Talimogene laherparepvec (T-Vec) is an HSV-1 based oncolytic virus that is currently in FDA approved for the treatment of recurrent melanoma (13). Over a hundred more are currently in the late and early stages of clinical testing. One challenge pertaining to oncolytic virus-based therapies is the induction of strong innate and adaptive anti-viral immune responses, especially the induction of type I interferons (IFN-I), which leads to clearing the virus before reaching its full therapeutic effect. In addition, patients previously vaccinated against and/or infected with related viruses have pre-existing T and B cell immunity including neutralizing antibodies which also results in fast virus clearance (14, 15). In stark contrast, the lymphocytic choriomeningitis virus (LCMV) is a non-oncolytic arenavirus currently in pre-clinical and clinical development, either as an anti-cancer agent or tumor vaccine vector, respectively. Infection with LCMV does not kill host cells by direct lysis and results in strong innate and adaptive immune responses also within the TME to eradicate the tumor. Compared to most oncolytic viruses, LCMV's replication is not curbed by IFN-I (16), and its late induction of neutralizing antibodies allows for a more persistent intra-tumoral virus load to maximize effects on the TME (17). Taken together, viruses such as oncolytic viruses and certain arenaviruses represent a rich resource of potential novel anti-cancer therapeutics and this review aims to summarize the recent application of arenaviruses in cancer therapy and the potential gaps to be filled where other therapies are ineffective.

The biology of arenaviruses

The *Arenaviridae* family consists of three genera, *Mammaarenavirus, Reptarenavirus* and *Hartmanivirus*, the first of which infects mammalian hosts. The *Mammaarenavirus* genus consists of 41 distinct viral species capable of infecting mammalian hosts and is geographically, genetically and epidemiologically sub-divided into Old and New World groups (18). Notable representatives of Old Word arenaviruses that will be mentioned in the current review include the LCMV strains, which were the first arenaviruses to be described in the 1930's. Examples of New World arenaviruses which, in contrast can cause severe Haemorrhagic fevers include for example the Junin virus (JUNV) (causing Argentine Haemorrhagic Fever, AHF) and the Tacaribe virus (19).

The genome of arenaviruses is bi-segmented and composed of two single-stranded negative sense RNAs. The arenavirus lifecycle detailed in Figure 1 is limited to the hosts' cytoplasm and viral entry can be clathrin-dependent. Viral entry is mediated by the surface receptor α-dystroglycan (αDG) and CD164 for LCMV as well as Lassa virus (LASV) (20), and the human transferrin receptor 1 (Tfr1) for the JUNV and Tacaribe viruses (21). The wide spectrum of pathogenicity among the arenaviruses has been attributed to several factors. Arenaviruses use different receptors including αDG, human transferrin receptor 1, the transmembrane protein neuropilin 2 (NRP2) (22) and possibly additional proteins for viral entry. Differences in receptor distribution determine cell tropism. LCMV, for instance, which uses the ubiquitously expressed αDG for viral entry, can infect many cell types. However, it has been recently suggested that some arenaviruses including LCMV and LASV may use a combination of receptors or host factors including heparan sulfate proteoglycans or CD164 for viral entry (23–27). Differences in binding affinity of LCMV strains to αDG were previously proven to correlate with virus persistence and disease outcome. The Armstrong, E350 and WE2.2 strains with low affinity to αDG preferentially infect cells within the red pulp of the spleen and were not detectable in mice 7, 14 or 30 days post infection (28). In contrast, the Clone 13, Traub, and the WE54 strains with high affinity to αDG replicate in the white pulp of the spleen and are able to persist in mice, leading to chronic infection (28, 29). Bonhomme et al., through deletion of multiple GP1 and GP2 glycosylation sites that occur in different LCMV strains, were able to demonstrate that posttranslational modification differences of these proteins play an important role in virus fitness and ability to

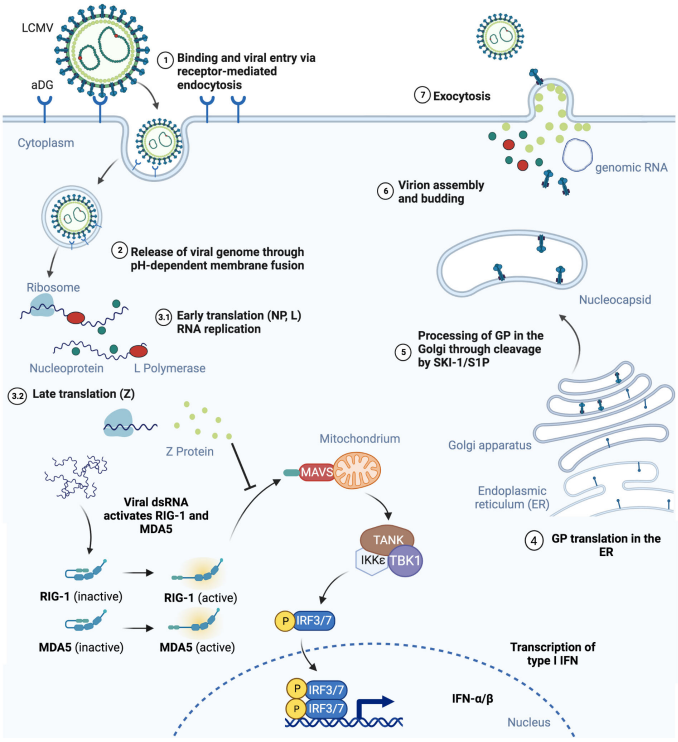

FIGURE 1
Schematic representation of mammalian cell infection by LCMV is shown. (1) LCMV endocytosis is αDG-mediated and (2) leads to the release of viral genome in the cell cytoplasm. (3) NP, L and Z proteins are produced. Virus RNA activates RIG-1 and MDA5, however binding to MAVS and its activation is blocked by Z protein, therefore inhibiting the INF pathway. (4) GP precursor translation takes place in the endoplasmic reticulum and (5) maturates in Golgi by SKI-1/S1P mediated cleavage. (6) NP, L and Z proteins together with viral RNA assembly into virions with GP on the surface and (7) bud out of the infected cell. Figure was created with BioRender.com.

infect epithelial cells, macrophages or primary neurons (30). In addition to this differential use of binding receptors between arenaviruses, effects incurred by virus binding can also elicit additional changes. LCMV binding to αDG for example can lead to membrane destabilization and receptor downregulation, which can influence the future course of viral infection (23, 31). Furthermore, differences in cellular requirements enabling endosomal trafficking dependent or not on cholesterol, clathrin or caveolin (32–34) and immune evasion mechanisms also determine the pathogenicity during the course of arenaviral infection.

The innate and adaptive immune responses triggered by arenaviruses are critical for eventual viral clearance and these include IFN-I induction and the mounting of effective effector $CD8^+$ T cell responses. Arenaviruses have developed several evolutionary mechanisms of evading immune detection. Binding to the retinoic acid-inducible gene I (RIG-I) and melanoma differentiation-associated gene 5 (MDA5) by the Z protein of New World arenaviruses prevents its association with mitochondrial antiviral signalling protein (MAVS) and blocks type I interferon beta (IFN-β) production (35). The NP protein in many arenaviruses including LCMV inhibits interferon regulatory factor 3 (IRF3) activation. Decreased IFN-β production has also been shown to occur through decreased PKR signalling (36–38). Eschli et al. demonstrated that the LCMV WE strain is only able to engage B cells with high viral loads due to a low frequency of GP1 specificity and sensitive epitope masking by glycosylation of the virus spike protein, which leads to weak antibody binding and, therefore, escape from early neutralisation (39). Taken together, considerable insights into the genetics, structure and life-cycle of arenaviruses has enabled their application into diverse research areas from investigating T cell dependent anti-viral immunity to their development as anti-tumor agents.

Arenaviruses as anti-tumor agents

Experimental, pre-clinical and clinical development of LCMV

For decades, LCMV has been the prototypic experimental arenavirus of choice for immunologists. Not only does infection with LCMV result in robust $CD8^+$ effector T cell responses but also in long-term immunity. Indeed, its wide experimental use has led to monumental discoveries such as MHC restriction and PD-1's role during T cell exhaustion (40). Checkpoint inhibition of the PD1-PD-L1 axis using monoclonal antibodies (mAb) such as the approved Nivolumab and Pembrolizumab has revolutionized the treatment landscape and ushered a new era of cancer immunotherapy (41, 42). Furthermore, by expressing LCMV-specific epitopes on tumor cells, it has been possible to study

various aspects of $CD8^+$ T cell mediated anti-tumor immunity (43, 44). In addition to being a useful biological tool, LCMV strains, through their immune-activating effects, have direct anti-tumoral effects (17).

The observation that LCMV influences tumor growth dates back to sixty years ago when Nadel and Haas tested the efficacy of different strains of LCMV against the L1210 leukemia model in guinea pigs and mice (45) (Figure 2). Guinea pigs subcutaneously administered LCMV as late as seven days post tumor inoculation survived longer than their uninfected counterparts although this was not recapitulated in mice who succumbed to these particular LCMV strains. Fifteen years later, another group treated mice with LCMV and found that it potentiated the chemotherapeutic effects of 5-Fluoruracil (5-FU) (46). These observations with LCMV and similar studies with the MP virus (47), which is antigenically, morphologically and serologically considered to be a strain of LCMV (48), led to the treatment of cancer patients with the MP virus in the 1970s. Three patients with far-advanced lymphoma were intravenously treated with a single dose of the MP virus. All patients had underlying complications and were already pre-treated with several rounds of chemotherapy. One of the patients died from underlying pulmonary bacterial infections, another from pulmonary failure and a third one from disease progression (49). It is difficult to ascertain potential efficacy in such a small cohort of patients with very advanced disease. However, there was another larger clinical trial composed of 18 patients with more diverse though still advanced and pre-treated metastatic malignancies where the MP virus was administered *via* the intravenous route (50). None of the patients experienced any virus-induced encephalitis and three patients were not successfully infected. Out of the remaining 15 patients, 6 patients experienced a beneficial clinical response and/or presented evidence of tumor burden decrease. Meanwhile, with the advent of sophisticated genetic approaches and an increased understanding of the molecular, biological and immunological basis of viruses, the ability to better apply arenaviruses as anti-cancer agents has increased.

Recently, it was shown that intravenous or peritumoral injection of the LCMV WE strain in several syngeneic or spontaneous murine and human xenograft models of cancer, including subcutaneous, endogenous hepatocellular carcinoma and spontaneous MT/*ret* melanoma led to regression or complete elimination of early-stage pre-established tumors (17). Kalkavan et al. also demonstrated that LCMV preferentially replicates in tumor cells and metastatic sites leading to robust immune infiltration with some accompanying replication in the liver. LCMV replication within the tumor persisted for at least thirty days post-tumor inoculation and tumor regression was dependent on IFN-I production by tumor-infiltrating monocytes. Importantly, IFN-I did not blunt LCMV replication within the tumor, allowing for sustained innate immune activation and clearance of LCMV from other organs. The preferential tumoral LCMV replication led to tumor regression through several proposed and interconnected enhanced innate and adaptive anti-tumor responses within the TME including local IFN-I production through the engagement of pattern recognition receptors, direct IFN-I anti-tumoral effects, reduced angiogenesis, recruitment of monocytes and cytotoxic $CD8^+$ T cells to the TME and enhanced MHC I antigen presentation (17) (Figure 3). LCMV WE was also demonstrated to be superior to oncolytic viruses, a chimeric variant of vesicular stomatitis virus (VSV-GP) and a recombinant TK-depleted vaccinia virus (rVACV). Furthermore, LCMV WE was suggested in this and another study to have a strong anti-tumoral effect, especially when combined with checkpoint inhibition (51). As many of the cancer cell lines tested in *in vivo* tumor models by Kalkavan et al. are responsive to the anti-tumoral effects of IFN-I and express elevated levels of interferon receptors, preferential replication of LCMV within the tumor cannot be attributed to defects in interferon signalling but rather to expression differences in host factors crucial for viral replication between normal and cancer cells (52). This is an important point as oncolytic viruses are generally sensitive to IFN-I and their efficient replication is usually dependent on tumors harboring defects in interferon signalling (53). Therefore, patients whose tumors are characterized by intact IFN-I signalling are less likely to respond to oncolytic viral therapy leaving a gap that could be filled with LCMV.

Other studies utilized the acute LCMV Armstrong (LCMV Arm) strain to activate the immune system (54–56). For example, the infection of melanoma tumor bearing mice with LCMV Arm significantly slowed tumor growth and also decreased tumor angiogenesis. The anti-tumoral effects were shown to be dependent on LCMV-Arm-induced upregulation of angiogenesis inhibitor thrombospondin-1 (TSP-1) in $CD4^+$ and $CD8^+$ T cells (54). In another study, mice with advanced melanoma experienced restored tumor MHC-I expression following LCMV WE treatment leading to enhanced anti-tumor $CD8^+$ T cell responses and tumor regression (57). The LCMV WE strain was also used to demonstrate the importance of NK cells and certain chemokines for an effective

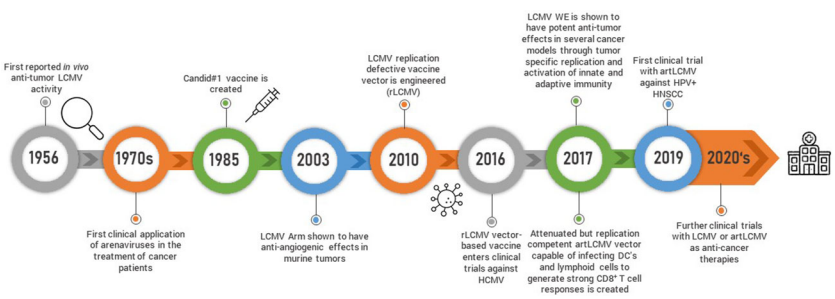

FIGURE 2
Schematic timeline representing arenavirus-based discoveries and research development is shown.

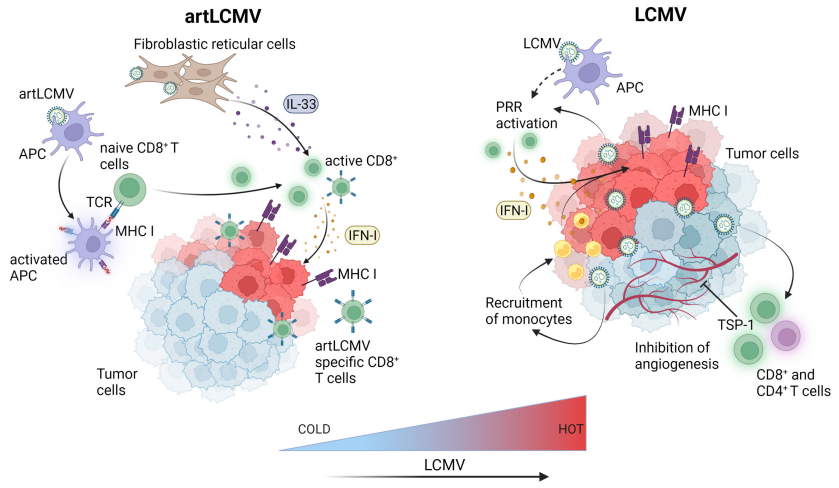

FIGURE 3
LCMV-based immunotherapies induce innate and adaptive immune responses within the tumor microenvironment. Attenuated but replicating artLCMV infects and activates APCs and delivers engineered tumor antigens for direct presentation to specific $CD8^+$ T cells thereby inducing adaptive immune responses. Fibroblastic reticular cell infection by artLCMV leads to IL-33 secretion, activating the alarmin pathway in $CD8^+$ T cells. LCMV directly replicates in tumor cells and APCs leading to pattern recognition receptors (PRR) activation and production of IFN-I in the TME. This leads to monocyte and cytotoxic $CD8^+$ T cell recruitment, increased antigen presentation and MHC-I upregulation on tumor cells. LCMV also induces angiogenesis inhibiting TSP-1 surface expression on $CD4^+$ and $CD8^+$ T cells. Figure was created with BioRender.com.

anti-tumoral response (58). Taken together, LCMV has been shown to efficiently re-direct the innate and adaptive immune system to target tumors. In murine tumor models, LCMV was demonstrated to be safe and effective through a variety of non-immunogenic and immunogenic tumor models. Current work is focused on increasing LCMV's tumor tropism to translate its strong potential as anti-cancer agent into an effective tumor treatment. Targeted evolution is used to increase LCMV's infectivity to tumor cells by retaining or decreasing its uptake into healthy cells and, therefore, healthy organs. This is achieved by a specific selection of tumor-prone virus mutations using the so-called Fast Evolution Platform. The overall aim is to maximize the inflammatory signals within the tumor tissue and thereby activate several anti-tumoral immune effector mechanisms. This approach is presently being developed by Abalos Therapeutics (59) (Table 1).

Genetically modified LCMV and other arenavirus vaccines

While the use of unmodified LCMV has been shown to be effective in controlling tumors, genetically modified LCMV used either as a vaccine or vector delivering tumor antigens is another promising approach. Flatz et al. engineered an LCMV based replication defective vaccine vector by successfully replacing the GP open reading frame portion of LCMV with vaccine antigens (rLCMV) (60). Insertion of up to 2.6 kilobases of foreign genetic material was possible and the vaccine was tested with several different cytotoxic T lymphocyte (CTL) epitopes including OVA (rLCMV-OVA) and GP33 (LCMV-GP33) to establish proof-of-principle efficacy and immunogenicity in several disease models. Robust and antigen specific $CD8^+$ T cells responses occurred when mice were vaccinated with rLCMV-OVA, and this was mediated through direct targeting and activation of dendritic cells (DCs) which are critical antigen presenting cells necessary for $CD8^+$ T cell activation. Mice inoculated with B16.F10 melanoma cells expressing the $CD8^+$ T cell epitope GP33 and treated with rLCMV-GP33 eight days post-inoculation survived longer than mice treated with adenovirus 5 GP33 (rAd-GP33) or vaccinia virus GP33 (VACC-GP33) vaccines. Importantly, unlike other viral-based vaccines including the adenovirus 5 against which rLCMV was directly compared, rLCMV failed to induce vector antibody immunity in mice and non-human primates (61) enabling repeated boosters. The rLCMV vaccine vector is being translated into the clinic and its

TABLE 1 Summary of current arenavirus-based clinical trials.

Virus	Targeted tumor	Current clinical stage	Study moderator
MVA	HPV16-positive	Phase II	Transgene
LCMV	Solid tumors	Pre-clinical	Abalos Therapeutics
rLCMV with rPICV	HPV16-positive HNSCC	Phase II	Hookipa Pharma
rLCMV with rPICV	Prostate	Phase I	Hookipa Pharma

incorporation into a vaccine against Cytomegalovirus (HB-101 Vaxwave®) has reached Phase II clinical testing.

Although the rLCMV-GP33 vaccine was shown to increase survival in tumor-bearing mice, it was reasoned that the ability to replicate and deliver anti-tumor signals to cells other than just DCs might prove even more efficacious against tumors. This led to the development of a replication competent but attenuated LCMV vector (artLCMV) capable of infecting not only DCs but also lymphoid stromal cells (62) (Figure 3). Unlike rLCMV, artLCMV, through spread and infection to lymphoid stromal cells, induced the IL-33 alarmin pathway which has been shown to be critical for effective anti-viral and other immune responses (63). The combined effect of generating strong $CD8^+$ T cell responses using a transplantable OVA-expressing tumor model, IL-33 alarmin signalling and IFN-I production (for 48 hrs) led to more potent and specific anti-tumor immunity and subsequent tumor control superior to that of the replication deficient rLCMV without neutralizing antibody production (62). However, responses were still hampered by self-tolerance and strong responses against vectorized non-self antigens at the expense of tumor specific ones. To overcome this competition between tumor and vector specific cytotoxic effector T lymphocytes (CTLs) Bonilla et al. designed a 2-vector therapy system based on two distantly related arenaviruses (LCMV and Pichinde virus (PICV)). This strategy was able to reshuffle immunodominance in favor of tumor specific CTLs, which led to more effective tumor control and protection against tumor rechallenge (64). Attenuated replicating vector arenaviruses (TheraT® platform) are in the clinical stages of commercial development for the treatment of prostate cancer (HB-301 TheraT®), HPV+ Head/Neck Cancer (single LCMV based HB-201 or in combination with PICV based HB-202 TheraT®) (Table 1). Much like the acute LCMV strains, the artLCMV platform stimulates innate immune responses and is also dependent on replication in antigen-presenting (APCs) cells to elicit its anti-tumor effects. The Phase I/II clinical trial (NCT NCT04180215) is an open-label study commenced in 2019 evaluating HB-201 and HB-201 and HB-202 as single or two-vector therapy in previously treated patients with advanced or metastatic HPV 16+ cancers, mainly head and neck. Recently, preliminary data from the trial reported the presence of E6/E7 specific $CD8^+$ T cell levels in the blood and a high infiltration of $CD8^+$ T cells in over 50% of patient tumor samples (65). One main disadvantage of this approach, however, is that this arenavirus platform currently only delivers the HPV16 epitope in the case of head and neck cancer, or targets the most common prostate cancer markers PAP, PSA, PSMA but cannot be used for other types of tumours unless novel antigens are specifically integrated.

Safety and dosing of LCMV and arenavirus-based vector vaccines

Although the numbers of LCMV infected people are not known as only the most severe infected cases are reported, serological studies indicate that around 5% of the American (66), 1.7% of the Spanish, 2.9% of the Dutch and 0.3% of the French populations (67) have LCMV specific antibodies, indicating previous exposure to the virus. While some arenaviruses cause fatal hemorrhagic fevers, symptoms caused by LCMV infections are comparatively mild and include influenza-like symptoms as well as dysesthesia (23). This initial phase of disease symptoms when occurring may be followed by a symptom-free period of a few days up to 3 weeks, before the beginning of a second phase. The latter is characterized by fever, headache, nausea and meningeal irritation and is usually followed by complete recovery. This has been corroborated by well-documented cases of infected laboratory workers (68–70). Although LCMV does not pose a serious health risk in the general population, infection during organ transplantation and pregnancy can be detrimental. In one published case, three organ recipients receiving kidneys and liver of a donor developed virus infection symptoms including fever and encephalopathy soon after transplantation leading to death within 36 days. Analysis of the viral protein sequences revealed 14 fragments consistent with arenaviruses most closely related to LCMV (71). In another case, all organ recipients developed illnesses symptomatic of virus infection and a liver recipient died 2-3 weeks post donation. LCMV was later found in the aortic tissue of the donor and the infection was confirmed in the recipients thirty-seven days after transplantation (72, 73). The source for the donor infection was later identified to be pet animals such as a hamster, corroborating reports that direct human to human transmission does not occur (74). All of these severe effects of an unrecognized LCMV infection may be attributed to the concurrent treatment of the transplantation patients with immune suppressive drugs thereby not enabling an efficient anti-viral immune response at the time of infection. Detrimental effects of LCMV can also be observed during congenital infection which can severely affect the survival and well-being of the children affected. The most common symptoms of congenital LCMV infection are chorioretinitis, hydrocephalus and ventriculomegaly (75).

Since in clinical LCMV applications, an intravenous (IV) route of administration is preferred, off-target replication in organs other than the intended tumor or lymphoid organs (in the case of LCMV-based vector vaccines) should be considered. Preclinically, subcutaneous injection of LCMV WE resulted in detectable virus in the skin and spleen 8 days post infection in mice (17). Even after intravenous infection of mice, although dose dependent increases of liver enzymes were measured, changes were in all cases transient and enzyme levels returned to background levels ten to fifteen days after infection (76). In the context of replication competent arenavirus vaccine vectors, detection of the vector was apparent in the spleen and liver of mice but was rapidly cleared without induction of organ damage (62). However, in certain mouse strains including the virus-sensitive FVB or NZ, infection with LCMV Clone13 but not with other variants, like Arm, does result in severe illness including thrombocytopenia and hepatocellular necrosis (77). Such severe disease symptoms can be avoided not only by choosing the right LCMV strain, but also by virus attenuation for example by reassorting the genome segments of two different LCMV strains (77). Therefore, virus strains for clinical development will have to be carefully chosen to avoid any potential for more severe disease effects and carefully evaluated in

respective animal studies. Taken together, preclinical *in vivo* studies suggest that for certain wildtype or recombinant LCMV strains while replication in off-target organs such as the liver and spleen occurs, the virus is rapidly cleared and does not persist long enough to induce adverse organ damage.

Clinically, the safety of administering therapeutic LCMV to potentially immune-suppressed and conceivably heavily pre-treated cancer patients needs to be carefully evaluated (49, 78). Previously, the administration of the MP LCMV strain to immunosuppressed cohorts with metastatic disease in the two clinical trials performed in the 1970s was generally well-tolerated and did not result in serious viraemia related side-effects (50). However, in the 1971 study after a single intravenous injection of the three advanced lymphoma patients, viral titers were detectible post-mortem in multiple organs in all the patients (49). Nevertheless, few virus-related adverse effects on normal tissues were observed pointing to a potentially favourable safety profile (50) which may even be further enhanced by the identification of tumor-tropic replication-competent strains. The above mentioned Phase I/II study is slated for completion in 2025, but initial reports of safety, tolerability, and immunogenicity are encouraging although so far 2 patients experienced dose-limiting toxicity involving Grade 4 hepatitis or Grade 4 encephalopathy (79, 80). A recent update presented at ASCO 2022, revealed plans to investigate a combination of HB-201 with pembrolizumab (81) in the Phase II portion of the trial.

Preclinically, LCMV and arenavirus vectors are able to elicit immune responses through several routes of administration including intravenous, intradermal and subcutaneous (ranging from 10^2-10^6 PFU per animal), with one dose often being sufficient to elicit effective anti-tumor immune responses in mice, albeit when evaluating tumor rechallenge and booster regimens, more doses may be required. Clinically, in the case of arenavirus vectors, both intravenous and intratumoral routes of administration have been applied, although the IV route enables secondary lymphoid organs to be reached. As LCMV and vector-LCMV neutralizing antibody production currently appears not a hindrance, repeated dosing where clinically necessary should be possible, although the potential for neutralizing anti-viral immune responses will have to be carefully explored during ongoing and coming clinical evaluation of LCMV cancer therapy.

Live-attenuated Junin vaccine (Candid#1) and other arenaviruses

Before the development of the Candid#1 vaccine, infection with the hemorrhagic fever (HR) causing Junin virus resulted in the highest levels of mortality (15-30%) of any other HR causing arenavirus (23). The Candid#1 is a live attenuated vaccine and was generated through serial passaging of the Junin virus in guinea pigs followed by suckling mice and finally in tissue culture. Although its commercial distribution is limited due to the relatively small affected Argentinian population, it has been an effective vaccine in protecting against Junin virus infection. Recent hints into the molecular mechanism of Candid#1 attenuation point to a single residue change F427I in the G2 transmembrane domain of the GP leading to decreased virulency (82). At the same time, this may limit its more wide-spread use as a vaccine due to the potential of back mutation, and therefore, other approaches to develop vaccines targeting arenaviruses inducing hemorrhagic fevers are currently exploited including the addition of more attenuating mutations (e.g., for Junin) (83) or genome reassorting from hemorrhagic and non-hemorrhagic arenavirus strains (e.g., Lassa and Mopeia) (84, 85).

Kalkavan et al., in addition to uncovering the already mentioned anti-tumoral effects of LCMV strain WE, found that, following injection, the Candid#1 vaccine also replicated within tumors and decreased xenograft tumor growth of human cancer cell lines in NOD.SCID mice (17). However, the *in vivo* anti-tumoral effects of Candid#1 occurred following direct intratumoral injections and it is currently unclear whether the attenuated virus would preferentially replicate in the tumor if applied by a more clinically relevant application route. An *in vitro* study found that Candid#1 was cytopathic and induced apoptosis in several human cancer cell lines in an interferon independent manner, linking the mechanism to RIG-I with higher viral replication in RIG-I deficient cell lines or after knocking it down (86). Apoptotic effects on normal cell lines however, were not tested and the study was limited in the number of cell lines used. Despite the preliminary nature of the above studies, they are nevertheless promising. The Candid#1 vaccine has already been successfully and safely used in humans, and next generation approaches are currently underway. Although approval from the Food and Drug Administration (FDA) in the US is still pending, it has been produced and used on a larger scale by the Argentinian government. As the attenuated phenotype of the Candid#1 vaccine appears to be based on the single substitution at residue 427 (F427I), the FDA's primary concern with the vaccine has been a potential reversion to its previously virulent phenotype. Indeed, serial passaging of the Candid#1 virus in cell culture can lead to reversion (87) and approaches in generating second-generation Candid#1 vaccines are focusing on inserting additional mutations into the virus' GPC in order to create a barrier to reversion (83, 87). It is also worth mentioning that the Tacaribe virus, which is another New World arenavirus closely related to the Junin virus, was found not to be virulent (88). Wolf et al. discovered that infection of cancer cell lines and primary macrophages with the Tacaribe virus causes caspase-dependent apoptosis (89). Although the apoptosis was shown to depend on active viral replication, it was not further mechanistically investigated. It would be interesting to extend this finding in an *in vivo* setting and explore whether the Tacaribe virus would preferentially replicate within tumors and also have anti-tumor effects.

Another interesting approach was presented in a study by Muik et al. that used an oncolytic VSV virus with an exchanged surface glycoprotein of LCMV origin (VSV-GP) as an anti-tumor agent. Oncolytic viruses are usually rapidly neutralised, whereas VSV-GP appears to avoid neutralizing humoral responses by failing to induce nAb against the LCMV spike protein (90). Other efforts focused on exchanging the VSV glycoprotein with another New World arenavirus, Lassa (VSV-Lassa-GPC). VSV-GP and VSV-Lassa-GPC have shown pre-clinical efficacy in tumor models (91), and VSV-GP is currently evaluated in a Phase I study alone or in combination with checkpoint therapy (92).

Concluding remarks and future perspectives

Arenaviruses, particularly the well-studied LCMV viruses, have a strong potential to make an impact in cancer therapy. The efficacy of LCMV, whether unmodified strains, recombinant strains with increased tumor cell tropism, or incorporated into a viral attenuated vaccine, in controlling tumors in a broad range of pre-clinical murine models of cancer has been demonstrated. As already shown by the multifaceted use of oncolytic viruses in cancer therapy, there appears a substantial potential for live replicating arenaviruses in the treatment of tumors. Unlike oncolytic viruses, LCMV preferentially replicates in a wide range of tumors and can robustly continue to do so even in tumors where interferon signalling is intact. Furthermore, induction of IFN-I by LCMV does not curb viral replication within the TME allowing for sustained immune activation and enabling control of the virus in normal tissues, thereby minimizing potential collateral damage and increasing the therapeutic index. The anti-viral immune responses elicited by LCMV in murine tumor models were shown to be instrumental in contributing to tumor regression and did not blunt the anti-tumor efficacy of the virus, which is another common challenge faced by oncolytic viruses. The production of neutralizing antibodies can suppress oncolytic virus efficacy but LCMV fails to elicit strong neutralizing antibody responses (39, 93). Instrumental to translating LCMV to the clinic will be a thorough safety evaluation, and a deeper understanding of the underlying mechanisms of tumor replication and anti-tumoral effects. Studies of viral entry receptor distribution in tumor cells and a closer examination of the specific host factors in tumor cells which enable LCMV replication might lead to further mechanistic insights and shed light on how to optimize LCMV treatments and uncover responders to therapy. The fact that LCMV variants were already administered to human patients decades ago resulting in responses in some patients is encouraging in paving the pathway to future applications of the virus as an anti-cancer therapeutic.

The artLCMV vaccine platform is one of the anti-cancer therapeutic approaches in pre-clinical and clinical development. The low seroprevalence of LCMV in the general population (67), coupled with weak neutralizing antibody production against LCMV (93) appears to allow for repeated application which is yet a substantial limitation of many other viral based vaccines and oncolytic viruses, and might enable higher patient response rates. The artLCMV's anti-tumoral mechanism of action depends on the infection of APCs to elicit $CD8^+$ T cell responses and to activate the IL33-alarmin pathway in lymphoid tissue. It remains to be further investigated whether effective anti-tumoral cytotoxic effector T lymphocyte (CTL) responses can be successfully recapitulated in a clinical setting in those tumors where the expression of tumor specific-antigens or neoantigens may be a limiting factor in the successful induction of CTL responses due to tumor heterogeneity, evasion mechanisms including loss of target antigen, downregulation of MHC molecules and T cell exhaustion (94).

On the other hand, LCMV as a cancer therapy currently developed in the absence of a vaccine antigen has the advantage that the concurrent administration of tumor-specific or neo-antigens is not required for an efficient anti-tumoral response. Although LCMV is not cytopathic, it induces strong innate and adaptive anti-tumoral responses including the local activation of pattern recognition receptors within the TME, which in turn allow for IFN-I and inflammatory cytokine production, immune cell infiltrating recruitment and the release of tumor neoantigens and subsequent generation of adaptive immune responses. The induction of innate immune responses can counteract immunosuppressive tumor-promoting mechanisms within the TME. This makes such LCMV strains more broadly applicable than the artLCMV platform and not contingent on treating tumors with well-defined stably expressing tumor antigens. Although still in their infancy, the use of other attenuated arenaviruses including live vaccines such as Candid#1 for the treatment of tumors might also hold promise especially if safer second-generation vaccines can be developed.

Finally, as with other virus based vaccines and oncolytic viruses, combinatorial approaches with other immunotherapies or anti-cancer agents will likely prove therapeutically effective, especially in treating poorly immune infiltrating cold tumors. The tumor TME of cold tumors is often characterized by high PD-L1 expression, low immune infiltrates including cytotoxic T cells and/or low expression of the antigen presentation machinery (95). That, when combined with low neoantigen levels makes these tumors largely unresponsive to immunotherapies. By contrast, tumors that are immunologically scored as "hot" are highly infiltrated with cytotoxic T cells and are more responsive to immunotherapies (3). Therefore, approaches such as arenavirus therapies that can successfully manipulate the TME towards an increased 'hot' phenotype (Figure 3) could not only lead to increased immunotherapeutic responses but open up previously poor candidate patient cohorts to immunotherapy treatment.

The first clinical trial combining an oncolytic virus therapy (T-Vec) with the anti PD-1 Pembrolizumab demonstrated that T-Vec promoted tumoral T cell infiltration improving Pembrolizumab's efficacy (96). Patients with advanced melanoma in a phase II randomized study receiving a combination of T-Vec with the anti-CTLA-4 antibody ipilimumab experienced significantly higher objective responses than patients receiving ipilimumab alone (97). Unfortunately, combination therapy failed phase III, as there was no significant improvement in the survival of patients treated with addition of T-Vec (98). Virus based vaccines such as viagenpumatucel-L (gp96-Ig-secreting allogeneic tumor-cell vaccine HS110) in combination with the anti-PD-1 Nivolumab in patients with non-small cell lung adenocarcinoma successfully completed a phase II clinical trial (61). However, one of the major obstacles missing from the arsenal of current immunotherapy combinations, especially for vaccines, is the ability to selectively and specifically activate tumor-killing immune infiltrates for long enough to overcome the metabolic, spatiotemporal and immune barriers imposed by the immunosuppressive cells within the TME such as M2 macrophages, myeloid derived suppressor cells (MDSC) and regulatory T cells (Treg's) which can cause anergy, exhaustion and senescence of cytotoxic lymphocytes as well as the induction of pro-tumoral inflammation. There exists a niche for LCMV-based arenavirus therapies, especially in the treatment of poorly infiltrating

cold tumors as well as tumors with intact interferon responses, both instances where viral vaccines and oncolytic viruses, respectively, might have limited efficacy. Finally, the potential use of LCMV-based arenavirus therapies could boost the response rates of immunotherapies such as CI's that rely not only on adequate $CD8^+$ T cell infiltration but de-repression of immunosuppressive mechanisms within the TME.

Author contributions

PS wrote sections of the manuscript, visualization, and editing. OS and ZL contributed editing and figures. AB proofread the manuscript and provided suggestions. AAP wrote, edited and supervised the study. All authors contributed to the article and approved the submitted version.

Funding

AAP acknowledges the support by Forschungskommission (2021-03), the Ilselore-Luckow-Stiftung and the José Carreras Foundation (DJCLS 18R/2021).

Acknowledgments

We would like to thank Abalos Therapeutics and especially Jörg Vollmer for his helpful suggestions both in terms of content and editing the manuscript.

Conflict of interest

The authors declare that the research was conducted in the absence of any commercial or financial relationships that could be construed as a potential conflict of interest.

Publisher's note

References

1. Marshall HT, Djamgoz MBA. Immuno-oncology: Emerging targets and combination therapies. *Front Oncol* (2018) 8:315. doi: 10.3389/fonc.2018.00315

2. Zhang J, Huang D, Saw PE, Song E. Turning cold tumors hot: From molecular mechanisms to clinical applications. *Trends Immunol* (2022) 43(7):523–45. doi: 10.1016/j.it.2022.04.010

3. Duan Q, Zhang H, Zheng J, Zhang L. Turning cold into hot: Firing up the tumor microenvironment. *Trends Cancer.* (2020) 6(7):605–18. doi: 10.1016/j.trecan.2020.02.022

4. Such L, Zhao F, Liu D, Thier B, Le-Trilling VTK, Sucker A, et al. Targeting the innate immunoreceptor RIG-I overcomes melanoma-intrinsic resistance to T cell immunotherapy. *J Clin Invest* (2020) 130(8):4266–81. doi: 10.1172/JCI131572

5. Oronsky B, Gastman B, Conley AP, Reid C, Caroen S, Reid T. Oncolytic adenoviruses: The cold war against cancer finally turns hot. *Cancers (Basel).* (2022) 14(19):4701. doi: 10.3390/cancers14194701

6. Chulpanova DS, Solovyeva VV, Kitaeva KV, Dunham SP, Khaiboullina SF, Rizvanov AA. Recombinant viruses for cancer therapy. *Biomedicines.* (2018) 6(4):94. doi: 10.3390/biomedicines6040094

7. Brun JL, Dalstein V, Leveque J, Mathevet P, Raulic P, Baldauf JJ, et al. Regression of high-grade cervical intraepithelial neoplasia with TG4001 targeted immunotherapy. *Am J obstetrics gynecology.* (2011) 204(2):169.e1–8. doi: 10.1016/j.ajog.2010.09.020

8. Neelapu SS, Locke FL, Bartlett NL, Lekakis LJ, Miklos DB, Jacobson CA, et al. Axicabtagene ciloleucel CAR T-cell therapy in refractory Large b-cell lymphoma. *New Engl J Med* (2017) 377(26):2531–44. doi: 10.1056/NEJMoa1707447

9. Maude SL, Laetsch TW, Buechner J, Rives S, Boyer M, Bittencourt H, et al. Tisagenlecleucel in children and young adults with b-cell lymphoblastic leukemia. *New Engl J Med* (2018) 378(5):439–48. doi: 10.1056/NEJMoa1709866

10. Chaurasiya S, Chen NG, Fong Y. Oncolytic viruses and immunity. *Curr Opin Immunol* (2018) 51:83–90. doi: 10.1016/j.coi.2018.03.008

11. Doniņa S, Strēle I, Proboka G, Auziņš J, Alberts P, Jonsson B, et al. Adapted ECHO-7 virus rigvir immunotherapy (oncolytic virotherapy) prolongs survival in melanoma patients after surgical excision of the tumour in a retrospective study. *Melanoma Res* (2015) 25(5):421–6. doi: 10.1097/CMR.0000000000000180

12. Liang M. Oncorine, the world first oncolytic virus medicine and its update in China. *Curr Cancer Drug targets.* (2018) 18(2):171–6. doi: 10.2174/1568009618666171129221503

13. Andtbacka RH, Kaufman HL, Collichio F, Amatruda T, Senzer N, Chesney J, et al. Talimogene laherparepvec improves durable response rate in patients with advanced melanoma. *J Clin Oncol* (2015) 33(25):2780–8. doi: 10.1200/JCO.2014.58.3377

14. Lemos de Matos A, Franco LS, McFadden G. Oncolytic viruses and the immune system: The dynamic duo. *Mol Ther Methods Clin Dev* (2020) 17:349–58. doi: 10.1016/j.omtm.2020.01.001

15. Niemann J, Woller N, Brooks J, Fleischmann-Mundt B, Martin NT, Kloos A, et al. Molecular retargeting of antibodies converts immune defense against oncolytic viruses into cancer immunotherapy. *Nat Commun* (2019) 10(1):3236. doi: 10.1038/s41467-019-11137-5

16. Lang PA, Recher M, Honke N, Scheu S, Borkens S, Gailus N, et al. Tissue macrophages suppress viral replication and prevent severe immunopathology in an interferon-i-dependent manner in mice. *Hepatol (Baltimore Md).* (2010) 52(1):25–32. doi: 10.1002/hep.23640

17. Kalkavan H, Sharma P, Kasper S, Helfrich I, Pandyra AA, Gassa A, et al. Spatiotemporally restricted arenavirus replication induces immune surveillance and type I interferon-dependent tumour regression. *Nat Commun* (2017) 8:14447. doi: 10.1038/ncomms14447

18. Hallam SJ, Koma T, Maruyama J, Paessler S. Review of mammarenavirus biology and replication. *Front Microbiol* (2018) 9:1751. doi: 10.3389/fmicb.2018.01751

19. Zapata JC, Salvato MS. Arenavirus variations due to host-specific adaptation. *Viruses.* (2013) 5(1):241–78. doi: 10.3390/v5010241

20. Cao W, Henry MD, Borrow P, Yamada H, Elder JH, Ravkov EV, et al. Identification of alpha-dystroglycan as a receptor for lymphocytic choriomeningitis virus and lassa fever virus. *Science.* (1998) 282(5396):2079–81. doi: 10.1126/science.282.5396.2079

21. Radoshitzky SR, Abraham J, Spiropoulou CF, Kuhn JH, Nguyen D, Li W, et al. Transferrin receptor 1 is a cellular receptor for new world haemorrhagic fever arenaviruses. *Nature.* (2007) 446(7131):92–6. doi: 10.1038/nature05539

22. Raaben M, Jae LT, Herbert AS, Kuehne AI, Stubbs SH, Chou YY, et al. NRP2 and CD63 are host factors for lujo virus cell entry. *Cell Host Microbe* (2017) 22(5):688–96.e5. doi: 10.1016/j.chom.2017.10.002

23. McLay L, Liang Y, Ly H. Comparative analysis of disease pathogenesis and molecular mechanisms of new world and old world arenavirus infections. *J Gen Virol* (2014) 95(Pt 1):1–15. doi: 10.1099/vir.0.057000-0

24. Fedeli C, Torriani G, Galan-Navarro C, Moraz ML, Moreno H, Gerold G, et al. Axl can serve as entry factor for lassa virus depending on the functional glycosylation of dystroglycan. *J Virol* (2018) 92(5):1363–6. doi: 10.1128/JVI.01613-17

25. Shimojima M, Kawaoka Y. Cell surface molecules involved in infection mediated by lymphocytic choriomeningitis virus glycoprotein. *J Vet Med Sci* (2012) 74(10):1363–6. doi: 10.1292/jvms.12-0176

26. Bakkers MJG, Moon-Walker A, Herlo R, Brusic V, Stubbs SH, Hastie KM, et al. CD164 is a host factor for lymphocytic choriomeningitis virus entry. *Proc Natl Acad Sci U S A.* (2022) 119(10):e2119676119. doi: 10.1073/pnas.2119676119

27. Volland A, Lohmuller M, Heilmann E, Kimpel J, Herzog S, von Laer D. Heparan sulfate proteoglycans serve as alternative receptors for low affinity LCMV variants. *PLoS Pathog* (2021) 17(10):e1009996. doi: 10.1371/journal.ppat.1009996

28. Smelt SC, Borrow P, Kunz S, Cao W, Tishon A, Lewicki H, et al. Differences in affinity of binding of lymphocytic choriomeningitis virus strains to the cellular receptor alpha-dystroglycan correlate with viral tropism and disease kinetics. *J Virol* (2001) 75 (1):448–57. doi: 10.1128/JVI.75.1.448-457.2001

29. Xu HC, Wang R, Shinde PV, Walotka L, Huang A, Poschmann G, et al. Slow viral propagation during initial phase of infection leads to viral persistence in mice. *Commun Biol* (2021) 4(1):508. doi: 10.1038/s42003-021-02028-x

30. Bonhomme CJ, Knopp KA, Bederka LH, Angelini MM, Buchmeier MJ. LCMV glycosylation modulates viral fitness and cell tropism. *PLoS One* (2013) 8(1):e53273. doi: 10.1371/journal.pone.0053273

31. Rojek JM, Campbell KP, Oldstone MB, Kunz S. Old world arenavirus infection interferes with the expression of functional alpha-dystroglycan in the host cell. *Mol Biol Cell* (2007) 18(11):4493–507. doi: 10.1091/mbc.e07-04-0374

32. Rojek JM, Perez M, Kunz S. Cellular entry of lymphocytic choriomeningitis virus. *J Virol* (2008) 82(3):1505–17. doi: 10.1128/JVI.01331-07

33. Martinez MG, Cordo SM, Candurra NA. Characterization of junin arenavirus cell entry. *J Gen Virol* (2007) 88(Pt 6):1776–84. doi: 10.1099/vir.0.82808-0

34. Moraz ML, Pythoud C, Turk R, Rothenberger S, Pasquato A, Campbell KP, et al. Cell entry of lassa virus induces tyrosine phosphorylation of dystroglycan. *Cell Microbiol* (2013) 15(5):689–700. doi: 10.1111/cmi.12078

35. Fan L, Briese T, Lipkin WI. Z proteins of new world arenaviruses bind RIG-I and interfere with type I interferon induction. *J Virol* (2010) 84(4):1785–91. doi: 10.1128/JVI.01362-09

36. Martinez-Sobrido L, Zuniga EI, Rosario D, Garcia-Sastre A, de la Torre JC. Inhibition of the type I interferon response by the nucleoprotein of the prototypic arenavirus lymphocytic choriomeningitis virus. *J Virol* (2006) 80(18):9192–9. doi: 10.1128/JVI.00555-06

37. Martinez-Sobrido L, Giannakas P, Cubitt B, Garcia-Sastre A, de la Torre JC. Differential inhibition of type I interferon induction by arenavirus nucleoproteins. *J Virol* (2007) 81(22):12696–703. doi: 10.1128/JVI.00882-07

38. King BR, Hershkowitz D, Eisenhauer PL, Weir ME, Ziegler CM, Russo J, et al. A map of the arenavirus nucleoprotein-host protein interactome reveals that junin virus selectively impairs the antiviral activity of double-stranded RNA-activated protein kinase (PKR). *J Virol* (2017) 91(15):e00763-17. doi: 10.1128/JVI.00763-17

39. Eschli B, Zellweger RM, Wepf A, Lang KS, Quirin K, Weber J, et al. Early antibodies specific for the neutralizing epitope on the receptor binding subunit of the lymphocytic choriomeningitis virus glycoprotein fail to neutralize the virus. *J Virol* (2007) 81(21):11650–7. doi: 10.1128/JVI.00955-07

40. Barber DL, Wherry EJ, Masopust D, Zhu B, Allison JP, Sharpe AH, et al. Restoring function in exhausted CD8 T cells during chronic viral infection. *Nature.* (2006) 439(7077):682–7. doi: 10.1038/nature04444

41. Robert C, Long GV, Brady B, Dutriaux C, Maio M, Mortier L, et al. Nivolumab in previously untreated melanoma without BRAF mutation. *N Engl J Med* (2015) 372 (4):320–30. doi: 10.1056/NEJMoa1412082

42. Topalian SL, Drake CG, Pardoll DM. Immune checkpoint blockade: A common denominator approach to cancer therapy. *Cancer Cell* (2015) 27(4):450–61. doi: 10.1016/j.ccell.2015.03.001

43. Prevost-Blondel A, Zimmermann C, Stemmer C, Kulmburg P, Rosenthal FM, Pircher H. Tumor-infiltrating lymphocytes exhibiting high ex vivo cytolytic activity fail to prevent murine melanoma tumor growth in vivo. *J Immunol* (1998) 161(5):2187–94. doi: 10.4049/jimmunol.161.5.2187

44. Prevost-Blondel A, Neuenhahn M, Rawiel M, Pircher H. Differential requirement of perforin and IFN-gamma in CD8 T cell-mediated immune responses against B16.F10 melanoma cells expressing a viral antigen. *Eur J Immunol* (2000) 30(9):2507–15. doi: 10.1002/1521-4141(200009)30:9<2507::AID-IMMU2507>3.0.CO;2-V

45. Haas VH, Nadel EM. Effect of the virus of lymphocytic choriomeningitis on the course of leukemia in guinea pigs and mice. *J Natl Cancer Inst* (1956) 17(2):221–31.

46. Eiselein J, Biggs MW. Observations with a variant of lymphocytic choriomeningitis virus in mouse tumors. *Cancer Res* (1970) 30(7):1953–7.

47. Molomut N, Padnos M. Inhibition of transplantable and spontaneous murine tumours by m-p virus. *Nature* (1965) 208(5014):948–&. doi: 10.1038/208948a0

48. Ofodile A, Padnos M, Molomut N, Duffy JL. Morphological and biological characteristics of the m-p strain of lymphocytic choriomeningitis virus. *Infect Immun* (1973) 7(2):309–12. doi: 10.1128/iai.7.2.309-312.1973

49. Horton J, Hotchin JE, Olson KB, Davies JN. The effects of MP virus infection in lymphoma. *Cancer Res* (1971) 31(8):1066–8.

50. Webb HE, Molomut N, Padnos M, Wetherley-Mein G. The treatment of 18 cases of malignant disease with an arenavirus. *Clin Oncol* (1975) 1(2):157–69.

51. Bhat H, Ali M, Hamdan TA. Arenavirus therapy in combination with checkpoint blockade as an effective way for better tumour clearance. *Cell Physiol Biochem* (2021) 55(6):726–38. doi: 10.33594/000000472

52. Panda D, Das A, Dinh PX, Subramaniam S, Nayak D, Barrows NJ, et al. RNAi screening reveals requirement for host cell secretory pathway in infection by diverse families of negative-strand RNA viruses. *Proc Natl Acad Sci U S A.* (2011) 108 (47):19036–41. doi: 10.1073/pnas.1113643108

53. Matveeva OV, Chumakov PM. Defects in interferon pathways as potential biomarkers of sensitivity to oncolytic viruses. *Rev Med Virol* (2018) 28(6):e2008. doi: 10.1002/rmv.2008

54. Schadler KL, Crosby EJ, Zhou AY, Bhang DH, Braunstein L, Baek KH, et al. Immunosurveillance by antiangiogenesis: Tumor growth arrest by T cell-derived thrombospondin-1. *Cancer Res* (2014) 74(8):2171–81. doi: 10.1158/0008-5472.CAN-13-0094

55. Rankin EB, Yu D, Jiang J, Shen H, Pearce EJ, Goldschmidt MH, et al. An essential role of Th1 responses and interferon gamma in infection-mediated suppression of neoplastic growth. *Cancer Biol Ther* (2003) 2(6):687–93. doi: 10.4161/cbt.2.6.557

56. Grusdat M, McIlwain DR, Xu HC, Pozdeev VI, Knievel J, Crome SQ, et al. IRF4 and BATF are critical for CD8$^+$ T-cell function following infection with LCMV. *Cell Death differentiation.* (2014) 21(7):1050–60. doi: 10.1038/cdd.2014.19

57. Zhou F, Kardash J, Bhat H, Duhan V, Friedrich S-K, Bezgovsek J, et al. Viral infection overcomes ineffectiveness of anti-tumoral CD8+ T cell mediated cytotoxicity. *bioRxiv* (2019). doi: 10.1101/591198

58. Bhat H, Zaun G, Hamdan TA, Lang J, Adomati T, Schmitz R, et al. Arenavirus induced CCL5 expression causes NK cell-mediated melanoma regression. *Front Immunol* (2020) 11:1849. doi: 10.3389/fimmu.2020.01849

59. Nettelbeck DM, Leber MF, Altomonte J, Angelova A, Beil J, Berchtold S, et al. Virotherapy in Germany-recent activities in virus engineering, preclinical development, and clinical studies. *Viruses* (2021) 13(8):1420. doi: 10.3390/v13081420

60. Flatz L, Hegazy AN, Bergthaler A, Verschoor A, Claus C, Fernandez M, et al. Development of replication-defective lymphocytic choriomeningitis virus vectors for the induction of potent CD8+ T cell immunity. *Nat Med* (2010) 16(3):339–45. doi: 10.1038/nm.2104

61. Penaloza MacMaster P, Shields JL, Alayo QA, Cabral C, Jimenez J, Mondesir J, et al. Development of novel replication-defective lymphocytic choriomeningitis virus vectors expressing SIV antigens. *Vaccine.* (2017) 35(1):1–9. doi: 10.1016/j.vaccine.2016.11.063

62. Kallert SM, Darbre S, Bonilla WV, Kreutzfeldt M, Page N, Muller P, et al. Replicating viral vector platform exploits alarmin signals for potent CD8(+) T cell-mediated tumour immunotherapy. *Nat Commun* (2017) 8:15327. doi: 10.1038/ncomms15327

63. Bonilla WV, Frohlich A, Senn K, Kallert S, Fernandez M, Johnson S, et al. The alarmin interleukin-33 drives protective antiviral CD8(+) T cell responses. *Science.* (2012) 335(6071):984–9. doi: 10.1126/science.1215418

64. Bonilla WV, Kirchhammer N, Marx AF, Kallert SM, Krzyzaniak MA, Lu M, et al. Heterologous arenavirus vector prime-boost overrules self-tolerance for efficient tumor-specific CD8 T cell attack. *Cell Rep Med* (2021) 2(3):100209. doi: 10.1016/j.xcrm.2021.100209

65. Edwards D, Schwendinger M, Katchar K, Schlienger K, Orlinger K, Matushansky I, et al. Abstract 3284: HB-201 and HB-202, an arenavirus-based immunotherapy, induces tumor T cell infiltration in patients with HNSCC and other HPV16+ tumors. *Cancer Res* (2022) 82(12_Supplement):3284. doi: 10.1158/1538-7445.AM2022-3284

66. Bonthius DJ. Lymphocytic choriomeningitis virus: An underrecognized cause of neurologic disease in the fetus, child, and adult. *Semin Pediatr neurology.* (2012) 19 (3):89–95. doi: 10.1016/j.spen.2012.02.002

67. de Lamballerie X, Fulhorst CF, Charrel RN. Prevalence of antibodies to lymphocytic choriomeningitis virus in blood donors in southeastern France. *Transfusion.* (2007) 47(1):172–3. doi: 10.1111/j.1537-2995.2007.01081.x

68. Baum SG, Lewis AMJr., Rowe WP, Huebner RJ. Epidemic nonmeningitic lymphocytic-choriomeningitis-virus infection. an outbreak in a population of laboratory personnel. *N Engl J Med* (1966) 274(17):934–6. doi: 10.1056/NEJM196604282741704

69. Dykewicz CA, Dato VM, Fisher-Hoch SP, Howarth MV, Perez-Oronoz GI, Ostroff SM, et al. Lymphocytic choriomeningitis outbreak associated with nude mice in a research institute. *JAMA.* (1992) 267(10):1349–53. doi: 10.1001/jama.1992.03480100055030

70. Dräger S, Marx AF, Pigny F, Cherpillod P, Eisermann P, Sendi P, et al. Lymphocytic choriomeningitis virus meningitis after needlestick injury: A case report. *Antimicrobial resistance infection control.* (2019) 8:77. doi: 10.1186/s13756-019-0524-4

71. Palacios G, Druce J, Du L, Tran T, Birch C, Briese T, et al. A new arenavirus in a cluster of fatal transplant-associated diseases. *N Engl J Med* (2008) 358(10):991–8. doi: 10.1056/NEJMoa073785

72. Schafer IJ, Miller R, Stroher U, Knust B, Nichol ST, Rollin PE, et al. Notes from the field: A cluster of lymphocytic choriomeningitis virus infections transmitted through organ transplantation - Iowa, 2013. *MMWR Morb Mortal Wkly Rep* (2014) 63(11):249. doi: 10.1111/ajt.12802

73. McCormick JB, King IJ, Webb PA, Scribner CL, Craven RB, Johnson KM, et al. Lassa fever. effective therapy with ribavirin. *N Engl J Med* (1986) 314(1):20–6. doi: 10.1056/NEJM198601023140104

74. Hoey J. Lymphocytic choriomeningitis virus. *CMAJ.* (2005) 173(9):1033. doi: 10.1503/cmaj.051184

75. Delaine M, Weingertner AS, Nougairede A, Lepiller Q, Fafi-Kremer S, Favre R, et al. Microcephaly caused by lymphocytic choriomeningitis virus. *Emerg Infect Dis* (2017) 23(9):1548–50. doi: 10.3201/eid2309.170775

76. Zinkernagel RM, Haenseler E, Leist T, Cerny A, Hengartner H, Althage A. T Cell-mediated hepatitis in mice infected with lymphocytic choriomeningitis virus. liver cell destruction by h-2 class I-restricted virus-specific cytotoxic T cells as a physiological correlate of the 51Cr-release assay? *J Exp Med* (1986) 164(4):1075–92. doi: 10.1084/jem.164.4.1075

77. Baccala R, Welch MJ, Gonzalez-Quintial R, Walsh KB, Teijaro JR, Nguyen A, et al. Type I interferon is a therapeutic target for virus-induced lethal vascular damage. *Proc Natl Acad Sci U S A.* (2014) 111(24):8925–30. doi: 10.1073/pnas.1408148111

78. Wilson JD, Webb HE, Molomut NM, Padnos M. Depression of pha response in patients during therapeutic infection with mp-virus. *Intervirology.* (1973) 2(1):41–7. doi: 10.1159/000149403

79. Ho AL, Posner MR, Niu J, Fu S, Leidner RS, Pearson AT, et al. First report of the safety/tolerability and preliminary antitumor activity of HB-201 and HB-202, an arenavirus-based cancer immunotherapy, in patients with HPV16+ cancers. *J Clin Oncol* (2021) 39(15_suppl):2502. doi: 10.1200/JCO.2021.39.15_suppl.2502

80. Katchar K, Schwendinger M, DaSilva D, Lauterbach H, Orlinger K, Qing X, et al. Abstract LB049: Preliminary analysis of immunogenicity of HB-201 and HB-202, an arenavirus-based cancer immunotherapy, in patients with advanced HPV16-positive cancers. *Cancer Res* (2021) 81(13_Supplement):LB049–LB. doi: 10.1158/1538-7445.AM2021-LB049

81. Fu S, Nabell L, Pearson AT, Leidner R, Adkins D, Posner MR, et al. Recommended phase 2 dose (RP2D) of HB-200 arenavirus-based cancer immunotherapies in patients with HPV16+ cancers. *J Clin Oncol* (2022) 40 (16_suppl):2517. doi: 10.1200/JCO.2022.40.16_suppl.2517

82. Albarino CG, Bird BH, Chakrabarti AK, Dodd KA, Flint M, Bergeron E, et al. The major determinant of attenuation in mice of the Candid1 vaccine for Argentine hemorrhagic fever is located in the G2 glycoprotein transmembrane domain. *J Virol* (2011) 85(19):10404–8. doi: 10.1128/JVI.00856-11

83. Gowen BB, Hickerson BT, York J, Westover JB, Sefing EJ, Bailey KW, et al. Second-generation live-attenuated Candid1 vaccine virus resists reversion and protects against lethal junin virus infection in Guinea pigs. *J Virol* (2021) 95(14):e0039721. doi: 10.1128/JVI.00397-21

84. Lukashevich IS. The search for animal models for lassa fever vaccine development. *Expert Rev Vaccines* (2013) 12(1):71–86. doi: 10.1586/erv.12.139

85. Lauterbach H, Schmidt S, Katchar K, Qing X, Iacobucci C, Hwang A, et al. Development and characterization of a novel non-lytic cancer immunotherapy using a recombinant arenavirus vector platform. *Front Oncol* (2021) 11:732166. doi: 10.3389/fonc.2021.732166

86. Kolokoltsova OA, Grant AM, Huang C, Smith JK, Poussard AL, Tian B, et al. RIG-I enhanced interferon independent apoptosis upon junin virus infection. *PLoS One* (2014) 9(6):e99610. doi: 10.1371/journal.pone.0099610

87. York J, Nunberg JH. Epistastic interactions within the junin virus envelope glycoprotein complex provide an evolutionary barrier to reversion in the live-attenuated Candid1 vaccine. *J Virol* (2018) 92(1):e01682-17. doi: 10.1128/JVI.01682-17

88. Carballal G, Calello MA, Laguens RP, Weissenbacher MC. Tacaribe virus: A new alternative for Argentine hemorrhagic fever vaccine. *J Med Virol* (1987) 23(3):257–63. doi: 10.1002/jmv.1890230308

89. Wolff S, Groseth A, Meyer B, Jackson D, Strecker T, Kaufmann A, et al. The new world arenavirus tacaribe virus induces caspase-dependent apoptosis in infected cells. *J Gen Virol* (2016) 97(4):855–66. doi: 10.1099/jgv.0.000403

90. Muik A, Stubbert LJ, Jahedi RZ, Geiβ Y, Kimpel J, Dold C, et al. Re-engineering vesicular stomatitis virus to abrogate neurotoxicity, circumvent humoral immunity, and enhance oncolytic potency. *Cancer Res* (2014) 74(13):3567–78. doi: 10.1158/0008-5472.CAN-13-3306

91. Wollmann G, Drokhlyansky E, Davis JN, Cepko C, van den Pol AN. Lassa-vesicular stomatitis chimeric virus safely destroys brain tumors. *J Virol* (2015) 89 (13):6711–24. doi: 10.1128/JVI.00709-15

92. Porosnicu M, Quinson AM, Crossley K, Luecke S, Lauer UM. Phase I study of VSV-GP (BI 1831169) as monotherapy or combined with ezabenlimab in advanced and refractory solid tumors. *Future Oncol (London England).* (2022) 18(24):2627–38. doi: 10.2217/fon-2022-0439

93. Recher M, Lang KS, Navarini A, Hunziker L, Lang PA, Fink K, et al. Extralymphatic virus sanctuaries as a consequence of potent T-cell activation. *Nat Med* (2007) 13(11):1316–23. doi: 10.1038/nm1670

94. Wirth TC, Kuhnel F. Neoantigen targeting-dawn of a new era in cancer immunotherapy? *Front Immunol* (2017) 8. doi: 10.3389/fimmu.2017.01848

95. Galon J, Bruni D. Approaches to treat immune hot, altered and cold tumours with combination immunotherapies. *Nat Rev Drug discovery.* (2019) 18(3):197–218. doi: 10.1038/s41573-018-0007-y

96. Ribas A, Dummer R, Puzanov I, VanderWalde A, Andtbacka RHI, Michielin O, et al. Oncolytic virotherapy promotes intratumoral T cell infiltration and improves anti-PD-1 immunotherapy. *Cell.* (2017) 170(6):1109–19. doi: 10.1016/j.cell.2017.08.027

97. Chesney J, Puzanov I, Collichio F, Singh P, Milhem MM, Glaspy J, et al. Randomized, open-label phase II study evaluating the efficacy and safety of talimogene laherparepvec in combination with ipilimumab versus ipilimumab alone in patients with advanced, unresectable melanoma. *J Clin Oncol* (2018) 36(17):1658. doi: 10.1200/JCO.2017.73.7379

98. Chesney JA, Ribas A, Long GV, Kirkwood JM, Dummer R, Puzanov I, et al. Randomized, double-blind, placebo-controlled, global phase III trial of talimogene laherparepvec combined with pembrolizumab for advanced melanoma. *J Clin Oncol* (2023) 41(3):528–40. doi: 10.1200/JCO.22.00343

frontiers | Frontiers in Immunology

TYPE Original Research
PUBLISHED 02 June 2023
DOI 10.3389/fimmu.2023.1070953

OPEN ACCESS

EDITED BY
Mazdak Ganjalikhani Hakemi,
Isfahan University of Medical Sciences, Iran

REVIEWED BY
Gholam Ali Kardar,
Tehran University of Medical Sciences, Iran
Tohid Kazemi,
Tabriz University of Medical Sciences, Iran

*CORRESPONDENCE
Xiaoying Huang
huangxiaoying@wzhospital.cn
Chang Yu
wzmcyc@126.com

RECEIVED 15 October 2022
ACCEPTED 22 May 2023
PUBLISHED 02 June 2023

CITATION
Wang N, Chai M, Zhu L, Liu J, Yu C and Huang X (2023) Development and validation of polyamines metabolism-associated gene signatures to predict prognosis and immunotherapy response in lung adenocarcinoma. *Front. Immunol.* 14:1070953. doi: 10.3389/fimmu.2023.1070953

Development and validation of polyamines metabolism-associated gene signatures to predict prognosis and immunotherapy response in lung adenocarcinoma

Ning Wang[1], Mengyu Chai[1], Lingye Zhu[1], Jingjing Liu[1], Chang Yu[2]* and Xiaoying Huang[1]*

[1]Division of Pulmonary Medicine, the First Affiliated Hospital of Wenzhou Medical University, Key Laboratory of Heart and Lung, Wenzhou, Zhejiang, China, [2]Intervention Department, the First Affiliated Hospital of Wenzhou Medical University, Wenzhou, Zhejiang, China

Background: Polyamines metabolism is closely related to tumor development and progression, as well as tumor microenvironment (TME). In this study, we focused on exploring whether polyamines metabolism-associated genes would provide prognosis and immunotherapy response prediction in lung adenocarcinoma (LUAD).

Methods: The expression profile data of polyamines metabolism-associated genes were acquired from the Cancer Genome Atlas (TCGA) database. Utilizing the least absolute shrinkage and selection operator (LASSO) algorithm, we created a risk score model according to polyamines metabolism-associated gene signatures. Meanwhile, an independent cohort (GSE72094) was employed to validate this model. Through the univariate and multivariate Cox regression analyses, the independent prognostic factors were identified. Subsequently, quantitative real-time polymerase chain reaction (qRT-PCR) was performed to detect their expression in LUAD cells. By consensus clustering analysis, polyamines metabolism-associated subgroups were determined in LUAD patients, with differential gene expression, prognosis, and immune characteristics analyses explored.

Results: A total of 59 polyamines metabolism genes were collected for this study, of which 14 genes were identified for the construction of risk score model using LASSO method. High- and low- risk groups of LUAD patients in TCGA cohort were distinguished *via* this model, and high-risk group presented dismal clinical outcomes. The same prognostic prediction of this model had been also validated in GSE72094 cohort. Meanwhile, three independent prognostic factors (PSMC6, SMOX, SMS) were determined for constructing the nomogram, and they were all upregulated in LUAD cells. In addition, two distinct subgroups (C1 and C2) were identified in LUAD patients. Comparing the two subgroups, 291 differentially expressed genes (DEGs) were acquired, mainly enriching in organelle fission, nuclear division, and cell cycle. Comparing to C1 subgroup, the patients in C2

subgroup had favorable clinical outcomes, increased immune cells infiltration, and effective immunotherapy response.

Conclusion: This study identified polyamines metabolism-associated gene signatures for predicting the patients' survival, and they were also linked to immune cells infiltration and immunotherapy response in LUAD patients.

KEYWORDS

lung adenocarcinoma, polyamines metabolism, prognosis, tumor microenvironment, immunotherapy response

1 Introduction

Polyamines metabolism participate in multiple cellular processes, such as gene regulation, cell proliferation and differentiation, cell death, and immune system function (1–3). The maintenance of polyamines homeostasis requires stringent cellular regulatory process, including biosynthesis, decomposition, and transport. Previous studies have uncovered that due to increased biosynthesis and transport, and decreased catabolism, high levels of polyamines widely occur in cancer cells suggesting an important interplay between polyamines metabolism and carcinogenesis (4, 5). Polyamines metabolism is dysregulated in many tumors, which is directly associated with the development and progression of cancers. Therefore, polyamines metabolism has been considered to be an attractive target for cancer therapy.

Cancer immunotherapy, an emerging and promising treatment strategy, utilizes the enhanced antitumor effects of immune system to kill cancer cells. Recently, striking progress has been made in cancer immunotherapy, which dramatically changed the paradigm of cancer treatment (6, 7). Immunotherapy has improved cancer patients' survival worldwide, however, most patients lack effective immune response resulting in non-sustainable disease control. Existing evidence reveals that the inadequate immune effector cells infiltration and the immunosuppressive status of immune cells in tumor microenvironment (TME) are the important mechanisms affecting the response to cancer immunotherapy. Immunosuppressive TME can hamper the antitumor actions of immune effector cells leading to the immune surveillance evasion of malignant cells, which is a vital obstacle to successful immunotherapy (8, 9). Therefore, understanding the potential regulatory mechanisms of the immune status in TME is critical for improving the efficacy of immunotherapy.

According to research findings, polyamines biosynthetic enzymes were upregulated in tumor tissues, and the elevated spermine and spermidine promoted tumor growth and correlated with immunosuppressive status of TME (10). In addition, many immune cell types in TME, including myeloid-derived suppressor cells (MDSCs), dendritic cells and M2 macrophages, translated from an immune-active to an immune-suppressive state affecting antitumor immunity owing to polyamines metabolic disorders (11). Considering the dependence of tumor cells on polyamines and the crucial biological function of polyamines in immune cells, targeting polyamines metabolic pathways are expected to be an important cancer therapeutic strategy. In particular, it will be extremely beneficial to explore biomarkers based on polyamines metabolism that can predict the response to immunotherapy in tumor patients.

Lung adenocarcinoma (LUAD), the most common subtype of lung cancer, has a dismal prognosis, with relatively high mortality rate in malignant tumor patients (12, 13). Despite advancements in traditional cancer treatments over the last few decades, there has limited improvements in patients' survival outcomes. Immunotherapy, especially immune checkpoint inhibitors (ICIs), has been considered as an important therapeutic option for LUAD patients with favorable improvement in survival (14, 15). Currently, PD-L1 expression is still considered as a biomarker for predicting the patients who will benefit from immune checkpoint blockade (ICB) therapy. However, many patients do not present a good response. It is, therefore, meaningful to identify the new biomarkers precisely predicting immunotherapy response.

In this study, we investigated the expression pattern of polyamines metabolism genes in LUAD, and screened out the significant gene signatures based on machine learning method to develop a risk score model, which could predict patients' survival. This model also was validated in another independent cohort, and the expression of prognostic factors were detect using qRT-PCR. Furthermore, the subgroups of LUAD patients classified by these significant gene signatures had different immune cells infiltration levels and immunotherapy response. This is the first study to explore the role of polyamines metabolism-related gene signatures

Abbreviations: AUC, area under the curve; BP, biological process; CC, cellular component; CI, confidence interval; DEGs, differentially expressed genes; GEO, Gene Expression Omnibus; GO, gene ontology; HR, hazard ratio; ICB, immune checkpoint blockade; ICIs, immune checkpoint inhibitors; KEGG, Kyoto encyclopedia of genes and genomes; LASSO, least absolute shrinkage and selection operator; MF, molecular function; LUAD, lung adenocarcinoma; OS, overall survival; PCA, principal components analysis; PPI, protein–protein interaction; qRT-PCR, quantitative reverse-transcription polymerase chain reaction; ROC, receiver operating characteristic; TCGA, the cancer genome atlas; TIDE, Tumor Immune Dysfunction and Exclusion; TME, tumor microenvironment.

in LUAD patients from the perspective of patients' prognosis and immunotherapy response.

2 Materials and methods

2.1 Data acquisition

RNA-sequencing expression profile data and matched clinical information of LUAD samples were collected from The Cancer Genome Atlas (TCGA) database (https://portal.gdc.cancer.gov/). Validation dataset (GSE72094) was obtained from Gene Expression Omnibus (GEO) database (http://www.ncbi.nlm.nih.gov/geo/). After standardized processing, the data was conducted for further analysis using R software. A total of 59 polyamines metabolism-associated genes were collected from MSigDB database (http://www.gsea-msigdb.org/). By searching the keyword "polyamines", the gene sets "REACTOME_METABOLISM_OF_ POLYAMINES" were discovered. The detail gene information is listed in Supplementary Materials.

2.2 Gene expression and protein–protein interaction network

We first investigated the expression levels of 59 polyamines metabolism-associated genes between tumor and normal tissues. Furthermore, PPI network was established based on STRING platform (https://string-db.org/) to analyze their interconnections (16).

2.3 Identification of polyamines metabolism-associated gene signatures for risk score model in LUAD

Based on LASSO algorithm using "glmnet" R package (17), the significant polyamines metabolism gene signatures were explored to construct the risk score model. Application of the optimal cut-off value, LUAD patients were distinguished into two groups: high- and low- risk groups, for further prognosis analysis. In addition, we verified the predictive ability of risk score model *via* the external independent dataset (GSE72094).

2.4 Prognosis analysis

We first respectively compared the prognosis between high- and low-risk groups in TCGA and GSE72094 LUAD cohorts using the "survival" package. Furthermore, the univariate and multivariate Cox regression analyses were carried out to recognize the independent prognostic factors from polyamines metabolism-associated genes in LUAD. Subsequently, these factors were used for establishing a prognostic nomogram *via* the "rms" package, which could be employed for survival (1-, 3-, 5-year) prediction of LUAD patients.

2.5 Receiver operating characteristic curve analysis

The predictive performance of gene expression was judged using ROC curve analysis conducted by the "pROC" package. The area under the curve (AUC) value was calculated for quantitative analysis according to previous methods (18).

2.6 Cell culture and qRT-PCR

Human bronchial epithelial cells (BEAS-2B) and human LUAD cells (H1975 and H2009) were acquired from the American Type Culture Collection (ATCC, United States). All cells were conventionally cultured and the total RNA was collected according to commercial kit methods. After reverse transcription *via* Hiscript III All-in-one RT Super mix Perfect for qPCR kit (Vazyme, China), qRT-PCR was conducted using Taq Pro Universal SYBR qPCR Master Mix kit (Vazyme, China). GAPDH served as an endogenous control. Primers were synthesized from Sangon Biotech (Shanghai, China) and the detail information of the sequences were provided in Supplementary Materials.

2.7 Recognition of the subgroups in LUAD patients *via* consensus clustering analysis

The consensus clustering analysis was applied to recognize the polyamines metabolism-associated subgroups in LUAD patients, which was conducted *via* the "ConsensusClusterPlus" package.

2.8 Differential gene analysis

Differential gene analysis was carried out to recognize the DEGs between the different subgroups *via* the "Limma" package (19) based on the criteria of adjusted $P < 0.05$ and Fold Change > 2. Then, volcano plot and heatmap were applied to display these differential genes.

2.9 Function enrichment analysis

GO enrichment, including the biological process (BP), cellular component (CC), and molecular function (MF), and KEGG enrichment of these significant polyamines metabolism genes were conducted. Additionally, function enrichment analyses of the upregulated DEGs in subgroups were carried out *via* the "ggplot2" and "ClusterProfiler" packages.

2.10 Clinicopathological features analysis

The association between the clinicopathological features such as age, TNM stage, and survival status in different subgroups of LUAD

patients was described using Sankey diagram *via* the "ggalluval" package. Moreover, overall survival analysis was performed in different subgroups of LUAD patients.

2.11 Somatic mutation analysis

Somatic mutation analysis in different subgroups were performed *via* the "Maftools" package. The whole somatic mutation landscape was displayed using waterfall plots.

2.12 Immune characteristics analysis

We first assessed the immune status of TME, including Immune Score, Stromal Score and ESTIMATE Score in different subgroups *via* "estiate" package. Furthermore, the immune cells infiltration status was investigated using MCP-counter (20) and xCell (21) algorithms performed by the "immunedeconv" package. Finally, we assessed the immunotherapy response to ICB in different subgroups by means of Tumor Immune Dysfunction and Exclusion (TIDE) algorithm (22).

3 Results

3.1 The expression of polyamines metabolism-related genes in LUAD

The entire study is conducted according to the summarizing flow chart (Figure 1). A total of 59 polyamines metabolism-related genes were collected from MSigDB database. The expression of these polyamines metabolism genes in normal and LUAD samples were first explored. As shown in Figure 2A, most of polyamines metabolism genes were overexpressed in LUAD samples. The STRING platform was employed to construct PPI network, investigating the connections among these polyamines metabolism-associated genes (Figure 2B).

3.2 Construction and validation of polyamines metabolism-associated risk score model in LUAD

The significant gene signatures were further narrowed down from 59 polyamines metabolism-associated genes using LASSO regression machine learning method in LUAD. The result showed a total of 14 significant gene signatures were eventually determined to establish the risk score model on the basis of the optimal λ value 0.02949 (Figures 3A, B). The risk score was calculated following equation: Risk Score = 0.036*PSMA4 + (-0.003)*PSME4 + 0.109*PSMC5 + 0.157*SMOX + 0.188*PSMC6 + (-0.011)*PSMA7 + (-0.117)*PSMD10 + 0.206*SMS + (-0.015)*AMD1 + (-0.044)*SAT1 + 0.224*PSMB7 + (-0.101)*AZIN2 + (-0.003)*PAOX + 0.028*PSMD2. According to the optimal cut-off value (4.26), the patients were divided into two groups with high and low risk. As shown in Figure 3C, the LUAD patients with high-risk scores presented high risk of death. Prognosis analysis indicated that high-risk patients had poor prognosis (P = 1.4 e-11, HR = 2.67, Figure 3D). Moreover, we discovered that except for high expression of AMD1 and SAT1 in normal samples, other genes (PSMA4, PSME4, PSMC5, SMOX, PSMC6, PSMA7, PSMD10, SMS, PSMB7, AZIN2, PAOX, PSMD2) were all upregulated in tumor samples (Figure 3E). Gene expression correlation analysis revealed that there presented a positive correlation among these genes (PSMA, PSME4, PSMC5, SMOX, PSMC6, PSMA7, PSMD10, SMS, AMD1, PSMB7, and PSMD2) (Figure 3F).

Next, an independent cohort (GSE72094) was utilized to validate the predictive effectiveness of risk score model in the prognosis of LUAD patients. Based on the optimal cut-off value (4.28), high and low risk groups were distinguished. We also

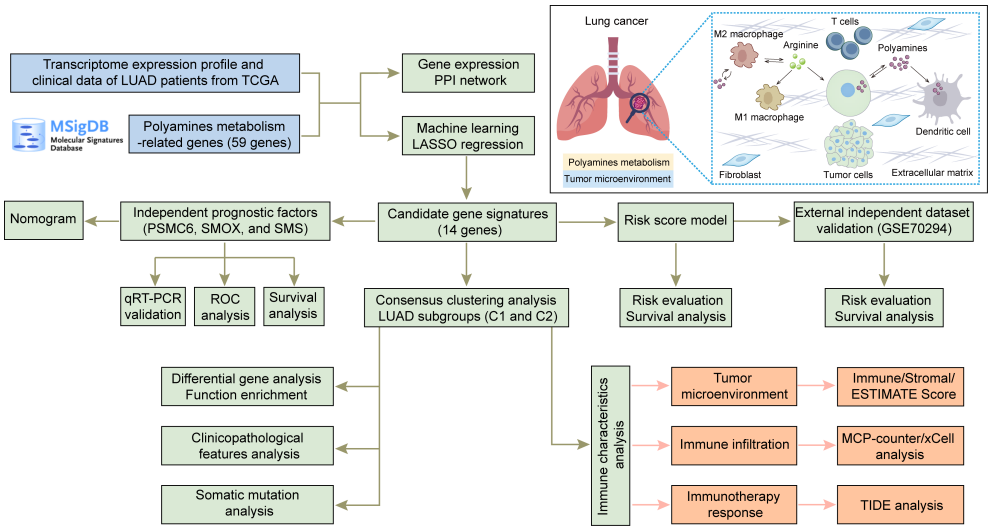

FIGURE 1
Flow diagram of the overall study and the pattern diagram of polyamines metabolism in tumor microenvironment.

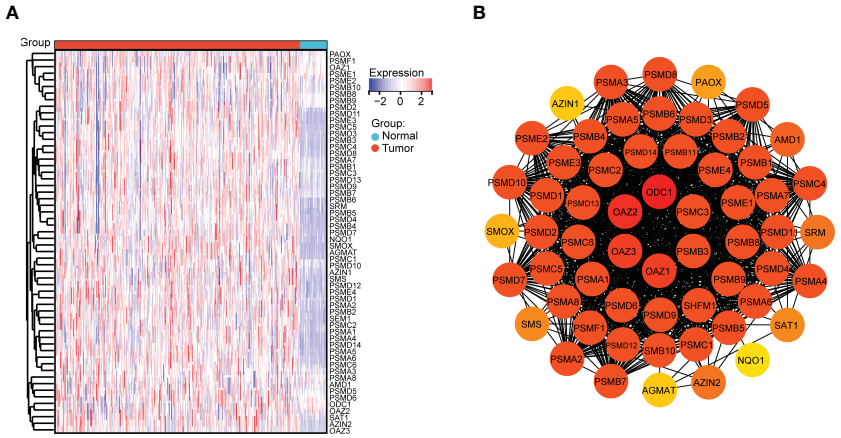

FIGURE 2
Gene expression and protein–protein interaction (PPI) network. **(A)** Heatmap depicting the expression of polyamines metabolism-associated genes between tumor and normal tissues based on TCGA database. Different colors represent the trend of gene expression in different tissues. **(B)** PPI network among polyamines metabolism-associated genes. Different depth color represents the degree score of the protein.

discovered that high-risk patients had poor prognosis (Figure 4A). Finally, the expression of 14 genes in high- and low- risk groups were exhibited *via* heatmap (Figure 4B).

3.3 Function enrichment analysis of the 14 gene signatures in risk score model

We next performed GO and KEGG enrichment analyses of the 14 gene signatures in risk score model respectively. As shown in Figures 5A–C, the Top5 enrichment results of BP, CC, and MF were exhibited. Moreover, KEGG analysis results indicated that these genes were primarily enriched in proteasome, arginine and proline metabolism, and metabolic pathways (Figure 5D).

3.4 Recognition of the independent prognostic factors and construction of the nomogram

Through univariate Cox regression analysis, we discovered that AZIN2, PSMA4, PSMB7, PSMC5, PSMC6, PSMD2, SMOX, and SMS were significantly correlated with patients' OS. The hazard ratio of AZIN2 (HR < 1, $P < 0.05$) favored patients' prognosis, and the other genes, including PSMA4, PSMB7, PSMC5, PSMC6, PSMD2, SMOX, and SMS, were all risk factors (HR > 1, $P < 0.05$) (Figure 6A). We further conducted the multivariate Cox regression analysis, and discovered that PSMC6, SMOX, and SMS were also significantly correlated with OS, all serving as risk factors (HR > 1, $P < 0.05$) (Figure 6B). Thus, comprehensive analyses revealed that PSMC6, SMOX, and SMS could be recognized as independent prognostic factors. Based on the three factors, we constructed a nomogram, providing a certain predictive effect of clinical prognosis (Figures 6C, D).

Next, we explored the expression levels of PSMC6, SMOX, and SMS in LUAD cell lines, and their diagnostic and prognostic values in LUAD patients, respectively. PSMC6, SMOX, and SMS were all upregulated in LUAD cell lines (H1975 and H2009), comparing to normal bronchial epithelial cells (BEAS-2B) (Figures 7A–C). ROC analysis revealed that the AUC values of PSMC6, SMOX, and SMS were 0.822, 0.818, and 0.802, respectively, suggesting they had certain diagnostic values (Figures 7D–F). Finally, survival analysis revealed that the patients with high expression of PSMC6, SMOX, and SMS presented poor prognosis (Figures 7G–I).

3.5 Consensus clustering analysis recognized polyamines metabolism-associated subgroups in LUAD

LUAD samples were divided into two different subgroups (C1 and C2) relying on consensus clustering analysis (Figures 8A–D). Subsequently, the expression of 14 genes between the two subgroups were displayed (Figure 8E). In addition, a total of 291 DEGs were screened out by comparing the two different subgroups, of which 199 DEGs were upregulated and 92 DEGs were downregulated (Figure 9A). The detail gene information is listed in Supplementary Materials. The expression of DEGs were displayed *via* heatmap (Figure 9B). Finally, function enrichment analyses revealed that GO analysis of upregulated DEGs mainly converged at organelle fission, nuclear division, mitotic nuclear division, and chromosome segregation (Figure 9C). The KEGG analysis of upregulated DEGs mainly converged at cell cycle (Figure 9D).

3.6 Comprehensive analysis of clinicopathological features, somatic mutation and immune landscape in the subgroups

We first analyzed the different clinicopathological features such as age, TNM stage, and survival status in C1 and C2 subgroups

10.3389/fimmu.2023.1070953

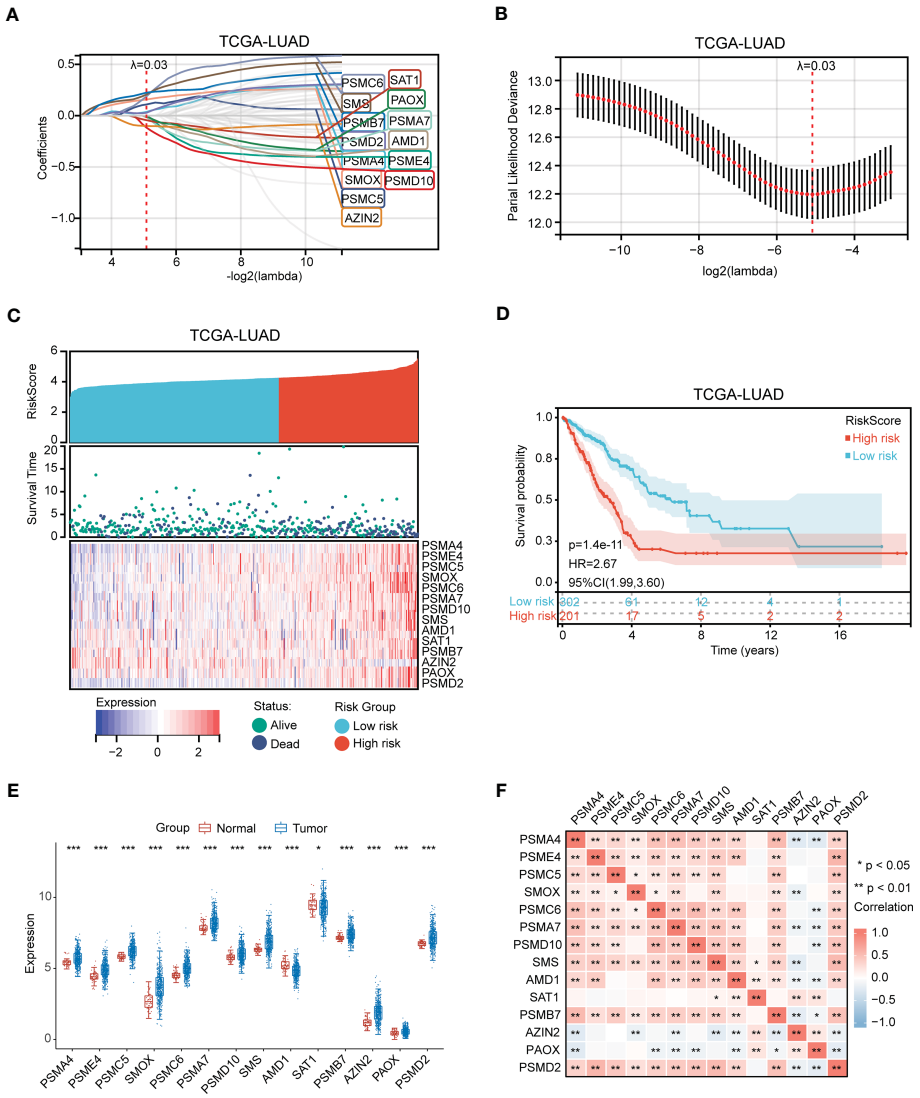

FIGURE 3
Identification of polyamines metabolism-associated gene signatures for risk score model. **(A)** Screening of the polyamines metabolism-associated gene signatures for risk score model using the LASSO algorithm. **(B)** The best log (Lambda) value in the model. **(C)** Heatmap depicting genes expression distribution and survival status in LUAD patients. **(D)** Kaplan-Meier plot depicting overall survival of high- and low- risk LUAD patients. **(E)** Box plot depicting the expression of gene signatures in risk score model. **(F)** Heatmap depicting the correlation among these gene signatures. Statistical analysis: $*P < 0.05$, $**P < 0.01$, and $***P < 0.001$.

using Sankey diagram (Figure 10A). Kaplan-Meier plots indicated that the patients in C1 subgroup presented a dismal prognosis in OS, comparing to C2 subgroup (Figure 10B). In addition, we discovered that there presented different genes mutation between C1 and C2 subgroups such as TP53, TTN, MUC16, and so on (Figure 10C).

Accumulating evidence reveals that polyamines metabolism is correlated with tumor immunosuppressive microenvironment and promotes tumor growth. In this research, we first investigated the composition of the tumor microenvironment between C1 and C2 subgroups. The result indicated that C2 subgroup presented a higher immune infiltration status than C1 subgroup (Figure 11A). We next assessed the infiltration levels of immune cells between C1 and C2 subgroups utilizing MCP-counter algorithm. The samples in C2 subgroup had significantly higher immune cells infiltration, such as neutrophil, T cell, B cell, and myeloid dendritic cell than those in C1 subgroup (Figures 11B, C). In addition, we performed another algorithm (xCell) analysis, and also noted that there were high infiltration levels of most of immune cells in C2 subgroup (Figures S1A, B). Finally, TIDE algorithm was applied to assess the immunotherapy response to ICB between C1 and C2 subgroups. High TIDE score reveals poor response to ICB and short survival. As shown in Figure 11D, the patients in C2 subgroup had relatively satisfied treatment response to immunotherapy.

4 Discussion

Metabolic reprogramming has been widely considered to be a key mechanism in tumorigenesis and progression (23, 24).

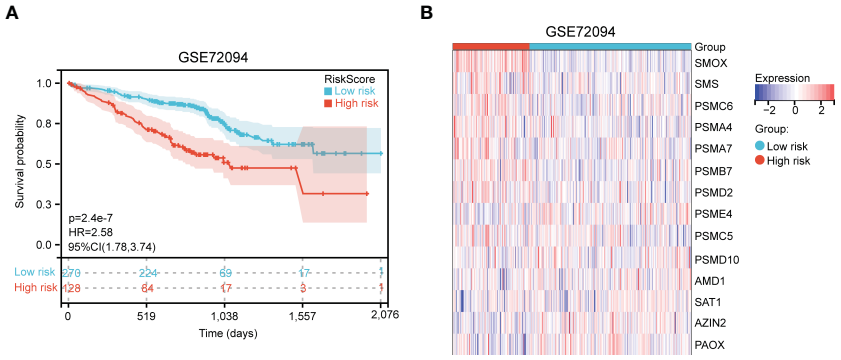

FIGURE 4
Validation of polyamines metabolism-associated risk score model in GSE72094 cohort. **(A)** Kaplan-Meier plot depicting overall survival of high- and low- risk LUAD patients in the independent cohort. **(B)** Heatmap depicting the expression of these gene signatures in risk score model in the independent cohort.

Metabolic reprogramming, an important hallmark of tumor cells, accelerates cell proliferation by regulating metabolism-related processes. Polyamines are not only involved in gene regulation, but also in a series of signal transduction processes, exerting a crucial role in cell proliferation and survival. Notably, dysregulation of polyamines metabolism leads to the elevation of polyamines in cancers, maintaining the growth and progression of tumor cells (25). Previous research have shown that polyamines dysregulation contributes to the progression of helicobacter pylori-induced gastric cancer (26). In addition, the study of potential regulatory mechanism of polyamines metabolism exerts the vital means for understanding the tumor evolving process (27). Therefore, polyamines metabolic pathway is a promising target for anti-tumor treatment.

Here, we discovered that most of polyamines metabolism-related genes were overexpressed in LUAD samples. In order to

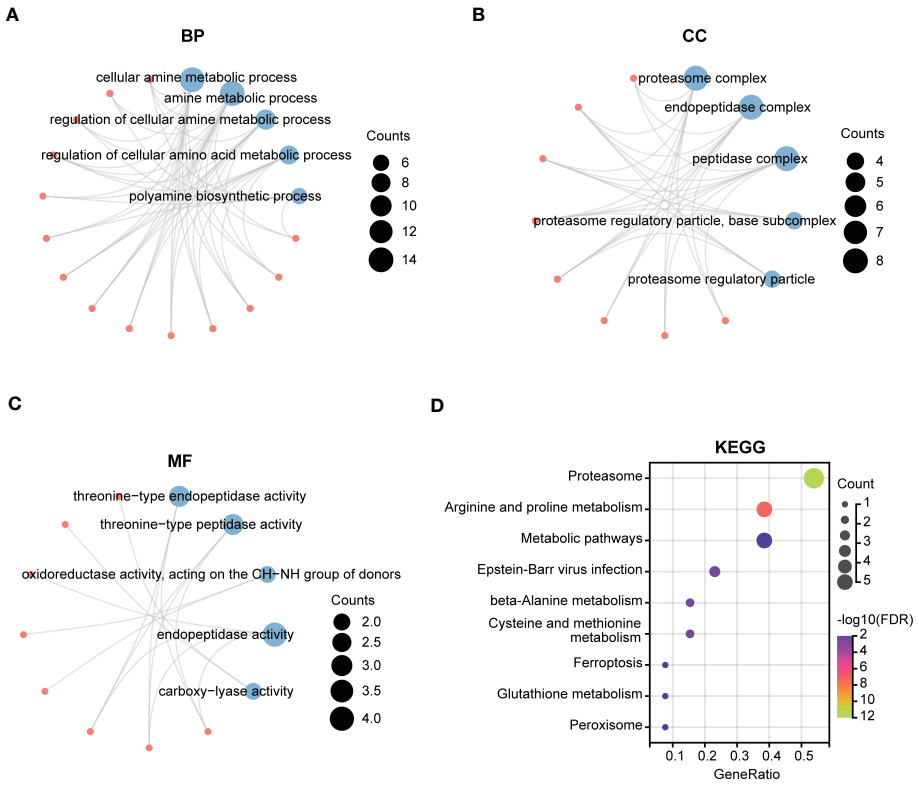

FIGURE 5
Function enrichment analysis of polyamines metabolism-associated gene signatures. **(A-C)** The top5 pathways of **(A)** BP (biological process), **(B)** CC (cellular component), and **(C)** MF (molecular function) in GO enrichment analysis of polyamines metabolism-associated gene signatures. **(D)** KEGG enrichment analysis of these gene signatures. The size of the circle means the number of enriched genes, and the larger the number, the larger the circle.

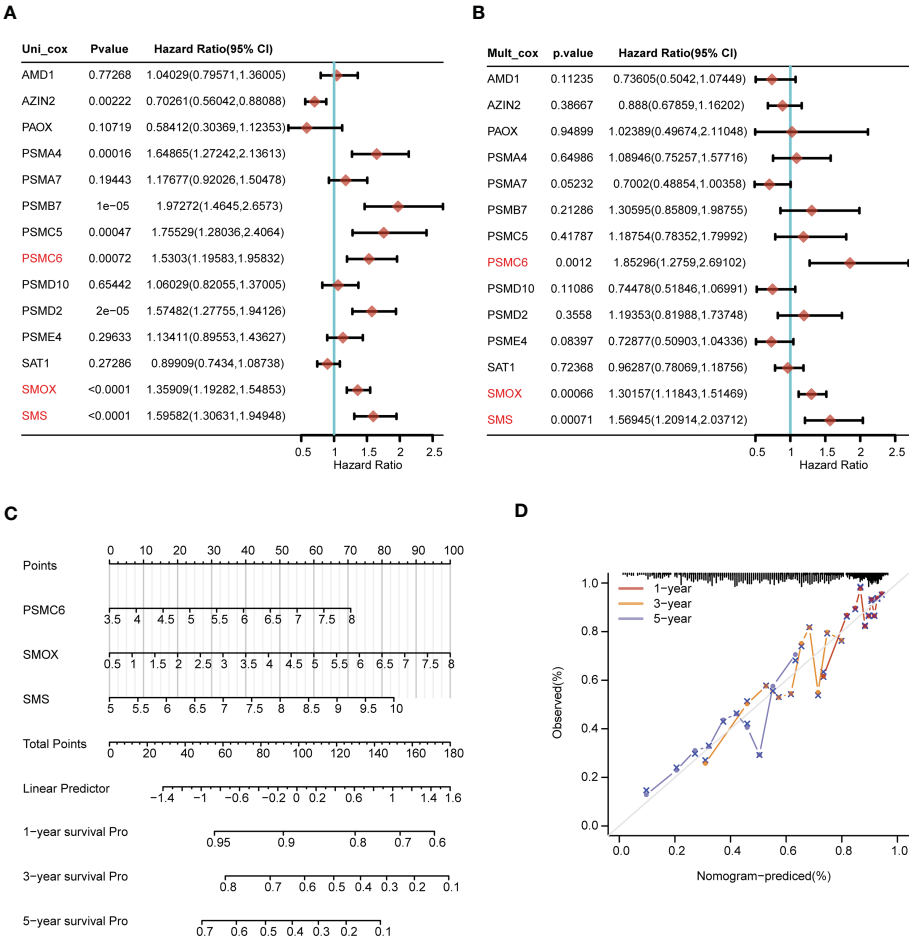

FIGURE 6
Construction of the nomogram predicting patients' survival in LUAD. **(A)** The univariate and **(B)** multivariate Cox regression analyses of polyamines metabolism-associated gene signatures for exploring the independent prognostic factors in LUAD. HR more than 1 indicates the risky gene, and HR less than 1 indicates the protective gene. **(C)** Construction of the nomogram for survival prediction (1-, 3-, 5-year) of LUAD patients. **(D)** Calibration curve of the nomogram.

clarify the association between polyamines metabolism and LUAD patients' prognosis, we developed a risk score model using polyamines metabolism genes *via* machine learning method, predicting the different prognosis of the high- and low- risk patients. Next, we further validated the predictive effects of this model using an independent cohort, and discovered that this model could also precisely predict the patients' prognosis. These results suggested that polyamines metabolism genes-constructed model presented a good prediction efficiency. Considering the heterogeneity among LUAD patients, subgroup analysis was a good strategy for in-depth study. Based on these genes in the model, the LUAD patients were divided into two distinct subgroups by means of consensus clustering method. The two subgroups also presented different prognosis, which verified again the predicted effects of these gene signatures. To sum up, polyamines metabolism-related gene signatures had significant predictive effects on the patients' prognosis.

In recent years, immunotherapy has been the fastest-growing antitumor therapy. Despite great advances have been made in the application of immune checkpoint blockade therapy in multiple cancers, only a minority of patients have durable responses (28). A more in-depth investigation of complex immune landscape in TME is crucial for identifying the influencing factors in immunotherapy response. New research has found that tumor metabolism not only exerts a vital role in maintaining tumor survival, but also influences immune cells function by releasing metabolites in TME. Metabolic competition between tumor cells and immune cells, limiting efficient supply of nutrients to immune cells, impedes the antitumor function of immune cells (29, 30). Thus, metabolic changes in TME have been recognized as one of the important influences on the effects of tumor immunotherapy. In the process of tumor development, most of the cellular components in TME undergo metabolic reprogramming, and cells metabolic state has important implications for anti-tumor immunotherapy (31). Recent researches have indicated that polyamine metabolism-associated pathways have a profound impact on tumor microenvironment, and perform a crucial role in immune surveillance (32). In addition, polyamine metabolism is involved in anti-tumor immunity, and the assessment of polyamine levels can be utilized to predict the response to immunotherapy (33).

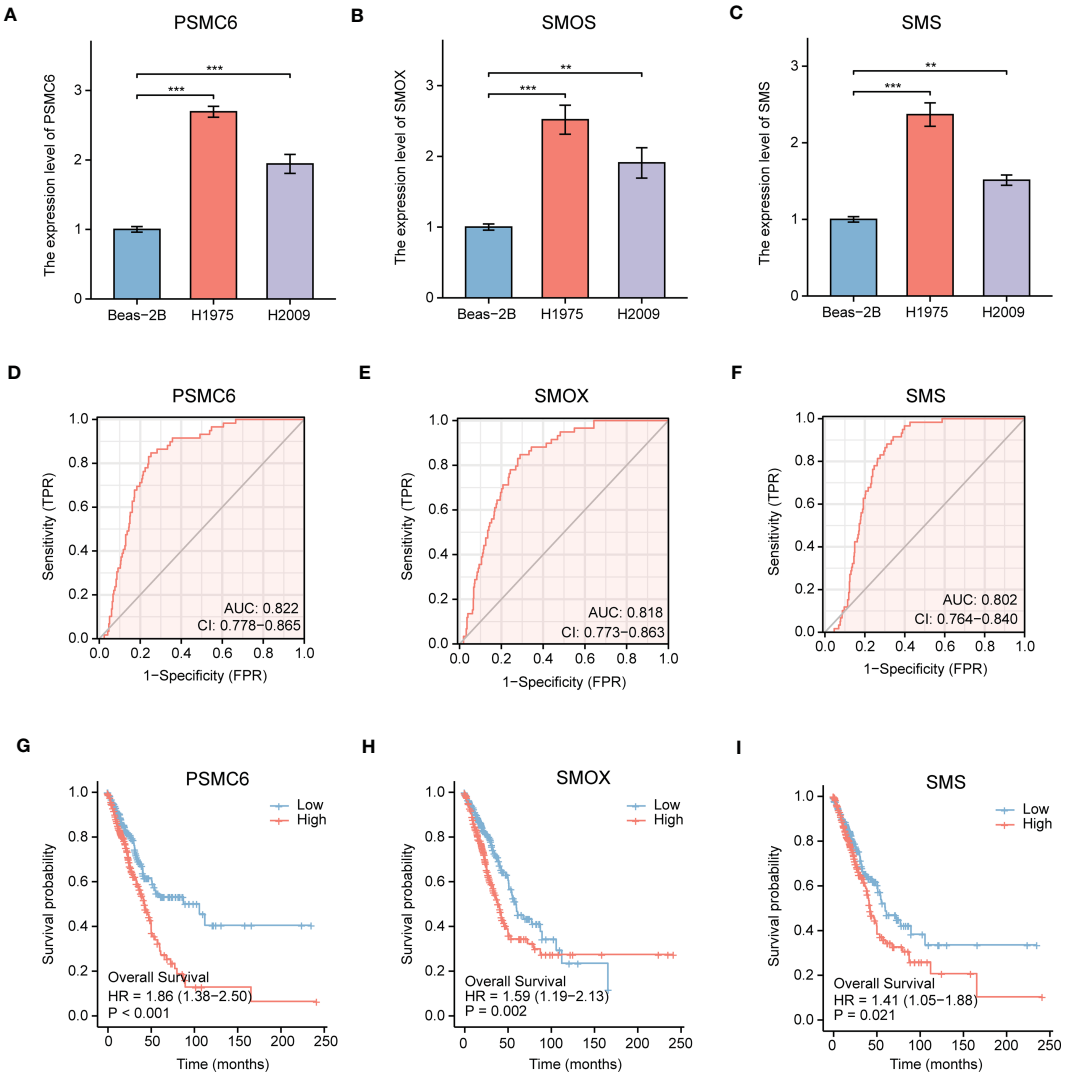

FIGURE 7
Comprehensive analysis of gene expression, diagnostic value, and prognosis analysis of the independent factors (PSMC6, SMOX, SMS). **(A-C)** The gene expression levels of **(A)** PSMC6, **(B)** SMOX, and **(C)** SMS in normal lung cells (Beas-2B) and LUAD cells (H1975 and H2009) by qRT-PCR. GAPDH serves as an endogenous control. **(D-F)** ROC curve analyses for **(D)** PSMC6, **(E)** SMOX, and **(F)** SMS expression in LUAD. The AUC value represents the predictive performance. **(G-I)** Kaplan-Meier plot depicting the predictive role of **(G)** PSMC6, **(H)** SMOX, and **(I)** SMS expression for patients' survival. Statistical analysis: $^{**}P < 0.01$ and $^{***}P < 0.001$.

Immune cells infiltration may be required for the response to ICB therapy, and immune cells status in TME also perform a critical role in tumor immunotherapy (34). The research on immune response mechanisms of "cold" tumors and "hot" tumors will contribute to more accurately recognizing the patient groups that benefit from immunotherapy. Polyamines participate in regulating antitumor immune responses, and high polyamines levels are associated with the immunosuppressive effects (35). Through reducing the levels of polyamines can attenuate the proliferation of tumor cells, while improve the immunogenicity of "cold" tumors. In our study, the patients in C2 subgroup possessed relatively high immune cells infiltration. In addition, they also had relatively satisfied immunotherapy response according to TIDE score. These results indicated that polyamines metabolism-associated gene signatures could be utilized to predict the immunotherapy response. Therefore, tumor cells relying on polyamines and the important physiological roles of polyamines in various immune cell types suggests that targeting polyamines metabolic pathways may become a crucial focus for improving the efficacy of immunotherapy.

In conclusion, this study first developed and validated the important biological function of polyamines metabolism gene signatures for judging prognosis in LUAD patients. More importantly, the candidate genes (PSMC6, SMOX, and SMS) were identified as independent prognostic factors, constructing the nomogram to predict the patients' prognosis. In addition, we

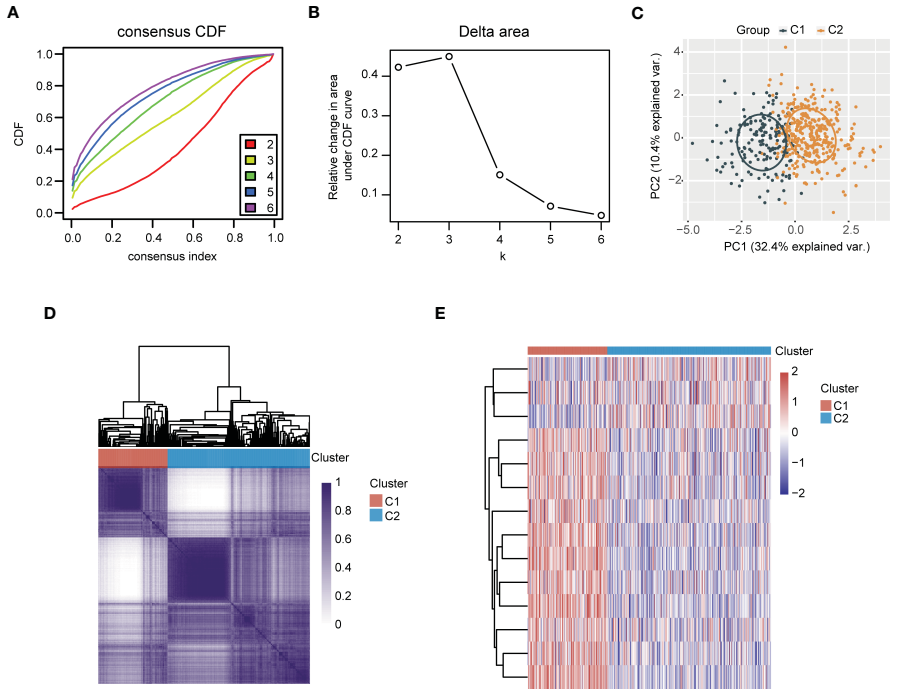

FIGURE 8
Recognition of polyamines metabolism-associated subgroups in LUAD patients through consensus clustering analysis. **(A)** Consensus clustering of the cumulative distribution function (CDF) curve. **(B)** The relative change in area under CDF curve. **(C)** Principal component analysis (PCA) of C1 and C2 subgroups. **(D)** Heatmap of consensus clustering (k = 2). **(E)** Heatmap depicting the expression of gene signatures in C1 and C2 subgroups of LUAD patients.

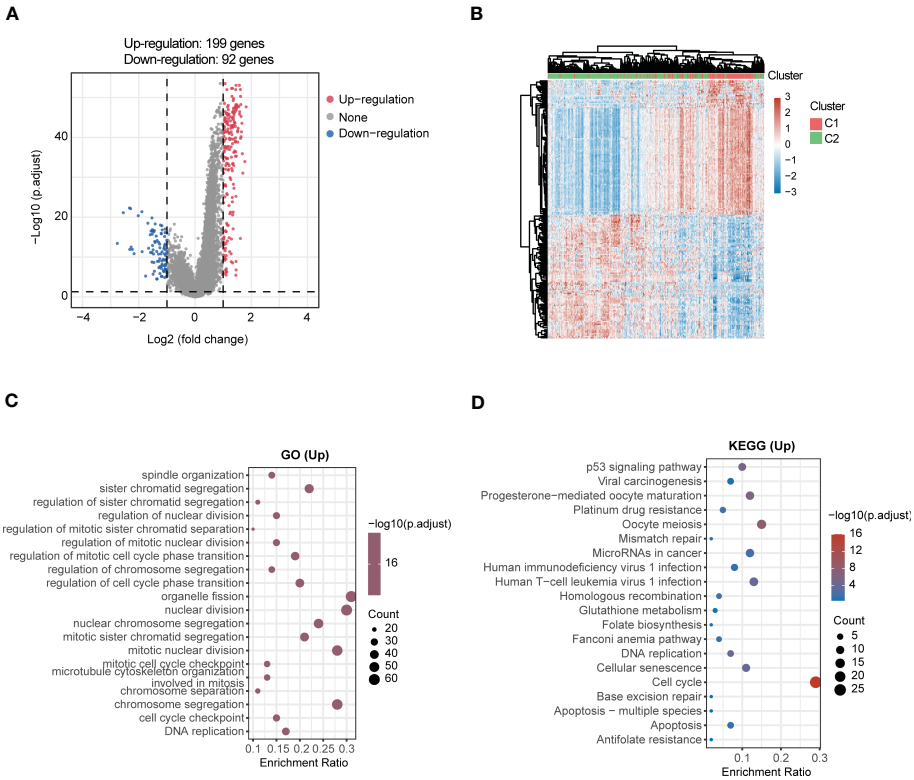

FIGURE 9
Comprehensive analysis of DEGs and function enrichment between the two subgroups in LUAD. **(A)** Volcano plot depicting DEGs between the two subgroups. Red means the upregulated genes, blue means the downregulated genes, and grey means not significant. **(B)** Heatmap of DEGs in the two subgroups. **(C)** GO and **(D)** KEGG enrichment analysis of the upregulated DEGs.

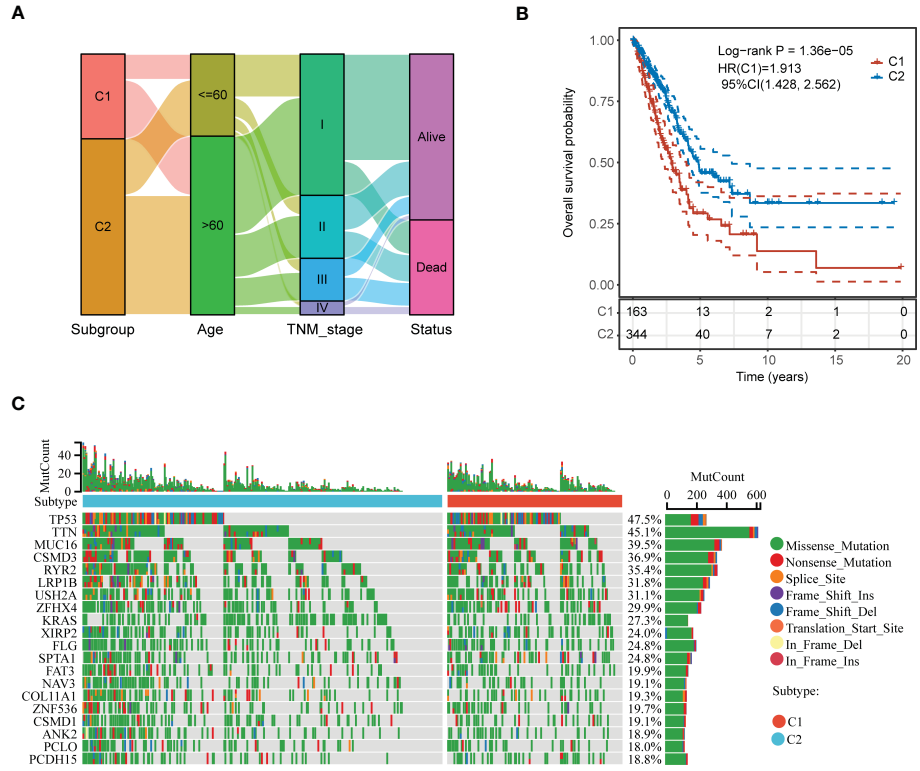

FIGURE 10
Comprehensive analysis of clinicopathological features and somatic mutation between the two subgroups of LUAD patients. **(A)** Sankey diagram depicting the different clinicopathological features in C1 and C2 subgroups of LUAD patients. **(B)** Kaplan-Meier plot depicting overall survival in C1 and C2 subgroups of LUAD patients. **(C)** Waterfall plot depicting the somatic mutation feature in C1 and C2 subgroups.

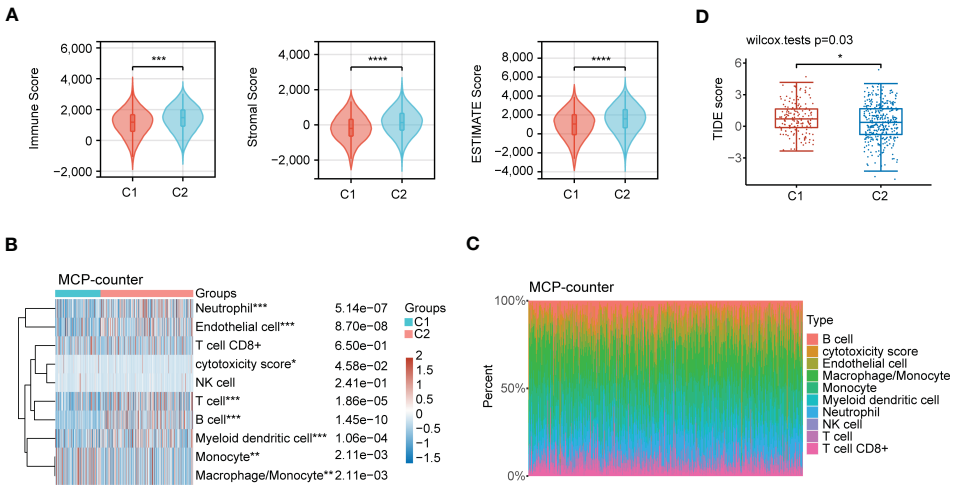

FIGURE 11
Immune characteristics analysis in the subgroups of LUAD patients. **(A)** Comprehensive analysis of the immune status in TME, including Immune Score, Stromal Score and ESTIMATE Score between C1 and C2 subgroups. **(B)** Heatmap depicting immune cells infiltration in C1 and C2 subgroups using MCP-counter algorithm. **(C)** Stacking plot depicting immune cell abundance in TME using MCP-counter algorithm. **(D)** The prediction of immunotherapy response between the two subgroups according to the TIDE score. Statistical analysis: *$P < 0.05$, **$P < 0.01$, ***$P < 0.001$, and ****$P < 0.0001$.

determined the expression levels of PSMC6, SMOX, and SMS in LUAD cell lines, and explored their diagnostic and prognostic values in LUAD patients using ROC and survival analyses. We also highlighted the correlation of polyamines metabolism-associated subgroups in LUAD patients with immune cells infiltration in TME, and the immunotherapy response. These observations portended that targeting the polyamines metabolic pathway may become a promising therapeutic strategy for LUAD patients.

Data availability statement

Publicly available datasets were analyzed in this study. This data can be found here: LUAD data was collected from The Cancer Genome Atlas (TCGA) database (https://portal.gdc.cancer.gov/); GSE72094 dataset was acquired from GEO database (http://www.ncbi.nlm.nih.gov/geo/).

Author contributions

XH and CY contributed to the design, supervision, and acquiring funding of this work. NW and LZ performed data collection, analysis, and experiments. MC and JL participated in data analysis and figure generation. NW wrote the manuscript. All authors contributed to the article and approved the submitted version.

Conflict of interest

The authors declare that the research was conducted in the absence of any commercial or financial relationships that could be construed as a potential conflict of interest.

Publisher's note

Supplementary material

The Supplementary Material for this article can be found online at: https://www.frontiersin.org/articles/10.3389/fimmu.2023.1070953/full#supplementary-material

SUPPLEMENTARY FIGURE 1
Analysis of immune cells infiltration between C1 and C2 subgroups of LUAD patients using xCell algorithm. **(A)** Heatmap depicting immune cells infiltration in C1 and C2 subgroups using xCell algorithm. **(B)** Stacking plot depicting immune cell abundance in TME using xCell algorithm.

References

1. Hesterberg RS, Cleveland JL, Epling-Burnette PK. Role of polyamines in immune cell functions. *Med Sci (Basel)* (2018) 6(1):22. doi: 10.3390/medsci6010022

2. Pegg AE. Functions of polyamines in mammals. *J Biol Chem* (2016) 291 (29):14904–12. doi: 10.1074/jbc.R116.731661

3. Dever TE, Ivanov IP. Roles of polyamines in translation. *J Biol Chem* (2018) 293 (48):18719–29. doi: 10.1074/jbc.TM118.003338

4. Casero RAJr, Murray Stewart T, Pegg AE. Polyamine metabolism and cancer: treatments, challenges and opportunities. *Nat Rev Cancer* (2018) 18(11):681–95. doi: 10.1038/s41568-018-0050-3

5. Guo Y, Ye Q, Deng P, Cao Y, He D, Zhou Z, et al. Spermine synthase and MYC cooperate to maintain colorectal cancer cell survival by repressing bim expression. *Nat Commun* (2020) 11(1):3243. doi: 10.1038/s41467-020-17067-x

6. Morris EC, Neelapu SS, Giavridis T, Sadelain M. Cytokine release syndrome and associated neurotoxicity in cancer immunotherapy. *Nat Rev Immunol* (2022) 22(2):85–96. doi: 10.1038/s41577-021-00547-6

7. Reck M, Remon J, Hellmann MD. First-line immunotherapy for non-Small-Cell lung cancer. *J Clin Oncol* (2022) 40(6):586–97. doi: 10.1200/JCO.21.01497

8. Devalaraja S, To T, Folkert IW, Natesan R, Alam MZ, Li M, et al. Tumor-derived retinoic acid regulates intratumoral monocyte differentiation to promote immune suppression. *Cell* (2020) 180(6):1098–1114.e16. doi: 10.1016/j.cell.2020.02.042

9. Di Blasio S, van Wigcheren GF, Becker A, van Duffelen A, Gorris M, Verrijp K, et al. The tumour microenvironment shapes dendritic cell plasticity in a human organotypic melanoma culture. *Nat Commun* (2020) 11(1):2749. doi: 10.1038/s41467-020-16583-0

10. Holbert CE, Cullen MT, Casero RAJr, Stewart TM. Polyamines in cancer: integrating organismal metabolism and antitumour immunity. *Nat Rev Cancer* (2022) 22(8):467–80. doi: 10.1038/s41568-022-00473-2

11. Latour YL, Gobert AP, Wilson KT. The role of polyamines in the regulation of macrophage polarization and function. *Amino Acids* (2020) 52(2):151–60. doi: 10.1007/s00726-019-02719-0

12. Sung H, Ferlay J, Siegel RL, Laversanne M, Soerjomataram I, Jemal A, et al. Global cancer statistics 2020: GLOBOCAN estimates of incidence and mortality worldwide for 36 cancers in 185 countries. *CA Cancer J Clin* (2021) 71(3):209–49. doi: 10.3322/caac.21660

13. Brody H. Lung cancer. *Nature* (2020) 587(7834):S7. doi: 10.1038/d41586-020-03152-0

14. Tagliamento M, Frelaut M, Baldini C, Naigeon M, Nencioni A, Chaput N, et al. The use of immunotherapy in older patients with advanced non-small cell lung cancer. *Cancer Treat Rev* (2022) 106:102394. doi: 10.1016/j.ctrv.2022.102394

15. Friedlaender A, Naidoo J, Banna GL, Metro G, Forde P, Addeo A. Role and impact of immune checkpoint inhibitors in neoadjuvant treatment for NSCLC. *Cancer Treat Rev* (2022) 104:102350. doi: 10.1016/j.ctrv.2022.102350

16. Szklarczyk D, Gable AL, Lyon D, Junge A, Wyder S, Huerta-Cepas J, et al. STRING v11: protein-protein association networks with increased coverage, supporting functional discovery in genome-wide experimental datasets. *Nucleic Acids Res* (2019) 47(D1):D607–13. doi: 10.1093/nar/gky1131

17. Ang YS, Rivas RN, Ribeiro A, Srivas R, Rivera J, Stone NR, et al. Disease model of GATA4 mutation reveals transcription factor cooperativity in human cardiogenesis. *Cell* (2016) 167(7):1734–1749.e22. doi: 10.1016/j.cell.2016.11.033

18. Wang N, Zhu L, Wang L, Shen Z, Huang X. Identification of SHCBP1 as a potential biomarker involving diagnosis, prognosis, and tumor immune microenvironment across multiple cancers. *Comput Struct Biotechnol J* (2022) 20:3106–19. doi: 10.1016/j.csbj.2022.06.039

19. Ritchie ME, Phipson B, Wu D, Hu Y, Law CW, Shi W, et al. Limma powers differential expression analyses for RNA-sequencing and microarray studies. *Nucleic Acids Res* (2015) 43(7):e47. doi: 10.1093/nar/gkv007

20. Becht E, Giraldo NA, Lacroix L, Buttard B, Elarouci N, Petitprez F, et al. Estimating the population abundance of tissue-infiltrating immune and stromal cell populations using gene expression. *Genome Biol* (2016) 17(1):218. doi: 10.1186/s13059-016-1070-5

21. Aran D, Hu Z, Butte AJ. xCell: digitally portraying the tissue cellular heterogeneity landscape. *Genome Biol* (2017) 18(1):220. doi: 10.1186/s13059-017-1349-1

22. Jiang P, Gu S, Pan D, Fu J, Sahu A, Hu X, et al. Signatures of T cell dysfunction and exclusion predict cancer immunotherapy response. *Nat Med* (2018) 24(10):1550–8. doi: 10.1038/s41591-018-0136-1

23. Rao S, Mondragón L, Pranjic B, Hanada T, Stoll G, Köcher T, et al. AIF-regulated oxidative phosphorylation supports lung cancer development. *Cell Res* (2019) 29(7):579–91. doi: 10.1038/s41422-019-0181-4

24. Gentric G, Kieffer Y, Mieulet V, Goundiam O, Bonneau C, Nemati F, et al. PML-regulated mitochondrial metabolism enhances chemosensitivity in human ovarian cancers. *Cell Metab* (2019) 29(1):156–173.e10. doi: 10.1016/j.cmet.2018.09.002

25. Lee CY, Su GC, Huang WY, Ko MY, Yeh HY, Chang GD, et al. Promotion of homology-directed DNA repair by polyamines. *Nat Commun* (2019) 10(1):65. doi: 10.1038/s41467-018-08011-1

26. McNamara KM, Gobert AP, Wilson KT. The role of polyamines in gastric cancer. *Oncogene* (2021) 40(26):4399–412. doi: 10.1038/s41388-021-01862-x

27. Novita Sari I, Setiawan T, Seock Kim K, Toni Wijaya Y, Won Cho K, Young Kwon H. Metabolism and function of polyamines in cancer progression. *Cancer Lett* (2021) 519:91–104. doi: 10.1016/j.canlet.2021.06.020

28. Gu SS, Wang X, Hu X, Jiang P, Li Z, Traugh N, et al. Clonal tracing reveals diverse patterns of response to immune checkpoint blockade. *Genome Biol* (2020) 21 (1):263. doi: 10.1186/s13059-020-02166-1

29. Riesenberg BP, Hunt EG, Tennant MD, Hurst KE, Andrews AM, Leddy LR, et al. Stress-mediated attenuation of translation undermines T-cell activity in cancer. *Cancer Res* (2022) 82(23):4386–99. doi: 10.1158/0008-5472.CAN-22-1744

30. Reinfeld BI, Rathmell WK, Kim TK, Rathmell JC. The therapeutic implications of immunosuppressive tumor aerobic glycolysis. *Cell Mol Immunol* (2022) 19(1):46–58. doi: 10.1038/s41423-021-00727-3

31. Lian X, Yang K, Li R, Li M, Zuo J, Zheng B, et al. Immunometabolic rewiring in tumorigenesis and anti-tumor immunotherapy. *Mol Cancer* (2022) 21(1):27. doi: 10.1186/s12943-021-01486-5

32. Matos A, Carvalho M, Bicho M, Ribeiro R. Arginine and arginases modulate metabolism, tumor microenvironment and prostate cancer progression. *Nutrients* (2021) 13(12):4503. doi: 10.3390/nu13124503

33. Chia TY, Zolp A, Miska J. Polyamine immunometabolism: central regulators of inflammation, cancer and autoimmunity. *Cells* (2022) 11(5):896. doi: 10.3390/cells11050896

34. Azizi E, Carr AJ, Plitas G, Cornish AE, Konopacki C, Prabhakaran S, et al. Single-cell map of diverse immune phenotypes in the breast tumor microenvironment. *Cell* (2018) 174(5):1293–1308.e36. doi: 10.1016/j.cell.2018.05.060

35. Lian J, Liang Y, Zhang H, Lan M, Ye Z, Lin B, et al. The role of polyamine metabolism in remodeling immune responses and blocking therapy within the tumor immune microenvironment. *Front Immunol* (2022) 13:912279. doi: 10.3389/fimmu.2022.912279

Frontiers in Immunology

Explores novel approaches and diagnoses to treat immune disorders.

The official journal of the International Union of Immunological Societies (IUIS) and the most cited in its field, leading the way for research across basic, translational and clinical immunology.

Discover the latest Research Topics

See more →

Frontiers

Avenue du Tribunal-Fédéral 34
1005 Lausanne, Switzerland
frontiersin.org

Contact us

+41 (0)21 510 17 00
frontiersin.org/about/contact